MALARIA TARGETING TOOLKIT: HOST-PARASITE INTERACTION

EDITED BY: Jing-wen Lin, Takeshi Annoura, Miguel Prudêncio and Deirdre A. Cunningham
PUBLISHED IN: Frontiers in Cellular and Infection Microbiology

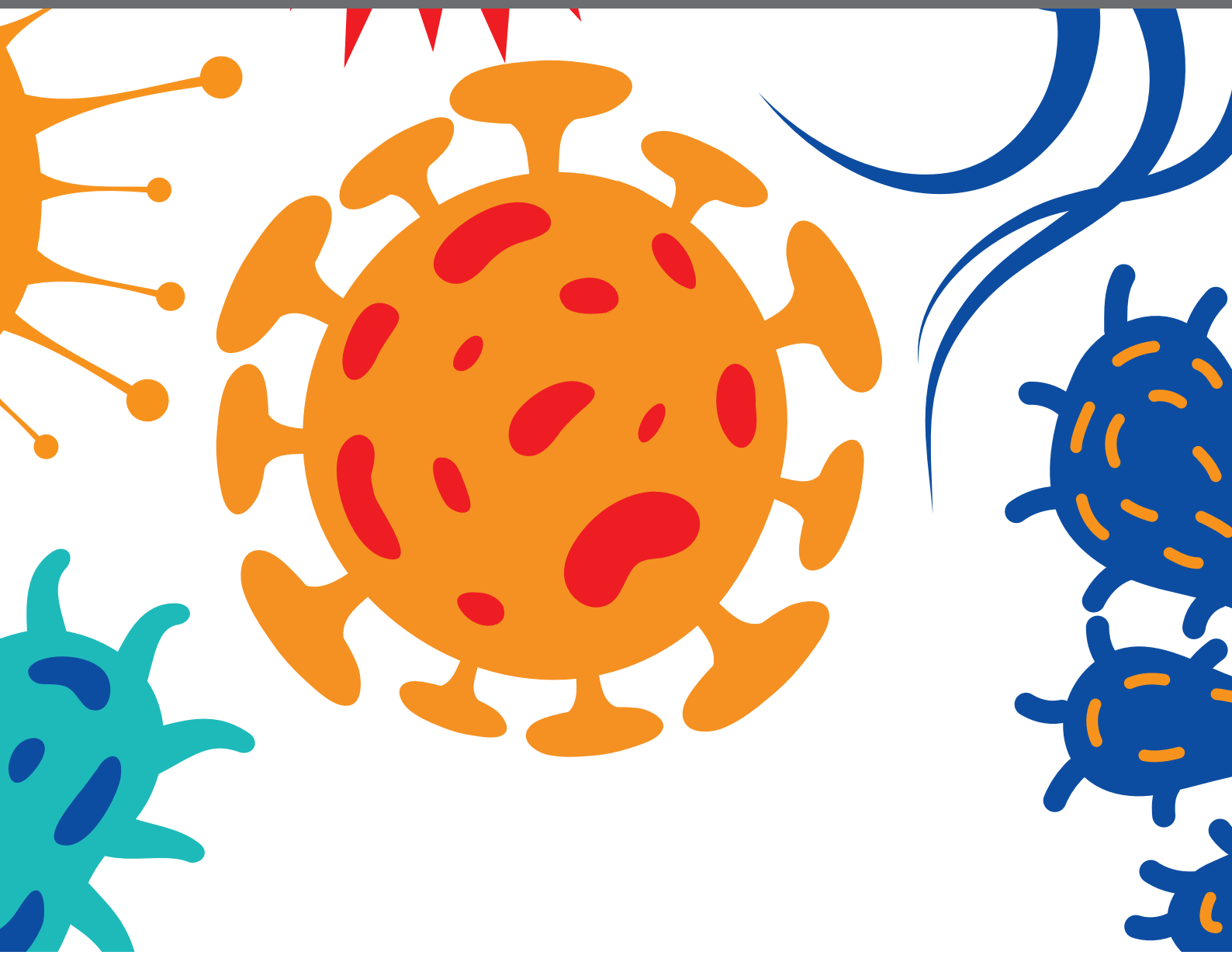

frontiers Research Topics

frontiers

ISSN 1664-8714
ISBN 978-2-88974-006-2
DOI 10.3389/978-2-88974-006-2

About Frontiers

Frontiers is more than just an open-access publisher of scholarly articles: it is a pioneering approach to the world of academia, radically improving the way scholarly research is managed. The grand vision of Frontiers is a world where all people have an equal opportunity to seek, share and generate knowledge. Frontiers provides immediate and permanent online open access to all its publications, but this alone is not enough to realize our grand goals.

Frontiers Journal Series

The Frontiers Journal Series is a multi-tier and interdisciplinary set of open-access, online journals, promising a paradigm shift from the current review, selection and dissemination processes in academic publishing. All Frontiers journals are driven by researchers for researchers; therefore, they constitute a service to the scholarly community. At the same time, the Frontiers Journal Series operates on a revolutionary invention, the tiered publishing system, initially addressing specific communities of scholars, and gradually climbing up to broader public understanding, thus serving the interests of the lay society, too.

Dedication to Quality

Each Frontiers article is a landmark of the highest quality, thanks to genuinely collaborative interactions between authors and review editors, who include some of the world's best academicians. Research must be certified by peers before entering a stream of knowledge that may eventually reach the public - and shape society; therefore, Frontiers only applies the most rigorous and unbiased reviews.
Frontiers revolutionizes research publishing by freely delivering the most outstanding research, evaluated with no bias from both the academic and social point of view. By applying the most advanced information technologies, Frontiers is catapulting scholarly publishing into a new generation.

What are Frontiers Research Topics?

Frontiers Research Topics are very popular trademarks of the Frontiers Journals Series: they are collections of at least ten articles, all centered on a particular subject. With their unique mix of varied contributions from Original Research to Review Articles, Frontiers Research Topics unify the most influential researchers, the latest key findings and historical advances in a hot research area! Find out more on how to host your own Frontiers Research Topic or contribute to one as an author by contacting the Frontiers Editorial Office: frontiersin.org/about/contact

MALARIA TARGETING TOOLKIT: HOST-PARASITE INTERACTION

Topic Editors:
Jing-wen Lin, Sichuan University, China
Takeshi Annoura, National Institute of Infectious Diseases (NIID), Japan
Miguel Prudêncio, Universidade de Lisboa, Portugal
Deirdre A. Cunningham, Francis Crick Institute, United Kingdom

Citation: Lin, J.-w., Annoura, T., Prudêncio, M., Cunningham, D. A., eds. (2021). Malaria Targeting Toolkit: Host-Parasite Interaction. Lausanne: Frontiers Media SA. doi: 10.3389/978-2-88974-006-2

Table of Contents

frontiers in Cellular and Infection Microbiology

EDITORIAL
published: 17 November 2021
doi: 10.3389/fcimb.2021.795494

Editorial: Malaria Targeting Toolkit: Host-Parasite Interactions

Tamasa Araki[1], *Jing-wen Lin*[2*], *Miguel Prudêncio*[3*], *Deirdre A. Cunningham*[4*] *and Takeshi Annoura*[1*]

[1] Department of Parasitology, National Institute of Infectious Diseases (NIID), Tokyo, Japan, [2] State Key Laboratory of Biotherapy, West China Hospital, Sichuan University and Collaborative Innovation Center for Biotherapy, Chengdu, China, [3] Instituto de Medicina Molecular, Faculdade de Medicina, Universidade de Lisboa, Lisboa, Portugal, [4] The Francis Crick Institute, London, United Kingdom

Keywords: ***Plasmodium***, **malaria, drug development, immune response, parasite virulence, host-parasite interactions**

OPEN ACCESS

Edited and reviewed by:
Tania F. De Koning-Ward, Deakin University, Australia

***Correspondence:**
Takeshi Annoura
annoura@niid.go.jp
Jing-wen Lin
lin.jingwen@scu.edu.cn
Miguel Prudêncio
mprudencio@medicina.ulisboa.pt
Deirdre A. Cunningham
Deirdre.Cunningham@crick.ac.uk

Specialty section:
This article was submitted to Parasite and Host, a section of the journal Frontiers in Cellular and Infection Microbiology

Received: *15 October 2021*
Accepted: *29 October 2021*
Published: *17 November 2021*

Citation:
Araki T, Lin J-w, Prudêncio M, Cunningham DA and Annoura T (2021) Editorial: Malaria Targeting Toolkit: Host-Parasite Interactions. Front. Cell. Infect. Microbiol. 11:795494. doi: 10.3389/fcimb.2021.795494

Editorial on the Research Topic

Malaria Targeting Toolkit: Host-Parasite Interaction

Malaria remains a serious threat to public health worldwide. Protozoan *Plasmodium* parasites, the etiological agents of malaria, are transmitted to their mammalian hosts by *Anopheles* mosquitoes. Despite decades of collective efforts, malaria remains one of the most devastating infectious diseases in the globe, with more than half of the world's population at risk of infection and more than 400 thousand annual deaths. Malaria is a complex disease with a broad spectrum of symptoms, ranging from mild forms to severe pathology, the latter occurring in patients with life-threatening anemia, cerebral malaria, metabolic acidosis, and multiorgan system failure. In order to provide new insights into the complex interplay between the parasite and its mammalian host during the liver or blood stages of *Plasmodium* infection, the identification of key parasite or host molecules that interact with each other or that critically influence the outcome of infection, and the understanding of immune responses to infection, remain a priority (**Figure 1**). The present Research Topic consists of 11 papers, including 3 reviews, 1 perspective, 1 brief research report, and 6 original research articles.

Dhangadamajhi and Singh described the role of plasma sphingosine 1-phosphate (S1P), recently shown to play an important role in the regulation of various physiological processes related to malaria pathogenesis. S1P is a bioactive lipid intermediate of sphingolipid metabolism that exists in intracellular (such as red blood cells and platelets) and circulating extracellular pools, with each pool having a different function. In this review, the authors summarised the significance of each of these pools in the context of malaria. They also discussed how the S1P content in the erythrocytes could be channelled towards future therapeutic opportunities for malaria.

An original research article revealed the role of the *Plasmodium berghei* quiescin sulfhydryl oxidase (PbQSOX), which is present in various eukaryotic species and catalyses the insertion of disulphide bonds into unfolded and reduced proteins. Zheng et al. show that PbQSOX is most abundantly expressed in ookinetes, and localizes in the cytoplasm and surface of ookinetes. Further, the authors showed that mosquitoes fed on Δpbqsox parasite-infected mice displayed a significant

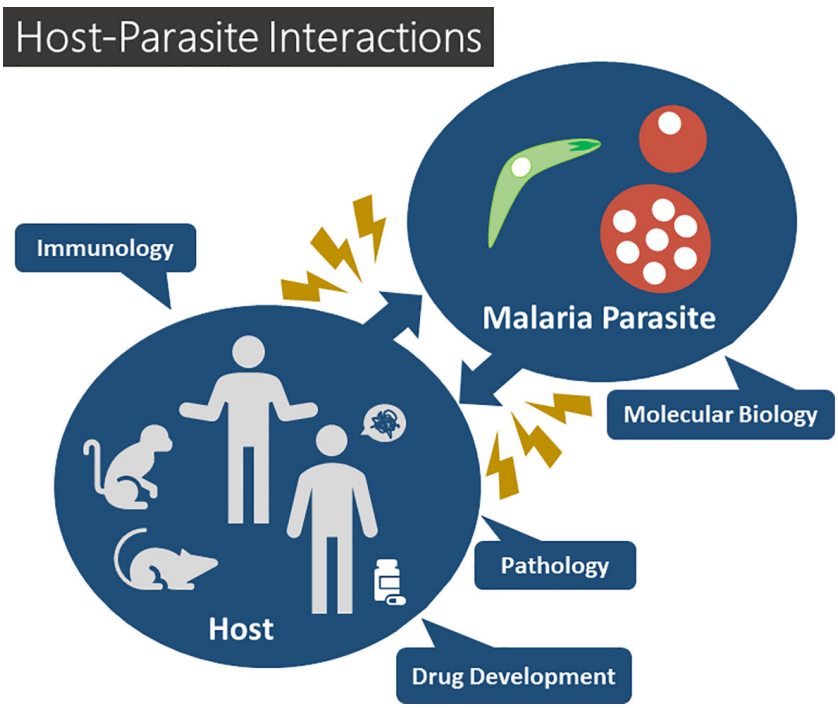

FIGURE 1 | Host-parasite interactions in malaria.

reduction in ookinete and oocyst numbers compared to those fed on wild-type parasite-infected mice. Furthermore, both polyclonal antisera and a monoclonal antibody against recombinant PbQSOX exhibited substantial transmission-blocking activities *in vitro* and in the mosquito feeding assays. These findings identified QSOX as a potential target for blocking parasite transmission.

Another article discussed the potential of chimeric *Plasmodium falciparum* (Pf) parasites expressing the *P. vivax* (Pv) circumsporozoite protein (CSP) as a tool for the investigation of vaccines against Pv. Chimeric rodent malaria parasites expressing Pf and Pv CSP have previously been used in the preclinical evaluation of CSP-based pre-erythrocytic vaccines. Miyazaki et al. have now generated chimeric *P. falciparum* parasites expressing both the endogenous PfCSP and the heterologous PvCSP. The authors showed that immunization of mice with these Pf-PvCSP sporozoites elicited the production of antibodies against the repeat regions of both PfCSP and PvCSP, supporting the use of the newly generated parasite line in the optimization of vaccines targeting PvCSP.

A review by He et al. discussed the 'conflicting' roles exhibited by type I interferons (IFN-ls) during malarial infections. IFN-Is are important cytokines that play a role in various infections, autoimmune diseases, and cancer. Both the liver and the blood stages of malaria parasites can stimulate IFN-I responses in their vertebrate host. The host's genetic background greatly influences IFN-I production during *Plasmodium* infections as well. Consequently, the effect of IFN-Is on parasitemia and disease symptoms are highly variable, depending on the combination of the parasite species/strains and the host. This review also summarized the major findings and progress in ligand recognition, signalling pathways, functions, and regulation of IFN-I responses during mammalian infections by *Plasmodium* parasites.

An article by Ito et al. showed that novel proteins of apical organelles in merozoites are involved in erythrocyte invasion by *Plasmodium falciparum*. The authors generated a panel of monoclonal antibodies against *P. falciparum* schizont-rich parasites and screened the antibodies using immunofluorescence assays. Five of the monoclonal antibodies were then used in immuno-affinity experiments to purify their target antigens. Afterwards, liquid chromatography-tandem mass spectrometry (LC-MS/MS) was used to identify these antigens. The authors further expand on a novel complex that was identified by immunoprecipitation, composed of *P. falciparum* rhoptry-associated membrane antigen (PfRAMA) and *P. falciparum* rhoptry neck protein 3 (PfRON3) and identified a region spanning amino acids Q221-E481 of PfRAMA that can associate with PfRON3 in the immature schizonts.

A mini-review provided exciting new insights on the cross-talk between the *Plasmodium* parasite and its mammalian host. Voorberg-van der Wel et al. zoomed in on new technologies using monkey malaria and other malaria parasite model systems that can provide the tools necessary to investigate host-parasite interactions of relapsing parasites. The authors proposed that learning more about hypnozoite and host cross-talks should help identify factors that promote the activation of these dormant

parasite reservoirs, leading to disease relapses, and may contribute to the identification of new tools aimed at eventually achieving malaria eradication.

A perspective topic authored by Oresegun et al. discussed underlying pathophysiological processes leading to a serious malaria infection. The authors described zoonotic malaria caused by *P. knowlesi* and proposed the use of this parasite as a model system specifically for severe malaria. Subsequently, a method to generate long-read third-generation *Plasmodium* genome sequence data from archived clinical samples was developed using the MinION platform. This research then developed a representative translational model for severe malaria that was informed by clinically relevant parasite diversity due to its ability to exploit the duality of *P. knowlesi* as a laboratory model and human pathogen.

Another article by Taku et al. discussed how the transport protein N-myristoylated adenylate kinase 2 (PfAK2) is transported and regulated by Rab GTPases from the endoplasmic reticulum (ER) to the cell's surface. Previously, the same group reported that the export of PfAK2, which lacked the PEXEL (*Plasmodium* export element) motif, was regulated by PfRab5b GTPase (Ebine et al., 2016). These authors now expand their findings and demonstrate that PfRab5b and the associated GTPases are involved in trafficking PfAK2 and PEXEL-positive Rifin from the ER. Two membrane trafficking GTPases, PfArf1 and PfRab1b, were also coimmunoprecipitated with PfRab5b and subjected to mass spec analysis. Their results showed that PfArf1 and PfRab1b colocalised with PfRab5b adjacent to the ER marker, PfBiP. Furthermore, results from the mutant analysis of PfArf1 and Rab1b suggest that PfArf1 was extensively involved in the transportation of PfAK2. The data showed that PfArf1 and PfRab1b are also involved in RIFIN transport, thereby indicating the sequential roles of PfArf1 and PfRab1b in cargo selection. The research is the first report on cargo selection of PfAK2 on the ER's subdomain by PfArf1.

The molecular mechanisms underlying the protection against malaria offered by the heterozygous carriage of the haemoglobin S mutation (HbAS), or sickle cell trait, are still poorly understood. The original article by Chauvet et al. investigated the proteome and phosphoproteome of red cell membrane extract from *P. falciparum*-infected and uninfected red blood cells (RBCs) from heterozygous S carriers (HbAS) and homozygous non-mutant (HbAA) donors. The authors identified proteins whose quantity or phosphorylation state varied according to infection status and/or host haemoglobin genotype. Changes due to the S trait, to *P. falciparum* infection, or both were highlighted. Proteins identified included erythrocyte membrane transporters, skeletal proteins, and parasite proteins such as RESA or MESA. Phosporylation state may influence multiple functions such as membrane interactions, nutrient transport, cytoadherence. This is the first report of phosphorylation patterns in HbAS RBCs, infected or uninfected, and thus provides clues to understanding the molecular mechanisms of malaria resistance and importantly also identified alterations in phosphorylation state solely due to the carrier status.

The original research article by Ikeda et al. employed a novel genetic tool, *P. berghei* mutator (PbMut), whose base substitution rate is 36.5 times higher than that of wild-type parasites, to analyse a mutant parasite line (PbMut-PPQ-R-P9) with reduced susceptibility to piperaquine (PPQ), unveiling a new mechanism of drug resistance in malaria parasites. Whole-genome sequence analysis of PbMut-PPQ-R-P9 clones revealed that eight nonsynonymous mutations were conserved in all clones, including N331I in PbCRT, which encodes the chloroquine resistance transporter (CRT). Furthermore, the PPQ susceptibility and growth rates observed in genome-edited parasites (PbCRT-N331I) were significantly lower than those of PbMut-PPQ-R-P9, implying that additional mutations in PbMut-PPQ-R9 parasites compensate for the fitness cost of the PbCRT (N331I) mutation and contribute to reduced PPQ susceptibility. In summary, PbMut served as a novel genetic tool for predicting gene mutations responsible for drug resistance. Nevertheless, further studies on PbMut-PPQ-R-P9, which are likely to reveal genetic changes that compensate for fitness costs owing to drug resistance acquisition, should be conducted.

This original research article clarifies *Plasmodium*'s mechanism of mRNA quality control and export using RNA-binding proteins of malaria parasites. Previous research had shown that nuclear poly(A) binding protein 2 (NAB2), THO complex subunit 4 (THO4), nucleolar protein 3 (NPL3), G-strand binding protein 2 (GBP2), and serine/arginine-rich splicing factor 1 (SR1) are involved in nuclear mRNA export (Eshar et al., 2015). Niikura et al. now found that NAB2 and SR1, but not THO4, NPL3, or GBP2, influence the asexual development of malaria parasites. In contrast, GBP2, but not NPL3, is involved in male and female gametocyte production; therefore, the authors focus on the contribution of GBP2 and NAB2 to the sexual and asexual development of malaria parasites. They found out that GBP2 interacts with ALBA4, DOZI, CITH, and with the phosphorylated adapter RNA export (PHAX) domain-containing protein, which plays a role in translational repression. Alternatively, NAB2 interacts with transportin and binds directly to 143 mRNAs, including those encoding 40S and 60S ribosomal proteins.

In summary, the articles in this Frontier's Research Topic "Malaria Targeting Toolkit: Host-Parasite Interactions" bring important new data as well as thoughtful insights about host-parasite interactions, parasite virulence, immune responses and molecular mechanisms of host resistance to parasites, and parasite resistance to drugs. Novel tools and methodologies are being developed, state-of-the-art techniques expanded, and many new insights gained, which will inform future malaria drug and vaccine development efforts.

AUTHOR CONTRIBUTIONS

TAr and TAn prepared the draft. TAr, JL, MP, DC, and TAn revised the draft and approved the final version of the draft. All authors contributed to the article and approved the submitted version.

FUNDING

This work was supported in part by a grant for Research on Emerging and Re-emerging Infectious Diseases from the Japan Agency for Medical Research and Development (AMED) (JP21fk0108096j0303, JP21fk0108138j0602, and JP21fk0108139j3002 to TAn), a grant from the Japan Society for the Promotion of Science (JSPS) (KAKENHI JP21K06999 to TAn) and a grant from The Chemo-Sero-Therapeutic Research Institute (90011100) to TAn. This work was supported in part by the National Natural Science Foundationof China (No. 31800772) to J-wL.

ACKNOWLEDGMENTS

We greatly thank all authors and reviewers for their contributions to this Research Topic as well as the editorial office for their support.

REFERENCES

Ebine, K., Hirai, M., Sakaguchi, M., Yahata, K., Kaneko, O., and Saito-Nakano, Y. (2016). Plasmodium Rab5b Is Secreted to the Cytoplasmic Face of the Tubovesicular Network in Infected Red Blood Cells Together With N-Acylated Adenylate Kinase 2. *Malaria J.* 15, 323. doi: 10.1186/s12936-016-1377-4

Eshar, S., Altenhofen, L., Rabner, A., Ross, P., Fastman, Y., Mandel-Gutfreund, Y., et al. (2015). Pfsr1 Controls Alternative Splicing and Steady-State RNA Levels in Plasmodium Falciparum Through Preferential Recognition of Specific RNA Motifs. *Mol. Microbiol.* 96 (6), 1283–1297. doi: 10.1111/mmi.13007

Conflict of Interest: The authors declare that the research was conducted in the absence of any commercial or financial relationships that could be construed as a potential conflict of interest.

frontiers in Cellular and Infection Microbiology

ORIGINAL RESEARCH
published: 26 June 2020
doi: 10.3389/fcimb.2020.00311

Characterization of a Sulfhydryl Oxidase From *Plasmodium berghei* as a Target for Blocking Parasite Transmission

Wenqi Zheng[1,2†], Fei Liu[1†], Feng Du[3], Fan Yang[1], Xu Kou[1,4], Yiwen He[1], Hui Feng[1], Qi Fan[5], Enjie Luo[3], Hui Min[1,6], Jun Miao[6], Liwang Cui[6] and Yaming Cao[1]**

[1] Department of Immunology, College of Basic Medical Sciences, China Medical University, Shenyang, China, [2] Department of Clinical Laboratory, Affiliated Hospital of Inner Mongolian Medical University, Hohhot, China, [3] Department of Pathogen Biology, College of Basic Medical Sciences, China Medical University, Shenyang, China, [4] Department of Animal Quarantine, College of Animal Husbandry and Veterinary Sciences, Liaoning Medical University, Jinzhou, China, [5] Dalian Institute of Biotechnology, Dalian, China, [6] Department of Internal Medicine, Morsani College of Medicine, University of South Florida, Tampa, FL, United States

Quiescin sulfhydryl oxidase (QSOX), present in a wide variety of eukaryotic species, catalyzes the insertion of disulfide bonds into unfolded, reduced proteins. Here we characterized the QSOX protein from the rodent malaria parasite *Plasmodium berghei* (PbQSOX), which is conserved in all sequenced malaria parasite species. The PbQSOX protein was not expressed in asexual erythrocytic stages, but was most abundantly expressed in ookinetes. Indirect immunofluorescence assays revealed PbQSOX was not only localized in cytoplasm of gametocytes, gametes and ookinetes, but also expressed on the surface of gametes and ookinetes. Western blot identified extracellular presence of PbQSOX in the culture medium of ookinetes suggestive of secretion. *Pbqsox* deletion (Δ*pbqsox*) did not affect asexual intraerythrocytic development, but reduced exflagellation of male gametocytes as well as formation and maturation of ookinetes. *Pbqsox* deletion also led to a significant increase in the reduced thiol groups of ookinete surface proteins, suggesting that it may play a role in maintaining the integrity of disulfide bonds of surface proteins, which might be needed for ookinete development. Mosquitoes that fed on Δ*pbqsox*-infected mice showed a significant reduction in ookinete and oocyst numbers compared to those fed on wild-type parasite-infected mice. Further, both polyclonal mouse antisera and a monoclonal antibody against the recombinant PbQSOX exhibited substantial transmission-blocking activities in *in vitro* and mosquito feeding assays, suggesting QSOX is a potential target for blocking parasite transmission.

Keywords: malaria, *Plasmodium berghei*, quiescin sulfhydryl oxidase, sexual development, transmission-blocking vaccine

OPEN ACCESS

Edited by:
Takeshi Annoura, National Institute of Infectious Diseases (NIID), Japan

Reviewed by:
Kazutoyo Miura, National Institute of Allergy and Infectious Diseases (NIAID), United States
Hirdesh Kumar, National Institute of Allergy and Infectious Diseases (NIAID), United States

***Correspondence:**
Liwang Cui
liwangcui@usf.edu
Yaming Cao
ymcao@mail.cmu.edu.cn

† These authors have contributed equally to this work

Specialty section:
This article was submitted to Parasite and Host, a section of the journal Frontiers in Cellular and Infection Microbiology

Received: *07 April 2020*
Accepted: *22 May 2020*
Published: *26 June 2020*

Citation:
Zheng W, Liu F, Du F, Yang F, Kou X, He Y, Feng H, Fan Q, Luo E, Min H, Miao J, Cui L and Cao Y (2020) Characterization of a Sulfhydryl Oxidase From Plasmodium berghei as a Target for Blocking Parasite Transmission. Front. Cell. Infect. Microbiol. 10:311. doi: 10.3389/fcimb.2020.00311

INTRODUCTION

Malaria is caused by protozoan parasites of the genus *Plasmodium* and transmitted via female *Anopheles* mosquitoes. Globally, an estimated 3.3 billion people are at risk of infection. According to World Malaria Report 2019, the global progress against malaria has stalled as the number of malaria cases rose from 217 million in 2016 to 228 million in 2018 (WHO, 2019). The emergence

of drug-resistant parasites and insecticide-resistant *Anopheles* are major limiting factors for malaria elimination, and calls for integrated approaches (Hemingway et al., 2016; Menard and Dondorp, 2017). One potential strategy involves the development of effective malaria vaccines (Genton, 2008). Among the vaccines targeting different parasite stages, transmission-blocking vaccines (TBVs) target sexual- and mosquito-stage parasites (i.e., gametocyte, gamete, zygote, and ookinete) as well as mosquito gut proteins (Wu et al., 2015; Kumar and Tolia, 2019).

The working principle of TBVs is that TBVs induce transmission-blocking (TB) antibodies in humans, which will arrest subsequent parasite development in the mosquito midgut, thus interrupting the transmission of the parasites to the vectors (Wu et al., 2015; Delves et al., 2018). Transmission of the malaria parasites to the vector is initiated by the sexual stage precursor cells, the gametocytes. Once gametocytes are ingested by a mosquito, gametogenesis is accomplished in 15–20 min, and the resultant male and female gametes will mate to form zygotes. Subsequent development from a zygote to a motile ookinete must be accomplished within 24 h so that the parasite can escape the hostile environment in the blood bolus. The gamete–ookinete stages are extracellular and are exposed to the mosquito-derived digestive enzymes and the resultant cytotoxic byproducts, as well as the immune responses from the human hosts (Sinden, 2002). To adapt to these environmental changes in the blood meal inside the mosquito midgut, the malaria parasite produces antioxidant proteins such as thioredoxin-1, peroxiredoxin-1 and 1-Cys peroxiredoxin-1, to ensure survival and escape of the ookinete (Turturice et al., 2013). However, it is not known whether other antioxidant proteins are involved in this process or how the ookinete deals with the oxidative damage of its surface proteins.

Quiescin sulfhydryl oxidase (QSOX) family enzymes, found in eukaryotes except fungi, specifically catalyze the direct and facile introduction of disulfide bonds into unfolded, reduced proteins with the reduction of a molecular oxygen, generating hydrogen peroxide: $2RSH+O_2 \rightarrow RS\text{-}SR+H_2O_2$ (Haque et al., 2012; Limor-Waisberg et al., 2013). Two moieties of the enzyme carry out the tandem actions of substrate oxidation and electron transfer: thioredoxin-fold (Trx) domain and a sulfhydral oxidase module related to the Erv/ALR enzyme family. A helix-rich region between the Trx and Erv/ALR domains adopts a structural fold similar to the Erv domain, and is thus known as the pseudo-Erv domain (ψErv) (Alon et al., 2010). Interestingly, metazoan QSOX enzymes have a second Trx-fold domain (Trx-2) between the active Trx domain and the ψErv domain, whereas this Trx-2 domain is absent in plant and protist QSOXs (Kodali and Thorpe, 2010; Haque et al., 2012; Limor-Waisberg et al., 2013). While the functional significance of QSOXs has been increasingly appreciated, recent studies have revealed that elevated human QSOX is strongly correlated with certain diseases including pancreatic cancer (Katchman et al., 2011), heart failure (Mebazaa et al., 2012), breast cancer (Soloviev et al., 2013; Poillet et al., 2014), and prostate tumorigenesis (Song et al., 2009).

In looking for additional antioxidant proteins, we paid attention to the QSOX family because there is a growing body of evidence showing that QSOXs are widely present in eukaryotes and may play essential roles in parasite growth and host–parasite interactions (Haque et al., 2012). The QSOX enzymes that catalyze the thiol redox reaction possess conserved as well as unique domains, making them worthwhile targets for new therapeutic development. Here we identified a QSOX member in all malaria parasite genomes and characterized QSOX in the rodent malaria parasite *Plasmodium berghei* (PbQSOX). We discovered that PbQSOX is required for parasite sexual development, especially for ookinete maturation. In addition, antibodies against PbQSOX showed obvious TB activities, indicating that PbQSOX may be a potential candidate for TB drug and vaccine development.

MATERIALS AND METHODS

Mice, Parasites, and Mosquitoes

Six- to eight-week-old female BALB/c mice were used for all experiments. *P. berghei* (ANKA strain 2.34) and all experimental lines were maintained in female BALB/c mice by serial mechanical passage (up to a maximum of eight passages) and used for challenge infection as described elsewhere (Blagborough and Sinden, 2009). Mouse infection was typically done by intraperitoneally (i.p.) injecting 5×10^6 *P. berghei*-infected red blood cells (iRBCs). Adult *Anopheles stephensi* (Hor strain) mosquitoes were maintained on a 10% (w/v) glucose solution at 25°C and 50–80% relative humidity with a 12-h light–dark cycle in an insectary. Animal use was conducted according to the guidelines of The Animal Usage Committee of China Medical University.

Sequence Analysis

The putative *pbqsox* amino acid sequence and its orthologs in other *Plasmodium* species in PlasmoDB (www.plasmodb.org) were used to BLAST search GenBank. Homologous genes in model organisms were retrieved and aligned by ClustalW. A cladogram of the full-length QSOX proteins was constructed using the maximum-likelihood method as implemented in MEGA5 (Tamura et al., 2011). The secondary structure of PbQSOX was predicted by PSIPRED (http://bioinf.cs.ucl.ac.uk/psipred/). Signal peptide and protein domain organization was determined using the SMART program (http://smart.embl-heidelberg.de/).

Expression and Purification of Recombinant PbQSOX (rPbQSOX)

For the expression of rPbQSOX, a *pbqsox* fragment encoding amino acids 24–516 without the predicted signal peptide was amplified from the *P. berghei* genomic DNA using forward primer *pbqsox*-F containing a *Bam*HI site and an enterokinase cleavage sequence (GACGACGACGACAAG) (Zhou et al., 2014), and reverse primer *pbqsox*-R containing a *Hin*dIII site (**Table S1**) and cloned into pET30a (+) vector. The final pET-30a (+)-*pbqsox* vector carried an N-terminal His•Tag®/thrombin/S•Tag™/ enterokinase sequence and the *pbqsox* fragment. The rPbQSOX was expressed in *Escherichia coli* BL-21 strain after induction with 1 mM isopropyl-β-D-thiogalactopyranoside at 20°C for 12 h. Proteins were purified

using Ni-NTA His•Bind Superflow (Novagen) under native conditions. After the final wash with 20 mM imidazole in 300 mM NaCl and 50 mM sodium phosphate buffer (pH 8.0), rPbQSOX was eluted with 250 mM imidazole in 300 mM NaCl and 50 mM sodium phosphate buffer (pH 8.0). The fractions containing rPbQSOX were extensively desalted in 0.1 M phosphate-buffered saline (PBS, pH 7.4) overnight at 4°C. Then the fusion rPbQSOX protein was digested by the recombinant enterokinase (Solarbio) at 25°C for 16 h to remove the tags. The mixture was further purified by Ni-NTA His•Bind Superflow to remove the His/S tag. The effluent containing liberated rPbQSOX was analyzed by 10% SDS-PAGE. A recombinant glutathione S-transferase (rGST) protein was expressed using the empty vector pGEX-4T-1 and used as negative controls for activity assay and immunization.

PbQSOX Activity Assay

The sulfhydral oxidase activity of rPbQSOX was determined at 25°C in 50 mM potassium phosphate buffer and 1 mM EDTA at pH 7.5 as described elsewhere (Raje et al., 2002; Zheng et al., 2012). The molar concentration of the enzyme was determined according to the molecular weight determined using the molar extinction coefficient from the ExPASy proteomics server (http://www.expasy.org/). Briefly, 500 nM of purified rPbQSOX or rGST (negative control) was assayed in a final assay mixture containing 1.4 μM horseradish peroxidase (HRP), 1 mM homovanillic acid (HVA) and 5.7 mM Tris [2-carboxyethyl] phosphine (TCEP) or 5 mM dithiothreitol (DTT) (Sigma). In this assay, the oxidase activity was determined as the fluorescence intensity of the HVA dimer, which was formed from HRP-mediated HVA oxidation by H_2O_2. H_2O_2 is produced when oxygen is reduced by QSOX using TECP or DTT as the substrate (Raje et al., 2002). Enzyme activity data were obtained by monitoring the fluorescence at 360 nm excitation and 485 nm emission at 10 min.

Purification of Different Stages of the Parasite

To purify schizonts, infected blood taken from mice on day 4 post infection (p.i.) were placed in a blood-stage culture medium [RPMI 1640 containing 20% (v/v) fetal bovine serum (FBS), 50 mg/L penicillin and streptomycin, 50 ml culture medium/0.5 ml blood] and incubated for 16 h at 37°C with shaking at 100 rpm. A Giemsa-stained blood smear from the culture was prepared and the relative abundance of schizonts determined. If appropriate, the culture was fractionated on 55% (v/v) Nycodenz–RPMI 1640 culture medium cushion. Gametocytes were purified according to a previous study (Beetsma et al., 1998) with modifications. Phenylhydrazine-treated mice were infected with *P. berghei*, and on day 4 p.i. mice were treated with 20 mg/L sulfadiazine (Sigma) in drinking water for 2 days. Blood was collected in blood-stage culture medium pre-warmed at 37°C to avoid premature activation of gametocytes, and the blood suspension was loaded on top of a 48% (v/v) Nycodenz/blood-stage culture medium cushion and centrifuged at 1,300 × g for 30 min without brake. The interface was recovered and washed twice in 10 ml of RPMI 1640 before activation for gamete formation. For ookinete culture, parasitemia was allowed to reach 1–3% and mice were bled by cardiac puncture under terminal anesthesia on day 3 p.i. as described (Sinden et al., 1985). Blood was passed through a CF11 cellulose powder (Whatman) column to deplete white blood cells. The eluate was diluted 1:10 with complete ookinete medium [RPMI 1640 containing 50 mg/L penicillin, 50 mg/L streptomycin, 100 mg/L neomycin, 20% (v/v) FBS and 1 mg/L heparin, pH 8.3] in a flask to a maximum depth of 1 cm and kept at 19°C for 24 h, after which the culture was checked for the presence of ookinetes by Giemsa staining. Cultured ookinetes were loaded on a 62% (v/v) Nycodenz/ookinete culture medium cushion and centrifuged at 1,300 × g for 30 min without brake. Ookinetes at the interface were recovered and washed twice in 10 ml of PBS (pH 7.4).

Quantitative Reverse Transcription-Polymerase Chain Reaction (qRT-PCR)

Total RNA was isolated from purified parasites using an RNA purification kit (Qiagen). cDNA was synthesized from 1 μg of total RNA using an RNA-to-cDNA kit (Takara). *Pbqsox* expression was determined by qRT-PCR using primers Pbqsox1 and Pbqsox2 (**Table S1**). qRT-PCR reactions consisted of 2 μl cDNA, 10 μl SYBR Green fast master mix (ThermoFisher), 0.5 μl each of the forward and reverse primers and 7 μl RNase-free water. Analysis was conducted using a 7500 Fast PCR System (ThermoFisher) with the following conditions: initial denaturation at 95°C for 20 s, followed by 40 cycles of 95°C for 5 s and 60°C for 30 s. The expression of *hsp70* (PBANKA_081890) was used as the internal reference with primers Hsp70F and Hsp70R (**Table S1**). Relative quantification of *pbqsox* expression was assessed using the $\Delta\Delta C_t$ method (Livak and Schmittgen, 2001).

Animal Immunization and Antibody Production

To obtain specific immune sera, purified rPbQSOX was mixed with complete Freund's adjuvant and used to subcutaneously immunize BALB/c mice (50 μg/mouse). Two booster immunizations of 25 μg of protein emulsified in incomplete Freund's adjuvant were done at 2-weeks intervals. Ten days after the last immunization, blood was collected from the mice by cardiac puncture and allowed to clot at room temperature to obtain the antisera.

Anti-rPbQSOX monoclonal antibody (mAb) was produced using spleen cells obtained from BALB/c mice immunized with rPbQSOX as described above and fused with Sp2/0-Ag14 myeloma cells (Kohler and Milstein, 1975). Hybridoma cells were generated by the polyethylene glycol method, selected in the hypoxanthine-aminopterin-thymidine medium, and screened by indirect antibody capture enzyme-linked immunosorbent assay (ELISA). The IgG fractions were prepared by ammonium sulfate precipitation and purified on a Protein A column. The mAb isotype was determined using the SBA Clonotyping™ System-HRP (Southern Biotechnology Associates) according to the manufacturer's instructions.

Western Blot

Purified schizonts, gametocytes and ookinetes were treated with 0.15% saponin to lyse erythrocytes and parasites were collected by centrifugation and washed once with PBS. Parasites were lysed in PBS containing 1% Triton X-100, 2% SDS, and protease inhibitors (Volkmann et al., 2012) for 30 min at room temperature. Equal amounts of the parasite lysates (10 μg/per lane) were separated on a 10% SDS-PAGE gel under reducing conditions. Proteins were transferred to a 0.22 μm PVDF membrane (Bio-Rad). The membrane was blocked with 5% skim milk in Tris-buffered saline (TBS) at 4°C for 12 h and then incubated with anti-rPbQSOX antisera diluted at 1:500 or anti-PbQSOX mAb diluted at 1:1,000 in TBS containing 0.1% Tween 20 (TBST) for 3 h. The mouse anti-PbHsp70 sera (1:500) were used to monitor protein loading. After three washes with TBST, the membrane was incubated for 2 h with HRP-conjugated goat anti-mouse IgG antibodies (Invitrogen) diluted 1:10,000 in TBST. After three washes with TBST, the proteins on the blot were visualized with a Pierce ECL Western Blotting Kit (ThermoFisher).

Indirect Immunofluorescence Assay (IFA)

Cells were washed once in PBS and fixed with 4% paraformaldehyde and 0.0075% glutaraldehyde (Sigma) in PBS for 30 min at room temperature (Tonkin et al., 2004). Fixed cells were washed once in PBS and then permeabilized with or without 0.1% Triton X-100 in PBS for 10 min. Cells were rinsed with 50 mM glycine in PBS and blocked with PBS containing 3% skim milk for 1 h at 37°C. Cells were incubated with mouse anti-rPbQSOX antisera (1:500) or anti-rPbQSOX mAb (1:500), or anti-Pbs21 mAb (1:500) in PBS containing 3% skim milk at 37°C for 1 h and washed three times with PBS. The parasites without permeabilization were then treated with 0.1% Triton X-100 and blocked with 3% bovine serum albumin/PBS for 60 min. After that, all parasites were incubated with rabbit antisera against PbMSP1, Pbg377, α-tubulin and PSOP25 as stage-specific markers for schizonts, female gametocytes/gametes, male gametocytes/gametes, and ookinetes, respectively (Liu et al., 2019). After the cells were washed thrice with PBS, Alexa-488 conjugated goat anti-mouse IgG secondary antibodies (1:500; Invitrogen) and Alexa-555 conjugated goat anti-rabbit IgG secondary antibodies (1:500; Abcam) were added and incubated for 1 h. Cells were mounted with Hoechst 33258 (1:1,000; Invitrogen). Negative controls were wild-type (WT) *P. berghei* ookinetes that were incubated with the anti-rGST sera or with the secondary antibodies only. WT ookinetes probed with the anti-Pbs21 mAb and anti-PSOP25 serum served as the positive controls. Parasites were visualized on a Nikon C2 fluorescence confocal laser scanning microscope (Nikon, Japan).

Generation of the *Pbqsox* Knockout Lines

To knock out *pbqsox*, an 824-bp upstream fragment containing the 5′ UTR was amplified from *P. berghei* genomic DNA using primers 5UTR-F and 5UTR-R (**Table S1**), and cloned in the plasmid PL0034 at the *Hin*dIII and *Pst*I sites upstream of the h*dhfr* cassette. Similarly, an 805-bp downstream fragment containing the 3′ UTR was amplified using primers 3UTR-F and 3UTR-R (**Table S1**), and inserted at the *Xho*I and *Eco*RI sites downstream of the h*dhfr* cassette. This would replace the *pbqsox* protein-coding region with the h*dhfr* expression cassette which confers resistance to pyrimethamine. The plasmid was linearized by *Hin*dIII/*Eco*RI digestion and transfected by electroporation into purified *P. berghei* schizonts (Janse et al., 2006). In two independent transfection experiments, the complete parasite suspension was injected intravenously via the tail vein into two mice. Starting at 24 h after injection of the transfected parasites, mice were treated with pyrimethamine (Sigma) in drinking water at 70 μg/ml for a period of 3–4 days. After parasite cloning by limiting dilution, the *pbqsox* deletion (Δ*pbqsox*) line was confirmed by integration-specific PCR (**Table S1**). The Δ*pbqsox* line was also confirmed by Western blot and IFA. For Western blot, WT and Δ*pbqsox* ookinetes were purified and incubated with the anti-rPbQSOX sera and anti-Hsp70 sera as described above. For IFA, Δ*pbqsox* ookinetes were incubated with anti-rPbQSOX sera after membrane permeabilization with Triton X-100.

Phenotypic Analysis of the Δ*pbqsox* Line

To determine whether deletion of *pbqsox* affects parasite growth, five mice were inoculated i.p. with 0.2 ml of infected blood containing either 5×10^6 WT or Δ*pbqsox* parasites. Asexual parasitemia was monitored from day 3 to day 7 p.i. using Giemsa-stained blood films. To evaluate the effect on gametocytogenesis and gametocyte activation, BALB/c mice were injected i.p. with 0.2 ml of 6 mg/ml phenylhydrazine in 0.9% NaCl 3 days prior to infection. Mice were inoculated i.p. with 0.2 ml of infected blood containing 5×10^6 iRBCs. Three days after infection, gametocytemia and gametocyte sex ratio were assessed by Giemsa-stained blood smears (Lal et al., 2009). Exflagellation centers of male gametocytes and formation of macrogametes were quantified as described (Tewari et al., 2010; van Dijk et al., 2010). Briefly, a volume (close to 10 μl) of gametocyte-infected blood adjusted to contain equal amounts of mature gametocytes based on the mature gametocyte count was obtained from the tail vein of each mouse and mixed immediately with ookinete culture medium in a final volume of 50 μl. The mixture was placed under a Vaseline-coated cover slip at 25°C and 15 min later exflagellation centers (male gamete interacting with RBCs) were counted over the next 10 min under a phase contrast microscope at 400× magnification. To count macrogametes, 10 μl of gametocyte-infected blood were mixed with ookinete culture medium at 25°C for 15 min. Then the macrogametes were labeled with anti-Pbs21 mAb (1:500) and Alexa-488-conjugated anti-mouse IgG antibodies (1:500) without membrane permeabilization. The culture was continued at 19°C for 24 h, harvested and labeled with mouse anti-Pbs21 mAb (1:500) and Alexa-488-conjugated anti-mouse IgG antibodies (1:500). Detailed analysis of ookinete differentiation was performed as described (Janse et al., 1985). Macrogametes, zygotes and different stages of ookinetes were counted under a fluorescence microscope at 1,000× magnification in 20 fields. The proportions of different cell shapes were calculated as the number of zygotes or ookinetes/(total number of macrogametes,

zygotes and different stage ookinetes) × 100% as described previously (Reininger et al., 2005).

For mosquito feeding, 4 day-old female *An. stephensi* mosquitoes were starved for 12 h and then allowed to feed on phenylhydrazine-treated mice infected with either WT or Δ*pbqsox* parasites for 30 min. Unfed mosquitoes were removed and engorged mosquitoes were maintained at 19–22°C and 50–80% relative humidity. The ookinete formation in the blood meal was analyzed at 24 h after blood feeding (Volkmann et al., 2012). For oocyst counts, midguts were dissected on day 10 and stained with 0.5% mercurochrome (Sigma) to determine the prevalence (proportion of infected mosquitoes) and intensity (number of oocysts per positive midgut) of infection (Usui et al., 2011).

Quantification of PbQSOX in Ookinete Culture Medium

Ookinetes were cultured as described above and the culture medium was collected by centrifugation at 1,300 × g for 10 min. To detect the presence of PbQSOX, culture medium (50 μl/lane) was separated on a 10% SDS-PAGE gel under reducing conditions and Western blots were performed as described above with the anti-rPbQSOX mAb (1:1,000 dilution). To quantify PbQSOX in the ookinete culture medium, a standard ELISA curve with purified rPbQSOX at 0.1, 0.2, 0.4, 0.6, 0.8, 1, and 1.6 μg/well was constructed. Then 50 μl of serially diluted ookinete culture medium (from a known number of the ookinetes) were added to each well of a Nunc MaxiSorp® flat-bottom 96-well plate. After coating of plate at 4°C for 12 h, the plate was sequentially incubated with anti-rPbQSOX mAb (1:1,000) and HRP-conjugated goat anti-mouse IgG antibodies (1:2,000, Invitrogen). Then the PbQSOX content of the WT ookinete culture medium was calculated according to the standard curve.

Quantification of Thiol Groups on Δ*pbqsox* Ookinetes by ThioGlo Staining

To quantify the amount of thiol groups on the ookinetes, 100 ookinetes from the WT and Δ*pbqsox* parasites were washed with PBS (pH 7.4) for four times. Then the samples were incubated with 6 μM of the ThioGlo fluorescent probe IV (Calbiochem) in the dark for 30 min at room temperature. The reaction was terminated by the addition of 2 μl of 2 M HCl, and the fluorescence was measured by using an ELISA plate reader with excitation at 400 nm and emission at 465 nm. Background fluorescence was subtracted from all fields (Ilani et al., 2013). The amount of thiol groups on both WT and Δ*pbqsox* ookinetes were compared.

In vitro Ookinete Conversion Inhibition Assay

Mice pre-treated with phenylhydrazine were infected as described above. On day 3 p.i., parasitemia was determined and exflagellation of male gametocytes was checked. Ten μl of infected blood were taken from each mouse and added to 90 μl ookinete medium containing anti-rPbQSOX antisera or anti-rGST sera as the control at final dilutions of 1:5, 1:10, and 1:50. Additionally, anti-rPbQSOX mAb was added to the ookinete culture at 10, 5, and 1 μg/100 μl of ookinete culture, respectively. The culture without mAb was used as a negative control. Ookinete cultures were incubated at 19°C for 24 h and the number of macrogametes, zygotes, retorts and ookinetes were counted as described above. Ookinete conversion rate were calculated as the number of ookinetes/the total number of (macrogametes, zygotes, retorts and ookinetes) × 100%.

In vivo TB Activity

For *in vivo* studies, three mice were immunized with the rPbQSOX as described above. Three mice in the control group were immunized with the rGST protein. Ten days after the last immunization, six immunized mice were infected with the WT *P. berghei* iRBCs to assess TB activity by the direct mosquito feeding assay. For the antibody transfer experiment, three mice were injected intravenously with either 150 μg of anti-rPbQSOX mAb/mouse or equal volume of PBS as control 1 h before mosquito feeding. Approximately 30 mosquitoes were dissected 10 days after feeding to determine the prevalence and intensity of infection.

Statistical Analysis

Statistical comparison between groups was performed with the GraphPad Prism 6.0 software. Parasitemia, gametocytemia, the amount of PbQSOX secreted by ookinetes and thiol contents were analyzed by the Student's *t* test and ANOVA. The number of exflagellation centers, macrogamete numbers and the intensity of infection (oocysts/midgut) were analyzed by the Mann–Whitney *U* test, while the proportions of cell shapes and ookinete conversion rate were analyzed by the Chi-square test. The prevalence of infection was analyzed by the Fisher's exact test using SPSS version 21.0. $P < 0.05$ was considered statistically significant.

RESULTS

Bioinformatic Analysis Identifies a Conserved QSOX Gene in *Plasmodium*

Search of the PlasmoDB for proteins involved in disulfide bond formation identified a QSOX-like protein in all sequenced *Plasmodium* genomes. This putative sulfhydryl oxidase protein in *P. berghei* (PBANKA_145540) encodes 516 amino acids, with a predicted molecular weight of 61.5 kDa. Analysis of the domain structures by SMART showed that the predicted protein contains a signal peptide, a highly conserved N-terminal Trx1 domain and C-terminal Erv/ALR domain, which is typical of QSOX enzymes (**Figure 1A**). Phylogenetic comparison with homologs in model organisms showed that all *Plasmodium* homologs formed a separate clade, most closely related to the plant *Arabidopsis thaliana* QSOX (**Figure 1B**). From the sequence alignment and predicted domains (**Figure 1B** and **Figure S1A**), *Plasmodium* QSOX-like proteins are different from the metazoan homologs in that it lacks the Trx2 domain completely. This feature closely resembles QSOX proteins in plants and protozoan

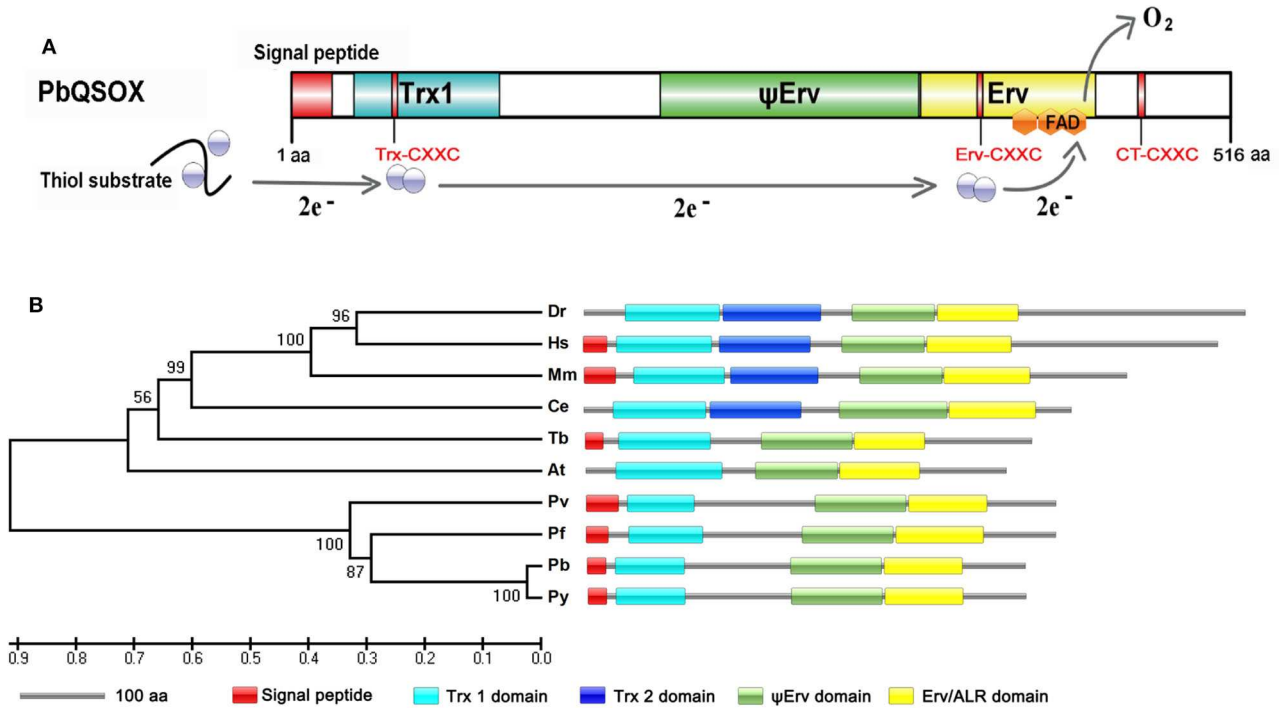

FIGURE 1 | Identification and phylogenetic analysis of PbQSOX. **(A)** Domain organization of PbQSOX protein and schematic representation of the electron transfer pathway through PbQSOX domains. Trx1, ψErv, and Erv/ALR domains are highlighted in blue, green and yellow, respectively. Within the oxidoreductase module of QSOX, two electrons are accepted from the substrate by the Trx-CXXC motif. From the Trx1 domain, the electrons are transferred to the Erv-CXXC motif at first, then to the FAD cofactor. Ultimately, two electrons are transferred to molecular oxygen through the FAD cofactor. **(B)** A maximum likelihood tree inferred from QSOXs in different species: *Arabidopsis thaliana* (At), *Caenorhabditis elegans* (Ce), *Danio rerio* (Dr), *Homo sapiens* (Hs), *Mus musculus* (Mm), *Plasmodium berghei* (Pb), *Plasmodium falciparum* (Pf), *Plasmodium vivax* (Pv), *Plasmodium yoelii* (Py), and *Trypanosoma brucei* (Tb). Protein domain architectures predicted with the SMART program are shown.

parasites (**Figure 1B**). The *Plasmodium* QSOX-like proteins have all three conserved CXXC motifs. Within the Trx1 domain, the most prevalent redox active Trx-CXXC motif is CGHC, whereas the corresponding PbQSOX sequence is CPAC, which is the same as in *Arabidopsis* (**Figure S1**). The Erv/ALR domain Erv-CXXC motif serves to communicate with the Trx-CXXC and interacts with the flavin adenine dinucleotide (FAD) co-factor (Haque et al., 2012), and this motif in PbQSOX is CRNC (**Figure S1A**). In addition, a C-terminal CXXC motif (CT-CXXC) is also highly retained in QSOX family enzymes (**Figure S1A**). Thus, the putative sulfhydryl oxidase protein in *P. berghei* has all these conserved features of the QSOX family, and is thus designated as the *P. berghei* quiescin sulfhydryl oxidase (PbQSOX).

The Recombinant PbQSOX Possesses Thiol Oxidase Activity

We wanted to determine whether PbQSOX possessed thiol oxidase activity, given it has the conserved domain structure typical of QSOX proteins. We expressed the rPbQSOX protein lacking the predicted signal peptide in *E. coli,* and purified the protein under native conditions. In addition, we also expressed and purified the rGST protein to serve as the control. SDS-PAGE analysis of rPbQSOX showed a homogeneous band of ~58 kDa, consistent with its predicted molecular size (**Figure 2A**). We tested rPbQSOX for thiol oxidase activity using the TCEP

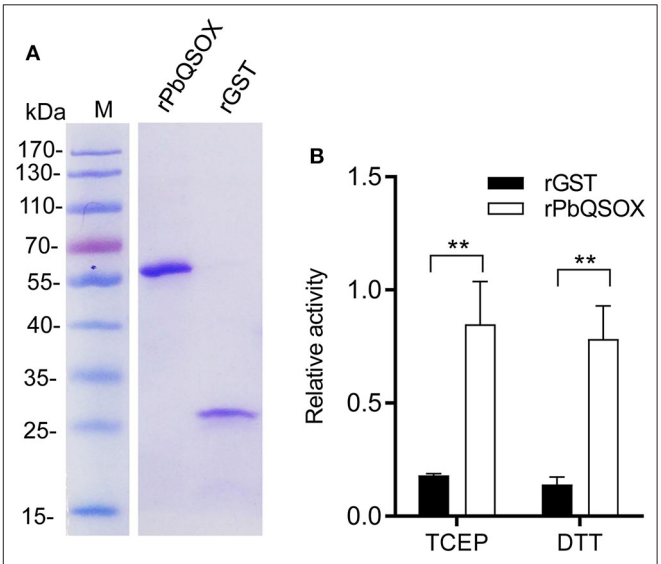

FIGURE 2 | Purification and the oxidase activity of rPbQSOX. **(A)** rPbQSOX and rGST protein were expressed and purified from *E. coli*. Molecular weight of rPbQSOX and the GST-tag protein are ~58 and 26 kDa, respectively. **(B)** The oxidase activities of rPbQSOX with TCEP and DTT as substrates. The oxidase activity was based on determining the rate of the H_2O_2 generation. Means were collated from three separate experiments. Recombinant GST (rGST) protein was used as a negative control. Error bars are standard deviations. $^{**}p < 0.01$.

and DTT as the substrates. QSOX oxidizes TCEP or DTT to produce H_2O_2, which can be detected by a luminescent reaction. As shown in **Figure 2B**, the rPbQSOX possessed obvious oxidase activity, consistent with its orthologs in other eukaryotes (Jaje et al., 2007; Kodali and Thorpe, 2010; Zheng et al., 2012).

PbQSOX Is Expressed Primarily in Sexual Stages

We next investigated the expression of PbQSOX during parasite development. Schizonts, gametocytes and ookinetes were purified on Nycodenz gradients (**Figure S2**) and used for qRT-PCR and Western blot analysis. *Pbqsox* transcripts were not detected in schizonts, but were detected in gametocytes and ookinetes, with the highest abundance in ookinetes (**Figure 3A**). To detect the PbQSOX protein expression, mice were immunized with rPbQSOX to produce both polyclonal antisera and a mAb. Western blot analysis of protein lysates from purified schizonts, gametocytes and ookinetes using both anti-PbQSOX mAb and the polyclonal antisera only detected a ∼61 kDa protein in gametocytes and ookinetes (**Figure 3B**). Consistent with the qRT-PCR result, the PbQSOX protein level was much higher in ookinetes than in gametocytes (**Figure 3B**).

PbQSOX Is Secreted and Associated With Plasma Membranes of Sexual Stages

The presence of a putative signal peptide in PbQSOX suggests that it may be a secreted protein. Examination of PbQSOX localization in different stages of *P. berghei* using the anti-PbQSOX mAb detected strong fluorescence in gametocytes, gametes and ookinetes, but not in schizonts or when only the secondary antibodies were used (**Figure 4**). Furthermore, the fluorescence in gametocytes was observed only after membrane permeabilization, suggesting that PbQSOX was localized in the cytoplasm. In exflagellating microgametes, fluorescence

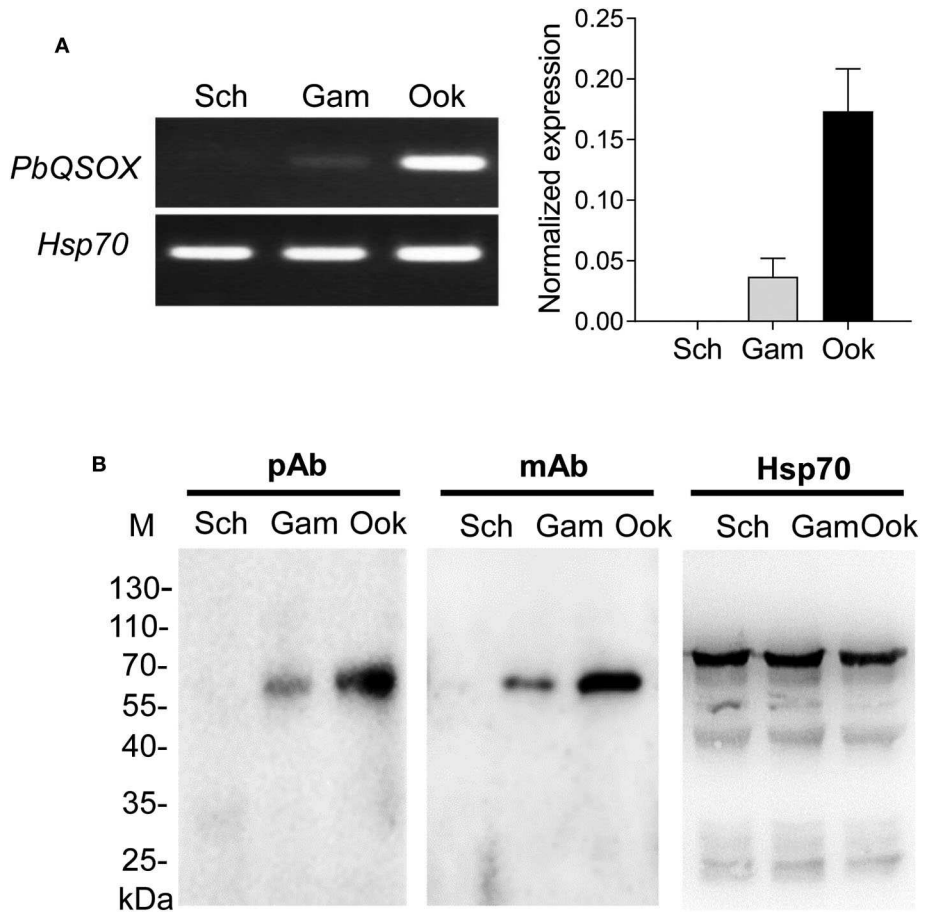

FIGURE 3 | PbQSOX expression during asexual and sexual development. **(A)** *Pbqsox* expression detected by qRT-PCR. Left panel: RT-PCR products of *pbqsox* (upper) and *hsp70* (lower) performed using RNA purified from schizonts (Sch), gametocytes (Gam) and ookinetes (Ook) were separated in 1% agarose gel to show the relative abundance of *pbqsox* transcripts in different stages. Right panel: Quantitation of the *pbqsox* mRNA in different stages by qRT-PCR with the mRNA levels normalized against the house-keeping gene *hsp70*. **(B)** Western blots of PbQSOX in different stages of the parasites. Lysates of schizonts (Sch), gametocytes (Gam), and ookinetes (Ook) at 10 μg/lane were probed with mouse anti-rPbQSOX antisera (pAb, 1:500) and monoclonal antibody (mAb, 1:1,000). Protein loading was estimated by using the antisera against Hsp70 (1:500).

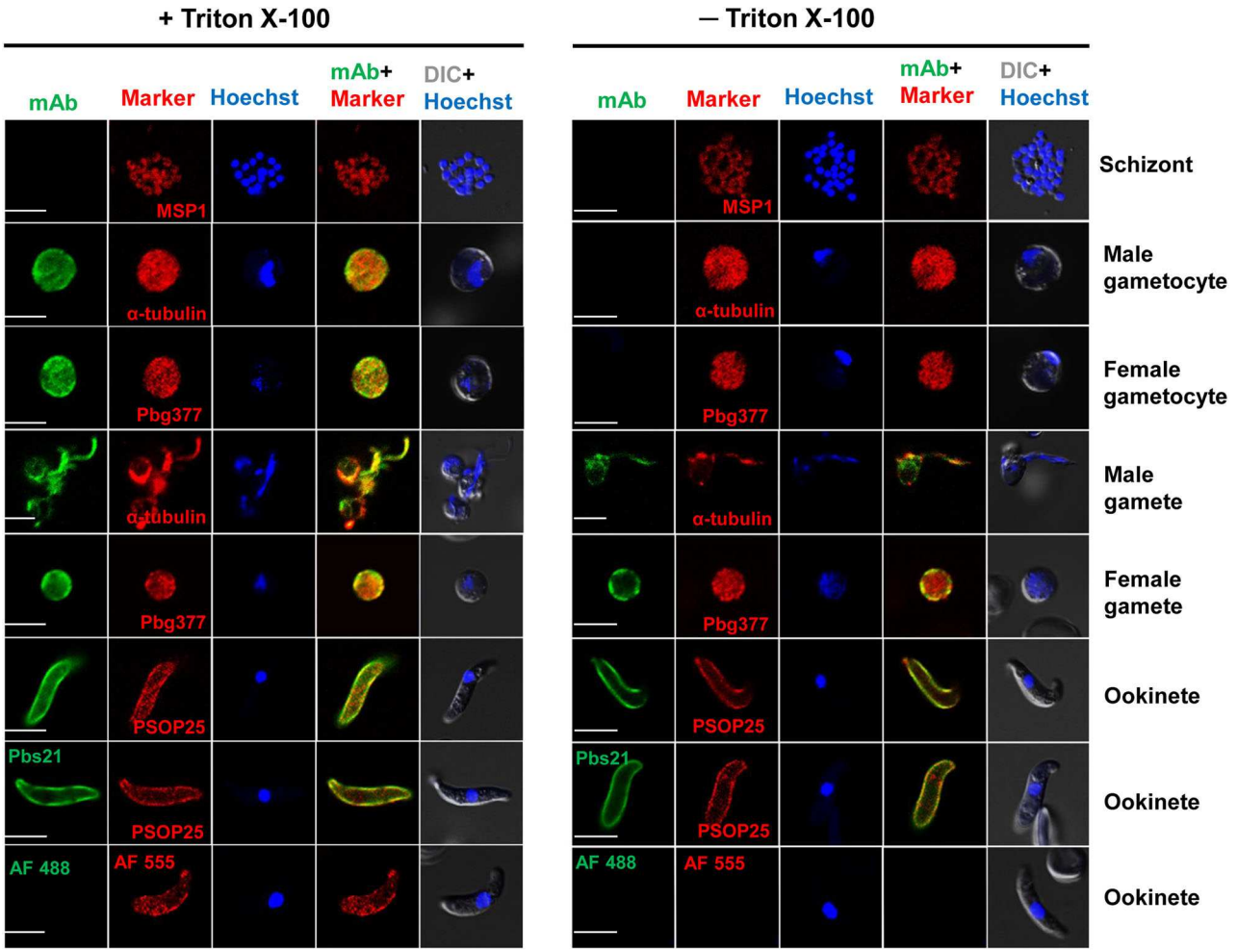

FIGURE 4 | Localization of PbQSOX by IFA. Cells treated with (left panel) or without (right panel) 0.1% Triton X-100 are compared. Anti-rPbQSOX mAb (1:500) was used as the primary antibodies. The antibodies against PbMSP1 for schizonts, Pbg377 for female gametocytes/gametes, α-tubulin for male gametocytes/gametes, and PSOP25 for ookinetes were used as stage-specific markers (red). Nuclei were stained with Hoechst (1:1,000) (blue). Pbs21 mAb was used as positive control for ookinete surface. WT ookinetes labeled only with the secondary antibodies (AF488, Alexa Fluor 488, and AF555, Alexa Fluor 555) were used as a negative control. Two right columns show the merge of PbQSOX + stage-specific marker and merge of nuclear stain (Hoeschst) + DIC (differential interference contrast). Scale bars = 5 μm.

was associated with both the flagella and residual body. In macrogametes and ookinetes, fluorescence was even detected without membrane permeabilization, suggesting PbQSOX was associated with the plasma membrane in these stages. The surface staining of ookinetes with the anti-rPbQSOX mAb was similar to that observed with the anti-Pbs21 mAb (**Figure 4**). A similar fluorescent pattern was observed using the anti-rPbQSOX polyclonal antisera (**Figure S3A**). No PbQSOX expression was detected in sporozoites (**Figure S3B**).

PbQSOX Is Required for Parasite Sexual Development

To determine the role of PbQSOX during the *Plasmodium* development, a *pbqsox* knockout line, Δ*pbqsox*, was generated using a double cross-over homologous recombination strategy (Janse et al., 2006). Pyrimethamine-resistant parasites were selected and cloned for genotype and phenotype analyses. Deletion of the *pbqsox* gene was confirmed by both integration-specific PCR, and Western blot (**Figure S4**).

To determine the effect of *pbqsox* deletion on parasite development, equal numbers of the WT- and Δ*pbqsox*-iRBCs were injected i.p. into BALB/c mice, and parasitemia was determined daily in Giemsa-stained thin blood smears, while gametocytemia and gametocyte sex ratio were determined on day 3 p.i. Consistent with the lack of PbQSOX expression in asexual erythrocytic stages, *pbqsox* deletion had no noticeable effect on asexual parasitemia (**Figure S5A**). In addition, it did not affect the gametocytogenesis, as gametocytemia (**Figure S5B**) and gametocyte sex ratio (**Figure S5C**) did not differ significantly between the WT and the Δ*pbqsox* parasites. Whereas, *pbqsox*

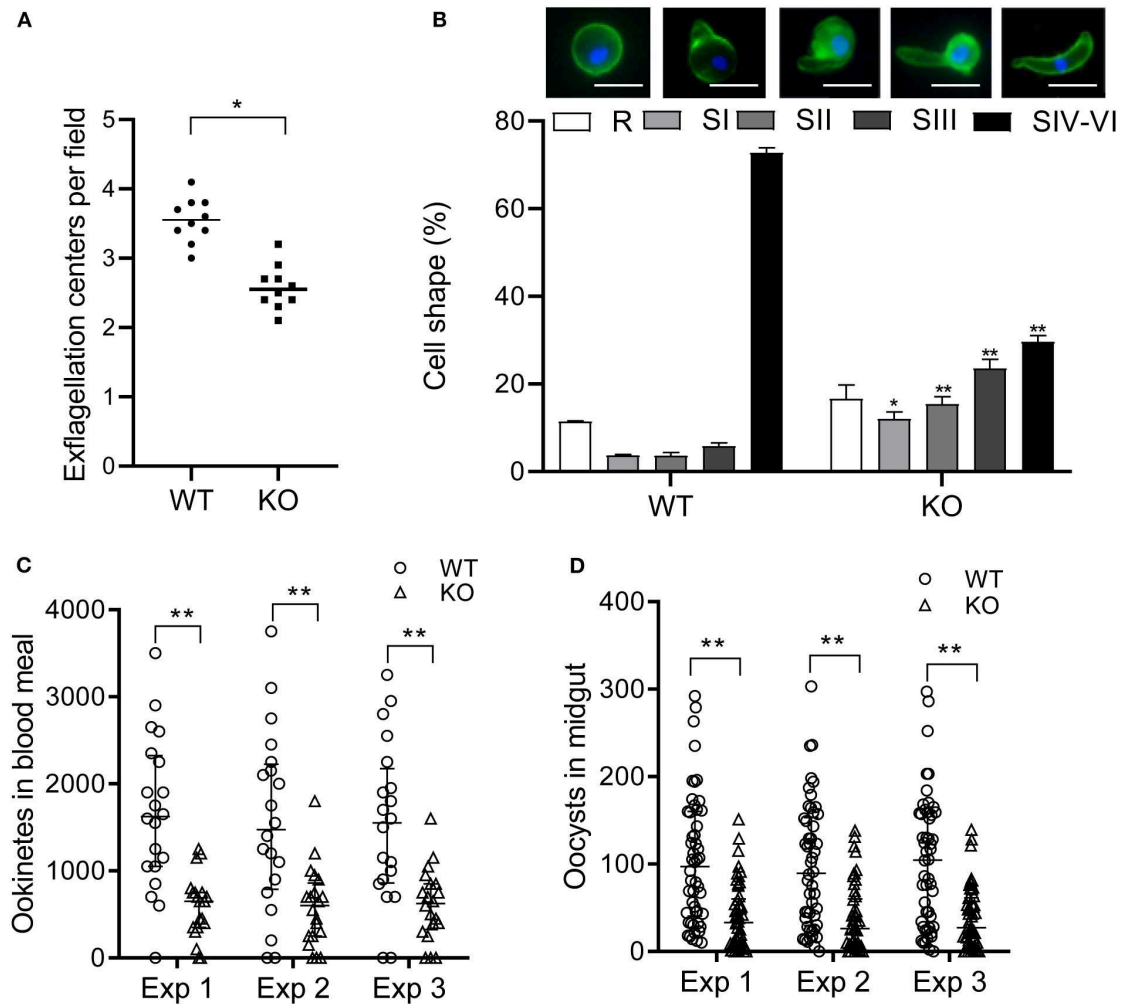

FIGURE 5 | Phenotypic analyses of the Δ*pbqsox* parasites. **(A)** Exflagellation of WT or Δ*pbqsox* (KO) microgametocytes. Exflagellation centers were counted under a phase contrast microscope at 400× magnification. Individual data points represent the number of exflagellation centers from each mouse. Horizontal bars indicate the median number of exflagellation centers. $^{**}p < 0.01$. **(B)** Ookinete stages in *in vitro* cultures of WT and Δ*pbqsox* (KO) parasites. Morphologies of ookinetes used for defining different stages are given above the graph. Scale bars = 5 μm. Means were obtained from three separate experiments. Error bars indicate standard error of the mean (SEM) within individual treatments. * and ** $p < 0.05$ and < 0.01, respectively, for comparison of the respective cell shapes between WT and KO. **(C)** Ookinete number in the blood meal per mosquito after feeding on WT- and Δ*pbqsox* (KO)-infected mice. Three independent experiments were performed. $^{**}p < 0.01$. Horizontal bars indicate the median with interquartile range of individual treatments. **(D)** Oocyst number per midgut in mosquitoes 10 days after blood feeding on WT- or Δ*pbqsox* (KO)-infected mice. Three independent experiments were performed. $^{**}p < 0.01$. Horizontal bars indicate the median with interquartile range of individual treatments.

deletion did not affect the formation of macrogametes (**Figure S5D**), it reduced the number of exflagellation centers by 28.0% ($p < 0.05$; **Figure 5A**). Subsequently, *in vitro* ookinete culture showed that ookinetes in the Δ*pbqsox* line retained normal morphology (**Figure S6A**), but the proportion of ookinetes (stage IV-VI) was reduced by 43.1% ($p < 0.01$; **Figure 5B**). Detailed analysis of ookinete differentiation showed that 12%, 15.4%, and 23.5% of the Δ*pbqsox* ookinetes arrested at stage I, II, and III, respectively, as compared to 3.7%, 3.6% and 5.8% at these stages for the wild-type control ($p < 0.01$; **Figure 5B**), suggesting that *pbqsox* deletion interfered with the zygote–ookinete maturation process.

The effect of *pbqsox* deletion on parasite development was further evaluated in mosquito feeding assays. *Anopheles stephensi* mosquitoes were allowed to feed on Δ*pbqsox*- and WT parasite-infected mice and the formation of ookinetes and oocysts were evaluated 24 h and 10 days post blood feeding, respectively. Consistent with the *in vitro* ookinete conversion result, the number of ookinetes formed in the blood bolus of mosquitoes feeding on Δ*pbqsox*-infected mice was 60.2–64.6% lower than that with the WT parasites ($p < 0.01$; **Figure 5C**, **Table 1**). Although there was no reduction in the prevalence of infected mosquitoes between Δ*pbqsox* and WT parasites (**Table 1**), there was a 61.8–62.8% reduction in oocyst number/midgut in

TABLE 1 | The effect of *pbqsox* deletion on ookinete and oocyst development in mosquitoes.

Exp*	Group	Ookinetes in blood meal at 24 h post feeding				Oocysts in midgut at 10 days post feeding					
		# Infected/ Dissected (%)	# ookinetes/ midgut [mean (range)]	% reduction of ookinetes[a]	P^b	# Infected/ Dissected (%)	% reduction of prevalence[c]	P^d	# oocysts/ midgut [mean (range)]	% reduction of oocyst density[e]	P^f
1	WT	19/20 (95)	1,663 (0–3,500)	64.6	0.000	50/50 (100)	6	0.241	103.9 (10–292)	62.8	0.000
	Δ*pbqsox*	18/20 (90)	587.5 (0–1,250)			47/50 (94)			38.6 (0–151)		
2	WT	18/20 (90)	1,560 (0–3750)	62.5	0.001	49/50 (98)	12	0.065	97.2 (0–303)	61.8	0.000
	Δ*pbqsox*	17/20 (85)	585 (0–1,800)			43/50 (86)			37.1 (0–138)		
3	WT	18/20 (90)	1,533 (0–3,250)	60.2	0.000	49/50 (98)	6	0.359	102.8 (0–297)	62.3	0.000
	Δ*pbqsox*	17/20 (85)	610 (0–1,600)			46/50 (92)			38.6 (0–139)		

**The study was performed in three experiments (Exp), and the numbers of ookinetes and oocysts in each midgut were determined at 24 h and 10 days post blood feeding, respectively.*
[a]% reduction in ookinetes was calculated as (mean $_{WT}$–mean $_{\Delta pbqsox}$)/mean $_{WT}$ × 100%.
[b]P values from Mann–Whitney U test for comparison between the WT and Δpbqsox groups.
[c]% reduction in prevalence was calculated as % prevalence $_{WT}$–% prevalence $_{\Delta pbqsox}$.
[d]P-values from Fisher's exact test for comparison between the WT and Δpbqsox groups.
[e]% reduction in oocysts was calculated as (mean $_{WT}$–mean $_{\Delta pbqsox}$)/mean $_{WT}$ × 100%.
[f]P -values from Mann–Whitney U test for comparison between the WT and Δpbqsox groups.

mosquitoes after feeding on Δ*pbqsox*-infected mice as compared to those fed on WT parasite-infected mice ($p < 0.01$; **Figure 5D**). Of note, the gross morphology of oocysts appeared normal in the Δ*pbqsox* parasites compared to the WT (**Figure S6B**). Together, these findings indicate that PbQSOX plays an important role in male gametogenesis, and ookinete maturation.

PbQSOX Is Required for Disulfide Bridges of Surface Proteins in Ookinetes

With the presence of a signal sequence and its association with the surface of ookinetes, we reasoned that PbQSOX might be secreted/shed into the medium. To detect secretion/shedding of PbQSOX, equal numbers (1×10^4) of WT and Δ*pbqsox* ookinetes were cultured in the ookinete culture medium for 24 h. Western blot analysis of concentrated culture medium detected PbQSOX in the culture of WT ookinetes, but not in the Δ*pbqsox* ookinetes (**Figure 6A**). Using the standard curve established with the rPbQSOX ELISA (**Figure 6B**), we estimated that the amount of PbQSOX secreted or shed by 1×10^4 WT ookinetes into the culture medium to be 0.38 ± 0.05 μg (**Figure 6C**).

We hypothesized that PbQSOX might be needed to maintain the integrity of disulfide bridges of surface proteins during sexual development, which is required for ookinete development and maturation. To evaluate this possible function, we quantified the surface thiol contents of the WT and Δ*pbqsox* ookinetes using ThioGlo™. The results showed that the thiol content was significantly higher on the Δ*pbqsox* ookinetes than that on the WT ookinetes ($p < 0.01$; **Figure 6D**), indicating the presence of more reduced proteins on the mutant ookinetes.

Antibodies Against PbQSOX Showed Obvious TB Activities

The surface association of PbQSOX with sexual stages prompted us to test whether antibodies against PbQSOX possess TB activities. Immunization of BALB/c mice with purified rPbQSOX elicited an effective antibody response. Antibody titers increased over time following the initial immunization, with substantial boosting observed in the two subsequent immunizations (data not shown). The anti-rPbQSOX mAb produced from a selected hybridoma line was purified, and the isotype was determined to be IgG2b. Both anti-rPbQSOX sera and mAb were then used in *in vitro* ookinete conversion and mosquito feeding assays.

Ookinete conversion was determined by culturing parasites for 24 h in an ookinete culture medium containing mouse anti-rPbQSOX sera or mAb. In both cases, the antisera and the mAb inhibited ookinete conversion in a dose-dependent manner. In ookinete cultures supplemented with the anti-rPbQSOX sera at 1:5, 1:10 and 1:50 dilutions, ookinete conversion rates were reduced by 66.9, 41.3, and 30.8%, respectively ($p < 0.01$), as compared with the anti-rGST control sera (**Figure 7A**). In cultures with the anti-rPbQSOX mAb added at 10, 5 and 1 μg/100 μl, ookinete conversion rates were reduced by 69.7, 54.1, and 29.3%, respectively ($p < 0.01$; **Figure 7B**).

To examine the TB effect of anti-rPbQSOX antibodies *in vivo*, mice were immunized with rPbQSOX or the control rGST protein. Ten days after the last immunization, six immunized mice in each group were infected with the WT *P. berghei* to assess TB activity by the direct feeding assay. On day 10 post feeding, mosquitoes were dissected and midgut oocysts were counted. Whereas the prevalence of infected mosquitoes was similar after feeding on rGST- and rPbQSOX-immunized mice (**Table 2**), oocyst density in mosquitoes that fed on rPbQSOX-immunized mice was reduced by 51.7, 48.1, and 55%, respectively, as compared to the rGST-immunized control mice (**Figure 7C**, **Table 2**). Next, we evaluated the TB effect of the anti-rPbQSOX mAb in an antibody transfer experiment, where mice infected with WT *P. berghei* were injected intravenously with either 150 μg of anti-rPbQSOX mAb/mouse or PBS 1 h before mosquito feeding. Compared with mosquitoes that fed on the control mice, those fed on mAb-transferred mice showed reductions in oocyst density by 64.6, 66.6, and 62.0%, respectively (**Figure 7D**, **Table 2**), although the

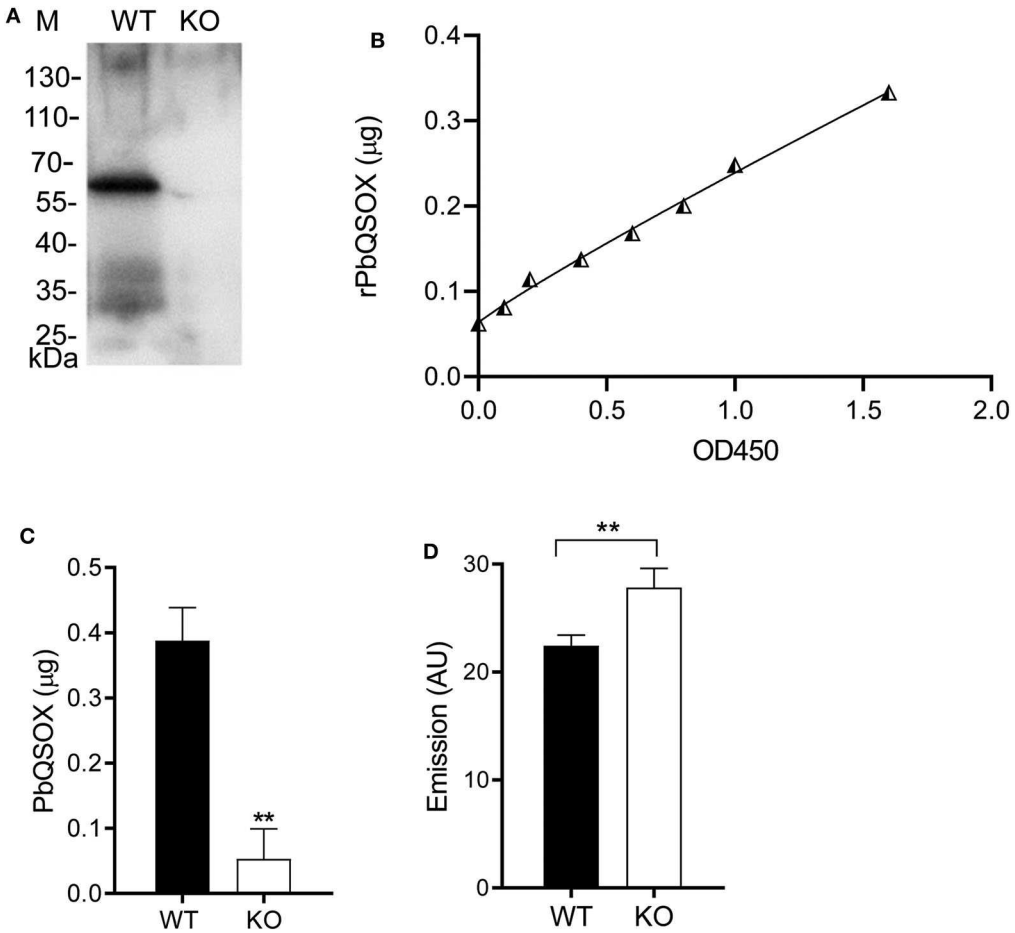

FIGURE 6 | PbQSOX secretion by cultured ookinetes and its potential effect on ookinete surface proteins. **(A)** Western blot analysis of culture supernatants of WT and Δ*pbqsox* (KO) ookinetes probed with anti-rPbQSOX mAb showing the presence of PbQSOX in culture medium. **(B)** Non-linear regression standard curve between rPbQSOX concentrations and optical density readings at OD450 by ELISA. The rPbQSOX at different dilutions was used to coat the wells of the ELISA plate and the standard curve was established to quantify PbQSOX in the ookinete culture medium. **(C)** Quantification of PbQSOX in culture medium. Culture supernatants of 1×10^4 WT and Δ*pbqsox* (KO) ookinetes were used to quantify the PbQSOX by ELISA. $^{**}p < 0.01$. Values represent the mean and SEM of three independent experiments. **(D)** Reactive thiol content on the WT and Δ*pbqsox* (KO) ookinetes. One hundred ookinetes from each group were labeled with ThioGlo. Emission (AU, arbitrary units) was measured using an ELISA plate reader (excitation at 400 nm and emission at 465 nm). Data indicate the mean and SEM from three independent experiments.

prevalence of infected mosquitoes was not different between the two groups.

DISCUSSION

During its development in the erythrocytes of the vertebrate host, the malaria parasite endures a substantial amount of intracellular oxidative stress resulting from hemoglobin catabolism (Muller, 2004), while inside the blood bolus after ingestion by a mosquito, it is exposed to extracellular oxidative insults from the digestive enzymes of the mosquito and immune factors of the vertebrate host (Sinden et al., 1996; Margos et al., 2001). The malaria parasite possesses two major antioxidant systems, the glutathione system and the thioredoxin system, to deal with these oxidative stresses (Muller, 2004). These antioxidant systems are not only important for the asexual development, but also are induced during ookinete development in the mosquito midgut (Turturice et al., 2013). Here, we identified QSOX as another antioxidant system involved in the regulation of the redox state and possibly folding of proteins in malaria parasites. QSOX is a specialized enzyme that catalyzes the introduction of disulfide bonds into unfolded reduced proteins (Thorpe et al., 2002; Thorpe and Coppock, 2007; Heckler et al., 2008). QSOX is conserved in *Plasmodium* and also other protozoan parasites such as trypanosomes, and the PbQSOX protein possesses thiol oxidase activity similar to vertebrate QSOX proteins (Kodali and Thorpe, 2010), despite the fact that protozoan QSOXs contain only a single thioredoxin domain.

Plasmodium QSOX appears to play an important role in sexual development of the parasite, since deletion of *pbqsox* resulted in defects in sexual development, leading to remarkable reductions in the numbers of mature ookinetes and oocysts. PbQSOX is expressed primarily during sexual development and is associated with the surface of gametes and ookinetes. In

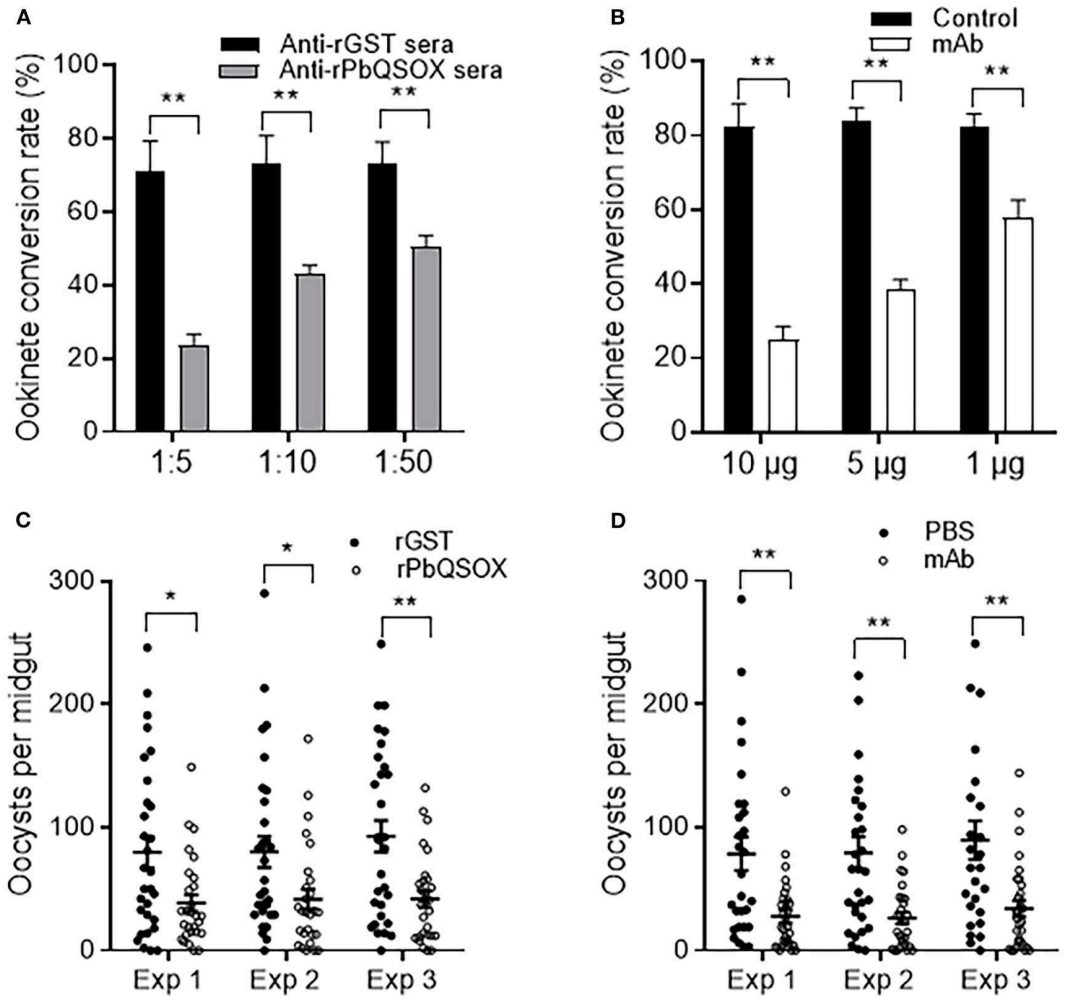

FIGURE 7 | Transmission-blocking activities of anti-rPbQSOX antibodies. **(A)** Effect of anti-rPbQSOX antisera on *P. berghei* ookinete formation *in vitro*. Anti-rGST sera were used as control. Sera were used at final dilutions of 1:5, 1:10, and 1:50. **(B)** Effect of anti-rPbQSOX mAb on *P. berghei* ookinete formation *in vitro*. Anti-rPbQSOX mAb was added at 10, 5 and 1 µg/100 µl in cultures. Cultures without mAb were used as a negative control. Means were collated from three separate experiments. Data in **A** and **B** indicate mean and SEM from three separate experiments. $^{**}p < 0.01$. **(C)** Direct mosquito feeding assay on mice immunized with rPbQSOX and rGST control. **(D)** Passive antibody transfer experiment to assess the TB activity of the anti-rPbQSOX mAb and PBS control. Data in **(C,D)** were from three independent experiments (Exp 1 – 3). Individual data points represent the number of oocysts found in individual mosquitoes 10 days post-feeding. Horizontal bars indicate the median with interquartile range of individual experiments. $^{*}p < 0.05$, $^{**}p < 0.01$.

addition, *P. berghei* ookinetes also secrete/shed large amounts of PbQSOX into the medium during *in vitro* culture. Analogously, QSOX enzymes have been found in secreted fluids including milk, semen, egg white and blood serum (Hoober et al., 1996; Benayoun et al., 2001; Zanata et al., 2005; Jaje et al., 2007). The extracellular QSOXs in different biological systems suggest they may play diverse roles (Limor-Waisberg et al., 2013). For instance, it was found that extracellular catalysis of disulfide bond formation by human QSOX1 is needed for laminin incorporation into the extracellular matrix, which is a prerequisite for tumor adhesion and metastasis (Ilani et al., 2013). In this context, we found that *pbqsox* deletion resulted in reduced numbers of mature ookinetes with concomitant accumulation of earlier stages, implying that PbQSOX is needed during ookinete development. The identification of significantly increased thiol groups on Δ*pbqsox* ookinetes as compared to those on the WT ookinetes indicates that PbQSOX plays a critical role in maintaining the structural integrity of ookinete surface proteins during the extracellular development of ookinetes. Further, whether PbQSOX is expressed and plays a role during liver stage development warrants future studies.

The abundant expression and critical function of PbQSOX during sexual development provide a potential target for blocking parasite transmission to mosquitoes. The expression of PbQSOX on both pre-fertilization and post-fertilization stages imply that antibodies against this protein may interrupt parasite transmission at multiple steps, e.g., preventing mating and formation of zygotes (Wu et al., 2015; Bechtsi and

TABLE 2 | *In vivo* evaluation of transmission–blocking effect of anti-rPbQSOX sera and monoclonal antibody (mAb).

Exp	Immunization groups							mAb transfer groups						
	Immunization	# Infected/ dissected (%)	% RP[a]	*P*[b]	# oocyst/midgut [mean (range)]	% ROD[c]	*P*[d]	Treatment	# Infected/ dissected (%)	% RP[a]	*P*[b]	# oocyst/midgut [mean (range)]	% ROD[c]	*P*[d]
1	rGST	28/30 (93.3)	0.5	1.000	79.8 (0–246)	51.7	0.021	PBS	28/28 (100)	10	0.261	78.4 (3–285)	64.6	0.002
	rPbQSOX	26/28 (92.8)			38.5 (0–149)			mAb	27/30 (90)			27.7 (0–129)		
2	rGST	29/30 (96.6)	7.8	0.530	80.3 (0–290)	48.1	0.013	PBS	29/30 (96.6)	10.4	0.330	79.1 (0–301)	66.6	0.001
	rPbQSOX	24/27 (88.8)			41.6 (0–172)			mAb	25/29 (86.2)			26.4 (0–98)		
3	rGST	29/30 (96.6)	3.8	0.951	92.9 (0–249)	55	0.003	PBS	25/26 (96.1)	9.5	0.440	89.5 (0–305)	62.0	0.002
	rPbQSOX	26/28 (92.8)			41.8 (0–132)			mAb	26/30 (86.6)			34.0 (0–144)		

[a] *RP: % reduction in prevalence was calculated as % prevalence* $_{rGST\ or\ PBS}$ *− % prevalence* $_{rPbQSOX\ or\ mAb}$.
[b] *P-values from Fisher's exact test for comparison between the control rGST or PBS and rPbQSOX immunization or mAb transfer groups.*
[c] *ROD: % reduction in oocyst intensity was calculated as (mean* $_{rGST\ or\ PBS}$ *− mean* $_{rPbQSOX\ or\ mAb}$*)/mean* $_{rGST\ or\ PBS}$ *× 100%.*
[d] *P-values from Mann–Whitney U test for comparison between control rGST or PBS and rPbQSOX immunization or mAb transfer groups.*

Waters, 2017) and subsequent transition and maturation of ookinetes (Guttery et al., 2015). We observed that anti-rPbQSOX antibodies significantly inhibited ookinete formation *in vitro*. The levels of inhibition at higher antiserum concentrations (1:5 dilution) compared favorably with that for the anti-*P. berghei* HAP2 serum, which inhibited ookinete formation up to ∼81% (Blagborough and Sinden, 2009). Moreover, we also observed PbQSOX on the surface of ookinetes, suggesting that anti-PbQSOX antibodies may also interfere with the invasion of the midgut epithelium and formation of oocysts (Smith and Barillas-Mury, 2016). In direct feeding experiments, oocyst density in mosquitoes that fed on rPbQSOX-immunized mice was also moderately reduced, which was similar to the TB efficiency of the ookinete secreted protein PSOP12 (Sala et al., 2015). Altogether, these results demonstrated evident TB activity of PbQSOX antibodies, which warrants further studies on the human malaria parasites.

In summary, we find that PbQSOX is a conserved *Plasmodium* protein and is required for parasite sexual development especially for ookinete maturation. PbQSOX is expressed primarily in both pre- and post-fertilization stages, and antibodies against PbQSOX showed obvious TB activities at ookinete steps, highlighting the TBV potential of PbQSOX.

DATA AVAILABILITY STATEMENT

The QSOX protein sequences were downloaded from the GenBank (https://www.ncbi.nlm.nih.gov/genbank/) with accession numbers NP_508419.1 (*Caenorhabditis elegans*), NP_001121836.1 (*Danio rerio*), NP_705787.1 (*Mus musculus*), NP_002817.2 (*Homo sapiens*), NP_565258.1 (*Arabidopsis thaliana*), and XP_011773962.1 (*Trypanosoma brucei*).

ETHICS STATEMENT

The animal study was reviewed and approved by The Animal Usage Committee of China Medical University.

AUTHOR CONTRIBUTIONS

LC and YC conceived the study. WZ and FL designed and performed experiments and data analysis, and drafted the paper. FD, XK, FY, YH, HF, and HM performed experiments and data analysis. QF, EL, and JM participated in data analysis and edited the paper. All authors contributed to the article and approved the submitted version.

FUNDING

This research was supported by grants R01AI099611 and R01AI150533 from the National Institutes of Health, USA. WZ was supported by a grant (81760367) from the National Natural Science Foundation of China. LC was supported by a grant U19AI089672 from the National Institute of Allergy and Infectious Diseases, NIH.

SUPPLEMENTARY MATERIAL

The Supplementary Material for this article can be found online at: https://www.frontiersin.org/articles/10.3389/fcimb.2020.00311/full#supplementary-material

REFERENCES

Alon, A., Heckler, E. J., Thorpe, C., and Fass, D. (2010). QSOX contains a pseudodimer of functional and degenerate sulfhydryl oxidase domains. *FEBS Lett.* 584, 1521–1525. doi: 10.1016/j.febslet.2010.03.001

Bechtsi, D. P., and Waters, A. P. (2017). Genomics and epigenetics of sexual commitment in Plasmodium. *Int. J. Parasitol.* 47, 425–434. doi: 10.1016/j.ijpara.2017.03.002

Beetsma, A. L., Van De Wiel, T. J., Sauerwein, R. W., and Eling, W. M. (1998). Plasmodium berghei ANKA: purification of large numbers

of infectious gametocytes. *Exp. Parasitol.* 88, 69–72. doi: 10.1006/expr.1998.4203

Benayoun, B., Esnard-Feve, A., Castella, S., Courty, Y., and Esnard, F. (2001). Rat seminal vesicle FAD-dependent sulfhydryl oxidase. Biochemical characterization and molecular cloning of a member of the new sulfhydryl oxidase/quiescin Q6 gene family. *J. Biol. Chem.* 276, 13830–13837. doi: 10.1074/jbc.M010933200

Blagborough, A. M., and Sinden, R. E. (2009). Plasmodium berghei HAP2 induces strong malaria transmission-blocking immunity *in vivo* and *in vitro*. *Vaccine* 27, 5187–5194. doi: 10.1016/j.vaccine.2009.06.069

Delves, M. J., Angrisano, F., and Blagborough, A. M. (2018). Antimalarial transmission-blocking interventions: past, present, and future. *Trends Parasitol.* 34, 735–746. doi: 10.1016/j.pt.2018.07.001

Genton, B. (2008). Malaria vaccines: a toy for travelers or a tool for eradication? *Expert Rev. Vaccines* 7, 597–611. doi: 10.1586/14760584.7.5.597

Guttery, D. S., Roques, M., Holder, A. A., and Tewari, R. (2015). Commit and transmit: molecular players in plasmodium sexual development and zygote differentiation. *Trends Parasitol.* 31, 676–685. doi: 10.1016/j.pt.2015.08.002

Haque, S. J., Majumdar, T., and Barik, S. (2012). Redox-assisted protein folding systems in eukaryotic parasites. *Antioxid. Redox Signal* 17, 674–683. doi: 10.1089/ars.2011.4433

Heckler, E. J., Rancy, P. C., Kodali, V. K., and Thorpe, C. (2008). Generating disulfides with the Quiescin-sulfhydryl oxidases. *Biochim. Biophys. Acta* 1783, 567–577. doi: 10.1016/j.bbamcr.2007.10.002

Hemingway, J., Ranson, H., Magill, A., Kolaczinski, J., Fornadel, C., Gimnig, J., et al. (2016). Averting a malaria disaster: will insecticide resistance derail malaria control? *Lancet* 387, 1785–1788. doi: 10.1016/S0140-6736(15)00417-1

Hoober, K. L., Joneja, B., White, H. B III, and Thorpe, C. (1996). A sulfhydryl oxidase from chicken egg white. *J. Biol. Chem.* 271, 30510–30516. doi: 10.1074/jbc.271.48.30510

Ilani, T., Alon, A., Grossman, I., Horowitz, B., Kartvelishvily, E., Cohen, S. R., et al. (2013). A secreted disulfide catalyst controls extracellular matrix composition and function. *Science* 341, 74–76. doi: 10.1126/science.1238279

Jaje, J., Wolcott, H. N., Fadugba, O., Cripps, D., Yang, A. J., Mather, I. H., et al. (2007). A flavin-dependent sulfhydryl oxidase in bovine milk. *Biochemistry* 46, 13031–13040. doi: 10.1021/bi7016975

Janse, C. J., Franke-Fayard, B., Mair, G. R., Ramesar, J., Thiel, C., Engelmann, S., et al. (2006). High efficiency transfection of Plasmodium berghei facilitates novel selection procedures. *Mol. Biochem. Parasitol.* 145, 60–70. doi: 10.1016/j.molbiopara.2005.09.007

Janse, C. J., Mons, B., Rouwenhorst, R. J., Van Der Klooster, P. F., Overdulve, J. P., and Van Der Kaay, H. J. (1985). *In vitro* formation of ookinetes and functional maturity of Plasmodium berghei gametocytes. *Parasitology 91*, 19–29. doi: 10.1017/S0031182000056481

Katchman, B. A., Antwi, K., Hostetter, G., Demeure, M. J., Watanabe, A., Decker, G. A., et al. (2011). Quiescin sulfhydryl oxidase 1 promotes invasion of pancreatic tumor cells mediated by matrix metalloproteinases. *Mol. Cancer Res.* 9, 1621–1631. doi: 10.1158/1541-7786.MCR-11-0018

Kodali, V. K., and Thorpe, C. (2010). Quiescin sulfhydryl oxidase from Trypanosoma brucei: catalytic activity and mechanism of a QSOX family member with a single thioredoxin domain. *Biochemistry* 49, 2075–2085. doi: 10.1021/bi902222s

Kohler, G., and Milstein, C. (1975). Continuous cultures of fused cells secreting antibody of predefined specificity. *Nature* 256, 495–497. doi: 10.1038/256495a0

Kumar, H., and Tolia, N. H. (2019). Getting in: The structural biology of malaria invasion. *PLoS Pathog.* 15:e1007943. doi: 10.1371/journal.ppat.1007943

Lal, K., Delves, M. J., Bromley, E., Wastling, J. M., Tomley, F. M., and Sinden, R. E. (2009). Plasmodium male development gene-1 (mdv-1) is important for female sexual development and identifies a polarised plasma membrane during zygote development. *Int. J. Parasitol.* 39, 755–761. doi: 10.1016/j.ijpara.2008.11.008

Limor-Waisberg, K., Ben-Dor, S., and Fass, D. (2013). Diversification of quiescin sulfhydryl oxidase in a preserved framework for redox relay. *BMC Evol. Biol.* 13:70. doi: 10.1186/1471-2148-13-70

Liu, F., Liu, Q., Yu, C., Zhao, Y., Wu, Y., Min, H., et al. (2019). An MFS-Domain Protein Pb115 Plays a Critical Role in Gamete Fertilization of the Malaria Parasite Plasmodium berghei. *Front. Microbiol.* 10:2193. doi: 10.3389/fmicb.2019.02193

Livak, K. J., and Schmittgen, T. D. (2001). Analysis of relative gene expression data using real-time quantitative PCR and the 2(-Delta Delta C(T)-) method. *Methods* 25, 402–408. doi: 10.1006/meth.2001.1262

Margos, G., Navarette, S., Butcher, G., Davies, A., Willers, C., Sinden, R. E., et al. (2001). Interaction between host complement and mosquito-midgut-stage Plasmodium berghei. *Infect. Immun.* 69, 5064–5071. doi: 10.1128/IAI.69.8.5064-5071.2001

Mebazaa, A., Vanpoucke, G., Thomas, G., Verleysen, K., Cohen-Solal, A., Vanderheyden, M., et al. (2012). Unbiased plasma proteomics for novel diagnostic biomarkers in cardiovascular disease: identification of quiescin Q6 as a candidate biomarker of acutely decompensated heart failure. *Eur. Heart. J.* 33, 2317–2324. doi: 10.1093/eurheartj/ehs162

Menard, D., and Dondorp, A. (2017). Antimalarial drug resistance: a threat to malaria elimination. *Cold Spring Harb. Perspect. Med.* 7:a025619. doi: 10.1101/cshperspect.a025619

Muller, S. (2004). Redox and antioxidant systems of the malaria parasite Plasmodium falciparum. *Mol. Microbiol.* 53, 1291–1305. doi: 10.1111/j.1365-2958.2004.04257.x

Poillet, L., Pernodet, N., Boyer-Guittaut, M., Adami, P., Borg, C., Jouvenot, M., et al. (2014). QSOX1 inhibits autophagic flux in breast cancer cells. *PLoS ONE* 9:e86641. doi: 10.1371/journal.pone.0086641

Raje, S., Glynn, N. M., and Thorpe, C. (2002). A continuous fluorescence assay for sulfhydryl oxidase. *Anal. Biochem.* 307, 266–272. doi: 10.1016/S0003-2697(02)00050-7

Reininger, L., Billker, O., Tewari, R., Mukhopadhyay, A., Fennell, C., Dorin-Semblat, D., et al. (2005). A NIMA-related protein kinase is essential for completion of the sexual cycle of malaria parasites. *J. Biol. Chem.* 280, 31957–31964. doi: 10.1074/jbc.M504523200

Sala, K. A., Nishiura, H., Upton, L. M., Zakutansky, S. E., Delves, M. J., Iyori, M., et al. (2015). The Plasmodium berghei sexual stage antigen PSOP12 induces anti-malarial transmission blocking immunity both *in vivo* and *in vitro*. *Vaccine* 33, 437–445. doi: 10.1016/j.vaccine.2014.11.038

Sinden, R. E. (2002). Molecular interactions between Plasmodium and its insect vectors. *Cell. Microbiol.* 4, 713–724. doi: 10.1046/j.1462-5822.2002.00229.x

Sinden, R. E., Butcher, G. A., Billker, O., and Fleck, S. L. (1996). Regulation of infectivity of Plasmodium to the mosquito vector. *Adv. Parasitol.* 38, 53–117. doi: 10.1016/S0065-308X(08)60033-0

Sinden, R. E., Hartley, R. H., and Winger, L. (1985). The development of plasmodium ookinetes *in vitro*: an ultrastructural study including a description of meiotic division. *Parasitology 91*, 227–244. doi: 10.1017/S0031182000057334

Smith, R. C., and Barillas-Mury, C. (2016). Plasmodium oocysts: overlooked targets of mosquito immunity. *Trends Parasitol.* 32, 979–990. doi: 10.1016/j.pt.2016.08.012

Soloviev, M., Esteves, M. P., Amiri, F., Crompton, M. R., and Rider, C. C. (2013). Elevated transcription of the gene QSOX1 encoding quiescin Q6 sulfhydryl oxidase 1 in breast cancer. *PLoS One* 8, e57327. doi: 10.1371/journal.pone.0057327

Song, H., Zhang, B., Watson, M. A., Humphrey, P. A., Lim, H., and Milbrandt, J. (2009). Loss of Nkx3.1 leads to the activation of discrete downstream target genes during prostate tumorigenesis. *Oncogene* 28, 3307–3319. doi: 10.1038/onc.2009.181

Tamura, K., Peterson, D., Peterson, N., Stecher, G., Nei, M., and Kumar, S. (2011). MEGA5: molecular evolutionary genetics analysis using maximum likelihood, evolutionary distance, and maximum parsimony methods. *Mol. Biol. Evol.* 28, 2731–2739. doi: 10.1093/molbev/msr121

Tewari, R., Straschil, U., Bateman, A., Bohme, U., Cherevach, I., Gong, P., et al. (2010). The systematic functional analysis of plasmodium protein kinases identifies essential regulators of mosquito transmission. *Cell Host Microbe.* 8, 377–387. doi: 10.1016/j.chom.2010.09.006

Thorpe, C., and Coppock, D. L. (2007). Generating disulfides in multicellular organisms: emerging roles for a new flavoprotein family. *J. Biol. Chem.* 282, 13929–13933. doi: 10.1074/jbc.R600037200

Thorpe, C., Hoober, K. L., Raje, S., Glynn, N. M., Burnside, J., Turi, G. K., et al. (2002). Sulfhydryl oxidases: emerging catalysts of protein disulfide bond formation in eukaryotes. *Arch. Biochem. Biophys.* 405, 1–12. doi: 10.1016/S0003-9861(02)00337-5

Tonkin, C. J., Van Dooren, G. G., Spurck, T. P., Struck, N. S., Good, R. T., Handman, E., et al. (2004). Localization of organellar proteins in

plasmodium falciparum using a novel set of transfection vectors and a new immunofluorescence fixation method. *Mol. Biochem. Parasitol.* 137, 13–21. doi: 10.1016/j.molbiopara.2004.05.009

Turturice, B. A., Lamm, M. A., Tasch, J. J., Zalewski, A., Kooistra, R., Schroeter, E. H., et al. (2013). Expression of cytosolic peroxiredoxins in Plasmodium berghei ookinetes is regulated by environmental factors in the mosquito bloodmeal. *PLoS Pathog.* 9:e1003136. doi: 10.1371/journal.ppat.1003136

Usui, M., Fukumoto, S., Inoue, N., and Kawazu, S. (2011). Improvement of the observational method for Plasmodium berghei oocysts in the midgut of mosquitoes. *Parasit. Vectors* 4, 118. doi: 10.1186/1756-3305-4-118

van Dijk, M. R., van Schaijk, B. C., Khan, S. M., van Dooren, M. W., Ramesar, J., Kaczanowski, S., et al. (2010). Three members of the 6-cys protein family of Plasmodium play a role in gamete fertility. *PLoS Pathog.* 6:e1000853. doi: 10.1371/journal.ppat.1000853

Volkmann, K., Pfander, C., Burstroem, C., Ahras, M., Goulding, D., Rayner, J. C., et al. (2012). The alveolin IMC1h is required for normal ookinete and sporozoite motility behaviour and host colonisation in Plasmodium berghei. *PLoS ONE* 7:e41409. doi: 10.1371/journal.pone.0041409

WHO (2019). *World Malaria Report 2019.* Available online at: https://www.who.int/publications-detail/world-malaria-report-2019

Wu, Y., Sinden, R. E., Churcher, T. S., Tsuboi, T., and Yusibov, V. (2015). Development of malaria transmission-blocking vaccines: from concept to product. *Adv. Parasitol.* 89, 109–152. doi: 10.1016/bs.apar.2015.04.001

Zanata, S. M., Luvizon, A. C., Batista, D. F., Ikegami, C. M., Pedrosa, F. O., Souza, E. M., et al. (2005). High levels of active quiescin Q6 sulfhydryl oxidase (QSOX) are selectively present in fetal serum. *Redox Rep.* 10, 319–323. doi: 10.1179/135100005X83699

Zheng, W., Zhang, W., Hu, W., Zhang, C., and Yang, Y. (2012). Exploring the smallest active fragment of HsQSOX1b and finding a highly efficient oxidative engine. *PLoS ONE* 7:e40935. doi: 10.1371/journal.pone.0040935

Zhou, C., Yan, Y., Fang, J., Cheng, B., and Fan, J. (2014). A new fusion protein platform for quantitatively measuring activity of multiple proteases. *Microb. Cell Fact.* 13:44. doi: 10.1186/1475-2859-13-44

Conflict of Interest: The authors declare that the research was conducted in the absence of any commercial or financial relationships that could be construed as a potential conflict of interest.

frontiers in Cellular and Infection Microbiology

REVIEW
published: 14 August 2020
doi: 10.3389/fcimb.2020.00353

Sphingosine 1-Phosphate in Malaria Pathogenesis and Its Implication in Therapeutic Opportunities

Gunanidhi Dhangadamajhi[1]* *and Shailja Singh*[2]

[1] Department of Biotechnology, North Orissa University, Baripada, India, [2] Special Centre for Molecular Medicine, Jawaharlal Nehru University, New Delhi, India

Sphingosine 1-Phosphate (S1P) is a bioactive lipid intermediate in the sphingolipid metabolism, which exist in two pools, intracellular and extracellular, and each pool has a different function. The circulating extracellular pool, specifically the plasma S1P is shown to be important in regulating various physiological processes related to malaria pathogenesis in recent years. Although blood cells (red blood cells and platelets), vascular endothelial cells and hepatocytes are considered as the important sources of plasma S1P, their extent of contribution is still debated. The red blood cells (RBCs) and platelets serve as a major repository of intracellular S1P due to lack, or low activity of S1P degrading enzymes, however, contribution of platelets toward maintaining plasma S1P is shown negligible under normal condition. Substantial evidences suggest platelets loss during *falciparum* infection as a contributing factor for severe malaria. However, platelets function as a source for plasma S1P in malaria needs to be examined experimentally. RBC being the preferential site for parasite seclusion, and having the ability of trans-cellular S1P transportation to EC upon tight cell-cell contact, might play critical role in differential S1P distribution and parasite growth. In the present review, we have summarized the significance of both the S1P pools in the context of malaria, and how the RBC content of S1P can be channelized in better ways for its possible implication in therapeutic opportunities to control malaria.

Keywords: sphingosine 1-phosphate, malaria, RBC, rosette, therapeutic

OPEN ACCESS

Edited by:
Jing-wen Lin,
Sichuan University, China

Reviewed by:
Viswanathan Natarajan,
University of Illinois at Chicago, United States
Tracey Lamb,
The University of Utah, United States

***Correspondence:**
Gunanidhi Dhangadamajhi
gunarmrc@gmail.com

Specialty section:
This article was submitted to Parasite and Host, a section of the journal Frontiers in Cellular and Infection Microbiology

Received: *18 March 2020*
Accepted: *08 June 2020*
Published: *14 August 2020*

Citation:
Dhangadamajhi G and Singh S (2020) Sphingosine 1-Phosphate in Malaria Pathogenesis and Its Implication in Therapeutic Opportunities. Front. Cell. Infect. Microbiol. 10:353. doi: 10.3389/fcimb.2020.00353

INTRODUCTION

Chemotherapeutics is the mainstay of malaria control in absence of high efficacy approved vaccine and ineffective vector control measures (Tibon et al., 2020). Unfortunately, parasite resistance to almost all the current pharmacotherapy is a major threat to control malaria. Despite high incidence, luckily, only a minority of individuals (1–2%) develop the malaria attributed complicacy. However, notable numbers (15–20%) of these patients still succumb to death even after effective antimalarial treatment (Dondorp et al., 2010; Newton et al., 2013) and thus requires the most urgent attention and intensive care. The complex interactions between the malaria parasite and human host leading to adhesion phenotypes (such as cyto-adherence, rosetting, and platelet mediated clumping), endothelial dysfunction, deregulation of the homeostasis system, host inflammatory response and nitric oxide (NO) production are thought to be the key events (van der Heyde et al., 2006; Yeo et al., 2008; Rowe et al., 2009). In other words, host response to malaria infection is of paramount importance in determining inter-individual variation in disease severity in malaria. Host response

in malaria research has primarily focused on protein component and lipids were usually appraised for their role in cell membrane formation or energy storage. Recently, Sphingosine 1-Phosphate (S1P), a pleiotropic lysophospholipid has been shown to affect various cellular pathways including the immune and vascular systems which are implicated in the pathology of severe malaria (Snider et al., 2010; Lou et al., 2011; Xiong et al., 2014). S1P is present in almost all cells and body fluids. However, it is one of the important components of blood, distributed differentially in blood cells and plasma, thereby regulating various physiological processes. In the present review, attempt has been made to highlight the current knowledge on S1P metabolism, cellular sources of plasma S1P, their transport and biological function based on the available literatures. In addition to this, we compiled the importance of S1P in the context of clinical malaria. Besides, RBC being the major source of S1P and preferential site for parasite seclusion, how RBC content of S1P could be channelized in a beneficial way for possible malaria control have been discussed.

S1P METABOLISM AND PLASMA SOURCE OF S1P

Shingosine, named after Sphinx, a Greek mythical creature of enigmatic activity is one of the important intermediate in sphingolipid metabolism. S1P is produced mostly through intracellular phosphorylation of sphingosine, a deacylated product of ceramide in various cell types by two isoform of sphingosine kinases (SPHK1 and SPHK2) (Ksiazek et al., 2015; Hatoum et al., 2017). Ceramide in turn is generated either from the condensation of serine and palmitoyl-CoA in a *de novo* pathway by serine palmitoyltransferase in the endoplasmic reticulum (ER), or from degradation of membrane sphingolipids (such as sphingomyelin and glycosphingolipids) in lysosomes or in the outer leaf-let of cellular membranes (Maceyka and Spiegel, 2014; Thuy et al., 2014; Ksiazek et al., 2015; Cantalupo and Di Lorenzo, 2016). The SPHK1 and SPHK2 kinases which phosphorylate sphingosine into S1P have different sub-cellular localization and tissue distribution (Maceyka et al., 2005). While SPHK1 is localized in cytosol (Pitson et al., 2005; Chan and Pitson, 2013) and highly substrate specific (Ksiazek et al., 2015), SPHK2 is mainly found in the nucleus, mitochondria, and ER (Cantalupo and Di Lorenzo, 2016) with broader range substrate specificity (Venkataraman et al., 2006; Maceyka and Spiegel, 2014). Further, of the two isoforms, only SPHK1 is shown to be released out of the endothelial cells constitutively, and the rate of extracellular S1P synthesis by SPHK1 is dependent on the level of spingosine present in the extracellular medium (Ancellin et al., 2002; Venkataraman et al., 2006; Takabe et al., 2008). However, its contribution as an additional source of plasma S1P in human is not clearly known. Moreover, it remains to be seen whether malaria infection has any impact on endothelial cell release of SPHK1 in extracellular milieu. It is established that S1P level in plasma and lymph is maintained relatively high compared to its concentration in tissues (Schwab et al., 2005; Peest et al., 2008; Takabe et al., 2008). Further, this differential gradient of S1P has been shown important in regulating various physiological function (Kerage et al., 2014; Cantalupo and Di Lorenzo, 2016; Cartier and Hla, 2019).

It is to be noted that blood harbors S1P in blood cells as well as in plasma (**Figure 1**). However, plasma S1P has a short half-life period (Venkataraman et al., 2008; Salous et al., 2013) which indicates its rapid clearance and instant replenishment in a well-regulated process. Although blood cells such as RBC and platelets, vascular endothelial cell, and hepatocytes are considered as the important sources of plasma S1P, their extent of contribution is still debated (Tani et al., 2007; Venkataraman et al., 2008). The balance between synthesis and export of S1P, and its intracellular or extracellular degradation by three types of enzymes is crucial in maintaining plasma level S1P. The intracellular degradation of S1P is carried out by two endoplasmic reticulum localized enzymes, such as (i) S1P phosphatases (SPP), which reversibly dephosphorylate S1P into sphingosine and (ii) S1P lyases (S1PL), which irreversibly inactivate S1P in to hexadecenal and ethanolamaine-1-phosphate (Bandhuvula and Saba, 2007; Liu et al., 2012). The degradation of S1P in extracellular space is carried out by the ecto-enzyme lipid phosphate phosphatases (LPP1 and LPP3) found in the plasma membrane of endothelial cell, and platelets (Yatomi et al., 2004; Zhao et al., 2007; Salous et al., 2013), which dephosphorylates most of the lipid phosphates including S1P. The S1P in the cell can also be dephosphorylated by another isoforms of LPP, the LPP2 which resides intra-cellularly (Kai et al., 2006). Of note, circulating S1P is rapidly dephosphorylated by LPPs into sphingosine (Zhao et al., 2007), where the latter is taken up by the blood cells and platelets (Tani et al., 2005; Ksiazek et al., 2015) for intracellular synthesis of S1P (Zhao et al., 2007). Besides, sphingosine can also be generated from membrane sphingolipids in these cells.

Of the various cell types, RBC synthesize S1P mainly via SPHK1, whereas platelets synthesize via SPHK2 and they both accumulate large amount of S1P due to lack of cellular organelles and S1P degrading enzymes (Hanel et al., 2007; Zhao et al., 2007; Bode et al., 2010; Urtz et al., 2015). Although the platelet content of S1P is relatively higher than that is in the RBC (Anada et al., 2007; Ito et al., 2007), the majority of S1P in the plasma pool of healthy individuals is contributed by RBC, possibly due to its largest share in total blood cell numbers (Hanel et al., 2007; Ito et al., 2007) and that the platelets release S1P only upon activation (Ohkawa et al., 2008; Ono et al., 2013). It is shown that human platelets can also constitutively release S1P without stimulation depending upon the presence of high albumin concentration in the plasma (Jonnalagadda et al., 2014). However, the observation of normal level of plasma S1P in thrombocytopenic or platelet-deficient mice (Pappu et al., 2007; Venkataraman et al., 2008) and non-correlation of platelet count with S1P level in human study (Ohkawa et al., 2008) suggest the contribution of platelet toward maintaining plasma S1P is negligible under normal condition. Interestingly, while genetic and pharmacological inhibition of *Sphk1* has shown reduction in plasma level of S1P by 50% (Kharel et al., 2011), similar studies with *Sphk2* (which encodes the major enzyme for platelet S1P synthesis) showed opposite results (Sensken et al., 2010; Kharel et al., 2012). This also supports the

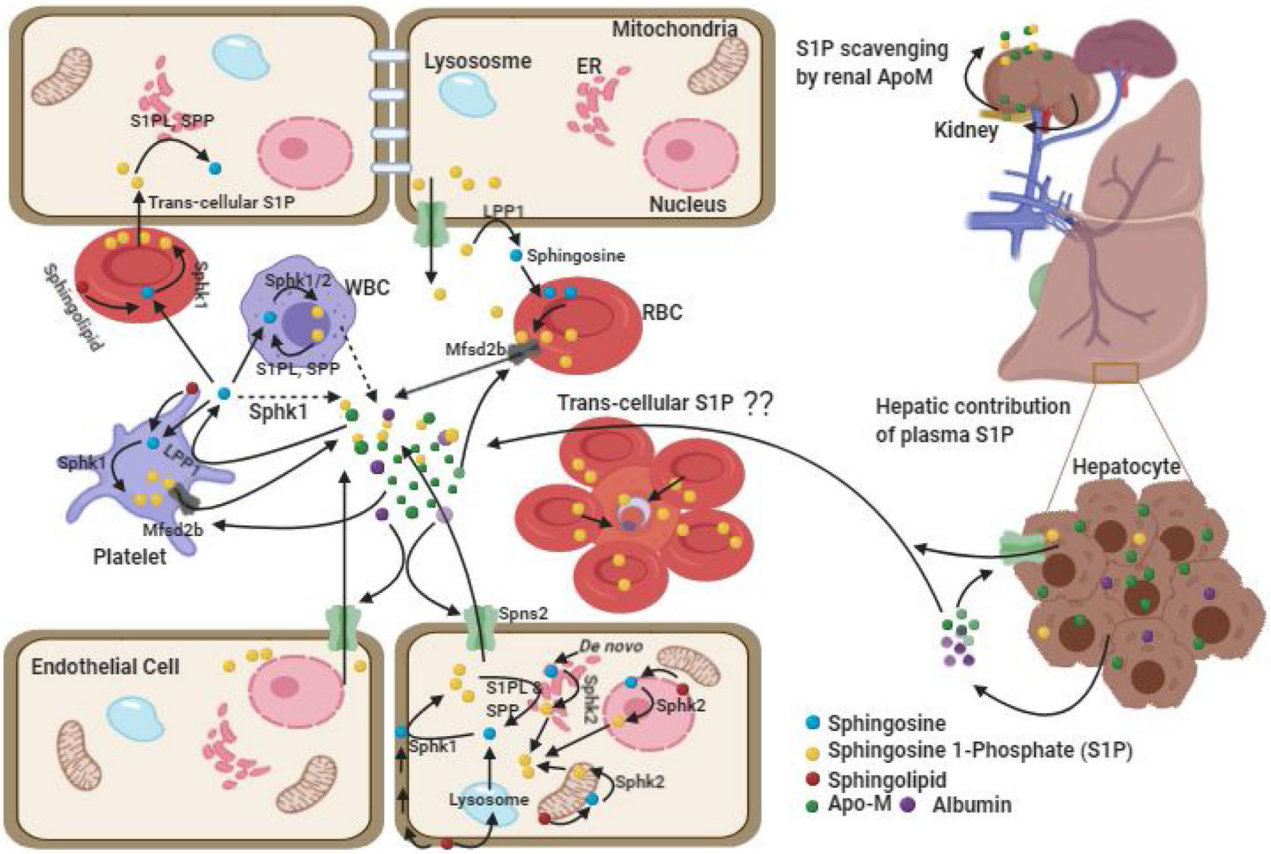

FIGURE 1 | Plasma Sources of cellular S1P. There are two pools of S1P, intracellular and extracellular each with different functions. The intracellular pool is synthesized upon incorporation of the substrate from plasma or its generation within the cell followed by phosphorylation by resident kinases such as SPHK1 in cytosol and SPHK2 in mitochondria, ER and nucleus. The intracellular S1P can be degraded by S1PL and SPP enzymes. The extra-cellular pool of S1P is predominantly maintained by cellular efflux of S1P facilitated by the acceptor molecules (ApoM-HDL and albumin) and possibly by endothelial cell secretion of SPHK1 which converts sphingosine in extracellular space into S1P (dashed arrow). RBCs play important role by functioning as a major reservoir for intracellular and extra-cellular S1P. In absence of acceptor molecule, RBC transports the S1P to EC and other cells through trans-cellular transportation after tight cell-cell contact. While, ECs have been demonstrated as alternative source for plasma S1P, platelets contributes to the extracellular pool only upon activation. Hepatocytes by secreting ApoM stimulate S1P export from hepatic and extra-hepatic cells, whereas kidney derived ApoM function to prevent urinal secretion of S1P and is metabolized in the kidney itself. The (??) in the figure depicts possible trans-cellular transportation of S1P from un-infected RBC to infected RBC in rosette.

non-significant role of platelets toward plasma S1P. In humans, although the cellular content of S1P in RBC of both anemic and healthy individuals is found to be comparable (Bode et al., 2010; Selim et al., 2011), significantly reduced plasma S1P level in anemic patients suggests the major role of RBC in contributing S1P in human blood (Hanel et al., 2007; Bode et al., 2010; Selim et al., 2011). This was further strengthened by the observation that in *Sphk1/Sphk2* deficient mice, transfusion of only wild type erythrocytes but not the platelets and leukocytes restored normal S1P level in plasma (Pappu et al., 2007). Further, significant correlation of RBC parameters with plasma S1P and the findings of higher plasma S1P in men, compared to women (Ohkawa et al., 2008) highlight RBC as the important source of blood S1P. Although gender difference in plasma S1P level was shown controversial in other studies (Hammad et al., 2010; Karuna et al., 2011), it is attributed to be due to remarkable decrease in plasma S1P post-menopause in women because of estrogen deficiency (Guo et al., 2014) and the inclusion of older age group in the study (Guo et al., 2014).

Spontaneous S1P efflux from vascular endothelial cells have also been documented similar to RBCs and could serve as an alternative source in replenishing plasma S1P at least in mice (Venkataraman et al., 2008; Fukuhara et al., 2012; Hisano et al., 2012). Shear stress and down regulation of intracellular S1P degrading enzymes have been shown to enhance S1P efflux from ECs (Venkataraman et al., 2008). However, it could not be replicated in human studies (Zhao et al., 2007). The contribution of WBCs toward plasma S1P is almost none and suggested to be due to its high rate of degradation than the rate of its release (Hanel et al., 2007; Salous et al., 2013). Consistent to this, no correlation between WBCs count with S1P has been found (Pappu et al., 2007; Ohkawa et al., 2008). The role of hepatocytes

in S1P homeostasis is related to its over expression of ApoM (Kurano et al., 2013; Nojiri et al., 2014), the major acceptor of circulating S1P which stimulates S1P export from hepatic and extra-hepatic cells (Liu et al., 2014; Huang et al., 2015). Although liver and kidney cells secrete ApoM (Zhang et al., 2003; Huang et al., 2015), plasma level of ApoM which mainly associates with HDL is predominantly secreted by liver cells. Liver derived ApoM play a major role in sphingolipid recycling, and in the maintenance of the plasma level of ApoM/S1P-enriched HDL besides whole body S1P distribution and homeostasis (Venkataraman et al., 2008; Christoffersen et al., 2011; Kurano et al., 2013). However, renal-ApoM by functioning as an S1P scavenger is metabolized in the kidney itself after re-absorption in the renal proximal tubule through the megalin receptor and prevent urinal secretion of S1P (Faber et al., 2006). Altogether, RBC is the major source of plasma S1P in humans but vascular EC and RBCs are equally important in maintaining blood S1P in mice.

EXPORT OF INTRACELLULAR S1P, ACCEPTOR MOLECULES AND THEIR EFFECT ON S1P FUNCTION

Having a polar head group, the export of cellular S1P to plasma is carried out through transporters like spinster homolog 2 (Spns2) from endothelial cells in a non-ATP dependent manner (Fukuhara et al., 2012; Hisano et al., 2012; Mendoza et al., 2012; Donoviel et al., 2015) or through major facilitator superfamily transporter 2b (Mfsd2b) from RBCs and platelets in an ATP dependent manner (Vu et al., 2017; Kobayashi et al., 2018). Moreover, being poorly water soluble, the release of S1P to plasma is facilitated by the presence of extracellular acceptor molecules such as HDL (most notably ApoM-HDL which carries 70% of S1P), or albumin (which carries 30% of S1P). Intracellular S1P efflux to plasma has been decreased upon dilution of plasma or prevented in serum/plasma free medium (Hanel et al., 2007; Venkataraman et al., 2008; Bode et al., 2010; Christoffersen et al., 2011; Karuna et al., 2011; Sutter et al., 2014). Further, in absence of the S1P acceptor molecules (albumin and ApoM) in plasma, RBC may contribute to S1PL degradable cellular pool of S1P through trans-cellular S1P transportation to EC and other tissue cells upon tight cell-cell contact (Bode et al., 2010). This indicates that RBC content of S1P and the acceptor molecules play critical role in differential distribution and degradation of S1P.

Recent studies have shown that the S1P efflux from EC, RBC, and platelets, and their effective circulation in the plasma and specific biological function is dependent on its association with the type of acceptor molecule. Of note, the rate of release of S1P from RBC is enhanced by the ApoM-HDL (Bode et al., 2010; Wilkerson et al., 2012; Yu et al., 2014) and from the platelets by albumin (Jonnalagadda et al., 2014). Further, functional differences in evoking intracellular signaling between ApoM-S1P and albumin-S1P exist (Wilkerson et al., 2012; Galvani et al., 2015; Obinata and Hla, 2019), albeit the reason for this remains poorly understood. It is suggested that while albumin is indiscriminating in binding to various small hydrophobic molecules including S1P (Obinata and Hla, 2019), ApoM has high affinity for S1P and is a specific chaperone that protects the bound S1P from degradation by LPP (Kimura et al., 2001; Christoffersen et al., 2011; Zhang et al., 2016). Moreover, ApoM-bound S1P in a context-dependent signaling has been shown to mediate prolonged receptor activation for several hours compared to transient activation by albumin in evoking downstream cascade (Wilkerson et al., 2012; Swendeman et al., 2017). While albumin-bound S1P has been found to be associated with diminished cAMP production and efficient $S1PR_1$-internalization (Galvani et al., 2015; Obinata and Hla, 2019), ApoM-S1P has been observed to regulate lymphopoiesis in bone marrow (Blaho et al., 2015) and maintain vascular integrity through anti-inflammatory responses in endothelial cells (Galvani et al., 2015; Sattler et al., 2015; Keul et al., 2019). Interestingly, engineered ApoM with long plasma half-life (about 90 h) and the potential to bind S1P (such as ApoM-Fc) was when intraperitoneally administered to the experimental model of stroke in mice, an increase in plasma S1P concentration by 30% was recorded post 24 h with protection from myocardial damage after ischemia, together with reduction of hypertension and brain infarct volume compared to the control ApoM of comparable half-life with no S1P binding ability (ApoM-Fc-TM) (Swendeman et al., 2017). Moreover, the association of low level HDL-S1P content with coronary artery disease (Sattler et al., 2010), and type II diabetes (Tong et al., 2014) in case-control human studies evidence for the potential beneficial role of ApoM-S1P in these diseases. However, it remains to be elucidated how plasma S1P level and the S1P bound receptors affect the pathological conditions in human malaria.

Although intracellular receptor for S1P is not well-characterized, it is shown to regulate important intracellular function like ubiquitination, histone deacetylation and gene expression, and respiration (Hait et al., 2009; Alvarez et al., 2010; Sun et al., 2016). On the other hand, the extracellular S1P exerts its diverse effects in an autocrine or paracrine manner through five G-protein coupled receptors [$S1PR_{1-5,}$ initially termed as endothelial differentiation gene (EDG)]. These S1PRs vary in their distribution and expression in response to various stimuli (Strub et al., 2010; Blaho and Hla, 2014). Of the five receptors ($S1PR_{1-5}$), $S1PR_{4-5}$ have much narrower patterns of expression compared to $S1PR_{1-3}$ receptors, with ubiquitous expression of $S1PR_1$ in the brain, kidney, lung, spleen and cardiovascular system (Strub et al., 2010; Blaho and Hla, 2014). While $S1PR_1$ regulates immune cell function including lymphocyte egress from lymph nodes (Liu et al., 2000; Schwab et al., 2005; Sanna et al., 2006), $S1PR_2$ is required for vestibular and auditory systems development (MacLennan et al., 2006; Ingham et al., 2016; Hofrichter et al., 2018), whereas $S1PR_3$ is required for regulation of heart rate (Forrest et al., 2004). Further, $S1PR_{1-3}$ receptors play an important role in angiogenesis and vascular permeability (Strub et al., 2010). A study involving triple knockout of $S1PR_{1-3}$ has led to the embryonic lethality in mice due to the massive vascular deficiencies (Kono et al., 2004). Since, vascular injury is common in severe *falciparum* malaria; we hypothesize for the possible involvement of $S1PR_{1-3}$ receptors including plasma level of S1P in severe malaria.

Although the S1P concentration in plasma and its subsequent effect on malaria could possibly be due to genetic variation, there is lack of information on mutations in genes affecting S1P synthesis (*Sphk1, Sphk2*), degradation (*Spl, Spp1, Spp2*) and signaling receptors ($S1pr_{1-3}$) leading to plasma level of S1P concentration and clinical outcome in malaria. Screening of functional genetic variations in these genes may be useful for better understanding of S1P biology in malaria.

S1P AND ITS ASSOCIATION WITH MALARIA

To date, only few studies have exploited the role of S1P in malaria. Recent studies have highlighted the dysregulation of the S1P pathway mostly in the pathogenesis of CM in mice (**Table 1**). Reduced plasma S1P has been found to be associated with malaria severity and impaired neuro-cognitive functions in mice (**Table 1**). In Ugandan children with CM, the plasma S1P level was significantly less compared to uncomplicated malaria (Finney et al., 2011) consistent to the results obtained in experimental malaria. Severe neurological sequelae are also common in human CM, often associated with death in children post-discharge from hospital (Idro et al., 2010; Oluwayemi et al., 2013). Of note, increased bio-availability of S1P has been shown to inhibit neurological signs and prolonged survival in experimental CM (Finney et al., 2011; Nacer et al., 2012, 2014) indicating S1P enrichment in plasma could be a rational means of new therapeutics strategy, although it has to be established in human studies. Further, the involvement of S1P receptors, specifically increased $S1PR_3$ concentration with mortality has been documented in acute lung injury (ALI)/acute respiratory distress syndrome (ARDS) patients (Sun et al., 2012), yet another severe complication of *falciparum* malaria which ranges from 5 to 25% of adults and 29% of pregnant women (Taylor et al., 2012). Anticipating implication of circulating $S1PR_3$ as a potential biomarker of severity in malaria induced ARDS, when the expression of the *Sphk1* and $S1PR_3$ proteins were investigated in malaria-associated ALI/ARDS, up-regulated expression of these were demonstrated in the lung tissues of experimental mice and human malaria patients (Punsawad and Viriyavejakul, 2019; Viriyavejakul and Punsawad, 2020). However, agreeing to evidence from previous studies (Finney et al., 2011; Punsawad and Viriyavejakul, 2017), plasma and lung tissues level of S1P was significantly less in malaria infected mice with ALI/ARDS) compared to non-ALI/ARDS and control (Punsawad and Viriyavejakul, 2019). Although the reason for S1P reduction remains unknown, it can be surmised that *Sphk1* and $S1pr_3$ expression in lung tissues do not contribute much for tissue fluids or plasma level of S1P. A recent knockout study in *Pseudomonas aeruginosa* induced lung inflammation revealing the pathogenic role of SPHK2 through epigenetic regulation of gene expression and intracellular S1P generation (Ebenezer et al., 2019) proposes the possible collusion of SPHK2 in malaria induced ARDS. Further studies with *Sphk1, Sphk2*, and $S1pr_3$ knockout mice or antagonists may help understanding their involvement in ALI/ARDS and unveil the reason for S1P reduction. These findings are of particular interest and indicate the possible protective nature of S1P in severe malaria; however the role of S1P in malaria is still unclear.

Endothelial dysfunction leading to loss of vascular integrity and leakage is the key to the pathogenesis of severe malaria (van der Heyde et al., 2006; Liles and Kain, 2014). Accelerated breakdown of endothelial glycocalyx leading to endothelial cell (EC) activation and exposure of EC surface receptors for parasite sequestration has been documented during severe malaria (Hempel et al., 2019; Yeo et al., 2019). Interestingly, inverse association of S1P with endothelial glycocalyx breakdown products have been demonstrated in Indonesian adults patients with *falciparum* infection (Yeo et al., 2019). Further, increased permeability of endothelial cells induced by sera from individuals with complicated *falciparum* malaria has been found to reverse with phosphorylated FTY720, an S1P agonist (Oggungwan et al., 2018). This indicates that S1P bioavailability could be instrumental in attenuating endothelial damage and ensuing protection from severe malaria. Previous study examining the impact of S1P bioavailability through S1P lyase deficiency in ECM has documented improved survival in mice (Finney et al., 2011), which further resolves the importance of S1P in effective therapeutics against malaria. Disruption of vascular integrity in the blood–brain barrier (BBB) is often associated with poor outcome in CM. Moreover, increased vascular integrity and significant survival advantage have been observed in murine model of CM upon prophylactic or early therapeutic treatment with FTY720. However, therapeutic intervention with FTY720 in later stage infection (3–5 days) in the same study was ineffective against ECM (Finney et al., 2011). Notably, administration of FTY720 in combination with sub curative dose of artesunate (the most potent antimalarial drug against all forms of severe malaria) in late stage infection resulted in improved survival from ECM with unaltered parasite burden compared to artesunate alone (Finney et al., 2011) indicating that the protective effect was especially through host response modulation. Artesunate is shown protective against malaria by its direct parasite killing activity and indirect immune-modulatory effect such as prevention of endothelial cell activation, cyto-adherence of parasite infected RBCs, and amelioration of blood–brain barrier (BBB) breakdown (Souza et al., 2012). Recent study documents artesunate mediated alleviation of BBB disruption to be through activation of $S1PR_1$, downstream phosphatidylinositol 3-kinase/AKT signaling, and stabilization of β-catenin (Zuo et al., 2017). Although FTY720 too activates S1PRs (except $S1PR_2$) initially, it down regulates $S1PR_1$ function through irreversible induction of $S1PR_1$ internalization and degradation (Oo et al., 2011). It remains unknown how FTY720 modulates the action of artesunate in improving survival from later stage ECM in combination treatment. Nonetheless, these findings are immensely important to include S1P agonists as potential adjunctive therapeutics for malaria treatment. It is suggested that reduced lymphocyte count in the blood due to impaired lymphocyte egress with significant restriction of immune cells infiltration into the brain upon FTY720 treatment as prophylactic or early therapeutic drug could be the contributing factor for protection against CM (Finney et al., 2011). However, in late stage treatment, when there was already advancement in leukocyte egress and subsequent recruitment to brain had begun

TABLE 1 | Association of S1P with experimental infection of malaria and clinical malaria in human.

S. No	Organism or cell	Experimentation	Findings	References
1	Human Erythrocytes	The *SPHK-1* activity and its phosphorylation status were compared between uninfected and *P. falciparum*-infected erythrocytes *in vitro* in different stages of asexual development.	A significant decrease in SPHK-1 phosphorylation and activity were observed in a time-dependent manner in *falciparum*-infected erythrocytes compared to uninfected RBCs.	(Sah et al., 2020)
2	Human Erythrocytes	Intracellular parasitic growth was assessed upon pharmacological inhibition of host cell *SPHK1* in *falciparum* infected RBCs	Intracellular reduction of S1P in erythrocytes impaired glycolysis, low level of lactate was released as bi-product; parasite growth was affected leading to cell death. Impaired glycolysis was attributed to be due to decreased translocation of GAPDH from membrane to site of function in cytosol in infected RBC.	(Sah et al., 2019)
3	DBA/2 mice	*Plasmodium berghei* ANKA infected mice were divided into two groups: with and without ALI/ARDS. Expression of the *SphK-1* and S1PR-3 proteins was investigated	Upregulated expression of the *SphK-1* and S1PR-3 proteins was observed in endothelial cells, alveolar epithelial cells and alveolar macrophages in the lung tissues of ALI/ARDS group compared to control group. However, S1P in plasma and lung tissues was significantly less in ALI/ARDS group compared to control mice.	(Punsawad and Viriyavejakul, 2019)
4	HUVECs	Endothelial cells were incubated with malaria infected and non-infected human sera for induction of permeability. Treatment with FTY720 before and after incubation of sera was evaluated for restoration of permeability.	Significantly high permeability was recorded after incubation with serum from complicated patients with *falciparum* malaria compared to uncomplicated *falciparum* patients and *vivax* infected patients. Treatment with FTY720 before and after incubation of sera significantly reduced and prevented sera induced increase in endothelial cell permeability	(Oggungwan et al., 2018)
5	CBA/CaJ mice	Mice were infected with *PbA* for induction of ECM and with *Plasmodium yoelii* for malarial hyperparasitemia without neurological impairment. Treatment with FTY720 was investigated to understand the pathogenesis	Recruitment of activated leukocytes (CD8+ T cells and ICAM+ macrophages), and neutrophils to post-capillary venules prevents venous blood efflux from the brains severely, which leads to vasogenic edema in ECM. Cells arrest in vasculature is likely to increase the intracranial pressure leading to poor clinical outcome. Treatment with FTY720 prevents these cells recruitment and protect from death in ECM.	(Nacer et al., 2014)
6	CBA/CaJ mice	Mice infected with *P. berghei ANKA* strains were evaluated for recovery upon FTY720 treatment (oral dose of 0.3 mg/kg/day, starting 1 day before infection)	*P. berghei* ANKA induced ECM with neurological signs, cerebral hemorrhages, and BBB dysfunction. FTY720 inhibited vascular leakage and neurological signs, stabilized BBB and prolonged survival to ECM.	(Nacer et al., 2012)
7	C57BL/6	Mice infected with *PbA* (ECM) were treated with FTY720 1 d prior to and 1, 3, or 5 d post-infection to evaluate the possible involvement of S1P in endothelial dysfunction and survival. In order to examine whether increased S1P bioavailability affect survival in ECM, parasite infected mice deficient of S1PL was compared with wild-type littermates	FTY720 treatment in 1 day–pre-infection and 1 day–post-infection improved BBB integrity in ECM compared to untreated infected mice, and day 3 post-infection treated mice. Lymphocyte counts were markedly reduced in blood and their infiltration (both $CD4^+$and $CD8^+$ cells) in the brain was decreased. Further, treatment with FTY720 suppressed endothelial dysfunction and reduced plasma level of IFNϒ. FTY720 in combination with sub-curative dose of artesunate treatment on 5d post-infection resulted in improved survival compared to artesunate therapy alone. Increased bioavailability of S1P due to S1PL deficiency in knockout mice was associated with improved outcome compared to wild-type littermates	(Finney et al., 2011)
8	Human	Plasma S1P levels was compared between *falciparum* infected Ugandan children with CM and UM to examine the significance of S1P in human malaria	Plasma level of S1P was significantly less in children with cerebral malaria compared to UM. Also hemoglobin and platelet levels were highly reduced in CM	(Finney et al., 2011)
9	Human	S1P levels in serum of adult Indian malaria patients (*falciparum* and *vivax* infected) were compared to healthy controls	S1P level was significantly less in malaria patients compared to healthy control. Complicated malaria patients had the lowest S1P level, and platelet count positively correlated with S1P level	(Sah et al., 2020)

(Continued)

TABLE 1 | Continued

S. No	Organism or cell	Experimentation	Findings	References
	Human	Autopsied patients who died with *P. falciparum* malaria were categorized into PE and Non-PE group, and cellular expression of SPHK-1 and S1PR-3 were investigated using immune histochemistry.	Over expression of both SPHK-1 and S1PR-3 proteins were observed in lung tissues of PE indicating their role in the pathogenesis of pulmonary complications in severe malaria.	(Viriyavejakul and Punsawad, 2020)
10	Human	Endothelial glycocalyx breakdown products, markers of endothelial dysfunction, parasite biomass, S1P and NO levels were compared between Indonesian adults with *falciparum* malaria (severe and moderately severe) and healthy control	Inverse correlation between S1P and breakdown products of endothelial glycocalyx was observed. Glycocalyx breakdown was associated with endothelial dysfunction, low NO bioavailability, increased parasite biomass, severity of malaria and risk of death.	(Yeo et al., 2019)
11	Human	Serum S1P levels were measured in Thai patients with *P. vivax*, uncomplicated *P. falciparum*, and complicated *P. falciparum* malaria on day 0 and on day 7. These values were compared to that of healthy control	Low serum S1P was associated with severity of malaria on day of admission which increased to significant level on day 7. Platelet count, hemoglobin and hematocrit values were positively correlated with serum S1P level in severe *falciparum* malaria patients	(Punsawad and Viriyavejakul, 2017)

GAPDH, Glyceraldehyde 3-phosphate dehydrogenase; SPHK1, Sphingosine kinase 1; ALI/ARDS, acute lung injury/acute respiratory distress syndrome; HUVEC, Human umbilical vein endothelial cell; ECM, Experimental cerebral malaria; BBB, Blood-brain-barrier; UM, Uncomplicated malaria; PE, Pulmonary edema; S1PL, Sphingosine-1-phosphate lyase.

(a process involved in CM pathology), attempt to recover mice could have been difficult (Finney et al., 2011; Nacer et al., 2012, 2014). Artesunate has been proven beneficial against late stage ECM independent of parasite killing and is attributed to be due to the reduction of endothelial dysfunction, and leuckocyte detachment from brain vasculature (Clemmer et al., 2011; Souza et al., 2012). Besides, IL-10 (which suppresses inflammation) producing T cells are augmented in artesunate treated mice (Thomé et al., 2016). Although there is rapid decrease in leukocyte accumulation in brain of artesunate treated ECM (Clemmer et al., 2011; Thomé et al., 2016), whether it is through the same mechanism of restricting leucocytes infiltration in to CNS as it for FTY720 is unknown. It is possible that FTY720 by down regulating $S1PR_1$ during late stage infection may lead to breach of BBB which may facilitate effective delivery of artesunate to central nervous system (CNS) for execution of immune-protective response against malaria. Some transient pharmacological inhibition studies of $S1PR_1$ in brain endothelial cell also highlight enhanced delivery and accumulation of therapeutics drugs in to the CNS (Cannon et al., 2012; Yanagida et al., 2017) supporting this hypothetical dysregulated $S1PR_1$ signaling axis as a possible target in modern therapeutics. Besides, S1P induction of NO release from endothelial cell (Igarashi et al., 2001) in mediating protective immune-response cannot be ruled out as the bioavailability of NO has been associated with resistance to malaria in previous clinical studies (Yeo et al., 2008; Dhangadamajhi et al., 2009). However, the effect of S1P and $S1PR_1$ signaling in human malaria has not been investigated in terms of NO production and subsequent clinical outcome.

Previous studies investigating the effects of *Plasmodium falciparum* infections on blood indices show reduction of platelet count (thrombocytopenia) and RBCs (anemia), the two major sources for plasma S1P to be frequent and are responsible for clinical severity with fatal outcome (Birhanu et al., 2017; Punsawad and Viriyavejakul, 2017; Dhangadamajhi et al., 2019). Further, platelet count has been delineated to resolve rapidly with recovery in the absence of any additional and specific treatment (Khan et al., 2012). Also, thrombocytopenia and anemia have been associated with a reduction in S1P level (Ono et al., 2013; Punsawad and Viriyavejakul, 2017). Although platelets release S1P into the blood circulation only after activation, whether such activation occurs during *falciparum* infection needs to be investigated. Based on significant correlation between platelet count and plasma S1P (Ono et al., 2013; Punsawad and Viriyavejakul, 2017), and their association with severity of malaria, it is reasonable to speculate the contribution of platelet to plasma S1P in malaria. On the other hand, S1P gradient and S1PR signaling (specifically through $S1PR_1$ and partly by $S1PR_4$ under stress) were shown essential for platelet formation from megakaryocytes and their shedding in to the circulation (Zhang et al., 2012). Therefore, reduced plasma S1P with impaired S1PR signaling during *falciparum* infection might affect thrombopoiesis and could be the cause of observed thrombocytopenia. Since, platelets harbor endothelial cell protective factors (Nachman and Rafii, 2008), their loss upon reduced S1P in plasma may contribute indirectly to endothelial dysfunction. Whether, platelets function as plasma source of S1P during *falciparum* infection and/or thrombocytopenia in malaria is a consequence of reduced S1P in plasma is yet to be investigated. Although low level of S1P in plasma is associated with cerebral malaria and ARDS (Finney et al., 2011), its concentration in other forms of sub-clinical severe malaria needs further investigation. Besides, the role of S1P in endothelial dysfunction, inflammation, and NO production is largely unknown in human malaria. Therefore, it is imperative to investigate the prognostic implications of S1P in the context of severe *falciparum* malaria for its possible utility as adjunctive therapeutics in severe malaria.

RBC AND MALARIA IN THE CONTEXT OF S1P

Owing to the major source of S1P in the blood and preferential site for parasite seclusion, the role of RBCs in the context of S1P is critical. In a recent *in vitro* study by our group, it was shown that erythrocytic inhibition of SPHK1 leading to reduced intracellular S1P level arrested parasite growth and ultimately to cell death possibly due to impaired glycolysis (Sah et al., 2019). It was suggested that the deprivation of intra-erythrocytic S1P hindered the binding of deoxy-Hb to plasma membrane thereby decreasing the translocation of the glycolytic enzyme, Glyceraldehyde 3-phosphate dehydrogenase (GAPDH) from the erythrocyte plasma membrane to the cytosol (Sun et al., 2016; Sah et al., 2019). This indicates that besides hemoglobin (major nutrient source for the intra-cellular malaria parasite), intra-erythrocytic level of S1P is important for parasite growth as well, at least for the smooth operation of glycolysis in order to meet its high energy demand. Further, RBC being the main repository for S1P due to its capability to import sphingosine from the plasma (Ito et al., 2007), high SPHK1 activity (Hanel et al., 2007; Pappu et al., 2007), and lack or low activity of S1P degrading enzymes (Ito et al., 2007; Selim et al., 2011) may render survival advantage to the obligatory parasite. In addition, metabolic acidosis, the common cause of severe *falciparum* malaria could be the consequence of S1P mediated glycolysis boost in parasite infected RBC which can lead to increased lactate production. However, the fact that plasma level of S1P is crucial, and its low level has been attributed to cause severe malaria. Although, anemia and thrombocytopenia (which are common during severe malaria) terrify the condition of reduced plasma S1P, there is no study conducted till date addressing whether erythrocytic content of S1P is maintained despite decreased plasma S1P level during severe malaria. Previous study documents RBC content of S1P in non-malaria anemic patients to be similar compared to healthy individual (Selim et al., 2011). Intriguingly, Knapp et al. have documented perpetual reduced plasma S1P concentration as a stimulant for enhanced SPHK1 expression in erythrocytes in myocardial infarction (Knapp et al., 2013). During malaria infection, due to prolonged reduction in plasma S1P, parasite infected and/or non-infected RBCs might also be induced for increased rate of S1P production. Besides, trans-cellular S1P transportation from un-infected RBC to infected RBCs in rosette can't be ruled out. Rosette formation (aggregation of uninfected RBCs around a parasite infected RBC) is shown to be virulent in malaria and is region specific (Rowe et al., 2009; Rout et al., 2012). However, what triggers rosette formation is unknown. It is possible that poor intracellular S1P in parasite infected RBC may favor its binding with un-infected RBCs in rosette for auxiliary S1P to the growing parasite through trans-cellular transportation. In a recent study, the observation of time dependent decrease in SPHK1 activity in infected RBC *in vitro* culture of *falciparum* parasite without affecting normal RBC (Sah et al., 2020) supports a possible acquisition of S1P from nearby uninfected cells. Investigation on this aspect would thus be helpful in better understanding on involvement of S1P in rosette formation and subsequent complicacy in severe malaria. Further, uptake of S1P carrier proteins by the infected erythrocytes during *in vitro* culture (El Tahir et al., 2003) or their significant loss from plasma in malaria infected patients compared to the healthy individual (Visser et al., 2013) suggests strategic reduction of S1P export to the plasma by the parasite during malaria infection. Therefore, we speculate that intra-erythrocytic level of S1P adequate for parasite growth might be maintained during malaria and that decreased S1P efflux to plasma due to insufficient acceptors (**Figure 2**) may lead to S1P mediated various patho-physiological conditions of malaria.

THERAPEUTIC OPPORTUNITIES

Up to now it is clear that Sphk1/S1P signaling nexus and maintenance of adequate S1P level in erythrocytes is essential for intra-cellular parasitic growth (Sah et al., 2019), whereas low plasma S1P concentration contributes to severe manifestation of malaria. Therefore, reduction of RBC content of S1P and/or augmentation of plasma S1P through efflux from cellular sources could be an adjunctive therapeutic opportunities against severe malaria. Since S1P level in body fluids and cellular compartments is tightly regulated by complex interplay of S1P metabolizing enzymes, transporters, chaperones, and signaling receptors, one or more of these could be induced, inhibited or modulated as per requirement for S1P-targeted therapeutic approaches. Amongst the various S1P receptors targeting agents, functional antagonist to $S1PR_1$ such as Fingolimod (also known as FTY720-P/Gilenya) and Siponimod (antagonist to $S1PR_1$ and $S1PR_5$) are FDA–approved drugs (Cartier and Hla, 2019). These drugs are shown to be effective against multiple sclerosis (MS), relapse remitting MS, neuro degenerative diseases, and cancer in several clinical trials (Cartier and Hla, 2019). Further, because of the acute agonistic action upon initial binding Fingolimod has also been reported to induce $S1PR_1$ in megakaryocytes resulting in rapid platelet release (Zhang et al., 2012). Keeping in view of the constructive role of FTY720 in maintaining vascular integrity, survival benefits against CM and importance of platelets biology in malaria pathogenesis, FTY720 and related drugs should also be evaluated for their effectiveness in human clinical trial of malaria.

Regulation or inhibition of metabolic enzymes, particularly SPHK1 in RBC and deprivation of RBC content of S1P could be a potent therapeutic against malaria infection. A recent article by Pulkoski-Gross and Obeid (2018) describes SPHK1 regulation at different levels starting from transcription to post-translational modification through the use of long non-coding RNAs, micro RNAs, small interfering RNAs, and physiological and pharmacological stimuli. However, RBC being devoid of nucleus and genetic material, these methods of regulation seem ineffective. On the other hand, requirement of membrane localization for the cytosol resident SPHK1 for its ultimate functioning leave a hope to examine inhibitors of SPHK1 interaction with membranes as possible drug compound. Inhibition of SPHK1 phosphorylation at serine 225 has enabled reduced translocation to membrane resulting into deregulated S1P in *Leishmaniasis* infected macrophages (Arish et al., 2018). Reduced SPHK1 activity in *falciparum* infected RBCs has also

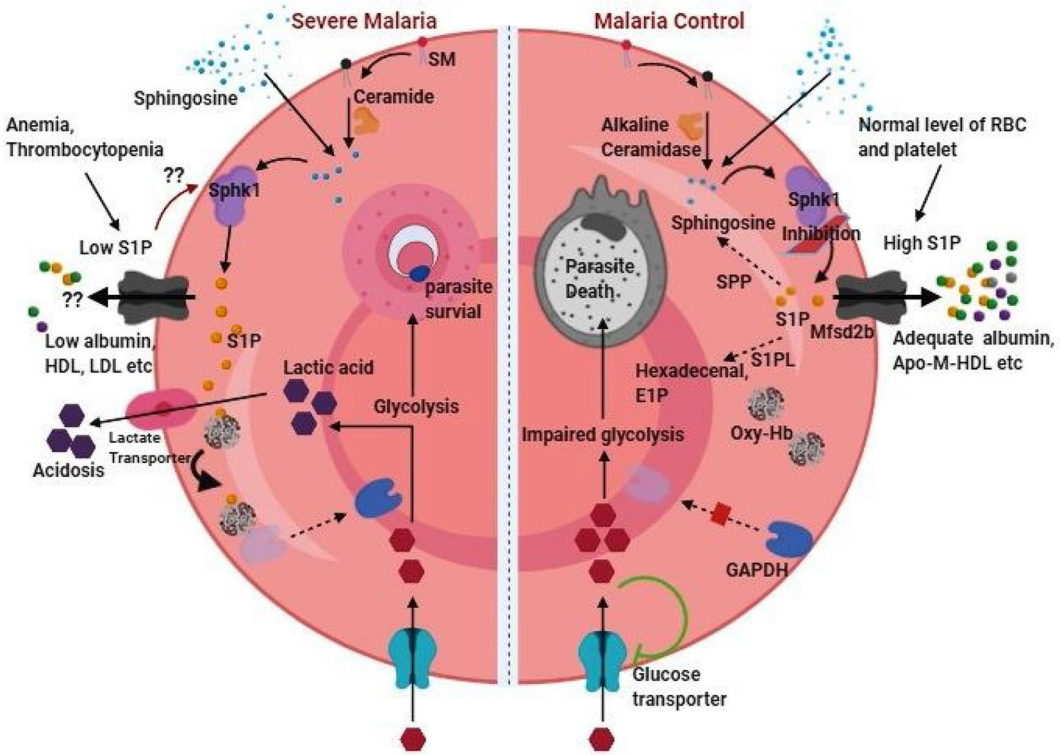

FIGURE 2 | RBC content of S1P as therapeutic target in malaria. RBC content of S1P can function as double-edged sword in malaria pathogenesis by provoking severe malaria (left half of the figure) or can be targeted for malaria control (right half of the figure). Thrombocytopenia and anemia, which are common in malaria indicates loss of two important sources of plasma S1P. Besides, depletion of acceptor molecules such as ApoM and albumin during malaria infection is expected to further harsh the condition of low plasma S1P level by reducing S1P efflux from these cellular sources. On the other hand, low level of plasma S1P might induces SPHK1 for phosphorylation of sphingosine synthesizing S1P in RBC. Sphingosine in RBC can be available as an intermediate of sphingolipid metabolism or directly be incorporated from the plasma. While intra-cellular S1P in RBC facilitate enhanced glycolysis essential for parasite growth, release of lactic acid byproduct leads to the severe condition of acidosis in malaria. Thus, malaria control (right half of the figure) can be achieved through S1P deprivation in parasite infected erythrocyte either by sphk1 inhibition, intracellular degradation by stimulation of S1P phosphatase and lyase, and/or promoting S1P exports in presence of adequate level of acceptor molecules. High plasma S1P has the beneficial role of protection against malaria. The (??) represents our hypothesis based on experimental evidences in different conditions or diseases.

been documented due to the lack of phosphorylation (Sah et al., 2020). Recently, GPCR proteins such as bradykinin receptors and muscarinic M3 receptor were shown to induce SPHK1 translocation to membrane (ter Braak et al., 2009; Bruno et al., 2018) and thus their inhibition would be provocative of future research. Further, cellular degradation of SPHK1 leading to loss of S1P in RBCs may also be an alternative approach of restricting intracellular parasite growth. Although on-target inhibition or degradation of SPHK1 is likely to preclude the possibility of trans-cellular S1P transport from uninfected RBCs to parasite infected RBC in rosette, undesirable degradation in other cell types may limit the use of these drugs. Further, this could also prevent participation of RBC as a source to plasma S1P as well hampering the protective effect of S1P against malaria. It is noteworthy that platelets production of S1P is largely mediated by SPHK2 (Urtz et al., 2015). Thus, platelet induction of S1P release could replenish plasma S1P and may play a crucial role in such case. Future studies in this aspect would render additional insights as to the role of RBC and platelets derived S1P in malaria. Of the several compounds, 2-(p-hydroxyanilino)-4-(p-chlorophenyl) thiazole (also known as SK1 II) has been shown to induce SPHK1 degradation through lysosomal pathway (Ren et al., 2010). Chloroquine (CQ), on the other hand, has been shown to reverse SK1 II mediated degradation of SPHK1 (Ren et al., 2010). CQ though does not affect *de novo* synthesis of S1P derivatives; it restores S1P level in the cell through disrupting autophagy or lyso-somal degradation of enzymes by increasing the lysomal pH. Therefore, investigation on whether SK1 II also has its effect in RBC/parasite infected RBC which lack lysosome, or whether CQ modulates SPHK1 function in these cells upon SK1 II treatment would be important for possible targeted degradation of SPHK1.

Stimulation of S1P degradation in parasite infected RBC would be another appreciable approach. Although, RBC was reported as incapable of degrading S1P due to lack of S1PL and SPP enzymes (Ito et al., 2007), low level of these enzymes have been detected (Selim et al., 2011). Further, marked reduction of S1P in prolong storage of RBC (Selim et al., 2011; Dong

et al., 2012) support the plausible S1P degradation in RBC. It is unknown whether expression of these S1P degrading enzymes are induced or affected by the malaria parasite. However, SPP induction in iRBCs would be helpful in two ways. First, S1P level in RBCs would be reduced as required for therapeutics because of its degradation into Sphingosine and phosphate. Second, increased intra-cellular content of sphingosine might play an additional role of inducing eryptosis due to phosphatidyl serine exposure at RBC surface (erythrocyte death characterized by cell shrinkage) as reported previously (Qadri et al., 2011). However, it is unknown whether sphingosine could induce eryptosis in iRBCs as well. Since RBC serves as important source for the plasma level of S1P, cellular depletion of S1P via facilitated import into plasma through chaperone proteins (especially through ApoM-HDL) would be of therapeutic interest. This perspective of intra-cellular S1P depletion would be valuable by affecting parasite growth in infected RBCs as well as increasing plasma level of S1P as required for protection. Although albumin too function as S1P acceptor, the observation of increased albumin in cerebrospinal fluid impairing BBB function of Malawian children with CM (Brown et al., 2001) and reported $S1PR_1$ internalization upon albumin-S1P binding precludes its utility in therapeutics use in malaria. Of note, administration of engineered ApoM with long plasma half-life has resulted into increased plasma concentration of S1P and cardiac protection with recovery from stroke in experimental mice (Swendeman et al., 2017). Similar study is warranted in experimental model of malaria and whether there is deprivation of the RBC content of S1P through increased efflux upon adequate bio-availability of engineered ApoM needs to be investigated. Because, parasite dependency on RBC content of S1P for survival in infected cell may complicate its export to plasma. Alternatively, induction of S1P transporters in RBC and platelets would be additional opportunity for S1P-targeted drug development in malaria.

CONCLUSION AND FUTURE PERSPECTIVES

In summary, S1P seems to play a double-edged sword in malaria pathogenesis. While intracellular content of S1P in infected RBCs is essential for parasite growth and development, its low level in plasma is associated with cerebral malaria in mouse model and human studies. However, how reduced S1P concentration in plasma affects other forms of sub-clinical severe malaria is yet to be materialized. Although diminished S1P concentration in plasma is likely to induce S1P synthesis in RBC, it is yet to be confirmed in parasite infected and/or non-infected RBCs through experimental studies in malaria. Further, whether S1P is involved in inducing rosette formation during *falciparum* infection would be important to understand rosette mediated complicacy in severe malaria. The fact that bioavailability of S1P is a tightly regulated process and its function is modulated by acceptor chaperones in the plasma. Thus, screening of functional variants in genes regulating S1P level in the plasma and S1P receptors, proportion of plasma S1P bound to albumin or ApoM HDL and their association with clinical manifestation of malaria would be helpful. Although kidney function to prevent urinal secretion of S1P, in malaria related renal failure (the most common severe complication after cerebral malaria), urinal detection of S1P could serve as a prognostic indicator and needs investigation in this line. Hitherto, substantial evidences suggest plasma S1P is crucial for differential manifestation of malaria. Therefore, selective inhibition of S1P synthesis in RBC, its degradation or abatement though supplementation of adequate acceptor molecules leading to augmented plasma level S1P may impair RBC growth of parasite and protect from severe malaria. Although the involvement of S1P in malaria pathogenesis has been studied only recently; more studies are warranted to answer several of these un-resolved questions before its implication as therapeutics.

AUTHOR CONTRIBUTIONS

GD: conceived the original idea, prepared all figures, and the first draft of manuscript. SS: interpreted the manuscript drafting for important intellectual content. All authors discussed and contributed to the final manuscript.

FUNDING

The present review is an upshot of the project proposal submitted to ICMR, Govt. of India for funding by both the authors. The funding agency has no role in designing, drafting, and decision to submit the review article for publication.

ACKNOWLEDGMENTS

We thankfully acknowledge the authors whose contribution have been cited and would like to apologize to those whose published articles could not be cited due to space constraints.

REFERENCES

Alvarez, S. E., Harikumar, K. B., Hait, N. C., Allegood, J., Strub, G. M., Kim, E. Y., et al. (2010). Sphingosine-1-phosphate is a missing cofactor for the E3 ubiquitin ligase TRAF2. *Nature* 465, 1084–1088. doi: 10.1038/nature09128

Anada, Y., Igarashi, Y., and Kihara, A. (2007). The immunomodulator FTY720 is phosphorylated and released from platelets. *Eur. J. Pharmacol.* 568, 106–111. doi: 10.1016/j.ejphar.2007.04.053

Ancellin, N., Colmont, C., Su, J., Li, Q., Mittereder, N., Chae, S.-S., et al. (2002). Extracellular export of sphingosine kinase-1 enzyme Sphingosine 1-phosphate generation and the induction of angiogenic vascular maturation. *J. Biol. Chem.* 277, 6667–6675. doi: 10.1074/jbc.M102841200

Arish, M., Husein, A., Ali, R., Tabrez, S., Naz, F., Ahmad, M. Z., et al. (2018). Sphingosine-1-phosphate signaling in *Leishmania donovani* infection in macrophages. *PLoS Negl. Trop. Dis.* 12:e0006647. doi: 10.1371/journal.pntd.0006647

Bandhuvula, P., and Saba, J. D. (2007). Sphingosine-1-phosphate lyase in immunity and cancer: silencing the siren. *Trends Mol. Med.* 13, 210–217. doi: 10.1016/j.molmed.2007.03.005

Birhanu, M., Asres, Y., Adissu, W., Yemane, T., Zemene, E., and Gedefaw, L. (2017). Hematological parameters and hemozoin-containing leukocytes and their association with disease severity among malaria infected children: a cross-sectional study at Pawe General Hospital, Northwest Ethiopia. *Interdiscip. Perspect. Infect. Dis*. 2017:8965729. doi: 10.1155/2017/8965729

Blaho, V. A., Galvani, S., Engelbrecht, E., Liu, C., Swendeman, S. L., Kono, M., et al. (2015). HDL-bound sphingosine-1-phosphate restrains lymphopoiesis and neuroinflammation. *Nature* 523, 342–346. doi: 10.1038/nature14462

Blaho, V. A., and Hla, T. (2014). An update on the biology of sphingosine 1-phosphate receptors. *J. Lipid Res*. 55, 1596–1608. doi: 10.1194/jlr.R046300

Bode, C., Sensken, S.-C., Peest, U., Beutel, G., Thol, F., Levkau, B., et al. (2010). Erythrocytes serve as a reservoir for cellular and extracellular sphingosine 1-phosphate. *J. Cell. Biochem*. 109, 1232–1243. doi: 10.1002/jcb.22507

Brown, H., Rogerson, S., Taylor, T., Tembo, M., Mwenechanya, J., Molyneux, M., et al. (2001). Blood-brain barrier function in cerebral malaria in Malawian children. *Am. J. Trop. Med. Hyg*. 64, 207–213. doi: 10.4269/ajtmh.2001.64.207

Bruno, G., Cencetti, F., Bernacchioni, C., Donati, C., Blankenbach, K. V., Thomas, D., et al. (2018). Bradykinin mediates myogenic differentiation in murine myoblasts through the involvement of SK1/Spns2/S1P2 axis. *Cell. Signal*. 45, 110–121. doi: 10.1016/j.cellsig.2018.02.001

Cannon, R. E., Peart, J. C., Hawkins, B. T., Campos, C. R., and Miller, D. S. (2012). Targeting blood-brain barrier sphingolipid signaling reduces basal P-glycoprotein activity and improves drug delivery to the brain. *Proc. Natl. Acad. Sci. U.S.A*. 109, 15930–15935. doi: 10.1073/pnas.1203534109

Cantalupo, A., and Di Lorenzo, A. (2016). S1P signaling and *de novo* biosynthesis in blood pressure homeostasis. *J. Pharmacol. Exp. Ther*. 358, 359–370. doi: 10.1124/jpet.116.233205

Cartier, A., and Hla, T. (2019). Sphingosine 1-phosphate: lipid signaling in pathology and therapy. *Science* 366:eaar5551. doi: 10.1126/science.aar5551

Chan, H., and Pitson, S. M. (2013). Post-translational regulation of sphingosine kinases. *Biochim. Biophys. Acta* 1831, 147–156. doi: 10.1016/j.bbalip.2012.07.005

Christoffersen, C., Obinata, H., Kumaraswamy, S. B., Galvani, S., Ahnström, J., Sevvana, M., et al. (2011). Endothelium-protective sphingosine-1-phosphate provided by HDL-associated apolipoprotein M. *Proc. Natl. Acad. Sci. U.S.A*. 108, 9613–9618. doi: 10.1073/pnas.1103187108

Clemmer, L., Martins, Y., Zanini, G., Frangos, J., and Carvalho, L. (2011). Artemether and artesunate show the highest efficacies in rescuing mice with late-stage cerebral malaria and rapidly decrease leukocyte accumulation in the brain. *Antimicrob. Agents Chemother*. 55, 1383–1390. doi: 10.1128/AAC.01277-10

Dhangadamajhi, G., Mohapatra, B. N., Kar, S. K., and Ranjit, M. (2009). Endothelial nitric oxide synthase gene polymorphisms and *Plasmodium falciparum* infection in Indian adults. *Infect. Immun*. 77, 2943–2947. doi: 10.1128/IAI.00083-09

Dhangadamajhi, G., Panigrahi, S., Roy, S., and Tripathy, S. (2019). Effect of *Plasmodium falciparum* infection on blood parameters and their association with clinical severity in adults of Odisha, India. *Acta Trop*. 190, 1–8. doi: 10.1016/j.actatropica.2018.10.007

Dondorp, A. M., Yeung, S., White, L., Nguon, C., Day, N. P., Socheat, D., et al. (2010). Artemisinin resistance: current status and scenarios for containment. *Nat. Rev. Microbiol*. 8, 272–280. doi: 10.1038/nrmicro2331

Dong, A., Sunkara, M., Panchatcharam, M., Salous, A., Selim, S., Morris, A. J., et al. (2012). Synergistic effect of anemia and red blood cells transfusion on inflammation and lung injury. *Adv. Hematol.* 2012:924042. doi: 10.1155/2012/924042

Donoviel, M. S., Hait, N. C., Ramachandran, S., Maceyka, M., Takabe, K., Milstien, S., et al. (2015). Spinster 2, a sphingosine-1-phosphate transporter, plays a critical role in inflammatory and autoimmune diseases. *FASEB J*. 29, 5018–5028. doi: 10.1096/fj.15-274936

Ebenezer, D. L., Berdyshev, E., Bronova, I. A., Tiruppathi, C., Kumarova, Y., Benevolenskaya, E. V., et al. (2019). *Pseudomonas aeruginosa* stimulates nuclearsphingosine-1-phosphate generation and epigenetic regulation of lung inflammatory injury. *Thorax* 74, 579–591. doi: 10.1136/thoraxjnl-2018-212378

El Tahir, A., Malhotra, P., and Chauhan, V. S. (2003). Uptake of proteins and degradation of human serum albumin by *Plasmodium falciparum*–infected human erythrocytes. *Malar. J*. 2:11. doi: 10.1186/1475-2875-2-11

Faber, K., Hvidberg, V., Moestrup, S. K., Dahlbäck, B., and Nielsen, L. B. (2006). Megalin is a receptor for apolipoprotein M, and kidney-specific megalin-deficiency confers urinary excretion of apolipoprotein M. *Mol. Endocrinol*. 20, 212–218. doi: 10.1210/me.2005-0209

Finney, C. A., Hawkes, C. A., Kain, D. C., Dhabangi, A., Musoke, C., Cserti-Gazdewich, C., et al. (2011). S1P is associated with protection in human and experimental cerebral malaria. *Mol. Med*. 17, 717–725. doi: 10.2119/molmed.2010.00214

Forrest, M., Sun, S.-Y., Hajdu, R., Bergstrom, J., Card, D., Doherty, G., et al. (2004). Immune cell regulation and cardiovascular effects of sphingosine 1-phosphate receptor agonists in rodents are mediated via distinct receptor subtypes. *J. Pharmacol. Exp. Ther*. 309, 758–768. doi: 10.1124/jpet.103.062828

Fukuhara, S., Simmons, S., Kawamura, S., Inoue, A., Orba, Y., Tokudome, T., et al. (2012). The sphingosine-1-phosphate transporter Spns2 expressed on endothelial cells regulates lymphocyte trafficking in mice. *J. Clin. Invest*. 122, 1416–1426. doi: 10.1172/JCI60746

Galvani, S., Sanson, M., Blaho, V. A., Swendeman, S. L., Obinata, H., Conger, H., et al. (2015). HDL-bound sphingosine 1-phosphate acts as a biased agonist for the endothelial cell receptor S1P1 to limit vascular inflammation. *Sci. Signal*. 8, 79–79. doi: 10.1126/scisignal.aaa2581

Guo, S., Yu, Y., Zhang, N., Cui, Y., Zhai, L., Li, H., et al. (2014). Higher level of plasma bioactive molecule sphingosine 1-phosphate in women is associated with estrogen. *Biochim. Biophys. Acta* 1841, 836–846. doi: 10.1016/j.bbalip.2014.02.005

Hait, N. C., Allegood, J., Maceyka, M., Strub, G. M., Harikumar, K. B., Singh, S. K., et al. (2009). Regulation of histone acetylation in the nucleus by sphingosine-1-phosphate. *Science* 325, 1254–1257. doi: 10.1126/science.1176709

Hammad, S. M., Pierce, J. S., Soodavar, F., Smith, K. J., Al Gadban, M. M., Rembiesa, B., et al. (2010). Blood sphingolipidomics in healthy humans: impact of sample collection methodology. *J. Lipid Res*. 51, 3074–3087. doi: 10.1194/jlr.D008532

Hanel, P., Andréani, P., and Graler, M. H. (2007). Erythrocytes store and release sphingosine 1-phosphate in blood. *FASEB J*. 21, 1202–1209. doi: 10.1096/fj.06-7433com

Hatoum, D., Haddadi, N., Lin, Y., Nassif, N. T., and Mc Gowan, E. M. (2017). Mammalian sphingosine kinase (SphK) isoenzymes and isoform expression: challenges for SphK as an oncotarget. *Oncotarget* 8, 36898–36929. doi: 10.18632/oncotarget.16370

Hempel, C., Sporring, J., and Kurtzhals, J. A. L. (2019). Experimental cerebral malaria is associated with profound loss of both glycan and protein components of the endothelial glycocalyx. *FASEB J*. 33, 2058–2071. doi: 10.1096/fj.201800657R

Hisano, Y., Kobayashi, N., Yamaguchi, A., and Nishi, T. (2012). Mouse SPNS2 functions as a sphingosine-1-phosphate transporter in vascular endothelial cells. *PLoS ONE* 7:e38941. doi: 10.1371/journal.pone.0038941

Hofrichter, M. A., Mojarad, M., Doll, J., Grimm, C., Eslahi, A., Hosseini, N. S., et al. (2018). The conserved p. Arg108 residue in S1PR2 (DFNB68) is fundamental for proper hearing: evidence from a consanguineous Iranian family. *BMC Med. Genet.* 19:81. doi: 10.1186/s12881-018-0598-5

Huang, L.-Z., Gao, J.-L., Pu, C., Zhang, P.-H., Wang, L.-Z., Feng, G., et al. (2015). Apolipoprotein M: research progress, regulation and metabolic functions. *Mol. Med. Rep*. 12, 1617–1624. doi: 10.3892/mmr.2015.3658

Idro, R., Kakooza-Mwesige, A., Balyejjussa, S., Mirembe, G., Mugasha, C., Tugumisirize, J., et al. (2010). Severe neurological sequelae and behaviour problems after cerebral malaria in Ugandan children. *BMC Res. Notes* 3:104. doi: 10.1186/1756-0500-3-104

Igarashi, J., Bernier, S. G., and Michel, T. (2001). Sphingosine 1-phosphate and activation of endothelial nitric-oxide synthase differential regulation of Akt and MAP kinase pathways by EDG and bradykinin receptors in vascular endothelial cells. *J. Biol. Chem*. 276, 12420–12426. doi: 10.1074/jbc.M008375200

Ingham, N. J., Carlisle, F., Pearson, S., Lewis, M. A., Buniello, A., Chen, J., et al. (2016). S1PR2 variants associated with auditory function in humans and endocochlear potential decline in mouse. *Sci. Rep*. 6:28964. doi: 10.1038/srep28964

Ito, K., Anada, Y., Tani, M., Ikeda, M., Sano, T., Kihara, A., et al. (2007). Lack of sphingosine 1-phosphate-degrading enzymes in erythrocytes. *Biochem. Biophys. Res. Commun*. 357, 212–217. doi: 10.1016/j.bbrc.2007.03.123

Jonnalagadda, D., Sunkara, M., Morris, A. J., and Whiteheart, S. W. (2014). Granule-mediated release of sphingosine-1-phosphate by activated platelets. *Biochim. Biophys. Acta* 1841, 1581–1589. doi: 10.1016/j.bbalip.2014.08.013

Kai, M., Sakane, F., Jia, Y.-J., Imai, S., Yasuda, S., and Kanoh, H. (2006). Lipid phosphate phosphatases 1 and 3 are localized in distinct lipid rafts. *J. Biochem.* 140, 677–686. doi: 10.1093/jb/mvj195

Karuna, R., Park, R., Othman, A., Holleboom, A. G., Motazacker, M. M., Sutter, I., et al. (2011). Plasma levels of sphingosine-1-phosphate and apolipoprotein M in patients with monogenic disorders of HDL metabolism. *Atherosclerosis* 219, 855–863. doi: 10.1016/j.atherosclerosis.2011.08.049

Kerage, D., Brindley, D., and Hemmings, D. (2014). Novel insights into the regulation of vascular tone by sphingosine 1-phosphate. *Placenta* 35, 86–92. doi: 10.1016/j.placenta.2013.12.006

Keul, P., Polzin, A., Kaiser, K., Gräler, M., Dannenberg, L., Daum, G., et al. (2019). Potent anti-inflammatory properties of HDL in vascular smooth muscle cells mediated by HDL-S1P and their impairment in coronary artery disease due to lower HDL-S1P: a new aspect of HDL dysfunction and its therapy. *FASEB J.* 33, 1482–1495. doi: 10.1096/fj.201801245R

Khan, S. J., Abbass, Y., and Marwat, M. A. (2012). Thrombocytopenia as an indicator of malaria in adult population. *Malar. Res. Treat.* 2012:405981. doi: 10.1155/2012/405981

Kharel, Y., Mathews, T. P., Gellett, A. M., Tomsig, J. L., Kennedy, P. C., Moyer, M. L., et al. (2011). Sphingosine kinase type 1 inhibition reveals rapid turnover of circulating sphingosine 1-phosphate. *Biochem. J.* 440, 345–353. doi: 10.1042/BJ20110817

Kharel, Y., Raje, M., Gao, M., Gellett, A. M., Tomsig, J. L., Lynch, K. R., et al. (2012). Sphingosine kinase type 2 inhibition elevates circulating sphingosine 1-phosphate. *Biochem. J.* 447, 149–157. doi: 10.1042/BJ20120609

Kimura, T., Sato, K., Kuwabara, A., Tomura, H., Ishiwara, M., Kobayashi, I., et al. (2001). Sphingosine 1-phosphate may be a major component of plasma lipoproteins responsible for the cytoprotective actions in human umbilical vein endothelial cells. *J. Biol. Chem.* 276, 31780–31785. doi: 10.1074/jbc.M104353200

Knapp, M., Lisowska, A., Zabielski, P., Musial, W., and Baranowski, M. (2013). Sustained decrease in plasma sphingosine-1-phosphate concentration and its accumulation in blood cells in acute myocardial infarction. *Prostaglandins Other Lipid Mediat.* 106, 53–61. doi: 10.1016/j.prostaglandins.2013.10.001

Kobayashi, N., Kawasaki-Nishi, S., Otsuka, M., Hisano, Y., Yamaguchi, A., and Nishi, T. (2018). MFSD2B is a sphingosine 1-phosphate transporter in erythroid cells. *Sci. Rep.* 8, 1–11. doi: 10.1038/s41598-018-23300-x

Kono, M., Mi, Y., Liu, Y., Sasaki, T., Allende, M. L., Wu, Y.-P., et al. (2004). The sphingosine-1-phosphate receptors S1P1, S1P2, and S1P3 function coordinately during embryonic angiogenesis. *J. Biol. Chem.* 279, 29367–29373. doi: 10.1074/jbc.M403937200

Ksiazek, M., Chacinska, M., Chabowski, A., and Baranowski, M. (2015). Sources, metabolism, and regulation of circulating sphingosine-1-phosphate. *J. Lipid Res.* 56, 1271–1281. doi: 10.1194/jlr.R059543

Kurano, M., Tsukamoto, K., Ohkawa, R., Hara, M., Iino, J., Kageyama, Y., et al. (2013). Liver involvement in sphingosine 1-phosphate dynamism revealed by adenoviral hepatic overexpression of apolipoprotein M. *Atherosclerosis* 229, 102–109. doi: 10.1016/j.atherosclerosis.2013.04.024

Liles, W. C., and Kain, K. C. (2014). Endothelial activation and dysfunction in the pathogenesis of microvascular obstruction in severe malaria—a viable target for therapeutic adjunctive intervention. *J. Infect. Dis.* 210, 163–164. doi: 10.1093/infdis/jiu035

Liu, M., Seo, J., Allegood, J., Bi, X., Zhu, X., Boudyguina, E., et al. (2014). Hepatic apolipoprotein M (apoM) overexpression stimulates formation of larger apoM/sphingosine 1-phosphate-enriched plasma high density lipoprotein. *J. Biol. Chem.* 289, 2801–2814. doi: 10.1074/jbc.M113.499913

Liu, X., Zhang, Q.-H., and Yi, G.-H. (2012). Regulation of metabolism and transport of sphingosine-1-phosphate in mammalian cells. *Mol. Cell. Biochem.* 363, 21–33. doi: 10.1007/s11010-011-1154-1

Liu, Y., Wada, R., Yamashita, T., Mi, Y., Deng, C.-X., Hobson, J. P., et al. (2000). Edg-1, the G protein–coupled receptor for sphingosine-1-phosphate, is essential for vascular maturation. *J. Clin. Invest.* 106, 951–961. doi: 10.1172/JCI10905

Loh, K. C., Baldwin, D., and Saba, J. D. (2011), Sphingolipid signaling and hematopoietic malignancies: to the rheostat and beyond. *Anticancer Agents Med. Chem.* 11, 782–793. doi: 10.2174/187152011797655159

Maceyka, M., Sankala, H., Hait, N. C., Le Stunff, H., Liu, H., Toman, R., et al. (2005). SphK1 and SphK2, sphingosine kinase isoenzymes with opposing functions in sphingolipid metabolism. *J. Biol. Chem.* 280, 37118–37129. doi: 10.1074/jbc.M502207200

Maceyka, M., and Spiegel, S. (2014). Sphingolipid metabolites in inflammatory disease. *Nature* 510, 58–67. doi: 10.1038/nature13475

MacLennan, A. J., Benner, S. J., Andringa, A., Chaves, A. H., Rosing, J. L., Vesey, R., et al. (2006). The S1P2 sphingosine 1-phosphate receptor is essential for auditory and vestibular function. *Hear. Res.* 220, 38–48. doi: 10.1016/j.heares.2006.06.016

Mendoza, A., Bréart, B., Ramos-Perez, W. D., Pitt, L. A., Gobert, M., Sunkara, M., et al. (2012). The transporter Spns2 is required for secretion of lymph but not plasma sphingosine-1-phosphate. *Cell Rep.* 2, 1104–1110. doi: 10.1016/j.celrep.2012.09.021

Nacer, A., Movila, A., Baer, K., Mikolajczak, S. A., Kappe, S. H., and Frevert, U. (2012). Neuroimmunological blood brain barrier opening in experimental cerebral malaria. *PLoS Pathog.* 8:e1002982. doi: 10.1371/journal.ppat.1002982

Nacer, A., Movila, A., Sohet, F., Girgis, N. M., Gundra, U. M., Loke, P., et al. (2014). Experimental cerebral malaria pathogenesis—hemodynamics at the blood brain barrier. *PLoS Pathog.* 10:e1004528. doi: 10.1371/journal.ppat.1004528

Nachman, R. L., and Rafii, S. (2008). Platelets, petechiae, and preservation of the vascular wall. *N. Engl. J. Med.* 359, 1261–1270. doi: 10.1056/NEJMra0800887

Newton, P. N., Stepniewska, K., Dondorp, A., Silamut, K., Chierakul, W., Krishna, S., et al. (2013). Prognostic indicators in adults hospitalized with falciparum malaria in Western Thailand. *Malar. J.* 12:229. doi: 10.1186/1475-2875-12-229

Nojiri, T., Kurano, M., Tokuhara, Y., Ohkubo, S., Hara, M., Ikeda, H., et al. (2014). Modulation of sphingosine-1-phosphate and apolipoprotein M levels in the plasma, liver and kidneys in streptozotocin-induced diabetic mice. *J. Diabetes Investig.* 5, 639–648. doi: 10.1111/jdi.12232

Obinata, H., and Hla, T. (2019). Sphingosine 1-phosphate and inflammation. *Int. Immunol.* 31, 617–625. doi: 10.1093/intimm/dxz037

Oggungwan, K., Glaharn, S., Ampawong, S., Krudsood, S., and Viriyavejakul, P. (2018). FTY720 restores endothelial cell permeability induced by malaria sera. *Sci. Rep.* 8, 1–6. doi: 10.1038/s41598-018-28536-1

Ohkawa, R., Nakamura, K., Okubo, S., Hosogaya, S., Ozaki, Y., Tozuka, M., et al. (2008). Plasma sphingosine-1-phosphate measurement in healthy subjects: close correlation with red blood cell parameters. *Ann. Clin. Biochem.* 45, 356–363. doi: 10.1258/acb.2007.007189

Oluwayemi, I. O., Brown, B. J., Oyedeji, O. A., and Oluwayemi, M. A. (2013). Neurological sequelae in survivors of cerebral malaria. *Pan Afr. Med. J.* 15:88. doi: 10.11604/pamj.2013.15.88.1897

Ono, Y., Kurano, M., Ohkawa, R., Yokota, H., Igarashi, K., Aoki, J., et al. (2013). Sphingosine 1-phosphate release from platelets during clot formation: close correlation between platelet count and serum sphingosine 1-phosphate concentration. *Lipids Health Dis.* 12:20. doi: 10.1186/1476-511X-12-20

Oo, M. L., Chang, S.-H., Thangada, S., Wu, M.-T., Rezaul, K., Blaho, V., et al. (2011). Engagement of S1P 1-degradative mechanisms leads to vascular leak in mice. *J. Clin. Invest.* 121, 2290–2300. doi: 10.1172/JCI45403

Pappu, R., Schwab, S. R., Cornelissen, I., Pereira, J. P., Regard, J. B., Xu, Y., et al. (2007). Promotion of lymphocyte egress into blood and lymph by distinct sources of sphingosine-1-phosphate. *Science* 316, 295–298. doi: 10.1126/science.1139221

Peest, U., Sensken, S.-C., Andréani, P., Hänel, P., Van Veldhoven, P. P., and Gräler, M. H. (2008). S1P-lyase independent clearance of extracellular sphingosine 1-phosphate after dephosphorylation and cellular uptake. *J. Cell. Biochem.* 104, 756–772. doi: 10.1002/jcb.21665

Pitson, S. M., Xia, P., Leclercq, T. M., Moretti, P. A., Zebol, J. R., Lynn, H. E., et al. (2005). Phosphorylation-dependent translocation of sphingosine kinase to the plasma membrane drives its oncogenic signalling. *J. Exp. Med.* 201, 49–54. doi: 10.1084/jem.20040559

Pulkoski-Gross, M. J., and Obeid, L. M. (2018). Molecular mechanisms of regulation of sphingosine kinase 1. *Biochim. Biophys. Acta* 1863, 1413–1422. doi: 10.1016/j.bbalip.2018.08.015

Punsawad, C., and Viriyavejakul, P. (2017). Reduction in serum sphingosine 1-phosphate concentration in malaria. *PLoS ONE* 12:e0180631. doi: 10.1371/journal.pone.0180631

Punsawad, C., and Viriyavejakul, P. (2019). Expression of sphingosine kinase 1 and sphingosine 1-phosphate receptor 3 in malaria-associated acute lung injury/acute respiratory distress syndrome in a mouse model. *PLoS ONE* 14:e0222098. doi: 10.1371/journal.pone.0222098

Qadri, S. M., Bauer, J., Zelenak, C., Mahmud, H., Kucherenko, Y., Lee, S. H., et al. (2011). Sphingosine but not sphingosine-1-phosphate stimulates suicidal erythrocyte death. *Cell. Physiol. Biochem*. 28, 339–346. doi: 10.1159/000331750

Ren, S., Xin, C., Pfeilschifter, J., and Huwiler, A. (2010). A novel mode of action of the putative sphingosine kinase inhibitor 2-(p-hydroxyanilino)-4-(p-chlorophenyl) thiazole (SKI II): induction of lysosomal sphingosine kinase 1 degradation. *Cell. Physiol. Biochem*. 26, 97–104. doi: 10.1159/000315110

Rout, R., Dhangadamajhi, G., Ghadei, M., Mohapatra, B. N., Kar, S. K., and Ranjit, M. (2012). Blood group phenotypes A and B are risk factors for cerebral malaria in Odisha, India. *Trans. R. Soc. Trop. Med. Hyg*. 106, 538–543. doi: 10.1016/j.trstmh.2012.05.014

Rowe, J. A., Claessens, A., Corrigan, R. A., and Arman, M. (2009). Adhesion of *Plasmodium falciparum*-infected erythrocytes to human cells: molecular mechanisms and therapeutic implications. *Expert Rev. Mol. Med*. 11:e16. doi: 10.1017/S1462399409001082

Sah, R. K., Pati, S., Saini, M., Boopathi, P. A., Kochar, S. K., Kochar, D. K., et al. (2020). Reduction of sphingosine kinase 1 phosphorylation and activity in *Plasmodium*-infected erythrocytes. *Front. Cell Dev. Biol*. 8:80. doi: 10.3389/fcell.2020.00080

Sah, R. K., Saini, M., Pati, S., and Singh, S. (2019). *Plasmodium falciparum* growth is regulated by Sphingosine 1 phosphate produced by Host Erythrocyte Membrane Sphingosine kinase 1. *bioRxiv* 756502. doi: 10.1101/756502

Salous, A. K., Panchatcharam, M., Sunkara, M., Mueller, P., Dong, A., Wang, Y., et al. (2013). Mechanism of rapid elimination of lysophosphatidic acid and related lipids from the circulation of mice. *J. Lipid Res*. 54, 2775–2784. doi: 10.1194/jlr.M039685

Sanna, M. G., Wang, S.-K., Gonzalez-Cabrera, P. J., Don, A., Marsolais, D., Matheu, M. P., et al. (2006). Enhancement of capillary leakage and restoration of lymphocyte egress by a chiral S1P 1 antagonist *in vivo*. *Nat. Chem. Biol*. 2, 434–441. doi: 10.1038/nchembio804

Sattler, K., Gräler, M., Keul, P., Weske, S., Reimann, C.-M., Jindrová, H., et al. (2015). Defects of high-density lipoproteins in coronary artery disease caused by low sphingosine-1-phosphate content: correction by sphingosine-1-phosphate—loading. *J. Am. Coll. Cardiol*. 66, 1470–1485. doi: 10.1016/j.jacc.2015.07.057

Sattler, K. J., Elbasan, S., Keul, P., Elter-Schulz, M., Bode, C., Gräler, M. H., et al. (2010). Sphingosine 1-phosphate levels in plasma and HDL are altered in coronary artery disease. *Basic Res. Cardiol*. 105, 821–832. doi: 10.1007/s00395-010-0112-5

Schwab, S. R., Pereira, J. P., Matloubian, M., Xu, Y., Huang, Y., and Cyster, J. G. (2005). Lymphocyte sequestration through S1P lyase inhibition and disruption of S1P gradients. *Science* 309, 1735–1739. doi: 10.1126/science.1113640

Selim, S., Sunkara, M., Salous, A. K., Leung, S. W., Berdyshev, E. V., Bailey, A., et al. (2011). Plasma levels of sphingosine 1-phosphate are strongly correlated with haematocrit, but variably restored by red blood cell transfusions. *Clin. Sci*. 121, 565–572. doi: 10.1042/CS20110236

Sensken, S.-C., Bode, C., Nagarajan, M., Peest, U., Pabst, O., and Gräler, M. H. (2010). Redistribution of sphingosine 1-phosphate by sphingosine kinase 2 contributes to lymphopenia. *J. Immunol*. 184, 4133–4142. doi: 10.4049/jimmunol.0903358

Snider, A. J., Gandy, K. A. O., and Obeid, L. M. (2010). Sphingosine kinase: role in regulation of bioactive sphingolipid mediators in inflammation. *Biochimie* 92, 707–715. doi: 10.1016/j.biochi.2010.02.008

Souza, M. C., Paixao, F. H. M., Ferraris, F. K., Ribeiro, I., and Henriques, M., das G.M. (2012). Artesunate exerts a direct effect on endothelial cell activation and NF-B translocation in a mechanism independent of *Plasmodium* killing. *Malar. Res. Treat*. 2012:679090. doi: 10.1155/2012/679090

Strub, G. M., Maceyka, M., Hait, N. C., Milstien, S., and Spiegel, S. (2010). "Extracellular and intracellular actions of sphingosine-1-phosphate," in *Sphingolipids as Signaling and Regulatory Molecules*, eds C. Chalfant and M. Del Poeta (New York, NY: Springer), 141–155. doi: 10.1007/978-1-4419-6741-1_10

Sun, K., Zhang, Y., D'Alessandro, A., Nemkov, T., Song, A., Wu, H., et al. (2016). Sphingosine-1-phosphate promotes erythrocyte glycolysis and oxygen release for adaptation to high-altitude hypoxia. *Nat. Commun*. 7, 1–13. doi: 10.1038/ncomms12086

Sun, X., Singleton, P. A., Letsiou, E., Zhao, J., Belvitch, P., Sammani, S., et al. (2012). Sphingosine-1–phosphate receptor−3 is a novel biomarker in acute lung injury. *Am. J. Respir. Cell Mol. Biol*. 47, 628–636. doi: 10.1165/rcmb.2012-0048OC

Sutter, I., Park, R., Othman, A., Rohrer, L., Hornemann, T., Stoffel, M., et al. (2014). Apolipoprotein M modulates erythrocyte efflux and tubular reabsorption of sphingosine-1-phosphate. *J. Lipid Res*. 55, 1730–1737. doi: 10.1194/jlr.M050021

Swendeman, S. L., Xiong, Y., Cantalupo, A., Yuan, H., Burg, N., Hisano, Y., et al. (2017). An engineered S1P chaperone attenuates hypertension and ischemic injury. *Sci. Signal*. 10:eaal2722. doi: 10.1126/scisignal.aal2722

Takabe, K., Paugh, S. W., Milstien, S., and Spiegel, S. (2008). "Inside-out" signaling of sphingosine-1-phosphate: therapeutic targets. *Pharmacol. Rev*. 60, 181–195. doi: 10.1124/pr.107.07113

Tani, M., Ito, M., and Igarashi, Y. (2007). Ceramide/sphingosine/sphingosine 1-phosphate metabolism on the cell surface and in the extracellular space. *Cell. Signal*. 19, 229–237. doi: 10.1016/j.cellsig.2006.07.001

Tani, M., Sano, T., Ito, M., and Igarashi, Y. (2005). Mechanisms of sphingosine and sphingosine 1-phosphate generation in human platelets. *J. Lipid Res*. 46, 2458–2467. doi: 10.1194/jlr.M500268-JLR200

Taylor, W. R., Hanson, J., Turner, G. D., White, N. J., and Dondorp, A. M. (2012). Respiratory manifestations of malaria. *Chest* 142, 492–505. doi: 10.1378/chest.11-2655

ter Braak, M., Danneberg, K., Lichte, K., Liphardt, K., Ktistakis, N. T., Pitson, S. M., et al. (2009). Gαq-mediated plasma membrane translocation of sphingosine kinase-1 and cross-activation of S1P receptors. *Biochim. Biophys. Acta* 1791, 357–370. doi: 10.1016/j.bbalip.2009.01.019

Thomé, R., de Carvalho, A. C., Alves da Costa, T., Ishikawa, L. L. W., Fraga-Silva, T. F. C., Sartori, A., et al. (2016). Artesunate ameliorates experimental autoimmune encephalomyelitis by inhibiting leukocyte migration to the central nervous system. *CNS Neurosci. Ther*. 22, 707–714. doi: 10.1111/cns.12561

Thuy, A. V., Reimann, C.-M., Hemdan, N. Y., and Gräler, M. H. (2014). Sphingosine 1-phosphate in blood: function, metabolism, and fate. *Cell. Physiol. Biochem*. 34, 158–171. doi: 10.1159/000362992

Tibon, N. S., Ng, C. H., and Cheong, S. L. (2020). Current progress in antimalarial pharmacotherapy and multi-target drug discovery. *Eur. J. Med. Chem*. 188:111983. doi: 10.1016/j.ejmech.2019.111983

Tong, X., Lv, P., Mathew, A. V., Liu, D., Niu, C., Wang, Y., et al. (2014). The compensatory enrichment of sphingosine-1-phosphate harbored on glycated high-density lipoprotein restores endothelial protective function in type 2 diabetes mellitus. *Cardiovasc. Diabetol*. 13:82. doi: 10.1186/1475-2840-13-82

Urtz, N., Gaertner, F., von Bruehl, M.-L., Chandraratne, S., Rahimi, F., Zhang, L., et al. (2015). Sphingosine 1-phosphate produced by sphingosine kinase 2 intrinsically controls platelet aggregation *in vitro* and *in vivo*. *Circ. Res*. 117, 376–387. doi: 10.1161/CIRCRESAHA.115.306901

van der Heyde, H. C., Nolan, J., Combes, V., Gramaglia, I., and Grau, G. E. (2006). A unified hypothesis for the genesis of cerebral malaria: sequestration, inflammation and hemostasis leading to microcirculatory dysfunction. *Trends Parasitol*. 22, 503–508. doi: 10.1016/j.pt.2006.09.002

Venkataraman, K., Lee, Y.-M., Michaud, J., Thangada, S., Ai, Y., Bonkovsky, H. L., et al. (2008). Vascular endothelium as a contributor of plasma sphingosine 1-phosphate. *Circ. Res*. 102, 669–676. doi: 10.1161/CIRCRESAHA.107.165845

Venkataraman, K., Thangada, S., Michaud, J., Oo, M. L., Ai, Y., Lee, Y.-M., et al. (2006). Extracellular export of sphingosine kinase-1a contributes to the vascular S1P gradient. *Biochem. J*. 397, 461–471. doi: 10.1042/BJ20060251

Viriyavejakul, P., and Punsawad, C. (2020). Overexpression of sphingosine kinase-1 and sphingosine-1-phosphate receptor-3 in severe *Plasmodium falciparum* malaria with pulmonary edema. *Biomed Res. Int*. 2020:3932569. doi: 10.1155/2020/3932569

Visser, B. J., Wieten, R. W., Nagel, I. M., and Grobusch, M. P. (2013). Serum lipids and lipoproteins in malaria-a systematic review and meta-analysis. *Malar. J*. 12:442. doi: 10.1186/1475-2875-12-442

Vu, T. M., Ishizu, A.-N., Foo, J. C., Toh, X. R., Zhang, F., Whee, D. M., et al. (2017). Mfsd2b is essential for the sphingosine-1-phosphate export in erythrocytes and platelets. *Nature* 550, 524–528. doi: 10.1038/nature24053

Wilkerson, B. A., Grass, G. D., Wing, S. B., Argraves, W. S., and Argraves, K. M. (2012). Sphingosine 1-phosphate (S1P) carrier-dependent regulation of endothelial barrier high density lipoprotein (HDL)-S1P prolongs endothelial barrier enhancement as compared with albumin-S1P via effects on levels, trafficking, and signaling of S1P1. *J. Biol. Chem*. 287, 44645–44653. doi: 10.1074/jbc.M112.423426

Xiong, Y., Yang, P., Proia, R. L., and Hla, T. (2014). Erythrocyte-derived sphingosine 1-phosphate is essential for vascular development. *J. Clin. Invest*. 124, 4823–4828. doi: 10.1172/JCI77685

Yanagida, K., Liu, C. H., Faraco, G., Galvani, S., Smith, H. K., Burg, N., et al. (2017). Size-selective opening of the blood–brain barrier by targeting endothelial sphingosine 1–phosphate receptor 1. *Proc. Natl. Acad. Sci. U.S.A*. 114, 4531–4536. doi: 10.1073/pnas.1618659114

Yatomi, Y., Yamamura, S., Hisano, N., Nakahara, K., Igarashi, Y., and Ozaki, Y. (2004). Sphingosine 1-phosphate breakdown in platelets. *J. Biochem*. 136, 495–502. doi: 10.1093/jb/mvh143

Yeo, T. W., Rooslamiati, I., Gitawati, R., Tjitra, E., Lampah, D. A., Kenangalem, E., et al. (2008). Pharmacokinetics of L-arginine in adults with moderately severe malaria. *Antimicrob. Agents Chemother*. 52, 4381–4387. doi: 10.1128/AAC.00421-08

Yeo, T. W., Weinberg, J. B., Lampah, D. A., Kenangalem, E., Bush, P., Chen, Y., et al. (2019). Glycocalyx breakdown is associated with severe disease and fatal outcome in *Plasmodium falciparum* malaria. *Clin. Infect. Dis*. 69, 1712–1720. doi: 10.1093/cid/ciz038

Yu, Y., Guo, S., Feng, Y., Feng, L., Cui, Y., Song, G., et al. (2014). Phospholipid transfer protein deficiency decreases the content of S1P in HDL via the loss of its transfer capability. *Lipids* 49, 183–190. doi: 10.1007/s11745-013-3850-y

Zhang, H., Pluhackova, K., Jiang, Z., and Böckmann, R. A. (2016). Binding characteristics of sphingosine-1-phosphate to ApoM hints to assisted release mechanism via the ApoM calyx-opening. *Sci. Rep*. 6:30655. doi: 10.1038/srep30655

Zhang, L., Orban, M., Lorenz, M., Barocke, V., Braun, D., Urtz, N., et al. (2012). A novel role of sphingosine 1-phosphate receptor S1pr1 in mouse thrombopoiesis. *J. Exp. Med*. 209, 2165–2181. doi: 10.1084/jem.20121090

Zhang, X.-Y., Dong, X., Zheng, L., Luo, G.-H., Liu, Y.-H., Ekström, U., et al. (2003). Specific tissue expression and cellular localization of human apolipoprotein M as determined by *in situ* hybridization. *Acta Histochem*. 105, 67–72. doi: 10.1078/0065-1281-00687

Zhao, Y., Kalari, S. K., Usatyuk, P. V., Gorshkova, I., He, D., Watkins, T., et al. (2007). Intracellular generation of sphingosine 1-phosphate in human lung endothelial cells: role of lipid phosphate phosphatase-1 and sphingosine kinase 1. *J. Biol. Chem*. 282, 14165–14177. doi: 10.1074/jbc.M701279200

Zuo, S., Ge, H., Li, Q., Zhang, X., Hu, R., Hu, S., et al. (2017). Artesunate protected blood–brain barrier via sphingosine 1 phosphate receptor 1/phosphatidylinositol 3 kinase pathway after subarachnoid hemorrhage in rats. *Mol. Neurobiol*. 54, 1213–1228. doi: 10.1007/s12035-016-9732-6

Conflict of Interest: The authors declare that the research was conducted in the absence of any commercial or financial relationships that could be construed as a potential conflict of interest.

frontiers in Cellular and Infection Microbiology

REVIEW
published: 02 December 2020
doi: 10.3389/fcimb.2020.594621

Type I Interferons and Malaria: A Double-Edge Sword Against a Complex Parasitic Disease

Xiao He[1†], *Lu Xia*[1,2†], *Keyla C. Tumas*[1], *Jian Wu*[1*†] *and Xin-Zhuan Su*[1*]

[1] *Malaria Functional Genomics Section, Laboratory of Malaria and Vector Research, National Institute of Allergy and Infectious Disease, National Institutes of Health, Bethesda, MD, United States,* [2] *Center for Medical Genetics, School of Life Sciences, Central South University, Changsha, China*

Type I interferons (IFN-Is) are important cytokines playing critical roles in various infections, autoimmune diseases, and cancer. Studies have also shown that IFN-Is exhibit 'conflicting' roles in malaria parasite infections. Malaria parasites have a complex life cycle with multiple developing stages in two hosts. Both the liver and blood stages of malaria parasites in a vertebrate host stimulate IFN-I responses. IFN-Is have been shown to inhibit liver and blood stage development, to suppress T cell activation and adaptive immune response, and to promote production of proinflammatory cytokines and chemokines in animal models. Different parasite species or strains trigger distinct IFN-I responses. For example, a *Plasmodium yoelii* strain can stimulate a strong IFN-I response during early infection, whereas its isogenetic strain does not. Host genetic background also greatly influences IFN-I production during malaria infections. Consequently, the effects of IFN-Is on parasitemia and disease symptoms are highly variable depending on the combination of parasite and host species or strains. Toll-like receptor (TLR) 7, TLR9, melanoma differentiation-associated protein 5 (MDA5), and cyclic GMP-AMP synthase (cGAS) coupled with stimulator of interferon genes (STING) are the major receptors for recognizing parasite nucleic acids (RNA/DNA) to trigger IFN-I responses. IFN-I levels *in vivo* are tightly regulated, and various novel molecules have been identified to regulate IFN-I responses during malaria infections. Here we review the major findings and progress in ligand recognition, signaling pathways, functions, and regulation of IFN-I responses during malaria infections.

Keywords: IFN-Is, *Plasmodium*, immune response, signaling pathways, virulence

OPEN ACCESS

Edited by:
Jing-wen Lin,
Sichuan University, China

Reviewed by:
Tracey Lamb,
The University of Utah, United States
Galadriel Hovel-Miner,
George Washington University, United States

****Correspondence:***
Jian Wu
jian.wu2@nih.gov
Xin-Zhuan Su
xsu@niaid.nih.gov

†These authors share first authorship

Specialty section:
This article was submitted to Parasite and Host, a section of the journal Frontiers in Cellular and Infection Microbiology

Received: *13 August 2020*
Accepted: *30 October 2020*
Published: *02 December 2020*

Citation:
He X, Xia L, Tumas KC, Wu J and Su X-Z (2020) Type I Interferons and Malaria: A Double-Edge Sword Against a Complex Parasitic Disease. Front. Cell. Infect. Microbiol. 10:594621. doi: 10.3389/fcimb.2020.594621

INTRODUCTION

Plasmodium parasites have a complex life cycle developing within a vertebrate host and a female *Anopheles* mosquito (**Figure 1**). Malaria infection begins with a mosquito bite injecting sporozoites into the skin of a vertebrate host. The sporozoites travel to the liver through the bloodstream and infect hepatocytes. In the liver, the parasites undergo multiple rounds of replication, resulting in thousands of merozoites (Prudencio et al., 2006). The merozoites are released into the blood where they rapidly infect red blood cells (RBCs) and begin intraerythrocytic cycle of replication, releasing

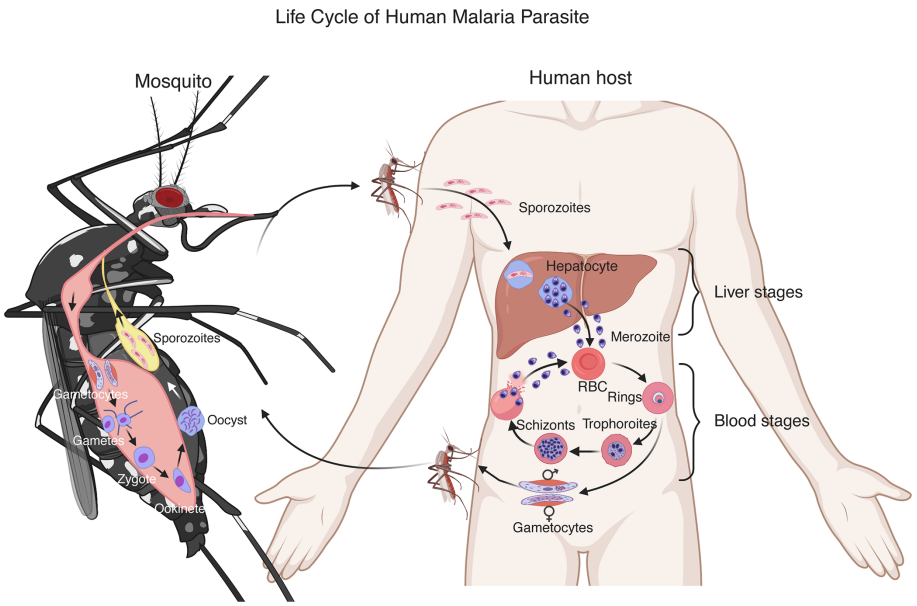

FIGURE 1 | Life cycle of a human malaria parasite. Malarial infection begins when an infected female *Anopheles* mosquito bites a human host and injects sporozoites into the skin. The sporozoites then travel through the bloodstream to invade hepatocytes. A sporozoite multiplies in the hepatocyte to generate thousands of merozoites. After being released from the liver, the merozoites invade red blood cells (RBCs) and develop to ring stage, trophozoite and schizont that contains 16–32 merozoites. The merozoites are released after rupture of infected RBCs to invade new erythrocytes. These blood stages of the parasite life cycle cause most malaria symptoms. A small number of merozoites develop into sexual stages, male and female gametocytes. Gametocytes are taken up by a second mosquito through a blood meal. In the mosquito midgut, the gametocytes differentiate into gametes, zygotes, ookinetes and then oocysts. A mature oocyst contains tens of thousands of sporozoites that migrate to the mosquito salivary glands to be injected into another human host to start a new cycle.

more merozoites to invade new RBCs. The erythrocytic development cycle takes approximately 24 h for *Plasmodium knowlesi* and rodent parasites such as *Plasmodium yoelii*, *Plasmodium berghei*, and *Plasmodium chabaudi*, 48 h for *Plasmodium falciparum*, *Plasmodium vivax*, and *Plasmodium ovale*, and 72 h for *Plasmodium malariae*. The asexual intraerythrocytic cycle is responsible for malaria symptoms (Crompton et al., 2014). During the development in RBCs, the parasites express various proteins on infected RBCs (iRBCs) and release a large amount of different materials into the bloodstream when iRBCs rupture, which trigger vigorous host immune responses and malaria signs or symptoms, including fever and chills, headache, anemia and possibly cerebral malaria.

Innate immunity is the first line of host defense against an invading pathogen. Interferons (IFNs) are produced by the host immune system and are well recognized for their role in antiviral infections. IFNs were initially described in 1957 as soluble glycoproteins with strong effects to "interfere" with the virus replication (Isaacs and Lindenmann, 1957; Isaacs et al., 1957). Today, three major groups of IFNs have been characterized: Type I IFN (IFN-I), IFN-II and IFN-III (Borden et al., 2007; Kotenko, 2011). IFN-Is consist of 13 IFN-α subtypes in humans (14 in mice), IFN-β, IFN-ω, IFN-κ, IFN-ϵ, IFN-ζ, IFN-δ, and IFN-τ (Pestka et al., 2004; Borden et al., 2007). Among them, IFN-α and IFN-β are the most abundant and well-studied. All IFN-I subtypes signal in an autocrine and paracrine fashion through heterodimeric IFN-I receptor (IFNAR) composed of two subunits, IFNAR1 (IFN-α/β receptor α chain) and IFNAR2 (IFN-α/β receptor β chain) (Uze et al., 2007; Boxx and Cheng, 2016). Binding of IFN-Is to IFNAR induces a cascade of downstream signaling events to initiate the transcription of hundreds of interferon-stimulated genes (ISGs) (**Figure 2**). ISGs include antimicrobial proteins, chemokines/cytokines and inflammation-inducing mediators. Many ISGs target critical molecules and pathways of a pathogen directly. Chemokines/cytokines and their receptors enable cell-to-cell communication and cell migration, whereas negative regulators of signaling pathways maintain a balanced IFN response and cellular homeostasis. Other ISGs encode for proapoptotic proteins, leading to cell death under certain conditions (Schneider et al., 2014; Lukhele et al., 2019).

IFN-Is are some of the most common cytokines produced by the host and play important roles in both protection and pathogenesis during malaria parasite infections (Angulo and Fresno, 2002; Stevenson and Riley, 2004; Schofield and Grau, 2005; Clark et al., 2008; Dunst et al., 2017; Gotz et al., 2017). At the early stage of infection, the parasites can be recognized by the host, which induces complex immune responses, including production of IFNs and pro-inflammatory cytokines (Scragg et al., 1999). The pathogen components recognized by host pathogen recognition receptors (PRRs) are called pathogen-associated molecular patterns (PAMPs). PAMPs are generally evolutionarily conserved molecules, including DNA, RNA, lipopolysaccharide (LPS), peptidoglycans, glycosylphosphatidylinositol (GPI), and some

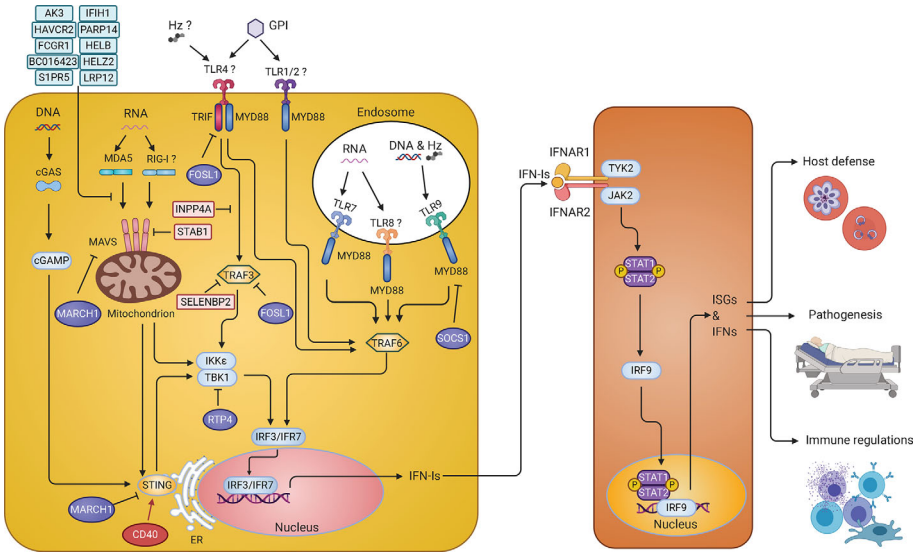

FIGURE 2 | IFN-I response and signaling pathways in malaria parasite infections. Parasite pathogen-associated molecular patterns (PAMPs) such as DNA and RNA are recognized by Toll-like receptors (TLRs) on the membrane of endosomes, including TLR7, TLR9, and possibly TLR8, and activate MYD88-TRAF6-IRF7 signaling cascade to stimulate production of IFN-Is. In the cytosol, parasite RNA is sensed by MDA5 (maybe RIG-I too) leading to the activation of MAVS-TBK1-IRF3 signaling and IFN-I production. Parasite DNA in the cytosol is sensed by cGAS, resulting in the activation of STING-TBK1-IRF3 signaling pathway to produce IFN-Is. On the cell surface, glycosylphosphatidylinositol (GPI) might be recognized by TLR4 and/or TLR1/2 that activates MYD88-TRAF6-IRF7 and TRIF-TBK1-IRF3 pathways to produce IFN-Is. Hemozoin (Hz) can form a complex with DNA and be recognized by TLR9 or with host fibrinogen and recognized by TLR4. Hz itself can also be sensed by NLR family pyrin domain containing 3 (NLRP3). However, recognition of Hz by these receptors mostly leads to the production of the proinflammatory cytokines. Many molecules (in light blue or light pink) are regulators that have been shown to inhibit IFN-I responses *in vitro*. The roles of CD40, FOSL1, MARCH1, and RTP4 in regulating IFN-I responses were further demonstrated *in vivo* during malaria parasite and/or viral (RTP4) infections. These regulators either can increase (CD40 in red) or decrease (FOSL1, MARCH1, and RTP4 in purple) IFN-I production through phosphorylation and/or ubiquitination of proteins in the IFN-I response pathways. The IFN-Is secreted by the cells bind to the IFNAR to activate the STAT1/STAT2-IRF9 pathway leading to transcription of ISGs that either directly act on parasites or modulate host immune responses. Infection of *Ifnar1*$^{-/-}$ mice will affect downstream IFN-I signaling but may not influence (and possibly stimulate) IFN-Is production.

proteins (Beutler, 2009; Takeuchi and Akira, 2010; Kawasaki and Kawai, 2014; Wu and Chen, 2014; Brubaker et al., 2015; Vijay, 2018). During infections, some host molecules that are normally not accessible to the host immune system can be 'released' and trigger immune responses. These molecules such as high mobility box 1 (HMGB1), heat shock proteins (HSPs), SP100 protein family, and uric acid crystal are called danger-associated molecular patterns (DAMPs) (Rubartelli and Lotze, 2007; Tang et al., 2012; Kaczmarek et al., 2013; Venereau et al., 2015). The host can detect PAMPs and DAMPs by a wide range of PRRs, leading to activation of downstream pathways and production of chemokines/cytokines. PRRs are present at many different cellular locations, including the outer plasma membrane, endosomal membrane luminal surface, mitochondria outer membrane and cytosol (Kawai and Akira, 2011; Kawasaki and Kawai, 2014; Wu and Chen, 2014). Toll-like receptors (TLRs), RIG-I-like receptors (RLRs), cyclic GMP-AMP synthase (cGAS), nucleotide-binding oligomerization domain (NOD)-like receptors (NLRs), and absent in melanoma 2 (AIM2) are common receptors that recognize PAMPs and host DAMPs to initiate IFN-I and inflammatory responses.

Initially identified as potent antiviral mediators, IFN-Is have been shown to play important roles against many pathogens, including bacteria, fungi, and protozoa (Ramirez-Ortiz et al., 2011; Beiting, 2014; Boxx and Cheng, 2016; Silva-Barrios and Stager, 2017). However, IFN-Is can also cause immunopathology in acute viral infections (Davidson et al., 2014) and lead to immunosuppression during chronic viral infections (Teijaro et al., 2013; Wilson et al., 2013). Similarly, in some bacterial infections, IFN-Is have been shown to exacerbate infections and promote secondary or chronic bacterial infections (Boxx and Cheng, 2016). Dual and opposing roles of IFN-Is have also been reported in many protozoan infections (Beiting, 2014; Silva-Barrios and Stager, 2017), including conflicting roles in malaria infections. Here we review and discuss IFN-I responses during malaria infections, including parasite ligands, host receptors, IFN-I induction and regulation, and their functions in disease pathology and protection.

SENSING MALARIA PARASITES: LIGANDS AND RECEPTORS

Many PRRs have been reported to recognize different malaria PAMPs or DAMPs to initiate the immune responses (**Figure 2**). TLRs, RLRs and cGAS have been shown to play important roles in IFN-I responses during malaria parasite infections, whereas NLRs and AIM2 largely contribute to activation of inflammasomes (Gazzinelli et al., 2014). Malaria parasite hemozoin (Hz), RNA, DNA, GPI as well as host derived uric acid crystal, peroxiredoxins and extracellular vesicles (EVs) are examples of PAMPs and

DAMPs that can induce IFN-I and inflammatory responses. TLRs consist of 10 members in humans (TLR1–TLR10) and 12 receptors in mice (TLR1–TLR9 and TLR11–TLR13) (Takeda et al., 2003; Nie et al., 2018). The RLRs are located at the cytoplasm and contain a DexD/H box RNA helicases domain that can detect RNA (Loo and Gale, 2011). There are three known RLRs: retinoic acid-inducible gene I (RIG-I), melanoma differentiation-associated protein 5 (MDA5), and DExH-box helicase 58 (DHX58 or LGP2). RIG-I and MDA5 are responsible for sensing double-stranded RNA (dsRNA), whereas DHX58 functions as a regulator of the RIG-I and MDA5 signaling pathways (Yoneyama et al., 2005). cGAS binds to microbial DNA and self-DNA in the cytoplasm and catalyzes the synthesis of cyclic guanosine monophosphate–adenosine monophosphate (cGAMP) (Sun et al., 2013). cGAMP acts as a second messenger to activate the downstream signal adaptor, stimulator of interferon genes (STING) (Wu et al., 2013).

TLR1, TLR2, TLR4, TLR6, TLR7 and TLR9 have been reported to recognize malaria ligands. TLR2 forms heterodimers with TLR1 or TLR6, and the heterodimers can bind to the distinct structure of parasite GPI (Campos et al., 2001; Krishnegowda et al., 2005). TLR4 can recognize parasite GPI as well as the peroxiredoxins and fibrinogen bound to Hz (Krishnegowda et al., 2005; Zhu et al., 2005; Barrera et al., 2011). TLR7 and TLR8 sense parasite RNA (Baccarella et al., 2013; Spaulding et al., 2016; Yu et al., 2016; Coch et al., 2019), and TLR9 recognizes parasite DNA and Hz-DNA complexes (Pichyangkul et al., 2004; Parroche et al., 2007; Wu et al., 2010; Gowda et al., 2011). The major cytosolic receptor for sensing malaria RNA is MDA5 (Liehl et al., 2014; Miller et al., 2014), although RIG-I has also been implicated to play a role in response to malaria infection (Wu et al., 2020). cGAS recognizes parasite DNA and leads to the production of IFN-Is (Yu et al., 2016; Gallego-Marin et al., 2018; Hahn et al., 2018). It is possible that different sensors are activated by parasite products at different developmental stages, leading to variation in levels of IFN-I subtypes over time. Additionally, different IFN-I subtypes can have different biological and immunological roles. For example, C57BL/6J mice infected with lymphocytic choriomeningitis virus (LCMV) Cl-13 strain produced both IFN-α and IFN-β. However, IFN-α was found to control early viral dissemination, whereas IFN-β could suppress T cell responses and delay clearance of persistent virus (Ng et al., 2015; Ng et al., 2016). Additionally, IFN-α and IFN-β were shown to have different activities against West Nile virus infection (Sheehan et al., 2015). Whether IFN-α and IFN-β play different roles in malaria parasite infections requires further investigations.

DNA Sensing and Signaling Pathways

Many studies have shown that endosomal TLR9 and cytoplasmic cGAS can recognize microbial DNA and host self-DNA in certain pathological conditions (**Figure 2**) (Pichyangkul et al., 2004; Beutler, 2009; Takeuchi and Akira, 2010). During malaria infections, TLR9 binds unmethylated CpG motifs of parasite DNA (Lamphier et al., 2006; Ohto and Shimizu, 2016). It is worth noting that *P. vivax* parasite that has a higher frequency of CpG motifs in the genome than *P. falciparum* parasite is also a stronger fever inducer (Anstey et al., 2012). Malaria parasites in the iRBCs or free merozoites are phagocytized by dendritic cells (DCs) and macrophages and enter the endosomes of these cells (Parroche et al., 2007; Wu et al., 2010; Gowda et al., 2011; Hirako et al., 2015). The endosomes then fuse to the lysosomes to form phagolysosomes and release DNA into the acidic environment. There, DNA can bind to TLR9 and activate the mitogen-activated protein kinase (MAPK)/nuclear factor kappa-light-chain-enhancer of activated B cells (NF-κB)/interferon regulatory transcription factor (IRF) 7 pathways, leading to the production of IFN-Is and proinflammatory chemokines/cytokines (Sasai et al., 2010; Kawai and Akira, 2011). For the IRF7 pathway, TLR9 recruits the toll/interleukin-1 receptor (TIR) domain containing adaptor protein (TIRAP) that binds to myeloid differentiation primary response 88 (MYD88) and interleukin-1 receptor-associated kinase 1 (IRAK1) (Kawagoe et al., 2008; Barton and Kagan, 2009; Kawai and Akira, 2010). The MYD88-IRAK1 complex further recruits tumor necrosis factor (TNF) receptor associated factor (TRAF) 3 and IRF7 that translocate into the nucleus to activate promoters of IFN-I genes (O'Neill et al., 2003; Kawai and Akira, 2008).

Parasite DNA can also enter the cytosol and activate cGAS and AIM2. cGAS synthesizes cGAMP that binds to STING (also known as MITA, ERIS or MPYS) (Ishikawa and Barber, 2008; Zhong et al., 2008; Sun et al., 2009; Jin et al., 2013) and triggers conformational changes of STING to form STING oligomers through side-by-side packing of the STING molecules (Shang et al., 2012). STING then translocates from the endoplasmic reticulum (ER) to the Golgi apparatus (Gui et al., 2019) to bind TANK binding kinase 1 (TBK1), leading to phosphorylation of interferon regulatory factor (IRF) 3 (Hornung and Latz, 2010). Phosphorylated IRF3 also translocates into the nucleus to activate IFN-I genes. DNA sensing by AIM2 generally triggers the production of inflammatory cytokines and activation of inflammasomes (Kalantari et al., 2014). Therefore, TLR9 and cGAS/STING are the major sensors for recognizing malaria parasite DNA for IFN-I responses.

RNA Sensing and Signaling Pathways

Parasite RNA from both liver and blood stages can be recognized by the host RNA sensors (**Figure 2**). During development in the liver, parasite RNA is mainly recognized by MDA5 (Liehl et al., 2014; Miller et al., 2014). MDA5 becomes activated after binding RNA and releases its caspase activation and recruitment domains (CARD) from the C-terminal regulatory domain (Cui et al., 2008). Activated MDA5 recruits mitochondrial antiviral-signaling protein (MAVS) through homotypic CARD-CARD domain interactions (Kawai et al., 2005; Meylan et al., 2005; Seth et al., 2005; Xu et al., 2005). MAVS forms prion-like structures and further recruit TRAF3, TBK1 and IκB kinase epsilon (IKKε) to phosphorylate IRF3 and IRF7, leading to IFN-I production (Hou et al., 2011; Jacobs and Coyne, 2013). MAVS can also bind to TRAF6 and activate NF-κB/IKK complex, resulting in the production of inflammatory cytokines (Belgnaoui et al., 2011). TLR7 and MDA5 can also sense parasite RNA from blood stages (Baccarella et al., 2013; Wu et al., 2014; Spaulding et al., 2016; Yu et al., 2016). Similar to TRL9, TLR7 activates the MYD88 and IRF7 pathway to produce IFN-Is (Baccarella et al., 2013; Yu et al., 2016). TLR7 and MDA5 are the major sensors for malaria parasite RNA for IFN-I responses.

Additionally, RNA polymerase III (pol III) was reported to convert AT rich viral DNA into dsRNA that can be recognized

by the RLRs (Chiu et al., 2009). Pol III deficiency led to reduced IFN-I production in Raw 264.7, but not in HEK293T cells (Sharma et al., 2011; Wu et al., 2014). This discrepancy is likely due to difference in gene expression between the two cell lines including the lack of TLR expression in the HEK293T cells (Hornung et al., 2002). Interestingly, RIG-I expression was detected in a study using trans-species expression quantitative trait locus (ts-eQTL) analysis after infection of 24 parasite progeny from a *P. y. yoelii* 17XNL × *P. y. nigeriensis* N67 cross (Wu et al., 2020). Additionally, messenger RNA (mRNA) and protein levels of IFN-β could be significantly suppressed by RNAi knockdown of the genes encoding MDA5, RIG-I, or RNA pol III after *P. yoelii* DNA stimulation (Wu et al., 2014). However, whether RIG-I and Pol III play a role in the recognition of parasite DNA or RNA *in vivo* requires further investigations.

Responses to GPI

GPI exists in many eukaryote species and is attached to a protein during posttranslational modification (Brown and Waneck, 1992). The major function of GPI is binding to certain functional proteins at the cell surfaces (Ferguson et al., 1999). GPI contains a conserved ethanolamine phosphate-substituted oligosaccharide moiety that links to phosphatidylinositol with an alpha glycosidic bond (Ropert and Gazzinelli, 2000). The structures of GPIs in different species vary, mainly in the lipid substituents, sugar chain length, or ethanolamine phosphate residues attached to the conserved glycan moiety. Malaria GPI is one of the earliest identified parasite PAMPs (Schofield and Hackett, 1993). The detailed structures of parasite GPI have been studied using biochemical analysis and mass spectrometry (Naik et al., 2000). The structures of parasite GPIs are different from human GPIs and can be recognized by the host's immune system. Studies have shown that malaria GPI is sensed by TLRs on the surface of macrophages or DCs, mainly through the TLR1-TLR2 heterodimers and TLR4 (Krishnegowda et al., 2005; Zhu et al., 2005; Lu et al., 2006; Zhu et al., 2009). Similar to TLR7 and TLR9, TLR1-TLR2 and TLR4 recruit MYD88 to activate the NF-κB and IRF7 pathways, leading to the production of IFN-Is and inflammatory cytokines. TLR4 can also recruit a protein called TIR-domain-containing adapter-inducing interferon-β (TRIF) that further forms a complex with IKKε and TBK1 to phosphorylate and activate IRF3 and IRF7 (Sweeney et al., 2004; Kawagoe et al., 2008; Beutler, 2009; Ning et al., 2011; Kawasaki and Kawai, 2014). However, the majority of studies on malaria GPI have focused on activation of inflammatory cytokines. One study shows that GPI can induce interferon-sensitive response element (ISRE) activation *in vitro*, which suggests that GPI may also stimulate IFN-I production *via* TLR4 (Yao et al., 2016). Since inflammatory responses by malaria infection can inhibit MYD88-IRF7-dependent IFN-I signaling (Yu et al., 2018), it is possible that the strong pro-inflammatory responses stimulated by parasite GPI can influence other IFN-I pathways indirectly.

Parasite Hz and Host Responses

Hz is a brown pigment that is formed during the digestion of hemoglobin in the digestive vacuole (DV) of blood stage parasites (Pandey and Tekwani, 1996; Arese and Schwarzer, 1997; Pagola et al., 2000; Jani et al., 2008; Olivier et al., 2014). Hz is captured by immune cells after rupture of iRBCs (Celada et al., 1983; Ho and Webster, 1989; Arese and Schwarzer, 1997). There is no known receptor for Hz; however, it can trigger immune responses in multiple ways. Hz carrying parasite DNA is a potent activator of TLR9, leading to production of ISGs and pro-inflammatory cytokines (Parroche et al., 2007). The parasite DNA does not colocalize with Hz that is synthesized in the DV (Jaramillo et al., 2009). Therefore, Hz probably binds DNA released from dead cells or DV. Hz can also form a complex with the host fibrinogen that is then recognized by TLR4 or CD11b/CD18-integrin on monocytes, leading to production TNF and reactive oxygen species (ROS) (Barrera et al., 2011).

Hz may cause immune cell dysfunction or apoptosis after phagocytosis by the monocytes or macrophages. Studies have shown that macrophages became functionally impaired after ingestion of *P. falciparum*-infected erythrocytes or isolated Hz due to a long-lasting oxidative burst (Schwarzer et al., 1992). Monocytes or macrophages ingesting a large amount of iRBC or Hz may undergo apoptotic death with low levels of cytokine production due to phagolysosomal acidification (Schwarzer et al., 2001; Wu et al., 2015b). Hz can also inhibit differentiation and maturation of human DC by impairing expression of major histocompatibility complex class II antigen (Schwarzer et al., 1998; Skorokhod et al., 2004). Hz induces phagolysosomal destabilization leading to release of lysosomal contents to the cytosol, including DNA or RNA to induce IFN-I responses. Additionally, Hz itself can activate the NLRP3 inflammasome through Lyn and Syk signaling pathways (Dostert et al., 2009; Olivier et al., 2014). An unidentified ligand released from the parasite lysosome (or DV) has been reported to activate NLRP12 inflammasome (Ataide et al., 2014). Overall, Hz is considered as a danger signal which can activate diverse pathways to influence IFN-I production and inflammatory responses (Dostert et al., 2009; Shio et al., 2009).

Extracellular Vesicles (EVs) and Host Responses

EVs are lipid bilayer-delimited particles derived from iRBCs or other host cells (Babatunde et al., 2020). Based on their size and biological functions, EVs are classified into two forms: exosomes and microvesicles. Exosomes are smaller vesicles ranging from 30 to 150 nm in diameter and are usually released by reticulocytes during differentiation and maturation (Johnstone et al., 1987). Microvesicles are larger vesicles with sizes of 150 nm to 1–2 μm in diameter and are produced by the plasma membrane budding and fission (Tricarico et al., 2017). EVs contain lipids, proteins, and nucleic acids (DNA and RNA) (Laulagnier et al., 2004; Nolte-'t Hoen et al., 2012; Tauro et al., 2012; Ridder et al., 2014; Sinha et al., 2014; Williams et al., 2014; Babatunde et al., 2018). Malaria parasite infection causes a strong inflammatory response, and inflammatory cytokines such as TNF-α can greatly contribute to the production of the EVs by almost all cell types (Combes et al., 1999; Freyssinet, 2003). Studies have shown that EVs containing parasite materials are potential triggers of proinflammatory innate immune responses (Couper et al., 2010). In animal models, blockage of EV production in mice resulted in complete resistance to cerebral malaria development (Combes et al., 2005; Penet et al., 2008). Transfer of

EVs from *P. berghei* ANKA-infected mice caused damages to the blood-brain barrier in the recipient mice (El-Assaad et al., 2014). Parasite DNA in the EVs can be detected by cGAS to activate the STING-dependent pathway leading to the production of IFN-Is and inflammatory cytokines (Sisquella et al., 2017). Parasite RNA in the EVs, on the other hand, will activate MDA5 and trigger the MAVS-dependent pathway to produce IFN-Is (Ye et al., 2018). EVs also contain microRNA (miRNA) and mRNA. mRNA can be translated into protein in the recipient cells; meanwhile, miRNA may regulate gene expression in the target cells (Ratajczak et al., 2006; Valadi et al., 2007). Similar to Hz, EVs and their contents can influence several host pathways, including IFN-I responses.

HOST CELLS PRODUCING IFN-IS

IFN-Is can be produced by several types of host cells during malaria infections. *Plasmodium* parasites reside in different cell types during their life cycle. In the liver, the parasites develop mostly in the hepatocytes, and large amount of parasite materials are synthesized and released within the hepatocytes. MDA5 in hepatocytes can recognize parasite RNA from liver stages leading to IFN-I production (Liehl et al., 2014; Miller et al., 2014). In the blood stage infections, IFN-I production is more complicated. The parasites reside in RBCs that lack PRRs and the machinery for IFN-I responses. Peripheral blood mononuclear cell (PBMC) cultures stimulated with iRBC can produce IFN-α *in vitro* (Montes de Oca et al., 2016). Other studies find that plasmacytoid dendritic cells (pDC) are the major source of IFN-Is (deWalick et al., 2007; Voisine et al., 2010). Splenic conventional dendritic cells (cDC) are an alternative source of IFN-Is (Voisine et al., 2010; Haque et al., 2014). Macrophages can also produce IFN-Is during blood stage infections (Spaulding et al., 2016; Yu et al., 2016). NK cells from healthy donors' PBMCs co-cultured with *P. falciparum* 3D7-infected erythrocytes upreguated IFN-α related genes (Grangeiro de Carvalho et al., 2011). Therefore, hepatocytes and DCs are the main sources of IFN-Is during liver and blood stage infections, although many other cell types may also contribute to the IFN-I production.

IFN-I RESPONSES TO LIVER STAGES

Although infection at the liver stages is generally asymptomatic, studies have shown that a complex series of immune events occur during liver stage development, including IFN-I responses (Liehl and Mota, 2012; Liehl et al., 2014; Miller et al., 2014). Transcriptomic analysis of liver stages showed an IFNAR1-dependent IFN-I response in hepatocytes, which was not restricted to *Plasmodium* species (*P. berghei* and *P. yoelii*) nor mouse host strains (BALB/c and C57BL/6) (Liehl et al., 2014). *Plasmodium* parasite RNA was reported to be recognized by MDA5 in hepatocytes (and possibly other receptors). Furthermore, the magnitude of IFN-I responses was parasite dose and replication dependent. Leukocytes were mobilized as effectors by IFN-Is to eliminate the parasites (Liehl et al., 2014) (**Figure 3A**). IFN-I signaling helps recruit NK cells and NKT cells, especially IFN-γ secreting CD1d-restricted NKT cells to eliminate the liver stage parasites (Miller et al., 2014). The IFN-I responses also benefit the host from an immediate liver stage reinfection by significantly reducing the liver parasite load as well as blood stage parasitemia (Liehl et al., 2015). Similarly, attenuated *P. yoelii* parasites that only develop to late liver-stage forms induce significant IFN responses (including IFN-Is and IFN-γ) and provide cross protection against a secondary liver stage infection (*P. yoelii* or *P. berghei*) (Miller et al., 2014). A distinct population of $CD11c^+$ cells was also observed to invade the liver at 36–40 h post *P. y. yoelii* 17XNL sporozoite inoculation (Kurup et al., 2019a). These monocyte derived $CD11c^+$ dendritic cells (DCs) showed strong IFN-I profiles, with highly upregulated expression of key molecules such as TLR7 and IRF7 in the IFN-I pathways. The $CD11c^+$ DCs acquired and presented parasite antigen by phagocytosing infected hepatocytes, to prime $CD8^+$ T cells, the major mediators in liver stage protection (Kurup et al., 2019a). *P. berghei* radiation-attenuated sporozoites (RAS) could also induce liver $CD8\alpha^+$ DCs that activated $CD8^+$ T cells in the liver (Jobe et al., 2009), although the activation level was much weaker than that induced by normal sporozoites (Parmar et al., 2018). The accumulation and activation of $CD8\alpha^+$ DCs was associated with higher-levels s of CCL-20, CCL-21, and IFN-Is (Parmar et al., 2018). Interestingly, a baculovirus-induced innate immunity also provided complete protection against subsequent *P. berghei* sporozoite infection or existing liver stage infection, and neutralization of IFN-α could abolish this effect (Emran et al., 2018). These studies provide mechanistic supports for some earlier observations that interferon inducers have better protection against *P. berghei* sporozoite-induced infection than that by blood stage infection (Jahiel et al., 1968a; Jahiel et al., 1968b; Jahiel et al., 1970). The prevalent pathways of IFN-I induction are through activation of cytosolic receptors that recognize parasite nucleic acids. A significant amount of parasite RNA was detected in non-hepatocytes during liver stage development (Kurup et al., 2019a), suggesting that DCs and other cells may also be sources of IFN-Is. Together, these studies show that during acute liver stage infection, parasite nucleic acids from the rapidly replicating sporozoites can trigger IFN-I responses and production. The IFN-Is then lead to an influx of leukocytes, including NK, NKT and DCs, to the liver and prime the adaptive immunity, especially $CD8^+$ T cells, to subsequently eliminate the parasites. Until now, only parasite RNA has been documented to induce IFN-Is in the hepatocytes. In addition, it has been reported that many sporozoites inoculated into the skin of a mouse migrated to the lymph-nodes and were phagocytosed by $CD8\alpha^+$ DCs to induce $CD8^+$ T cell responses (Radtke et al., 2015), but whether this process also triggers IFN-I responses requires further investigations.

Sterile protection against *Plasmodium* infection can be achieved through exposure to radiation- or genetically-attenuated sporozoites that are able to infect but cannot replicate within the hepatocyte, or through exposure to sporozoites under chloroquine chemoprophylaxis (Mo and McGugan, 2018). It appears that IFN-Is are part of protective immunity during normal or attenuated sporozoite infection; however, the roles of IFN-Is in infections by sporozoites attenuated by various methods has not been well

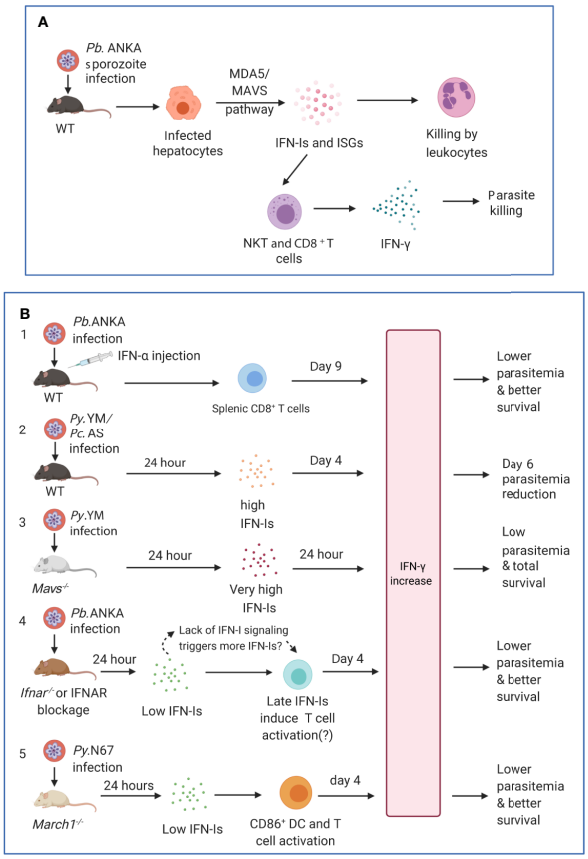

FIGURE 3 | Timing and levels of interferon production may determine the outcomes of malaria parasite infections. **(A)** The protection against liver stages relies on the activation of innate immunity involving IFN-I responses and immune cell infiltration. Infection of C57BL/6 mice with *P. berghei* ANKA liver-stages induces an IFN-I response through MDA5 signaling pathway in hepatocytes. Infiltrating leukocytes (macrophages and neutrophils) are mobilized to the vicinity of infected hepatocytes by IFN-I signaling (Liehl et al., 2014). IFN-γ–secreting immune cells, in particular CD1d-restricted NKT cells, are also likely the main players responsible for the innate elimination during liver stage (Miller et al., 2014). **(B)** Several models show that IFN-Is likely function through regulating IFN-γ production, T cell activation, and adaptive immune response to influence parasitemia and disease severity during blood stage infections. First, several studies showed that injections of IFN-α and/or IFN-β were protective (**Supplementary Table 1**). C57BL/6 mice infected with *P. berghei* ANKA and injected with IFN-α had significantly (P <0.05) higher levels of IFN-γ (772 ± 73 pg/ml, day 9 pi) than those receiving diluent (180 ± 14 pg/ml), reduced parasitemia, and better host survival (Vigario et al., 2007). Second, C57BL/6 mice infected with *P. y. nigeriensis* N67 or *P. chabaudi* AS had elevated levels of IFN-α (~320 and ~450 pg/ml, respectively) 24 h pi (Kim et al., 2012; Wu et al., 2020). *Mavs*$^{-/-}$ mice infected with *P. y. nigeriensis* N67 or *Ifnar*$^{-/-}$ mice infected *P. chabaudi* AS had increased day 6 parasitemia (parasitemia increases in *Ifnar*$^{-/-}$ mice may not be significant but had reduced ability to resolve parasitemia later) (Voisine et al., 2010; Kim et al., 2012; Wu et al., 2014). IFN-Is appear to work with IFN-γ in controlling parasitemia during early infection. Compared with *P. y. yoelii* YM infected WT C57BL/6 mice that produced very low IFN-Is 24 h pi, *P. y. nigeriensis* N67-infected mice had significantly higher IFN-α/β, IFN-γ and IL-6 24 h pi (Wu et al., 2020). Additionally, *Ifnar1*$^{-/-}$*Ifngr1*$^{-/-}$ mice infected with *P. chabaudi* AS exhibited higher mortality than WT or *Ifnar1*$^{-/-}$ mice and were not able to completely clear parasites (Kim et al., 2012). Third, *Mavs*$^{-/-}$ mice infected with *P. y. yoelii* YM produced very high levels of IFN-α (~2,800 pg/ml), IFN-β (~2,000 pg/ml) and IFN-γ (>1,200 pg/ml) 24 h pi and all survived the infections (Yu et al., 2016). All these models suggested early production (24 h) of IFN-α/β and IFN-γ can help control parasitemia and may improve host survival. Fourth, in *P. berghei* ANKA-infected WT C57BL/6 mice, low levels of IFN-α/β were observed 24 h after pi (Haque et al., 2011; Haque et al., 2014). Depletion or blockage of IFN-I signaling using *Ifnar*$^{-/-}$ mice or anti-IFNAR antibody treatment results in higher levels of IFN-γ, better parasite control, and improved host survival (Haque et al., 2011; Haque et al., 2014). Interestingly, higher levels of IFN-α were observed in WT mice 48 h pi (~70 pg/ml IFN-α vs ~20 pg/ml at 24 h) and day 4 pi (~200 mg/ml IFN-α), suggesting that blockage of IFN-I signaling may stimulate IFN-I response. Unfortunately, the IFN-I levels in *Ifnar*$^{-/-}$ mice or mice treated with anti-IFNAR were not measured at additional time points. Similarly, anti-IFNAR antibody treatment of C57BL/6 mice infected with *P. y. yoelii* 17XNL significantly reduced days 16 and 21 parasitemia through inhibition of T regulatory 1 response, enhancement of Tfh cell accumulation and better humoral immunity (Zander et al., 2016). Again, the levels of IFN-Is in the anti-IFNAR treated animals were not reported. Serum levels of IFN-γ between anti-IFNAR antibody treated and non-treated mice were similar at day 16 pi when parasitemia began to show significant difference. It is possible that the lack of IFN-I signaling in these models prompts the system to produce more IFN-Is, and that IFN-Is and IFN-γ work together through regulating immune cell populations and antibody production to control the infections. Fifth, *March1*$^{-/-}$ mice infected with *P. y. nigeriensis* N67 (or *P. y. yoelii* YM) had low levels of IFN-Is 24 h pi but had significantly increased IFN-γ and IL-10 day 4 pi due to decreased degradation of CD86/MHCII and T cell activation, leading to reduced parasitemia and better host survival (Wu et al., 2020). IFN-γ was shown to be a key player in controlling parasitemia and host survival. These observations suggest key roles of early IFN-Is (24 h pi) and IFN-γ in later stages of infection (day 4 or later) and emphasize the importance of measuring IFN-Is, IFN-γ, and other cytokines during the course of blood infection for better understanding of protection mechanisms mediated by IFNs. *Pb*.ANKA, *P. berghei* ANKA; *Py*.N67, *P. y. nigeriensis* N67; *Py*.YM, *P. y. yoelii* YM; *Pc*.AS, *P. chabaudi* AS.

studied. Late liver stage-arresting and replication-competent (LARC) of genetically-attenuated sporozoites have been shown to provide good cross-stage and cross-species protection in mice (Butler et al., 2011; Vaughan et al., 2018). However, a recent study using *P. yoelii* LARC sporozoites showed that the liver stage-engendered IFN-I signaling impaired hepatic $CD8^+$ T cell responses, which is critical for liver stage protection. Compared with wildtype (WT) mice, *Ifnar1*$^{-/-}$ mice exhibited superior protection due to greater $CD8^+$ T cell memory and superior $CD8^+$ T effector function (Minkah et al., 2019). However, the protective immune mechanisms in the *Ifnar1*$^{-/-}$ mice after infections with WT and LARC sporozoites can be quite different, and the observations in IFN-1 signaling-deficient mice infected with defective sporozoites may not represent the true protective immunity in normal malaria infections.

IFN-IS IN BLOOD STAGE INFECTIONS

Confounding roles of IFN-Is have been reported during bacterial and viral infections (Carrero, 2013). IFN-Is can be protective against bacterial and viral infections by promoting the induction of TNF-α, nitric oxide, and other cytokines. In contrast, IFN-I signaling can also induce suppression of adaptive immune responses during chronic infection with LCMV and acute infections with intracellular bacteria (Carrero, 2013). During malaria blood stage infections, both positive and negative effects of IFN-Is on protection have also been reported in different rodent malaria models and in human infections, which may mirror the observations in acute and chronic infections of bacteria and viruses.

Malaria Blood Stage Infection Stimulates IFN-Is Responses

A single sporozoite can generate thousands of merozoites that are released to the bloodstream to invade RBCs. In 1968, almost 10 years after the discovery of IFNs, IFNs were reported to be present in the serum of *P. berghei*-infected mice (Huang et al., 1968). However, in a later study, no IFN activity was detected in adult human sera during malaria infection (majority *P. vivax* infection) using virus titration assay (Rytel et al., 1973). Another early study found that acute *P. falciparum* infection induced strong IFN-I responses, especially IFN-α, in children, which was correlated with both parasitemia and NK cell activity (Ojo-Amaize et al., 1981). The differences in these studies could be due to variation in parasite species, infection stage, the time of measurement, as well as host age. Lack of sensitive methods to directly measure IFN-Is at the time of the studies could also be another reason. Later, human *P. falciparum* schizonts and parasite lysate were shown to activate human pDC and murine DCs to produce IFN-Is through the TLR-9 dependent pathway, and elevated serum levels of IFN-Is were detected in *P. falciparum* patients (Pichyangkul et al., 2004). Similarly, *P. berghei* blood stage infection led to IFN-I production by both mouse pDCs and cDCs (deWalick et al., 2007). Blood stage *P. yoelii* infection induced IFN-I responses by cDC *via* the MDA5 pathway (Wu et al., 2014). In a transcriptomic study of infections with multiple *P. yoelii* strains, TLR3/7, TLR9, cGAS, MDA5, and RIG-I were shown to be the upstream regulators significantly activated on day 1 after *P. y. nigeriensis* N67 infection (Xia et al., 2018). pDCs were primed by activated $CD169^+$ macrophages upon STING-mediated sensing of parasites in the bone marrow to generate a robust IFN-I responses in *P. y. yoelii* YM blood stage infection (Spaulding et al., 2016). In controlled human malaria infection (CHMI), IFN-Is could be produced throughout the course of infection (Montes de Oca et al., 2016). However, induction of IFN-I production is parasite strain dependent; for example, *P. yoelii nigeriensis* N67 can stimulate an early peak of IFN-Is, whereas mice infected with *P. y. nigeriensis* N67C or *P. y. yoelii* YM produce low levels of IFN-Is (Wu et al., 2014; Wu et al., 2015a; Wu et al., 2020). The parasitemia in mice infected with *P. y. nigeriensis* N67, *P. y. nigeriensis* N67C and *P. y. yoelii* YM strains are similar at 24 h pi (Pattaradilokrat et al., 2014), suggesting that the differences in IFN-I levels are unlikely due to variation in parasitemia. A C741Y amino acid substitution in the protein trafficking domain of the *P. y. nigeriensis* N67 erythrocyte binding-like (PyEBL) protein was shown to affect host immune response, including IFN-I pathways, T cell activation and IgG switching by enhancing phosphatidylserine (PS) exposure on iRBC surface and phagocytosis (Peng et al., 2020). Other genes including those in a locus of parasite chromosome 13 were also significantly linked to expression of many ISGs (Wu et al., 2015a).

Protective IFN-I Responses Against Parasitemia and Host Mortality

IFN-Is have been shown to be protective against blood stage malaria parasites including suppression of parasitemia and/or improved host survival (**Figure 3B**). Upon activation of IFN-I signaling, ISGs including chemokines/cytokines and other inflammation-inducing mediators are produced to eliminate parasites residing in the host RBCs. Mice deficient of MDA5 or MAVS had compromised ability to control parasitemia day 6 after injection of *P. y. nigeriensis* N67 iRBCs (Wu et al., 2014). A strong IFN-I transcriptional signature was also found in circulating neutrophils from *P. vivax*-infected patients and in *P. chabaudi*-infected mice (Rocha et al., 2015). IFN-I signaling recruited neutrophils that contributed to parasite control but also caused liver damage (Rocha et al., 2015). By blocking STING- and/or MAVS-mediated IFN-I signaling, strong early TLR7-mediated IFN-I responses during *P. y. yoelii* YM blood stage infection helped the host control the parasitemia as well as lower mortality (Yu et al., 2016) (**Figure 3B**). In addition, increased transcription of ISGs in pDCs was reported after *P. chabaudi* blood stage infection or *in vitro* iRBC stimulation, although minimal effects of pDCs or IFN-I signaling on *P. chabaudi* AS infection were observed (Voisine et al., 2010). The dynamics of parasitemia and host survival are different between mice infected with *P. y. nigeriensis* N67 and *P. chabaudi* AS, but these infections shared elevated levels of IFN-Is 24 h pi (300–500 pg/ml) (Kim et al., 2012; Wu et al., 2020) and reduced days 6 and 7 parasitemia (the differences in parasitemia for some *P. chabaudi* AS infections may not be statistically significant) (Voisine et al., 2010; Kim et al., 2012; Wu et al., 2020). It is important to note that different mouse strains were used in the studies (129Sv/Ev, C57BL/6, BALB/c for *P. chabaudi* and C57BL/6 for *P. yoelii* infections). In addition, TLR7 signaling was the major pathway for IFN-I response in

P. chabaudi AS infection, whereas MDA5 was the major RNA sensor in *P. y. nigeriensis* N67 infections (Baccarella et al., 2013; Wu et al., 2014). The differences in parasitemia control and host survival in mice infected with different strains of *P. chabaudi* and *P. yoelii* could also be partly due to variations in immune mechanisms controlling these infections. In *P. chabaudi* infection, $CD4^+$ T cells appear to play a major role in protective immunity, although B cells and antibodies can also contribute to the protection, including B cell regulation of Th cell responses during primary infection (Langhorne et al., 1990; von der Weid et al., 1994; Xu et al., 2000). For some *P. yoelii* infections, the defense mechanism is mostly mediated by humoral factors in the absence of demonstrable cell-mediated immunity (Murphy and Lefford, 1979; Freeman and Parish, 1981). IFN-Is have also been shown to enhance humoral immunity and promote isotype switching by stimulating dendritic cells *in vivo* (Le Bon et al., 2001). A substitution of C741Y in the *P. y. nigeriensis* N67 was indeed linked to increased levels of IFN-α/β, T helper cell differentiation, and antibody isotype switching (Peng et al., 2020). Stimulation of an early IFN-I response may influence the direction of host immune responses such as $CD4^+$ T cell activation and later antibody production. Whether and how IFN-Is regulate host immune mechanisms, including T cell activation and antibody production require additional investigation.

Furthermore, continuous injection of purified recombinant human IFN-α suppressed blood stage parasitemia for two *P. yoelii* strains (265 BY and 17XNL) by inhibiting the production of reticulocytes, which were preferentially invaded by these parasite strains, but not for the strain of *P. vinckei petteri* that infects only mature red blood cells (Vigario et al., 2001). Constant human recombinant IFN-α treatment also resulted in enhanced survival, which was associated with an IFN-γ–mediated decrease of parasitemia, expression of intracellular adhesion molecule-1 (ICAM-1 or CD54) in the brain, and $CD8^+$ T cells sequestration (Vigario et al., 2007) (**Figure 3B**). ICAM-1 is a cell surface glycoprotein that is typically expressed on endothelial and immune cells; it plays an important role in cell-cell adhesion, extravasation, signal transduction, and inflammation (Bui et al., 2020). Increased expression of ICAM-I in the brain microvasculature has been implicated in the development of cerebral malaria (CM). Absence of ICAM-1 correlates with a decrease of macrophage and iRBC sequestration in the brain and lung capillaries leading to a less severe thrombocytopenia and reduced mortality (Favre et al., 1999). In addition, administration of murine IFN-β after *P. berghei* ANKA infection increased host survival and improved blood–brain barrier function without altering systemic parasitemia. Injection of IFN-β also downregulated CXCL9 and ICAM-1 expression in the brain, reduced serum TNF-α level, and decreased T-cell infiltration in the brain (Morrell et al., 2011). The observations of protection in different parasite models are quite diverse. It is too early to draw a general conclusion on protective mechanisms. More studies on protection mechanisms are required.

IFN-I Suppression of DC and T Cell Activation

DCs play a central role as a bridge between innate and acquired immunity (Wykes and Good, 2008). IFN-Is were shown to modulate DC function and impair the development of protective IFN-γ producing $CD4^+$ T-bet^+ T cells for parasite control during *P. berghei* ANKA and *P. chabaudi* AS infections (Haque et al., 2011; Haque et al., 2014). $CD4^+$ T cells have been shown to produce IFN-γ and macrophage colony-stimulating factor (M-CSF or CSF1) that are important for the activation and expansion of $CD169^+$ macrophages to control malaria blood-stage infection (Fontana et al., 2016; Kurup et al., 2019b). IFN-I signaling impaired $CD8^-$ cDC function to prime IFN-γ-producing T helper type 1 (Th1) cells for parasite control (Haque et al., 2014), and IFN-I signaling deficiency promoted $CD4^+$ T-cell-dependent parasite control thus reducing the onset of severe clinical symptoms and fatal cerebral pathology (Haque et al., 2011) (**Figure 3B**). IFN-Is and IFN-γ were involved in activation-induced cDC death during *P. berghei* ANKA infection (Tamura et al., 2015). In a non-lethal *P. y. yoelii* 17XNL blood stage infection, IFN-Is directly induced T-bet and Blimp-1 expression to promote T regulatory 1 (Tr1) cell responses (Zander et al., 2016). The Tr1 cells then secreted interleukin 10 (IL-10) and IFN-γ to restrict T follicular helper (Tfh) cell accumulation and limit parasite-specific antibody responses. Furthermore, IFN-Is were shown to suppress innate immune cell function and IFN-γ production by parasite-specific $CD4^+$ T cells as well as to promote the development of IL-10-producing Tr1 cells (Montes de Oca et al., 2016). On the other hand, IFNAR1-deficiency accelerated humoral immune response and parasite control by boosting the inducible T cell co-stimulator (ICOS) signaling (Sebina et al., 2016). IFNAR1-signalling also impaired germinal center B-cell formation, Ig-class switching, and Tfh cell differentiation thus impeding the resolution of non-lethal blood-stage infection of *P. y. yoelii* 17XNL and *P. chabaudi* AS.

IFN-Is Promote Inflammation and Host Death

In other studies, IFN-I signaling appears to promote production of inflammatory cytokines/chemokines and pathogenesis of experimental cerebral malaria (ECM). Key mediators of ECM, including *P. berghei* ANKA-induced brain sequestration of $CXCR3^+$-activated $CD8^+$ T cells, granzyme B, IFN-γ, CXCL9, and CXCL10, were attenuated in IFN-I signaling deficient mice (Palomo et al., 2013). Microglia from mice infected with *P. berghei* ANKA showed signature of IFN-I signaling that was responsible for activation of microglia, production of CXCL9, CXCL10, CCL8 and CCL12 and pathogenesis of ECM (Capuccini et al., 2016). Similarly, mice lacking IFN-I receptor ($Ifnar1^{-/-}$) had a significant decrease in inflammatory response with low levels of IL-6, CCL2, CCL3, CXCL1, CXCL10 and IFN-α and survived *P. y. yoelii* YM infection (Spaulding et al., 2016). IFNAR1 deficiency protected mice from ECM after *P. berghei* ANKA infection, and IFNAR1 signaling unleashed $CD8^+$ T cell effector capacity that was crucial for ECM development (Ball et al., 2013). Deficiency of ubiquitin specific peptidase 15 (USP15), an IFN-I positive regulator, also protected mice from ECM and neuroinflammation (Torre et al., 2017). These studies, particularly *P. berghei* ANKA infections, suggest that IFN-I signaling, likely at days 3–6 pi, promotes inflammatory responses and ECM, and that high levels of IFN-γ, CXCL9, CXCL10, and $CD8^+$ T cells likely contribute to the host death. On the other hand, the lethal parasite *P. y. yoelii* YM grows quickly in C57BL/6 mice with limited immune response before

mouse death with high parasitemia (~90%) on day 7 pi. High IFN-I levels 24 h pi in the *P. y. yoelii* YM-infected *Mavs*$^{-/-}$ mice also lead to increased level of IFN-γ and host survival, suggesting that increased inflammatory responses help control parasitemia and enhance host survival (Yu et al., 2016). Therefore, protection in terms of host survival depends on parasite/host models. If an infection induces a strong inflammatory response such as *P. berghei* ANKA infection, blockage of IFN-I signaling may reduce inflammation and enhance host survival. For an infection that does not induce a strong inflammatory response, higher levels of IFN-Is and IFN-γ as well as an elevated inflammatory response may instead inhibit parasitemia and enhance survival. Because immune responses are dynamic, measurements of cytokines/chemokines and cell populations will vary at different time points during the course of infection, which can contribute to reports of contradictory results.

IFN-I RESPONSES IN HUMAN INFECTIONS

Studying IFN-I responses in human malaria infections have been mainly based on association of disease severity and/or IFN-I levels in the blood with gene expression level and/or genetic polymorphisms in genes playing a role in IFN-I responses. Microarray, RNA sequencing, single-cell sequencing, and genetic association can be important tools for studying IFN-I responses in human malaria infections. However, host immune responses, including IFN-I responses, will be highly variable among patients because the majority of clinical malaria infections in endemic regions carry multiple parasite strains with diverse genetic backgrounds (Conway et al., 1991; O'Brien et al., 2016; Zhu et al., 2019). Other factors such as the time of infection (usually unknown) and host genetic background will greatly influence the level and dynamics of IFN-I responses.

Consistent with observations in some studies using *P. berghei* ANKA infections (Vigario et al., 2001; Vigario et al., 2007), IFN-Is, particularly IFN-α, appear to be protective in human infections of *P. falciparum*. The pre-antimalarial treatment levels of IFN-α were significantly lower in children with severe malaria than those with mild malaria (Luty et al., 2000). Similarly, lower circulating IFN-α was observed in children with severe malaria anemia (SMA) in Kenya, and two polymorphisms in IFN-α promoters [IFN-α2 (A173T) and IFN-α8 (T884A)] leading to reduced IFN-α production were associated with increased susceptibility to SMA and mortality (Kempaiah et al., 2012). Mild *P. falciparum* malaria following an episode of severe malaria was reported to be associated with induction of the IFN-I pathway in Malawian Children (Krupka et al., 2012). Patients with mild *P. falciparum* malaria in Rwanda had upregulated levels of IFN-Is, IFN-γ, complement system components, and nitric oxide (Subramaniam et al., 2015). These observations suggest a protective role of IFN-Is in malaria disease severity.

In contrast, IFN-I responses have also been associated with immune suppression and severe diseases in human malaria infections. Association between IFNAR1 variants and CM in children from Africa was observed; variants with lower IFNAR1 expression were associated with protection, whereas variants with increased IFNAR1 expression were associated with CM (Aucan et al., 2003; Khor et al., 2007; Ball et al., 2013; Feintuch et al., 2018). This is consistent with the observations that blocking IFNAR signaling can protect infected mice from severe disease symptoms. However, the dynamics of IFN-I levels during infection are unknown. Association between IFNAR1 and malaria susceptibility was also observed in Indian populations (Kanchan et al., 2015). But how these IFNAR1 variants regulate IFN-I responses to affect CM development requires further investigation. Dual transcriptome analyses of the host and parasite genes on samples from 46 malaria-infected Gambian children showed that disease severity was associated with increased expression of granulopoiesis and interferon-γ-related genes as well as with inadequate suppression of IFN-I signaling genes (Lee et al., 2018).

POTENTIAL EXPLANATIONS FOR THE CONFLICTING ROLES OF IFN-IS

IFN-I signaling can be protective leading to suppression of parasitemia and better survival or can inhibit DC and T cell activation to dampen adaptive response during malaria parasite infections. The effects or mechanisms of IFN-Is on parasitemia control and disease severity are complex, depending on both species of parasites and their hosts (parasite and host genetics), the timing and levels of IFN-I production, and possibly the subtypes of IFN-Is. Although the mechanisms of IFN-I in regulating host responses to infections of different malaria parasite species are diverse, some major themes can be established (**Figure 3** and **Supplementary Table S1**). IFN-Is are protective if high levels of IFN-Is are produced early (24 h pi) during an infection. *P. berghei* ANKA-infected C57BL/6 mice injected with IFN-α had significantly ($P < 0.05$) higher levels of IFN-γ (772 ± 73 pg/ml, day 9 pi) than those receiving diluent (180 ± 14 pg/ml), reduced parasitemia, and better host survival (Vigario et al., 2007). Elevated levels of IFN-Is (300–500 mg/ml IFN-α) can reduce early (day 6) parasitemia as seen in *P. y. nigeriensis* N67 and *P. chabaudi* AS infections (Voisine et al., 2010; Wu et al., 2014; Wu et al., 2020). In another study, the effect of *Ifnar1*$^{-/-}$ on *P. chabaudi* AS parasitemia may not be significant, but the day 6 parasitemia is higher in the *Ifnar1*$^{-/-}$ than those of WT mice (Kim et al., 2012). The protection mechanisms for these infections are largely unknown, probably associated with increased IFN-γ expression at later stages of infection. Additionally, the levels of IFN-γ and IL-6 were also higher in mice with elevated early IFN-Is than infections with low IFN-Is, suggesting that IFN-γ, IL-6 and other cytokines may contribute to the reduction of parasitemia and better host survival (Yu et al., 2016; Wu et al., 2020). In another model, *P. y. yoelii* YM infection of STING or MAVS deficient mice produced much higher peaks of IFN-α/β (~2,500 pg/ml IFN-α and ~1,200 pg/ml IFN-β in MAVS knockout mice) than those observed in WT mice infected with *P. y. nigeriensis* N67 infection 24 h pi, which may provide stronger inhibition of parasite

growth, leading to higher survival rates (Yu et al., 2016). In all the cases, IFN-I levels were quickly downregulated to background level after 24 h pi. These observations suggest a positive linkage between early peaks of IFN-Is and parasitemia control. It remains to be determined why *P. y. nigeriensis* N67 infection induces an early IFN-I responses, whereas other parasites such as *P. y. nigeriensis* N67C and *P. y. yoelii* YM infections stimulate only low levels of IFN-Is (~60 pg/ml IFN-α and almost no IFN-β in YM infection) in C57BL/6 mice. Additionally, the molecular mechanism of downregulation of the 24 h IFN-I peak is still unknown.

On the other hand, blockage of IFN-I signaling has also been shown to increase DC and T cell activation and inflammation, which can promote survival or mortality depending on parasite species or strains. IFN-Is can cause immunopathology in acute viral infections (Davidson et al., 2014) and mediate immunosuppression during chronic viral infections (Teijaro et al., 2013; Wilson et al., 2013). Therefore, chronically elevated IFN-Is may explain the observations of immune suppression in various reports of malaria infections. In one study showing inhibition of DC and T cell activation by IFN-I signaling, *Ifnar1*$^{-/-}$ mice or multiple injections of anti-IFNAR antibodies were used (Zander et al., 2016), which is different from infection of wild type mice. In another study, infection of C57BL/6J mice with *P. y. yoelii* YM produced low level of IFN-α (20–70 pg/ml), as reported in other studies (Yu et al., 2016; Wu et al., 2020); however, infection of *Sting*$^{Gt/Gt}$ mice did not produce high levels of IFN-Is as observed in the study of (Yu et al., 2016). The reason for the discrepancy is unknown. Some possibilities include the uses of different sources of mice and parasite strains. Similarly, low levels of IFN-α/β were also observed in *P. berghei* ANKA-infected WT C57BL/6 mice 24 h pi (Haque et al., 2011; Haque et al., 2014). Again, depletion or blockage of IFN-I signaling resulted in higher levels of IFN-γ, better parasite control and improved host survival (Haque et al., 2011; Haque et al., 2014). Interestingly, higher levels of IFN-α were observed in wild type mice 48 h pi (~70 pg/ml IFN-α vs ~20 pg/ml at 24 h) and day 4 pi (~200 mg/ml IFN-α). Generally, studies suggesting IFN-I suppression of T cell activation or enhancement of inflammatory chemokines/cytokines used *Ifnar1*$^{-/-}$ mice or multiple injections of anti-IFNAR antibodies, which are different from infections having a short time increase in IFN-I level. In these models, the absence of IFN-I signaling due to deficiency of IFNAR or antibody blockage may prompt the host to increase IFN-I production through autocrine feedback mechanisms, leading to activation and/or inhibition of alternative immune pathways that would not occur in infections with normal IFN-I signaling. Indeed, it has been shown that production of IFN-α/β early (24 h pi) during LCMV infection of mice was dependent upon the IFN-α/βR and STAT1, and in the absence of IFN-α/βR and the STAT1, an alternative delayed pathway dependent on a functional IFN-γR was activated to produce IFN-α/β at 48 h pi (Malmgaard, 2004). Additionally, the alternative pathway for induction of IFN-α/β exists in IFN-α/βR$^{-/-}$ and STAT1$^{-/-}$ mice but is absent in IFN-γR$^{-/-}$ mice, suggesting that IFN-γ was involved in the alternative pathway. Similar alternative pathways could exist in the *Plasmodium*-infected *Ifnar1*$^{-/-}$ mice. However, no systematic measurement of IFN-I levels during infection were done in the studies using *Ifnar1*$^{-/-}$ mice or injections of anti-IFNAR antibodies. If the feedback alternative pathways of IFN-I responses exist in the infected *Ifnar1*$^{-/-}$ mice, then high IFN-I levels may still play a role in protection through some unknown/alternative mechanisms. Measurements of the dynamic IFN-I levels during malaria infections will be important in order to understand the roles of IFN-Is in malaria infections.

In summary, an early IFN-I response (24 h pi) can be protective through suppression of parasitemia. Disruption of IFN-I signaling through IFNAR deficiency can be beneficial to the host; however, the levels of IFN-Is during the infections are mostly unknown. Whether elevated levels of IFN-Is are protective against severe diseases likely depends on parasite species/strains and host genetic background. It appears that all the protective effects are mediated through adequate levels of IFN-γ, proper activation of immune cells, and production of antibodies. How an early IFN-I response or the absence of IFN-I signaling regulates IFN-γ and antibody responses during malaria parasite infections require additional investigations.

REGULATION OF IFN-I RESPONSES DURING MALARIA PLASMODIUM INFECTIONS

IFN-Is regulate many arms of the host immune responses; chronically elevated IFN-Is can suppress adaptive immunity and may also promote autoimmune diseases (Chen et al., 2020). Therefore, the levels of IFN-Is are also closely regulated by various mechanisms such as ubiquitination, phosphorylation and ADP-ribosylation of molecules in the IFN-I response pathways (Takaoka and Yamada, 2019; Zheng and Gao, 2020). Many molecules have been shown to amplify IFN-I signaling, including induction of STAT1 and IRF9 expression by IFN-γ and interleukin-6 (IL-6) (Ivashkiv and Donlin, 2014). There are also proteins such as suppressor of cytokine signaling 1 and 3 (SOCS1 and SOCS3) and ubiquitin carboxy-terminal hydrolase 18 (USP18) or microRNAs (miRNAs) that can suppress IFN-I responses (Yoshimura et al., 2007; Sarasin-Filipowicz et al., 2009). Because IFN-I responses during malaria infections shared the same pathways as those of viral infections, it can be expected that many regulatory mechanisms of IFN-I production in malaria parasite and virus infections are similar. However, malaria parasites are more complex organisms than viruses, and as a result, IFN-I responses and regulation during malaria parasite infections are likely more sophisticated than those of viruses.

All IFN-I response pathways use downstream transcription factors such as IRFs that regulate gene expression of IFNs. Using IRF deficient mice, many of these IRFs have been shown to play important roles in parasitemia control, disease severity, and ECM symptoms (Gun et al., 2014). Three single nucleotide polymorphisms (SNPs) in the IRF1 gene were shown to be correlated with blood parasite levels in malaria patients from west African, and one SNP (rs10065633) was associated with severe disease (Mangano et al., 2008). However, the molecular

mechanisms regulating IFN-I responses during human malaria infections remain largely unknown. Recently, several studies using *P. yoelii* parasites begin to shed light on the mechanisms of IFN-I response regulation. A large number of host genes that interact with many genetic loci on the 14 chromosomes of *P. yoelii*, including clusters of genes involved in IFN-I responses, were identified using ts-eQTL (Wu et al., 2015a). Among the genes identified, a set of randomly selected putative ISGs (*Ak3*, *Fosl1*, *Inpp4a*, *Havcr2*, *Fcgr1*, *Bc016423*, *S1pr5*, *Parp14*, *Satb1*, *Selenbp2*, *Helb*, *Helz2*, and *Lrp12*) were found to inhibit luciferease signals driven by IFN-β promoter, suggesting being negative regulators of the IFN-I signaling pathways (**Figure 2**). As mentioned above, *P.y. nigeriensis* N67 infection stimulates peaks of IFN-α/β approximately 24 h pi, and the IFN-I level quickly declines to background level soon after. These negative regulators likely play a role in the decline of the IFN-I levels. Selected genes from this study were further functionally characterized *in vivo* and *in vitro*. For example, CD40 (or TNF receptor superfamily member 5, TNFRSF5), a receptor expressed on the surfaces of many cell types, was shown to enhance STING protein level and STING-mediated IFN-I responses by affecting STING ubiquitination (Yao et al., 2016). On the other hand, the FOS-like antigen 1 (FOSL1), known as a component of FOS transcription factor, was shown to act as a negative regulator of IFN-I responses (Cai et al., 2017). After poly(I:C) or iRBC stimulation, FOSL1 translocated from the nucleus to the cytoplasm, where it interacted with TRAF3 and TRIF to reduce IRF3 phosphorylation and IFN-I production (**Figure 2**). Therefore, FOSL1 acts as a negative regulator of IFN-I response as well as a transcription factor, depending on its cellular location (Cai et al., 2017). Receptor transporter protein 4 gene (*Rtp4*) gene, another gene identified from the same ts-eQTL analysis, was clustered with ISGs such as *Oas2*, *Dhx58*, *Ifit3*, *Usp18*, *Isg15*, and *Ifi35* (Wu et al., 2015a). RTP4 is induced by IFN-Is and binds to the TBK1 complex where it negatively regulates TBK1 signaling by interfering with the expression and phosphorylation of both TBK1 and IRF3 (He et al., 2020). Interestingly, RTP4 may have a specific role in brain pathology because mice deficient of RTP4 have lower West Nile virus titers in the brain and reduced hemorrhages in the cerebellum of *P. berghei* ANKA-infected mice compared with those of WT mice. Using the same ts-eQTL approach but with mRNAs collected 24 h after infection, a gene called *March1*, a member of the membrane-associated ring-CH-type finger 1 family, was also found to be clustered with ISGs (*Oas1d* and *Isg20*) (Wu et al., 2020). MARCH1 was shown to interact with STING, MAVS, and various regulators of the IFN-I pathways to regulate IFN responses likely through protein ubiquitination. *March1*$^{-/-}$ mice infected with *P. y. nigeriensis* N67 or *P. y. yoelii* YM had significantly reduced serum IFN-I levels day 1 pi, but had increased number of CD86^{+}DC and elevated levels of IFN-γ day 4 pi, and survived longer than WT mice. The results suggest that MARCH1 is an important immune regulator affecting IFN-I responses, T cell activation, and adaptive immunity. Studying malaria infections also reveals a cross regulation mechanism of two different IFN-I response pathways (**Figure 2**). It was found that STING- and MAVS-mediated low level IFN-I responses induced the negative regulator SOCS1 that in turn inhibited the more powerful TLR7/MYD88-mediated IFN-I responses in pDCs during *P. y. yoelii* YM blood stage infection (Yu et al., 2016). Additionally, activation of the AIM2, NLRP3 or adaptor caspase-1 inflammsome pathways enhances IL-1β–mediated MYD88-TRAF3-IRF3 signaling and upregulation of SOCS1 that can inhibit MYD88-IRF7 signaling and IFN-I production in pDCs (Yu et al., 2018). These studies identify several regulators and mechanisms of IFN-I responses during malaria infections, which also contributes to our understanding of IFN-I signaling and regulation in general.

Molecules from malaria parasites may also modulate host IFN-I responses, although little is known about the mechanism of immune modulation by the parasites. A genetic locus on chromosome 13 of *P. yoelii* was significantly linked to expression of a large number ISGs, suggesting one or more parasite genes in the lcous may influnce host IFN-I responses (Wu et al., 2015a). Additionally, a C741Y amino acid substitution in the *P. yoelii* erythrocyte binding-like (PyEBL) protein appears to affect host IFN-I responses. The parasite carrying 741Y PyEBL (*P. y. nigeriensis* N67) stimulates higher levels of early IFN-Is than *P. y. nigeriensis* N67C that has 741C PyEBL (Peng et al., 2020; Wu et al., 2020). The substitution also altered host transcritomic responses, including genes in IFN-I responses, T helper cell activation, and IgG isotype switching (Peng et al., 2020). These observations indicate that parasite molecules can also modulate host IFN-I responses. However, parasite molecules that can stimulate and regulate IFN-I responses remain largely unknown.

CONCLUSIONS

Malaria parasite infection stimulates complex and differentially regulated immune responses, dependent on parasite and host species or strains. The parasite PAMPs and DAMPs are recognized by a number of host receptors. Asymptomatic liver stage infection induces the IFN-I responses, which reaches its peak during late liver stage when the parasite undergoes massive replication. The IFN-I signaling recruits and promotes the immune cells to control the liver stage infection. Parasite RNA appears to be the major ligand to elicit IFN-I responses in the hepatocytes, although parasite DNA may also stimulate IFN-I responses at this stage. It would be interesting to investigate whether parasite DNA and other host sensors are involved in the liver stage IFN-I response. After entering the bloodstream, sporozoites are phagocytized by DCs, which may trigger IFN-I responses in these DCs and lead to a positive feedback loop of IFN-I production. IFN-Is have been shown to be protective as well as deleterious in the blood stage parasite infections. Elevated level of IFN-Is or injection of IFN-Is can lead to the clearance of parasites and/or improved host survival rate. Parasite clearance could be mediated by phagocytosis and/or lysis of iRBCs activated by IFN-I signaling. However, deficiency in IFN-I signaling may also enhance DC function, T cell activation, and adaptive immune responses, which may reduce or aggravate disease severity depending on parasite strains and host genetic background. If an infection

causes strong inflammatory response with severe disease symptoms (such as *P. y. nigeriensis N67C* and *P. berghei ANKA*), persistent elevated IFN-I levels may help alleviate disease symptoms by inhibiting T cell activation and suppressing inflammatory responses. Additionally, in many cases of rodent malaria infections (such as *P. y. yoelii* YM infection), the IFN-I levels are low, possibly due to mechanisms of immune evasion or inhibition of immune responses. An early strong IFN-I response can help suppress the rapid parasite growth, buying time for the host to develop protective immunity. Therefore, the roles of IFN-Is in malaria protection are dependent on parasite strains, host genetic background, and the level and timing of IFN-I production.

AUTHOR CONTRIBUTIONS

XH, LX, KT, JW, and X-ZS wrote the manuscript. JW and X-ZS conceived and designed the paper. JW created **Figure 1**. XH created **Figure 2** and **Figure 3**. All authors contributed to the article and approved the submitted version.

FUNDING

This work was supported by the Division of Intramural Research, National Institute of Allergy and Infectious Diseases (NIAID), National Institutes of Health (NIH), USA.

ACKNOWLEDGMENTS

We thank Diane Cooper, MS, of the NIH library for manuscript editing assistance.

SUPPLEMENTARY MATERIAL

The Supplementary Material for this article can be found online at: https://www.frontiersin.org/articles/10.3389/fcimb.2020.594621/full#supplementary-material

REFERENCES

Angulo, I., and Fresno, M. (2002). Cytokines in the pathogenesis of and protection against malaria. *Clin. Diagn. Lab. Immunol.* 9 (6), 1145–1152. doi: 10.1128/cdli.9.6.1145-1152.2002

Anstey, N. M., Douglas, N. M., Poespoprodjo, J. R., and Price, R. N. (2012). *Plasmodium vivax*: clinical spectrum, risk factors and pathogenesis. *Adv. Parasitol.* 80, 151–201. doi: 10.1016/B978-0-12-397900-1.00003-7

Arese, P., and Schwarzer, E. (1997). Malarial pigment (haemozoin): a very active 'inert' substance. *Ann. Trop. Med. Parasitol.* 91 (5), 501–516. doi: 10.1080/00034989760879

Ataide, M. A., Andrade, W. A., Zamboni, D. S., Wang, D., Souza Mdo, C., Franklin, B. S., et al. (2014). Malaria-induced NLRP12/NLRP3-dependent caspase-1 activation mediates inflammation and hypersensitivity to bacterial superinfection. *PloS Pathog.* 10 (1), e1003885. doi: 10.1371/journal.ppat.1003885

Aucan, C., Walley, A. J., Hennig, B. J., Fitness, J., Frodsham, A., Zhang, L., et al. (2003). Interferon-alpha receptor-1 (IFNAR1) variants are associated with protection against cerebral malaria in the Gambia. *Genes Immun.* 4 (4), 275–282. doi: 10.1038/sj.gene.6363962

Babatunde, K. A., Mbagwu, S., Hernandez-Castaneda, M. A., Adapa, S. R., Walch, M., Filgueira, L., et al. (2018). Malaria infected red blood cells release small regulatory RNAs through extracellular vesicles. *Sci. Rep.* 8, 884. doi: 10.1038/s41598-018-19149-9

Babatunde, K. A., Subramanian, B. Y., Ahouidi, A. D., Murillo, P. M., Walch, M., and Mantel, P. Y. (2020). Role of Extracellular Vesicles in Cellular Cross Talk in Malaria. *Front. Immunol.* 11, 22. doi: 10.3389/fimmu.2020.00022

Baccarella, A., Fontana, M. F., Chen, E. C., and Kim, C. C. (2013). Toll-Like Receptor 7 Mediates Early Innate Immune Responses to Malaria. *Infect. Immun.* 81 (12), 4431–4442. doi: 10.1128/Iai.00923-13

Ball, E. A., Sambo, M. R., Martins, M., Trovoada, M. J., Benchimol, C., Costa, J., et al. (2013). IFNAR1 controls progression to cerebral malaria in children and CD8+ T cell brain pathology in *Plasmodium berghei*-infected mice. *J. Immunol.* 190 (10), 5118–5127. doi: 10.4049/jimmunol.1300114

Barrera, V., Skorokhod, O. A., Baci, D., Gremo, G., Arese, P., and Schwarzer, E. (2011). Host fibrinogen stably bound to hemozoin rapidly activates monocytes via TLR-4 and CD11b/CD18-integrin: a new paradigm of hemozoin action. *Blood* 117 (21), 5674–5682. doi: 10.1182/blood-2010-10-312413

Barton, G. M., and Kagan, J. C. (2009). A cell biological view of Toll-like receptor function: regulation through compartmentalization. *Nat. Rev. Immunol.* 9 (8), 535–542. doi: 10.1038/nri2587

Beiting, D. P. (2014). Protozoan parasites and type I interferons: a cold case reopened. *Trends Parasitol.* 30 (10), 491–498. doi: 10.1016/j.pt.2014.07.007

Belgnaoui, S. M., Paz, S., and Hiscott, J. (2011). Orchestrating the interferon antiviral response through the mitochondrial antiviral signaling (MAVS) adapter. *Curr. Opin. Immunol.* 23 (5), 564–572. doi: 10.1016/j.coi.2011.08.001

Beutler, B. A. (2009). TLRs and innate immunity. *Blood* 113 (7), 1399–1407. doi: 10.1182/blood-2008-07-019307

Borden, E. C., Sen, G. C., Uze, G., Silverman, R. H., Ransohoff, R. M., Foster, G. R., et al. (2007). Interferons at age 50: past, current and future impact on biomedicine. *Nat. Rev. Drug Discov.* 6 (12), 975–990. doi: 10.1038/nrd2422

Boxx, G. M., and Cheng, G. (2016). The Roles of Type I Interferon in Bacterial Infection. *Cell Host Microbe* 19 (6), 760–769. doi: 10.1016/j.chom.2016.05.016

Brown, D., and Waneck, G. L. (1992). Glycosyl-phosphatidylinositol-anchored membrane proteins. *J. Am. Soc. Nephrol.* 3 (4), 895–906.

Brubaker, S. W., Bonham, K. S., Zanoni, I., and Kagan, J. C. (2015). Innate immune pattern recognition: a cell biological perspective. *Annu. Rev. Immunol.* 33, 257–290. doi: 10.1146/annurev-immunol-032414-112240

Bui, T. M., Wiesolek, H. L., and Sumagin, R. (2020). ICAM-1: A master regulator of cellular responses in inflammation, injury resolution, and tumorigenesis. *J. Leukoc. Biol.* 108 (3), 787–799. doi: 10.1002/JLB.2MR0220-549R

Butler, N. S., Schmidt, N. W., Vaughan, A. M., Aly, A. S., Kappe, S. H., and Harty, J. T. (2011). Superior antimalarial immunity after vaccination with late liver stage-arresting genetically attenuated parasites. *Cell Host Microbe* 9 (6), 451–462. doi: 10.1016/j.chom.2011.05.008

Cai, B., Wu, J., Yu, X., Su, X. Z., and Wang, R. F. (2017). FOSL1 Inhibits Type I Interferon Responses to Malaria and Viral Infections by Blocking TBK1 and TRAF3/TRIF Interactions. *mBio* 8 (1), e02161–16. doi: 10.1128/mBio.02161-16

Campos, M. A., Almeida, I. C., Takeuchi, O., Akira, S., Valente, E. P., Procopio, D. O., et al. (2001). Activation of Toll-like receptor-2 by glycosylphosphatidylinositol anchors from a protozoan parasite. *J. Immunol.* 167 (1), 416–423. doi: 10.4049/jimmunol.167.1.416

Capuccini, B., Lin, J., Talavera-Lopez, C., Khan, S. M., Sodenkamp, J., Spaccapelo, R., et al. (2016). Transcriptomic profiling of microglia reveals signatures of cell activation and immune response, during experimental cerebral malaria. *Sci. Rep.* 6:39258. doi: 10.1038/srep39258

Carrero, J. A. (2013). Confounding roles for type I interferons during bacterial and viral pathogenesis. *Int. Immunol.* 25 (12), 663–669. doi: 10.1093/intimm/dxt050

Celada, A., Cruchaud, A., and Perrin, L. H. (1983). Phagocytosis of *Plasmodium falciparum*-parasitized erythrocytes by human polymorphonuclear leukocytes. *J. Parasitol.* 69 (1), 49–53. doi: 10.2307/3281273

Chen, H. J., Tas, S. W., and de Winther, M. P. J. (2020). Type-I interferons in atherosclerosis. *J. Exp. Med.* 217 (1), e20190459. doi: 10.1084/jem.20190459

Chiu, Y. H., MacMillan, J. B., and Chen, Z. J. J. (2009). RNA Polymerase III Detects Cytosolic DNA and Induces Type I Interferons through the RIG-I Pathway. *Cell* 138 (3), 576–591. doi: 10.1016/j.cell.2009.06.015

Clark, I. A., Alleva, L. M., Budd, A. C., and Cowden, W. B. (2008). Understanding the role of inflammatory cytokines in malaria and related diseases. *Travel Med. Infect. Dis.* 6 (1-2), 67–81. doi: 10.1016/j.tmaid.2007.07.002

Coch, C., Hommertgen, B., Zillinger, T., Dassler-Plenker, J., Putschli, B., Nastaly, M., et al. (2019). Human TLR8 Senses RNA From *Plasmodium falciparum*-Infected Red Blood Cells Which Is Uniquely Required for the IFN-gamma Response in NK Cells. *Front. Immunol.* 10, 371. doi: 10.3389/fimmu.2019.00371

Combes, V., Simon, A. C., Grau, G. E., Arnoux, D., Camoin, L., Sabatier, F., et al. (1999). In vitro generation of endothelial microparticles and possible prothrombotic activity in patients with lupus anticoagulant. *J. Clin. Invest.* 104 (1), 93–102. doi: 10.1172/Jci4985

Combes, V., Coltel, N., Alibert, M., van Eck, M., Raymond, C., Juhan-Vague, I., et al. (2005). ABCA1 gene deletion protects against cerebral malaria - Potential pathogenic role of microparticles in neuropathology. *Am. J. Pathol.* 166 (1), 295–302. doi: 10.1016/S0002-9440(10)62253-5

Conway, D. J., Greenwood, B. M., and McBride, J. S. (1991). The epidemiology of multiple-clone *Plasmodium falciparum* infections in Gambian patients. *Parasitol* 103 Pt 1, 1–6. doi: 10.1017/s0031182000059217

Couper, K. N., Barnes, T., Hafalla, J. C. R., Combes, V., Ryffel, B., Secher, T., et al. (2010). Parasite-Derived Plasma Microparticles Contribute Significantly to Malaria Infection-Induced Inflammation through Potent Macrophage Stimulation. *PloS Pathog.* 6 (1), e1000744. doi: 10.1371/journal.ppat.1000744

Crompton, P. D., Moebius, J., Portugal, S., Waisberg, M., Hart, G., Garver, L. S., et al. (2014). Malaria immunity in man and mosquito: insights into unsolved mysteries of a deadly infectious disease. *Annu. Rev. Immunol.* 32, 157–187. doi: 10.1146/annurev-immunol-032713-120220

Cui, S., Eisenacher, K., Kirchhofer, A., Brzozka, K., Lammens, A., Lammens, K., et al. (2008). The C-terminal regulatory domain is the RNA 5 '-triphosphate sensor of RIG-I. *Mol. Cell* 29 (2), 169–179. doi: 10.1016/j.molcel.2007.10.032

Davidson, S., Crotta, S., McCabe, T. M., and Wack, A. (2014). Pathogenic potential of interferon alphabeta in acute influenza infection. *Nat. Commun.* 5, 3864. doi: 10.1038/ncomms4864

deWalick, S., Amante, F. H., McSweeney, K. A., Randall, L. M., Stanley, A. C., Haque, A., et al. (2007). Cutting edge: conventional dendritic cells are the critical APC required for the induction of experimental cerebral malaria. *J. Immunol.* 178 (10), 6033–6037. doi: 10.4049/jimmunol.178.10.6033

Dostert, C., Guarda, G., Romero, J. F., Menu, P., Gross, O., Tardivel, A., et al. (2009). Malarial hemozoin is a Nalp3 inflammasome activating danger signal. *PloS One* 4 (8), e6510. doi: 10.1371/journal.pone.0006510

Dunst, J., Kamena, F., and Matuschewski, K. (2017). Cytokines and Chemokines in Cerebral Malaria Pathogenesis. *Front. Cell Infect. Microbiol.* 7:324. doi: 10.3389/fcimb.2017.00324

El-Assaad, F., Wheway, J., Hunt, N. H., Grau, G. E. R., and Combes, V. (2014). Production, Fate and Pathogenicity of Plasma Microparticles in Murine Cerebral Malaria. *PloS Pathog.* 10 (3), e1003839. doi: 10.1371/journal.ppat.1003839

Emran, T. B., Iyori, M., Ono, Y., Amelia, F., Yusuf, Y., Islam, A., et al. (2018). Baculovirus-Induced Fast-Acting Innate Immunity Kills Liver-Stage *Plasmodium*. *J. Immunol.* 201 (8), 2441–2451. doi: 10.4049/jimmunol.1800908

Favre, N., Da Laperousaz, C., Ryffel, B., Weiss, N. A., Imhof, B. A., Rudin, W., et al. (1999). Role of ICAM-1 (CD54) in the development of murine cerebral malaria. *Microbes Infect.* 1 (12), 961–968. doi: 10.1016/s1286-4579(99)80513-9

Feintuch, C. M., Tare, A., Cusumano, L. R., Benayoun, J., Ryu, S., Sixpence, A., et al. (2018). Type I Interferon Receptor Variants in Gene Regulatory Regions are Associated with Susceptibility to Cerebral Malaria in Malawi. *Am. J. Trop. Med. Hyg.* 98 (6), 1692–1698. doi: 10.4269/ajtmh.17-0887

Ferguson, M. A. J., Brimacombe, J. S., Brown, J. R., Crossman, A., Dix, A., Field, R. A., et al. (1999). The GPI biosynthetic pathway as a therapeutic target for African sleeping sickness. *Biochim. Biophys. Acta Mol. Basis Dis.* 1455 (2-3), 327–340. doi: 10.1016/S0925-4439(99)00058-7

Fontana, M. F., de Melo, G. L., Anidi, C., Hamburger, R., Kim, C. Y., Lee, S. Y., et al. (2016). Macrophage Colony Stimulating Factor Derived from CD4+ T Cells Contributes to Control of a Blood-Borne Infection. *PloS Pathog.* 12 (12), e1006046. doi: 10.1371/journal.ppat.1006046

Freeman, R. R., and Parish, C. R. (1981). *Plasmodium yoelii*: antibody and the maintenance of immunity in BALB/c mice. *Exp. Parasitol.* 52 (1), 18–24. doi: 10.1016/0014-4894(81)90056-4

Freyssinet, J. M. (2003). Cellular microparticles: what are they bad or good for? *J. Thromb. Haemost.* 1 (7), 1655–1662. doi: 10.1046/j.1538-7836.2003.00309.x

Gallego-Marin, C., Schrum, J. E., Andrade, W. A., Shaffer, S. A., Giraldo, L. F., Lasso, A. M., et al. (2018). Cyclic GMP-AMP Synthase Is the Cytosolic Sensor of *Plasmodium falciparum* Genomic DNA and Activates Type I IFN in Malaria. *J. Immunol.* 200 (2), 768–774. doi: 10.4049/jimmunol.1701048

Gazzinelli, R. T., Kalantari, P., Fitzgerald, K. A., and Golenbock, D. T. (2014). Innate sensing of malaria parasites. *Nat. Rev. Immunol.* 14 (11), 744–757. doi: 10.1038/nri3742

Gotz, A., Tang, M. S., Ty, M. C., Arama, C., Ongoiba, A., Doumtabe, D., et al. (2017). Atypical activation of dendritic cells by *Plasmodium falciparum*. *Proc. Natl. Acad. Sci. U.S.A.* 114 (49), E10568–E10577. doi: 10.1073/pnas.1708383114

Gowda, N. M., Wu, X. Z., and Gowda, D. C. (2011). The Nucleosome (Histone-DNA Complex) Is the TLR9-Specific Immunostimulatory Component of *Plasmodium falciparum* That Activates DCs. *PloS One* 6 (6), e20398. doi: 10.1371/journal.pone.0020398

Grangeiro de Carvalho, E., Bonin, M., Kremsner, P. G., and Kun, J. F. (2011). *Plasmodium falciparum*-infected erythrocytes and IL-12/IL-18 induce diverse transcriptomes in human NK cells: IFN-alpha/beta pathway versus TREM signaling. *PloS One* 6 (9), e24963. doi: 10.1371/journal.pone.0024963

Gui, X., Yang, H., Li, T., Tan, X., Shi, P., Li, M., et al. (2019). Autophagy induction via STING trafficking is a primordial function of the cGAS pathway. *Nature* 567 (7747), 262–266. doi: 10.1038/s41586-019-1006-9

Gun, S. Y., Claser, C., Tan, K. S., and Renia, L. (2014). Interferons and interferon regulatory factors in malaria. *Mediators Inflammation* 2014:243713. doi: 10.1155/2014/243713

Hahn, W. O., Butler, N. S., Lindner, S. E., Akilesh, H. M., Sather, D. N., Kappe, S. H., et al. (2018). cGAS-mediated control of blood-stage malaria promotes *Plasmodium*-specific germinal center responses. *JCI Insight* 3 (2), e94142. doi: 10.1172/jci.insight.94142

Haque, A., Best, S. E., Ammerdorffer, A., Desbarrieres, L., de Oca, M. M., Amante, F. H., et al. (2011). Type I interferons suppress CD4(+) T-cell-dependent parasite control during blood-stage *Plasmodium* infection. *Eur. J. Immunol.* 41 (9), 2688–2698. doi: 10.1002/eji.201141539

Haque, A., Best, S. E., Montes de Oca, M., James, K. R., Ammerdorffer, A., Edwards, C. L., et al. (2014). Type I IFN signaling in CD8- DCs impairs Th1-dependent malaria immunity. *J. Clin. Invest.* 124 (6), 2483–2496. doi: 10.1172/JCI70698

He, X., Ashbrook, A. W., Du, Y., Wu, J., Hoffmann, H. H., Zhang, C., et al. (2020). RTP4 inhibits IFN-I response and enhances experimental cerebral malaria and neuropathology. *Proc. Natl. Acad. Sci. U.S.A.* 117 (32), 19465–19474. doi: 10.1073/pnas.2006492117

Hirako, I. C., Gallego-Marin, C., Ataide, M. A., Andrade, W. A., Gravina, H., Rocha, B. C., et al. (2015). DNA-Containing Immunocomplexes Promote Inflammasome Assembly and Release of Pyrogenic Cytokines by CD14+ CD16 + CD64high CD32low Inflammatory Monocytes from Malaria Patients. *mBio* 6 (6), e01605–e01615. doi: 10.1128/mBio.01605-15

Ho, M., and Webster, H. K. (1989). Immunology of human malaria. A cellular perspective. *Parasite Immunol.* 11 (2), 105–116. doi: 10.1111/j.1365-3024.1989.tb00652.x

Hornung, V., and Latz, E. (2010). Intracellular DNA recognition. *Nat. Rev. Immunol.* 10 (2), 123–130. doi: 10.1038/nri2690

Hornung, V., Rothenfusser, S., Britsch, S., Krug, A., Jahrsdorfer, B., Giese, T., et al. (2002). Quantitative expression of toll-like receptor 1-10 mRNA in cellular subsets of human peripheral blood mononuclear cells and sensitivity to CpG oligodeoxynucleotides. *J. Immunol.* 168 (9), 4531–4537. doi: 10.4049/jimmunol.168.9.4531

Hou, F. J., Sun, L. J., Zheng, H., Skaug, B., Jiang, Q. X., and Chen, Z. J. (2011). MAVS Forms Functional Prion-like Aggregates to Activate and Propagate Antiviral Innate Immune Response (vol 146, pg 448, 2011). *Cell* 146 (5), 841–841. doi: 10.1016/j.cell.2011.08.013

Huang, K. Y., Schultz, W. W., and Gordon, F. B. (1968). Interferon induced by *Plasmodium berghei*. *Science* 162 (3849), 123–124. doi: 10.1126/science.162.3849.123

Isaacs, A., and Lindenmann, J. (1957). Virus interference. I. The interferon. *Proc. R. Soc. Lond. B Biol. Sci.* 147 (927), 258–267. doi: 10.1098/rspb.1957.0048

Isaacs, A., Lindenmann, J., and Valentine, R. C. (1957). Virus interference. II. Some properties of interferon. *Proc. R. Soc. Lond. B Biol. Sci.* 147 (927), 268–273. doi: 10.1098/rspb.1957.0049

Ishikawa, H., and Barber, G. N. (2008). STING is an endoplasmic reticulum adaptor that facilitates innate immune signalling. *Nature* 455 (7213), 674–678. doi: 10.1038/nature07317

Ivashkiv, L. B., and Donlin, L. T. (2014). Regulation of type I interferon responses. *Nat. Rev. Immunol.* 14 (1), 36–49. doi: 10.1038/nri3581

Jacobs, J. L., and Coyne, C. B. (2013). Mechanisms of MAVS Regulation at the Mitochondrial Membrane. *J. Mol. Biol.* 425 (24), 5009–5019. doi: 10.1016/j.jmb.2013.10.007

Jahiel, R. I., Nussenzweig, R. S., Vanderberg, J., and Vilcek, J. (1968a). Anti-malarial effect of interferon inducers at different stages of development of *Plasmodium berghei* in the mouse. *Nature* 220 (5168), 710–711. doi: 10.1038/220710a0

Jahiel, R. I., Vilcek, J., Nussenzweig, R., and Vanderberg, J. (1968b). Interferon inducers protect mice against *plasmodium berghei* malaria. *Science* 161 (3843), 802–804. doi: 10.1126/science.161.3843.802

Jahiel, R. I., Vilcek, J., and Nussenzweig, R. S. (1970). Exogenous interferon protects mice against *Plasmodium berghei* malaria. *Nature* 227 (5265), 1350–1351. doi: 10.1038/2271350a0

Jani, D., Nagarkatti, R., Beatty, W., Angel, R., Slebodnick, C., Andersen, J., et al. (2008). HDP-a novel heme detoxification protein from the malaria parasite. *PloS Pathog.* 4 (4), e1000053. doi: 10.1371/journal.ppat.1000053

Jaramillo, M., Bellemare, M. J., Martel, C., Shio, M. T., Contreras, A. P., Godbout, M., et al. (2009). Synthetic *Plasmodium*-like hemozoin activates the immune response: a morphology - function study. *PloS One* 4 (9), e6957. doi: 10.1371/journal.pone.0006957

Jin, L., Getahun, A., Knowles, H. M., Mogan, J., Akerlund, L. J., Packard, T. A., et al. (2013). STING/MPYS mediates host defense against *Listeria* monocytogenes infection by regulating Ly6C(hi) monocyte migration. *J. Immunol.* 190 (6), 2835–2843. doi: 10.4049/jimmunol.1201788

Jobe, O., Donofrio, G., Sun, G., Liepinsh, D., Schwenk, R., and Krzych, U. (2009). Immunization with radiation-attenuated *Plasmodium berghei* sporozoites induces liver cCD8alpha+DC that activate CD8+T cells against liver-stage malaria. *PloS One* 4 (4), e5075. doi: 10.1371/journal.pone.0005075

Johnstone, R. M., Adam, M., Hammond, J. R., Orr, L., and Turbide, C. (1987). Vesicle Formation during Reticulocyte Maturation - Association of Plasma-Membrane Activities with Released Vesicles (Exosomes). *J. Biol. Chem.* 262 (19), 9412–9420.

Kaczmarek, A., Vandenabeele, P., and Krysko, D. V. (2013). Necroptosis: the release of damage-associated molecular patterns and its physiological relevance. *Immunity* 38 (2), 209–223. doi: 10.1016/j.immuni.2013.02.003

Kalantari, P., DeOliveira, R. B., Chan, J., Corbett, Y., Rathinam, V., Stutz, A., et al. (2014). Dual Engagement of the NLRP3 and AIM2 Inflammasomes by *Plasmodium*-Derived Hemozoin and DNA during Malaria. *Cell Rep.* 6 (1), 196–210. doi: 10.1016/j.celrep.2013.12.014

Kanchan, K., Jha, P., Pati, S. S., Mohanty, S., Mishra, S. K., Sharma, S. K., et al. (2015). Interferon-gamma (IFNG) microsatellite repeat and single nucleotide polymorphism haplotypes of IFN-alpha receptor (IFNAR1) associated with enhanced malaria susceptibility in Indian populations. *Infect. Genet. Evol.* 29, 6–14. doi: 10.1016/j.meegid.2014.10.030

Kawagoe, T., Sato, S., Matsushita, K., Kato, H., Matsui, K., Kumagai, Y., et al. (2008). Sequential control of Toll-like receptor-dependent responses by IRAK1 and IRAK2. *Nat. Immunol.* 9 (6), 684–691. doi: 10.1038/ni.1606

Kawai, T., and Akira, S. (2008). Toll-like receptor and RIG-I-like receptor signaling. *Ann. N. Y. Acad. Sci.* 1143, 1–20. doi: 10.1196/annals.1443.020

Kawai, T., and Akira, S. (2010). The role of pattern-recognition receptors in innate immunity: update on Toll-like receptors. *Nat. Immunol.* 11 (5), 373–384. doi: 10.1038/ni.1863

Kawai, T., and Akira, S. (2011). Toll-like Receptors and Their Crosstalk with Other Innate Receptors in Infection and Immunity. *Immunity* 34 (5), 637–650. doi: 10.1016/j.immuni.2011.05.006

Kawai, T., Takahashi, K., Sato, S., Coban, C., Kumar, H., Kato, H., et al. (2005). IPS-1, an adaptor triggering RIG-I- and Mda5-mediated type I interferon induction. *Nat. Immunol.* 6 (10), 981–988. doi: 10.1038/ni1243

Kawasaki, T., and Kawai, T. (2014). Toll-like receptor signaling pathways. *Front. Immunol.* 5:461. doi: 10.3389/fimmu.2014.00461

Kempaiah, P., Anyona, S. B., Raballah, E., Davenport, G. C., Were, T., Hittner, J. B., et al. (2012). Reduced interferon (IFN)-alpha conditioned by IFNA2 (-173) and IFNA8 (-884) haplotypes is associated with enhanced susceptibility to severe malarial anemia and longitudinal all-cause mortality. *Hum. Genet.* 131 (8), 1375–1391. doi: 10.1007/s00439-012-1175-1

Khor, C. C., Vannberg, F. O., Chapman, S. J., Walley, A., Aucan, C., Loke, H., et al. (2007). Positive replication and linkage disequilibrium mapping of the chromosome 21q22.1 malaria susceptibility locus. *Genes Immun.* 8 (7), 570–576. doi: 10.1038/sj.gene.6364417

Kim, C. C., Nelson, C. S., Wilson, E. B., Hou, B., DeFranco, A. L., and DeRisi, J. L. (2012). Splenic red pulp macrophages produce type I interferons as early sentinels of malaria infection but are dispensable for control. *PloS One* 7 (10), e48126. doi: 10.1371/journal.pone.0048126

Kotenko, S. V. (2011). IFN-lambdas. *Curr. Opin. Immunol.* 23 (5), 583–590. doi: 10.1016/j.coi.2011.07.007

Krishnegowda, G., Hajjar, A. M., Zhu, J., Douglass, E. J., Uematsu, S., Akira, S., et al. (2005). Induction of proinflammatory responses in macrophages by the glycosylphosphatidylinositols of *Plasmodium falciparum*: cell signaling receptors, glycosylphosphatidylinositol (GPI) structural requirement, and regulation of GPI activity. *J. Biol. Chem.* 280 (9), 8606–8616. doi: 10.1074/jbc.M413541200

Krupka, M., Seydel, K., Feintuch, C. M., Yee, K., Kim, R., Lin, C. Y., et al. (2012). Mild *Plasmodium falciparum* malaria following an episode of severe malaria is associated with induction of the interferon pathway in Malawian children. *Infect. Immun.* 80 (3), 1150–1155. doi: 10.1128/IAI.06008-11

Kurup, S. P., Anthony, S. M., Hancox, L. S., Vijay, R., Pewe, L. L., Moioffer, S. J., et al. (2019a). Monocyte-Derived CD11c(+) Cells Acquire *Plasmodium* from Hepatocytes to Prime CD8 T Cell Immunity to Liver-Stage Malaria. *Cell Host Microbe* 25 (4), 565–577 e566. doi: 10.1016/j.chom.2019.02.014

Kurup, S. P., Butler, N. S., and Harty, J. T. (2019b). T cell-mediated immunity to malaria. *Nat. Rev. Immunol.* 19 (7), 457–471. doi: 10.1038/s41577-019-0158-z

Lamphier, M. S., Sirois, C. M., Verma, A., Golenbock, D. T., and Latz, E. (2006). TLR9 and the recognition of self and non-self nucleic acids. *Oligonucleotide Ther.* 1082, 31–43. doi: 10.1196/annals.1348.005

Langhorne, J., Simon-Haarhaus, B., and Meding, S. J. (1990). The role of CD4+ T cells in the protective immune response to *Plasmodium chabaudi in vivo*. *Immunol. Lett.* 25 (1-3), 101–107. doi: 10.1016/0165-2478(90)90099-c

Laulagnier, K., Motta, C., Hamdi, S., Roy, S., Fauvelle, F., Pageaux, J. F., et al. (2004). Mast cell- and dendritic cell-derived exosomes display a specific lipid composition and an unusual membrane organization. *Biochem. J.* 380 (Pt 1), 161–171. doi: 10.1042/BJ20031594

Le Bon, A., Schiavoni, G., D'Agostino, G., Gresser, I., Belardelli, F., and Tough, D. F. (2001). Type i interferons potently enhance humoral immunity and can promote isotype switching by stimulating dendritic cells in vivo. *Immunity* 14 (4), 461–470. doi: 10.1016/s1074-7613(01)00126-1

Lee, H. J., Georgiadou, A., Walther, M., Nwakanma, D., Stewart, L. B., Levin, M., et al. (2018). Integrated pathogen load and dual transcriptome analysis of systemic host-pathogen interactions in severe malaria. *Sci. Transl. Med.* 10 (447), eaar3619. doi: 10.1126/scitranslmed.aar3619

Liehl, P., and Mota, M. M. (2012). Innate recognition of malarial parasites by mammalian hosts. *Int. J. Parasitol.* 42 (6), 557–566. doi: 10.1016/j.ijpara.2012.04.006

Liehl, P., Zuzarte-Luis, V., Chan, J., Zillinger, T., Baptista, F., Carapau, D., et al. (2014). Host-cell sensors for *Plasmodium* activate innate immunity against liver-stage infection. *Nat. Med.* 20 (1), 47–53. doi: 10.1038/nm.3424

Liehl, P., Meireles, P., Albuquerque, I. S., Pinkevych, M., Baptista, F., Mota, M. M., et al. (2015). Innate immunity induced by *Plasmodium* liver infection inhibits malaria reinfections. *Infect. Immun.* 83 (3), 1172–1180. doi: 10.1128/IAI.02796-14

Loo, Y. M., and Gale, M. (2011). Immune Signaling by RIG-I-like Receptors. *Immunity* 34 (5), 680–692. doi: 10.1016/j.immuni.2011.05.003

Lu, Z. Y., Serghides, L., Patel, S. N., Degousee, N., Rubin, B. B., Krishnegowda, G., et al. (2006). Disruption of JNK2 decreases the cytokine response to *Plasmodium falciparum* glycosylphosphatidylinositol in vitro and confers protection in a cerebral malaria model. *J. Immunol.* 177 (9), 6344–6352. doi: 10.4049/jimmunol.177.9.6344

Lukhele, S., Boukhaled, G. M., and Brooks, D. G. (2019). Type I interferon signaling, regulation and gene stimulation in chronic virus infection. *Semin. Immunol.* 43, 101277. doi: 10.1016/j.smim.2019.05.001

Luty, A. J., Perkins, D. J., Lell, B., Schmidt-Ott, R., Lehman, L. G., Luckner, D., et al. (2000). Low interleukin-12 activity in severe *Plasmodium falciparum* malaria. *Infect. Immun.* 68 (7), 3909–3915. doi: 10.1128/iai.68.7.3909-3915.2000

Malmgaard, L. (2004). Induction and regulation of IFNs during viral infections. *J. Interferon Cytokine Res.* 24 (8), 439–454. doi: 10.1089/1079990041689665

Mangano, V. D., Luoni, G., Rockett, K. A., Sirima, B. S., Konate, A., Forton, J., et al. (2008). Interferon regulatory factor-1 polymorphisms are associated with the control of *Plasmodium falciparum* infection. *Genes Immun.* 9 (2), 122–129. doi: 10.1038/sj.gene.6364456

Meylan, E., Curran, J., Hofmann, K., Moradpour, D., Binder, M., Bartenschlager, R., et al. (2005). Cardif is an adaptor protein in the RIG-I antiviral pathway and is targeted by hepatitis C virus. *Nature* 437 (7062), 1167–1172. doi: 10.1038/nature04193

Miller, J. L., Sack, B. K., Baldwin, M., Vaughan, A. M., and Kappe, S. H. I. (2014). Interferon-Mediated Innate Immune Responses against Malaria Parasite Liver Stages. *Cell Rep.* 7 (2), 436–447. doi: 10.1016/j.celrep.2014.03.018

Minkah, N. K., Wilder, B. K., Sheikh, A. A., Martinson, T., Wegmair, L., Vaughan, A. M., et al. (2019). Innate immunity limits protective adaptive immune responses against pre-erythrocytic malaria parasites. *Nat. Commun.* 10 (1), 3950. doi: 10.1038/s41467-019-11819-0

Mo, A. X., and McGugan, G. (2018). Understanding the Liver-Stage Biology of Malaria Parasites: Insights to Enable and Accelerate the Development of a Highly Efficacious Vaccine. *Am. J. Trop. Med. Hyg.* 99 (4), 827–832. doi: 10.4269/ajtmh.17-0895

Montes de Oca, M., Kumar, R., Rivera, F. L., Amante, F. H., Sheel, M., Faleiro, R. J., et al. (2016). Type I Interferons Regulate Immune Responses in Humans with Blood-Stage *Plasmodium falciparum* Infection. *Cell Rep.* 17 (2), 399–412. doi: 10.1016/j.celrep.2016.09.015

Morrell, C. N., Srivastava, K., Swaim, A., Lee, M. T., Chen, J., Nagineni, C., et al. (2011). Beta interferon suppresses the development of experimental cerebral malaria. *Infect. Immun.* 79 (4), 1750–1758. doi: 10.1128/IAI.00810-10

Murphy, J. R., and Lefford, M. J. (1979). Host defenses in murine malaria: evaluation of the mechanisms of immunity to *Plasmodium yoelii* infection. *Infect. Immun.* 23 (2), 384–391. doi: 10.1128/IAI.23.2.384-391.1979

Naik, R. S., Branch, O. H., Woods, A. S., Vijaykumar, M., Perkins, D. J., Nahlen, B. L., et al. (2000). Glycosylphosphatidylinositol anchors of *Plasmodium falciparum*: Molecular characterization and naturally elicited antibody response that may provide immunity to malaria pathogenesis. *J. Exp. Med.* 192 (11), 1563–1575. doi: 10.1084/jem.192.11.1563

Ng, C. T., Sullivan, B. M., Teijaro, J. R., Lee, A. M., Welch, M., Rice, S., et al. (2015). Blockade of interferon Beta, but not interferon alpha, signaling controls persistent viral infection. *Cell Host Microbe* 17 (5), 653–661. doi: 10.1016/j.chom.2015.04.005

Ng, C. T., Mendoza, J. L., Garcia, K. C., and Oldstone, M. B. (2016). Alpha and Beta Type 1 Interferon Signaling: Passage for Diverse Biologic Outcomes. *Cell* 164 (3), 349–352. doi: 10.1016/j.cell.2015.12.027

Nie, L., Cai, S. Y., Shao, J. Z., and Chen, J. (2018). Toll-Like Receptors, Associated Biological Roles, and Signaling Networks in Non-Mammals. *Front. Immunol.* 9:1523. doi: 10.3389/fimmu.2018.01523

Ning, S., Pagano, J. S., and Barber, G. N. (2011). IRF7: activation, regulation, modification and function. *Genes Immun.* 12 (6), 399–414. doi: 10.1038/gene.2011.21

Nolte-'t Hoen, E. N. M., Buermans, H. P. J., Waasdorp, M., Stoorvogel, W., Wauben, M. H. M., and 't Hoen, P. A. C. (2012). Deep sequencing of RNA from immune cell-derived vesicles uncovers the selective incorporation of small non-coding RNA biotypes with potential regulatory functions. *Nucleic Acids Res.* 40 (18), 9272–9285. doi: 10.1093/nar/gks658

Ohto, U., and Shimizu, T. (2016). Structural aspects of nucleic acid-sensing Toll-like receptors. *Biophys. Rev.* 8 (1), 33–43. doi: 10.1007/s12551-015-0187-1

Ojo-Amaize, E. A., Salimonu, L. S., Williams, A. I., Akinwolere, O. A., Shabo, R., Alm, G. V., et al. (1981). Positive correlation between degree of parasitemia, interferon titers, and natural killer cell activity in *Plasmodium falciparum*-infected children. *J. Immunol.* 127 (6), 2296–2300.

Olivier, M., Van Den Ham, K., Shio, M. T., Kassa, F. A., and Fougeray, S. (2014). Malarial pigment hemozoin and the innate inflammatory response. *Front. Immunol.* 5:25. doi: 10.3389/fimmu.2014.00025

O'Brien, J. D., Iqbal, Z., Wendler, J., and Amenga-Etego, L. (2016). Inferring Strain Mixture within Clinical *Plasmodium falciparum* Isolates from Genomic Sequence Data. *PloS Comput. Biol.* 12 (6), e1004824. doi: 10.1371/journal.pcbi.1004824

O'Neill, L. A., Brown, Z., and Ward, S. G. (2003). Toll-like receptors in the spotlight. *Nat. Immunol.* 4 (4):299. doi: 10.1038/ni0403-299

Pagola, S., Stephens, P. W., Bohle, D. S., Kosar, A. D., and Madsen, S. K. (2000). The structure of malaria pigment beta-haematin. *Nature* 404 (6775), 307–310. doi: 10.1038/35005132

Palomo, J., Fauconnier, M., Coquard, L., Gilles, M., Meme, S., Szeremeta, F., et al. (2013). Type I interferons contribute to experimental cerebral malaria development in response to sporozoite or blood-stage *Plasmodium berghei* ANKA. *Eur. J. Immunol.* 43 (10), 2683–2695. doi: 10.1002/eji.201343327

Pandey, A. V., and Tekwani, B. L. (1996). Formation of haemozoin/beta-haematin under physiological conditions is not spontaneous. *FEBS Lett.* 393 (2-3), 189–193. doi: 10.1016/0014-5793(96)00881-2

Parmar, R., Patel, H., Yadav, N., Parikh, R., Patel, K., Mohankrishnan, A., et al. (2018). Infectious Sporozoites of *Plasmodium berghei* Effectively Activate Liver CD8alpha(+) Dendritic Cells. *Front. Immunol.* 9:192. doi: 10.3389/fimmu.2018.00192

Parroche, P., Lauw, F. N., Goutagny, N., Latz, E., Monks, B. G., Visintin, A., et al. (2007). Malaria hemozoin is immunologically inert but radically enhances innate responses by presenting malaria DNA to Toll-like receptor 9. *Proc. Natl. Acad. Sci. U.S.A.* 104 (6), 1919–1924. doi: 10.1073/pnas.0608745104

Pattaradilokrat, S., Li, J., Wu, J., Qi, Y., Eastman, R. T., Zilversmit, M., et al. (2014). Plasmodium genetic loci linked to host cytokine and chemokine responses. *Genes Immun.* 15 (3), 145–152. doi: 10.1038/gene.2013.74

Penet, M. F., Abou-Hamdan, M., Coltel, N., Cornille, E., Grau, G. E., de Reggi, M., et al. (2008). Protection against cerebral malaria by the low-molecular-weight thiol pantethine. *Proc. Natl. Acad. Sci. U. S. A.* 105 (4), 1321–1326. doi: 10.1073/pnas.0706867105

Peng, Y. C., Qi, Y., Zhang, C., Yao, X., Wu, J., Pattaradilokrat, S., et al. (2020). *Plasmodium yoelii* Erythrocyte-Binding-like Protein Modulates Host Cell Membrane Structure, Immunity, and Disease Severity. *mBio* 11 (1), e02995–e02919. doi: 10.1128/mBio.02995-19

Pestka, S., Krause, C. D., and Walter, M. R. (2004). Interferons, interferon-like cytokines, and their receptors. *Immunol. Rev.* 202, 8–32. doi: 10.1111/j.0105-2896.2004.00204.x

Pichyangkul, S., Yongvanitchit, K., Kum-Arb, U., Hemmi, H., Akira, S., Krieg, A. M., et al. (2004). Malaria blood stage parasites activate human plasmacytoid dendritic cells and murine dendritic cells through a toll-like receptor 9-dependent pathway. *J. Immunol.* 172 (8), 4926–4933. doi: 10.4049/jimmunol.172.8.4926

Prudencio, M., Rodriguez, A., and Mota, M. M. (2006). The silent path to thousands of merozoites: the *Plasmodium* liver stage. *Nat. Rev. Microbiol.* 4 (11), 849–856. doi: 10.1038/nrmicro1529

Radtke, A. J., Kastenmuller, W., Espinosa, D. A., Gerner, M. Y., Tse, S. W., Sinnis, P., et al. (2015). Lymph-node resident CD8alpha+ dendritic cells capture antigens from migratory malaria sporozoites and induce CD8+ T cell responses. *PloS Pathog.* 11 (2), e1004637. doi: 10.1371/journal.ppat.1004637

Ramirez-Ortiz, Z. G., Lee, C. K., Wang, J. P., Boon, L., Specht, C. A., and Levitz, S. M. (2011). A nonredundant role for plasmacytoid dendritic cells in host defense against the human fungal pathogen *Aspergillus fumigatus*. *Cell Host Microbe* 9 (5), 415–424. doi: 10.1016/j.chom.2011.04.007

Ratajczak, J., Miekus, K., Kucia, M., Zhang, J., Reca, R., Dvorak, P., et al. (2006). Embryonic stem cell-derived microvesicles reprogram hematopoietic progenitors: evidence for horizontal transfer of mRNA and protein delivery. *Leukemia* 20 (5), 847–856. doi: 10.1038/sj.leu.2404132

Ridder, K., Keller, S., Dams, M., Rupp, A. K., Schlaudraff, J., Del Turco, D., et al. (2014). Extracellular vesicle-mediated transfer of genetic information between the hematopoietic system and the brain in response to inflammation. *J. Neuroimmunol.* 275 (1-2), 165–165. doi: 10.1016/j.jneuroim.2014.08.444

Rocha, B. C., Marques, P. E., Leoratti, F. M. S., Junqueira, C., Pereira, D. B., Antonelli, L., et al. (2015). Type I Interferon Transcriptional Signature in Neutrophils and Low-Density Granulocytes Are Associated with Tissue Damage in Malaria. *Cell Rep.* 13 (12), 2829–2841. doi: 10.1016/j.celrep.2015.11.055

Ropert, C., and Gazzinelli, R. T. (2000). Signaling of immune system cells by glycosylphosphatidylinositol (GPI) anchor and related structures derived from parasitic protozoa. *Curr. Opin. Microbiol.* 3 (4), 395–403. doi: 10.1016/s1369-5274(00)00111-9

Rubartelli, A., and Lotze, M. T. (2007). Inside, outside, upside down: damage-associated molecular-pattern molecules (DAMPs) and redox. *Trends Immunol.* 28 (10), 429–436. doi: 10.1016/j.it.2007.08.004

Rytel, M. W., Rose, H. D., and Stewart, R. D. (1973). Absence of circulating interferon in patients with malaria and with American trypanosomiasis. *Proc. Soc. Exp. Biol. Med.* 144 (1), 122–123. doi: 10.3181/00379727-144-37539

Sarasin-Filipowicz, M., Wang, X., Yan, M., Duong, F. H., Poli, V., Hilton, D. J., et al. (2009). Alpha interferon induces long-lasting refractoriness of JAK-STAT

signaling in the mouse liver through induction of USP18/UBP43. *Mol. Cell Biol.* 29 (17), 4841–4851. doi: 10.1128/MCB.00224-09

Sasai, M., Linehan, M. M., and Iwasaki, A. (2010). Bifurcation of Toll-like receptor 9 signaling by adaptor protein 3. *Science* 329 (5998), 1530–1534. doi: 10.1126/science.1187029

Schneider, W. M., Chevillotte, M. D., and Rice, C. M. (2014). Interferon-stimulated genes: a complex web of host defenses. *Annu. Rev. Immunol.* 32, 513–545. doi: 10.1146/annurev-immunol-032713-120231

Schofield, L., and Grau, G. E. (2005). Immunological processes in malaria pathogenesis. *Nat. Rev. Immunol.* 5 (9), 722–735. doi: 10.1038/nri1686

Schofield, L., and Hackett, F. (1993). Signal transduction in host cells by a glycosylphosphatidylinositol toxin of malaria parasites. *J. Exp. Med.* 177 (1), 145–153. doi: 10.1084/jem.177.1.145

Schwarzer, E., Turrini, F., Ulliers, D., Giribaldi, G., Ginsburg, H., and Arese, P. (1992). Impairment of macrophage functions after ingestion of *Plasmodium falciparum*-infected erythrocytes or isolated malarial pigment. *J. Exp. Med.* 176 (4), 1033–1041. doi: 10.1084/jem.176.4.1033

Schwarzer, E., Alessio, M., Ulliers, D., and Arese, P. (1998). Phagocytosis of the malarial pigment, hemozoin, impairs expression of major histocompatibility complex class II antigen, CD54, and CD11c in human monocytes. *Infect. Immun.* 66 (4), 1601–1606. doi: 10.1128/IAI.66.4.1601-1606.1998

Schwarzer, E., Bellomo, G., Giribaldi, G., Ulliers, D., and Arese, P. (2001). Phagocytosis of malarial pigment haemozoin by human monocytes: a confocal microscopy study. *Parasitol* 123 (Pt 2), 125–131. doi: 10.1017/s0031182001008216

Scragg, I. G., Hensmann, M., Bate, C. A., and Kwiatkowski, D. (1999). Early cytokine induction by *Plasmodium falciparum* is not a classical endotoxin-like process. *Eur. J. Immunol.* 29 (8), 2636–2644. doi: 10.1002/(SICI)1521-4141(199908)29:08<2636::AID-IMMU2636>3.0.CO;2-Y

Sebina, I., James, K. R., Soon, M. S., Fogg, L. G., Best, S. E., Labastida Rivera, F., et al. (2016). IFNAR1-Signalling Obstructs ICOS-mediated Humoral Immunity during Non-lethal Blood-Stage *Plasmodium* Infection. *PloS Pathog.* 12 (11), e1005999. doi: 10.1371/journal.ppat.1005999

Seth, R. B., Sun, L. J., Ea, C. K., and Chen, Z. J. J. (2005). Identification and characterization of MAVS, a mitochondrial antiviral signaling protein that activates NF-kappa B and IRF3. *Cell* 122 (5), 669–682. doi: 10.1016/j.cell.2005.08.012

Shang, G., Zhu, D., Li, N., Zhang, J., Zhu, C., Lu, D., et al. (2012). Crystal structures of STING protein reveal basis for recognition of cyclic di-GMP. *Nat. Struct. Mol. Biol.* 19 (7), 725–727. doi: 10.1038/nsmb.2332

Sharma, S., DeOliveira, R. B., Kalantari, P., Parroche, P., Goutagny, N., Jiang, Z., et al. (2011). Innate immune recognition of an AT-rich stem-loop DNA motif in the *Plasmodium falciparum* genome. *Immunity* 35 (2), 194–207. doi: 10.1016/j.immuni.2011.05.016

Sheehan, K. C., Lazear, H. M., Diamond, M. S., and Schreiber, R. D. (2015). Selective Blockade of Interferon-alpha and -beta Reveals Their Non-Redundant Functions in a Mouse Model of West Nile Virus Infection. *PloS One* 10 (5), e0128636. doi: 10.1371/journal.pone.0128636

Shio, M. T., Eisenbarth, S. C., Savaria, M., Vinet, A. F., Bellemare, M. J., Harder, K. W., et al. (2009). Malarial hemozoin activates the NLRP3 inflammasome through Lyn and Syk kinases. *PloS Pathog.* 5 (8), e1000559. doi: 10.1371/journal.ppat.1000559

Silva-Barrios, S., and Stager, S. (2017). Protozoan Parasites and Type I IFNs. *Front. Immunol.* 8:14. doi: 10.3389/fimmu.2017.00014

Sinha, A., Ignatchenko, V., Ignatchenko, A., Mejia-Guerrero, S., and Kislinger, T. (2014). In-depth proteomic analyses of ovarian cancer cell line exosomes reveals differential enrichment of functional categories compared to the. NCI 60 proteome. *Biochem. Biophys. Res. Commun.* 445 (4), 694–701. doi: 10.1016/j.bbrc.2013.12.070

Sisquella, X., Ofir-Birin, Y., Pimentel, M. A., Cheng, L., Abou Karam, P., Sampaio, N. G., et al. (2017). Malaria parasite DNA-harbouring vesicles activate cytosolic immune sensors. *Nat. Commun.* 8, 1985. doi: 10.1038/s41467-017-02083-1

Skorokhod, O. A., Alessio, M., Mordmuller, B., Arese, P., and Schwarzer, E. (2004). Hemozoin (malarial pigment) inhibits differentiation and maturation of human monocyte-derived dendritic cells: a peroxisome proliferator-activated receptor-gamma-mediated effect. *J. Immunol.* 173 (6), 4066–4074. doi: 10.4049/jimmunol.173.6.4066

Spaulding, E., Fooksman, D., Moore, J. M., Saidi, A., Feintuch, C. M., Reizis, B., et al. (2016). STING-Licensed Macrophages Prime Type I IFN Production by Plasmacytoid Dendritic Cells in the Bone Marrow during Severe *Plasmodium yoelii* Malaria. *PloS Pathog.* 12 (10), e1005975. doi: 10.1371/journal.ppat.1005975

Stevenson, M. M., and Riley, E. M. (2004). Innate immunity to malaria. *Nat. Rev. Immunol.* 4 (3), 169–180. doi: 10.1038/nri1311

Subramaniam, K. S., Spaulding, E., Ivan, E., Mutimura, E., Kim, R. S., Liu, X., et al. (2015). The T-Cell Inhibitory Molecule Butyrophilin-Like 2 Is Up-regulated in Mild *Plasmodium falciparum* Infection and Is Protective During Experimental Cerebral Malaria. *J. Infect. Dis.* 212 (8), 1322–1331. doi: 10.1093/infdis/jiv217

Sun, W., Li, Y., Chen, L., Chen, H., You, F., Zhou, X., et al. (2009). ERIS, an endoplasmic reticulum IFN stimulator, activates innate immune signaling through dimerization. *Proc. Natl. Acad. Sci. U.S.A.* 106 (21), 8653–8658. doi: 10.1073/pnas.0900850106

Sun, L., Wu, J., Du, F., Chen, X., and Chen, Z. J. (2013). Cyclic GMP-AMP synthase is a cytosolic DNA sensor that activates the type I interferon pathway. *Science* 339 (6121), 786–791. doi: 10.1126/science.1232458

Sweeney, S. S., Hammaker, D., and Firestein, G. S. (2004). Novel functions of the IKK-related kinase IKK in RA: Regulation of c-jun and metalloproteinases. *Arthritis Rheum.* 50 (9), S654–S654.

Takaoka, A., and Yamada, T. (2019). Regulation of signaling mediated by nucleic acid sensors for innate interferon-mediated responses during viral infection. *Int. Immunol.* 31 (8), 477–488. doi: 10.1093/intimm/dxz034

Takeda, K., Kaisho, T., and Akira, S. (2003). Toll-like receptors. *Annu. Rev. Immunol.* 21, 335–376. doi: 10.1146/annurev.immunol.21.120601.141126

Takeuchi, O., and Akira, S. (2010). Pattern Recognition Receptors and Inflammation. *Cell* 140 (6), 805–820. doi: 10.1016/j.cell.2010.01.022

Tamura, T., Kimura, K., Yui, K., and Yoshida, S. (2015). Reduction of conventional dendritic cells during *Plasmodium* infection is dependent on activation induced cell death by type I and II interferons. *Exp. Parasitol.* 159, 127–135. doi: 10.1016/j.exppara.2015.09.010

Tang, D., Kang, R., Coyne, C. B., Zeh, H. J., and Lotze, M. T. (2012). PAMPs and DAMPs: signal 0s that spur autophagy and immunity. *Immunol. Rev.* 249 (1), 158–175. doi: 10.1111/j.1600-065X.2012.01146.x

Tauro, B. J., Greening, D. W., Mathias, R. A., Ji, H., Mathivanan, S., Scott, A. M., et al. (2012). Comparison of ultracentrifugation, density gradient separation, and immunoaffinity capture methods for isolating human colon cancer cell line LIM1863-derived exosomes. *Methods* 56 (2), 293–304. doi: 10.1016/j.ymeth.2012.01.002

Teijaro, J. R., Ng, C., Lee, A. M., Sullivan, B. M., Sheehan, K. C., Welch, M., et al. (2013). Persistent LCMV infection is controlled by blockade of type I interferon signaling. *Science* 340 (6129), 207–211. doi: 10.1126/science.1235214

Torre, S., Polyak, M. J., Langlais, D., Fodil, N., Kennedy, J. M., Radovanovic, I., et al. (2017). USP15 regulates type I interferon response and is required for pathogenesis of neuroinflammation. *Nat. Immunol.* 18 (1), 54–63. doi: 10.1038/ni.3581

Tricarico, C., Clancy, J., and D'Souza-Schorey, C. (2017). Biology and biogenesis of shed microvesicles. *Small GTPases* 8 (4), 220–232. doi: 10.1080/21541248.2016.1215283

Uze, G., Schreiber, G., Piehler, J., and Pellegrini, S. (2007). The receptor of the type I interferon family. *Curr. Top. Microbiol. Immunol.* 316, 71–95. doi: 10.1007/978-3-540-71329-6_5

Valadi, H., Ekstrom, K., Bossios, A., Sjostrand, M., Lee, J. J., and Lotvall, J. O. (2007). Exosome-mediated transfer of mRNAs and microRNAs is a novel mechanism of genetic exchange between cells. *Nat. Cell Biol.* 9 (6), 654–U672. doi: 10.1038/ncb1596

Vaughan, A. M., Sack, B. K., Dankwa, D., Minkah, N., Nguyen, T., Cardamone, H., et al. (2018). A *Plasmodium* Parasite with Complete Late Liver Stage Arrest Protects against Preerythrocytic and Erythrocytic Stage Infection in Mice. *Infect. Immun.* 86 (5), e00088–18. doi: 10.1128/IAI.00088-18

Venereau, E., Ceriotti, C., and Bianchi, M. E. (2015). DAMPs from Cell Death to New Life. *Front. Immunol.* 6:422. doi: 10.3389/fimmu.2015.00422

Vigario, A. M., Belnoue, E., Cumano, A., Marussig, M., Miltgen, F., Landau, I., et al. (2001). Inhibition of *Plasmodium yoelii* blood-stage malaria by interferon alpha through the inhibition of the production of its target cell, the reticulocyte. *Blood* 97 (12), 3966–3971. doi: 10.1182/blood.v97.12.3966

Vigario, A. M., Belnoue, E., Gruner, A. C., Mauduit, M., Kayibanda, M., Deschemin, J. C., et al. (2007). Recombinant human IFN-alpha inhibits cerebral malaria and reduces parasite burden in mice. *J. Immunol.* 178 (10), 6416–6425. doi: 10.4049/jimmunol.178.10.6416

Vijay, K. (2018). Toll-like receptors in immunity and inflammatory diseases: Past, present, and future. *Int. Immunopharmacol.* 59, 391–412. doi: 10.1016/j.intimp.2018.03.002

Voisine, C., Mastelic, B., Sponaas, A. M., and Langhorne, J. (2010). Classical CD11c+ dendritic cells, not plasmacytoid dendritic cells, induce T cell responses to *Plasmodium chabaudi* malaria. *Int. J. Parasitol.* 40 (6), 711–719. doi: 10.1016/j.ijpara.2009.11.005

von der Weid, T., Kitamura, D., Rajewsky, K., and Langhorne, J. (1994). A dual role for B cells in *Plasmodium chabaudi chabaudi* (AS) infection? *Res. Immunol.* 145 (6), 412–419. doi: 10.1016/s0923-2494(94)80170-3

Williams, C., Rodriguez-Barrueco, R., Silva, J. M., Zhang, W. J., Hearn, S., Elemento, O., et al. (2014). Double-stranded DNA in exosomes: a novel biomarker in cancer detection. *Cell Res.* 24 (6), 766–769. doi: 10.1038/cr.2014.44

Wilson, E. B., Yamada, D. H., Elsaesser, H., Herskovitz, J., Deng, J., Cheng, G., et al. (2013). Blockade of chronic type I interferon signaling to control persistent LCMV infection. *Science* 340 (6129), 202–207. doi: 10.1126/science.1235208

Wu, J., and Chen, Z. J. (2014). Innate immune sensing and signaling of cytosolic nucleic acids. *Annu. Rev. Immunol.* 32, 461–488. doi: 10.1146/annurev-immunol-032713-120156

Wu, X. Z., Gowda, N. M., Kumar, S., and Gowda, D. C. (2010). Protein-DNA Complex Is the Exclusive Malaria Parasite Component That Activates Dendritic Cells and Triggers Innate Immune Responses. *J. Immunol.* 184 (8), 4338–4348. doi: 10.4049/jimmunol.0903824

Wu, J., Sun, L., Chen, X., Du, F., Shi, H., Chen, C., et al. (2013). Cyclic GMP-AMP is an endogenous second messenger in innate immune signaling by cytosolic DNA. *Science* 339 (6121), 826–830. doi: 10.1126/science.1229963

Wu, J., Tian, L., Yu, X., Pattaradilokrat, S., Li, J., Wang, M., et al. (2014). Strain-specific innate immune signaling pathways determine malaria parasitemia dynamics and host mortality. *Proc. Natl. Acad. Sci. U.S.A.* 111 (4), E511–E520. doi: 10.1073/pnas.1316467111

Wu, J., Cai, B., Sun, W., Huang, R., Liu, X., Lin, M., et al. (2015a). Genome-wide Analysis of Host-*Plasmodium yoelii* Interactions Reveals Regulators of the Type I Interferon Response. *Cell Rep.* 12 (4), 661–672. doi: 10.1016/j.celrep.2015.06.058

Wu, X., Gowda, N. M., and Gowda, D. C. (2015b). Phagosomal Acidification Prevents Macrophage Inflammatory Cytokine Production to Malaria, and Dendritic Cells Are the Major Source at the Early Stages of Infection: Implication for malaria protective immunity development. *J. Biol. Chem.* 290 (38), 23135–23147. doi: 10.1074/jbc.M115.671065

Wu, J., Xia, L., Yao, X., Yu, X., Tumas, K. C., Sun, W., et al. (2020). The E3 ubiquitin ligase MARCH1 regulates antimalaria immunity through interferon signaling and T cell activation. *Proc. Natl. Acad. Sci. U.S.A.* 117 (28), 16567–16578. doi: 10.1073/pnas.2004332117

Wykes, M. N., and Good, M. F. (2008). What really happens to dendritic cells during malaria? *Nat. Rev. Microbiol.* 6 (11), 864–870. doi: 10.1038/nrmicro1988

Xia, L., Wu, J., Pattaradilokrat, S., Tumas, K., He, X., Peng, Y. C., et al. (2018). Detection of host pathways universally inhibited after *Plasmodium yoelii* infection for immune intervention. *Sci. Rep.* 8 (1), 15280. doi: 10.1038/s41598-018-33599-1

Xu, H., Hodder, A. N., Yan, H., Crewther, P. E., Anders, R. F., and Good, M. F. (2000). CD4+ T cells acting independently of antibody contribute to protective immunity to *Plasmodium chabaudi* infection after apical membrane antigen 1 immunization. *J. Immunol.* 165 (1), 389–396. doi: 10.4049/jimmunol.165.1.389

Xu, L. G., Wang, Y. Y., Han, K. J., Li, L. Y., Zhai, Z. H., and Shu, H. B. (2005). VISA is an adapter protein required for virus-triggered IFN-beta signaling. *Mol. Cell* 19 (6), 727–740. doi: 10.1016/j.molcel.2005.08.014

Yao, X., Wu, J., Lin, M., Sun, W., He, X., Gowda, C., et al. (2016). Increased CD40 Expression Enhances Early STING-Mediated Type I Interferon Response and Host Survival in a Rodent Malaria Model. *PloS Pathog.* 12 (10), e1005930. doi: 10.1371/journal.ppat.1005930

Ye, W. J., Chew, M., Hou, J., Lai, F., Leopold, S. J., Loo, H. L., et al. (2018). Microvesicles from malaria-infected red blood cells activate natural killer cells via MDA5 pathway. *PloS Pathog.* 14 (10), e1007298. doi: 10.1371/journal.ppat.1007298

Yoneyama, M., Kikuchi, M., Matsumoto, K., Imaizumi, T., Miyagishi, M., Taira, K., et al. (2005). Shared and unique functions of the DExD/H-box helicases RIG-I, MDA5, and LGP2 in antiviral innate immunity. *J. Immunol.* 175 (5), 2851–2858. doi: 10.4049/jimmunol.175.5.2851

Yoshimura, A., Naka, T., and Kubo, M. (2007). SOCS proteins, cytokine signalling and immune regulation. *Nat. Rev. Immunol.* 7 (6), 454–465. doi: 10.1038/nri2093

Yu, X., Cai, B., Wang, M., Tan, P., Ding, X., Wu, J., et al. (2016). Cross-Regulation of Two Type I Interferon Signaling Pathways in Plasmacytoid Dendritic Cells Controls Anti-malaria Immunity and Host Mortality. *Immunity* 45 (5), 1093–1107. doi: 10.1016/j.immuni.2016.10.001

Yu, X., Du, Y., Cai, C., Cai, B., Zhu, M., Xing, C., et al. (2018). Inflammasome activation negatively regulates MyD88-IRF7 type I IFN signaling and anti-malaria immunity. *Nat. Commun.* 9 (1), 4964. doi: 10.1038/s41467-018-07384-7

Zander, R. A., Guthmiller, J. J., Graham, A. C., Pope, R. L., Burke, B. E., Carr, D. J., et al. (2016). Type I Interferons Induce T Regulatory 1 Responses and Restrict Humoral Immunity during Experimental Malaria. *PloS Pathog.* 12 (10), e1005945. doi: 10.1371/journal.ppat.1005945

Zheng, Y., and Gao, C. (2020). Fine-tuning of antiviral innate immunity by ubiquitination. *Adv. Immunol.* 145, 95–128. doi: 10.1016/bs.ai.2019.11.004

Zhong, B., Yang, Y., Li, S., Wang, Y. Y., Li, Y., Diao, F., et al. (2008). The adaptor protein MITA links virus-sensing receptors to IRF3 transcription factor activation. *Immunity* 29 (4), 538–550. doi: 10.1016/j.immuni.2008.09.003

Zhu, J., Krishnegowda, G., and Gowda, D. C. (2005). Induction of proinflammatory responses in macrophages by the glycosylphosphatidylinositols of *Plasmodium falciparum*: the requirement of extracellular signal-regulated kinase, p38, c-Jun N-terminal kinase and NF-kappaB pathways for the expression of proinflammatory cytokines and nitric oxide. *J. Biol. Chem.* 280 (9), 8617–8627. doi: 10.1074/jbc.M413539200

Zhu, J. Z., Wu, X. Z., Goel, S., Gowda, N. M., Kumar, S., Krishnegowda, G., et al. (2009). MAPK-activated Protein Kinase 2 Differentially Regulates *Plasmodium falciparum* Glycosylphosphatidylinositol-induced Production of Tumor Necrosis Factor-alpha and Interleukin-12 in Macrophages. *J. Biol. Chem.* 284 (23), 15750–15761. doi: 10.1074/jbc.M901111200

Zhu, S. J., Hendry, J. A., Almagro-Garcia, J., Pearson, R. D., Amato, R., Miles, A., et al. (2019). The origins and relatedness structure of mixed infections vary with local prevalence of *P. falciparum* malaria. *Elife* 8, e40845. doi: 10.7554/eLife.40845

Conflict of Interest: The authors declare that the research was conducted in the absence of any commercial or financial relationships that could be construed as a potential conflict of interest.

frontiers in Cellular and Infection Microbiology

ORIGINAL RESEARCH
published: 17 December 2020
doi: 10.3389/fcimb.2020.591046

Generation of a Genetically Modified Chimeric *Plasmodium falciparum* Parasite Expressing *Plasmodium vivax* Circumsporozoite Protein for Malaria Vaccine Development

Yukiko Miyazaki[1‡], Catherin Marin-Mogollon[1‡], Takashi Imai[1,2], António M. Mendes[3], Rianne van der Laak[4], Angelika Sturm[4], Fiona J. A. Geurten[1], Shinya Miyazaki[1], Severine Chevalley-Maurel[1], Jai Ramesar[1], Surendra K. Kolli[1], Hans Kroeze[1], Roos van Schuijlenburg[1], Ahmed M. Salman[5], Brandon K. Wilder[6], Arturo Reyes-Sandoval[5], Koen J. Dechering[4], Miguel Prudêncio[3], Chris J. Janse[1], Shahid M. Khan[1†] and Blandine Franke-Fayard[1]*

[1] Department of Parasitology, Leiden University Medical Center, Leiden, Netherlands, [2] Department of Infectious Diseases and Host Defense, Gunma University Graduate School of Medicine, Maebashi, Japan, [3] Instituto de Medicina Molecular João Lobo Antunes, Faculdade de Medicina, Universidade de Lisboa, Lisboa, Portugal, [4] TropIQ Health Sciences, Nijmegen, Netherlands, [5] The Jenner Institute, Nuffield Department of Medicine, University of Oxford, Oxford, United Kingdom, [6] Vaccine and Gene Therapy Institute, Oregon Health and Science University, Portland, Oregon, United States

Chimeric rodent malaria parasites with the endogenous circumsporozoite protein (*csp*) gene replaced with *csp* from the human parasites *Plasmodium falciparum* (*Pf*) and *P. vivax* (*Pv*) are used in preclinical evaluation of CSP vaccines. Chimeric rodent parasites expressing *Pf*CSP have also been assessed as whole sporozoite (WSP) vaccines. Comparable chimeric *P. falciparum* parasites expressing CSP of *P. vivax* could be used both for clinical evaluation of vaccines targeting *Pv*CSP in controlled human *P. falciparum* infections and in WSP vaccines targeting *P. vivax* and *P. falciparum*. We generated chimeric *P. falciparum* parasites expressing both *Pf*CSP and *Pv*CSP. These *Pf-Pv*CSP parasites produced sporozoite comparable to wild type *P. falciparum* parasites and expressed *Pf*CSP and *Pv*CSP on the sporozoite surface. *Pf-Pv*CSP sporozoites infected human hepatocytes and induced antibodies to the repeats of both *Pf*CSP and *Pv*CSP after immunization of mice. These results support the use of *Pf-Pv*CSP sporozoites in studies optimizing vaccines targeting *Pv*CSP.

Keywords: malaria, *Plasmodium falciparum*, *Plasmodium vivax*, circumsporozoite protein (CSP), chimeric parasites, vaccines

OPEN ACCESS

Edited by:
Nicolas Blanchard, INSERM U1043 Centre de Physiopathologie de Toulouse Purpan, France

Reviewed by:
Georgina Nuri Montagna, Consejo Nacional de Investigaciones Científicas y Técnicas (CONICET), Argentina
Giulia Costa, Max Planck Institute for Infection Biology, Germany

****Correspondence:***
Blandine Franke-Fayard
bfranke@lumc.nl

[†]Deceased

[‡]These authors have contributed equally to this work

Specialty section:
This article was submitted to Parasite and Host, a section of the journal Frontiers in Cellular and Infection Microbiology

Received: *03 August 2020*
Accepted: *11 November 2020*
Published: *17 December 2020*

Citation:
Miyazaki Y, Marin-Mogollon C, Imai T, Mendes AM, van der Laak R, Sturm A, Geurten FJA, Miyazaki S, Chevalley-Maurel S, Ramesar J, Kolli SK, Kroeze H, van Schuijlenburg R, Salman AM, Wilder BK, Reyes-Sandoval A, Dechering KJ, Prudêncio M, Janse CJ, Khan SM and Franke-Fayard B (2020) Generation of a Genetically Modified Chimeric Plasmodium falciparum Parasite Expressing Plasmodium vivax Circumsporozoite Protein for Malaria Vaccine Development. Front. Cell. Infect. Microbiol. 10:591046. doi: 10.3389/fcimb.2020.591046

INTRODUCTION

Plasmodium falciparum (Pf) and *P. vivax* (*Pv*) are two major human malaria parasites that threaten public health, mainly in tropical areas. Malaria parasites are transmitted by *Anopheles* mosquitoes where they develop into infectious sporozoites that reside in the salivary glands. After a bite of an infected mosquito, sporozoites enter the blood stream of the mammalian host and migrate to the

liver where they invade hepatocytes. Inside hepatocytes, parasites replicate to form thousands of daughter merozoites, which are released into the blood and invade erythrocytes. The pre-erythrocytic stages of *Plasmodium* parasites, i.e. sporozoites and liver stages, are attractive targets of leading malaria vaccine candidates, including RTS,S, the most advanced subunit vaccine against *P. falciparum* tested in Phase III clinical trials (Kester et al., 2009; Cohen et al., 2010; Agnandji et al., 2012; Olotu et al., 2016). RTS,S is based on the circumsporozoite protein (CSP), a major surface protein expressed by *Plasmodium* sporozoites and early liver stages which plays a critical role in sporozoite formation, invasion of mosquito salivary glands and invasion of host hepatocytes (Ménard, 2000; Sinnis and Coppi, 2007; Coppi et al., 2011). This protein contains a highly conserved central repeat region flanked by N- and C -terminal regions. B-cell responses to *Pf*CSP target predominantly the protein's central NANP repeat region, generating antibodies capable of protecting animal models from *Plasmodium* infection and NANP antibodies induced by RTS,S immunization are associated with clinical protection (White et al., 2013; Foquet et al., 2014; Sack et al., 2014; Triller et al., 2017). CSP from *P. vivax* also contains an immunogenic central repeat region with two major *Pv*CSP alleles, VK210 and VK247 considered as important targets for a vaccine (Yadava and Waters, 2017). So far pre-erythrocytic subunit vaccines targeting CSP, including RTS,S, have shown low to modest protective efficacy in clinical trials and in field studies (Agnandji et al., 2015; Hoffman et al., 2015; Clemens and Moorthy, 2016; Long and Zavala, 2016; Olotu et al., 2016; Healer et al., 2017; Mahmoudi and Keshavarz, 2017) emphasizing the need to improve CSP-based vaccination approaches which requires efficient preclinical and clinical evaluation of different vaccines. Clinical evaluation of *P. falciparum* vaccines is greatly aided by the ability to vaccinate individuals and then examine vaccine efficacy in controlled human malaria infections (CHMI) (Sauerwein et al., 2011; Spring et al., 2014; Bijker et al., 2016; Stanisic et al., 2018). Although CHMI for *P. vivax* has been developed (Arévalo-Herrera et al., 2016; Bennett et al., 2016; Payne et al., 2017; Hall et al., 2019), the lack of a continuous *in vitro* culture system for *P. vivax* blood stages limits the availability of *P. vivax* sporozoites for clinical human infections. In addition, since *P. vivax* forms dormant hypnozoites in the liver, which can causing infection relapses, safe and effective means for clearance of hypnozoites are essential for *P. vivax* CHMI studies (Payne et al., 2017).

In multiple preclinical studies, the evaluation of the efficacy of CSP-based vaccines and anti-CSP antibodies has been performed using chimeric rodent malaria parasites expressing CSP from either *P. falciparum* or *P. vivax* (Espinosa et al., 2013; Gimenez et al., 2017; Salman et al., 2017; Vijayan et al., 2017; de Camargo et al., 2018; Marques et al., 2020). The availability of comparable chimeric *P. falciparum* parasites expressing *Pv*CSP would permit the analysis of protective efficacy of *Pv*CSP-based vaccines in clinical studies using *P. falciparum*-based CHMI, bypassing the need for *P. vivax* sporozoite production and hypnozoite elimination. However, in contrast to efficient *Pv*CSP expression and sporozoite production in chimeric rodent parasites, we found that chimeric *P. falciparum* lines with the *Pf*CSP gene replaced by *Pv*CSP, failed to produce salivary gland sporozoites, indicating that *Pv*CSP cannot fully complement the role of *Pf*CSP in *P. falciparum* sporozoite formation (Marin-Mogollon et al., 2018). To develop chimeric *P. falciparum* sporozoites expressing *Pv*CSP, we therefore aimed at generating a chimeric *P. falciparum* line expressing both the endogenous *Pf*CSP and an engineered *Pv*CSP. It has been shown that introducing the *P. falciparum csp* gene as an additional copy into the genome of the rodent parasite *P. berghei* (*Pb*) results in development of viable and infective sporozoites, expressing both *Pb*CSP and *Pf*CSP in pre-erythrocytic stages (Mendes et al., 2018a; Mendes et al., 2018b; Reuling et al., 2020). We used CRISPR/Cas9 gene editing to introduce a chimeric *Pvcsp* gene, containing repeats of both the VK210 and VK247 alleles, into the *Pfp47* locus of the *P. falciparum* NF54 genome. We found that these *Pf-Pv*CSP chimeric *P. falciparum* parasites produced viable, motile sporozoites expressing both *Pf*CSP and chimeric *Pv*CSP at the sporozoite surface that are infectious to primary human hepatocytes. Immunization of mice with these sporozoites resulted in induction of antibodies against the repeats of both *Pf*CSP and chimeric *Pv*CSP. These results not only show promise for the use of *Pf-Pv*CSP sporozoites in clinical CHMI studies for optimization of vaccines targeting *Pv*CSP, but also suggest that such chimeric sporozoites can be used in whole, attenuated sporozoite vaccination approaches, capable of inducing cross-protective immune responses against both *P. falciparum* and *P. vivax*.

MATERIALS AND METHODS

In Vitro Cultivation of *P. falciparum* Blood Stages

Wild type *P. falciparum* NF54 (WT NF54) parasites (Ponnudurai et al., 1981) were obtained from the Radboud University Medical Center (Nijmegen, The Netherlands). Parasites were cultured in RPMI-1640 culture medium supplemented with L-glutamine and 25mM HEPES (Gibco Life Technologies), 50 mg/L hypoxanthine (Sigma), 0.225% $NaHCO_3$ and 10% human serum at a 5% hematocrit under 4% O_2, 3% CO_2 and 93% N_2 gas-conditions at 75 rpm at 37°C in a semi-automated culture system (Infers HT Multitron and Watson Marlow 520U) as previously described (Mogollon et al., 2016). Fresh human serum and human red blood cells (RBC) were obtained from the Dutch National Blood Bank (Sanquin Amsterdam, the Netherlands; permission granted from donors for the use of blood products for malaria research and microbiology tested for safety). Production of genetically modified parasites and characterization of these parasites throughout their life cycle, including mosquito transmission, was performed under GMO permits IG 17-230_II-k and IG 17-135_III.

Laboratory Animals and Ethics Statement

Female C57BL/6Jico mice (6–7 weeks; Charles River, NL) were used. All animal experiments were granted a licence by the Competent Authority after an advice on the ethical evaluation by the Animal

Experiments Committee Leiden (AVD1160020171625). All experiments were performed in accordance with the Experiments on Animals Act (Wod, 2014), the applicable legislation in the Netherlands and in accordance with the European guidelines (EU directive no. 2010/63/EU) regarding the protection of animals used for scientific purposes. All experiments were performed in a licenced establishment for the use of experimental animals (LUMC). Mice were housed in individually ventilated cages furnished with autoclaved aspen woodchip, fun tunnel, wood chew block and nestlets at 21 ± 2°C under a 12:12 h light-dark cycle at a relative humidity of 55 ± 10%.

Anopheles Rearing

Mosquitoes from a colony of *Anopheles stephensi* (line Nijmegen SDA500) were used. Larval stages were reared in water trays at a temperature of 28 ± 1°C and a relative humidity of 80%. Adult females were transferred to incubators with a temperature of 28 ± 0.2°C and a relative humidity of 80%. For the transmission experiments, 3- to 5-day-old mosquitoes were used.

Generation of the Chimeric Pf-PvCSP Parasites

Chimeric *P. falciparum* parasites expressing both *Pf*CSP and chimeric *Pv*CSP (*Pv*CSP-chi), were generated using the previously described pLf0019 construct (Mogollon et al., 2016) (**Figure S1**), containing the *cas9* gene, together with the gRNA-donor DNA containing plasmid, pLf0109, targeting *Pfp47* which contains the *Pvcsp-chi* expression cassette. The pLf0019 construct contains a blasticidin (*bsd*) drug-selectable marker cassette and the pLf0109 gRNA-donor DNA construct contains a *hdhfr-yfcu* drug-selectable marker cassette for selection with WR99210 and 5-fluorocytocine (5-FC)(**Figure S1**). To generate pLf0109, the plasmid pLf0047 (Marin-Mogollon et al., 2019), containing two homology regions and a gRNA expression cassette targeting *Pf*p47 (PF3D7_1346800), was modified by introducing a *Pvcsp-chi* expression cassette, which was commercially synthesized (Integrated DNA Technologies, Inc.; see **Figure S2**). This *Pvcsp-chi* expression cassette contains a codon-optimized *Pvcsp* open reading frame (ORF) containing the N- and C-terminal regions of the *Pvc*sp VK210 allele that flank a chimeric repeat sequence comprising repeats of both the VK210 allele (three times the repeat GDRADGQPA/GDRAAGQPA) and the VK247 allele (three times the repeat ANGAGNQPG/ANGAGDQPG). The ORF of *Pvcsp-chi* is flanked by *Eco*RV/*Eco*RI restriction sites and cloned into pLf0040 (cut *Eco*RV/*Eco*RI) (Marin-Mogollon et al., 2018) which contains 967bp of the promoter regions of *Pfcsp* (PF3D7_0304600) and 917bp of 3'UTR of *Pfcsp* resulting in intermediate plasmid T24 (**Figure S1**). This plasmid was digested with *Apa*I/*Sac*II to obtain the complete *Pvc*sp-*chi* expression cassette containing the *Pfc*sp promoter, the *Pvcsp-chi* ORF with the chimeric VK210/VK247 repeats, and the *Pfc*sp 3'UTR. This expression cassette was inserted into vector pLf0047 (**Figure S1**) using the same restriction enzymes (*Apa*I/*Sac*II) resulting in the final construct pLf0109. Plasmids for transfection were isolated from 250 ml cultures of *Escherichia coli* XL10-Gold Ultracompetent Cells (Stratagene, NL) by maxi-prep (PureYield™ Plasmid Maxiprep System (Promega, NL) to generate 25–50 μg of DNA used per transfection. Transfection of WT *Pf*NF54 parasites was performed using the 'spontaneous uptake method' as previously described (Miyazaki et al., 2020). Briefly uninfected RBC (300 μl of packed RBCs) were transfected with the constructs pLf0019 and pLf0109 (a mixture of 25 μg of each circular plasmid in 200 μl cytomix) using the Gene Pulser Xcell electroporator (BioRad) with a single pulse (310 V, 950 μF). Subsequently, the transfected RBCs were washed with complete RPMI1640 medium and mixed with WT *Pf*NF54 infected RBC (iRBC) with a parasitemia of 0.5% and a hematocrit of 5%. These cells were transferred into a 10 ml culture flask and the cultures were maintained under standard conditions in the semi-automated culture system (Mogollon et al., 2016). Selection of transfected parasites was performed by applying double-positive drug pressure from day 3 after transfection using the drugs WR99210 (2.6 nM) and BSD (5 μg/ml). The positive drug pressure was maintained until parasites were detectable in thin blood-smears (at day 15 after transfection). Subsequently, the parasites were maintained in drug-free medium for 2–4 days until the parasitemia reached over 10%, followed by applying negative selection by addition of 5-FC (1 μM) as described before (Mogollon et al., 2016) in order to eliminate parasites that retained the donor DNA construct as episomal plasmid and to enrich for the transfected parasites containing the donor DNA integrated into the genome. Negative drug pressure in the cultures was maintained until thin blood-smears were parasite-positive (after 7 days). After the negative selection, iRBC were harvested from cultures for genotyping by diagnostic PCR and Southern blot analysis. Subsequently, selected parasites were cloned by limiting dilution as previously described (Marin-Mogollon et al., 2018). Briefly, serial dilutions were performed with uninfected RBC in complete medium (1% hematocrit and 20% serum) and cultured in a total volume of 100 μl incubated in 96-well plates, resulting in 8 rows with the following numbers of iRBC per well: 100, 10, 5, 2.5, 1.25, 0.6, 0.3, 0.15. Plates were incubated in a Candle Jar at 37°C and culture medium was changed every other day. Every 5 days RBC were added resulting in an increase of the hematocrit from 1% to 5%. At days 10 to 11, samples were collected for thick smear analysis from the rows with the highest numbers (100 and 10) of iRBC/well. At day 21 thick smears were made from samples from all rows. Clones were selected from dilutions/row with less than 40% of the wells being parasite-positive. These clones were transferred in 10 ml culture flasks at 5% hematocrit under standard culture conditions in the semi-automated culture system for collection of parasites for further genotype and phenotype analyses (see next section).

Genotyping of Pf-PvCSP Parasites

Diagnostic PCR and Southern blot analysis of digested DNA were performed from material isolated from iRBC obtained from 10 ml cultures, pelleted by centrifugation (1500 g, 5 min). RBC were then lysed with 5 ml of cold (4°C) erythrocyte lysis buffer (10× stock solution 1.5 M NH_4Cl, 0.1 M $KHCO_3$, 0.01 M Na_2EDTA; pH 7.4; (Janse et al., 2006)) and parasites were treated with proteinase-K before DNA isolation by standard

phenol-chloroform methods. Correct integration of the donor construct was analyzed by long-range PCR (LR-PCR) (primers P1/P3) and standard PCR amplification of the *Pvcsp-chi* gene (primers P4/P5), the *Pfp47* gene (primers P6/P7) and the fragment for 5' integration (5'int; primers P1/P2). The PCR fragments were amplified using KOD Hot start polymerase following standard conditions with an annealing temperature of 52°C for 15 s, 55°C for 15 s, and 63°C for 25 s and an elongation step of 68°C for 4 min for LR-PCR and with an annealing temperature of 50°C for 10 s, 55°C for 10 s, and 60°C for 10 s and an elongation step of 68°C for 1 min for the other PCRs. Southern blot analysis was performed with genomic DNA digested with *Hpa*I and *Eco*RI (4 h at 37°C) to confirm integration of the replacement of the *Pfp47* gene by the *Pvcsp-chi* expression cassette. Digested DNA was hybridized with probes targeting the *Pfp47* homology region 1 (HR1), amplified from WT *Pf*NF54 genomic DNA by PCR using the primers P8/P9 and a second probe targeting ampicillin (Amp) gene, amplified from plasmid pLf0109 by PCR using the primers P10/P11.

Phenotype analysis Pf-PvCSP parasites: blood stages, gametocytes, oocysts, and sporozoites

The growth rate of asexual blood stages of the *Pf-Pv*CSP was determined in 10 ml cultures maintained in the semi-automated culture system under standard culture conditions. Briefly, a culture with 0.1% parasitemia was established in complete culture medium at a hematocrit of 5%. Medium was changed twice daily and the culture was maintained for a period of 3 days without refreshing RBC. For determination of the course of parasitemia, triplicate samples of 100 µl were collected daily from all cultures and cells pelleted by centrifugation (9485 g; 30 s) and stained with Giemsa. *P. falciparum* gametocytes cultures were generated using standard culture conditions as previously described (Marin-Mogollon et al., 2018) with some modifications. Briefly, parasites from asexual stage cultures were diluted to a final parasitemia of 0.5%, and cultures were followed during 14 days without adding new RBC. At day 14, gametocyte development was analyzed by counting male/female gametocytes (stage V) in Giemsa stained blood smears. To assess exflagellation, 20 µl samples of the *P. falciparum* gametocyte cultures at day 14 were diluted 1:1 with Fetal Calf Serum (FCS) at room temperature and exflagellation centers were examined and quantified 10–20 min after activation in a Bürker cell counter.

For analysis of oocyst and sporozoite production, *A. stephensi* mosquitoes were fed when cultures contained mature stage V gametocytes and showed more than 80 exflagellating parasites per 10^5 erythrocytes. Mosquito feeding was performed using the standard membrane feeding assay (SMFA) (Ponnudurai et al., 1989). Oocysts were analyzed between day 10 and 12 and salivary gland sporozoites were counted at day 18 and 21 after feeding. Oocyst were counted in 10–30 midguts, dissected in a droplet of mercurochrome (1%) in distilled water on a glass slide. Midguts were covered with a coverslip and oocyst images were recorded from dissected midgut in PBS 1 X (100× magnification). For counting sporozoites, salivary glands from 30–60 mosquitoes were dissected and homogenized using a grinder in 100 µl of RPMI pH 7.2 and sporozoites were analyzed in a Bürker cell counter using phase-contrast microscopy.

Analysis of PvCSP-chi and PfCSP Expression in Sporozoites

To analyze CSP expression in fixed *Pf-Pv*CSP and WT *Pf*NF54 salivary gland sporozoites by indirect immunofluorescence assay (IFA), samples of purified salivary gland sporozoites (20 µl) were placed on a 8-well black cell-line diagnostic microscope slide (Thermo Scientific, NL), dried for 10 min, and fixed with 4% paraformaldehyde for 30 min at room temperature. After fixation the slides were washed three times with PBS and permeabilized with 20 µl of 0.5% triton in PBS and then blocked with 10% of FCS in PBS for 1h. Fixed cells were washed with PBS and incubated overnight at 4°C with the following monoclonal CSP antibodies: mouse anti-*Pf*CSP (mAb 2A10, MRA-183; 1:200 dilution of 1 mg/ml stock solution); mouse anti-*Pv*CSP VK210 (mAb 2F2; MRA-184; (Salman et al., 2017); 1:200 dilution of 109 µg/ml stock solution) and mouse anti-*Pv*CSP VK247 (mAb 2E10.E9; MRA-185; (Salman et al., 2017); 1:200 dilution of 125 µg/ml stock solution. Subsequently, cells were rinsed three times with PBS and incubated with the secondary antibodies Alexa FLuor®488/594-conjugated chicken anti-mouse (Invitrogen Detection technologies, NL at 1:500 dilution). Finally, the cells were washed again three times with PBS and stained with the DNA-specific dye Hoechst-33342 at a final concentration of 10 µM. Fixed cells were covered with 1–2 drops of an anti-fading agent (Image-iT™ FX, Life technologies), and a coverslip placed on the cells and sealed with nail polish. Stained cells were analyzed for fluorescence using a Leica fluorescence MDR microscope (100× magnification). Pictures were recorded with a DC500 digital camera microscope using Leica LAS X software with the following exposure times: Alexa 488: 1.0 s; Alexa 594: 0.6 s; Hoechst 0.2 s; bright field 0.62 s (1× gain) or with a Leica SP8 upright confocal microscope.

To analyze CSP expression of live *Pf-Pv*CSP and WT *Pf*NF54 salivary gland sporozoites by indirect immunofluorescence assay (IFA), samples of 2×10^5 salivary gland sporozoites were aliquoted in 1.5 ml Eppendorf tubes and were incubated with the corresponding antibody (mouse anti-*Pf*CSP, mouse anti-*Pv*CSP VK210 or mouse anti-*Pv*CSPVK247 (1:100 dilution) in 100 µl of 1% (v/v) FCS in PBS 1×, for 1 h on ice. Subsequently, sporozoites were rinsed with 1.5 ml of 1% (v/v) FCS in PBS and pelleted by centrifugation at 9300 g for 4 min at 4°C. The sporozoite pellet was then resuspended in 100 µl 1% FCS in PBS containing the secondary antibodies; anti–mouse IgG Alexa 488 (1:200) and incubated for 1 h on ice. Sporozoites were rinsed with 1.5 ml of 1% (v/v) FCS in PBS and pelleted by centrifugation at 9300 g for 4 min at 4°C, and the resulting pellet was resuspended in 40 µl of PBS. Of the cell suspension containing sporozoites 20 µl was placed per well of an 8-well black cell-line diagnostic microscope slide (Thermo Scientific), incubated 30 min at room temperature (RT), and fixed with 80 µl of 4% PFA in PBS 1× for 30 min at RT. Finally, the wells were washed twice with PBS and stained with 10 µM Hoechst 33342 in PBS for 15 min at RT. For microscopy analysis, the preparations were

covered with 1–2 drops of an anti-fading agent (Image-iT™ FX, Life technologies), and a coverslip was placed onto the cells and sealed with nail polish. Stained cells were analyzed for fluorescence using a Leica fluorescence MDR microscope (100× magnification). Pictures were recorded with a DC500 digital camera microscope using Leica LAS X software with the following exposure times: Alexa 488: 0.7 s; Hoechst 0.136 s; bright field 0.62 s (1× gain).

Sporozoite Gliding Assay

Sporozoite motility was determined using a sporozoite gliding assay (Stewart and Vanderberg, 1988; van Schaijk et al., 2008). Glass slides were placed in a 24 wells plate (Thermofisher, DK) and coated with an anti-*Pf*CSP monoclonal 3SP2 (courtesy of Dr. M. McCall, Radboudumc, The Netherlands; 5 µg/ml in PBS) using 200 µl per slide, and left overnight at RT. The next day freshly isolated WT *Pf*NF54 and *Pf-Pv*CSP sporozoites, collected in RPMI (Thermofisher, Gibco 42401-018) with 10% FCS (Capricornscientific, FBS-12A CP15-1439) at RT were added to anti-*Pf*CSP coated slides that were washed with PBS. Per slide 30.000 sporozoites were added (in 200 µl RPMI with 10% FCS) and these glass slides were incubated for 2.5 h at 37°C under 5% CO_2 conditions. Slides were then washed three times with PBS and fixed with 4% PFA (Thermo Scientific, NL) for 20 min at RT. Then, the slides were washed three times with PBS and blocked with 1% BSA (Roche diagnostic, DE) in PBS for 15 min. After BSA blocking, the slides were washed three times with PBS, and the primary antibody anti-Pf-3SP2 or anti-*Pv*CSP-VK210 Mab (mAb 2F2) (10 µg/ml) was added and incubated for 45 min at RT. Slides were then washed three times with PBS, and incubated with a secondary antibody goat anti-mouse Alexa fluor 488 (Invitrogen Thermofisher, Oregon, A11001) Mab (diluted 500 times in PBS) for 45 min (RT, in the dark). Finally, slides were washed three times with PBS in the dark, air dried until the slides were almost dry and mounted with Coverslips (with Image iT FX signal Enhancer; Invitrogen Thermofisher, USA) and examined with a Leica DMR fluorescent microscope with standard GFP filter for the gliding trails at 63× magnification. The percentage of gliding was calculated in 8–10 fields, measuring the number of gliding trails for the WT *Pf*NF54 sporozoites in comparison with the gliding trails for the *Pf-Pv*CSP sporozoites. The mean and standard deviation were determined for the percentage of gliding trail sporozoites.

In Vitro Infection of Primary Human Hepatocytes by Sporozoites

In vitro primary human hepatocyte maturation assay was performed as described in (Marin-Mogollon et al., 2019) with few adaptations. Cryopreserved primary human hepatocytes, obtained from Xenothech, were thawed according to the manufacturer and seeded at a density of 60,000 cells/well in a collagen-coated 96-well clear-bottomed black plate for 2 days. Medium was refreshed daily (hepatocyte medium: Williams's E medium supplemented with 10% heat inactivated fetal bovine serum, 1% penicillin-streptomycin, 1% fungizone, 0.1 lU/ml insulin, 70 µM hydrocortisone). Per well, 7 x 10^4 freshly dissected *Pf-Pv*CSP and WT *Pf*NF54 sporozoites were added to the hepatocyte monolayer. After a quick spin (10 min at 1900 g), the plate was incubated at 37°C under 5% CO2. The medium was replaced with fresh hepatocyte culture medium 3 h post-invasion, and daily for 4 days thereafter. Then, hepatocytes were fixed with ice-cold methanol for at least 10 min on ice. A standard IFA was performed using an anti-*Pf*HSP70 primary antibody (StressMarq) with an Alexa fluor 594 (Invitrogen) secondary antibody and DAPI for nuclear staining. High content imaging was performed, using the ImageXpress Pico system (Molecular Devices). Number of parasites, number of hepatocytes and size of parasites were determined using the CRX software (Molecular Devices) and data analyzed using the GraphPad software.

Rodent Immunization With Sporozoites and Antibody Production

For generation of sporozoite-extracts for immunization, salivary gland sporozoites were isolated as described in the previous sections. Aliquots of 10^5 sporozoites in 50 µl PBS were made and stored at −80°C. After two rounds of freezing and thawing, 10^5 sporozoites in 200 µl PBS were used to immunize mice by intravenous injection. Groups of six C57BL/6 mice were immunized three times with sporozoites at a 7-day interval, and blood was collected in heparinized capillaries from all mice by orbital vein puncture 1 day prior to the first and third immunization and one week after the last immunization. Plasma was collected after centrifugation of the blood samples (1500 g for 8 min at 4°C) and stored at −20°C until further analysis.

For assessment of anti-CSP antibody titers (total IgG), enzyme-linked immunosorbent assays (ELISAs) were performed. High protein-binding capacity 96-well ELISA plates (Nunc MaxiSorp™ flat-bottom) were coated with synthetic peptides (Sigma) based on the repeat sequences of *Pf*CSP and *Pv*CSP. Specifically, plates were coated with peptides with the amino acid sequence (NANP)4NVDPC for *Pf*CSP, the amino sequence GD RAD GQP AGD RAA GQP A for the *Pv*CSP VK210 and the amino sequence ANGAGNQPG ANGAGDQPG for the *Pv*CSP VK247. The plates were coated overnight at 4°C with a peptide concentration of 5 µg/ml in PBS with a volume of 50 µl per well. Plates were washed three times with 0.05% Tween20/BS (PBST) and blocked with 200 µl of PBST with 5% milk for 30 min at RT. Plates were then washed one additional time and plasma samples were diluted 1:50 in 1% milk PBST and a 3-point 1:3 dilution was carried out for each sample. After 3h incubation at RT, plates were washed three times with PBST and incubated for 1h at RT with the secondary antibody, horseradish peroxidase-labelled goat anti-mouse IgG (GE Healthcare UK) at a dilution of 1:2000. After six PBST washes, the reaction was developed by adding BD OptEIA™ TMB Substrate Reagent and incubating for 1 to 5 min at RT, before stopping the reaction by adding 50 µl Stop solution (2N H_2SO_4). Absorbance was immediately measured at 450 nm using a Tecan Infinite M200 plate reader. Data were analyzed in relation to a standard titration curve of at least 8 points starting a dilution of 1.5u/ml

of the corresponding mouse monoclonal antibody: mouse anti-*Pf*CSP (mAb 2A10, MRA-183); mouse anti-*Pv*CSP VK210 (mAb 2F2; MRA-184) and mouse anti-*Pv*CSP VK247 (mAb 2E10.E9; MRA-185). All monoclonal antibodies were produced from hybridoma cell lines obtained from BEI Resources, NIAID, and kindly provided by Elizabeth Nardin.

Statistics

Data were analyzed using GraphPad Prism software version 8.1.1 (GraphPad Software, Inc). Significance difference analyses between WT *Pf*NF54 and *Pf-Pv*CSP lines were performed using the unpaired Student's t-test. The value of $p < 0.05$ was considered statistically significant (* $p < 0.01$, ** $p < 0.001$, *** $p < 0.0001$).

RESULTS

Generation of Chimeric *Plasmodium falciparum* Sporozoites Expressing PfCSP and Chimeric PvCSP

We have previously shown that chimeric *P. falciparum* parasites with the *Pfcsp* gene replaced by the two major *Pvcsp* alleles, VK210 and VK247, do not produce salivary gland sporozoites and most oocysts degenerate before formation of sporozoites (Marin-Mogollon et al., 2018). It has been shown that viable and infectious rodent *P. berghei* sporozoites can be engineered to express CSP proteins from two different *Plasmodium* species. These chimeric sporozoites were generated by introducing a *P. falciparum csp* gene as an additional copy into the *P. berghei* genome (Mendes et al., 2018a; Mendes et al., 2018b; Reuling et al., 2020). Based on this observation we aimed at generating chimeric *P. falciparum* sporozoites expressing both *Pf*CSP and an chimeric *Pv*CSP protein (*Pv*CSP-chi). Using CRISPR/Cas9 gene editing, a chimeric *P. falciparum* line (*Pf-Pv*CSP) was created that contains the *Pvcsp-chi* gene under the control of 967 bp of the *Pfcsp* gene promoter region. This expression cassette was introduced into the neutral *Pfp47* locus (*PF*3D7_1346800) of the genome of *P. falciparum* NF54 wild type (WT) parasites. The *Pfp47* locus was selected as it is suitable for introducing transgenes without compromising parasite development in the blood and liver stages or in *A. stephensi* mosquitoes (Talman et al., 2010; Vaughan et al., 2012; Vos et al., 2015; Marin-Mogollon et al., 2019; Miyazaki et al., 2020). The WT *Pf*NF54 parasites were transfected with two plasmids: a previously described construct containing the Cas9 expression cassette with the *blasticidin* (*bsd*) drug-selectable marker cassette (pLf0019) and a donor DNA construct (pLf0109) designed to target the *Pfp47* locus. The donor construct contains the *Pvcsp-chi* expression cassette flanked by two homology regions of *Pfp47*, the *Pfp47* sgRNA sequence and a h*dhfr*-y*fcu* drug-selectable marker cassette (see **Figures 1A**, **S1**, **S2** and *Materials and Methods* section for details of the generation of the constructs). This *Pvcsp-chi* gene contains the N- and C-terminal regions of the *Pvcsp* VK210 allele that flank a chimeric repeat sequence comprising repeats of both the VK210 allele (three times the repeat GDRADGQPA/GDRAAGQPA) and the VK247 allele (three times the repeat ANGAGNQPG/ANGAGDQPG). Transfection of WT *Pf*NF54 parasites was performed using the 'spontaneous uptake method'. Briefly, uninfected RBC were first transfected with the constructs pLf0019 and pLf0109. Subsequently, the transfected RBCs were mixed with WT *Pf*NF54 infected RBC (iRBC). Selection of transfected parasites containing both plasmids was performed by applying double-positive selection with the drugs Blasticidin and WR99210 until parasites were detectable by thin blood-smear analysis. Subsequently negative drug selection with 5-fluorocytosine was applied to enrich the parasites in which the *Pvcsp-chi* gene expression cassette was integrated into the genome by double cross-over homologous recombination. Next drug-selected parasites were cloned by limiting dilution. Diagnostic (long range) PCR and Southern analyses of three clones (*Pf-Pv*CSP cl1, cl3, and cl4) confirmed correct double crossover integration of the *Pvcsp-chi* gene expression into the *Pfp47* locus in the genome of all *Pf-Pv*CSP clones (**Figures 1B, C**). Two *Pf-Pv*CSP clones (cls 1, 3) were selected for further phenotype characterization.

Pf-PvCSP Parasites Produce Sporozoites in *Anopheles stephensi* Mosquitoes

The *in vitro* growth of *Pf-Pv*CSP (cl3) blood stages was comparable to that of the parental WT *Pf*NF54 blood stage parasites (**Figure 1D**). *Pf-Pv*CSP parasites produced numbers of mature gametocytes in standardized gametocyte cultures similar to those of the parental line (**Table 1; Figure S3**) and male gametocytes underwent exflagellation upon activation. Using SMFA, *A. stephensi* mosquitoes were infected with gametocytes of either WT *Pf*NF54 or *Pf-Pv*CSP parasites. The number of oocysts in mosquito midguts was determined at days 10 to 12 after infection and the number of sporozoites in salivary glands was analyzed at days 18 to 24 after infection. These analyses revealed that *Pf-Pv*CSP parasites produced comparable number of oocysts and salivary gland sporozoites to those of the parental parasites (**Table 1; Figures S3** and **S4**). Approximately 90% of *Pf-Pv*CSP oocysts already contained sporozoites at days 10 to 12 which is in contrast to the two previously created chimeric *P. falciparum* lines with the *Pfcsp* gene replaced by the *Pvcsp* alleles vk210 and vk247. Most of the oocysts of these replacement lines degenerated before the formation of sporozoites (Marin-Mogollon et al., 2018). The presence of *Pf-Pv*CSP sporozoites in salivary glands (**Table 1**) indicated that *Pf*CSP retains its normal function in the formation of sporozoites, and that expression of *Pv*CSP-chi in these sporozoites does not appear to interfere with sporozoite formation and invasion of salivary glands.

Pf-PvCSP Sporozoites Express PfCSP As Well As PvCSP-chi on Their Surface

To analyze the expression of *Pv*CSP-chi and *Pf*CSP in salivary gland sporozoites of the *Pf-Pv*CSP line, we first performed an immunofluorescence on fixed/permeabilized sporozoites with antibodies specific for the repeat sequences of either *Pv*CSP VK210, *Pv*CSP VK247 or *Pf*CSP. All *Pf-Pv*CSP sporozoites analyzed (n=2 exp.) reacted with all three antibodies whereas WT *Pf*NF54 sporozoites reacted only with anti-*Pf*CSP antibodies (**Figure 2**), indicating that all *Pf-Pv*CSP sporozoites expressed both the *Pf*CSP and *Pv*CSP-chi proteins.

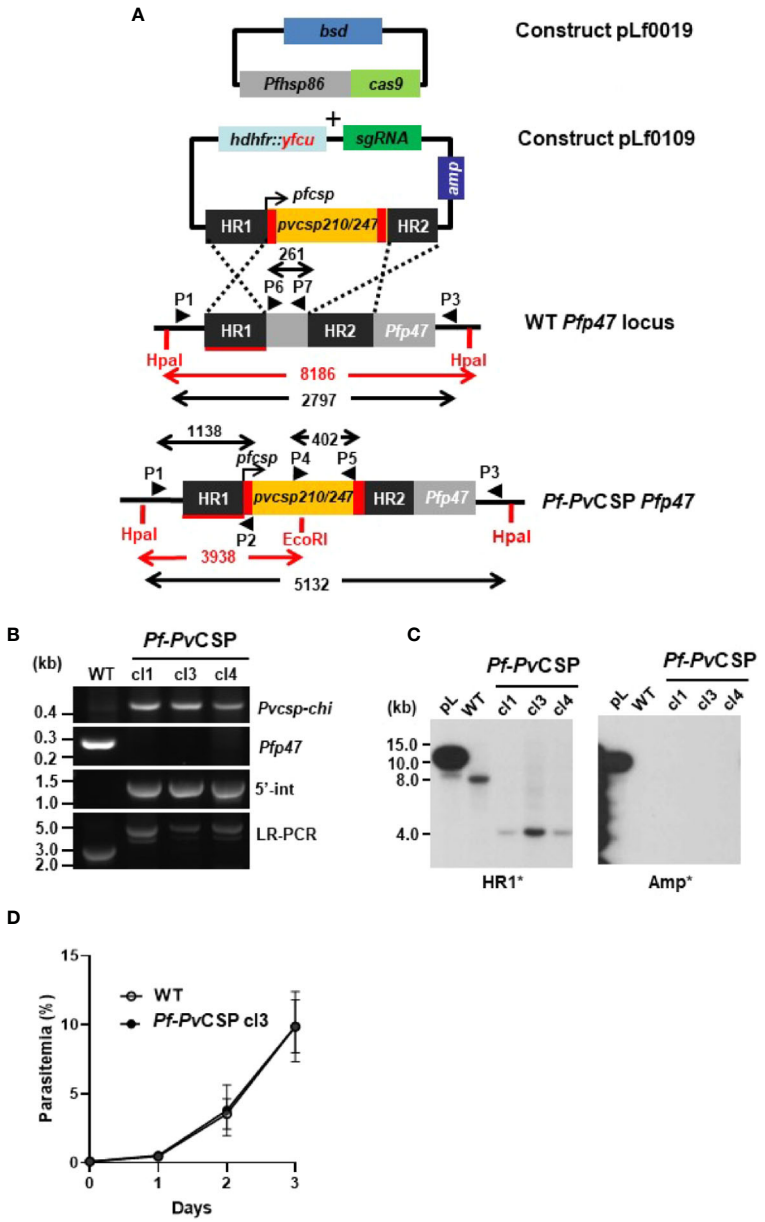

FIGURE 1 | Generation and genotyping of the chimeric *Pf-Pv*CSP parasites. A schematic representation of the Cas9 (plasmid Leiden *falciparum* (pLf) 0019) and donor DNA plasmids (pLf0109) constructs used to introduce the *Pvcsp* chimeric (*Pvcsp-chi*) expression cassette into the *Pf*NF54 *p47* gene locus. The *Pvcsp-chi* gene contains a chimeric repeat region of VK210 and VK247 alleles and is under the control of the promoter of the *Pfcsp* gene. The *p47* homology regions (HR1, HR2) used to introduce the donor DNA, location of primers (P), sizes of restriction fragments (*Hpa*I and *Eco*RI; in red), and PCR amplicons (in black) are indicated. WT, wild type; *bsd*, blasticidin selectable marker (bsd); h*dhfr::yfcu*, in donor plasmid. **(B)** Diagnostic PCRs confirming the correct integration of the *Pvcsp-chi* expression cassette into the *Pfp47* locus. Diagnostic PCR: part of *Pvcsp-chi* open reading frame (primers P4/P5); part of *Pfp47* open reading frame (primers P6/P7); 5'-integration of the plasmid into the *Pf-Pv*CSP-chi genome (5'-Int; primers P1/P2); LR-PCR (primers P1/P3). **(C)** Southern analysis of *Hpa*I and *Eco*RI restricted DNA of WT, and chimeric *Pf-Pv*CSP parasites confirms the specific integration of the *Pvcsp* genes into the *Pfp47* gene locus. **(D)** Growth of asexual blood-stages of *Pf-Pv*CSP cl3 and WT *Pf*NF54. Parasitemia (mean and S.D of 3 independent cultures) is shown during a 3-day culture period (in the semi-automated culture system). Cultures were initiated with a parasitemia of 0.1%.

We next investigated whether *Pv*CSP-chi protein is expressed at the surface of sporozoites, by performing IFA of live salivary gland sporozoites. Similarly to the results of IFA using fixed/permeabilized sporozoites, live *Pf-Pv*CSP sporozoites reacted with anti-*Pv*CSP VK210, anti-*Pv*CSP VK247 and anti-*Pf*CSP antibodies whereas WT *Pf*NF54 sporozoites reacted only to anti-*Pf*CSP antibodies (**Figure 3A**). This result demonstrates that the *Pv*CSP-chi protein is expressed at the surface of *Pf-Pv*CSP sporozoites.

TABLE 1 | Gametocyte, oocyst, and sporozoite production of *Pf-Pv*CSP and WT NF54 lines.

Parasites		Gams (%) male/female mean (SD)[a]	Exfl. No mean (SD)[b]	Exfl. Males (%) Mean (SD)[c]	Infected/dissected mosquitoes	Oocysts No mean (SD)[d]	Spz No mean[e]
WT	exp. 1	0.45/0.57	366	80	16/18	62	32 K
NF54	exp. 2	0.47/0.67	401	85	9/12	47	21 K
	exp. 3	0.52/0.63	201	38	11/12	40	54 K
		(0.03/0.04)	(87)	(21)		(9.3)	
***Pf-Pv*CSP**							
Clone 1	exp. 1	0.8/1.1	623	76	16/16	44	17 K
Clone 3	exp. 1	0.6/1.1	696	100	16/16	63	18 K
	exp. 2	0.3/0.4	641	100	18/18	52	20 K
	exp. 3	0.7/1.0	485	65	9/9	48	46 K
		(0.2/0.3)	(89)	(17)		(6.4)	

[a]*Mean percentage of stage V male and female gametocytes (per 100 red blood cells) in day 14 gametocyte cultures in one to three experiments (exp.) with standard deviation (SD).*
[b]*Mean number of exflagellating male gametocytes (per 10^5 red blood cells) at 10–20 min after activation in day 14 gametocyte cultures.*
[c]*Mean percentage of exflagellating stage V male gametocytes in day 14 gametocyte cultures (1–3 exp.) with standard deviation (SD).*
[d]*Mean number of oocyst per mosquito at days 10 to 12 after feeding (1–3 exp. per line; 10–30 mosquitoes per exp.).*
[e]*Mean number of salivary gland sporozoites per mosquito at days 18–24 after feeding. Range corresponds to the mean number of sporozoites in multiple experiments (1–3 exp. per line; 50–90 mosquitoes per exp.). See* ***Figure S3*** *for a graphic representation of the data of independent experiments.*

As CSP is shed during parasite gliding motility, we next assessed if *Pv*CSP is also shed similarly to *Pf*CSP by *Pf-Pv*CSP sporozoites. CSP-trails in a sporozoite gliding assay also reacted with both anti-*Pf*CSP and anti *Pv*CSP VK210 antibodies (**Figure 3B**), confirming surface expression of *Pv*CSP-chi and revealing shedding of *Pv*CSP-chi during gliding. Comparable gliding trails were observed in WT *Pf*NF54 and *Pf-Pv*CSP sporozoites using anti-*Pf*CSP antibody (**Figure 3B**), with a percentage of 85% gliding trails in WT *Pf*NF54 sporozoites (with a range of 28–65 gliding trails per field, Stdev. 2.6) and 87.0% gliding trails in *Pf-Pv*CSP sporozoites (with a range of 23–43 gliding trails per field, Stdev 7,6.).

Pf-PvCSP Sporozoites Infect Primary Human Hepatocytes

We next assessed the *in vitro* infectivity of *Pf-Pv*CSP sporozoites to primary human hepatocytes. At day 4 post infection of primary human hepatocytes with either WT or *Pf-Pv*CSP sporozoites, the cells were fixed, and liver stages were stained with an anti-*Pf*HSP70 antibody. *Pf-Pv*CSP sporozoites showed comparable efficiency of hepatocyte infection to WT *Pf*NF54 sporozoites (**Figure 4**). *Pf-Pv*CSP and WT *Pf*NF54 also displayed similar liver stage sizes at day 4 post infection (**Figure 4**). These results demonstrate that expression of *Pv*CSP-chi at the surface of *Pf-Pv*CSP sporozoites did not reduce parasite *in vitro* invasion and development in primary human hepatocytes.

Immunization of Mice with Pf-PvCSP Sporozoites Induce Antibodies Against Repeats of Both PfCSP and PvCSP-chi

We then analyzed the capacity of the *Pf-Pv*CSP sporozoites to elicit the production of antibodies against the repeat sequences of *Pf*CSP and *Pv*CSP-chi by immunizing mice with killed *Pf-Pv*CSP and WT *Pf*NF54 sporozoites. Groups of six C57BL/6 mice were intravenously injected with 10^5 freeze-thaw killed sporozoites, three times with a 7-day interval, and blood was collected from all mice 1 day prior to the first and third immunization and 1 week after the last immunization (**Figure 5A**). Plasma of these mice was tested for antigen-specific antibody production by ELISA using plates that were coated with the following repeat sequences; (NANP)4NVDPC for *Pf*CSP; GD RAD GQP AGD RAA GQP A for *Pv*CSP VK210; and ANGAGNQPG ANGAGDQPG for *Pv*CSP VK247 strain.

Plasma samples of mice immunized with either WT *Pf*NF54 or *Pf-Pv*CSP sporozoites reacted strongly to the *Pf*CSP repeat sequences after the second and third immunization with no significant differences in total IgG between the two groups of mice (**Figure 5B**), indicating comparable immunogenicity of the *Pf*CSP repeat sequences in WT *Pf*NF54 or *Pf-Pv*CSP sporozoites. In contrast, only mice immunized with *Pf-Pv*CSP sporozoites showed significantly increased antibody titers specific for the repeat sequences of *Pv*CSP VK210 and *Pv*CSP VK247 whereas no significant increase was observed in WT *Pf*NF54-immunized mice (**Figure 5B**). Although the total IgG against the *Pv*CSP repeats was lower than that against the *Pf*CSP repeats, these results show that exposure to *Pf-Pv*CSP sporozoites can induce the production of antibodies against *Pf*CSP, as well as against both *Pv*CSP repeat variants.

DISCUSSION

In this study we describe a chimeric *P. falciparum* line, *Pf-Pv*CSP, which expresses CSP from both *P. falciparum* and *P. vivax*. We demonstrate that chimeric parasites produce sporozoites in similar numbers to those of the parental WT *Pf*NF54 line and that both CSPs expressed in the chimeric parasites are present at the sporozoite surface and shed during gliding. Our results show that *Pf-Pv*CSP sporozoites are infectious to primary human hepatocytes. These observations support the notion that the presence of the chimeric *Pv*CSP protein at the surface of *P. falciparum* sporozoites does not affect sporozoite viability and infectivity. The formation of infective sporozoites expressing CSP of two different *Plasmodium* species has been previously

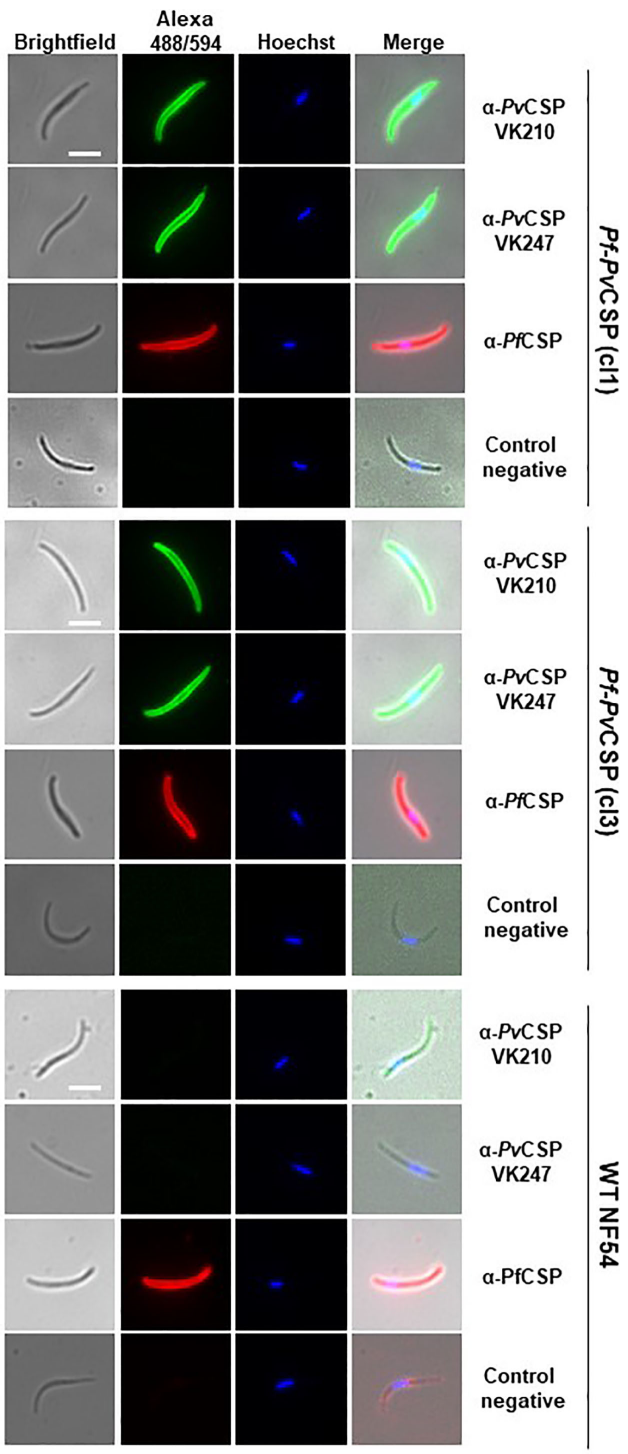

FIGURE 2 | Immunofluorescence analyses of *Pv*CSP and *Pf*CSP expression in fixed *Pf-Pv*CSP salivary gland sporozoites. Fixed permeabilized sporozoites of *Pf-Pv*CSP (clone 1 and clone 3) and WT *Pf*NF54 parasites stained with mouse anti-*Pv*CSPVK210, anti-*Pv*CSP VK247 (green; alexa 488) and anti-*Pf*CSP antibodies (red; alexa 594). Nuclei stained with the Hoechst-33342. Control negative, corresponds to the incubation without the primary antibody (2 experiments). Scale bar is 5 μm.

demonstrated in studies using *P. berghei* expressing *Pf*CSP (Mendes et al., 2018b). However, the viability and infectivity of these chimeric *Pb-PfCSP* sporozoites is expected, since *Pf*CSP can fully complement the multiple functions of *Pb*CSP as shown in replacement *P. berghei* lines with the endogenous *Pb*CSP replaced by *Pf*CSP (Triller et al., 2017; Flores-Garcia et al., 2019). This is distinct from *Pv*CSP, since previous attempts to functionally complement *Pf*CSP, by replacing the *Pfcsp* gene with two *Pvcsp alleles*, were unsuccessful (Marin-Mogollon et al., 2018). It is known that CSP fulfills multiple functions, both in the process of sporozoite formation and in later processes of sporozoite invasion of salivary glands, migration through the human skin and invasion of hepatocytes (Sinnis and Coppi, 2007; Vaughan et al., 2008; Ejigiri and Sinnis, 2009; Coppi et al., 2011; Vaughan and Kappe, 2017).

Although the previously generated gene-replacement *Pf-PvCSP* parasites were able to produce normal numbers of oocysts, no salivary gland sporozoite were formed and most oocyst degenerated before sporozoite formation, a phenotype that is comparable to *P. falciparum* mutants lacking the *Pfcsp* gene (Marin-Mogollon et al., 2018). Collectively, these observations indicate that *Pv*CSP is unable to fully complement the role of *Pf*CSP in the process of sporozoite formation inside oocysts but that the simultaneous expression of *Pv*CSP with *Pf*CSP in sporozoites of chimeric parasites does not hamper the formation of infectious sporozoites. The lack of full complementation of *Pf*CSP by *Pv*CSP in the process of sporozoite formation may result from the inability of *Pv*CSP to interact with other *P. falciparum* proteins that are involved in (the initial steps of) sporozoite formation.

Our studies of immunization of mice with the chimeric *Pf-PvCSP* sporozoites shows that antibodies are induced against the repeat sequences of both *Pf*CSP and the *Pv*CSP-chi protein, including antibody responses against both *Pv*CSP alleles, VK210 and VK247. Interestingly, although IgG responses against *Pf*CSP were significantly higher than against *Pv*CSP, anti- *Pf*CSP titers were comparable for mice immunized with either WT *Pf*NF54 sporozoites or *Pf-PvCSP* sporozoites. These observations indicate that the presence of *Pv*CSP does not affect the immunogenicity of *Pf*CSP with respect to IgG responses against the NANP/NVDP repeats. The lower IgG responses against the two *Pv*CSP repeats compared to the *Pf*CSP NANP/NVDP repeats can be caused by different factors. The *Pv*CSP-chi protein contains only 3 copies of the VK247 and VK210 repeats, while the *P. falciparum* NF54 CSP protein contains 38 NANP and 4 NVDP repeats (Bowman et al., 1999; Oyen et al., 2018). In addition, although we provide evidence of the presence of *Pv*CSP at the surface of the *Pf-Pv*CSP sporozoites and in gliding trails, the total amount of *Pf*CSP and *Pv*CSP in the *Pf-Pv*CSP sporozoites is unknown and may differ for the two proteins. The lower IgG responses might also result from a lower intrinsic immunogenicity of the *Pv*CSP repeats compared to the *P. falciparum* NANP/NVDP repeats. The repeat regions of CSP of the *P. vivax* strains VK210 and VK247 consist of 10–11 copies of the repeats GDRA(A/D)GQPA or ANGA (G/D)(N/D)QPG, respectively (de Souza-Neiras et al., 2007)] and are not cross reactive (Hall et al., 2019). Of note, our study employed freeze-thaw killed sporozoites to immunize mice; it is

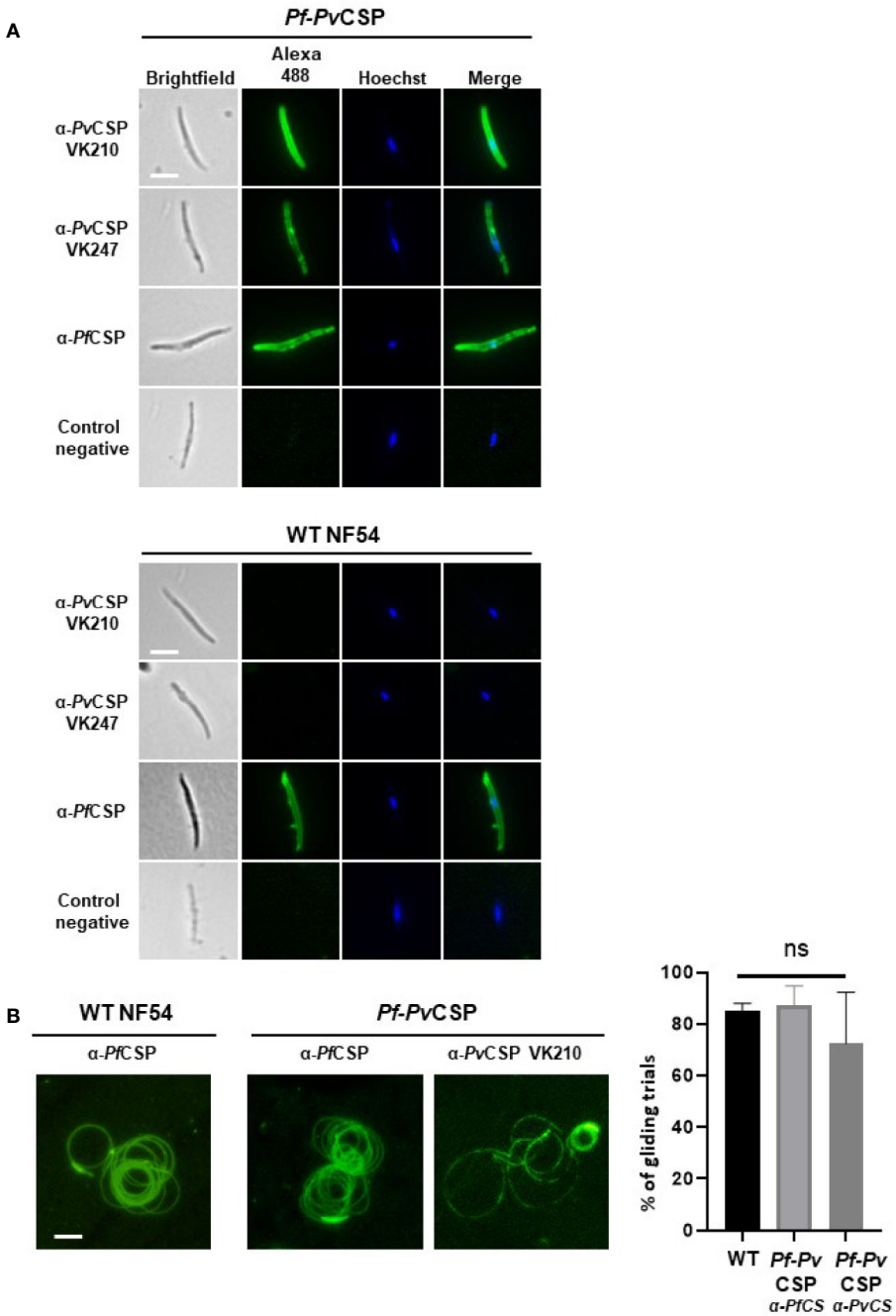

FIGURE 3 | Immunofluorescence analyses of *Pv*CSP and *Pf*CSP expression of live *Pf-Pv*CSP salivary gland sporozoites. **(A)** Live sporozoites of *Pf-Pv*CSP and WT *Pf*NF54 parasites labelled with mouse anti-*Pv*CSPVK210, anti-*Pv*CSP VK247 and anti-*Pf*CSP antibodies (green; alexa 488). Nuclei stained with the Hoechst-33342. Control negative, corresponds to the incubation without the primary antibody (2 experiments). Scale bar is 5 μm. **(B)** Typical sporozoite gliding trails of *Pf-Pv*CSP and WT *Pf*NF54 sporozoites stained with mouse anti-*Pv*CSPVK210 and anti-*Pf*CSP antibodies (left) and percentage of gliding trials (right) using primary antibody anti-Pf-3SP2 and anti-*Pv*CSPVK210 (1 experiment). Scale bar is 15 μm. ns, not significant, as determined by One-way ANOVA test (GraphPad).

therefore possible that antibody responses against *Pf*CSP and *Pv*CSP-chi proteins might be different when immunization is performed with live sporozoites.

Despite the differences in the repeat regions of *P. falciparum* and *P. vivax* CSP, both these proteins have been shown to be immunogenic and antibody levels against these repeats appear to be associated with protective immunity in animal malaria models and in humans (Porter et al., 2013; Foquet et al., 2014; Schwenk et al., 2014; Yadava et al., 2014; White et al., 2015; Gimenez et al., 2017; Atcheson et al., 2018; de Camargo et al., 2018; Dobaño et al., 2019).

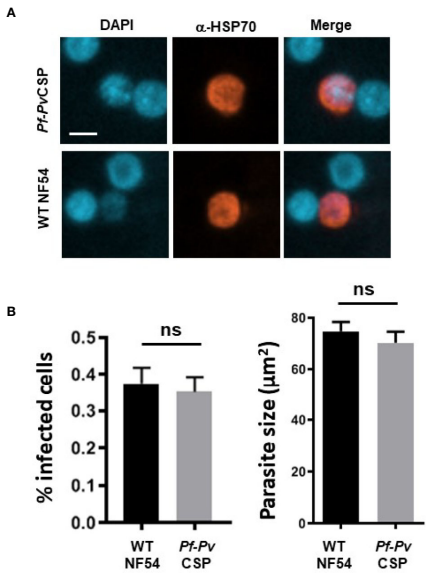

FIGURE 4 | *In vitro* infection of primary human hepatocytes by *Pf-Pv*CSP sporozoites. **(A)** Representative images of liver stage development in primary human hepatocytes 4 days after infection with *Pf-Pv*CSP and WT *Pf*NF54 sporozoites. Liver stages were stained with anti-*Pf*HSP70 antibodies and nuclei were stained with DAPI (1 experiment). Scale bar is 10 µm. **(B)** Percentage of infected hepatocytes (left) and size of liver stages (right) at day 4 after infection of hepatocytes by *Pf-Pv*CSP and WT NF54 sporozoites. The size was measured by determining the area of the parasite cytoplasm using the red-positive (anti-HSP70) area (µm^2). n.s., not significant, as determined by unpaired t-test (GraphPad).

However, due to differences in methodologies for inducing and analyzing antibody production after immunization with full-length CSP proteins or the respective repeat sequences, the relative immunogenicity of the *Pf*CSP and *Pv*CSP repeats in both animal models and in humans is largely unknown. To our knowledge, no studies exist that have compared the immunogenicity of different CSP repeat sequences of the two human *Plasmodium* species using similar immunization approaches and delivery systems. In comparative *P. vivax* and *P. falciparum* CHMI studies, it has been found that the CSP of both species induced cross-reactive antibodies (Hall et al., 2019). However, it is unknown whether the observed cross-reactivity resulted from the repeat sequences or from other epitopes in the N- or C-terminal region of the CSP molecules. In future studies it will be relevant to analyze infections in the FRG huHep mouse model (repopulated with human RBCs) to show that *Pf-Pv*CSP can form infectious liver merozoites. This would enable the use of this model for testing the efficacy of anti-*Pv*CSP antibodies.

Combined, our observations regarding the expression and immunogenicity of the *Pv*CSP on the surface of *P. falciparum* sporozoites hold promise for the use of the chimeric *Pf-Pv*CSP sporozoites for clinical evaluation of vaccines targeting *Pv*CSP in clinical CHMI studies. The use of such parasites would bypass the need for *P. vivax* sporozoite production and measures for hypnozoite removal (Payne et al., 2017). In addition, such chimeric sporozoites might also be used in whole, attenuated sporozoite vaccination approaches (Bijker et al., 2015; Goswami et al., 2020). Vaccination with chimeric, attenuated sporozoites might induce cross-protective immune responses against both *P. falciparum* and *P. vivax*.

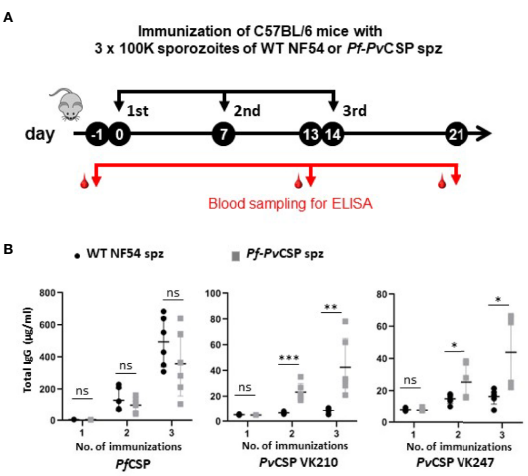

FIGURE 5 | Antibody production against repeat sequences of PfCSP and PvCSP-chi in mice after immunization with *Pf-Pv*CSP and WT *Pf*NF54 sporozoites. **(A)** Schematic representation of the immunization protocol. Groups of six C57BL/6 mice were immunized three times with killed sporozoites with a 7-day interval and blood was collected from all mice by orbital vein puncture 1 day before the first and third immunization and one week after the last immunization (one experiment). **(B)** Total IgG titers against *Pf*CSP and *Pv*CSP repeat sequences in plasma prior, during and after immunization. Enzyme-linked immunosorbent assays were performed with plasma samples collected from mice as shown in **(A)** to assess total IgG titers specific for the repeat sequences of *Pf*CSP ((NANP)4NVDPC) and two variants of *Pv*CSP(GD RAD GQP AGD RAA GQP A for *Pv*CSP VK210; ANGAGNQPG ANGAGDQPG for the *Pv*CSP VK247. Mean and standard error of the mean and *$p < 0.05$; **$p < 0.01$; ***$p < 0.001$, as determined by unpaired t-test analysis.

AUTHOR'S NOTE

This paper is dedicated to the memory of our friend and colleague, SMK, who initiated the studies described in this paper and recently passed away.

DATA AVAILABILITY STATEMENT

The raw data supporting the conclusions of this article will be made available by the authors, without undue reservation.

ETHICS STATEMENT

The animal study was reviewed and approved by Animal Experiments Committee Leiden (AVD1160020171625). All experiments were performed in accordance with the Experiments on Animals Act (Wod, 2014), the applicable legislation in the Netherlands and in accordance with the European guidelines (EU directive no. 2010/63/EU) regarding the protection of animals used for scientific purposes.

AUTHOR CONTRIBUTIONS

CM-M, BF-F, CJ, and SMK came up with the study concept and design. YM, CM-M, TI, AM, RL, AS, FG, SM, SC-M, JR, SK, HK, RS, AR-S, MP, CJ, and BF-F acquired the data. YM, CM-M, AM, MP, CJ, and BF-F conducted analysis and interpretation of the data. YM, CM-M, BF-F, and CJ wrote the draft of the manuscript. YM, CM-M, SM, AM, MP, RS, CJ, and BF-F critically revised the manuscript for important intellectual content. AM, KD, BW, and RS provided technical and/or material support. BF-F and CJ supervised the study. All authors reviewed the manuscript. All authors contributed to the article and approved the submitted version.

FUNDING

CM-M was, in part, supported by Colciencias Ph.D. fellowship (Call 568 from 2012 Resolution 01218 Bogotá, Colombia). TI was, in part, supported by Uehara Memorial Foundation grant. Work performed at IMM was supported by Fundação para a Ciência e Tecnologia (FCT-Portugal)'s grants PTDC/BBB-BMD/2695/2014 and PTDC-SAU-INF-29550-2017. AR-S is supported by the MRC-DPFS grant MR/N019008/1.

ACKNOWLEDGMENTS

We would like to acknowledge Els Baalbergen for the mosquito breeding.

SUPPLEMENTARY MATERIAL

The Supplementary Material for this article can be found online at: https://www.frontiersin.org/articles/10.3389/fcimb.2020.591046/full#supplementary-material

SUPPLEMENTARY FIGURE 1 | Plasmid maps of plasmids used in this study.

SUPPLEMENTARY FIGURE 2 | Plasmid map of pLf0109 and sequence of the commercially synthesized *Pvcsp-chi* gene. This gene that contains a codon-optimized *Pvcsp* open reading frame containing the N- and C-terminal regions of the *Pv*csp VK210 allele that flank a chimeric repeat sequence comprising repeats of both the VK210 allele (three times the repeat GDRADGQPA/GDRAAGQPA) and the VK247 allele (three times the repeat ANGAGNQPG/ANGAGDQPG).

SUPPLEMENTARY FIGURE 3 | Percentage of male exflagellating gametocytes and number of oocyst and sporozoites of *Pf-Pv*CSP cl3 and WT *Pf*NF54 parasites. **(A)** Percentage of stage V exflagellating male gametocytes in day 14 gametocyte cultures (3 experiments). Each dot correspond to an independent experiment. **(B)** Number of oocyst per mosquito at day 10 after feeding (n=3). Each dot correspond to the number of oocysts per midgut. **(C)** Number of sporozoites per mosquito at day 18–24 after feeding (n=3). Each dot corresponds to the mean number of sporozoites per mosquito. Mean and standard error of the mean. n.s., not significant (unpaired t-test; Graphpad).

SUPPLEMENTARY FIGURE 4 | Sporozoite formation in oocysts of *Pf-Pv*CSP and WT *Pf*NF54 parasites. Representative images of oocyst during development **(A)** and sporozoite formation **(B)** in oocysts (day 10) from WT NF54 parasites and *Pf-Pv*CSP parasites that express both *Pf*CSP and *Pv*CSP-chi. **(A)** Complete midgut and magnified area (×5). Scale bar: 200 μm (upper row) and 20 μm (lower row). **(B)** Sporozoite formation in an unstained oocyst. Scale bar: 20 μm.

SUPPLEMENTARY TABLE 1 | Primers used in this study.

REFERENCES

Agnandji, S. T., Lell, B., Fernandes, J. F., Abossolo, B. P., Methogo, B. G., Kabwende, A. L., et al. (2012). A phase 3 trial of RTS,S/AS01 malaria vaccine in African infants. *N. Engl. J. Med.* 367, 2284–2295. doi: 10.1056/NEJMoa1208394

Agnandji, S. T., Fernandes, J. F., Bache, E. B., and Ramharter, M. (2015). Clinical development of RTS,S/AS malaria vaccine: a systematic review of clinical Phase I-III trials. *Future Microbiol.* 10, 1553–1578. doi: 10.2217/fmb.15.90

Arévalo-Herrera, M., Vásquez-Jiménez, J. M., Lopez-Perez, M., Vallejo, A. F., Amado-Garavito, A. B., Céspedes, N., et al. (2016). Protective Efficacy of Plasmodium vivax Radiation-Attenuated Sporozoites in Colombian Volunteers: A Randomized Controlled Trial. *PLoS Negl. Trop. Dis.* 10, e0005070. doi: 10.1371/journal.pntd.0005070

Atcheson, E., Bauza, K., Salman, A. M., Alves, E., Blight, J., Viveros-Sandoval, M. E., et al. (2018). Tailoring a Plasmodium vivax Vaccine To Enhance Efficacy through a Combination of a CSP Virus-Like Particle and TRAP Viral Vectors. *Infect. Immun.* 86, 1–16. doi: 10.1128/IAI.00114-18

Bennett, J. W., Yadava, A., Tosh, D., Sattabongkot, J., Komisar, J., Ware, L. A., et al. (2016). Phase 1/2a Trial of Plasmodium vivax Malaria Vaccine Candidate VMP001/AS01B in Malaria-Naive Adults: Safety, Immunogenicity, and Efficacy. *PLoS Negl. Trop. Dis.* 10, e0004423. doi: 10.1371/journal.pntd.0004423

Bijker, E. M., Borrmann, S., Kappe, S. H., Mordmuller, B., Sack, B. K., and Khan, S. M. (2015). Novel approaches to whole sporozoite vaccination against malaria. *Vaccine* 33, 7462–7468. doi: 10.1016/j.vaccine.2015.09.095

Bijker, E. M., Sauerwein, R. W., and Bijker, W. E. (2016). Controlled human malaria infection trials: How tandems of trust and control construct scientific knowledge. *Soc. Stud. Sci.* 46, 56–86. doi: 10.1177/0306312715619784

Bowman, S., Lawson, D., Basham, D., Brown, D., Chillingworth, T., Churcher, C. M., et al. (1999). The complete nucleotide sequence of chromosome 3 of Plasmodium falciparum. *Nature* 400, 532–538. doi: 10.1038/22964

Clemens, J., and Moorthy, V. (2016). Implementation of RTS,S/AS01 Malaria Vaccine–The Need for Further Evidence. *N. Engl. J. Med.* 374, 2596–2597. doi: 10.1056/NEJMe1606007

Cohen, J., Nussenzweig, V., Nussenzweig, R., Vekemans, J., and Leach, A. (2010). From the circumsporozoite protein to the RTS, S/AS candidate vaccine. *Hum. Vaccin.* 6, 90–96. doi: 10.4161/hv.6.1.9677

Coppi, A., Natarajan, R., Pradel, G., Bennett, B. L., James, E. R., Roggero, M. A., et al. (2011). The malaria circumsporozoite protein has two functional domains, each with distinct roles as sporozoites journey from mosquito to mammalian host. *J. Exp. Med.* 208, 341–356. doi: 10.1084/jem.20101488

de Camargo, T. M., de Freitas, E. O., Gimenez, A. M., Lima, L. C., De Almeida Caramico, K., Françoso, K. S., et al. (2018). Prime-boost vaccination with recombinant protein and adenovirus-vector expressing Plasmodium vivax circumsporozoite protein (CSP) partially protects mice against Pb/Pv sporozoite challenge. *Sci. Rep.* 8, 1118. doi: 10.1038/s41598-017-19063-6

de Souza-Neiras, W. C., De Melo, L. M., and Machado, R. L. (2007). The genetic diversity of Plasmodium vivax–a review. *Mem. Inst. Oswaldo Cruz* 102, 245–254. doi: 10.1590/S0074-02762007000300002

Dobaño, C., Sanz, H., Sorgho, H., Dosoo, D., Mpina, M., Ubillos, I., et al. (2019). Concentration and avidity of antibodies to different circumsporozoite epitopes correlate with RTS,S/AS01E malaria vaccine efficacy. *Nat. Commun.* 10, 2174. doi: 10.1038/s41467-019-10195-z

Ejigiri, I., and Sinnis, P. (2009). Plasmodium sporozoite-host interactions from the dermis to the hepatocyte. *Curr. Opin. Microbiol.* 12, 401–407. doi: 10.1016/j.mib.2009.06.006

Espinosa, D. A., Yadava, A., Angov, E., Maurizio, P. L., Ockenhouse, C. F., and Zavala, F. (2013). Development of a chimeric Plasmodium berghei strain expressing the repeat region of the P. vivax circumsporozoite protein for in vivo evaluation of vaccine efficacy. *Infect. Immun.* 81, 2882–2887. doi: 10.1128/IAI.00461-13

Flores-Garcia, Y., Herrera, S. M., Jhun, H., Pérez-Ramos, D. W., King, C. R., Locke, E., et al. (2019). Optimization of an in vivo model to study immunity to Plasmodium falciparum pre-erythrocytic stages. *Malar. J.* 18, 426. doi: 10.1186/s12936-019-3055-9

Foquet, L., Hermsen, C. C., Van Gemert, G. J., Van Braeckel, E., Weening, K. E., Sauerwein, R., et al. (2014). Vaccine-induced monoclonal antibodies targeting circumsporozoite protein prevent Plasmodium falciparum infection. *J. Clin. Invest.* 124, 140–144. doi: 10.1172/JCI70349

Gimenez, A. M., Lima, L. C., Françoso, K. S., Denapoli, P. M. A., Panatieri, R., Bargieri, D. Y., et al. (2017). Vaccine Containing the Three Allelic Variants of the Plasmodium vivax Circumsporozoite Antigen Induces Protection in Mice after Challenge with a Transgenic Rodent Malaria Parasite. *Front. Immunol.* 8, 1275. doi: 10.3389/fimmu.2017.01275

Goswami, D., Betz, W., Locham, N. K., Parthiban, C., Brager, C., Schäfer, C., et al. (2020). A replication-competent late liver stage-attenuated human malaria parasite. *JCI Insight* 5 (13), 1–19 doi: 10.1172/jci.insight.135589

Hall, C. E., Hagan, L. M., Bergmann-Leitner, E., Tosh, D. M., Bennett, J. W., Regules, J. A., et al. (2019). Mosquito Bite-Induced Controlled Human Malaria Infection with Plasmodium vivax or P. falciparum Generates Immune Responses to Homologous and Heterologous Preerythrocytic and Erythrocytic Antigens. *Infect. Immun.* 87, 1–15. doi: 10.1128/IAI.00541-18

Healer, J., Cowman, A. F., Kaslow, D. C., and Birkett, A. J. (2017). Vaccines to Accelerate Malaria Elimination and Eventual Eradication. *Cold Spring Harb. Perspect. Med.* 7, 1–17. doi: 10.1101/cshperspect.a025627

Hoffman, S. L., Vekemans, J., Richie, T. L., and Duffy, P. E. (2015). The March Toward Malaria Vaccines. *Am. J. Prev. Med.* 49, S319–S333. doi: 10.1016/j.amepre.2015.09.011

Janse, C. J., Franke-Fayard, B., Mair, G. R., Ramesar, J., Thiel, C., Engelmann, S., et al. (2006). High efficiency transfection of Plasmodium berghei facilitates novel selection procedures. *Mol. Biochem. Parasitol.* 145, 60–70. doi: 10.1016/j.molbiopara.2005.09.007

Kester, K. E., Cummings, J. F., Ofori-Anyinam, O., Ockenhouse, C. F., Krzych, U., Moris, P., et al. (2009). Randomized, double-blind, phase 2a trial of falciparum malaria vaccines RTS,S/AS01B and RTS,S/AS02A in malaria-naive adults: safety, efficacy, and immunologic associates of protection. *J. Infect. Dis.* 200, 337–346. doi: 10.1086/600120

Long, C. A., and Zavala, F. (2016). Malaria vaccines and human immune responses. *Curr. Opin. Microbiol.* 32, 96–102. doi: 10.1016/j.mib.2016.04.006

Mahmoudi, S., and Keshavarz, H. (2017). Efficacy of phase 3 trial of RTS, S/AS01 malaria vaccine: The need for an alternative development plan. *Hum. Vaccin. Immunother.* 13, 2098–2101. doi: 10.1080/21645515.2017.1295906

Marin-Mogollon, C., Van Pul, F. J. A., Miyazaki, S., Imai, T., Ramesar, J., Salman, A. M., et al. (2018). Chimeric Plasmodium falciparum parasites expressing Plasmodium vivax circumsporozoite protein fail to produce salivary gland sporozoites. *Malar. J.* 17, 288. doi: 10.1186/s12936-018-2431-1

Marin-Mogollon, C., Salman, A. M., Koolen, K. M. J., Bolscher, J. M., Van Pul, F. J. A., Miyazaki, S., et al. (2019). A P. falciparum NF54 Reporter Line Expressing mCherry-Luciferase in Gametocytes, Sporozoites, and Liver-Stages. *Front. Cell Infect. Microbiol.* 9, 96. doi: 10.3389/fcimb.2019.00096

Marques, R. F., Gimenez, A. M., Aliprandini, E., Novais, J. T., Cury, D. P., Watanabe, I. S., et al. (2020). Protective Malaria Vaccine in Mice Based on the Plasmodium vivax Circumsporozoite Protein Fused with the Mumps Nucleocapsid Protein. *Vaccines (Basel)* 8, 1–19. doi: 10.3390/vaccines8020190

Ménard, R. (2000). The journey of the malaria sporozoite through its hosts: two parasite proteins lead the way. *Microbes Infect.* 2, 633–642. doi: 10.1016/S1286-4579(00)00362-2

Mendes, A. M., Machado, M., Goncalves-Rosa, N., Reuling, I. J., Foquet, L., Marques, C., et al. (2018a). A Plasmodium berghei sporozoite-based vaccination platform against human malaria. *NPJ Vaccines* 3, 33. doi: 10.1038/s41541-018-0068-2

Mendes, A. M., Reuling, I. J., Andrade, C. M., Otto, T. D., Machado, M., Teixeira, F., et al. (2018b). Pre-clinical evaluation of a P. berghei-based whole-sporozoite malaria vaccine candidate. *NPJ Vaccines* 3, 54. doi: 10.1038/s41541-018-0091-3

Miyazaki, S., Yang, A. S. P., Geurten, F. J. A., Marin-Mogollon, C., Miyazaki, Y., Imai, T., et al. (2020). Generation of Novel Plasmodium falciparum NF135 and NF54 Lines Expressing Fluorescent Reporter Proteins Under the Control of Strong and Constitutive Promoters. *Front. Cell Infect. Microbiol.* 10, 270. doi: 10.3389/fcimb.2020.00270

Mogollon, C. M., Van Pul, F. J., Imai, T., Ramesar, J., Chevalley-Maurel, S., De Roo, G. M., et al. (2016). Rapid Generation of Marker-Free P. falciparum Fluorescent Reporter Lines Using Modified CRISPR/Cas9 Constructs and Selection Protocol. *PLoS One* 11, e0168362. doi: 10.1371/journal.pone.0168362

Olotu, A., Fegan, G., Wambua, J., Nyangweso, G., Leach, A., Lievens, M., et al. (2016). Seven-Year Efficacy of RTS,S/AS01 Malaria Vaccine among Young African Children. *N. Engl. J. Med.* 374, 2519–2529. doi: 10.1056/NEJMoa1515257

Oyen, D., Torres, J. L., Cottrell, C. A., Richter King, C., Wilson, I. A., and Ward, A. B. (2018). Cryo-EM structure of P. falciparum circumsporozoite protein with a vaccine-elicited antibody is stabilized by somatically mutated inter-Fab contacts. *Sci. Adv.* 4, eaau8529. doi: 10.1126/sciadv.aau8529

Payne, R. O., Griffin, P. M., Mccarthy, J. S., and Draper, S. J. (2017). Plasmodium vivax Controlled Human Malaria Infection - Progress and Prospects. *Trends Parasitol.* 33, 141–150. doi: 10.1016/j.pt.2016.11.001

Ponnudurai, T., Leeuwenberg, A. D., and Meuwissen, J. H. (1981). Chloroquine sensitivity of isolates of Plasmodium falciparum adapted to in vitro culture. *Trop. Geogr. Med.* 33, 50–54. doi: 10.1017/s0031182000062065

Ponnudurai, T., Lensen, A. H., Van Gemert, G. J., Bensink, M. P., Bolmer, M., and Meuwissen, J. H. (1989). Infectivity of cultured Plasmodium falciparum gametocytes to mosquitoes. *Parasitology* 98 Pt 2, 165–173. doi: 10.1017/S0031182000062065

Porter, M. D., Nicki, J., Pool, C. D., Debot, M., Illam, R. M., Brando, C., et al. (2013). Transgenic parasites stably expressing full-length Plasmodium falciparum circumsporozoite protein as a model for vaccine down-selection in mice using sterile protection as an endpoint. *Clin. Vaccine Immunol.* 20, 803–810. doi: 10.1128/CVI.00066-13

Reuling, I. J., Mendes, A. M., De Jong, G. M., Fabra-García, A., Nunes-Cabaço, H., Van Gemert, G. J., et al. (2020). An open-label phase 1/2a trial of a genetically modified rodent malaria parasite for immunization against Plasmodium falciparum malaria. *Sci. Transl. Med.* 12, 1–13. doi: 10.1126/scitranslmed.aay2578

Sack, B. K., Miller, J. L., Vaughan, A. M., Douglass, A., Kaushansky, A., Mikolajczak, S., et al. (2014). Model for in vivo assessment of humoral protection against malaria sporozoite challenge by passive transfer of monoclonal antibodies and immune serum. *Infect. Immun.* 82, 808–817. doi: 10.1128/IAI.01249-13

Salman, A. M., Montoya-Diaz, E., West, H., Lall, A., Atcheson, E., Lopez-Camacho, C., et al. (2017). Rational development of a protective P. vivax vaccine evaluated with transgenic rodent parasite challenge models. *Sci. Rep.* 7, 46482. doi: 10.1038/srep46482

Sauerwein, R. W., Roestenberg, M., and Moorthy, V. S. (2011). Experimental human challenge infections can accelerate clinical malaria vaccine development. *Nat. Rev. Immunol.* 11, 57–64. doi: 10.1038/nri2902

Schwenk, R., Debot, M., Porter, M., Nikki, J., Rein, L., Spaccapelo, R., et al. (2014). IgG2 antibodies against a clinical grade Plasmodium falciparum CSP vaccine antigen associate with protection against transgenic sporozoite challenge in mice. *PLoS One* 9, e111020. doi: 10.1371/journal.pone.0111020

Sinnis, P., and Coppi, A. (2007). A long and winding road: the Plasmodium sporozoite's journey in the mammalian host. *Parasitol. Int.* 56, 171–178. doi: 10.1016/j.parint.2007.04.002

Spring, M., Polhemus, M., and Ockenhouse, C. (2014). Controlled human malaria infection. *J. Infect. Dis.* 209(Suppl 2), S40–S45. doi: 10.1093/infdis/jiu063

Stanisic, D. I., Mccarthy, J. S., and Good, M. F. (2018). Controlled Human Malaria Infection: Applications, Advances, and Challenges. *Infect. Immun.* 86, 1–17. doi: 10.1128/IAI.00479-17

Stewart, M. J., and Vanderberg, J. P. (1988). Malaria sporozoites leave behind trails of circumsporozoite protein during gliding motility. *J. Protozool.* 35, 389–393. doi: 10.1111/j.1550-7408.1988.tb04115.x

Talman, A. M., Blagborough, A. M., and Sinden, R. E. (2010). A Plasmodium falciparum strain expressing GFP throughout the parasite's life-cycle. *PLoS One* 5, e9156. doi: 10.1371/journal.pone.0009156

Triller, G., Scally, S. W., Costa, G., Pissarev, M., Kreschel, C., Bosch, A., et al. (2017). Natural Parasite Exposure Induces Protective Human Anti-Malarial Antibodies. *Immunity* 47, 1197–1209.e1110. doi: 10.1016/j.immuni.2017.11.007

van Schaijk, B. C., Janse, C. J., Van Gemert, G. J., Van Dijk, M. R., Gego, A., Franetich, J. F., et al. (2008). Gene disruption of Plasmodium falciparum p52 results in attenuation of malaria liver stage development in cultured primary human hepatocytes. *PLoS One* 3, e3549. doi: 10.1371/journal.pone.0003549

Vaughan, A. M., and Kappe, S. H. I. (2017). Malaria Parasite Liver Infection and Exoerythrocytic Biology. *Cold Spring Harb. Perspect. Med.* 7, 1–21. doi: 10.1101/cshperspect.a025486

Vaughan, A. M., Aly, A. S., and Kappe, S. H. (2008). Malaria parasite pre-erythrocytic stage infection: gliding and hiding. *Cell Host Microbe* 4, 209–218. doi: 10.1016/j.chom.2008.08.010

Vaughan, A. M., Mikolajczak, S. A., Camargo, N., Lakshmanan, V., Kennedy, M., Lindner, S. E., et al. (2012). A transgenic Plasmodium falciparum NF54 strain that expresses GFP-luciferase throughout the parasite life cycle. *Mol. Biochem. Parasitol.* 186, 143–147. doi: 10.1016/j.molbiopara.2012.10.004

Vijayan, A., Mejías-Pérez, E., Espinosa, D. A., Raman, S. C., Sorzano, C. O. S., Zavala, F., et al. (2017). A Prime/Boost PfCS14K(M)/MVA-sPfCS(M) Vaccination Protocol Generates Robust CD8(+) T Cell and Antibody Responses to Plasmodium falciparum Circumsporozoite Protein and Protects Mice against Malaria. *Clin. Vaccine Immunol.* 24, 1–16. doi: 10.1128/CVI.00494-16

Vos, M. W., Stone, W. J., Koolen, K. M., Van Gemert, G. J., Van Schaijk, B., Leroy, D., et al. (2015). A semi-automated luminescence based standard membrane feeding assay identifies novel small molecules that inhibit transmission of malaria parasites by mosquitoes. *Sci. Rep.* 5, 18704. doi: 10.1038/srep18704

White, M. T., Bejon, P., Olotu, A., Griffin, J. T., Riley, E. M., Kester, K. E., et al. (2013). The relationship between RTS,S vaccine-induced antibodies, $CD4^+$ T cell responses and protection against Plasmodium falciparum infection. *PLoS One* 8, e61395. doi: 10.1371/journal.pone.0061395

White, M. T., Verity, R., Griffin, J. T., Asante, K. P., Owusu-Agyei, S., Greenwood, B., et al. (2015). Immunogenicity of the RTS, S/AS01 malaria vaccine and implications for duration of vaccine efficacy: secondary analysis of data from a phase 3 randomised controlled trial. *Lancet Infect. Dis.* 15, 1450–1458. doi: 10.1016/S1473-3099(15)00239-X

Yadava, A., and Waters, N. C. (2017). Rationale for Further Development of a Vaccine Based on the Circumsporozoite Protein of Plasmodium vivax. *PLoS Negl. Trop. Dis.* 11, e0005164. doi: 10.1371/journal.pntd.0005164

Yadava, A., Hall, C. E., Sullivan, J. S., Nace, D., Williams, T., Collins, W. E., et al. (2014). Protective efficacy of a Plasmodium vivax circumsporozoite protein-based vaccine in Aotus nancymaae is associated with antibodies to the repeat region. *PLoS Negl. Trop. Dis.* 8, e3268. doi: 10.1371/journal.pntd.0003268

Conflict of Interest: KD holds stock in TropIQ Health Sciences. RL, AS and KD were employed by TropIQ Health Sciences.

The remaining authors declare that the research was conducted in the absence of any commercial or financial relationships that could be construed as a potential conflict of interest.

frontiers in Cellular and Infection Microbiology

BRIEF RESEARCH REPORT
published: 18 January 2021
doi: 10.3389/fcimb.2020.605367

Identification of a Novel RAMA/RON3 Rhoptry Protein Complex in *Plasmodium falciparum* Merozoites

Daisuke Ito[1,2‡], Jun-Hu Chen[3‡], Eizo Takashima[1], Tomoyuki Hasegawa[1†], Hitoshi Otsuki[2], Satoru Takeo[4], Amporn Thongkukiatkul[5], Eun-Taek Han[6] and Takafumi Tsuboi[1*]*

[1] Division of Malaria Research, Proteo-Science Center, Ehime University, Matsuyama, Japan, [2] Division of Medical Zoology, Department of Microbiology and Immunology, Faculty of Medicine, Tottori University, Yonago, Japan, [3] National Institute of Parasitic Diseases, Chinese Center for Disease Control and Prevention, Shanghai, China, [4] Division of Tropical Diseases and Parasitology, Department of Infectious Diseases, Faculty of Medicine, Kyorin University, Mitaka, Japan, [5] Department of Biology, Faculty of Science, Burapha University, Chonburi, Thailand, [6] Department of Medical Environmental Biology and Tropical Medicine, Kangwon National University School of Medicine, Chuncheon, South Korea

Malaria causes a half a million deaths annually. The parasite intraerythrocytic lifecycle in the human bloodstream is the major cause of morbidity and mortality. Apical organelles of merozoite stage parasites are involved in the invasion of erythrocytes. A limited number of apical organellar proteins have been identified and characterized for their roles during erythrocyte invasion or subsequent intraerythrocytic parasite development. To expand the repertoire of identified apical organellar proteins we generated a panel of monoclonal antibodies against *Plasmodium falciparum* schizont-rich parasites and screened the antibodies using immunofluorescence assays. Out of 164 hybridoma lines, 12 clones produced monoclonal antibodies yielding punctate immunofluorescence staining patterns in individual merozoites in late schizonts, suggesting recognition of merozoite apical organelles. Five of the monoclonal antibodies were used to immuno-affinity purify their target antigens and these antigens were identified by liquid chromatography-tandem mass spectrometry (LC-MS/MS). Two known apical organelle protein complexes were identified, the high-molecular mass rhoptry protein complex (PfRhopH1/Clags, PfRhopH2, and PfRhopH3) and the low-molecular mass rhoptry protein complex (rhoptry-associated proteins complex, PfRAP1, and PfRAP2). A novel complex was additionally identified by immunoprecipitation, composed of rhoptry-associated membrane antigen (PfRAMA) and rhoptry neck protein 3 (PfRON3) of *P. falciparum*. We further identified a region spanning amino acids Q_{221}-E_{481} within the PfRAMA that may associate with PfRON3 in immature schizonts. Further investigation will be required as to whether PfRAMA and PfRON3 interact directly or indirectly.

Keywords: *Plasmodium falciparum*, merozoite, monoclonal antibody, rhoptry, rhoptry-associated membrane antigen, rhoptry neck protein 3

OPEN ACCESS

Edited by:
Takeshi Annoura, National Institute of Infectious Diseases (NIID), Japan

Reviewed by:
Danny Wilson, University of Adelaide, Australia
Dave Richard, Laval University, Canada

***Correspondence:**
Takafumi Tsuboi
tsuboi.takafumi.mb@ehime-u.ac.jp
Eun-Taek Han
ethan@kangwon.ac.kr

†Present address:
Tomoyuki Hasegawa, Division of Applied Protein Research, the Advanced Research Support Center (ADRES), Ehime University, Matsuyama, Japan

‡*These authors have contributed equally to this work*

Specialty section:
This article was submitted to Parasite and Host, a section of the journal Frontiers in Cellular and Infection Microbiology

Received: *12 September 2020*
Accepted: *27 November 2020*
Published: *18 January 2021*

Citation:
Ito D, Chen J-H, Takashima E, Hasegawa T, Otsuki H, Takeo S, Thongkukiatkul A, Han E-T and Tsuboi T (2021) Identification of a Novel RAMA/RON3 Rhoptry Protein Complex in Plasmodium falciparum Merozoites. Front. Cell. Infect. Microbiol. 10:605367. doi: 10.3389/fcimb.2020.605367

INTRODUCTION

Malaria causes approximately a half a million deaths annually, mainly *via* infection with *Plasmodium falciparum* (WHO, 2019). To initiate intraerythrocytic development in humans, *P. falciparum* merozoites invade erythrocytes. Merozoite apical organelles—rhoptries, micronemes, exonemes, and dense granules—have been studied for their role in erythrocyte invasion. Before invasion some organelle components are discharged on the surface of merozoite. Once the merozoite recognizes and forms a tight junction between the erythrocyte membrane and its apical pole, the apical organelles discharge their protein contents into the moving junction and developing parasitophorous vacuole (PV). The apical organelles disappear after merozoite internalization within an erythrocyte, suggesting transient roles of their molecular contents during merozoite invasion (Cowman and Crabb, 2006). The apical organelles have thereby inspired analysis of the biological and immunological characteristics of their component proteins, as well as their candidacies for vaccine and drug development (Preiser et al., 2000; Kats et al., 2006; Kaneko, 2007).

Numerous rhoptry bulb proteins have been identified, including the high-molecular weight (HMW) proteins that form a complex consisting of PfRhopH1/Clag, PfRhopH2, and PfRhopH3 (Campbell et al., 1984; Holder et al., 1985; Lustigman et al., 1988; Sam-Yellowe et al., 1998; Kaneko et al., 2001; Kaneko et al., 2005); and the low-molecular weight complex (LMW) proteins consisting of PfRAP1, PfRAP2, and PfRAP3 (Ridley et al., 1990; Saul et al., 1992; Baldi et al., 2002). These protein complexes have been implicated in erythrocyte invasion (Siddiqui et al., 1987; Cooper et al., 1988; Harnyuttanakorn et al., 1992) and channel-mediated nutrient uptake (Counihan et al., 2017; Ito et al., 2017; Sherling et al., 2017). Another rhoptry bulb protein, rhoptry-associated membrane antigen (PfRAMA), is involved in rhoptry biogenesis, the merozoite invasion process, formation of the PV, and interacts with both PfRAP1 and PfRhopH3 (Topolska et al., 2004; Richard et al., 2009). The proteins were identified using monoclonal antibodies generated against parasite extracts (Campbell et al., 1984; Ridley et al., 1990; Saul et al., 1992; Doury et al., 1994; Sam-Yellowe et al., 2001) or proteomic analyses of purified merozoite rhoptries (Sam-Yellowe et al., 2004; Sanders et al., 2005; Gilson et al., 2006; Sanders et al., 2007). In addition to the rhoptry bulb proteins, the merozoite rhoptry neck proteins PfRON2, PfRON4, and PfRON5 form a moving junction complex together with a micronemal protein, PfAMA1, in *P. falciparum* (Collins et al., 2009; Richard et al., 2010). Therefore, the PfRON2/PfAMA1 complex proteins are highlighted as novel asexual blood-stage malaria vaccine candidates (Srinivasan et al., 2014).

A limited number of merozoite apical organellar proteins in micronemes, rhoptries, exonemes, and dense granules have been extensively assessed for their role in erythrocyte invasion and growth (Counihan et al., 2013; Cowman et al., 2017). The identification of novel merozoite apical organellar proteins is essential for the cumulative understanding of erythrocyte invasion, and therefore we attempted to expand the repertoire of apical organellar proteins and their partner molecules. In this study we have generated monoclonal antibodies (mAbs) against *P. falciparum* schizont-rich antigens that recognize the apical region of merozoites. We report here the immunofluorescence assay-based characterization of 12 newly obtained mAbs which react with apical organelles, and the identification of immunoaffinity-purified target antigens by liquid chromatography-tandem mass spectrometry (LC-MS/MS) analysis. We additionally describe the identification and validation of a novel PfRAMA/PfRON3 rhoptry protein complex of *P. falciparum*.

Abbreviations: BSA, bovine serum albumin; DAPI, 4′,6-diamidino-2-phenylindole; EDTA, ethylenediaminetetraacetic acid; ELISA, enzyme-linked immunosorbent assay; IFA, immunofluorescence assay; IgG, immunoglobulin G; MAb, monoclonal antibody; PBS, phosphate buffered saline; SDS-PAGE, sodium dodecyl sulfate- polyacrylamide gel electrophoresis; GPI, glycosylphosphatidylinositol; Pf, *P. falciparum*; PV, parasitophorous vacuole; AMA1, apical merozoite protein 1; RAMA, rhoptry-associated membrane antigen; RAP, rhoptry-associated protein; RON, rhoptry neck protein; RhopH, high-molecular weight rhoptry protein; Clag, cytoadherence-linked asexual gene; WGCFS, wheat germ cell-free protein synthesis system.

MATERIALS AND METHODS

Parasite Culture

P. falciparum NF54 strain asexual stage parasites were maintained in continuous culture of human erythrocytes (blood group O^+) obtained from the Japanese Red Cross Society, essentially as described (Ito et al., 2013; Morita et al., 2017).

Fractionation of Schizont-Rich Parasites and Soluble Antigen Preparation

To obtain parasite specimens, mature schizonts were enriched to 65%–75% parasitemia *via* 65% Percoll-sorbitol centrifugation (Dluzewski et al., 1984). The pellets were treated with tetanolysin (3 μg/ml, Biological Laboratories, Campbell, CA) to remove hemoglobin without loss of parasite proteins present in the PV space as described (Hiller et al., 2003; Lopez-Estrano et al., 2003), and washed with phosphate-buffered saline (PBS) containing cOmplete protease inhibitor cocktail (Roche, Mannheim, Germany). Schizont-rich parasites (~10^8) were disrupted by sonication (10 s pulse, 30 s rest, repeated 10 times) on ice in PBS supplemented with cOmplete protease inhibitor cocktail. Undisrupted cells and debris were removed by centrifugation at 21,600 × *g* for 15 min at 4°C. The resulting supernatant fractions were stored at −80°C and subsequently used as soluble antigen for mouse immunization, enzyme-linked immunosorbent assays (ELISA), and western blot analyses.

Monoclonal Antibody Production

Mouse monoclonal antibodies (mAbs) were produced at Kitayama Labes (Ina, Japan). Briefly, three BALB/c mice (female) 8-weeks old were immunized in their foot pads with 50 μg of soluble antigen of *P. falciparum* mature schizonts, formulated with Freund's complete adjuvant for the first immunization and with Freund's incomplete adjuvant 2 weeks later. Six weeks after the second immunization an intravenous

boost with the same amount of soluble fraction in PBS was administered, and lymphocytes from the inguinal lymph nodes were used to fuse with P3-X63-Ag8-U1 myeloma cells to produce hybridoma cells. Culture supernatants from hybridomas were initially screened for reactivity against immunogen by ELISA and secondarily with indirect immunofluorescence assays (IFA) using mature *P. falciparum* schizonts as antigen. Positive hybridoma cells were cloned by two rounds of limiting dilution and the antibody isotypes were determined using a monoclonal antibody isotyping kit (Santa Cruz Biotechnology, Santa Cruz, CA). Cloned cell lines were expanded as ascites in mice primed with Pristane (Wako, Osaka, Japan), and immunoglobulin G (IgG) was purified from ascitic fluid using a MAbTrap kit (GE Healthcare, Camarillo, CA).

Immunofluorescence Assays

Thin smears of schizont-rich *P. falciparum*-infected erythrocytes were prepared and stored at −80°C. The smears were thawed, fixed with 4% paraformaldehyde at room temperature for 10 min, permeabilized with PBS containing 0.1% Triton X-100 at room temperature for 15 min, and blocked with PBS containing 5% non-fat dry milk at 37°C for 30 min. The smears were then incubated with both mouse monoclonal antibodies and rabbit polyclonal antibodies as counter staining at 37°C for 1 h, followed by incubation at 37°C for 30 min with both Alexa Fluor 488-conjugated goat anti-mouse IgG and Alexa Fluor 546-conjugated goat anti-rabbit IgG (Invitrogen, Carlsbad, CA) as secondary antibodies (1:500). Nuclei were stained with 4′,6-diamidino-2-phenylindole (2 μg/ml, DAPI). Slides were mounted in ProLong Gold Antifade (Invitrogen) and viewed under a 63× oil-immersion lens. High-resolution image capture and processing was performed using a confocal scanning laser microscope (LSM5 PASCAL or LSM710; Carl Zeiss MicroImaging, Thornwood, NY). Images were processed in Adobe Photoshop (Adobe Systems, San José, CA).

Immunoelectron Microscopy

Parasites were fixed and embedded in LR White resin (Polysciences, Warrington, PA) and ultrathin sections were immunostained as described (Ito et al., 2011). Samples were examined with a transmission electron microscope (JEM-1230, JEOL, Tokyo, Japan).

SDS-PAGE and Western Blot Analysis

Parasite soluble antigens were extracted in SDS-PAGE loading buffer, incubated at 4°C for 6 h, and subjected to electrophoresis under non-reducing and reducing conditions on 12.5% polyacrylamide gels (ATTO, Tokyo, Japan). Proteins were then transferred to 0.2 μm PVDF membranes (GE Healthcare). The proteins were immunostained with antibodies followed by horseradish peroxidase conjugated secondary antibody (GE Healthcare) and visualized with Immobilon Western Chemiluminescent HRP Substrate (Millipore, Billerica, MA) on a LAS 4000 Mini luminescent-image analyzer (GE Healthcare). The relative molecular masses of the proteins were estimated with reference to Precision Plus Protein Standards (BioRad, Hercules, CA).

Affinity Purification of Target Proteins and Identification by Liquid Chromatography-Tandem Mass Spectrometry

Preparations of enriched late *P. falciparum* parasite schizonts were lysed for 1 h in extraction buffer [50 mM Tris–HCl, 0.2 M NaCl, 5 mM EDTA, 0.2% Nonidet P-40 (NP40; Nacalai Tesque, Kyoto, Japan), pH 7.4, containing 1 μg/ml leupeptin, 1 μg/ml pepstatin A, and 1 mM 4-(2-aminoethyl)-benzenesulfonyl fluoride hydrochloride (Wako)]. The lysate was centrifuged at 15,000 × *g* for 10 min at 4°C, and then target proteins were purified from the parasite lysate by affinity chromatography using a monoclonal antibody-conjugated Formyl-Cellulofine (Seikagaku-Kogyo, Japan) column as described (Kaneko et al., 2001). The following experiments were conducted at APRO SCIENCE (Naruto, Japan). Briefly, the purified protein was resolved by 10% SDS-PAGE under reducing conditions, and the expected individual target bands were excised from the gels. The extracted protein from each band was then digested overnight with trypsin (Thermo Fisher Scientific), and the resulting peptide fragments were fractionated by reverse phase high-performance liquid chromatography (EASY-nLC 1200, Thermo Fisher Scientific) and analyzed on a Q Exactive Plus mass spectrometer (Thermo Fisher Scientific). The obtained peptide mass fingerprints were used to search a *P. falciparum* protein sequence database (PlasmoDB, http://plasmodb.org) using the MASCOT program (Perkins et al., 1999).

Production of Recombinant PfRAMA Proteins and Antisera

The *pframa* (PF3D7_0707300) nucleotide sequence of the strain 3D7 was obtained from PlasmoDB. To generate specific antibodies, three regions of *pframa* were amplified and expressed as recombinant proteins using the wheat germ cell-free protein synthesis system (WGCFS, CellFree Sciences, Matsuyama, Japan) as described (Tsuboi et al., 2008). Briefly, the constructs included full-length PfRAMA (PfRAMA_FL) excluding the signal peptide and GPI-anchor signal sequences (encompassing 768 aa, D_{32} to I_{799}), the N-terminal region of PfRAMA (PfRAMA_N, encompassing 214 aa, D_{32} to D_{245}), and the C-terminal region of PfRAMA (PfRAMA_p60, encompassing 277 aa, K_{482} to F_{758}). Target regions were PCR amplified from *P. falciparum* NF54 blood-stage cDNA using sense primers with an XhoI restriction site and antisense primers with a BamHI site (in lowercase letters in the primer sequences below); specifically, PfRAMA-sense (5'-ctcgagGATCATAATATTAAGAATAATAATTGTATTA-3'), PfRAMA_FL-antisense (5'-ggatccCTATTTACTTATCAATTGTTTCTCTTCCTTA-3'), PfRAMA_N-antisense (5'-ggatccCTAATCGTCGTAATCATATTCTTCGCT-3'), PfRAMA_p60-sense (5'- ctcgagAAAAAAATGGTCTTTTATGATTTATAC-3'), and PfRAMA_p60-antisense (5'- ggatccCTAGAAAATTTTATTATTATTTTCTAATAATGT-3'). The amplified fragments were then restricted and ligated into the WGCFS vector pEU-E01-G(TEV)-N2 to fuse a GST-tag and TEV recognition site at the N-terminus of the target sequences (CellFree Sciences). The recombinant GST-PfRAMA proteins were captured using a glutathione-Sepharose 4B column (GE Healthcare), and the recombinant proteins were

eluted by on-column cleavage with 60 U of AcTEV protease (Invitrogen). The detailed methods are described (Ito et al., 2011). To generate antisera against each recombinant PfRAMA protein, immunization was performed at Kitayama Labes (Ina, Japan). Briefly, two female BALB/c mice were immunized subcutaneously with 20 μg of purified PfRAMA with Freund's adjuvant. A Japanese white rabbit was also immunized subcutaneously with 250 μg of purified PfRAMA with Freund's adjuvant. All immunizations were performed 3 times at 3-week intervals, and then antisera were collected 2 weeks after the third immunization. We used additional mouse and rabbit polyclonal antibodies: anti-PfAMA1 (PF3D7_1133400), Q_{25}-K_{546}; anti-PfRON3_2 (PF3D7_1252100), D_{1686}-K_{1884}; and anti-PfRAP1 (PF3D7_1410400), M_1-D_{782} that were generated and validated previously (Ito et al., 2011).

Immunoprecipitation

Immunoprecipitation was carried out as described (Ito et al., 2011). Briefly, proteins were extracted from late schizont pellets in PBS with 1% Triton X-100 containing cOmplete protease inhibitor cocktail. After centrifugation the supernatants (50 μl) were preincubated at 4°C for 1 h with 40 μl of 50% protein G-conjugated beads (GammaBind Plus Sepharose, GE Healthcare) in NETT buffer (50 mM Tris–HCl, 0.15 M NaCl, 1 mM EDTA, and 0.5% Triton X-100) supplemented with 0.5% BSA (fraction V, Sigma-Aldrich). Aliquots of recovered supernatants were incubated with purified IgG from rabbit polyclonal antibody, and then 40 μl of a 50% protein G-conjugated bead suspension was added. After 1 h incubation at 4°C, the beads were washed once with NETT–0.5% BSA, once with NETT, once with high-salt NETT (0.5 M NaCl), once with NETT, and once with low-salt NETT (0.05 M NaCl and 0.17% Triton X-100). Finally, proteins were eluted from the protein G-conjugated beads with 0.1 M glycine–HCl (pH 2.5), and then immediately neutralized with 1 M Tris pH 9.0. The supernatants were used for western blot analysis using mouse antibodies.

RESULTS

Monoclonal Antibody Production and Apical Organelle Recognition by Immunofluorescence Assays

Out of the 164 ELISA positive mAbs obtained against immunogens, only 12 (~7%) reacted by IFA against late schizont parasites with a punctate staining pattern suggestive of recognition of merozoite apical organelles (**Figure 1**). To predict target organelles, dual labeling IFA was performed with PfRAP1 as a rhoptry bulb marker and PfAMA1 as a microneme marker. All 12 selected mAbs colocalized with PfRAP1 but not with PfAMA1, suggesting recognition of the merozoite rhoptry bulb (**Figure 1**).

Monoclonal Antibodies Recognized Distinct Parasite Antigens by Western Blot Analysis

To classify target antigens recognized by the 12 mAbs, we first determined the mAb isotype from the culture supernatant and then each mAb was purified from mouse ascitic fluid using a MAbTrap kit (GE Healthcare). We were unable to obtain purified mAbs from two clones, 2B2 and 3D6 (**Supplementary Figure 1**). Western blot analysis of schizont-rich parasite lysates was then performed with purified mAb to confirm reactivity and to predict the molecular weights of the target parasite native antigens. The mAb clone 4A3 (IgG1 isotype) reacted with antigens of approximately 60 and 52 kDa size; 4H3 (IgG1) with 100 and 95 kDa antigens; 1C2 (IgG1) with a 150 kDa antigen; 1G5 (IgG2a) with 170, 60, 45, 40, and 30 kDa antigens; 4F6 (IgG1) with a 47 kDa antigen; 2B6 (IgG1) with a 60 kDa antigen; 3F10 (IgG1) with 100 and 52 kDa antigens; and 4E6 (IgG1) with 60 and 50 kDa antigens. The mAb clones 2E5 (IgG1) and 2E4 (IgG1) did not react with parasite antigens under this condition. Overall, eight western blot-positive mAbs recognized distinct parasite antigens (**Supplementary Figure 1**).

Target Antigen Identification by Liquid Chromatography-Tandem Mass Spectrometry From Immunoaffinity-Purified Parasite Proteins

We successfully obtained 5 mAb clones from mouse ascites in sufficient quantity to generate immunoaffinity columns. To identify target proteins recognized by the mAbs, schizont-rich parasite extracts were immunoaffinity-purified by affinity columns conjugated with each mAb followed by LC-MS/MS analysis. The mAbs were categorized based on whether they recognized LMW or HMW rhoptry protein complexes, or other proteins.

Monoclonal Antibodies 4F6 and 4H3 Recognize the Low-Molecular Weight PfRAP Complex Proteins

Western blot analysis of parasite lysates indicated that mAb 4F6 recognized a distinct antigen from that recognized by 4H3 (**Supplementary Figure 1**), but the SDS-PAGE banding patterns of the immunoaffinity-purified proteins looked similar using either a 4F6 or 4H3 column (**Figure 2A**). To identify which bands were specifically recognized, the immunoaffinity-purified materials were analyzed by western blot by staining independently with each mAb. **Figure 2B** shows that 4F6 recognizes a single band around 47 kDa under reducing conditions in separated proteins immunoaffinity-purified by either 4F6 (**Figure 2B**, lane 1) or 4H3 (**Figure 2B**, lane 2), and 4H3 recognized multiple bands around 100 kDa under non-reducing conditions. HMW bands recognized only under non-reducing conditions were likely non-specific reaction with secondary antibody because these bands were also visible in the negative controls (**Figure 2B**, PBS/T). By LC-MS/MS analyses we identified the 4F6 immunoprecipitates as PfRAP1 and PfRAP2 (**Figure 2C**). Taken together, the target antigens of both mAbs are the described LMW rhoptry protein complex (**Table 1**, **Supplementary Tables 1, 2**, and **Figure 2C**).

Monoclonal Antibodies 1C2 and 4E6 Recognize the High-Molecular Weight PfRhopH Complex Proteins

MAb 1C2 recognized a distinct antigen from that identified by 4E6 in western blots of parasite lysates (**Supplementary Figure 1**). A

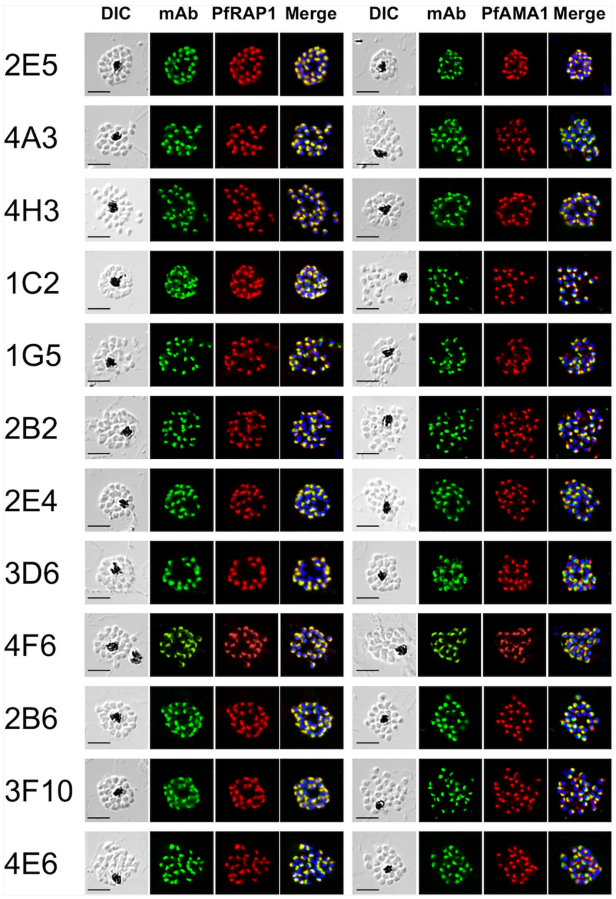

FIGURE 1 | Monoclonal antibodies react with the apical end of *P. falciparum* merozoites. Mature schizont stage parasites were dual-labeled with each mouse mAb and rabbit antisera against either PfRAP1 (rhoptry body marker) or PfAMA1 (microneme marker). Nuclei were visualized with DAPI in the merged images shown in the right most panels. DIC, differential interference contrast microscopy. Merge, created by merging the IFA and nuclear-staining images. A representative image out of at least three independent experiments is shown for each mAb. Bars represent 5 µm.

single major band around 140 kDa was visible in SDS-PAGE in the immunoaffinity-purified proteins using a 1C2 column, whereas triple major bands were visible in the immunoaffinity-purified proteins using a 4E6 column (**Figure 2D**). The immunoaffinity-purified materials were analyzed by western blot by independently staining with each mAb. **Figure 2E** shows that 1C2 recognized a single band around 140 kDa under reducing conditions of separated proteins immunoaffinity-purified by either 1C2 (**Figure 2E**, 1C2, lane 1) or 4E6 (**Figure 2E**, 1C2, lane 2). In contrast, we could not identify target antigen bands by western blot with 4E6 staining, perhaps because of the lower reactivity of the mAb 4E6 under reducing conditions (**Figure 2E**, 4E6). By LC-MS/MS analyses, we identified that mAb 1C2 dominantly recognized PfRhopH2 (**Figure 2F**, lane 1C2) and associated PfRhopH complex partners Clag 9 and PfRhopH3 as minor bands. In contrast, mAb 4E6 dominantly recognized PfRhopH3 (**Figure 2F**, lane 4E6) and associated PfRhopH complex partners as minor bands (Clag 3.1, Clag 3.2, and Clag 9). Taken together, the target antigens of both mAbs are within the HMW rhoptry protein complex (**Table 1**, **Supplementary Tables 1, 2**, and **Figure 2F**).

Monoclonal Antibody 1G5 Recognizes the PfRAMA Protein

MAb 1G5 recognized a major band around 60 kDa with multiple bands between 170 and 30 kDa in western blots of parasite lysates (**Supplementary Figure 1**). A single major band around 60 kDa was also visible in SDS-PAGE of the immunoaffinity-purified proteins using a 1G5 column (**Figure 2G**). The immunoaffinity-purified materials were analyzed by western blot and 1G5 staining. **Figure 2H** shows that 1G5 recognizes a major band around 60 kDa and at least seven additional bands between 100 kDa and 30 kDa, suggesting that those bands are proteolytically cleaved fragments from a single molecule. The SDS-PAGE results using a 10% gel at APRO SCIENCE showed that a major band around 60 kDa and a high-molecular weight band were identified (**Figure 2I**). LC-MS/MS determined that 1G5 recognizes PfRAMA (**Figure 2I**) and that an associated PfRON3 protein is also identified. Taken together, PfRAMA was the target antigen of mAb 1G5, and these data suggest that PfRAMA forms a protein complex with PfRON3 (**Table 1**, **Supplementary Tables 1, 2**, and **Figure 2I**).

Complex Formation Between PfRAMA and PfRON3 Proteins in the Early Schizont Stage

To confirm the specificity of polyclonal anti-RAMA antibodies western blot analyses of schizont-rich parasite lysates were performed under non-reducing (NR) and reducing (R) conditions. Rabbit and mouse anti-PfRAMA_FL and anti-PfRAMA_p60 antibodies recognized both PfRAMA_FL at the expected molecular weight of 170 kDa (**Figure 3A**, arrow) and PfRAMA_p60 at the expected molecular weight of 60 kDa (**Figure 3A**, arrowhead); however, anti-PfRAMA_N antibodies recognized only PfRAMA_FL (**Figure 3A**, arrow). In addition, anti-PfRAMA_FL rabbit antibodies recognized the rhoptry bulb by IEM (**Figure 3B**), and confirmed that the anti-PfRAMA antibodies specifically recognized PfRAMA. We also confirmed the specificity of the anti-PfRON3_2 rabbit antibody as rhoptry bulb localization (**Figure 3C**).

Immunoprecipitation assays were performed to validate the PfRAMA interaction with PfRON3. First, we immunoprecipitated PfRON3, PfRAMA, and PfAMA1 proteins in schizont-rich parasite lysates using rabbit anti-PfRON3_2, anti-PfRAMA_FL, and anti-PfAMA1 antibodies. By western blot analyses the immunoprecipitates were probed with mouse anti-PfRAMA_FL antibodies (**Figure 3D**). We observed that anti-PfRON3_2 antibody could coimmunoprecipitate both PfRAMA_FL (**Figure 3D**, arrow) and PfRAMA_p60 (**Figure 3D**, arrowhead). The signal intensity of the PfRAMA_FL band was relatively stronger than that of PfRAMA_p60 in PfRON3_2 immunoprecipitates, suggesting that PfRON3 formed a more stable complex with PfRAMA_FL than PfRAMA_p60. By comparison, anti-PfAMA1 antibodies as a negative control did not immunoprecipitate PfRAMA. As a reverse experiment we immunoprecipitated PfRON3 and

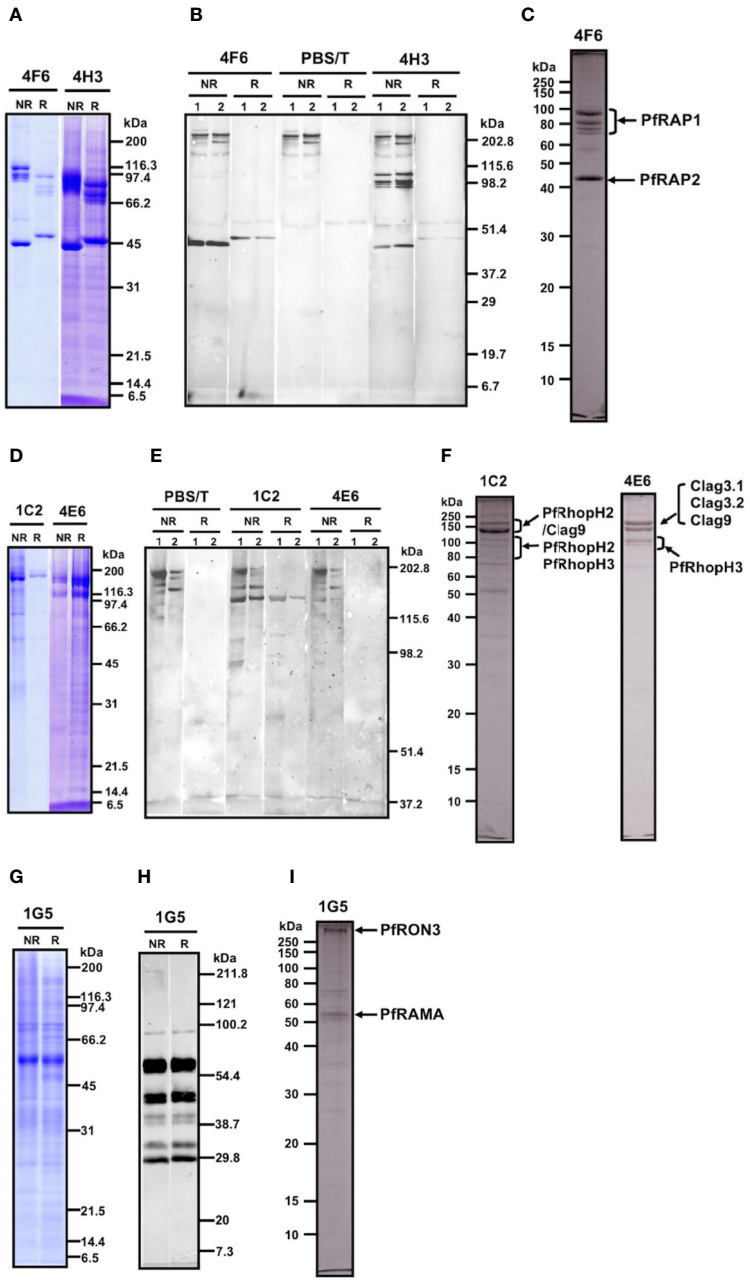

FIGURE 2 | **(A–C)** Analyses of the immunoaffinity-purified proteins using affinity columns conjugated with either mAb 4F6 or 4H3. **(A)** The elution fractions were resolved by 12.5% SDS-PAGE under reducing or non-reducing conditions. **(B)** Western blot analyses of elution fractions. Elution fractions from 4F6 (lane 1) and 4H3 (lane 2) affinity columns were resolved by 12.5% SDS-PAGE and the proteins were probed with either mAb 4F6 or 4H3. PBS/T serves as a negative control staining. **(C)** Protein bands used for the LC-MS/MS analyses. The elution fraction from the 4F6 column was resolved by 10% SDS-PAGE under reducing conditions and the target bands (arrows) were excised from the gel. Proteins identified by LC-MS/MS are indicated. **(D–F)** Analyses of the immunoaffinity-purified proteins using affinity columns conjugated with either mAb 1C2 or 4E6. **(D)** The elution fractions were resolved by 12.5% SDS-PAGE under reducing or non-reducing conditions. **(E)** Western blot analyses of elution fractions. The elution fractions from the 1C2 (lane 1) and 4E6 (lane 2) affinity columns were resolved by 7.5% SDS-PAGE and the proteins were probed with either mAb 1C2 or 4E6. PBS/T serves as a negative control staining. **(F)** Protein bands used for the LC-MS/MS analyses. The elution fractions from the 1C2 and 4E6 columns were resolved by 10% SDS-PAGE under reducing conditions and the target bands (arrows) were excised from the gel. Proteins identified by LC-MS/MS are indicated. **(G–I)**. Analyses of the immunoaffinity-purified proteins using an affinity column conjugated with mAb 1G5. **(G)** The elution fraction was resolved by 12.5% SDS-PAGE under reducing or non-reducing conditions. **(H)** Western blot analysis of elution fraction. Elution fractions from the 1G5 affinity column were resolved by 12.5% SDS-PAGE and the proteins were probed with mAb 1G5. **(I)** Protein bands used for the LC-MS/MS analyses. The elution fraction from the 1G5 column was resolved by 10% SDS-PAGE under reducing conditions and the target bands (arrows) were excised from the gel. Proteins identified by LC-MS/MS are indicated.

TABLE 1 | LC-MS/MS analysis of immunoaffinity-purified proteins with each monoclonal antibody from *Plasmodium falciparum* schizont lysates.

mAbs	Protein	MW (kDa)	%[a]	PlasmoDB ID	Peptide sequences identified[b]	Score[c]
4F6	PfRAP2	46.7	43	PF3D7_0501600	^{52}LSMWVYFIYNHFSSADELIK^{71}//^{314}QFDYALFHKTYSIPNLK^{330}	996
	PfRAP1	90.0	41	PF3D7_1410400	^{181}SASVAGIVGADEEAPPAPKNTLTPLEELYPTNVNLFNYKYSLNNMEENIN ILKNEGDLVAQKEEFEYDENMEK^{253}//^{712}MKTDMLSLQNEESK^{725}	1420
1C2	PfRhopH2	162.6	27	PF3D7_0929400	^{52}YLYMDEYLSEGDKATFEK^{69}/^{1193}LFVTEGTLEYLLLDK^{1207}	1792
	Clag9	160.4	9	PF3D7_0935800	^{35}SILDNDELYNSLSNLENLLLQTLEQDELK^{63}//^{1259}ENVVQEVQEDK^{1269}	317
	PfRhopH3	104.8	21	PF3D7_0905400	^{111}EYEEPFVNPVMK^{122}//^{824}TTDNTYKEMEELEEAEGTSNLK^{845}	622
4E6	PfRhopH3	104.8	36	PF3D7_0905400	^{52}GNGPDAGSFLDFVDEPEQFYWFVEHFLSVK^{81}//^{793}STSAASTSDEISGSEGPS TESTSTGNQGEDKTTDNTYKEMEELEEAEGTSNLK^{845}	1063
	Clag3.1	167.2	20	PF3D7_0302500	^{78}LILESLEKDK^{87}//^{1390}MNEADSADSDDEKDSDTPDDELMISR^{1415}	992
	Clag3.2	167.5	15	PF3D7_0302200	^{37}NENANVNTPENLNK LLNEYDNIEQLK^{62}// ^{964}TMFAAFQMLFSTMLSNNVDNLDK^{986}	858
	Clag9	160.4	12	PF3D7_0935800	^{35}SILDNDELYNSLSNLENLLLQTLEQDELKIPIMK^{68}//^{1244}EGAYEEAMVSR^{1254}	483
1G5	PfRAMA	103.6	11	PF3D7_0707300	^{589}YLDDLIDEEQTIKDAVK^{605}//^{735}INDELLTDQGPNEDTLLENNNK^{756}	401
	PfRON3	263.0	3	PF3D7_1252100	^{374}NLGTGFFDFSNSLFK^{388}//^{1558}FLADSNIPSIPYQGFSVR^{1575}	156

[a]*Percent peptide coverage (%) is shown for each protein. All regions covered by identified peptides are shown in red text in* ***Supplementary Table 1****.* [b]*Representative two peptide sequences with higher scores among all the identified peptides are shown. The number represents the position at the N- and C-terminus of each peptide ("//").* [c]*Score is a sum of the scores of all the identified peptides. Each peptide score is* $-10 \times Log_{10}(P)$*, where P is the probability that the observed match is a random event. Peptide scores greater than 27 indicate identity or extensive homology (P < 0.05). RAP, rhoptry-associated protein; RhopH, high-molecular mass rhoptry protein complex; Clag, cytoadherence-linked asexual gene; RAMA, rhoptry-associated membrane antigen; RON, rhoptry neck protein.*

PfRAMA proteins in the same parasite lysates using rabbit anti-PfRON3_2, anti-PfRAMA_p60, and anti-PfRAMA_FL antibodies and probed with mouse anti-PfRON3_2 antibodies as above (**Figure 3E**). We observed that anti-PfRAMA_FL antibody could coimmunoprecipitate PfRON3 (**Figure 3E**, arrow); however, anti-PfRAMA_p60 could not (**Figure 3E**). These results confirmed that PfRAMA (except for the PfRAMA_p60 region which is known to associate with PfRAP1, PfRhopH3, and PfSortilin) formed a protein complex with PfRON3.

IFA was performed to investigate in which developmental stages PfRAMA interacts with PfRON3. By immunostaining with anti-PfRON3_2 and anti-PfRAMA_FL antibodies, PfRON3, and PfRAMA were colocalized mostly in the cytoplasm in early schizonts (**Figure 3F**, ES), and in a patchy pattern in each merozoite in late schizonts (**Figure 3F**, LS) suggesting rhoptry localization. In contrast, when PfRAMA was immunostained with anti-PfRAMA_N antibodies, PfRON3, and PfRAMA also colocalized mostly in the cytoplasm in early schizonts (**Figure 3G**, ES); however, a lack of staining in late schizonts (**Figure 3G**, LS) suggested that the PfRAMA_N region was not present in the merozoite rhoptry in mature schizonts. These results suggest that the PfRAMA_N region may form a protein complex with PfRON3 in the early schizont stage.

DISCUSSION

Identification of novel apical organellar proteins of merozoite are essential for understanding merozoite invasion into erythrocytes as well as providing new vaccine candidates for study. Here we generated 12 mAbs which recognize merozoite apical organelles. Immunoaffinity-purification combined with LC-MS/MS identified target antigens of 5 mAbs as PfRAP1, PfRAP2, PfRhopH2, PfRhopH3, and PfRAMA. Although these five antigens are known rhoptry bulb proteins (Counihan et al., 2013), the identification of a novel PfRAMA/PfRON3 rhoptry protein complex in the *P. falciparum* merozoite is emphasized.

PfRAMA is a rhoptry bulb protein which is expressed relatively early before the *de novo* formation of rhoptries. After proteolytic cleavage a PfRAMA_p60 fragment is formed and localizes in the merozoite rhoptry bulb in the late schizont stage (Smythe et al., 1988; Topolska et al., 2004). Thereafter, PfRAMA_p60 localizes to the rhoptry but not on the surface of the free merozoite. When the merozoite attaches to the erythrocyte, the discharged PfRAMA_p60 binds to the erythrocyte surface. Subsequently, PfRAMA_p60 is localized in the PV membrane during merozoite invasion (Smythe et al., 1988; Topolska et al., 2004).

To elucidate the function of PfRAMA two studies demonstrated by fluorescent resonance energy transfer (FRET) and immunoprecipitation that PfRAMA interacts with both PfRAP1 and PfRhopH3 (Topolska et al., 2004; Richard et al., 2009). Recently the PfRAMA-PfRAP1 complex was also suggested as a cargo for the *Plasmodium* orthologue of sortilin (Hallee et al., 2018b). To further investigate the role of PfRAMA, Sherling et al., (2019) generated a PfRAMA conditional knockdown parasite line. Contrary to previous findings (Topolska et al., 2004; Richard et al., 2009; Hallee et al., 2018b), the PfRAMA knockdown parasites presented correct trafficking of PfRAP1 and PfRhopH3. In addition, several other rhoptry bulb proteins, such as PfRAP2, PfRh5, Clag3.1, and PfRhopH2 also localized correctly to the rhoptry in the transgenic parasites. Therefore, their findings were inconsistent with the proposed rhoptry bulb-specific protein escorter role of PfRAMA (Hallee et al., 2018b). Furthermore, although the knockdown parasites showed that some RON proteins—PfRON2, PfRON3, and PfRON4—were diminished in mature schizonts, the rhoptry neck proteins PfRON12 and Rh2b were normally localized in the rhoptry (Sherling et al., 2019). While PfRON3 is now known as a rhoptry body protein (Ito et al., 2011) (**Figure 3C**), they suggested that the mislocalization of the above RON proteins may be due to abnormal rhoptry neck biogenesis. In this study we identified by immunoprecipitation an interaction of PfRON3 with PfRAMA_FL but not with PfRAMA_p60 (**Figures 3D, E**). We also showed their colocalization when stained with anti-PfRAMA_FL

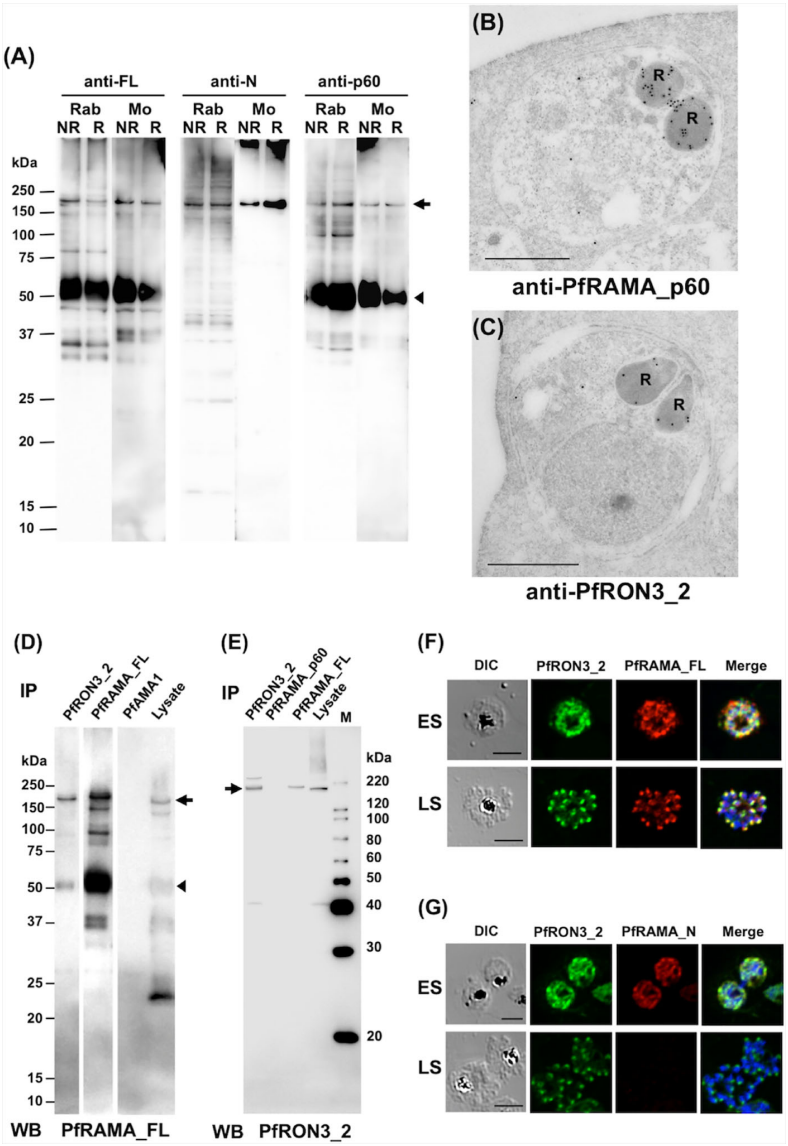

FIGURE 3 | **(A)** Specificity of anti-PfRAMA antibodies by western blot analyses. Proteins from schizont-rich parasites were extracted and separated by 12.5% SDS-PAGE under non-reducing (NR) or reducing (R) conditions. Using either anti-PfRAMA_FL, anti-PfRAMA_N, or anti-PfRAMA_p60 antibodies obtained from rabbits (Rab) and mice (Mo), a band of approximately 170 kDa (arrow) was detected as a signal of PfRAMA_FL and a 60-kDa band (arrowhead) was detected as a signal of PfRAMA_p60. **(B)** PfRAMA localization by IEM is shown. A representative image out of eight independent sections is shown of a merozoite in a schizont-infected erythrocyte probed with rabbit anti-PfRAMA_p60 antibody and subsequently with a secondary antibody conjugated with gold particles. The black dots indicate signals from gold particles localized in the rhoptry bulb. R, rhoptry. **(C)** PfRON3 localization shown by IEM. A representative image out of 16 independent sections is shown of a merozoite in a schizont-infected erythrocyte probed with rabbit anti-PfRON3_2 antibody and subsequently with a secondary antibody conjugated with gold particles. The black dots indicate signals from gold particles localized in the rhoptry bulb. R, rhoptry. Bars = 500 nm. **(D)** PfRAMA_FL interacts with PfRON3. NP-40 extracts of schizont-rich parasites (Lysate) were immunoprecipitated (IP) with rabbit sera against PfRON3 (anti-PfRON3_2), PfRAMA (anti-PfRAMA_FL), or PfAMA1 (anti-PfAMA1), then stained with mouse antisera (WB) against PfRAMA_FL. This panel is a representative result of two independent experiments. **(E)** PfRAMA_FL but not PfRAMA_p60 interacts with PfRON3. NP-40 extracts of schizont-rich parasites (Lysate) were immunoprecipitated (IP) with rabbit sera against PfRON3 (anti-PfRON3_2), PfRAMA (anti-PfRAMA_p60), or PfRAMA (anti-PfRAMA_FL), then stained with mouse antisera (WB) against PfRON3_2. M, molecular weight marker. This panel is a representative result of two independent experiments. **(F)** Co-localization of PfRON3 and PfRAMA. Immature early schizont (ES) or mature late schizont (LS) stage parasites were dual-labeled with rabbit antibodies against PfRON3_2 and mouse antibodies against PfRAMA_FL. Nuclei were visualized with DAPI in merged images shown in the right most panels. DIC, differential interference contrast microscopy. Merge, the image created by merging the IFA and nuclear-staining images. Bars represent 5 μm. **(G)** Co-localization of PfRON3 and PfRAMA. Immature early schizont (ES) or mature late schizont (LS) stage parasites were dual-labeled with rabbit antibodies against PfRON3_2 and mouse antibodies against PfRAMA_N. Nuclei were visualized with DAPI in merged images shown in the right most panels. DIC, differential interference contrast microscopy. Merge, the image created by merging the IFA and nuclear-staining images. Bars represent 5 μm.

and PfRON3 antibodies but not with anti-PfRAMA_N antibodies in the mature schizont stage (**Figures 3F, G**). These results suggest that the association between PfRAMA and PfRON3 occurs in the immature schizont stage, and thereafter the two proteins dissociate when the N-terminal region of PfRAMA (downstream from the PfRAMA_N region) is proteolytically degraded in the mature schizont (Smythe et al., 1988; Topolska et al., 2004). In addition, we previously reported that PfRON3 interacts with PfRON2 and PfRON4, but not with PfAMA1 (Ito et al., 2011), suggesting that a portion of PfRON3 is involved in the formation of a RON complex (PfRON2, 3, and 4), but not in the moving junction complex (PfRON2, 4, 5, and PfAMA1) (Ito et al., 2011). Taken together, the absence of PfRAMA affects the trafficking of its associated RONs, and this could potentially explain the abnormal rhoptry neck biogenesis as observed by Sherling et al., (2019).

To predict the PfRON3 associating region in PfRAMA, the PfRAMA knockdown parasite generated by Sherling et al., (2019) provided us with useful information. The knockdown parasite with abnormal PfRON3 trafficking resulted in expression of the N-terminal 220 residues of the protein but lacking the C-terminal region spanning aa V_{315}–S_{840}. This C-terminal 526-residue protein was previously shown to interact with both PfRAP1 and PfSortilin (Topolska et al., 2004; Richard et al., 2009; Hallee et al., 2018a; Hallee et al., 2018b). Additional evidence is that our anti-PfRAMA_p60 (K_{482} to F_{758}) antibodies failed to immunoprecipitate PfRON3 (**Figure 3E**). Taken together, the PfRAMA residues spanning aa Q_{221}-E_{481} may be important for the trafficking of PfRON3 to the rhoptries. Further investigation will be required as to whether PfRAMA and PfRON3 interact directly or indirectly, such as by using a surface plasmon resonance approach with recombinant proteins.

DATA AVAILABILITY STATEMENT

The raw data supporting the conclusions of this article will be made available by the authors, without undue reservation.

ETHICS STATEMENT

Ethical review and approval was not required for the animal study because all the immunization for mouse monoclonal antibodies and rabbit polyclonal antibodies were done at Kitayama Labes company (Ina, Japan) under their ethics standards, and we purchased the generated antibodies from the Kitayama Labes company. So our IRB approval was not needed.

AUTHOR CONTRIBUTIONS

TT and E-TH conceived and designed the experiments. DI, J-HC, ET, TH, AT, and E-TH conducted experiments. DI, J-HC, ET, HO, ST, AT, E-TH, and TT analyzed the data. DI, J-HC, ET, E-TH, and TT wrote the manuscript. All authors contributed to the article and approved the submitted version.

FUNDING

This work was supported in part by JSPS KAKENHI (Grant Nos. JP17H06873, JP18H02651, JP18K19455, JP19K22535, and JP20H03481) and Takeda Science Foundation. This work was also supported in part by the National Research Foundation of Korea Grant funded by the Korean Government (2015R1A4A1038666 and 2017R1A2A2A05069562). The funders had no role in the study design, data collection and analysis, decision to publish, or preparation of the manuscript.

ACKNOWLEDGMENTS

We thank Keizo Oka and Masachika Shudo in the Advanced Research Support Center (ADRES), Ehime University, for the technical assistance, and Dr. Thomas J. Templeton for critical reading of the manuscript. We also thank the Japanese Red Cross Society for providing human erythrocytes and plasma for culturing *P. falciparum*.

SUPPLEMENTARY MATERIAL

The Supplementary Material for this article can be found online at: https://www.frontiersin.org/articles/10.3389/fcimb.2020.605367/full#supplementary-material

SUPPLEMENTARY FIGURE 1 | Characterization and isotyping of each monoclonal antibody reacting with the apical end of *P. falciparum* merozoites. To characterize target antigens recognized by the 12 mAbs, the mAb isotypes were determined using the culture supernatant and each mAb was purified from mouse ascitic fluid using a MAbTrap kit (GE Healthcare). The summary of the western blot analyses (12.5% SDS-PAGE gel) and isotyping are presented in the right side of this figure. MAb name with isotype in parenthesis and reacted bands are shown in kDa. N/A, unable to obtain purified mAbs; Negative, no band detected in western blot analysis; PBS/T, negative control stained with PBS/T; NR, nonreducing condition; and R, reducing condition.

REFERENCES

Baldi, D. L., Good, R., Duraisingh, M. T., Crabb, B. S., and Cowman, A. F. (2002). Identification and disruption of the gene encoding the third member of the low-molecular-mass rhoptry complex in Plasmodium falciparum. *Infect. Immun.* 70, 5236–5245. doi: 10.1128/iai.70.9.5236-5245.2002

Campbell, G. H., Miller, L. H., Hudson, D., Franco, E. L., and Andrysiak, P. M. (1984). Monoclonal antibody characterization of Plasmodium falciparum antigens. *Am. J. Trop. Med. Hyg.* 33, 1051–1054. doi: 10.4269/ajtmh.1984.33.1051

Collins, C. R., Withers-Martinez, C., Hackett, F., and Blackman, M. J. (2009). An inhibitory antibody blocks interactions between components of the malarial invasion machinery. *PloS Pathog.* 5, e1000273. doi: 10.1371/journal.ppat.1000273

Cooper, J. A., Ingram, L. T., Bushell, G. R., Fardoulys, C. A., Stenzel, D., Schofield, L., et al. (1988). The 140/130/105 kilodalton protein complex in the rhoptries of

Plasmodium falciparum consists of discrete polypeptides. *Mol. Biochem. Parasitol.* 29, 251–260. doi: 10.1016/0166-6851(88)90080-1

Counihan, N. A., Kalanon, M., Coppel, R. L., and De Koning-Ward, T. F. (2013). Plasmodium rhoptry proteins: why order is important. *Trends Parasitol.* 29, 228–236. doi: 10.1016/j.pt.2013.03.003

Counihan, N. A., Chisholm, S. A., Bullen, H. E., Srivastava, A., Sanders, P. R., Jonsdottir, T. K., et al. (2017). Plasmodium falciparum parasites deploy RhopH2 into the host erythrocyte to obtain nutrients, grow and replicate. *Elife* 6, e23217. doi: 10.7554/eLife.23217

Cowman, A. F., and Crabb, B. S. (2006). Invasion of red blood cells by malaria parasites. *Cell* 124, 755–766. doi: 10.1016/j.cell.2006.02.006

Cowman, A. F., Tonkin, C. J., Tham, W. H., and Duraisingh, M. T. (2017). The Molecular Basis of Erythrocyte Invasion by Malaria Parasites. *Cell Host. Microbe* 22, 232–245. doi: 10.1016/j.chom.2017.07.003

Dluzewski, A. R., Ling, I. T., Rangachari, K., Bates, P. A., and Wilson, R. J. (1984). A simple method for isolating viable mature parasites of Plasmodium falciparum from cultures. *Trans. R. Soc. Trop. Med. Hyg.* 78, 622–624. doi: 10.1016/0035-9203(84)90221-9

Doury, J. C., Bonnefoy, S., Roger, N., Dubremetz, J. F., and Mercereau-Puijalon, O. (1994). Analysis of the high molecular weight rhoptry complex of Plasmodium falciparum using monoclonal antibodies. *Parasitology* 108 (Pt 3), 269–280. doi: 10.1017/s0031182000076113

Gilson, P. R., Nebl, T., Vukcevic, D., Moritz, R. L., Sargeant, T., Speed, T. P., et al. (2006). Identification and stoichiometry of glycosylphosphatidylinositol-anchored membrane proteins of the human malaria parasite Plasmodium falciparum. *Mol. Cell Proteomics* 5, 1286–1299. doi: 10.1074/mcp.M600035-MCP200

Hallee, S., Boddey, J. A., Cowman, A. F., and Richard, D. (2018a). Evidence that the Plasmodium falciparum Protein Sortilin Potentially Acts as an Escorter for the Trafficking of the Rhoptry-Associated Membrane Antigen to the Rhoptries. *mSphere* 3, e00551–e00517. doi: 10.1128/mSphere.00551-17

Hallee, S., Counihan, N. A., Matthews, K., De Koning-Ward, T. F., and Richard, D. (2018b). The malaria parasite Plasmodium falciparum Sortilin is essential for merozoite formation and apical complex biogenesis. *Cell Microbiol.* 20, e12844. doi: 10.1111/cmi.12844

Harnyuttanakorn, P., Mcbride, J. S., Donachie, S., Heidrich, H. G., and Ridley, R. G. (1992). Inhibitory monoclonal antibodies recognise epitopes adjacent to a proteolytic cleavage site on the RAP-1 protein of Plasmodium falciparum. *Mol. Biochem. Parasitol.* 55, 177–186. doi: 10.1016/0166-6851(92)90138-a

Hiller, N. L., Akompong, T., Morrow, J. S., Holder, A. A., and Haldar, K. (2003). Identification of a stomatin orthologue in vacuoles induced in human erythrocytes by malaria parasites. A role for microbial raft proteins in apicomplexan vacuole biogenesis. *J. Biol. Chem.* 278, 48413–48421. doi: 10.1074/jbc.M307266200

Holder, A. A., Freeman, R. R., Uni, S., and Aikawa, M. (1985). Isolation of a Plasmodium falciparum rhoptry protein. *Mol. Biochem. Parasitol.* 14, 293–303. doi: 10.1016/0166-6851(85)90057-x

Ito, D., Han, E. T., Takeo, S., Thongkukiatkul, A., Otsuki, H., Torii, M., et al. (2011). Plasmodial ortholog of Toxoplasma gondii rhoptry neck protein 3 is localized to the rhoptry body. *Parasitol. Int.* 60, 132–138. doi: 10.1016/j.parint.2011.01.001

Ito, D., Hasegawa, T., Miura, K., Yamasaki, T., Arumugam, T. U., Thongkukiatkul, A., et al. (2013). RALP1 is a rhoptry neck erythrocyte-binding protein of Plasmodium falciparum merozoites and a potential blood-stage vaccine candidate antigen. *Infect. Immun.* 81, 4290–4298. doi: 10.1128/IAI.00690-13

Ito, D., Schureck, M. A., and Desai, S. A. (2017). An essential dual-function complex mediates erythrocyte invasion and channel-mediated nutrient uptake in malaria parasites. *Elife* 6, e23485. doi: 10.7554/eLife.23485

Kaneko, O., Tsuboi, T., Ling, I. T., Howell, S., Shirano, M., Tachibana, M., et al. (2001). The high molecular mass rhoptry protein, RhopH1, is encoded by members of the clag multigene family in Plasmodium falciparum and Plasmodium yoelii. *Mol. Biochem. Parasitol.* 118, 223–231. doi: 10.1016/s0166-6851(01)00391-7

Kaneko, O., Yim Lim, B. Y., Iriko, H., Ling, I. T., Otsuki, H., Grainger, M., et al. (2005). Apical expression of three RhopH1/Clag proteins as components of the Plasmodium falciparum RhopH complex. *Mol. Biochem. Parasitol.* 143, 20–28. doi: 10.1016/j.molbiopara.2005.05.003

Kaneko, O. (2007). Erythrocyte invasion: vocabulary and grammar of the Plasmodium rhoptry. *Parasitol. Int.* 56, 255–262. doi: 10.1016/j.parint.2007.05.003

Kats, L. M., Black, C. G., Proellocks, N. I., and Coppel, R. L. (2006). Plasmodium rhoptries: how things went pear-shaped. *Trends Parasitol.* 22, 269–276. doi: 10.1016/j.pt.2006.04.001

Lopez-Estrano, C., Bhattacharjee, S., Harrison, T., and Haldar, K. (2003). Cooperative domains define a unique host cell-targeting signal in Plasmodium falciparum-infected erythrocytes. *Proc. Natl. Acad. Sci. U.S.A.* 100, 12402–12407. doi: 10.1073/pnas.2133080100

Lustigman, S., Anders, R. F., Brown, G. V., and Coppel, R. L. (1988). A component of an antigenic rhoptry complex of Plasmodium falciparum is modified after merozoite invasion. *Mol. Biochem. Parasitol.* 30, 217–224. doi: 10.1016/0166-6851(88)90090-4

Morita, M., Takashima, E., Ito, D., Miura, K., Thongkukiatkul, A., Diouf, A., et al. (2017). Immunoscreening of Plasmodium falciparum proteins expressed in a wheat germ cell-free system reveals a novel malaria vaccine candidate. *Sci. Rep.* 7, 46086. doi: 10.1038/srep46086

Perkins, D. N., Pappin, D. J., Creasy, D. M., and Cottrell, J. S. (1999). Probability-based protein identification by searching sequence databases using mass spectrometry data. *Electrophoresis* 20, 3551–3567. doi: 10.1002/(SICI)1522-2683(19991201)20:18<3551::AID-ELPS3551>3.0.CO;2-2

Preiser, P., Kaviratne, M., Khan, S., Bannister, L., and Jarra, W. (2000). The apical organelles of malaria merozoites: host cell selection, invasion, host immunity and immune evasion. *Microbes Infect.* 2, 1461–1477. doi: 10.1016/s1286-4579(00)01301-0

Richard, D., Kats, L. M., Langer, C., Black, C. G., Mitri, K., Boddey, J. A., et al. (2009). Identification of rhoptry trafficking determinants and evidence for a novel sorting mechanism in the malaria parasite Plasmodium falciparum. *PloS Pathog.* 5, e1000328. doi: 10.1371/journal.ppat.1000328

Richard, D., Macraild, C. A., Riglar, D. T., Chan, J. A., Foley, M., Baum, J., et al. (2010). Interaction between Plasmodium falciparum apical membrane antigen 1 and the rhoptry neck protein complex defines a key step in the erythrocyte invasion process of malaria parasites. *J. Biol. Chem.* 285, 14815–14822. doi: 10.1074/jbc.M109.080770

Ridley, R. G., Takacs, B., Lahm, H. W., Delves, C. J., Goman, M., Certa, U., et al. (1990). Characterisation and sequence of a protective rhoptry antigen from Plasmodium falciparum. *Mol. Biochem. Parasitol.* 41, 125–134. doi: 10.1016/0166-6851(90)90103-s

Sam-Yellowe, T. Y., Del Rio, R. A., Fujioka, H., Aikawa, M., Yang, J. C., Yakubu, Z., et al. (1998). Isolation of merozoite rhoptries, identification of novel rhoptry-associated proteins from Plasmodium yoeliiberghei, and conserved interspecies reactivity of organelles and proteins with P. falciparum rhoptry-specific antibodies. *Exp. Parasitol.* 89, 271–284. doi: 10.1006/expr.1998.4280

Sam-Yellowe, T. Y., Fujioka, H., Aikawa, M., Hall, T., and Drazba, J. A. (2001). A Plasmodium falciparum protein located in Maurer's clefts underneath knobs and protein localization in association with Rhop-3 and SERA in the intracellular network of infected erythrocytes. *Parasitol. Res.* 87, 173–185. doi: 10.1007/pl00008572

Sam-Yellowe, T. Y., Florens, L., Wang, T., Raine, J. D., Carucci, D. J., Sinden, R., et al. (2004). Proteome analysis of rhoptry-enriched fractions isolated from Plasmodium merozoites. *J. Proteome Res.* 3, 995–1001. doi: 10.1021/pr049926m

Sanders, P. R., Gilson, P. R., Cantin, G. T., Greenbaum, D. C., Nebl, T., Carucci, D. J., et al. (2005). Distinct protein classes including novel merozoite surface antigens in Raft-like membranes of Plasmodium falciparum. *J. Biol. Chem.* 280, 40169–40176. doi: 10.1074/jbc.M509631200

Sanders, P. R., Cantin, G. T., Greenbaum, D. C., Gilson, P. R., Nebl, T., Moritz, R. L., et al. (2007). Identification of protein complexes in detergent-resistant membranes of Plasmodium falciparum schizonts. *Mol. Biochem. Parasitol.* 154, 148–157. doi: 10.1016/j.molbiopara.2007.04.013

Saul, A., Cooper, J., Hauquitz, D., Irving, D., Cheng, Q., Stowers, A., et al. (1992). The 42-kilodalton rhoptry-associated protein of Plasmodium falciparum. *Mol. Biochem. Parasitol.* 50, 139–149. doi: 10.1016/0166-6851(92)90251-e

Sherling, E. S., Knuepfer, E., Brzostowski, J. A., Miller, L. H., Blackman, M. J., and Van Ooij, C. (2017). The Plasmodium falciparum rhoptry protein RhopH3 plays essential roles in host cell invasion and nutrient uptake. *Elife* 6, e23239. doi: 10.7554/eLife.23239

Sherling, E. S., Perrin, A. J., Knuepfer, E., Russell, M. R. G., Collinson, L. M., Miller, L. H., et al. (2019). The Plasmodium falciparum rhoptry bulb protein RAMA

plays an essential role in rhoptry neck morphogenesis and host red blood cell invasion. *PloS Pathog.* 15, e1008049. doi: 10.1371/journal.ppat.1008049

Siddiqui, W. A., Tam, L. Q., Kramer, K. J., Hui, G. S., Case, S. E., Yamaga, K. M., et al. (1987). Merozoite surface coat precursor protein completely protects Aotus monkeys against Plasmodium falciparum malaria. *Proc. Natl. Acad. Sci. U.S.A.* 84, 3014–3018. doi: 10.1073/pnas.84.9.3014

Smythe, J. A., Coppel, R. L., Brown, G. V., Ramasamy, R., Kemp, D. J., and Anders, R. F. (1988). Identification of two integral membrane proteins of Plasmodium falciparum. *Proc. Natl. Acad. Sci. U.S.A.* 85, 5195–5199. doi: 10.1073/pnas.85.14.5195

Srinivasan, P., Ekanem, E., Diouf, A., Tonkin, M. L., Miura, K., Boulanger, M. J., et al. (2014). Immunization with a functional protein complex required for erythrocyte invasion protects against lethal malaria. *Proc. Natl. Acad. Sci. U.S.A.* 111, 10311–10316. doi: 10.1073/pnas.1409928111

Topolska, A. E., Lidgett, A., Truman, D., Fujioka, H., and Coppel, R. L. (2004). Characterization of a membrane-associated rhoptry protein of Plasmodium falciparum. *J. Biol. Chem.* 279, 4648–4656. doi: 10.1074/jbc.M307859200

Tsuboi, T., Takeo, S., Iriko, H., Jin, L., Tsuchimochi, M., Matsuda, S., et al. (2008). Wheat germ cell-free system-based production of malaria proteins for discovery of novel vaccine candidates. *Infect. Immun.* 76, 1702–1708. doi: 10.1128/IAI.01539-07

WHO (2019). *World Malaria Report 2019* (Geneva, Switzerland: WHO Press).

Conflict of Interest: The authors declare that the research was conducted in the absence of any commercial or financial relationships that could be construed as a potential conflict of interest.

The reviewer DW declared a past co-authorship with several of the authors ET and TT to the handling editor.

frontiers in Cellular and Infection Microbiology

MINI REVIEW
published: 29 January 2021
doi: 10.3389/fcimb.2020.606033

Modeling Relapsing Malaria: Emerging Technologies to Study Parasite-Host Interactions in the Liver

Annemarie Voorberg-van der Wel, Clemens H. M. Kocken and Anne-Marie Zeeman *

Department of Parasitology, Biomedical Primate Research Center, Rijswijk, Netherlands

Recent studies of liver stage malaria parasite-host interactions have provided exciting new insights on the cross-talk between parasite and its mammalian (predominantly rodent) host. We review the latest state of the art and and zoom in on new technologies that will provide the tools necessary to investigate host-parasite interactions of relapsing parasites. Interactions between hypnozoites and hepatocytes are particularly interesting because the parasite can remain in a quiescent state for prolonged periods of time and triggers for reactivation have not been irrefutably identified. If we learn more about the cross-talk between hypnozoite and host we may be able to identify factors that encourage waking up these dormant parasite reservoirs and help to achieve the total eradication of malaria.

Keywords: malaria, parasite-host interaction, plasmodium, cynomolgi, hypnozoite, relapse

OPEN ACCESS

Edited by:
Jing-wen Lin,
Sichuan University, China

Reviewed by:
Glenn McConkey,
University of Leeds, United Kingdom
Fred David Mast,
Seattle Children's Research Institute, United States

***Correspondence:**
Anne-Marie Zeeman
zeeman@bprc.nl

Specialty section:
This article was submitted to Parasite and Host, a section of the journal Frontiers in Cellular and Infection Microbiology

Received: *14 September 2020*
Accepted: *04 December 2020*
Published: *29 January 2021*

Citation:
Voorberg-van der Wel A, Kocken CHM and Zeeman AM (2021) Modeling Relapsing Malaria: Emerging Technologies to Study Parasite-Host Interactions in the Liver. Front. Cell. Infect. Microbiol. 10:606033. doi: 10.3389/fcimb.2020.606033

INTRODUCTION

Malaria, caused by *Plasmodium* parasites, remains a very serious infectious disease, killing over 400,000 people per year (WHO, 2019). With a complex life-cycle in mosquito and vertebrate hosts, the parasite has to interact with its hosts to be able to survive and multiply. In the vertebrate host, the parasite has life-cycle stages initially in the liver and subsequently in the blood. Five malaria species can infect humans, *Plasmodium 8falciparum, vivax, ovale, malariae* (Hay et al., 2004), and the recently added zoonotic parasite *P. knowlesi* (Yegneswaran et al., 2009). Most of the fatal malaria infections are caused by *P. falciparum*, but also infection with *P. vivax*, the second most important human malaria parasite, can result in death (Price et al., 2007). *P vivax*, as well as a few other primate malarias form dormant stages called hypnozoites in the liver, that after months or even years can re-activate to yield new malaria episodes, without new infections through mosquito bites. This hidden reservoir of parasites complicates future malaria eradication. Liver stage biology, and

Abbreviations: P., plasmodium; FACS, fluorescence-activated cell sorting; FASII, fatty acid synthesis (in apicoplast); RNAseq, Ribonucleic acid sequencing; PVM, parasitophorous vacuolar membrane; UIS3, Up-regulated in sporozoites; huHep, human hepatocytes; 3D, three dimensional.

especially hypnozoite biology, remains obscure as the liver stages are relatively inaccessible. Here we review recent progress in studies on liver stage parasite-host interactions in general and zoom in on new technologies that will allow detailed biological studies on dormant liver stages and their interaction with the host.

PARASITE-HOST INTERACTIONS INSIDE THE LIVER; THE RODENT MODELS

The rodent malarias *Plasmodium berghei, Plasmodium yoelii, Plasmodium chabaudi*, and *Plasmodium vinckei* have played a pivotal role in understanding malaria biology [reviewed in (De Niz and Heussler, 2018)]. In the absence of prolonged blood stage cultures, these systems are almost exclusively *in vivo* based. Different mouse strains each have their own characteristics and the creation of transgenic mice has enabled studies that pinpoint specific parasite-host interactions (Liehl et al., 2014). The combination with highly efficient transfection systems for these parasite species (Mikolajczak et al., 2008; Matz and Kooij, 2015) renders the rodent malarias invaluable for studying parasite-host interactions *in vivo*.

Particularly liver stage research has greatly benefitted from the rodent models. Once sporozoites have switched from traversal to invasion (Coppi et al., 2007), the rodent malaria parasites show unprecedented multiplication inside hepatocytes. Within about 2 days, liver stage development is completed and thousands of merozoites are formed. Characterization of the liver stage parasites has been technically challenging due to their inaccessible location for experimentation. With robust *in vitro* parasite liver stage cultures established in many labs, more information has become available as to how the parasite manages to perform this daunting task.

The first comprehensive transcriptomic analysis for liver stages, which was combined with a proteomic survey, was described for *P. yoelii* (Tarun et al., 2008). The development of genetically engineered parasites allowed FACS isolation of liver stage infected hepatocytes. This revealed that liver stage schizonts express a wide range of metabolic pathways, including the liver stage-specific FASII pathway. Further in-depth RNAseq analyses performed at different timepoints during *P. berghei* liver stage development identified genes predominantly expressed in liver stages and showed that liver stage development was accompanied by differential expression of hundreds of parasite genes which may be regulated by a variety of posttranscriptional and posttranslational mechanisms (Caldelari et al., 2019; Shears et al., 2019).

While malaria liver stage development is a clinically silent phase of the life cycle, it has become clear that the hepatocyte does respond to the presence of the parasite in various ways. Transcriptional profiling of hepatoma cells early after infection with *P. berghei* showed an initial stress response of the cell to the presence of the parasite, which was followed by altered host cell metabolic responses to meet the requirements of parasite multiplication while maintaining parasite survival (Albuquerque et al., 2009). The parasite appears to prolong survival of the host cell by protecting it against extrinsic apoptosis (van de Sand et al., 2005; Kaushansky et al., 2013a), for example by suppression of host cell p53 (Kaushansky et al., 2013b) and by upregulating the "cellular inhibitor of apoptosis" protein (cIAP) (Ebert et al., 2020). Furthermore, the parasite has developed mechanisms to protect itself against elimination by autophagy of the host cell (Prado et al., 2015; Agop-Nersesian et al., 2017; Real et al., 2018). While autophagy can have detrimental effects, the liver stage parasite also appears to benefit from a non-canonical form of autophagy, termed *Plasmodium* Associated Autophagic-Response (PAAR) which was shown to support liver stage development (Agop-Nersesian et al., 2017; Coppens, 2017; Wacker et al., 2017; Evans et al., 2018).

That the malaria parasite is sensed by its host has also become evident by the specific type I interferon response that is triggered by liver stage malaria parasites following rodent liver infection (Liehl et al., 2014). In a rodent malaria model, it was shown that this response could inhibit malaria reinfections (Liehl et al., 2015). Similarly, host responses elicited during blood stage infection may impair liver stage infection. This appears to be mediated by the iron-regulatory hormone hepcidin, which restricts iron availability in the liver and thereby inhibits liver stage growth of the parasite (Portugal et al., 2011). This points to the importance of metal homeostasis during liver stage development, which is also highlighted by detrimental effects on liver stage parasites caused by gene knockouts of parasite metal transporters (Sahu et al., 2014; Kenthirapalan et al., 2016).

The parasite has been shown to recruit various host cell proteins in order to sustain its development, including GLUT1 (Meireles et al., 2017), aquaporin-3 (Posfai et al., 2018; Posfai et al., 2020) and protein traffic modulators such as COPB2 and GGA1 (Raphemot et al., 2019). Many of the host factors involved are recruited to the host-parasite interface in the liver cell, the parasitophorous vacuole membrane (PVM). Most interactions between host cell proteins and parasite proteins located at the PVM have remained elusive. To date, only a few connections between parasite antigens and hepatocyte proteins have been described. "Up-regulated in sporozoites protein" UIS3 has been shown to interact with liver fatty acid binding protein 1 (LFABP1) (Mueller et al., 2005; Mikolajczak et al., 2007), suggesting fatty acid scavenging from the host cell. Furthermore, *P. berghei* Exported protein 1 (EXP-1) was shown to interact with host Apolipoprotein H (ApoH) (Sa et al., 2017). These interactions have only been described for rodent malaria and possibly different parasite-host combinations require different interactions. This is highlighted by the finding that *P. falciparum* EXP-1 did not appear to interact with human ApoH (Sa et al., 2017).

Clearly, rodent models have been and will continue to play an important role in dissecting various aspects of malaria liver stage biology. However, it will be important to determine how the findings in these models translate to the human parasites, as has already been done for only a limited set of proteins, such as aquaporin-3 (Posfai et al., 2020) and Mucin-13 (LaMonte et al., 2019). While the rodent malaria studies allow investigations into the biology of developing liver stages, these parasite species do

not develop into hypnozoites and thus do not enable studies on hypnozoite biology and hypnozoite-hepatocyte interaction.

P. VIVAX PARASITE-HOST INTERACTIONS INSIDE THE LIVER

Studying *P. vivax* parasite-host interactions in the liver is hampered by the fact that *P. vivax* develops only in primates. *P. vivax* liver stages were studied in humans, as described by Shortt and Garnham in 1948 (Shortt et al., 1948), in which liver biopsies were taken from a volunteer at day 6/7 post infection by the bites of ~1700 mosquitoes. They demonstrated the existence of a liver tissue stage in the *P. vivax* malaria life-cycle, similar to their observations in monkeys infected with *P. cynomolgi* sporozoites that they published shortly prior to the human experiment (Shortt and Garnham, 1948a). They observed large liver schizonts responsible for primary disease, but unfortunately did not find the hypnozoites, which were described only in 1980 by Krotoski (in liver biopsies from *P. cynomolgi*-infected monkeys) (Krotoski et al., 1980). A lot of knowledge has been gained from early experimental human infections regarding relapse patterns and the clinical profile of *P. vivax*, but these types of experiments are nowadays restricted. Although sporozoite-derived controlled human infections with *P. vivax* are allowed (under strict supervision) and can be highly significant to test new drugs or vaccines, volunteers are usually cured at low blood stage parasitemia (Herrera et al., 2011; Arevalo-Herrera et al., 2016). Relapses are not studied in this model and studying the liver stage parasites by taking liver biopsies from these volunteers is not performed. The best non-human model for *P. vivax* infections used to be the chimpanzee, and after finding the first hypnozoites in *P. cynomolgi*-infected rhesus monkeys, *P. vivax* hypnozoites were discovered in liver biopsies taken from *P. vivax*-infected chimps (Krotoski et al., 1982a). Nowadays animal experiments on apes are banned, so this model is no longer available (Hutson, 2010).

Other primate models for *P. vivax*, like Saimiri or Aotus monkeys have been primarily used for schizonticidal drugs and vaccine efficacy studies [reviewed in (Joyner et al., 2015)] but to be able to detect (low level) blood stage parasites caused by relapses animals need to be splenectomized, and pattern and frequency of relapses appear to be difficult to predict in these animal models (Joyner et al., 2015).

An important step for *in vivo P. vivax* research was achieved by the development of the FRG huHep chimeric mouse. This model is suitable to study the pre-erythrocytic stages of *P. vivax*, including hypnozoites, and can be used to test the activity of potential radical cure drugs that would kill hypnozoites (Mikolajczak et al., 2015). Blood stage parasites can be observed when injecting the FRG huHep mice with human reticulocytes around the time that the merosomes will be released from the mature liver schizonts, but this becomes very complicated if one wants to study relapses. Also, these mice are severely immunocompromised and will not completely reflect the human response to malaria infection or drug treatment. Thus, this model may not be suitable to study parasite-host interactions of relapsing malaria.

Studying parasite-host interactions *in vitro* may sound a bit counterintuitive, but some processes can be fairly easily studied in an *in vitro* setting, like the hepatocyte's response to infection, activity of anti-relapse compounds and monitoring reactivation of the dormant stages. Primary human hepatocytes or hepatoma-derived cell lines (Hollingdale et al., 1984; Mazier et al., 1984; Sattabongkot et al., 2006; Chattopadhyay et al., 2010) are used as monoculture to study *P. vivax* liver stages *in vitro*. Recently, Roth et al. (Roth et al., 2018) have described a system using cryopreserved human primary hepatocytes and patient-derived sporozoites with high infection rates. This system should be helpful in the identification of new hypnozoite targeting compounds, as well as studying hypnozoites and reactivation as well as hepatocyte responses to infection. However, all of these models are dependent on patient material for the infection of mosquitoes. This means that there can be large variation between the different experiments, both in infection rate as well as in hypnozoite ratios (Roth et al., 2018). The variation caused by the different lots of hepatocytes is reduced when using cryopreserved cells, but variation caused by different patient-derived parasite isolates can't be tackled. This can be circumvented by using the *P. cynomolgi*-monkey model for relapsing malaria (described below). Additional advantages for this model are that *in vitro* and *in vivo* experiments can be performed with the same well-characterized parasite and the availability of a robust transfection procedure for this parasite. *P. cynomolgi* can be genetically modified using episomes, centromere-containing constructs (for stable retention of the episome) and by single crossover integration into the genome (Kocken et al., 1999; Akinyi et al., 2012; Voorberg-van der Wel et al., 2013; Voorberg-van der Wel et al., 2020). Transfection of *P.vivax* is also possible, but is more difficult due to the restrictions (as described above) when working with small monkeys like Aotus and Saimiri (Pfahler et al., 2006; Moraes Barros et al., 2015), and so far the papers describing *P. vivax* transfection only show proof of concept.

P. CYNOMOLGI, THE MONKEY SISTER PARASITE OF *P. VIVAX*

The monkey malaria parasite *P. cynomolgi* is considered to be an important model for the relapsing human malaria *P. vivax*, as it is phylogenetically closely related (Tachibana et al., 2012) and shares many biological characteristics (**Table 1**). Not only liver stage parasites, but also hypnozoites were first identified in the liver of rhesus monkeys that had been infected with high numbers of *P. cynomolgi* sporozoites (Shortt and Garnham, 1948a; Krotoski, 1985).

Monkeys infected with *P. cynomolgi* sporozoites have shown similar pathology as *P. vivax*-infected humans, including anemia and thrombocytopenia (Joyner et al., 2016; Joyner et al., 2017). In

TABLE 1 | Comparison of biological characteristics of *P. vivax* and *P. cynomolgi*.

	P. vivax	*P. cynomolgi*
Characteristics life cycle		
Asexual blood stage cycle	48 h (Garnham, 1966) Schüffners dots (Garnham, 1966)	48 h (Garnham, 1966) Schüffners dots (Garnham, 1966)
Early development gametocytes (time to maturation)	Yes, 2–3 days (Bousema and Drakeley, 2011; Ngotho et al., 2019)	Yes, 58 h (Hawking et al., 1968)
Invasion	Reticulocytes (Noulin et al., 2013)	Reticulocytes (in humans; in monkeys also normocytes) (Kosaisavee et al., 2017)
Pre-erythrocytic stage	8 days (Fairley, 1946)	8–10 days (Shortt and Garnham, 1948b)
Hypnozoites	Yes (Krotoski et al., 1982a)	Yes (Krotoski et al., 1982b)
Relapse pattern	Short latency and long latency (White, 2011)	Short latency (Schmidt, 1986)
Research tools		
In vitro blood stage culture	No	Yes (but no transmission yet) (Chua et al., 2019b)
In vitro liver stage culture	Yes (Gural et al., 2018b; Roth et al., 2018)	Yes (Dembele et al., 2011)
In vivo drug screening model	Limited (Mikolajczak et al., 2015)	Yes (Schmidt, 1983)
In vivo relapse model	Anecdotal (Joyner et al., 2015)	Yes (Schmidt, 1986)
Transfection technology	Proof of concept (Pfahler et al., 2006; Moraes Barros et al., 2015)	Episomes; centromeres; single crossover (Kocken et al., 1999; Akinyi et al., 2012; Voorberg-van der Wel et al., 2013; Voorberg-van der Wel et al., 2020)
Genome sequenced	Yes (Carlton et al., 2008)	Yes (Tachibana et al., 2012; Pasini et al., 2017)

addition, it was shown that *P. cynomolgi* relapses can be clinically silent. This is likely to be due to the rapid development of memory B cell responses that help to clear asexual blood stage parasites but not gametocytes (Joyner et al., 2019).

Moreover, *P. cynomolgi* showed drug activity profiles that were highly similar to *P. vivax* (Schmidt et al., 1982b). This led to large scale drug screening studies with *P. cynomolgi* sporozoite-induced infections in rhesus monkeys as central step in efforts [which initially also used patients undergoing *P. vivax* malaria therapy as well as prison inmate volunteers (Coatney, 1985)] to find new hypnozoite-killing drugs (Davidson et al., 1981; Schmidt et al., 1982b; Schmidt, 1983; Dutta et al., 1989; Deye et al., 2012).

The *in vivo* data have been crucial for the discovery of the liver stages and for assessing the effects of drugs targeting these stages. However, experimentation and throughput are limited for ethical and economic reasons and, apart from the 8-aminoquinolines, other compounds killing hypnozoites have not been identified. Therefore, higher throughput approaches in order to find new, more potent and less toxic drugs that cure relapsing infections are needed (Wells et al., 2010; Campo et al., 2015). Knowledge of liver stage biology may reveal new targets for drug development, which may be more efficient than random screening approaches.

The advent of *in vitro* culture techniques for malaria liver stage parasites, including *P. cynomolgi*, (Millet et al., 1988) has greatly increased opportunities for the development of drug screening platforms and to begin to study parasite-host interactions. For *P. cynomolgi*, a low-throughput 96-well based assay system which enabled testing of compounds that are active against hypnozoites was developed, in which hypnozoites could be distinguished from developing forms (schizonts) by their size and differential sensitivity against selected drugs (Dembele et al., 2011).

Using this assay, a PI4 kinase inhibitor (McNamara et al., 2013) was identified showing high activity against early hypnozoites (Zeeman et al., 2014). This translated to *in vivo* prophylactic, but not radical cure activity (Zeeman et al., 2016), illustrating that young hypnozoites may be different from maturing hypnozoites. This is in line with earlier *in vivo* work which showed that when *P. cynomolgi* infected rhesus monkeys were treated at different timepoints with only 1 or 2 dosages of primaquine, it appeared that some phases (mainly early stages) of liver stage development were more vulnerable for the activity of the drug than others (Schmidt et al., 1982a).

The culture system was further improved through the addition of a Matrigel cover, which makes it possible to culture the *P. cynomolgi* exoerythrocytic forms for prolonged periods of time, revealing possible events of hypnozoite reactivation (Dembele et al., 2014). Recently, a 3D spheroid-culture system was reported that allows long-term cultivation of *P. cynomolgi* liver stages including full maturation of liver schizonts and invasion of red blood cells. While mimicking the *in vivo* microenvironment of the liver the 3D-structure of the spheroids renders it difficult to image and quantitate parasite load, presenting an obstacle for the use of this technology for high-throughput screening (Chua et al., 2019a). However, such a 3D-platform may be suitable for studying parasite-host interactions, with optimal *in vitro* hepatocyte quality, mimicking the *in vivo* situation.

In an attempt to characterize hypnozoites at the transcript level, *P. cynomolgi* day 7 hypnozoites and schizonts were collected by Laser Capture Microdissection (LCM) (Cubi et al., 2017). Two hypnozoite samples were obtained, containing a total of 45 and 59 hypnozoites, respectively (Cubi et al., 2017). Given the low levels of hypnozoite RNA in these small-sized samples, low read counts were obtained. Some ApiAP2 transcription factors were identified that were upregulated in hypnozoites. Further functional studies are needed to confirm the roles of these proteins.

P. cynomolgi has the advantage that it can be genetically manipulated (Kocken et al., 1999; Akinyi et al., 2012). By

including a centromere (Iwanaga et al., 2010) in the construct, reporter lines have been developed which enable live visualization and purification of hypnozoites and liver stage schizonts (Voorberg-van der Wel et al., 2013). This has allowed a comprehensive transcriptomics analysis of day 6/7 and day 9 hypnozoites and schizonts (Voorberg-van der Wel et al., 2017; Bertschi et al., 2018). This revealed that developing schizonts are metabolically highly active, while hypnozoites continue to shut down transcription, except for pathways involved in the maintenance of genome stability, glycolysis and the pentose phosphate pathway. A marker for hypnozoites was not identified but Liver Stage Protein-2 was found to be schizont-specific and to be expressed very early on during schizogeny (Gupta et al., 2019). Rhesus host responses to *P. cynomolgi* infection and development in cultured hepatocytes have not yet been reported.

Using a *P. cynomolgi* reporter line that constitutively expresses GFP and shows mCherry expression when schizogony occurs, reactivation of hypnozoites *in vitro* was observed (Voorberg-van der Wel et al, 2020). This provides strong proof for the hypnozoite theory of relapse and allows screening of compounds that induce activation. If such compounds can be identified, "wake-and-kill" strategies can be envisaged in which hypnozoite activation is evoked, followed by killing of developing forms by currently available drugs.

The trigger for hypnozoite activation has remained enigmatic (**Box 1**) and the parasite-host interactions involved are elusive. Hypnozoite activation may be epigenetically controlled (Dembele et al., 2014). Furthermore, it has been suggested that activation may be triggered by mosquito bites (Hulden and Hulden, 2011), infectious disease (Shanks and White, 2013; Commons et al., 2019), or blood transfusion (Shanks and Waller, 2019). The *P. cynomolgi* fluorescent reporter line now offers the opportunity to investigate if/which molecules may stimulate hypnozoite activation. It must be realized, however, that in the context of the current *in vitro* platform it may be difficult to mimic the complex bodily reactions possibly involved in this. Moereover, reactivation events in culture are rare, making it challenging to isolate reactivating hypnozoites to study parasite and host transcriptomics.

Another question mark is how the hypnozoite survives for such a long time in a hepatocyte. Under normal conditions, the life-span of hepatocytes is estimated to be 6–12 months (Seeger and Mason, 2000). If the late recurrences [800–1,000 days after infection; (Schmidt, 1986)] of *P. cynomolgi* sporozoite induced infections in rhesus monkeys derive from activated hypnozoites, then how is this possible? Does the hypnozoite extend the longevity of the hepatocyte, or does it end up in a new hepatocyte after cell division?

BOX 1 | Outstanding questions:

Hypnozoite-host interaction

*How do the findings in the rodent liver stage models with respect to parasite-host interactions relate to the primate malarias?

*Which parasite-host interactions occur in the liver stage development of primate malarias?

*What are the differences between *in vitro* and *in vivo* parasites in terms of parasite-host interactions?

*How does the hypnozoite hide from the host immune system?

Hypnozoite-dormancy

*Do hypnozoites preferentially develop in a certain type of hepatocyte?

*How can a hypnozoite remain in the liver for prolonged times (longer than the generally estimated lifespan of hepatocytes)

*When does hypnozoite commitment occur?

*Which parasite/host molecules are involved in maintaining hypnozoite dormancy?

Hypnozoite-reactivation

*What is the mechanism behind hypnozoite activation?

*Is there a trigger involved or is it stochastic, *via* a biological clock, or a combination of this?

NEWLY EMERGING TECHNOLOGIES

Liver stage parasites reside inside hepatocytes, located inside the liver. Given this multilayered, inaccessible location it has proven difficult to study this stage of the parasite life cycle. Furthermore, the existence of two forms of the parasite in some primate species, hypnozoites and schizonts, adds another layer of complexity to this. Much knowledge of parasite-host interactions of liver stage parasites has already been gained in the rodent malarias, although most likely this information represents only the tip of the iceberg. It will be important to determine whether this information can be translated to the primate malaria species. On top of this, virtually nothing is known about the interactions that take place between the hypnozoite stage of development and its host cell (**Figure 1**). Tools to study this are vital and have only recently begun to emerge, benefitting from technologies that have already been developed for the rodent malarias.

The development of liver stage cultures has greatly facilitated liver stage research. Some systems use hepatoma-derived cell lines (Hollingdale et al., 1984; Mazier et al., 1984; Sattabongkot et al., 2006; Chattopadhyay et al., 2010). While this provides a constant source of host cells, these cells differ in a number of aspects from primary hepatocytes (Tripathi et al., 2020), including a lower metabolic activity (Castell et al., 2006) and a high dependence on glucose uptake (Meireles et al., 2017). Therefore, care should be taken to validate results that mimic the natural situation. The importance of metabolic activity of hepatocytes was investigated for *P. falciparum* (Yang et al., 2020 BioRXiv, non peer-reviewed paper). This study indicates that *P. falciparum* liver stage development is strongly influenced by the differential metabolic activity of human hepatocytes derived from different zones of the liver.

The drawback of cultures using primary hepatocytes is that after about 12 days of culture the hepatocyte quality starts to deteriorate (Voorberg-van der Wel et al., 2020), which precludes analyses of hypnozoite activation. Approaches to overcome this issue include the addition of a Matrigel cover (Dembele et al., 2014), co-cultivation of human primary hepatocytes with fibroblasts (March et al., 2013; Gural et al., 2018a) or through the use of specific 384-well plates coated with collagen (Roth et al., 2018). Nucleic-acid mediated gene silencing has been successful in this type of systems, having the potential of exploring functional parasite-host interactions (Mancio-Silva L et al., 2019).

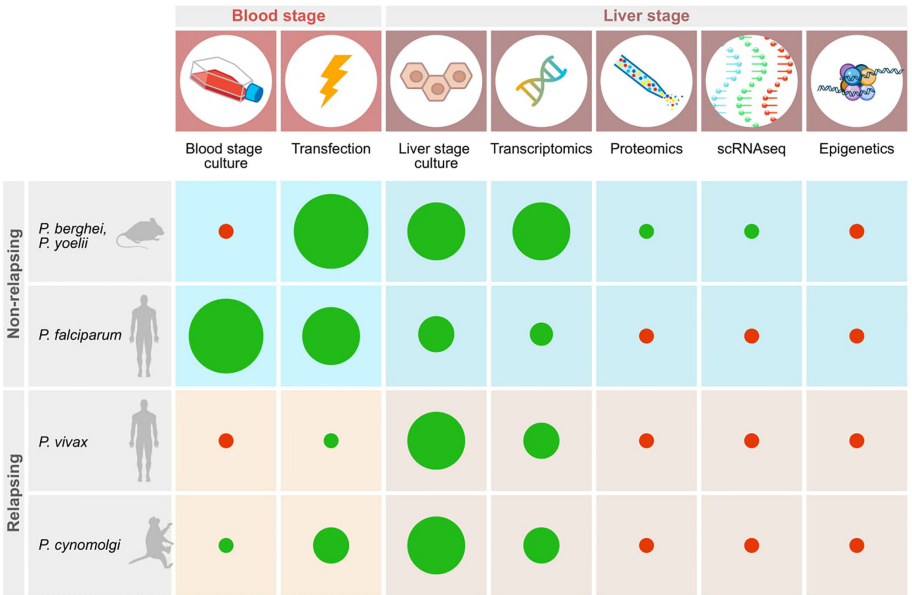

FIGURE 1 | Schematic representation of important technologies available for studying relapsing and non-relapsing malaria parasites. Red dots indicate the absence of tools, green dots show that techniques have been established. The size of the diameter of the dots schematically indicates how widely the technology has been adopted based on published reports.

The advent of three-dimensional (3D) cell culture methods has opened up ways to develop cultures that mimic the *in vivo* physiological conditions to a greater extent. Proof-of-concept of this type of technology has already been shown, involving the use of hepatic spheroids using various hepatoma cell lines for culturing *P. berghei* (Arez et al., 2019) and using primary hepatocytes for *P. cynomolgi* (Chua et al., 2019a). Full development was shown for both parasite species, and cultures could be maintained for prolonged periods of time [up to 60 days in case of the simian spheroids (Chua et al., 2019a)]. While further improvements in terms of infection rate and by adding more cell types to create organoid like features is warranted, this type of systems provide new opportunities to study hypnozoite activation *in vitro* under conditions that are resembling *the vivo* situation.

More continuous, stable sources with truly hepatocyte features may be derived using newly emerging stem cell technologies. Proof of concept liver stage infections have already been shown using human induced Pluripotent Stem Cell (iPSC) derived hepatocyte-like cells (Ng et al., 2015) and chemically differentiated mouse embryonic stem cell (ESC)-based cells (Tripathi et al., 2020). These systems are attractive, since they not only provide a virtually unlimited source of hepatocytes, but the stem cells are also amenable to genetic manipulation thus allowing validation of genes important for parasite-host interactions in liver cells. In this way it was shown that the host adipose triglyceride lipase gene was dispensable for *P. berghei* liver stage development (Tripathi et al., 2020).

Little is known about host molecules involved in hypnozoite/liver stage development. Given that the first hypnozoite transcriptomes have become available (Cubi et al., 2017; Voorberg-van der Wel et al., 2017; Bertschi et al., 2018), a Dual-RNAseq approach can be envisaged whereby not only the transcriptome of the parasite, but also that of the host cell can be determined (LaMonte et al., 2019).

Information about transcriptional profiles of individual parasites can be obtained by a new technique called single cell RNA sequencing (scRNA-seq). Although technically challenging, researchers have accomplished (Poran et al., 2017) and optimized (Reid et al., 2018) a method for single cell RNA sequencing of malaria parasites. Using this new technique, individual parasites of all stages of the *P. berghei* life cycle were sorted and a transcriptional profile was generated, including difficult samples such as rings, which have low levels of RNA, and ookinetes, which are hard to sort (Howick et al., 2019). When application of scRNA-seq and other newly emerging "omics" approaches [e.g. lipidomics, metabolomics, proteomics, epigenomics (Cowell and Winzeler, 2018)] to relapsing malaria species (and more specifically to dormant liver stages) becomes feasible, these studies will likely shed more light onto genes involved in hypnozoite dormancy/activation.

The capacity to genetically modify parasite genes is key to study genes that may be involved in parasite host-interactions essential for hypnozoites. At the moment, such studies can only realistically be envisaged using the primate malaria *P. cynomolgi*. Lines that express reporter genes in *P. cynomolgi* liver stages have already been engineered (Voorberg-van der Wel et al., 2020), opening up studies that investigate phenotypic consequences of overexpression of gene candidates that may be involved in hypnozoite development. However, the *P. cynomolgi* transfection system is still in its infancy and only limited studies have been reported. Further development is warranted, because full

exploitation of the capacity to genetically modify a relapsing parasite species will be vital for studying parasite-host interactions of hypnozoites with their host cell. Transfection systems have already been further optimized in other malaria species and it is expected that tools successful in these parasites, such as Crispr/Cas9 gene modification reviewed in (Lee et al., 2019), conditional (over)expression using DiCre (Jones et al., 2016) will be applicable to *P. cynomolgi* as well. Development of transfection tools may greatly benefit from the recently developed blood stage culture for this parasite (Chua et al., 2019b), extending the range of conditions that can be tested avoiding the use of donor and recipient monkeys.

AUTHOR CONTRIBUTIONS

All authors listed have made a substantial, direct, and intellectual contribution to the work and approved it for publication.

FUNDING

Some of the work presented here was supported by funding from the Medicines for Malaria Venture, and the Bill and Melinda Gates Foundation, grant number OPP1141292.

REFERENCES

Agop-Nersesian, C., De Niz, M., Niklaus, L., Prado, M., Eickel, N., and Heussler, V. T. (2017). Shedding of host autophagic proteins from the parasitophorous vacuolar membrane of Plasmodium berghei. *Sci. Rep.* 7 (1), 2191. doi: 10.1038/s41598-017-02156-7

Akinyi, S., Hanssen, E., Meyer, E. V., Jiang, J., Korir, C. C., Singh, B., et al. (2012). A 95 kDa protein of Plasmodium vivax and P. cynomolgi visualized by three-dimensional tomography in the caveola-vesicle complexes (Schuffner's dots) of infected erythrocytes is a member of the PHIST family. *Mol. Microbiol.* 84 (5), 816–831. doi: 10.1111/j.1365-2958.2012.08060.x

Albuquerque, S. S., Carret, C., Grosso, A. R., Tarun, A. S., Peng, X., Kappe, S. H., et al. (2009). Host cell transcriptional profiling during malaria liver stage infection reveals a coordinated and sequential set of biological events. *BMC Genomics* 10, 270. doi: 10.1186/1471-2164-10-270

Arevalo-Herrera, M., Vasquez-Jimenez, J. M., Lopez-Perez, M., Vallejo, A. F., Amado-Garavito, A. B., Cespedes, N., et al. (2016). Protective Efficacy of Plasmodium vivax Radiation-Attenuated Sporozoites in Colombian Volunteers: A Randomized Controlled Trial. *PloS Negl. Trop. Dis.* 10 (10), e0005070. doi: 10.1371/journal.pntd.0005070

Arez, F., Rebelo, S. P., Fontinha, D., Simao, D., Martins, T. R., Machado, M., et al. (2019). Flexible 3D Cell-Based Platforms for the Discovery and Profiling of Novel Drugs Targeting Plasmodium Hepatic Infection. *ACS Infect. Dis.* 5 (11), 1831–1842. doi: 10.1021/acsinfecdis.9b00144

Bertschi, N. L., Voorberg-van der Wel, A., Zeeman, A. M., Schuierer, S., Nigsch, F., Carbone, W., et al. (2018). Transcriptomic analysis reveals reduced transcriptional activity in the malaria parasite Plasmodium cynomolgi during progression into dormancy. *Elife* 7. doi: 10.7554/eLife.41081

Bousema, T., and Drakeley, C. (2011). Epidemiology and infectivity of Plasmodium falciparum and Plasmodium vivax gametocytes in relation to malaria control and elimination. *Clin. Microbiol. Rev.* 24 (2), 377–410. doi: 10.1128/CMR.00051-10

Caldelari, R., Dogga, S., Schmid, M. W., Franke-Fayard, B., Janse, C. J., Soldati-Favre, D., et al. (2019). Transcriptome analysis of Plasmodium berghei during exo-erythrocytic development. *Malar. J.* 18 (1), 330. doi: 10.1186/s12936-019-2968-7

Campo, B., Vandal, O., Wesche, D. L., and Burrows, J. N. (2015). Killing the hypnozoite–drug discovery approaches to prevent relapse in Plasmodium vivax. *Pathog. Glob. Health* 109 (3), 107–122. doi: 10.1179/2047773215Y.0000000013

Carlton, J. M., Adams, J. H., Silva, J. C., Bidwell, S. L., Lorenzi, H., Caler, E., et al. (2008). Comparative genomics of the neglected human malaria parasite Plasmodium vivax. *Nature* 455 (7214), 757–763. doi: 10.1038/nature07327

Castell, J. V., Jover, R., Martinez-Jimenez, C. P., and Gomez-Lechon, M. J. (2006). Hepatocyte cell lines: their use, scope and limitations in drug metabolism studies. *Expert Opin. Drug Metab. Toxicol.* 2 (2), 183–212. doi: 10.1517/17425255.2.2.183

Chattopadhyay, R., Velmurugan, S., Chakiath, C., Andrews Donkor, L., Milhous, W., Barnwell, J. W., et al. (2010). Establishment of an in vitro assay for assessing the effects of drugs on the liver stages of Plasmodium vivax malaria. *PloS One* 5 (12), e14275. doi: 10.1371/journal.pone.0014275

Chua, A. C. Y., Ananthanarayanan, A., Ong, J. J. Y., Wong, J. Y., Yip, A., Singh, N. H., et al. (2019a). Hepatic spheroids used as an in vitro model to study malaria relapse. *Biomaterials* 216, 119221. doi: 10.1016/j.biomaterials.2019.05.032

Chua, A. C. Y., Ong, J. J. Y., Malleret, B., Suwanarusk, R., Kosaisavee, V., Zeeman, A. M., et al. (2019b). Robust continuous in vitro culture of the Plasmodium cynomolgi erythrocytic stages. *Nat. Commun.* 10 (1), 3635. doi: 10.1038/s41467-019-11332-4

Coatney, G. R. (1985). Reminiscences: my forty-year romance with malaria. *Trans. Nebraska Acad. Sci.* XIII, 5–11.

Commons, R. J., Simpson, J. A., Thriemer, K., Hossain, M. S., Douglas, N. M., Humphreys, G. S., et al. (2019). Risk of Plasmodium vivax parasitaemia after Plasmodium falciparum infection: a systematic review and meta-analysis. *Lancet Infect. Dis.* 19 (1), 91–101. doi: 10.1016/S1473-3099(18)30596-6

Coppens, I. (2017). How Toxoplasma and malaria parasites defy first, then exploit host autophagic and endocytic pathways for growth. *Curr. Opin. Microbiol.* 40, 32–39. doi: 10.1016/j.mib.2017.10.009

Coppi, A., Tewari, R., Bishop, J. R., Bennett, B. L., Lawrence, R., Esko, J. D., et al. (2007). Heparan sulfate proteoglycans provide a signal to Plasmodium sporozoites to stop migrating and productively invade host cells. *Cell Host. Microbe* 2 (5), 316–327. doi: 10.1016/j.chom.2007.10.002

Cowell, A., and Winzeler, E. (2018). Exploration of the Plasmodium falciparum Resistome and Druggable Genome Reveals New Mechanisms of Drug Resistance and Antimalarial Targets. *Microbiol. Insights* 11, 117863611 8808529. doi: 10.1177/1178636118808529

Cubi, R., Vembar, S. S., Biton, A., Franetich, J. F., Bordessoulles, M., Sossau, D., et al. (2017). Laser capture microdissection enables transcriptomic analysis of dividing and quiescent liver stages of Plasmodium relapsing species. *Cell Microbiol.* 19 (8). doi: 10.1111/cmi.12735

Davidson, D. E. Jr., Ager, A. L., Brown, J. L., Chapple, F. E., Whitmire, R. E., and Rossan, R. N. (1981). New tissue schizontocidal antimalarial drugs. *Bull. World Health Organ* 59 (3), 463–479.

De Niz, M., and Heussler, V. T. (2018). Rodent malaria models: insights into human disease and parasite biology. *Curr. Opin. Microbiol.* 46, 93–101. doi: 10.1016/j.mib.2018.09.003

Dembele, L., Gego, A., Zeeman, A. M., Franetich, J. F., Silvie, O., Rametti, A., et al. (2011). Towards an in vitro model of Plasmodium hypnozoites suitable for drug discovery. *PloS One* 6 (3), e18162. doi: 10.1371/journal.pone.0018162

Dembele, L., Franetich, J. F., Lorthiois, A., Gego, A., Zeeman, A. M., Kocken, C. H., et al. (2014). Persistence and activation of malaria hypnozoites in long-term primary hepatocyte cultures. *Nat. Med.* doi: 10.1038/nm.3461

Deye, G. A., Gettayacamin, M., Hansukjariya, P., Im-erbsin, R., Sattabongkot, J., Rothstein, Y., et al. (2012). Use of a rhesus Plasmodium cynomolgi model to screen for anti-hypnozoite activity of pharmaceutical substances. *Am. J. Trop. Med. Hyg.* 86 (6), 931–935. doi: 10.4269/ajtmh.2012.11-0552

Dutta, G. P., Puri, S. K., Bhaduri, A. P., and Seth, M. (1989). Radical curative activity of a new 8-aminoquinoline derivative (CDRI 80/53) against Plasmodium cynomolgi B in monkeys. *Am. J. Trop. Med. Hyg.* 41 (6), 635–637. doi: 10.4269/ajtmh.1989.41.635

Ebert, G., Lopaticki, S., O'Neill, M. T., Steel, R. W. J., Doerflinger, M., Rajasekaran, P., et al. (2020). Targeting the Extrinsic Pathway of Hepatocyte Apoptosis Promotes

Clearance of Plasmodium Liver Infection. *Cell Rep.* 30 (13), 4343–4354.e4344. doi: 10.1016/j.celrep.2020.03.032

Evans, R. J., Sundaramurthy, V., and Frickel, E. M. (2018). The Interplay of Host Autophagy and Eukaryotic Pathogens. *Front. Cell Dev. Biol.* 6, 118. doi: 10.3389/fcell.2018.00118

Fairley, N. H. (1946). Researches on paludrine (M.4888) in malaria; an experimental investigation undertaken by the L.H.Q. Medical Research Unit (A.I.F.) Cairns, Australia. *Trans. R. Soc. Trop. Med. Hyg.* 40 (2), 105–162. doi: 10.1016/0035-9203(46)90052-1

Garnham, P. C. C. (1966). *Malaria parasites and other haemosporidia* (Oxford: Blackwell).

Gupta, D. K., Dembele, L., Voorberg-van der Wel, A., Roma, G., Yip, A., Chuenchob, V., et al. (2019). The Plasmodium liver-specific protein 2 (LISP2) is an early marker of liver stage development. *Elife* 8. doi: 10.7554/eLife.43362

Gural, N., Mancio-Silva, L., Miller, A. B., Galstian, A., Butty, V. L., Levine, S. S., et al. (2018a). In Vitro Culture, Drug Sensitivity, and Transcriptome of Plasmodium Vivax Hypnozoites. *Cell Host. Microbe* 23 (3), 395–406. doi: 10.1016/j.chom.2018.01.002

Gural, N., Mancio-Silva, L., Miller, A. B., Galstian, A., Butty, V. L., Levine, S. S., et al. (2018b). In Vitro Culture, Drug Sensitivity, and Transcriptome of Plasmodium Vivax Hypnozoites. *Cell Host. Microbe* 23 (3), 395–406 e394. doi: 10.1016/j.chom.2018.01.002

Hawking, F., Worms, M. J., and Gammage, K. (1968). 24- and 48-hour cycles of malaria parasites in the blood; their purpose, production and control. *Trans. R. Soc. Trop. Med. Hyg.* 62 (6), 731–765. doi: 10.1016/0035-9203(68)90001-1

Hay, S. I., Guerra, C. A., Tatem, A. J., Noor, A. M., and Snow, R. W. (2004). The global distribution and population at risk of malaria: past, present, and future. *Lancet Infect. Dis.* 4 (6), 327–336. doi: 10.1016/S1473-3099(04)01043-6S1473309904010436

Herrera, S., Solarte, Y., Jordan-Villegas, A., Echavarria, J. F., Rocha, L., Palacios, R., et al. (2011). Consistent safety and infectivity in sporozoite challenge model of Plasmodium vivax in malaria-naive human volunteers. *Am. J. Trop. Med. Hyg.* 84 (2 Suppl), 4–11. doi: 10.4269/ajtmh.2011.09-0498

Hollingdale, M. R., Nardin, E. H., Tharavanij, S., Schwartz, A. L., and Nussenzweig, R. S. (1984). Inhibition of entry of Plasmodium falciparum and P. vivax sporozoites into cultured cells; an in vitro assay of protective antibodies. *J. Immunol.* 132 (2), 909–913.

Howick, V. M., Russell, A. J. C., Andrews, T., Heaton, H., Reid, A. J., Natarajan, K., et al. (2019). The Malaria Cell Atlas: Single parasite transcriptomes across the complete Plasmodium life cycle. *Science* 365 (6455). doi: 10.1126/science.aaw2619

Hulden, L., and Hulden, L. (2011). Activation of the hypnozoite: a part of Plasmodium vivax life cycle and survival. *Malar. J.* 10, 90. doi: 10.1186/1475-2875-10-90

Hutson, S. (2010). Following Europe's lead, Congress moves to ban ape research. *Nat. Med.* 16 (10):1057. doi: 10.1038/nm1010-1057a

Iwanaga, S., Khan, S. M., Kaneko, I., Christodoulou, Z., Newbold, C., Yuda, M., et al. (2010). Functional identification of the Plasmodium centromere and generation of a Plasmodium artificial chromosome. *Cell Host. Microbe* 7 (3), 245–255. doi: 10.1016/j.chom.2010.02.010

Jones, M. L., Das, S., Belda, H., Collins, C. R., Blackman, M. J., and Treeck, M. (2016). A versatile strategy for rapid conditional genome engineering using loxP sites in a small synthetic intron in Plasmodium falciparum. *Sci. Rep.* 6:21800. doi: 10.1038/srep21800

Joyner, C., Barnwell, J. W., and Galinski, M. R. (2015). No more monkeying around: primate malaria model systems are key to understanding Plasmodium vivax liver-stage biology, hypnozoites, and relapses. *Front. Microbiol.* 6, 145. doi: 10.3389/fmicb.2015.00145

Joyner, C., Moreno, A., Meyer, E. V., Cabrera-Mora, M., Ma, H. C., Kissinger, J. C., et al. (2016). Plasmodium cynomolgi infections in rhesus macaques display clinical and parasitological features pertinent to modelling vivax malaria pathology and relapse infections. *Malar. J.* 15 (1), 451. doi: 10.1186/s12936-016-1480-6

Joyner, C. J., Consortium, T. M., Wood, J. S., Moreno, A., Garcia, A., and Galinski, M. (2017). Case Report: Severe and Complicated Cynomolgi Malaria in a Rhesus Macaque Resulted in Similar Histopathological Changes as Those Seen in Human Malaria. *Am. J. Trop. Med. Hyg.* 97 (2), 548–555. doi: 10.4269/ajtmh.16-0742

Joyner, C. J., Brito, C. F. A., Saney, C. L., Joice Cordy, R., Smith, M. L., Lapp, S. A., et al. (2019). Humoral immunity prevents clinical malaria during Plasmodium relapses without eliminating gametocytes. *PloS Pathog.* 15 (9), e1007974. doi: 10.1371/journal.ppat.1007974

Kaushansky, A., Metzger, P. G., Douglass, A. N., Mikolajczak, S. A., Lakshmanan, V., Kain, H. S., et al. (2013a). Malaria parasite liver stages render host hepatocytes susceptible to mitochondria-initiated apoptosis. *Cell Death Dis.* 4, e762. doi: 10.1038/cddis.2013.286

Kaushansky, A., Ye, A. S., Austin, L. S., Mikolajczak, S. A., Vaughan, A. M., Camargo, N., et al. (2013b). Suppression of host p53 is critical for Plasmodium liver-stage infection. *Cell Rep.* 3 (3), 630–637. doi: 10.1016/j.celrep.2013.02.010

Kenthirapalan, S., Waters, A. P., Matuschewski, K., and Kooij, T. W. (2016). Functional profiles of orphan membrane transporters in the life cycle of the malaria parasite. *Nat. Commun.* 7:10519. doi: 10.1038/ncomms10519

Kocken, C. H., van der Wel, A., and Thomas, A. W. (1999). Plasmodium cynomolgi: transfection of blood-stage parasites using heterologous DNA constructs. *Exp. Parasitol.* 93 (1), 58–60. doi: 10.1006/expr.1999.4430

Kosaisavee, V., Suwanarusk, R., Chua, A. C. Y., Kyle, D. E., Malleret, B., Zhang, R., et al. (2017). Strict tropism for CD71(+)/CD234(+) human reticulocytes limits the zoonotic potential of Plasmodium cynomolgi. *Blood* 130 (11), 1357–1363. doi: 10.1182/blood-2017-02-764787

Krotoski, W. A., Krotoski, D. M., Garnham, P. C. C., Bray, R. S., Killick-Kendrick, R., Draper, C. C., et al. (1980). Relapses in primate malaria: discovery of two populations of exoerythrocytic stages. *Br. Med. J.* 280 (6208), 153–154. doi: 10.1136/bmj.280.6208.153-a

Krotoski, W. A., Collins, W. E., Bray, R. S., Garnham, P. C., Cogswell, F. B., Gwadz, R. W., et al. (1982a). Demonstration of hypnozoites in sporozoite-transmitted Plasmodium vivax infection. *Am. J. Trop. Med. Hyg.* 31 (6), 1291–1293. doi: 10.4269/ajtmh.1982.31.1291

Krotoski, W. A., Garnham, P. C., Bray, R. S., Krotoski, D. M., Killick-Kendrick, R., Draper, C. C., et al. (1982b). Observations on early and late post-sporozoite tissue stages in primate malaria. I. Discovery of a new latent form of Plasmodium cynomolgi (the hypnozoite), and failure to detect hepatic forms within the first 24 hours after infection. *Am. J. Trop. Med. Hyg.* 31 (1), 24–35. doi: 10.4269/ajtmh.1982.31.24

Krotoski, W. A. (1985). Discovery of the hypnozoite and a new theory of malarial relapse. *Trans. R. Soc. Trop. Med. Hyg.* 79 (1), 1–11. doi: 10.1016/0035-9203(85)90221-4

LaMonte, G. M., Orjuela-Sanchez, P., Calla, J., Wang, L. T., Li, S., Swann, J., et al. (2019). Dual RNA-seq identifies human mucosal immunity protein Mucin-13 as a hallmark of Plasmodium exoerythrocytic infection. *Nat. Commun.* 10 (1), 488. doi: 10.1038/s41467-019-08349-0

Lee, M. C. S., Lindner, S. E., Lopez-Rubio, J. J., and Llinas, M. (2019). Cutting back malaria: CRISPR/Cas9 genome editing of Plasmodium. *Brief Funct. Genomics* 18 (5), 281–289. doi: 10.1093/bfgp/elz012

Liehl, P., Zuzarte-Luis, V., Chan, J., Zillinger, T., Baptista, F., Carapau, D., et al. (2014). Host-cell sensors for Plasmodium activate innate immunity against liver-stage infection. *Nat. Med.* 20 (1), 47–53. doi: 10.1038/nm.3424

Liehl, P., Meireles, P., Albuquerque, I. S., Pinkevych, M., Baptista, F., Mota, M. M., et al. (2015). Innate immunity induced by Plasmodium liver infection inhibits malaria reinfections. *Infect. Immun.* 83 (3), 1172–1180. doi: 10.1128/IAI.02796-14

Mancio-Silva L, F. H., Miller, A. B., Milstein, S., Liebow, A., Haslett, P., Sepp-Lorenzino, L., et al. (2019). Improving Drug Discovery by Nucleic Acid Delivery in Engineered Human Microlivers. *Cell Metab.* 29 (3), 727–735. doi: 10.1016/j.cmet.2019.02.003

March, S., Ng, S., Velmurugan, S., Galstian, A., Shan, J., Logan, D. J., et al. (2013). A microscale human liver platform that supports the hepatic stages of Plasmodium falciparum and vivax. *Cell Host. Microbe* 14 (1), 104–115. doi: 10.1016/j.chom.2013.06.005

Matz, J. M., and Kooij, T. W. (2015). Towards genome-wide experimental genetics in the in vivo malaria model parasite Plasmodium berghei. *Pathog. Glob. Health* 109 (2), 46–60. doi: 10.1179/2047773215Y.0000000006

Mazier, D., Landau, I., Druilhe, P., Miltgen, F., Guguen-Guillouzo, C., Baccam, D., et al. (1984). Cultivation of the liver forms of Plasmodium vivax in human hepatocytes. *Nature* 307 (5949), 367–369. doi: 10.1038/307367a0

McNamara, C. W., Lee, M. C., Lim, C. S., Lim, S. H., Roland, J., Nagle, A., et al. (2013). Targeting Plasmodium PI(4)K to eliminate malaria. *Nature* 504 (7479), 248–253. doi: 10.1038/nature12782

Meireles, P., Sales-Dias, J., Andrade, C. M., Mello-Vieira, J., Mancio-Silva, L., Simas, J. P., et al. (2017). GLUT1-mediated glucose uptake plays a crucial role during Plasmodium hepatic infection. *Cell Microbiol.* 19 (2). doi: 10.1111/cmi.12646

Mikolajczak, S. A., Jacobs-Lorena, V., MacKellar, D. C., Camargo, N., and Kappe, S. H. (2007). L-FABP is a critical host factor for successful malaria liver stage development. *Int. J. Parasitol.* 37 (5), 483–489. doi: 10.1016/j.ijpara.2007.01.002

Mikolajczak, S. A., Aly, A. S., Dumpit, R. F., Vaughan, A. M., and Kappe, S. H. (2008). An efficient strategy for gene targeting and phenotypic assessment in the Plasmodium yoelii rodent malaria model. *Mol. Biochem. Parasitol.* 158 (2), 213–216. doi: 10.1016/j.molbiopara.2007.12.006

Mikolajczak, S. A., Vaughan, A. M., Kangwanrangsan, N., Roobsoong, W., Fishbaugher, M., Yimamnuaychok, N., et al. (2015). Plasmodium vivax liver stage development and hypnozoite persistence in human liver-chimeric mice. *Cell Host. Microbe* 17 (4), 526–535. doi: 10.1016/j.chom.2015.02.011

Millet, P., Fisk, T. L., Collins, W. E., Broderson, J. R., and Nguyen-Dinh, P. (1988). Cultivation of exoerythrocytic stages of Plasmodium cynomolgi, P. knowlesi, P. coatneyi, and P. inui in Macaca mulatta hepatocytes. *Am. J. Trop. Med. Hyg.* 39 (6), 529–534. doi: 10.4269/ajtmh.1988.39.529

Moraes Barros, R. R., Straimer, J., Sa, J. M., Salzman, R. E., Melendez-Muniz, V. A., Mu, J., et al. (2015). Editing the Plasmodium vivax genome, using zinc-finger nucleases. *J. Infect. Dis.* 211 (1), 125–129. doi: 10.1093/infdis/jiu423

Mueller, A. K., Labaied, M., Kappe, S. H., and Matuschewski, K. (2005). Genetically modified Plasmodium parasites as a protective experimental malaria vaccine. *Nature* 433 (7022), 164–167. doi: 10.1038/nature03188

Ng, S., Schwartz, R. E., March, S., Galstian, A., Gural, N., Shan, J., et al. (2015). Human iPSC-derived hepatocyte-like cells support Plasmodium liver-stage infection in vitro. *Stem Cell Rep.* 4 (3), 348–359. doi: 10.1016/j.stemcr.2015.01.002

Ngotho, P., Soares, A. B., Hentzschel, F., Achcar, F., Bertuccini, L., and Marti, M. (2019). Revisiting gametocyte biology in malaria parasites. *FEMS Microbiol. Rev.* 43 (4), 401–414. doi: 10.1093/femsre/fuz010

Noulin, F., Borlon, C., Van Den Abbeele, J., D'Alessandro, U., and Erhart, A. (2013). 1912-2012: a century of research on Plasmodium vivax in vitro culture. *Trends Parasitol.* 29 (6), 286–294. doi: 10.1016/j.pt.2013.03.012

Pasini, E. M., Bohme, U., Rutledge, G. G., Voorberg-Van der Wel, A., Sanders, M., Berriman, M., et al. (2017). An improved Plasmodium cynomolgi genome assembly reveals an unexpected methyltransferase gene expansion. *Wellcome Open Res.* 2, 42. doi: 10.12688/wellcomeopenres.11864.1

Pfahler, J. M., Galinski, M. R., Barnwell, J. W., and Lanzer, M. (2006). Transient transfection of Plasmodium vivax blood stage parasites. *Mol. Biochem. Parasitol.* 149 (1), 99–101. doi: 10.1016/j.molbiopara.2006.03.018

Poran, A., Notzel, C., Aly, O., Mencia-Trinchant, N., Harris, C. T., Guzman, M. L., et al. (2017). Single-cell RNA sequencing reveals a signature of sexual commitment in malaria parasites. *Nature* 551 (7678), 95–99. doi: 10.1038/nature24280

Portugal, S., Carret, C., Recker, M., Armitage, A. E., Goncalves, L. A., Epiphanio, S., et al. (2011). Host-mediated regulation of superinfection in malaria. *Nat. Med.* 17 (6), 732–737. doi: 10.1038/nm.2368

Posfai, D., Sylvester, K., Reddy, A., Ganley, J. G., Wirth, J., Cullen, Q. E., et al. (2018). Plasmodium parasite exploits host aquaporin-3 during liver stage malaria infection. *PloS Pathog.* 14 (5), e1007057. doi: 10.1371/journal.ppat.1007057

Posfai, D., Maher, S. P., Roesch, C., Vantaux, A., Sylvester, K., Peneau, J., et al. (2020). Plasmodium vivax Liver and Blood Stages Recruit the Druggable Host Membrane Channel Aquaporin-3. *Cell Chem. Biol.* 27 (6), 719–727 e715. doi: 10.1016/j.chembiol.2020.03.009

Prado, M., Eickel, N., De Niz, M., Heitmann, A., Agop-Nersesian, C., Wacker, R., et al. (2015). Long-term live imaging reveals cytosolic immune responses of host hepatocytes against Plasmodium infection and parasite escape mechanisms. *Autophagy* 11 (9), 1561–1579. doi: 10.1080/15548627.2015.1067361

Price, R. N., Tjitra, E., Guerra, C. A., Yeung, S., White, N. J., and Anstey, N. M. (2007). Vivax malaria: neglected and not benign. *Am. J. Trop. Med. Hyg.* 77 (6 Suppl), 79–87. doi: 10.4269/ajtmh.2007.77.79

Raphemot, R., Toro-Moreno, M., Lu, K. Y., Posfai, D., and Derbyshire, E. R. (2019). Discovery of Druggable Host Factors Critical to Plasmodium Liver-Stage Infection. *Cell Chem. Biol.* 26 (9), 1253–1262.e1255. doi: 10.1016/j.chembiol.2019.05.011

Real, E., Rodrigues, L., Cabal, G. G., Enguita, F. J., Mancio-Silva, L., Mello-Vieira, J., et al. (2018). Plasmodium UIS3 sequesters host LC3 to avoid elimination by autophagy in hepatocytes. *Nat. Microbiol.* 3 (1), 17–25. doi: 10.1038/s41564-017-0054-x

Reid, A. J., Talman, A. M., Bennett, H. M., Gomes, A. R., Sanders, M. J., Illingworth, C. J. R., et al. (2018). Single-cell RNA-seq reveals hidden transcriptional variation in malaria parasites. *Elife* 7. doi: 10.7554/eLife.33105

Roth, A., Maher, S. P., Conway, A. J., Ubalee, R., Chaumeau, V., Andolina, C., et al. (2018). A comprehensive model for assessment of liver stage therapies targeting Plasmodium vivax and Plasmodium falciparum. *Nat. Commun.* 9 (1), 1837. doi: 10.1038/s41467-018-04221-9

Sa, E. C. C., Nyboer, B., Heiss, K., Sanches-Vaz, M., Fontinha, D., Wiedtke, E., et al. (2017). Plasmodium berghei EXP-1 interacts with host Apolipoprotein H during Plasmodium liver-stage development. *Proc. Natl. Acad. Sci. U. S. A.* 114 (7), E1138–E1147. doi: 10.1073/pnas.1606419114

Sahu, T., Boisson, B., Lacroix, C., Bischoff, E., Richier, Q., Formaglio, P., et al. (2014). ZIPCO, a putative metal ion transporter, is crucial for Plasmodium liver-stage development. *EMBO Mol. Med.* 6 (11), 1387–1397. doi: 10.15252/emmm.201403868

Sattabongkot, J., Yimamnuaychoke, N., Leelaudomlipi, S., Rasameesoraj, M., Jenwithisuk, R., Coleman, R. E., et al. (2006). Establishment of a human hepatocyte line that supports in vitro development of the exo-erythrocytic stages of the malaria parasites Plasmodium falciparum and P. vivax. *Am. J. Trop. Med. Hyg.* 74 (5), 708–715. doi: 10.4269/ajtmh.2006.74.708

Schmidt, L. H., Fradkin, R., Genther, C. S., and Hughes, H. B. (1982a). Delineation of the Potentials of Primaquine as a Radical Curative and Prophylactic Drug. *Am. J. Trop. Med. Hyg.* 31(3 (3 (Pt 2), 666–680. doi: 10.4269/ajtmh.1982.31.666

Schmidt, L. H., Fradkin, R., Genther, C. S., Rossan, R. N., and Squires, W. (1982b). Responses of Sporozoite-Induced and Trophozoite-Induced Infections to Standard Antimalarial Drugs. *Am. J. Trop. Med. Hyg.* 31(3 (3 (Pt 2), 646–665. doi: 10.4269/ajtmh.1982.31.646

Schmidt, L. H. (1983). Appraisals of compounds of diverse chemical classes for capacities to cure infections with sporozoites of Plasmodium cynomolgi. *Am. J. Trop. Med. Hyg.* 32 (2), 231–257. doi: 10.4269/ajtmh.1983.32.231

Schmidt, L. H. (1986). Compatibility of relapse patterns of Plasmodium cynomolgi infections in rhesus monkeys with continuous cyclical development and hypnozoite concepts of relapse. *Am. J. Trop. Med. Hyg.* 35 (6), 1077–1099. doi: 10.4269/ajtmh.1986.35.1077

Seeger, C., and Mason, W. S. (2000). Hepatitis B virus biology. *Microbiol. Mol. Biol. Rev.* 64 (1), 51–68. doi: 10.1128/mmbr.64.1.51-68.2000

Shanks, G., and Waller, M. (2019). Blood transfusion as a possible initiator of *Plasmodium vivax* relapse through increased heme metabolism leading to hepatocyte apoptosis. *Poster Presentation ICPVR Paris*.

Shanks, G. D., and White, N. J. (2013). The activation of vivax malaria hypnozoites by infectious diseases. *Lancet Infect. Dis.* 13 (10), 900–906. doi: 10.1016/S1473-3099(13)70095-1

Shears, M. J., Sekhar Nirujogi, R., Swearingen, K. E., Renuse, S., Mishra, S., Jaipal Reddy, P., et al. (2019). Proteomic Analysis of Plasmodium Merosomes: The Link between Liver and Blood Stages in Malaria. *J. Proteome Res.* 18 (9), 3404–3418. doi: 10.1021/acs.jproteome.9b00324

Shortt, H. E., Garnham, P. C., Covell, G., Shute, P. G., et al. (1948). The pre-erythrocytic stage of human malaria, Plasmodium vivax. *Br. Med. J.* 1 (4550):547. doi: 10.1136/bmj.1.4550.547

Shortt, H. E., and Garnham, P. C. (1948a). Demonstration of a persisting exo-erythrocytic cycle in Plasmodium cynomolgi and its bearing on the production of relapses. *Br. Med. J.* 1 (4564), 1225–1228. doi: 10.1136/bmj.1.4564.1225

Shortt, H. E., and Garnham, P. C. (1948b). The pre-erythrocytic development of Plasmodium cynomolgi and Plasmodium vivax. *Trans. R. Soc. Trop. Med. Hyg.* 41 (6), 785–795. doi: 10.1016/s0035-9203(48)80006-4

Tachibana, S., Sullivan, S. A., Kawai, S., Nakamura, S., Kim, H. R., Goto, N., et al. (2012). Plasmodium cynomolgi genome sequences provide insight into Plasmodium vivax and the monkey malaria clade. *Nat. Genet.* 44 (9), 1051–1055. doi: 10.1038/ng.2375

Tarun, A. S., Peng, X., Dumpit, R. F., Ogata, Y., Silva-Rivera, H., Camargo, N., et al. (2008). A combined transcriptome and proteome survey of malaria parasite

liver stages. *Proc. Natl. Acad. Sci. U. S. A.* 105 (1), 305–310. doi: 10.1073/pnas.0710780104

Tripathi, J., Segeritz, C. P., Griffiths, G., Bushell, W., Vallier, L., Skarnes, W. C., et al. (2020). A Novel Chemically Differentiated Mouse Embryonic Stem Cell-Based Model to Study Liver Stages of Plasmodium berghei. *Stem Cell Rep.* 14 (6), 1123–1134. doi: 10.1016/j.stemcr.2020.04.010

van de Sand, C., Horstmann, S., Schmidt, A., Sturm, A., Bolte, S., Krueger, A., et al. (2005). The liver stage of Plasmodium berghei inhibits host cell apoptosis. *Mol. Microbiol.* 58 (3), 731–742. doi: 10.1111/j.1365-2958.2005.04888.x

Voorberg-van der Wel, A., Zeeman, A. M., van Amsterdam, S. M., van den Berg, A., Klooster, E. J., Iwanaga, S., et al. (2013). Transgenic fluorescent Plasmodium cynomolgi liver stages enable live imaging and purification of Malaria hypnozoite-forms. *PloS One* 8 (1), e54888. doi: 10.1371/journal.pone.0054888

Voorberg-van der Wel, A., Roma, G., Gupta, D. K., Schuierer, S., Nigsch, F., Carbone, W., et al. (2017). A comparative transcriptomic analysis of replicating and dormant liver stages of the relapsing malaria parasite Plasmodium cynomolgi. *Elife* 6. doi: 10.7554/eLife.29605

Voorberg-van der Wel, A. M., Zeeman, A. M., Nieuwenhuis, I. G., van der Werff, N. M., Klooster, E. J., Klop, O., et al. (2020). A dual fluorescent Plasmodium cynomolgi reporter line reveals in vitro malaria hypnozoite reactivation. *Commun. Biol. Press*. doi: 10.1038/s42003-019-0737-3.

Wacker, R., Eickel, N., Schmuckli-Maurer, J., Annoura, T., Niklaus, L., Khan, S. M., et al. (2017). LC3-association with the parasitophorous vacuole membrane of Plasmodium berghei liver stages follows a noncanonical autophagy pathway. *Cell Microbiol.* 19 (10). doi: 10.1111/cmi.12754

Wells, T. N., Burrows, J. N., and Baird, J. K. (2010). Targeting the hypnozoite reservoir of Plasmodium vivax: the hidden obstacle to malaria elimination. *Trends Parasitol.* 26 (3), 145–151. doi: 10.1016/j.pt.2009.12.005

White, N. J. (2011). Determinants of relapse periodicity in Plasmodium vivax malaria. *Malar. J.* 10, 297. doi: 10.1186/1475-2875-10-297

WHO (2019). *World Malaria Report 2019*. Available at: https://www.who.int/publications/i/item/world-malaria-report-2019.

Yegneswaran, B., Alcid, D., and Mohan, J. (2009). Plasmodium knowlesi: an important yet overlooked human malaria parasite. *Mayo. Clin. Proc.* 84 (7), 664; author reply 664. doi: 10.4065/84.7.664

Zeeman, A. M., van Amsterdam, S. M., McNamara, C. W., Voorberg-van der Wel, A., Klooster, E. J., van den Berg, A., et al. (2014). KAI407, a Potent Non-8-Aminoquinoline Compound That Kills Plasmodium cynomolgi Early Dormant Liver Stage Parasites In Vitro. *Antimicrob. Agents Chemother.* 58 (3), 1586–1595. doi: 10.1128/AAC.01927-13

Zeeman, A. M., Lakshminarayana, S. B., van der Werff, N., Klooster, E. J., Voorberg-van der Wel, A., Kondreddi, R. R., et al. (2016). PI4 Kinase Is a Prophylactic but Not Radical Curative Target in Plasmodium vivax-Type Malaria Parasites. *Antimicrob. Agents Chemother.* 60 (5), 2858–2863. doi: 10.1128/AAC.03080-15

Conflict of Interest: The authors declare that the research was conducted in the absence of any commercial or financial relationships that could be construed as a potential conflict of interest.

frontiers in Cellular and Infection Microbiology

ORIGINAL RESEARCH
published: 02 February 2021
doi: 10.3389/fcimb.2020.610200

Rab5b-Associated Arf1 GTPase Regulates Export of N-Myristoylated Adenylate Kinase 2 From the Endoplasmic Reticulum in *Plasmodium falciparum*

Izumi Taku[1,2], *Tomohiro Hirai*[1,2], *Takashi Makiuchi*[3], *Naoaki Shinzawa*[4], *Shiroh Iwanaga*[4†], *Takeshi Annoura*[1], *Kisaburo Nagamune*[1,5], *Tomoyoshi Nozaki*[6] *and Yumiko Saito-Nakano*[1*]

[1] Department of Parasitology, National Institute of Infectious Diseases, Tokyo, Japan, [2] Graduate School of Life and Environmental Sciences, University of Tsukuba, Ibaraki, Japan, [3] Department of Parasitology, Tokai University School of Medicine, Isehara, Japan, [4] Department of Environmental Parasitology, Graduate School of Medical and Dental Sciences, Tokyo Medical and Dental University, Tokyo, Japan, [5] Faculty of Life and Environmental Sciences, University of Tsukuba, Ibaraki, Japan, [6] Graduate School of Medicine, The University of Tokyo, Tokyo, Japan

Plasmodium falciparum extensively remodels human erythrocytes by exporting hundreds of parasite proteins. This remodeling is closely linked to the *Plasmodium* virulence-related functions and immune evasion. The N-terminal export signal named PEXEL (*Plasmodium* export element) was identified to be important for the export of proteins beyond the PVM, however, the issue of how these PEXEL-positive proteins are transported and regulated by Rab GTPases from the endoplasmic reticulum (ER) to the cell surface has remained poorly understood. Previously, we identified new aspects of the trafficking of N-myristoylated adenylate kinase 2 (PfAK2), which lacks the PEXEL motif and is regulated by the PfRab5b GTPase. Overexpression of PfRab5b suppressed the transport of PfAK2 to the parasitophorous vacuole membrane and PfAK2 was accumulated in the punctate compartment within the parasite. Here, we report the identification of PfRab5b associated proteins and dissect the pathway regulated by PfRab5b. We isolated two membrane trafficking GTPases PfArf1 and PfRab1b by coimmunoprecipitation with PfRab5b and *via* mass analysis. PfArf1 and PfRab1b are both colocalized with PfRab5b adjacent to the ER in the early erythrocytic stage. A super-resolution microgram of the indirect immunofluorescence assay using PfArf1 or PfRab1b- expressing parasites revealed that PfArf1 and PfRab1b are localized to different ER subdomains. We used a genetic approach to expresses an active or inactive mutant of PfArf1 that specifically inhibited the trafficking of PfAK2 to the parasitophorous vacuole membrane. While expression of PfRab1b mutants did not affect in the PfAK2 transport. In contrast, the export of the

OPEN ACCESS

Edited by:
Tania F. De Koning-Ward, Deakin University, Australia

Reviewed by:
Danny Wilson, University of Adelaide, Australia
Gordon Langsley, INSERM U1016 Institut Cochin, France

***Correspondence:**
Yumiko Saito-Nakano
yumiko@nih.go.jp

†Present address:
Shiroh Iwanaga, Department of Molecular Protozoology, Research Institute for Microbial Diseases, Osaka University, Osaka, Japan

Specialty section:
This article was submitted to Parasite and Host, a section of the journal Frontiers in Cellular and Infection Microbiology

Received: *25 September 2020*
Accepted: *17 December 2020*
Published: *02 February 2021*

Citation:
Taku I, Hirai T, Makiuchi T, Shinzawa N, Iwanaga S, Annoura T, Nagamune K, Nozaki T and Saito-Nakano Y (2021) Rab5b-Associated Arf1 GTPase Regulates Export of N-Myristoylated Adenylate Kinase 2 From the Endoplasmic Reticulum in Plasmodium falciparum. Front. Cell. Infect. Microbiol. 10:610200. doi: 10.3389/fcimb.2020.610200

PEXEL-positive protein Rifin was decreased by the expression of the inactive mutant of PfRab1b or PfArf1. These data indicate that the transport of PfAK2 and Rifin were recognized at the different ER subdomain by the two independent GTPases: PfAK2 is sorted by PfArf1 into the pathway for the PV, and the export of Rifin might be sequentially regulated by PfArf1 and PfRab1b.

Keywords: *Plasmodium falciparum*, Rab5b, Arf1, Rab1b, AK2, Rifin, ERD2

INTRODUCTION

Secretory proteins are synthesized in the endoplasmic reticulum (ER) and are delivered to their destinations *via* the Golgi apparatus. ER-to-Golgi trafficking is highly conserved among eukaryotes, and two types of Ras super families of GTPases, the Sar/Arf and Rab families, mediate protein sorting and transport as molecular switches between these organelles (Suda et al., 2018; Kurokawa and Nakano, 2019). A guanine nucleotide exchange factor (GEF) acts on GDP-bound form of GTPase to convert it to a GTP-bound active state, and a GTPase accelerating protein (GAP) binds to the GTPase to catalyze hydrolysis of the bound GTP to GDP and thereby convert the GTPase back to its inactive state (Hutagalung and Novick, 2011). The GTPase cycle between GDP-and GTP-bound forms causes conformational changes and specific effector molecules are recruited to the GTP-bound active form to complete various membrane trafficking events (Stenmark, 2009; Donaldson and Jackson, 2011). Many regulatory functions performed by the proteins in the Sar/Arf and Rab families were identified by their interaction with diverse effector proteins that select cargo, promote vesicle movement, and verify the correct site for fusion (Hutagalung and Novick, 2011).

The Sar/Arf and Rab families of GTPases regulate the bidirectional transport between ER and the Golgi in mammalian cells and land plants (Brandizzi and Barlowe, 2013). Newly synthesized secretory proteins translocate into the ER lumen using the N-terminal signal peptide (Nickel and Rabouille, 2009). The ER luminal chaperone BiP assists in folding newly synthesized proteins to maintain protein homeostasis (Craig et al., 1993). Activation of the ER-localized GTPase Sar1 and its GTP hydrolysis triggers the recruitment of the COPII coat component and causes the enrichment of cargo proteins into the ER exit sites (ERES) where COPII-coated vesicles form (Kung et al., 2012; Yorimitsu and Sato, 2012). The COPII machinery performs two critical functions: first, Sar1 and the inner layer Sec23–Sec24 COPII subunits bind to and select specific cargo for packaging; second, polymerization of the outer layer of Sec13–Sec31 COPII subunits occurs into a cage structure to drive vesicle formation (Bi et al., 2007). After uncoating of the COPII coat, diffusive vesicles are anchored to *cis*-Golgi membranes by the extended coiled-coil domain that tethers factor protein p115, the yeast homolog of Uso1, as well as the multi-subunit TRAPPI (transport protein particle I) complex that activates Rab1 GTPase (Cai et al., 2007). The fusion of vesicles depends on the assembly of integral membrane SNARE complexes between the donor and acceptor membranes (Allan et al., 2000). In contrast, a heptameric complex COPI-coated vesicle facilitates the retrieval of escaped ER luminal proteins that contain KDEL signals, which are recognized by the resident KDEL receptor ERD2 in the *cis*-Golgi, and by SNARE proteins (Lewis et al., 1990; Semenza et al., 1990). Once Arf1 is activated by the GEF which contains a conserved Sec7 domain, the membrane-localized Arf1 recruits the COPI coat to the *cis*-Golgi membranes (Zhao et al., 1999). The COPI subunits recognize the sorting motifs of transmembrane cargo proteins and are incorporated into nascent COPI vesicles and subsequently retrieve cargo proteins to the ER (Eugster et al., 2000). Most Rab and Arf GTPases carry lipid modifications that are necessary for membrane recruitment. In the case of Rab, a carboxy-terminal geranylgeranylation (20-carbon unsaturated fatty acid) group at the C-terminal cysteine residue is responsible for the membrane attachment of the Rab-GTP form (Leung et al., 2006). In contrast, the N-terminal glycine residue of Arf is myristoylated (14-carbon saturated fatty acids) (Pasqualato et al., 2002).

Plasmodium falciparum is the causative agent of malaria, and it extensively remodels the human erythrocytes in which it resides (de Koning-Ward et al., 2016). The remodeling process is conducted by hundreds of proteins exported from the parasites into the host cell compartment, and these enable virulence-related functions including cytoadherence to the vascular endothelium, immune evasion, and nutrient uptake (Miller et al., 2013). Many of the exported proteins contain a five amino acid motif termed the *Plasmodium* export element (PEXEL) which is found ~20 amino acids downstream of the signal peptide (Hiller et al., 2004; Marti et al., 2004). The PEXEL motif is removed in the ER lumen of the parasite by the ER resident aspartic protease plasmepsin V before exit of the ER (Boddey et al., 2010; Russo et al., 2010). All repertoires of COPII and COPI components are conserved in the *Plasmodium* spp. (Kibria et al., 2019), suggesting that the early secretory system of *Plasmodium* may resemble that in higher eukaryotes. Several studies have reported that the fungal metabolite brefeldin A (BFA), which inhibits the Golgi-localized GEF Arf1, disrupts the accurate export of PEXEL-containing proteins (Akompong et al., 2002; Chang et al., 2008), indicating that these proteins are trafficked through the classical ER-Golgi pathway. Subsequently, the exported proteins are transported across the parasite plasma membrane and the parasitophorous vacuole membrane (PVM) *via* the multimeric *Plasmodium* translocon of exported proteins (PTEX) into the erythrocyte cytosol (de Koning-Ward et al., 2009). In these *Plasmodium* trafficking systems, the roles of small GTPases are poorly understood such that the subcellular

localization and function of only one Sar1 and six Rab GTPases has been being characterized functionally; i.e., PfSar1, PfRab1a, PfRab5a, PfRab5b, PfRab6, PfRab7, and PfRab11A (Adisa et al., 2001; Struck et al., 2005; Elliott et al., 2008; Agop-Nersesian et al., 2009; Rached et al., 2012; Krai et al., 2014; Ebine et al., 2016; Morse et al., 2016). However, effectors and binding proteins have only been identified for PfRab11A (Agop-Nersesian et al., 2009). Further, PfRab11A is associated with the myosin-tail-interacting-protein and is crucial for the parasite invasion of host cells (Agop-Nersesian et al., 2009).

Several exported proteins lacking an N-terminal PEXEL motif and are called PEXEL-negative proteins (PNEPs). These are also translocate through PTEX for export into the erythrocyte cytosol (Spielmann and Gilberger, 2010; Elsworth et al., 2014). For example, the skeleton binding protein 1 (SBP1), which is a PEXEL-negative transmembrane protein, is supposed to export *via* the classical secretory pathway, because the truncated SBP1 internalized in the perinuclear staining corresponding to the ER (Saridaki et al., 2009). However, recent report that SBP1 was included within electron-dense materials in the parasite cytoplasm (Iriko et al., 2020), strongly suggests that the presence of alternate export pathways except for the classical ER-to-Golgi transport pathway in the parasite trafficking system. *Plasmodium falciparum* adenylate kinase 2 (PfAK2), which lacks a signal peptide and the PEXEL motif, but is modified *via* myristoylation (14-carbon) and palmitoylation (16-carbon saturated fatty acid) at the N-terminal glycine and cysteine residues respectively, is transported to the parasite PVM (Rahlfs et al., 2009; Thavayogarajah et al., 2015; Ebine et al., 2016). Previously, we have reported that trafficking of PfAK2 to the PVM was repressed and the PfAK2 accumulated in the punctate structure within the parasite cytoplasm due to the overexpression of PfRab5b, indicating that PfRab5b is involved in the transport of PfAK2 to the PVM (Ebine et al., 2016). PfRab5b possesses a structurally unique motif that is similar to PfAK2, which lacks a C-terminal geranylgeranylation modification, while retaining the N-terminal myristoylation and palmitoylation motifs (Ezougou et al., 2014). In rodent malaria *P. berghei*, gene-deletion of PbRab5b was unsuccessful, indicating *Plasmodium* Rab5b is essential for the blood stage growth (Ezougou et al., 2014). Subcellular localization of PfRab5b is proximal to the region of the BiP-positive ER, and segregated from COPII subunit Sec13-positive ERES (Ebine et al., 2016). Interestingly, the inhibition of transport was observed in PfAK2, however the PEXEL-positive erythrocyte vesicle protein 1 (PfEVP1) and SBP1 were correctly exported upon the overexpression of PfRab5b (Ebine et al., 2016). These findings suggested that PfRab5b may regulate the transport of PfAK2 by the COPII independent non-classical pathway (Ebine et al., 2016).

Currently, none of GTPase, which regulates the trafficking of PNEPs including PfAK2, is elucidated, A bioinformatic technique previously identified casein kinase1 (CK1) as a PfRab5b binding protein (Rached et al., 2012); however, it remains unclear how PfRab5b is involved in the selective transport of PfAK2. To understand the mechanisms underlying the PfRab5b-dependent specific trafficking pathway, we isolated PfRab5b associated proteins using coimmunoprecipitation and mass analysis approaches. Among the candidate proteins, we found that the PfArf1 and PfRab1b GTPases were colocalized with PfRab5b in the compartment close to the ER. Indirect immunofluorescence assay for PfArf1- or PfRab1b- expressing parasites using super-resolution microscopy revealed that PfArf1 and PfRab1b were localized to different ER subdomains. Further, using a genetic approach to express an active or inactive mutant indicated that PfArf1, but not PfRab1b, was involved in the transport of PfAK2 to the PVM. Unexpectedly, PfRab1b participates in the trafficking of the PEXEL-positive export protein Rifin. Our data suggest that the trafficking pathways of PfAK2 and Rifin are separated in the PfArf1-positive ER subdomain, and this is the first report for the identification of GTPase which regulates transport of PfAK2 in *Plasmodium*.

MATERIALS AND METHODS

Ethics Statement

Human RBCs and plasma were obtained as donations from anonymized individuals at the Japanese Red Cross Society (no. 28J0023).

Strain Culture and Transfection

Plasmodium falciparum line MS822 (Nakazawa et al., 2011) was cultured as described previously (Alexandre et al., 2011), and transfection was performed as described (Deitsch et al., 2001; Alexandre et al., 2011). Transfected parasites were selected with 5 nM of WR99210-HCl (a kind gift from D Jacobus) or 2.5 μg/ml of blasticidin S-HCl (BSD, Funakoshi). Transfectants were selected 2 weeks after the addition of drugs.

Plasmid Construction

The vector pCHD43(II) (Sakura et al., 2013; Ebine et al., 2016) was used to express PfRab5b-yellow fluorescent protein (YFP)-FLAG (Watanabe et al., 2020), PfRab5b-YFP, and PfRab5b-YFP-destabilization domain (DD) (Armstrong and Goldberg, 2007) from the constitutive *P. falciparum* chloroquine resistance transporter promoter. To construct PfRab5b-YFP/pCHD43(II), the DD domain was removed from the PfRab5b-YFP-DD/pCHD43(II) construct using the PrimeSTAR Mutagenesis Basal Kit (TaKaRa Bio). A tandem repeat of the FLAG tag was inserted after the YFP coding region of PfRab5b-YFP/pCHD43(II) using PCR amplification with overlapping oligonucleotides to construct PfRab5b-YFP-FLAG/pCHD43(II) (**Supplementary Figure 1A**). The artificial centromere plasmid PfCenV-ef1-double, whose expression was regulated under the *Plasmodium berghei* elongation factor 1 (Pbef1α) and maintained by the *P. falciparum* centromere of chromosome 5, was used to stably express PfRab5b and PfArf1 or PfRab1b (Iwanaga et al., 2012). Fusion construct of PfRab5b^{Q94L}-YFP-DD was inserted into the NcoI site, and PfArf1-red fluorescent protein (RFP) or RFP-PfRab1b encoding genes were ligated into the NdeI site of

PfCenV-ef1-double, respectively (**Supplementary Figure 1B**). For expression of AK2-RFP or Rifin-RFP, fragments were inserted into the NdeI site of PfCenV-ef1-double. The AK2-RFP fragment was amplified from PfAK2-RFP/pCHD43(II)-BSD. A fragment of Rifin (PlasmoDB accession number PFA0745w) was amplified from gDNA from the *P. falciparum* 3D7 line (Walliker et al., 1987). The fusion construct consisting of PEXEL signal (1–51 aa) of the Rifin-RFP-transmembrane domain (102–336 aa) has been described previously (Marti et al., 2004). PfArf1 and PfRab1b fragments were amplified using cDNA from the *P. falciparum* 3D7 line and the episomal plasmids expressing PfArf1-YFP-DD or DD-YFP-PfRab1b were inserted into pCHD43(II)-BSD (Ebine et al., 2016). To construct constitutively active or inactive PfArf1 (Q71L and T31N) and PfRab1b (Q67L and S22N) mutants, the PrimeSTAR Mutagenesis Basal Kit was used to introduce point mutations (**Supplementary Figure 1C**). The former substitution at specific sites in the guanine nucleotide consensus domains of human Ras^{Q61L} impaired GTP hydrolysis activity (Haubruck and McCormick, 1991), and the latter substitution of human Ras^{S17A} alter the guanine nucleotide binding affinity for GTP to GDP (Feig and Cooper, 1988), respectively. The oligonucleotides used are listed in **Supplementary Table 1**.

Coimmunoprecipitation Assay and Mass Spectrometry Analysis

Transgenic parasites carrying the PfRab5b-YFP or PfRab5b-YFP-FLAG with pCHD43(II) episomal plasmids were cultured in 250 ml medium (5% hematocrit, 7% parasitemia), and infected red blood cells (iRBCs) were collected by centrifugation at 560 × g for 5 min and permeabilized using 0.075% saponin in phosphate buffered saline (PBS) for 30 min on ice. Samples were crosslinked using 0.5 mM 3,3'-dithiodipropionic acid di (N-hydroxysuccinimide ester) (DSP) (Sigma-Aldrich, St. Louis) for 30 min at room temperature, and were subsequently quenched by the addition of 50 mM Tris-HCl (pH 7.5) according to the manufacturer's protocol. Next, the samples were solubilized with 250 µl of 1.0% Triton X-100 in PBS and kept on ice for 20 min. The insoluble fraction was removed by centrifugation at 9,100 × g for 5 min, and the supernatant fractions were incubated with Protein G Sepharose (GE Healthcare) at 4°C for 60 min to reduce non-specific binding during coimmunoprecipitation. The PfRab5b protein complex was immunoprecipitated using anti-FLAG antibody conjugated agarose (EZview Red Anti-FLAG M2 Affinity Gel, Sigma-Aldrich) at 4°C for 3.5 h, and the immunoprecipitated was washed thrice with 1.0% Triton X-100 in PBS. The PfRab5b protein complexes were eluted with 50 µl of 0.2 mg/ml FLAG peptide (Sigma-Aldrich) in PBS containing 50 mM DTT and 10 mM EDTA at 4°C for 16 h. The eluted proteins were separated *via* 12% SDS-PAGE and visualized using silver staining. The in-gel trypsin digestion of proteins, liquid chromatography, and time-of-flight tandem mass spectrometry (LC-ToF MS/MS) (Orbitrap, Thermo Fisher Scientific, Waltham, MA, USA) were performed as described previously (Makiuchi et al., 2013). The quantitative value, normalized with unweighted spectrum counts, was used to estimate relative quantities of proteins in the samples. Specific binding proteins were selected by the following criteria: 1) peptide fold enrichment that showed >3.5 higher in PfRab5b-YFP-FLAG samples compared with those in the PfRab5b-YFP control were selected. 2) Protein with >3.5 higher in PfRab5b-YFP-FLAG samples with no value in the PfRab5b-YFP control were selected. 3) Proteins those involved in cytosolic proteins such as proteasome and ribosomal proteins were removed from the list.

Indirect Immunofluorescence Assay

Transgenic parasites carrying the PfRab5b, PfArf1, or PfRab1b mutant proteins fused with a DD system with artificial centromere plasmid PfCenV-ef1a-double were stabilized with 0.5 µM Shld1 for 24 h (Clontech) (Armstrong and Goldberg, 2007). Next, cultures were synchronized by the 5% sorbitol for 10 min at room temperature. After washing, ring-rich parasites were cultured until indicated erythrocytic stages under the 0.5 µM Shld1. Infected erythrocytes were collected and fixed with 4% paraformaldehyde (Thermo) in PBS at 4°C for more than 12 h. Fixed samples were permeabilized with 0.5% Triton X-100 in PBS for 30 min and blocked with 3% skim milk prepared with PBS for 10 min. Primary antibodies were used at the following dilutions: anti-BiP (1:100, kindly gift from Prof. Kita) and anti-ERD2 (1:100) (Elmendorf and Haldar, 1993). Alexa 488-conjugated anti-mouse IgG (1:10,000, Molecular Probes) was used as the secondary antibody. The number of parasites that showed colocalization of the RFP and PfERD2 or BiP signals was counted in 20–30 trophozoites from three independent experiments. A test for statistical significance was performed using the Student *t*-test.

Reciprocal Coimmunoprecipitation and Immunoblot Analysis

Transgenic parasites carrying the PfArf1-RFP, or PfArf1-RFP and $PfRab5b^{Q94L}$-YFP-DD with artificial centromere plasmids PfCenV-ef1a-double were cultured in 250 ml medium (5% hematocrit, 5.4% parasitemia), and collected iRBCs were permeabilized with saponin-PBS. The iRBCs were crosslinked with 2 mM DSP in 500 µl PBS for 30 min at room temperature with rotation. Samples were quenched with 50 mM Tris-HCl (pH7.5) for 15 min at room temperature with rotation, and then washed two times with 50 mM Tris-HCl (pH7.5). The sample pellets were resuspended in 500 µl lysis buffer (50 mM Tris-HCl, 150 mM NaCl, Complete protease inhibitor (Roche), 1% TritonX-100, (pH7.5) and homogenized by 30-times pipetting subsequently incubated on ice for 20 min. After unbroken cells were removed by centrifugation at 2,000 × g for 5 min, the supernatants were transferred to new tubes and incubated with 20 µl Protein G Sepharose (Sigma-Aldrich) for 30 min at room temperature to reduce non-specific binding during coimmunoprecipitation. After centrifugation at 800 × g for 5 min, the supernatant was reacted with 5 µg rabbit anti-RFP polyclonal antibody (GeneTex, GTX127897) at 4°C for over night and precipitated with 30 µl Protein G Sepharose for 1 h at room temperature. The Protein G Sepharose was washed with

1 ml lysis buffer for three times, and protein complexes were eluted with 40 µl of SDS sample buffer (250 mM Tris-HCl, 8% SDS, 8% 2-mercaptoethanol, 40% glycerol, 0.00 4% bromophenol blue, pH 6.8) at 95°C for 5 min. Bound proteins were eluted and loaded on 12% SDS-PAGE gels, followed by immunoblotting using mouse anti-GFP monoclonal antibody (1:100, Merck, 11814460001, clone 7.1 and 13.1) and mouse anti-RFP monoclonal antibody (1:200, Cell Biolabs AKR-021, clone RF5R), mouse anti-Hsp90 monoclonal antibody (1:500, Sigma, clone AC-16), and anti-mouse IgG conjugated HRP-linked antibody (1:10000, Cell Singling, 7076S).

Microscopy Techniques

Images were acquired using an LSM700 or LSM780 confocal laser-scanning microscope (Zeiss, Germany). For distance measurements between PfBiP and PfArf1 or PfRab1b, super-resolution imaging was performed using the Zeiss LSM880 with Airyscan confocal laser-scanning microscope, that is equipped with an oil-immersion 100× objective lens (alpha Plan-Apochromat 100×/1.46 oil DIC M27 Elyra) (Zeiss, Germany). The background fluorescence from the non-transfected parasites was set as baseline. All images were acquired in the same laser voltage and gain (exposure time). Raw data were processed using the Zeiss Zen2 software to measure fluorescent intensities. The images were analyzed using the Zeiss Zen2 software or Fiji-ImageJ software (Schindelin et al., 2012). Scoring of images was judged by the blinded two experienced microscopists.

RESULTS

Coimmunoprecipitation of PfRab5b-YFP-FLAG to Isolate PfRab5b Associated Candidate Proteins

Previous studies have shown that PfRab5b is localized adjacent to the ER and is involved in the trafficking of the N-myristoylated protein AK2 to the PVM (Ebine et al., 2016). In general, transport of newly synthesized transmembrane or luminal proteins from the ER is regulated by the Sar1 family of GTPases, but not by the Rab family (Nakano and Muramatsu, 1989). Proteins are packed into COPII-coated vesicles at the ERES and trafficked to the *cis*-Golgi cisternae under the control of the Rab1 and Arf1 GTPases (Balch et al., 1992; Martinez et al., 2016). To investigate the mechanism controlled by PfRab5b from the ER, we attempted to identify PfRab5b interacting proteins by coimmunoprecipitation. Lysates prepared from PfRab5b expressing parasites, which were C-terminally fused with the YFP and FLAG-tags (PfRab5b-YFP-FLAG) or a negative control PfRab5b-YFP (**Supplementary Figure 1A**), were immunoprecipitated with an anti-FLAG antibody and eluted using the FLAG peptide. The eluted samples were analyzed *via* LC-ToF MS/MS, and 677 peptides were identified from the PfRab5b-YFP-FLAG expressing lysate (**Supplementary Table 2**). Six candidate proteins showing a 3.5–fold change in the expression of PfRab5b-YFP-FLAG relative to PfRab5b-YFP were obtained. These included the ADP-ribosylation factor (PfArf GTPase) (PF3D7_1020900), erythrocyte binding antigen-181 (EBA181) (PF3D7_0102500), protein transport protein SEC7 (PfSec7) (PF3D7_1442900), early transcribed membrane protein 10.2 (ETRAMP10.2) (PF3D7_1033200), PfRab1b GTPase (PF3D7_0512600), and the PVM protein S16 (Pfs16) (PF3D7_0406200) (**Table 1**). In other organisms, the Arf GTPase, Sec7, and Rab1b are involved in the transport from the *cis*-Golgi to the ER (Monetta et al., 2007). Another *Plasmodium*-specific candidate protein EBA181 is a ligand localized on the surface of merozoites and plays an important role in the entry of parasites into erythrocytes by binding to surface receptors on erythrocyte cell membranes (Gilberger et al., 2003). ETRAMP10.2 is expressed at an early point of the intraerythrocytic stage and is localized at the parasite periphery, which is assumed to be the PVM (Spielmann et al., 2003). The Pfs16 is expressed in gametocytes and is localized at the parasite periphery, similar to ETRAMP10.2 (Bruce et al., 1994). In this study, we focused on the functions of the PfArf and PfRab1b GTPases to elucidate the mechanism of intracellular transport mediated by PfRab5b. Studies on the other candidate proteins will be described elsewhere.

PfArf1 and PfRab1b Colocalize With PfRab5b

In the *P. falciparum* genome, 11 Rab GTPase-encoding genes have been identified (Quevillon et al., 2003). Among them, PfRab1a and PfRab1b have been reported as two human Rab1 homologs (Quevillon et al., 2003). PfRab1a is localized to the ER and regulates trafficking from the ER to the apical organelles known as rhoptries (Morse et al., 2016). However, there are no reports for PfRab1b function and its subcellular localization. For the Sar/Arf family, the Sar1 homolog PfSar1 alone has been shown to localize the ER and define network membranes surrounding the parasite nuclei (Adisa et al., 2007). A BLASTP search revealed the presence of six Sar/Arf proteins in the *P. falciparum* 3D7 genome database (**Supplementary Figure 2A**). Amino acid sequencing showed that five of these proteins are Arf family GTPases (PF3D7_1020900, PF3D7-1034700, PF3D7_1442000, Pf3D7_0920500, Pf3D7_1316200), and one is a Sar1 homolog (PF3D7_0416800) based on the conserved effector sequence and the overall amino acid identities (**Supplementary Figure 2C**). PF3D7_1020900, which was obtained as PfRab5b interacting protein (**Table 1**), showed the highest identity (75%) to human Arf1 among the *Plasmodium* and human Arf families (**Supplementary Figure 2B**). Thus, the PfRab5b-associated protein candidate PF3D7_1020900 is a *Plasmodium* Arf1 homolog and was annotated as PfArf1 (GenBank Accession number, BR001667).

The intracellular colocalization of PfRab5b with PfArf1 or PfRab1b was demonstrated using double-expressing parasites. First, the constitutively active mutant PfRab5b^{Q94L} was fused with YFP and a DD (PfRab5b^{Q94L}-YFP-DD) and expressed in a Shld1 ligand-dependent manner (Armstrong and Goldberg, 2007; Ebine et al., 2016). The Q-to-L substitution in the conserved GTP binding consensus domain impairs intrinsic GTPase activity which favor formation of the active GTP-

TABLE 1 | Candidates for PfRab5b associated proteins.

Annotation	Gene ID	PlasmoDB ID	Molecular weight (kDa)	Normalized relative ratio against common peptidesPfRab5b-YFP-FLAG/PfRab5b-YFP (fold enrichment)
Rab5b	Q76NM7	PF3D7_1310600	23	72.8/1.16 (62.7)
Arf1	Q7KQL3	PF3D7_1020900	21	7.90/1.16 (6.80)
EBA181	Q8I2B4	PF3D7_0102500	181	7.90/1.16 (6.80)
Sec7	Q8IL42	PF3D7_1442900	405	11.4/2.32 (4.91)
ETRAMP10.2	Q8IJ76	PF3D7_1033200	39	5.27/1.16 (4.53)
Rab1b	Q7K6A8	PF3D7_0512600	23	4.39/1.16 (3.78)
Pfs16	Q6ZMA7	PF3D7_0406200	17	3.51/0 (N/A)

bound form to small GTPases (Der et al., 1986: Stenmark et al., 1994). As conventional Rab GTPases are modified with C-terminal geranyl-geranylation (Joberty et al., 1993), PfRab1b was fused with the N-terminal RFP (RFP-PfRab1b). In contrast, Arf1 is modified with N-terminal myristoylation (Sewell and Kahn, 1988), and PfArf1 was fused with a C-terminus RFP fusion (PfArf1-RFP). PfRab5b^{Q94L}-YFP-DD and RFP-PfRab1b, or PfArf1-RFP were placed under the control of the Pbef1α dual promoter and the constructs were transformed into parasites (**Supplementary Figure 1B**). Immunoblots using an anti-RFP antibody showed the 48 and 50 kDa bands of PfArf1-RFP and RFP-PfRab1b, respectively (**Supplementary Figure 3**). The anti-GFP antibody detected a 62 kDa band corresponding to PfRab5b^{Q94L}-YFP-DD, indicating that the full length of fusion constructs were expressed (**Supplementary Figure 3**). In the mononuclear early trophozoite stage, 2 or 3 nuclear late trophozoite, and multinucleated early schizont stages, the RFP signals of PfArf1-RFP and RFP-PfRab1b were observed as juxtanuclear punctate structures, and these colocalized with the YFP fluorescence from PfRab5b^{Q94L}-YFP-DD (**Figures 1A, B**). Previous report showed that PfRab5b localized near the parasite plasma membrane at the schizont stage (Ezougou et al., 2014). We additionally showed the localization of PfRab5b to the ER and PVM between ring and late schizont stages (Ebine et al., 2016). Thus we focus on the localization of PfArf1 and PfRab1b between early trophozoite and early schizont stages. PfRab5b^{Q94L}-YFP-DD showed good colocalization with PfArf1-RFP (average Pearson's correlation coefficient: $R = 0.51 \pm 0.088$. n = 10 parasites). PfRab1b-RFP showed mild colocalization with PfRab5b^{Q94L}-YFP-DD, as analyzed by YFP and RFP signals (average Pearson's correlation coefficient: $R = 0.34 \pm 0.05$, n = 10 parasites). This result indicated that PfArf1-RFP rather than PfRab1b-RFP closely associated to PfRab5b^{Q94L}-YFP-DD (**Supplementary Figure 4**). The interaction of PfRab5b^{Q94L}-YFP and RFP-PfArf1 was confirmed by reciprocal coimmunoprecipitation of RFP-PfArf1 and PfRab5b^{Q94L}-YFP double-expressing parasites with anti-RFP antibody (**Figure 1C**). The immunoprecipitated PfRab5b^{Q94L}-YFP was recognized as 62 kDa band using mouse anti-GFP antibody together with RFP-PfArf1 visualized with mouse anti-RFP antibody, while the negative control marker cytosolic protein Hsp90 was not detected in the sample. The interaction between PfRab5b^{Q94L}-YFP and PfRab1b-RFP was not confirmed in this reciprocal coimmunoprecipitation (data not shown).

PfArf1 and PfRab1b Were Localized in Different Subdomains of the ER and the *cis*-Golgi

In an analysis conducted previously, we have shown that PfRab5b was localized adjacent to the ER (Ebine et al., 2016), which was labeled with the ER luminal chaperone PfBiP (Kumar et al., 1991; Kumar and Zheng, 1992). To examine the subcellular localization of PfArf1 and PfRab1b, which were colocalized with PfRab5b (**Figure 1B**), PfArf1-RFP, or RFP-PfRab1b expressing parasites (**Supplementary Figure 1C**) were stained with the anti-PfBiP antibody. Punctate structure signals for PfArf1-RFP and RFP-PfRab1b were closely localized with the PfBiP signals (**Figure 2A**). More than 70% of PfArf1-RFP expressing parasites showed colocalization of the PfArf1-RFP and PfBiP signals (71 ± 11%). This proportion is higher than that of RFP-PfRab1b and PfBiP in RFP-PfRab1b expressing parasites (46 ± 7%, $p < 0.05$) (**Figure 2B**). This result was unexpected because the Arf1 and Rab1 GTPases were previously reported to be localized and targeted to the *cis*-Golgi in most other organisms (Stearns et al., 1990; Moyer et al., 2001). Next, PfArf1-RFP and RFP-PfRab1b expressing parasites were stained with an anti-PfERD2 antibody, which stained the *Plasmodium* homolog of the *cis*-Golgi membrane protein ERD2 (Lewis and Pelham, 1990; Elmendorf and Haldar, 1993). Most of the PfArf1-RFP expressing parasites did not show colocalization of the PfArf1-RFP and PfERD2 signals (32 ± 9%) (**Figures 2C, D**). The ratio of PfRab1b colocalization with PfERD2 was increased to 59 ± 3% in PfRab1b-RFP expressing parasites ($p < 0.05$) (**Figures 2C, D**). These results indicate that both PfArf1 and PfRab1b simultaneously localize to the ER and *cis*-Golgi in this organism; however, the subcellular localization of fraction differed between PfArf1 and PfRab1b, as most of the PfArf1 was localized to the proximal region of the ER, and half of PfRab1b was individually localized to the ER and the *cis*-Golgi.

Detailed analysis using super-resolution microscopy enabled the identification of the distinct subcellular localization of PfArf1 and PfRab1b on the ER, and whether both GTPases localize to the same subdomain or reside in distinct regions. The immunostained slides were processed with a super-resolution microscope LSM880 with Airyscan and processed with Zeiss Zen2 software, which provides a lateral resolution of 140 nm, to analyze the precise cellular locations of the proteins. Peak signal intensities of the most proximal staining between PfBiP and PfArf1-RFP (**Figure 3A**) or PfRab1b (**Figure 3B**) were calculated. The average distance from PfBiP was closer to

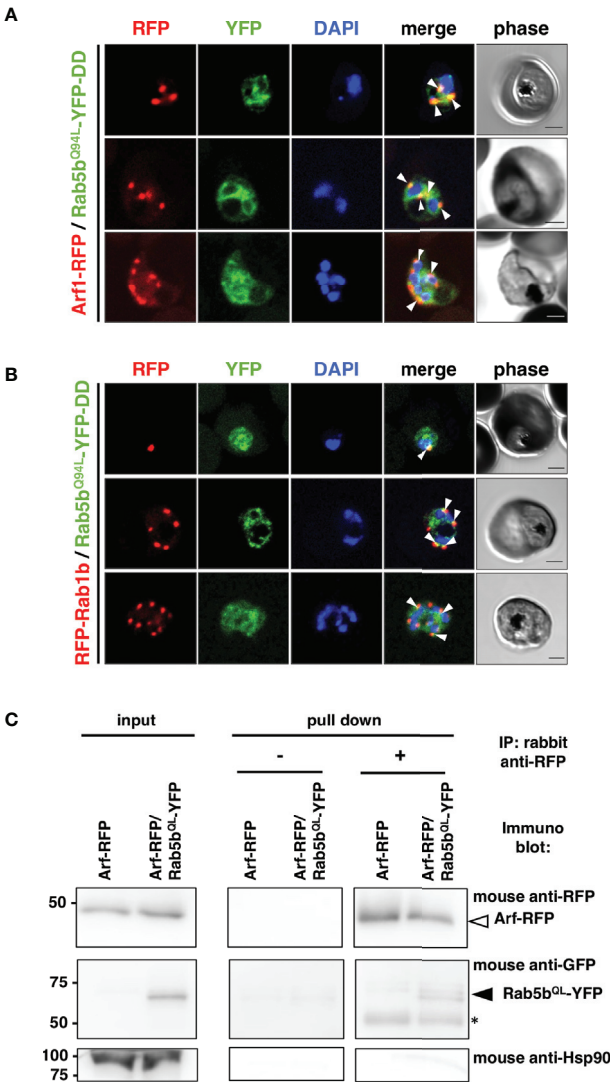

FIGURE 1 | Association of PfRab5b and PfArf1 GTPases rather than PfRab1b in adjacent to the nucleus. Transformant parasites carrying the PfArf1-RFP (**A**, red) or PfRab1b-RFP (**B**, red) constructs with PfRab5b^{Q94L}-YFP-DD (green) under the dual Pfef1α promoter were stabilized with Shld1, and were then used in the immunofluorescence assay. The fluorescence of RFP and YFP was captured. Arrowheads indicate the colocalization of PfArf1 and PfRab1b with PfRab5b^{Q94L}. The nuclei were stained with DAPI (blue). Representative images showing mononuclear early trophozoite (upper), two nuclear late trophozoite (middle), and multinucleated early schizont (lower) stages are shown. White arrowheads indicate the colocalization of PfRab5b^{Q94L}-YFP-DD and PfArf1-RFP or PfRab1b-RFP. The bars indicate 2 μm. **(C)** Reciprocal immuoprecipitation experiments of PfArf1-RFP *via* interaction with PfRab5b^{Q94L}-YFP-DD. PfRab5b^{Q94L}-YFP-DD and PfArf1-RFP double-expressing parasites were crosslinked with DSP as described in *Materials and Methods*, and immunoprecipitated with rabbit anti-RFP antibody (IP: +). Immunoprecipitated PfArf-RFP (a white arrowhead) and PfRab5b^{Q94L}-YFP-DD (a black arrowhead) was visualized with mouse anti-RFP or anti-GFP antibodies, respectively. In the absence of rabbit anti-RFP antibody during immnoprecipitation (IP: –), neither PfArf-RFP nor PfRab5b^{Q94L}-YFP-DD was detected. Anti-Hsp90 antibody was used as a negative control. Two 50 kDa bands in pull down fraction (an asterisk) were non specific recognition of secondary antibody against anti-rabbit IgG.

PfArf1-RFP than to RFP-PfRab1 (PfArf1-RFP: 0.33 ± 0.08 μm *vs.* RFP-PfRab1 0.45 ± 0.11 μm, $p < 0.001$) (**Figure 3C**). These data indicate the presence of compartmentalization in the ER or ER adjacent novel membrane structures, and PfArf1 showed significant localization close to the PfBiP-positive ER rather than PfRab1b.

PfArf1 and PfRab1b Are Involved in the Transport of the PEXEL-Positive Transmembrane Protein Rifin

Blood stage parasites export several proteins into the host erythrocyte cytosol and the PV (Sargeant et al., 2006; van Ooij et al., 2008). The PEXEL sequence is a five-residue motif in the

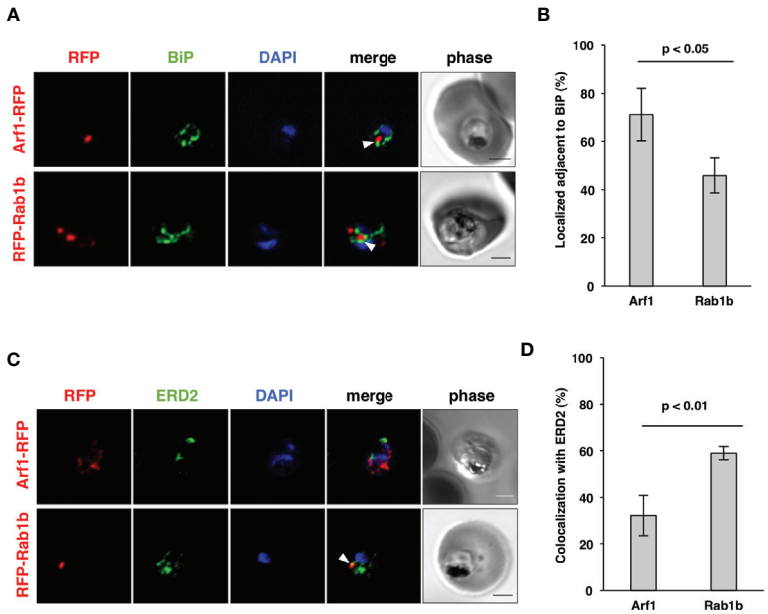

FIGURE 2 | Localization of PfArf1 and PfRab1b in juxtaposition to the ER and the *cis*-Golgi. **(A)** Synchronized parasites, expressing PfArf1-RFP (upper, red) or RFP-PfRab1b (lower, red), were fixed at early trophozoite stage and subjected to the indirect immunofluorescence analysis with anti-PfBiP antibody (green) and DAPI (blue). The fluorescence of PfArf1-RFP and RFP-PfRab1b is shown. PfBiP was stained with an anti-PfBiP antibody. Both PfArf1-RFP and RFP-PfRab1b localized adjacent to the PfBiP signal (arrowheads). **(B)** Rate of colocalization of PfArf1-RFP and RFP-PfRab1b with PfBiP. The number of parasites that showed colocalization of the RFP and PfBiP signals was counted in 20–30 trophozoites from three independent experiments. Error bars indicate the standard deviations of three replicates. A test for statistical significance was performed using the Student *t*-test. **(C)** Indirect immunofluorescence analysis of the localization of PfArf1-RFP (upper, red), RFP-PfRab1b (lower, red), the *cis*-Golgi-marker PfERD2 (green), and DAPI (blue). The fluorescence from RFP-PfRab1b colocalized with the PfERD2 signal (arrowhead), but not with PfArf1-RFP. The bars indicate 2 μm. **(D)** Rate of colocalization of PfArf1-RFP and RFP-PfRab1b with PfERD2. The number of parasites that showed colocalization of the RFP and PfERD2 signals was counted in 20–30 trophozoites from three independent experiments. A test for statistical significance was performed using the Student *t*-test.

downstream N-terminal signal peptide, and it has been detected in many exported proteins (Hiller et al., 2004; Marti et al., 2004). PEXEL-positive proteins have been suggested to pass through the classical ER/Golgi pathway (Akompong et al., 2002). However, the presence of several PNEPs indicates the existence of an alternative export pathway (Möskes et al., 2004; Thavayogarajah et al., 2015). We have previously shown that overexpression of PfRab5b did not disrupt the export of the PEXEL-positive transmembrane protein EVP1 to the iRBC cytosol (Ebine et al., 2016). To examine whether PfArf1 and PfRab1b are involved in trafficking of PEXEL-positive export proteins, we chose a Rifin variant PFA0745w, whose fusion construct with YFP was secreted into the erythrocyte cytosol (Marti et al., 2004). The N-terminal PEXEL domain and the C-terminal transmembrane region were fused with RFP (Rifin-RFP) and co-expressed with the PfArf1 and PfRab1b mutant constructs, whose expression was driven by the Shld1 ligand (**Supplementary Figure 1D**). In parasites expressing the PfArf1^{WT}-YFP-DD and active mutant PfArf1^{Q71L}-YFP-DD constructs, Rifin-RFP signals were detected in the iRBC plasma membrane and at the parasite periphery (PfArf1^{WT}: 91 ± 4%, PfArf1^{Q71L}: 88 ± 6%) (**Figures 4A, B**). In contrast, the export of Rifin-RFP was reduced in the inactive PfArf1^{T31N}-YFP-DD expressing parasites (53 ± 12%) (**Figures 4A, B**), suggesting that PfArf1 is involved in PEXEL-positive Rifin transport. Similarly, the expression of wild-type DD-YFP-PfRab1b and the active mutant DD-YFP-PfRab1b^{Q67L} did not show differences for the export of Rifin-RFP (PfRab1b^{WT}: 89 ± 2%, PfRab1b^{Q67L}: 90 ± 10%), whereas the expression of the inactive mutant DD-YFP-PfRab1b^{S22N} reduced the export activity (39 ± 9%) (**Figures 4C, D**).

PfArf1, But Not PfRab1b, Regulates the Export of N-Acylated Adenylate Kinase 2 to the PVM

Adenylate kinase 2 (PfAK2) is an N-terminal myristoylated and palmitoylated protein, which lacks the signal peptide and a transmembrane domain. It localizes to the parasite plasma membrane face to the PV (Thavayogarajah et al., 2015; Ebine et al., 2016), suggesting that PfAK2 was not transported through the classical ER/Golgi-dependent pathway. We have previously reported that overexpression of PfRab5b-YFP-DD disrupted the transport of PfAK2-RFP to the PVM (Ebine et al., 2016). Overexpression of PfRab5b-YFP-DD altered the peripheral staining of PfAK2-RFP in the parasite cytoplasmic staining pattern, indicating that PfRab5b might be involved in the

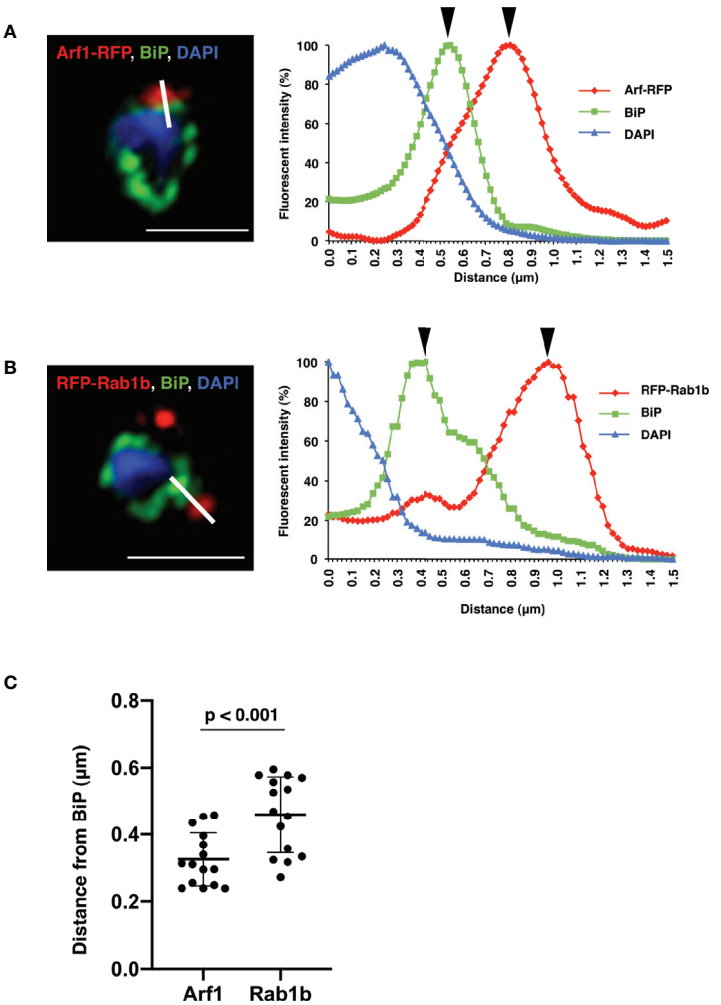

FIGURE 3 | Super-resolution imaging showing the fine differences between PfBiP and PfArf1 or PfRab1b. Synchronized parasites, expressing PfArf1-RFP **(A,** red**)** or RFP-PfRab1 **(B**, red**)**, were sampled at early trophozoite stage and fixed and subjected indirect immunofluorescence analysis with the anti-PfBiP antibody (green) and DAPI (blue). Fluorescence intensities along the bold white lines are indicated in the graphs on the right. The fluorescence intensity was calculated as the percentage of the highest signal intensities. Black arrowheads depict the peaks of RFP and PfBiP intensities. The bars indicate 2 μm. **(C)** The smallest calculated distances between **(A, B)** in 15 independent parasites were plotted, and the average (bold bars) and standard deviation (thin bars) are indicated. A test for statistical significance was evaluated using the Student's *t*-test.

transport of PfAK2 (Ebine et al., 2016). Therefore, we examined whether the overexpression of PfArf1 perturbs the transport of PfAK2-RFP to the PVM. Parasites that double-expressed PfAK2-RFP and PfArf1^{WT}, or the constitutively active PfArf1^{Q71L} or inactive PfArf1^{T31N} mutants (**Figure 1A**), whose expression is driven by the Shld1 ligand were established (**Supplementary Figure 1D**). The PfArf1^{Q71L} and PfArf1^{T31N} mutants are corresponding to human Arf1^{Q71L} and Arf1^{T31N}, respectively (Dascher and Balch, 1994: Teal et al., 1994). Expression of PfArf1^{Q71L} or PfArf1^{T31N} mutants for 48 h did not show growth defect (**Supplementary Figure 5**). In the PfArf1^{WT}-YFP-DD expressing parasite, all PfAK2-RFP signals were localized at the parasite periphery, indicating a typical PVM staining pattern (**Figure 5A**). In contrast, the active mutant PfArf1^{Q71L}-YFP-DD expressing parasites reduced PfAK2-RFP targeting to the PVM (38 ± 6.7%). Several parasites showed a faint RFP signal and a punctate RFP signal within the parasite cytoplasm (faint: 35 ± 7.1%, punctate: 27 ± 7.7%, respectively) (**Figures 5A, B**). In the inactive PfArf1^{T31N}-YFP-DD expressing parasite, the transport of PfAK2-RFP was reduced to 58 ± 6.8%, and further, 13 ± 7.2% and 29 ± 11% of the parasites showed a faint RFP signal and a punctate pattern in the cytoplasm, respectively (**Figures 5A, B**). The faint signal of PfAK2-RFP was more abundant in PfArf1^{Q71L}-YFP-DD than in PfArf1^{T31N}-YFP-DD ($p < 0.05$). These results indicate that PfArf1 is directly involved in the trafficking of PfAK2 to the PVM. The specific role of PfArf1 in the transport of PfAK2 was highlighted by the co-expression of PfRab1b mutants (**Figure 5C**). In the co-

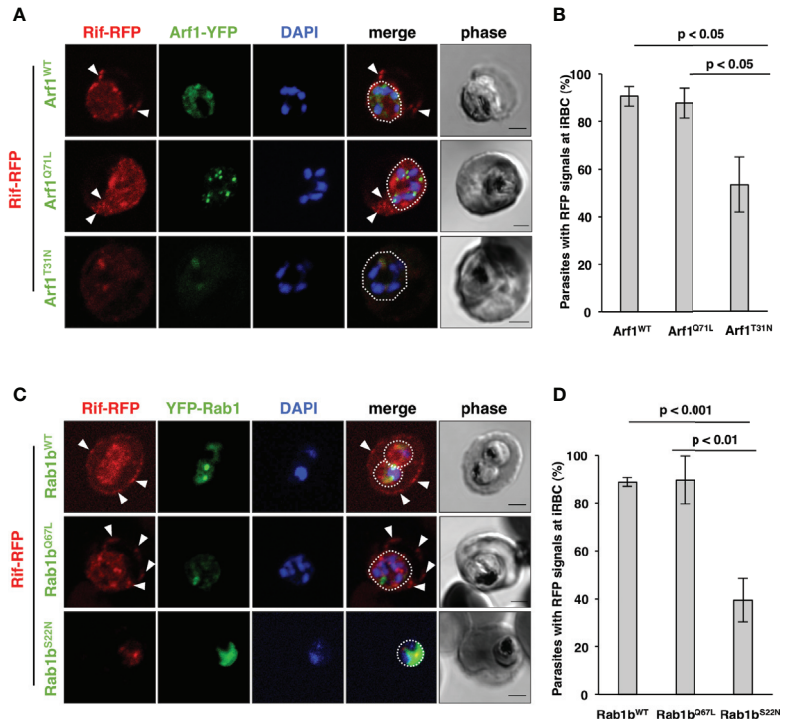

FIGURE 4 | PfArf1 and PfRab1b regulated the export of PEXEL-positive Rifin to the erythrocyte cytoplasm. Parasites expressing Rifin-RFP and PfArf1-YFP-DD **(A, B)** or DD-YFP-PfRab1b **(C, D)** were examined *via* the immunofluorescence assay. Fluorescence signals from RFP (red), YFP (green), and DAPI (blue) are shown. Wild-type PfArf1 or PfRab1b (upper panels), active mutant PfArf1^{Q71L} or PfRab1b^{Q67L} (middle panels), and the inactive mutant PfArf1^{T31N} or PfRab1b^{S22N} (lower panels) are shown. White dotted lines indicate the parasite plasma membrane. The arrowheads indicate dot-like exported Rifin-RFP signals. The bars indicate 2 μm. The rate of parasites that showed a Rifin-RFP signal was detected in the erythrocyte cytoplasm in PfArf1-RFP **(B)** and RFP-PfRab1b **(D)** expressing cells are shown in graphs. Thirty individual early trophozoites and early schizonts were counted from three independent experiments. Infected RBCs, recognized by the DAPI and YFP signals under the microscope, were imaged by the laser microcopy, and then analyzed for the localization of RFP and whether Rifin-RFP was exported to the iRBC. The statistical significance was determined using the Student's *t*-test.

expression with the wild-type DD-YFP-PfRab1b, active DD-YFP-PfRab1b^{Q67L}, or the inactive DD-YFP-PfRab1b^{S22N} constructs, which corresponds human Rab1b^{Q67L} and Rab1b^{S22N}, respectively (Tisdale et al., 1992), the transport of PfAK2-RFP was not inhibited and all parasites showed a peripheral pattern for their expression (PfRab1b^{WT}: 99 ± 2%, PfRab1b^{Q67L}: 96 ± 4%, PfRab1b^{S22N}: 94 ± 3%) (**Figures 5C, D**). Expression of Rab1b^{Q67L} and Rab1b^{S22N} mutants for 48 h did not show growth defect (**Supplementary Figure 5**). These results suggest that PfArf1 is extensively involved in the transport of the N-acylated protein PfAK2 to the PVM.

DISCUSSION

Isolation of PfArf1 and PfRab1b as PfRab5b Associated Proteins

In this study, we demonstrated the isolation of PfRab5b proteins using a coimmunoprecipitation approach. We identified two GTPases, PfRab1b and the human Arf1 homolog PfArf1, that colocalized with PfRab5b and were associated with the ER marker PfBiP in erythrocytic stage parasites. Further, we demonstrated that PfArf1 and PfRab1b are closely located near the ER, but the precise localization differed as shown by super-resolution microscopy, suggesting that the ER-Golgi interface in *Plasmodium* is highly compartmentalized. Additionally, we provide direct cell biological evidence that PfArf1 and PfRab1b are involved in different types of cargo selection. PfArf1 regulates the transport of N-acylated PfAK2 to the PVM, whereas PfRab1b controls the trafficking of the PEXEL-positive exported protein Rifin in the erythrocyte cytosol. Thus, PfRab5b and its associated GTPases are involved in the sorting of several families of exported proteins in the different ER subdomains.

Rab GTPase recycles GTP-bound active and GDP-bound inactive forms (Hutagalung and Novick, 2011). To immunoprecipitate efficiently, we used DSP cross-linker, whose spacer arm length 12.0 Å, before the coimmunoprecipitation to fix the PfRab5b-nucleotide bound state. Such approach, the use of cross-linker before coimmunoprecipitation, identifies many (> 100) proteins in LC-ToF MS/MS (Watanabe et al., 2020). Our approach also identified 677 proteins and PfArf1 was listed as highly enriched proteins among 677 proteins (**Supplementary**

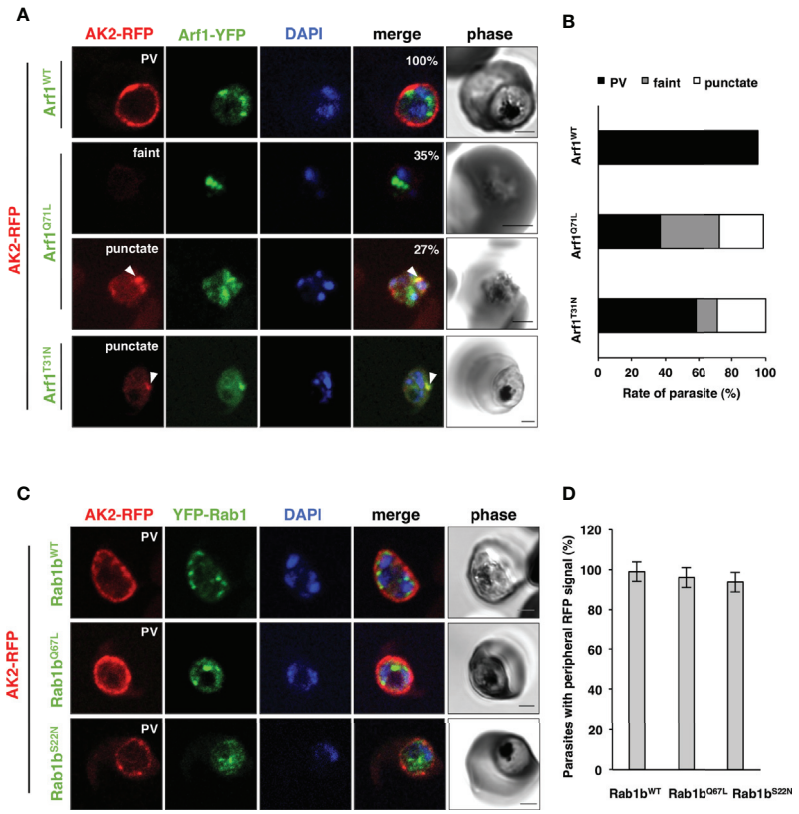

FIGURE 5 | The specific role of PfArf1 in the transport of N-acylated PfAK2 to the PVM. Parasites expressing PfAK2-RFP and PfArf1-YFP-DD **(A, B)** or DD-YFP-PfRab1b **(C, D)** were examined using the immunofluorescence assay. Fluorescence signals from RFP (red), YFP (green), and DAPI (blue) are shown. Wild-type PfArf1 or PfRab1b (upper panels), the active mutant PfArf1^{Q71L} or PfRab1b^{Q67L} (middle panels), and the inactive mutant PfArf1^{T31N} or PfRab1b^{S22N} (lower panels) are shown. Representative images for PfAK2-RFP are shown and are divided into three patterns: peripheral PVM staining (PVM), faint signal (faint), and dot-like punctate signal within the parasites (punctate). The bars indicate 2 μm. The parasites that showed a signal for PfAK2-RFP were classified into three patterns based on the PfArf1-RFP expressing cells **(B)** and then shown in bar graph. The rate of parasites showing peripheral staining for PfAK2-RFP in RFP-PfRab1b expressing cells **(D)**. Thirty individual early trophozoites and early schizonts were counted from three independent experiments. Infected RBCs, recognized by the DAPI and YFP signals under the microscope, were imaged by the laser microcopy, and then analyzed for the localization of RFP signal as PV, faint, and punctate. The statistical significance was determined using the Student's *t*-test.

Table 2). Contrary, a casein kinase CK1, which is identified as PfRab5b binding protein by bioinformatic technique (Rached et al., 2012), was not enriched in our approach (Accession Number, C6S3F7-1, **Supplementary Table 2**). Colocalization of PfRab5b and CK1 at parasite periphery was reported in schizont stage (Ezougou et al., 2014). These observations suggested that PfRab5b and CK1 may localized to different membrane subdomain on PVM in schizont stage. Further biological and biochemical studies are needed to prove direct and indirect interaction between PfRab5b and effector proteins.

PfArf1 Exports the N-Myristoylated Protein PfAK2 to the PVM

The regulatory mechanisms underlying the trafficking of acylated proteins are not clearly understood in *Plasmodium* and other organisms. Dual acylated proteins are first myristoylated at the ER membrane by N-myristoyl transferase after palmitoylation by a palmitoyltransferase, and the acylated proteins are then trafficked to the apical organelle and parasite plasma membrane surface (Cabrera et al., 2012). For other proteins, such as the *Plasmodium falciparum* calcium-dependent protein kinase 1 (PfCDPK1) and the *Drosophila* transgultaminase A (TG-A), the dual acylated proteins are packed into multivesicular bodies and are subsequently exported to the apical organelle or extracellular space *via* the unconventional ER-Golgi-independent pathway (Möskes et al., 2004; Shibata et al., 2017). We have previously shown that the transport of N-myristoyl PfAK2 to the PVM was inhibited by the overexpression of PfRab5b, and that PfAK2 accumulated in the punctate structure within the parasite cytoplasm together with PfRab5b, indicating that PfRab5b and PfAK2 were included in the internal vesicle of the multivesicular body and were then transported to the PVM (Ebine et al., 2016). In this study, we have shown that PfArf1, but not PfRab1b, is involved in the regulation of PfAK2 (**Figures 4** and **5**). Our results indicated that the expression of active or inactive PfArf1 mutants inhibited

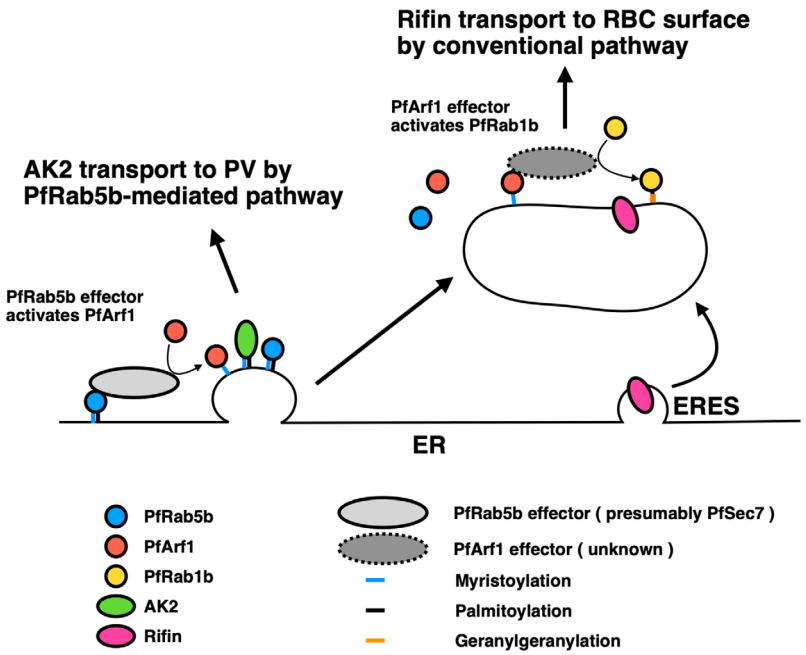

FIGURE 6 | A proposed model for the two pathways regulated by PfArf1 and PfRab1b. PfRab5b (blue circle) recruited PfArf1 (red circle) probably through the binding to PfArf1 activating protein (light grey ellipse) on the ER membrane (**Figure 1**). Membrane targeted PfArf1 selected the N-acylated AK2 and sorted into the pathway for the PV (**Figure 5**). According to the partial involvement of PfArf1-positive membrane for the selection of PEXEL-positive Rifin (**Figure 4**), and PfRab1b (yellow circle) localized to distant membrane from the ER (**Figure 3**), PfArf1-positive membrane might be matured into PfRab1b-positive compartment. PfRab1b-positive compartment selected and further transport the PEXEL-positive Rifin to the RBC surface. ER, endoplasmic reticulum; ERES, endoplasmic reticulum exit site; PV, parasitophorous vacuole; RBC, red blood cell.

PfAK2 transport to PVM (**Figure 5A**), whereas the expression of active or inactive PfRab1b mutants had no effect (**Figure 5C**). These results suggest that GTP hydrolysis by PfArf1 is required for proper PfAK2 recognition and further transport. For mammalian Arf1, it has been biochemically demonstrated that GTP hydrolysis by human Arf1 promotes the selective cargo selection from the Golgi membrane, and the concentration of cargo proteins into the COPI-coated vesicles (Lanoix et al., 1999). This observation indicated that the role of GTP hydrolysis in cargo selection is similar between PfArf1 and the human Arf1.

Presence of Subdomains Near the ER and the Sequential Roles of PfArf1 and PfRab1b in Cargo Selection

Both PfArf1 and PfRab1b are localized close to the ER as punctate structures in the early erythrocytic stage (**Figure 1B**). The punctate structure near the ER was observed in other proteins, such as the COPII coat components PfSec13 and PfSec24 (Lee et al., 2008; Struck et al., 2008) and in another PfRab1 isotype PfRab1a (Morse et al., 2016). Previously, we have shown that PfRab5b did not colocalize with the COPII component PfSec13 (Struck et al., 2008; Ebine et al., 2016), suggesting that PfArf1 and PfRab1b might be localized in different domains from the COPII vesicle budding site, the ERES. In this study, the results indicate that the PfArf1 signal was not completely consistent with that for PfRab1b and was localized to different membrane subdomains around the ER (**Figure 3**). These findings suggest that the previously reported COPII component, PfArf1, and PfRab1b might be localized to an independent subdomain and may have different roles in the transport of cargo proteins and cargo selection from the ER. PfRab1b was involved in the transport of the PEXEL-positive export protein, Rifin, and the expression of the inactive PfRab1b mutant showed decreased activity of Rifin export to erythrocyte cytosol (**Figures 4C, D**). In contrast, the expression of the active PfRab1b mutant did not inhibit Rifin export, indicating that the GTP-bound state of PfRab1b may be necessary for the proper functioning of PfRab1b. A similar observation was reported in mammalian Rab5 during endosome fusion, where it was demonstrated that the GTP-bound mutant form showed the same effect as the wild-type Rab (Barbieri et al., 1996).

Interestingly, the export of Rifin was also decreased by the expression of inactive mutants of PfArf1, but not the active GTP-fixed mutant and the wild-type PfArf1, which cycles GTP- and GDP-bound states (**Figures 4A, B**). This result suggests that the GTP-bound state of PfArf1, but not GDP-fixed mutant, is necessary for the export of Rifin, or for the correct activity of PfRab1b. Although not included in this study, it is notable that a Sec7 domain containing protein was listed as a candidate for the

PfRab5b binding protein using mass analysis (**Table 1**). The 200 amino acid residue Sec7 domain is conserved among eukaryote and has the guanine nucleotide exchange activity toward Arf (Arf GEF) (Cherifils et al., 1998). Sec7 binds GDP-bound wild-type Arf GTPase and promotes the exchange of GDP for GTP. In other organisms, Sec7 is involved in the "Rab cascade": activated GTPase triggers the recruitment of GEF for the downstream GTPase, and thus a series of GTPase activations is feasible (Barr, 2013). For example, in *Saccharomyces cerevisiae*, Ypt1 (in yeast Rab1) and the Arf-like GTPase Arl1 recruit Sec7 to the Golgi membrane, and subsequently Arf1 is activated by the GEF activity of membrane-localized Sec7, following the stimulation of Ypt31 (yeast Rab11) on the trans-Golgi membrane for cargo sorting to secretory vesicles (McDonold and Fromme, 2014). Thus, we generated a sequential hypothetical model of PfArf1 and PfRab1b adjacent to the ER that is presented in **Figure 6**. Membrane-localized PfRab5b may recruit PfSec7 to exchange GDP for GTP of PfArf1 in the adjacent ER subdomain, where the N-myristoylated protein PfAK2 is selected and packed into the pathway destined for the PVM. This is based on the finding that colocalization of the active mutant of PfRab5b and PfArf1 (**Figure 1**), and wild-type PfArf1 is necessary for the transport of PfAK2 (**Figure 5A**). It has been shown that *Plasmodium* PfArf1 possesses GTPase activity *in vitro* (Stafford et al., 1996) and that PfSec7 accelerated the nucleotide exchange activity against PfArf1 (Baumgartner et al., 2001). Thus, the PfArf1 may colocalize with PfSec7 adjacent to the ER. The role of PfSec7 in intracellular traffic remains elusive, and further studies are needed to unravel the regulation of PfAK2 transport together with PfArf1. Subsequently, the PfArf1 positive membrane matures and recruits PfRab1b at the membrane. This model is based on our results that indicate that PfRab1b localizes to the different subdomains of PfArf1 that are adjacent to the ER (**Figures 1B** and **3**), and that the sequential recruitment of different GTPases to the membrane occurs *via* Sec7 (McDonold and Fromme, 2014). In this hypothesis, PfSec7 could not recruit on the membrane in GDP-fixed PfArf1 mutant and may showed the defect in the function of downstream PfRab1b, suggesting expression of inactive mutant of PfArf1 showed the reduction of the export of Rifin (**Figures 4A, B**). The Rab1 positive membrane subdomain near the ER is found in mammalian tubulovesicular membrane clusters of the ER-Golgi intermediate compartment (ERGIC) (Appenzeller-Herzog and Hauri, 2006). ERGIC clusters lie close to the COPII-positive ERES. Transport from the ER to the ERGIC is controlled by COPII coat vesicles, and Rab1 is involved in membrane tethering at the ERGIC in anterograde transport (Allan et al., 2000). Sorting in the ERGIC involves another protein coat of COPI and the Arf family (Goldberg, 2000). Thus, ERGIC is a sorting and recycling platform for the transport between the ER and Golgi in mammalian cells. In *Plasmodium*, the PfRab1b-positive compartment was involved in the export of the PEXEL-positive protein Rifin (**Figure 4**) and this suggests the existence of a novel sorting compartment for PEXEL-positive cargo proteins. The model shown in **Figure 6** indicates the segregation of the subdomain for sorting of different cargo proteins. Conversely, the expression of active and inactive PfRab1b mutants did not affect the export of PfAK2 (**Figure 5**).

Transport to the Golgi and the Presence of a Few Parts of PfArf1 on the PfERD2-Positive Golgi Membrane

In most mammalian secretory cells, electron microscopy has revealed the presence of ribosome-coated rough ER and partly smooth surfaced structures in the vicinity of the Golgi complex (Saraste and Kuismanen, 1992). Golgi is displayed as stacks of flattened cisternae, which are often laterally linked into a ribbon-like structure (Zhang and Wang, 2016). In contrast, the ER and Golgi of malarial parasites are not well characterized and are reported to be loosely associated vesicles (Aikawa, 1971). To overcome the difficulty in the visualization of ER and the Golgi, we used super-resolution fluorescence microscopy (**Figure 3**) and quantified the number of colocalized parasites (**Figures 2–5**). In this study, about 70% of parasites showed colocalization of PfArf1 and the ER marker PfBiP, and 30% showed colocalization with the *cis*-Golgi marker PfERD2 (**Figure 2**). These results may explain the following two possibilities. One; PfArf1 is a Golgi resident which is involved in retrograde trafficking from the Golgi. This model is based on reports from mammalian and yeast models, where Arf1 is involved in different steps of cargo sorting together with specific effector or Sec7 containing proteins such as retrograde traffic from the *cis*-Golgi to the ER, or the secretory pathway from the *trans*-Golgi (Donaldson and Jackson, 2011). As it is not yet characterized, the Golgi resident PfArf1 may be involved in retrograde trafficking to the ER because the homolog of ERD2 is present and localized to the Golgi in *Plasmodium* (Elmendorf and Haldar, 1993). ERD2 retrieves the conserved C-terminal tetrapeptide sequence HDEL-containing ER luminal proteins from the *cis*-Golgi in yeast and mammalian cells (Hsu et al., 1992; Townsley et al., 1994). A second possibility is the presence of the Golgi subdomain in *Plasmodium*. The *Plasmodium* ERD2 was previously reported to colocalize with the Golgi re-assembly stacking protein (GRASP) (Struck et al., 2005), and PfArf1 was shown to be colocalized with GRASP in the early trophozoite stage (Thavayogarajah et al., 2015). Therefore, it appears that PfArf1, GRASP, and PfERD2 are colocalized in the same Golgi membrane. However, mammalian GRASP55 is present in the *medial*/*trans*-cisternae of Golgi stacks as shown by cryo-immunoelectron microscopy (Langreth et al., 1978). Thus, this may be the reason for the Golgi-stacked protein GRASP and HDEL-receptor ERD2 to colocalize in the same Golgi subdomain in *Plasmodium*.

CONCLUSION AND FUTURE PERSPECTIVES

In conclusion, our results show that PfArf1 mediates the transport of N-myristoylated PfAK2 from the adjacent ER, and PfRab1b, which localizes differently than PfArf1, is involved in the export of PEXEL-positive Rifin to the erythrocyte cytosol. Currently, the mechanism how PfArf1 recognize cargo protein at the ER

subdomain and sort to the pathway for the PVM, remains elusive. In other cases, there are very few reports on trafficking of dual acylated protein *via* a multivesicular body (Möskes et al., 2004; Shibata et al., 2017). In mammalian cells, myristoylated and palmitoylated GFP localized to the membrane subdomain enriched with cholesterol and ganglioside at the plasma membrane (McCabe and Berthiaume, 2001). It may plausible that PfArf1 together with PfRab5b and unidentified effector proteins organize the acylated cargo-recognition subdomain at the ER lipid subdomain. Consideration of the two facts that PfRab5b is essential for the growth (Ezougou et al., 2014; Ebine et al., 2016) and N-myristoyl transferase is a promising drug target for malaria (Schlott et al., 2018), suggests that elucidation of further molecular mechanism on PfArf1 and its regulatory proteins may help the plasmodium biology as well as pathogenesis.

DATA AVAILABILITY STATEMENT

The data sets presented in this study can be found in online repositories. The names of the repository/repositories and accession number(s) can be found in the article/**Supplementary Material**.

AUTHOR CONTRIBUTIONS

IT, TH, and YS-N conceived the study. IT, TH, TM, NS, SI, and YS-N designed and performed experiments and data analysis. IT, TM, TA, and YS-N drafted the paper. TA, KN, and TN participated in data analysis and edited the paper. YS-N acquired grants. All authors contributed to the article and approved the submitted version.

FUNDING

This research was funded by Grants-in-Aid for Scientific Research (C) (JP19K07531 to YS-N) from the Ministry of Education, Culture, Sports, Science and Technology (MEXT), and a grant from The Naito Foundation to YS-N.

ACKNOWLEDGMENTS

We thank Kiyoshi Kita (Nagasaki University) for providing the anti-PfBiP antibody, Osamu Kaneko (Nagasaki University) for the pCHD43(II) episomal plasmid, Daniel E Goldberg (Washington University School of Medicine) for the YFP-FKBP episomal plasmid, and Shusuke Nakazawa (Nagasaki University) for the *P. falciparum* MS822 line. The *P. falciparum* 3D7 line was obtained from MR4 (contributed by D. J. Carucci, MRA-102). We thank the Japanese Red Cross Society for providing human RBCs and plasma, and Jacobus Pharmaceuticals for WR99210. We thank all members of the Department of Parasitology, NIID, for various discussions related to the study.

SUPPLEMENTARY MATERIAL

The Supplementary Material for this article can be found online at: https://www.frontiersin.org/articles/10.3389/fcimb.2020.610200/full#supplementary-material

Supplementary Table 1 | List of oligonucleotide sequences used for plasmid construction.

Supplementary Table 2 | List of proteins detected from immunoprecipitated samples prepared from PfRab5b-YFP-FLAG and PfRab5b-YFP expressing parasites using anti-FLAG antibody. The most enriched proteins were shown in red and listed in **Table 1**.

Supplementary Figure 1 | Schematic structure of the constructs used in this study. **(A)** Episomal vector pCHD43(II) (Sakura et al., 2013; Ebine et al., 2016) was modulated to express a fusion fragment of PfRab5b-YFP-FLAG or (upper) or PfRab5b- YFP (lower). **(B)** The artificial centromere plasmid PfCenV-ef1-double was inserted two fragments in NcoI and NdeI sites, whose expression is regulated under the *Plasmodium berghei* elongation factor 1 (Pbef1α). In NcoI site, PfRab5b-YFP-DD was inserted and RFP-PfArf1 (upper) or PfRab1b-RFP (lower) was inserted in the NdeI site. **(C)** RFP-PfArf1 (upper) or PfRab1b-RFP (lower) was inserted in the NdeI site of the centromere plasmid for the single expression. **(D)** To double express GTPase (PfArf1 and PfRab1b) and cargo proteins (PfAK2 and Rifin), PfArf1-YFP-DD (upper, left) or DD-YFP-PfRab1b (lower, left) fragment was inserted into episomal plasmid pCHD43(II), whose hDHFR cassette was replaced with a blasticidin S-resistance cassette (Ebine et al., 2016). Cargo proteins, PfAK2-RFP (upper, right) or Rifin-RFP (lower, right) fusion constructs, were inserted into PfCenV-ef1-double of NdeI site. Each GTPase and cargo protein construct was transfected into the parasite, and simultaneously selected with WR99210 and blasticidin S. proCRT, the constitutive *P. falciparum* chloroquine resistance transporter promoter: PbDT, *Plasmodium berghei* dihydrofolate reductase terminator proPfCAM, *P. falciparum* calmodulin promoter, hDHFR, human dihydrofolate reductase: PfHRPII, *P. falciparum* histidine-rich protein II termiator: rep20, element to improve episomal segregation at mitosis: PfCenV, the centromere of chromosome 5: BSD, blasticidin S.

Supplementary Figure 2 | Pf3D7_1020900 is a mammalian homolog of Arf1. **(A)** Amino acid percentage identity matrix of the six *Plasmodium* Sar/Arf familiy of GTPases and human Arf1 and Sar1. *Plasmodium* protein sequences for the Sar/Arf family of GTPases were retrieved from the PlasmoDB genome database (release 46, Nov 2019) using the Pathema Bioinformatics Resource Center (https://plasmodb.org/plasmo/) (Collaborative, 2001). *Plasmodium* Sar/Arf homologs were retrieved *via* the BLASTP algorithm using the human Arf1 and Sar1 GTPases as queries in the *P. falciparum* 3D7 database. **(B)** Sequence alignment of *Homo sapiens* Arf1 and Sar1 and six *Plasmodium* Sar1/Arf families of proteins. Amino acid sequences were aligned using Clustal Omega (EMBL-EBI, Welcome Genome Campus). The N-terminus myristoylation site with a glycine residue specific for the Arf family and the GTP-binding consensus boxes are indicated in blue and red boxes, respectively (Pereira-Leal and Seabra, 2000). The effector regions of the Arf/Arf-like (Arl) and Sar1 families are indicated in light blue and magenta, respectively. Note that PF3D7_1442000 and PF3D7_1316200 lack an N-terminal glycine residue. PF3D7_0920500 and PF3D7_1316200 are missing the second GTP-binding box. Two conserved residues, that are substituted to create constitutively active and inactive mutants, are indicated by black and white arrowheads, respectively. **(C)** Amino acid percentage identity matrix of Pf3D7_1020900 and the five human Arf1.

Supplementary Figure 3 | Immunoblots showing the expression of full length of PfArf1-RFP, and RFP-PfRab1b. Parasite lysates expressing PfRab5b^{Q94L}-YFP-DD and Arf1-RFP or RFP-PfRab1b were subjected to immunoblot analysis using anti-RFP and anti-GFP antibodies. Anti-Hsp90 antibody was used as a loading control. Mock is the non-transformant parasite.

Supplementary Figure 4 | Pearson's correlation coefficient between PfRab5b^{Q94L}-YFP-DD and PfArf1-RFP or RFP-PfRab1b. The fluorescence intensities of the merged YFP and RFP signals were analyzed using Fiji-Image J software to generate Pearson correlation coefficients. The scatter plot represents Pearson correlation coefficients values from ten independent parasites, which are

obtained from three independent transfectants. The statistical significance was determined using Student's t-test.

Supplementary Figure 5 | Expressions of PfArf1 or PfRab1b mutants showed no effect on parasites growth. The population doubling time of non-transformant MS822 line, PfArf1 and PfRab1b mutants were measured for 2 days cultivation from three independent assays. The average (bar graph) and the standard deviation (thin bar) are indicated. Mock was cultured without drugs and PfArf1, PfRab1b mutants were cultured with BSD. Except from MS822 line, transformed parasite were cultured in the presence of 2.5 μg/ml of BSD and the expressions of PfArf1 and PfRab1b mutants were stabilized by 0.5 μM Shld1. A statistical significance was evaluated using Student's *t*-test.

REFERENCES

Adisa, A., Albano, F. R., Reeder, J., Foley, M., and Tilley, L. (2001). Evidence for a role for a *Plasmodium falciparum* homologue of Sec31p in the export of proteins to the surface of malaria parasite-infected erythrocytes. *J. Cell Sci.* 114, 3377–3386.

Adisa, A., Frankland, S., Rug, M., Jackson, K., Maier, A. G., Walsh, P., et al. (2007). Re-assessing the locations of components of the classical vesicle-mediated trafficking machinery in transfected *Plasmodium falciparum*. *Int. J. Parasitol.* 37, 1127–1141. doi: 10.1016/j.ijpara.2007.02.009

Agop-Nersesian, C., Naissant, B., Rached, F. B., Rauch, M., Kretzschmar, A., Thiberge, S., et al. (2009). Rab11A-controlled assembly of the inner membrane complex is required for completion of apicomplexan cytokinesis. *PloS Pathog.* 5, 1–15. doi: 10.1371/journal.ppat.1000270

Aikawa, M. (1971). Parasitological review. *Plasmodium*: the fine structure of malarial parasites. *Exp. Parasitol.* 30, 284–320. doi: 10.1016/0014-4894(71)90094-4

Akompong, T., Kadekoppala, M., Harrison, T., Oksman, A., Goldberg, D. E., Fujioka, H., et al. (2002). Trans expression of a *Plasmodium falciparum* histidine-rich protein II (HRPII) reveals sorting of soluble proteins in the periphery of the host erythrocyte and disrupts transport to the malarial food vacuole. *J. Biol. Chem.* 277, 28923–28933. doi: 10.1074/jbc.M201968200

Alexandre, J. S. F., Yahata, K., Kawai, S., Torii, M., and Kaneko, O. (2011). PEXEL-independent trafficking of *Plasmodium falciparum* SURFIN4.2 to the parasite-infected red blood cell and Maurer's clefts. *Parasitol. Int.* 60, 313–320. doi: 10.1016/j.parint.2011.05.003

Allan, B. B., Moyer, B. D., and Balch, W. E. (2000). Rab1 recruitment of p115 into a cis-SNARE complex: Programming budding COPII vesicles for fusion. *Science* 289, 444–448. doi: 10.1126/science.289.5478.444

Appenzeller-Herzog, C., and Hauri, H.-P. (2006). The ER-Golgi intermediate compartment (ERGIC): In search of its identity and function. *J. Cell Sci.* 119, 2173–2183. doi: 10.1242/jcs.03019

Armstrong, C. M., and Goldberg, D. E. (2007). An FKBP destabilization domain modulates protein levels in *Plasmodium falciparum*. *Nat. Methods* 4, 1007–1009. doi: 10.1038/nmeth1132

Balch, W. E., Kahn, R. A., and Schwaninger, R. (1992). ADP-ribosylation factor is required for vesicular trafficking between the endoplasmic reticulum and the cis-Golgi compartment. *J. Biol. Chem.* 267, 13053–13061. doi: 10.1016/S0021-9258(18)42380-0

Barbieri, M. A., Li, G., Mayorga, L. S., and Stahl, P. D. (1996). Characterization of Rab5:Q79L-stimulated endosome fusion. *Arch. Biochem. Biophys.* 326, 64–72. doi: 10.1006/abbi.1996.0047

Barr, F. A. (2013). Rab GTPases and membrane identity: Causal or inconsequential? *J. Cell Biol.* 202, 191–199. doi: 10.1083/jcb.201306010

Baumgartner, F., Wiek, S., Paprotka, K., Zauner, S., and Lingelbach, K. (2001). A point mutation in an unusual Sec7 domain is linked to brefeldin A resistance in a *Plasmodium falciparum* line generated by drug selection. *Mol. Microbiol.* 41, 1151–1158. doi: 10.1046/j.1365-2958.2001.02572.x

Bi, X., Mancias, J. D., and Goldberg, J. (2007). Insights into COPII coat nucleation from the structure of Sec23•Sar1 complexed with the active fragment of Sec31. *Dev. Cell* 13, 635–645. doi: 10.1016/j.devcel.2007.10.006

Boddey, J. A., Hodder, A. N., Günther, S., Gilson, P. R., Patsiouras, H., Kapp, E. A., et al. (2010). An aspartyl protease directs malaria effector proteins to the host cell. *Nature* 463, 627–631. doi: 10.1038/nature08728

Brandizzi, F., and Barlowe, C. (2013). Organization of the ER-Golgi interface for membrane traffic control. *Nat. Rev. Mol. Cell Biol.* 14, 382–392. doi: 10.1038/nrm3588

Bruce, M. C., Carter, R. N., Nakamura, K., Aikawa, M., and Carter, R. (1994). Cellular location and temporal expression of the *Plasmodium falciparum* sexual stage antigen Pfs16. *Mol. Biochem. Parasitol.* 65, 11–22. doi: 10.1016/0166-6851(94)90111-2

Cabrera, A., Herrmann, S., Warszta, D., Santos, J. M., John Peter, A. T., Kono, M., et al. (2012). Dissection of minimal sequence requirements for rhoptry membrane targeting in the malaria parasite. *Traffic* 13, 1335–1350. doi: 10.1111/j.1600-0854.2012.01394.x

Cai, H., Yu, S., Menon, S., Cai, Y., Lazarova, D., Fu, C., et al. (2007). TRAPPI tethers COPII vesicles by binding the coat subunit Sec23. *Nature* 445, 941–944. doi: 10.1038/nature05527

Chang, H. H., Falick, A. M., Carlton, P. M., Sedat, J. W., DeRisi, J. L., and Marletta, M. A. (2008). N-terminal processing of proteins exported by malaria parasites. *Mol. Biochem. Parasitol.* 160, 107–115. doi: 10.1016/j.molbiopara.2008.04.011

Cherifils, J., Ménétrey, J., Mathieu, M., Le Bras, G., Sylviane, R., Béraud-Dufour, S., et al. (1998). Structure of the Sec7 domain of the Arf exchange factor ARNO. *Nature* 392, 101–105. doi: 10.1038/32210

Collaborative, T. P. G. D. (2001). PlasmoDB: An integrative database of the *Plasmodium falciparum* genome. Tools for accessing and analyzing finished and unfinished sequence data. *Nucleic Acids Res.* 29, 66–69. doi: 10.1093/nar/29.1.66

Craig, E. A., Gambill, B. D., and Nelson, R. J. (1993). Heat shock proteins: Molecular chaperones of Protein Biogenesis. *Microbiol. Rev.* 57, 402–414. doi: 10.1016/0307-4412(91)90087-O

Dascher, C., and Balch, W. E. (1994). Dominant inhibitory mutants of ARF1 block endoplasmic reticulum to Golgi transport and trigger disassembly of the Golgi apparatus. *J. Biol. Chem.* 269 (2), 1437–1448. doi: 10.1016/S0021-9258(17)42277-0

de Koning-Ward, T. F., Gilson, P. R., Boddey, J. A., Rug, M., Smith, B. J., Papenfuss, A. T., et al. (2009). A newly discovered protein export machine in malaria parasites. *Nature* 459, 945–949. doi: 10.1038/nature08104

de Koning-Ward, T. F., Dixon, M. W. A., Tilley, L., and Gilson, P. R. (2016). *Plasmodium* species: Master renovators of their host cells. *Nat. Rev. Microbiol.* 14, 494–507. doi: 10.1038/nrmicro.2016.79

Deitsch, K. W., Driskill, C. L., and Wellems, T. E. (2001). Transformation of malaria parasites by the spontaneous uptake and expression of DNA from human erythrocytes. *Nucleic Acids Res.* 29, 850–853. doi: 10.1093/nar/29.3.850

Der, C. J., Finkel, T., and Cooper, G. M. (1986). Biological and biochemical properties of human rasH genes mutated at codon 61. *Cell* 44 (1), 167–176. doi: 10.1016/0092-8674(86)90495-2

Donaldson, J. G., and Jackson, C. L. (2011). ARF family G proteins and their regulators: Roles in membrane transport, development and disease. *Nat. Rev. Mol. Cell Biol.* 12, 362–375. doi: 10.1038/nrm3117

Ebine, K., Hirai, M., Sakaguchi, M., Yahata, K., Kaneko, O., and Saito-Nakano, Y. (2016). *Plasmodium* Rab5b is secreted to the cytoplasmic face of the tubovesicular network in infected red blood cells together with N-acylated adenylate kinase 2. *Malar. J.* 15, 1–17. doi: 10.1186/s12936-016-1377-4

Elliott, D. A., McIntosh, M. T., Hosgood, H. D., Chen, S., Zhang, G., Baevova, P., et al. (2008). Four distinct pathways of hemoglobin uptake in the malaria parasite *Plasmodium falciparum*. *Proc. Natl. Acad. Sci. U. S. A.* 105, 2463–2468. doi: 10.1073/pnas.0711067105

Elmendorf, H. G., and Haldar, K. (1993). Identification and localization of ERD2 in the malaria parasite *Plasmodium falciparum*: Separation from sites of sphingomyelin synthesis and implications for organization of the Golgi. *EMBO J.* 12, 4763–4773. doi: 10.1002/j.1460-2075.1993.tb06165.x

Elsworth, B., Matthews, K., Nie, C. Q., Kalanon, M., Charnaud, S. C., Sanders, P. R., et al. (2014). PTEX is an essential nexus for protein export in malaria parasites. *Nature* 511, 587–591. doi: 10.1038/nature13555

Eugster, A., Frigerio, G., Dale, M., and Duden, R. (2000). COP I domains required for coatomer integrity, and novel interactions with ARF and ARF-GAP. *EMBO J.* 19, 3905–3917. doi: 10.1093/emboj/19.15.3905

Ezougou, C. N., Ben-Rached, F., Moss, D. K., Lin, J. W., Black, S., Knuepfer, E., et al. (2014). *Plasmodium falciparum* Rab5B is an N-terminally myristoylated rab GTPase that is targeted to the parasite's plasma and food vacuole membranes. *PloS One* 9, 1–9. doi: 10.1371/journal.pone.0087695

Feig, L. A., and Cooper, G. M. (1988). Inhibition of NIH 3T3 cell proliferation by a mutant ras protein with preferential affinity for GDP. *Mol. Cell Biol.* 8 (8), 3235–3243. doi: 10.1128/mcb.8.8.3235

Gilberger, T.-W., Thompson, J. K., Triglia, T., Good, R. T., Duraisingh, M. T., and Cowman, A. F. (2003). A novel erythrocyte binding antigen-175 paralogue from *Plasmodium falciparum* defines a new trypsin-resistant receptor on human erythrocytes. *J. Biol. Chem.* 278, 14480–14486. doi: 10.1074/jbc.M211446200

Goldberg, J. (2000). Decoding of sorting signals by coatomer through a GTPase switch in the COPI coat complex. *Cell* 100, 671–679. doi: 10.1016/S0092-8674(00)80703-5

Haubruck, H., and McCormick, F. (1991). Ras p21: effects and regulation. *Biochim. Biophys. Acta* 1072, 215–229. doi: 10.1016/0304-419x(91)90015-d

Hiller, N. L., Bhattacharjee, S., van Ooij, C., Liolios, K., Harrison, T., Lopez-Estraño, C., et al. (2004). A host-targeting signal in virulence proteins reveals a secretome in malarial infection. *Science* 306, 1934–1937. doi: 10.1126/science.1102737

Hsu, V. W., Shah, N., and Klausner, R. D. (1992). A brefeldin A-like phenotype is induced by the overexpression of a human ERD-2-like protein, ELP-1. *Cell* 69, 625–635. doi: 10.1016/0092-8674(92)90226-3

Hutagalung, A. H., and Novick, P. J. (2011). Role of Rab GTPases in membrane traffic and cell physiology. *Physiol. Rev.* 91, 119–149. doi: 10.1152/physrev.00059.2009

Iriko, H., Ishino, T., Tachibana, M., Omoda, A., Torii, M., and Tsuboi, T. (2020). Skeleton binding protein 1 (SBP1) of *Plasmodium falciparum* accumulates in electron-dense material before passing through the parasitophorous vacuole membrane. *Parasitol. Int.* 75, 1–4. doi: 10.1016/j.parint.2019.102003

Iwanaga, S., Kato, T., Kaneko, I., and Yuda, M. (2012). Centromere plasmid: A new genetic tool for the study of *Plasmodium falciparum*. *PloS One* 7, 1–9. doi: 10.1371/journal.pone.0033326

Joberty, G., Tavitian, A., and Zahraoui, A. (1993). Isoprenylation of Rab proteins possessing a C-terminal CaaX motif. *FEBS Lett.* 330, 323–328. doi: 10.1016/0014-5793(93)80897-4

Kibria, K. M. K., Ferdous, J., Sardar, R., Panda, A., Gupta, D., Mohmmed, A., et al. (2019). A genome-wide analysis of coatomer protein (COP) subunits of apicomplexan parasites and their evolutionary relationships. *BMC Genomics* 20, 1–13. doi: 10.1186/s12864-019-5463-1

Krai, P., Dalal, S., and Klemba, M. (2014). Evidence for a Golgi-to-endosome protein sorting pathway in *Plasmodium falciparum*. *PloS One* 9, 1–12. doi: 10.1371/journal.pone.0089771

Kumar, N., and Zheng, H. (1992). Nucleotide sequence of a *Plasmodium falciparum* stress protein with similarity to mammalian 78-kDa glucose-regulated protein. *Mol. Biochem. Parasitol.* 56, 353–356. doi: 10.1016/0166-6851(92)90187-o

Kumar, N., Koski, G., Harada, M., Aikawa, M., and Zheng, H. (1991). Induction and localization of *Plasmodium falciparum* stress proteins related to the heat shock protein 70 family. *Mol. Biochem. Parasitol.* 48, 47–58. doi: 10.1016/0166-6851(91)90163-Z

Kung, L. F., Pagant, S., Futai, E., D'Arcangelo, J. G., Buchanan, R., Dittmar, J. C., et al. (2012). Sec24p and Sec16p cooperate to regulate the GTP cycle of the COPII coat. *EMBO J.* 31, 1014–1027. doi: 10.1038/emboj.2011.444

Kurokawa, K., and Nakano, A. (2019). The ER exit sites are specialized ER zones for the transport of cargo proteins from the ER to the Golgi apparatus. *J. Biochem.* 165, 109–114. doi: 10.1093/jb/mvy080

Langreth, S. G., Jensen, J. B., Reese, R. T., and Trager, W. (1978). Fine structure of human malaria in vitro. *J. Protozool.* 25, 443–452. doi: 10.1111/j.1550-7408.1978.tb04167.x

Lanoix, J., Ouwendijk, J., Chung-Chih, L., Stark, A., Love, H. D., Ostermann, J., et al. (1999). GTP hydrolysis by arf-1 mediates sorting and concentration of Golgi resident enzymes into functional COP I vesicles. *EMBO J.* 18, 4935–4948. doi: 10.1093/emboj/18.18.4935

Lee, M. C. S., Moura, P. A., Miller, E. A., and Fidock, D. A. (2008). *Plasmodium falciparum* Sec24 marks transitional ER that exports a model cargo via a diacidic motif. *Mol. Microbiol.* 68, 1535–1546. doi: 10.1111/j.1365-2958.2008.06250.x

Leung, K. F., Baron, R., and Seabra, M. C. (2006). Geranylgeranylation of Rab GTPases. *J. Lipid Res.* 47, 467–475. doi: 10.1194/jlr.R500017-JLR200

Lewis, M. J., and Pelham, H. R. B. (1990). A human homologue of the yeast HDEL receptor. *Nature* 348, 162–163. doi: 10.1038/348162a0

Lewis, M. J., Sweet, D. J., and Pelham, H. R. B. (1990). The ERD2 gene determines the specificity of the luminal ER protein retention system. *Cell* 61, 1359–1363. doi: 10.1016/0092-8674(90)90699-F

Makiuchi, T., Mi-Ichi, F., Nakada-Tsukui, K., and Nozaki, T. (2013). Novel TPR-containing subunit of TOM complex functions as cytosolic receptor for *Entamoeba* mitosomal transport. *Sci. Rep.* 3, 1–7. doi: 10.1038/srep01129

Marti, M., Good, R. T., Rug, M., Knuepfer, E., and Cowman, A. F. (2004). Targeting malaria virulence and remodeling proteins to the host erythrocyte. *Science* 306, 1930–1933. doi: 10.1126/science.1102452

Martinez, H., García, I. A., Sampieri, L., and Alvarez, C. (2016). Spatial-temporal study of Rab1b dynamics and function at the ER-Golgi interface. *PloS One* 11, 1–24. doi: 10.1371/journal.pone.0160838

McCabe, J. B., and Berthiaume, L. G. (2001). N-terminal protein acylation confers localization to cholesterol, sphingolipid-enriched membranes but not to lipid rafts/caveolae. *Mol. Biol. Cell* 12, 3601–3617. doi: 10.1091/mbc.12.11.3601

McDonold, C. M., and Fromme, J. C. (2014). Four GTPases differentially regulate the Sec7 Arf-GEF to direct traffic at the trans-Golgi network. *Dev. Cell* 30, 759–767. doi: 10.1016/j.devcel.2014.07.016

Miller, L. H., Ackerman, H. C., Su, X. Z., and Wellems, T. E. (2013). Malaria biology and disease pathogenesis: Insights for new treatments. *Nat. Med.* 19, 156–167. doi: 10.1038/nm.3073

Monetta, P., Slavin, I., Romero, N., and Alverez, C. (2007). Rab1b Interacts with GBF1 and modulates both ARF1 dynamics and COPI association. *Mol. Biol. Cell* 18, 2400–2410. doi: 10.1091/mbc.E06

Morse, D., Webster, W., Kalanon, M., Langsley, G., and McFadden, G.II (2016). *Plasmodium falciparum* Rab1A localizes to rhoptries in schizonts. *PloS One* 11, 1–13. doi: 10.1371/journal.pone.0158174

Möskes, C., Burghaus, P. A., Wernli, B., Sauder, U., Dürrenberger, M., and Kappes, B. (2004). Export of *Plasmodium falciparum* calcium-dependent protein kinase 1 to the parasitophorous vacuole is dependent on three N-terminal membrane anchor motifs. *Mol. Microbiol.* 54, 676–691. doi: 10.1111/j.1365-2958.2004.04313.x

Moyer, B. D., Allan, B. B., and Balch, W. E. (2001). Rab1 interaction with a GM130 effector complex regulates COPII vesicle cis-Golgi tethering. *Traffic* 2, 268–276. doi: 10.1034/j.1600-0854.2001.1o007.x

Nakano, A., and Muramatsu, M. (1989). A novel GTP-binding protein, sar1p, is involved in transport from the endoplasmic reticulum to the Golgi apparatus. *J. Cell Biol.* 109, 2677–2691. doi: 10.1083/jcb.109.6.2677

Nakazawa, S., Culleton, R., and Maeno, Y. (2011). In vivo and in vitro gametocyte production of *Plasmodium falciparum* isolates from Northern Thailand. *Int. J. Parasitol.* 41, 317–323. doi: 10.1016/j.ijpara.2010.10.003

Nickel, W., and Rabouille, C. (2009). Mechanisms of regulated unconventional protein secretion. *Nat. Rev. Mol. Cell Biol.* 10, 148–155. doi: 10.1038/nrm2617

Pasqualato, S., Renault, L., and Cherfils, J. (2002). Arf, Arl, Arp and Sar proteins: A family of GTP-binding proteins with a structural device for "front-back" communication. *EMBO Rep.* 3, 1035–1041. doi: 10.1093/embo-reports/kvf221

Pereira-Leal, J. B., and Seabra, M. C. (2000). The mammalian Rab family of small GTPases: definition of family and subfamily sequence motifs suggests a mechanism for functional specificity in the Ras superfamily. *J. Mol. Biol.* 301 (4), 1077–1087. doi: 10.1006/jmbi.2000.4010

Quevillon, E., Spielmann, T., Brahimi, K., Chattopadhyay, D., Yeramian, E., and Langsley, G. (2003). The *Plasmodium falciparum* family of Rab GTPases. *Gene* 306, 13–25. doi: 10.1016/S0378-1119(03)00381-0

Rached, F., Ndjembo-Ezougou, C., Chandran, S., Talabani, H., Yera, H., Dandavate, V., et al. (2012). Construction of a *Plasmodium falciparum* Rab-interactome identifies CK1 and PKA as Rab-effector kinases in malaria parasites. *Biol. Cell* 104, 34–47. doi: 10.1111/boc.201100081

Rahlfs, S., Koncarevic, S., Iozef, R., Mwongela Mailu, B., Savvides, S. N., Schirmer, R. H., et al. (2009). Myristoylated adenylate kinase-2 of *Plasmodium falciparum* forms a heterodimer with myristoyltransferase. *Mol. Biochem. Parasitol.* 163, 77–84. doi: 10.1016/j.molbiopara.2008.09.008

Russo, I., Babbitt, S., Muralidharan, V., Butler, T., Oksman, A., and Goldberg, D. E. (2010). Plasmepsin V licenses *Plasmodium* proteins for export into the host erythrocyte. *Nature* 463, 632–636. doi: 10.1038/nature08726

Sakura, T., Yahata, K., and Kaneko, O. (2013). The upstream sequence segment of the C-terminal cysteine-rich domain is required for microneme trafficking of *Plasmodium falciparum* erythrocyte binding antigen 175. *Parasitol. Int.* 62, 157–164. doi: 10.1016/j.parint.2012.12.002

Saraste, J., and Kuismanen, E. (1992). Pathways of protein sorting and membrane traffic between the rough endoplasmic reticulum and the Golgi complex. *Semin. Cell Biol.* 3, 343–355. doi: 10.1016/1043-4682(92)90020-v

Sargeant, T. J., Marti, M., Caler, E., Carlton, J. M., Simpson, K., Speed, T. P., et al. (2006). Lineage-specific expansion of proteins exported to erythrocytes in malaria parasites. *Genome Biol.* 7, R12. doi: 10.1186/gb-2006-7-2-r12

Saridaki, T., Fröhlich, K. S., Braun-Breton, C., and Lanzer, M. (2009). Export of PfSBP1 to the *Plasmodium falciparum* Maurer's Clefts. *Traffic* 10, 137–152. doi: 10.1111/j.1600-0854.2008.00860.x

Schindelin, J., Arganda-Carreras, I., Frise, E., Kaynig, V., Longair, M., Pietzsch, T., et al. (2012). Fiji: An open-source platform for biological-image analysis. *Nat. Methods* 9, 676–682. doi: 10.1038/nmeth.2019

Schlott, A. C., Holder, A. A., and Tate, E. W. (2018). N -myristoylation as a drug target in malaria: Exploring the role of N -myristoyltransferase substrates in the inhibitor mode of action. *ACS Infect. Dis.* 4, 449–457. doi: 10.1021/acsinfecdis.7b00203

Semenza, J. C., Hardwick, K. G., Dean, N., and Pelham, H. R. B. (1990). ERD2, a yeast gene required for the receptor-mediated retrieval of luminal ER proteins from the secretory pathway. *Cell* 61, 1349–1357. doi: 10.1016/0092-8674(90)90698-E

Sewell, J. L., and Kahn, R. A. (1988). Sequences of the bovine and yeast ADP-ribosylation factor and comparison to other GTP-binding proteins. *Proc. Natl. Acad. Sci. U. S. A.* 85, 4620–4624. doi: 10.1073/pnas.85.13.4620

Shibata, T., Hadano, J., Kawasaki, D., Dong, X., Kawabata, S.II, and Sllner, T. (2017). *Drosophila* TG-A transglutaminase is secreted via an unconventional Golgi-independent mechanism involving exosomes and two types of fatty acylations. *J. Biol. Chem.* 292, 10723–10734. doi: 10.1074/jbc.M117.779710

Spielmann, T., and Gilberger, T.-W. (2010). Protein export in malaria parasites: do multiple export motifs add up to multiple export pathways? *Trends Parasitol.* 26, 6–10. doi: 10.1016/j.pt.2009.10.001

Spielmann, T., Fergusen, D. J. P., and Beck, H.-P. (2003). etramps, a new *Plasmodium falciparum* gene family coding for developmentally regulated and highly charged membrane proteins located at the parasite– host cell interface. *Mol. Biol. Cell* 14, 1529–1544. doi: 10.1091/mbc.e02-04-0240

Stafford, W. H. L., Stockley, R. W., Ludbrook, S. B., and Holder, A. A. (1996). Isolation, expression and characterization of the gene for an ADP-ribosylation factor from the human malaria parasite, *Plasmodium falciparum*. *Eur. J. Biochem.* 242, 104–113. doi: 10.1111/j.1432-1033.1996.0104r.x

Stearns, T., Willingham, M. C., Botstein, D., and Kahn, R. A. (1990). ADP-ribosylation factor is functionally and physically associated with the Golgi complex. *Proc. Natl. Acad. Sci. U. S. A.* 87, 1238–1242. doi: 10.1073/pnas.87.3.1238

Stenmark, H., Parton, R. G., Steele-Mortimer, O., Lütcke, A., Gruenberg, J., and Zerial, M. (1994). Inhibition of rab5 GTPase activity stimulates membrane fusion in endocytosis. *EMBO J.* 15;13 (6), 1287–1296. doi: 10.1002/j.1460-2075.1994.tb06381.x

Stenmark, H. (2009). Rab GTPases as coordinators of vesicle traffic. *Nat. Rev. Mol. Cell Biol.* 10, 513–525. doi: 10.1038/nrm2728

Struck, N. S., de Souza Dias, S., Langer, C., Marti, M., Pearce, J. A., Cowman, A. F., et al. (2005). Re-defining the Golgi complex in *Plasmodium falciparum* using the novel Golgi marker PfGRASP. *J. Cell Sci.* 118, 5603–5613. doi: 10.1242/jcs.02673

Struck, N. S., Herrmann, S., Schmuck-Barkmann, I., De Souza Dias, S., Haase, S., Cabrera, A. L., et al. (2008). Spatial dissection of the cis- and trans-Golgi compartments in the malaria parasite *Plasmodium falciparum*. *Mol. Microbiol.* 67, 1320–1330. doi: 10.1111/j.1365-2958.2008.06125.x

Suda, Y., Kurokawa, K., and Nakano, A. (2018). Regulation of ER-Golgi transport dynamics by GTPases in budding yeast. *Front. Cell Dev. Biol.* 5:122. doi: 10.3389/fcell.2017.00122

Teal, S. B., Hsu, V. W., Peters, P. J., Klausner, R. D., and Donaldson, J. G. (1994). An activating mutation in ARF1 stabilizes coatomer binding to Golgi membranes. *J. Biol. Chem.* 4;269 (5), 3135–3138. doi: 10.1016/S0021-9258(17)41837-0

Thavayogarajah, T., Gangopadhyay, P., Rahlfs, S., Becker, K., Lingelbach, K., Przyborski, J. M., et al. (2015). Alternative protein secretion in the malaria parasite *Plasmodium falciparum*. *PloS One* 10, 1–18. doi: 10.1371/journal.pone.0125191

Tisdale, E. J., Bourne, J. R., Khosravi-Far, R., Der, C. J., and Balch, W. E. (1992). GTP-binding mutants of rab1 and rab2 are potent inhibitors of vesicular transport from the endoplasmic reticulum to the Golgi complex. *J. Cell Biol.* 119 (4), 749–761. doi: 10.1083/jcb.119.4.749

Townsley, F. M., Frigerio, G., and Pelham, H. R. B. (1994). Retrieval of HDEL proteins is required for growth of yeast cells. *J. Cell Biol.* 127, 21–28. doi: 10.1083/jcb.127.1.21

van Ooij, C., Tamez, P., Bhattacharjee, S., Hiller, N. L., Harrison, T., Liolios, K., et al. (2008). The malaria secretome: From algorithms to essential function in blood stage infection. *PloS Pathog.* 4, 1–15. doi: 10.1371/journal.ppat.1000084

Walliker, D., Quakyi, I. A., Wellems, T. E., Mccutchan, T. F., Szarfman, A. N. A., London, W. T., et al. (1987). Genetic analysis of the human malaria parasite *Plasmodium falciparum*. *Science* 236, 1661–1666. doi: 10.1126/science.3299700

Watanabe, N., Nakada-Tsukui, K., and Nozaki, T. (2020). Two isotypes of phosphatidylinositol 3-phosphate-binding sorting nexins play distinct roles in trogocytosis in *Entamoeba histolytica*. *Cell. Microbiol.* 22, 1–16. doi: 10.1111/cmi.13144

Yorimitsu, T., and Sato, K. (2012). Insights into structural and regulatory roles of Sec16 in COPII vesicle formation at ER exit sites. *Mol. Biol. Cell* 23, 2930–2942. doi: 10.1091/mbc.E12-05-0356

Zhang, X., and Wang, Y. (2016). GRASPs in Golgi structure and function. *Front. Cell Dev. Biol.* 3, 84. doi: 10.3389/fcell.2015.00084

Zhao, L., Helms, J. B., Brunner, J., and Wieland, F. T. (1999). GTP-dependent binding of ADP-ribosylation factor to coatomer in close proximity to the binding site for dilysine retrieval motifs and p23. *J. Biol. Chem.* 274, 14198–14203. doi: 10.1074/jbc.274.20.14198

Conflict of Interest: The authors declare that the research was conducted in the absence of any commercial or financial relationships that could be construed as a potential conflict of interest.

frontiers in Cellular and Infection Microbiology

PERSPECTIVE
published: 02 March 2021
doi: 10.3389/fcimb.2021.607686

Plasmodium knowlesi – Clinical Isolate Genome Sequencing to Inform Translational Same-Species Model System for Severe Malaria

Damilola R. Oresegun, Cyrus Daneshvar and Janet Cox-Singh *

Division of Infection, School of Medicine, University of St Andrews, St Andrews, United Kingdom

Malaria is responsible for unacceptably high morbidity and mortality, especially in Sub-Saharan African Nations. Malaria is caused by member species' of the genus *Plasmodium* and despite concerted and at times valiant efforts, the underlying pathophysiological processes leading to severe disease are poorly understood. Here we describe zoonotic malaria caused by *Plasmodium knowlesi* and the utility of this parasite as a model system for severe malaria. We present a method to generate long-read third-generation *Plasmodium* genome sequence data from archived clinical samples using the MinION platform. The method and technology are accessible, affordable and data is generated in real-time. We propose that by widely adopting this methodology important information on clinically relevant parasite diversity, including multiple gene family members, from geographically distinct study sites will emerge. Our goal, over time, is to exploit the duality of *P. knowlesi* as a well-used laboratory model and human pathogen to develop a representative translational model system for severe malaria that is informed by clinically relevant parasite diversity.

Keywords: *Plasmodium knowlesi*, MinION, parasite virulence, severe malaria, translational model system

OPEN ACCESS

Edited by:
Takeshi Annoura, National Institute of Infectious Diseases (NIID), Japan

Reviewed by:
Celio Geraldo Freire-de-Lima, Federal University of Rio de Janeiro, Brazil
Guan Zhu, Jilin University, China
Chaturong Putaporntip, Chulalongkorn University, Thailand

***Correspondence:**
Janet Cox-Singh
jcs26@st-andrews.ac.uk

Specialty section:
This article was submitted to Parasite and Host, a section of the journal Frontiers in Cellular and Infection Microbiology

Received: *17 September 2020*
Accepted: *27 January 2021*
Published: *02 March 2021*

Citation:
Oresegun DR, Daneshvar C and Cox-Singh J (2021) Plasmodium knowlesi – Clinical Isolate Genome Sequencing to Inform Translational Same-Species Model System for Severe Malaria. Front. Cell. Infect. Microbiol. 11:607686. doi: 10.3389/fcimb.2021.607686

BACKGROUND

Malaria is a vector-borne disease that has impacted human health in tropical and sub-tropical regions since ancient time and continues to outwit human endeavors to control and eradicate. Malaria parasites, genus *Plasmodium*, have a highly complex lifecycle, intimately dependant on an invertebrate mosquito host for the diploid sexual stage of reproduction and equally dependant on specific vertebrate hosts for asexual replication and transmission. Lifecycle complexity, including adaptation to specific vertebrate hosts, invertebrate host restriction to particular Anopheline vector species with spatial and ecological niche requirement may augur unfavourably for *Plasmodium* spp. survival in a dynamic world. Yet, despite sustained efforts, human malaria persists to the extent that the altruistic World Health Organization (WHO) malaria eradication goal of the 1950s, was downgraded to country and at times species-specific elimination https://www.who.int/malaria/areas/elimination/en/. Even so, eradication is not a forgotten dream and may well be achievable within a new 30-year time-frame (Feachem et al., 2019).

The human host-adapted *Plasmodium* species; *Plasmodium falciparum*, *Plasmodium vivax*, *Plasmodium malariae*, and *Plasmodium ovale*, two sub-species (Sutherland et al., 2010) are responsible for most of the reported cases of malaria. *P. falciparum*, in particular, and *P. vivax* are responsible for the global health burden of disease. *P. falciparum* infections carry a high level of morbidity and mortality in adults and children. Severe malaria manifests variously, for example as severe malaria with coma, acute kidney injury and severe malarial anaemia (Plewes et al., 2018; White, 2018; World-Health-Organization, 2019). Understanding the underlying pathophysiology of severe malaria is thwarted by the absence of a translational model system. In practice, malaria elimination remains the most effective strategic method to reduce indigenous transmission of *P. falciparum* and/or *P. vivax* and consequently the impact of severe malaria. Malaria elimination is a long-term goal and in the meantime people will continue to be infected and succumb to severe malaria.

Malaria elimination status is awarded to each country by the WHO even though the country need not necessarily be malaria free. A case in point is Malaysia where indigenous human-host adapted *Plasmodium* species transmission is zero and malaria elimination status was expected to be awarded to Malaysia by the WHO in 2020 (Liew et al., 2018; Jiram et al., 2019; Noordin et al., 2020) https://www.who.int/malaria/areas/elimination/e2020/malaysia/en/. However, malaria - the disease, persists in Malaysia, particularly in the eastern states of Sabah and Sarawak where for the past 20 years *Plasmodium knowlesi*, a malaria parasite of macaque monkeys, has been regularly diagnosed in symptomatic patients in Sabah and Sarawak (Lee et al., 2009a; Barber et al., 2017; Cooper et al., 2020; Raja et al., 2020).

Plasmodium knowlesi Malaria

As one millennium closed and a new one began, a substantial number of cases of *P. knowlesi* were identified in the human population in the Kapit division of Sarawak Malaysia Borneo (Singh et al., 2004). The entry of *P. knowlesi* into the human population became apparent as the number of cases of *P. falciparum* and *P. vivax* declined in response to robust control programmes. Up to that point *P. knowlesi*, a parasite morphologically similar to both *P. malariae* and the early trophozoites of *P. falciparum*, was misdiagnosed by routine microscopy (Lee et al., 2009b). Misdiagnosis as *P. falciparum* had little clinical consequence as both infections require urgent treatment and management. Misdiagnosis as the more benign *P. malariae* resulted in delayed treatment and the development of severe disease and preventable fatality (Cox-Singh et al., 2008).

There is no indication that the cases of *P. knowlesi* malaria are decreasing, 69% of the 16,500 reported cases of malaria in Malaysia between 2013 and 2017 were caused by *P. knowlesi* (Raja et al., 2020) (Hussin et al., 2020). In 2018, more than 4,000 cases of malaria were reported in Malaysia and with *P. falciparum* and *P. vivax* close to elimination, *P. knowlesi* accounted for most of those (World-Health-Organization, 2019; Chin et al., 2020).

P. knowlesi malaria is also widespread across South East Asia where the natural habitat supports sylvan transmission – areas where the specific Anopheline vectors of *P. knowlesi*, the natural macaque hosts and the parasites co-exist and where humans enter these habitats (Singh and Daneshvar, 2013; Shearer et al., 2016). Zoonotic malaria is unlikely to fill the void left by the removal of *P. falciparum* and *P. vivax*, however, communities living close to and individuals who enter the jungle transmission areas for work or leisure activities are at risk of this newly emergent potentially life threatening disease.

P. knowlesi malaria is associated with severe disease in 10 – 12% of cases with death in vulnerable and untreated individuals (Cox-Singh et al., 2008; Daneshvar et al., 2009; William et al., 2011; Rajahram et al., 2012; Grigg et al., 2018; Hussin et al., 2020). Although *P. knowlesi* infections are associated with hyperparasitaemia, severe malaria caused by *P. knowlesi* occurs across a wide spectrum of parasitaemia. Relatively low parasite counts, ≥15,000 parasites/μl carry a high risk of severe disease (Willmann et al., 2012; Cooper et al., 2020). Severe *P. knowlesi* malaria is characterised by one or more of the WHO criteria for severe malaria including; anaemia, acute kidney injury, acute and late-onset respiratory distress, hypotension, jaundice, and metabolic acidosis (Cox-Singh et al., 2008; Daneshvar et al., 2009; Cox-Singh et al., 2010; Barber et al., 2011; World-Health-Organization, 2013; Grigg et al., 2018). Indeed, until the discovery of zoonotic malaria caused by *P. knowlesi*, severe malaria was the preserve of *P. falciparum* and severe malaria guidelines written for *P. falciparum* infection. With few tools to study the pathways to severe malaria and the absence of a comparator disease, assigning clinical cause and effect in malaria was roadblocked.

Even so characterising and untangling the combined contribution of human host response and pathogen to disease presentation and outcome is inherently complex, in the literal sense. The human race survives and often thrives in a harsh microbial world (Numbers, 2011). Of the many microbes only a few are pathogenic, and even-then not uniformly so. Host innate immune function is key to infectivity with co-factors, including age, co-morbidity and co-evolution influencing disease outcomes. Such disease determinants are poorly defined, yet critical to understand, as witnessed in the ongoing Coronavirus pandemic (Mills et al., 2015; Loy et al., 2017; Mandl et al., 2018; Petersen et al., 2020). Human host diversity and response to infection, including response to infection with potentially virulent malaria parasites, is outside of the scope of this article. Rather we focus on determining clinically relevant *Plasmodium* spp. genetic diversity and propose a model system to test for association between parasite genetic diversity and clinical outcome (**Figure 1**).

It is also perhaps worth noting here that in general, disease phenotype precision remains a limiting factor in genome-wide associations studies (GWAS) and an area that lags behind available technologies (MacRae, 2019). No different is the study of parasite genetic characters associated with disease

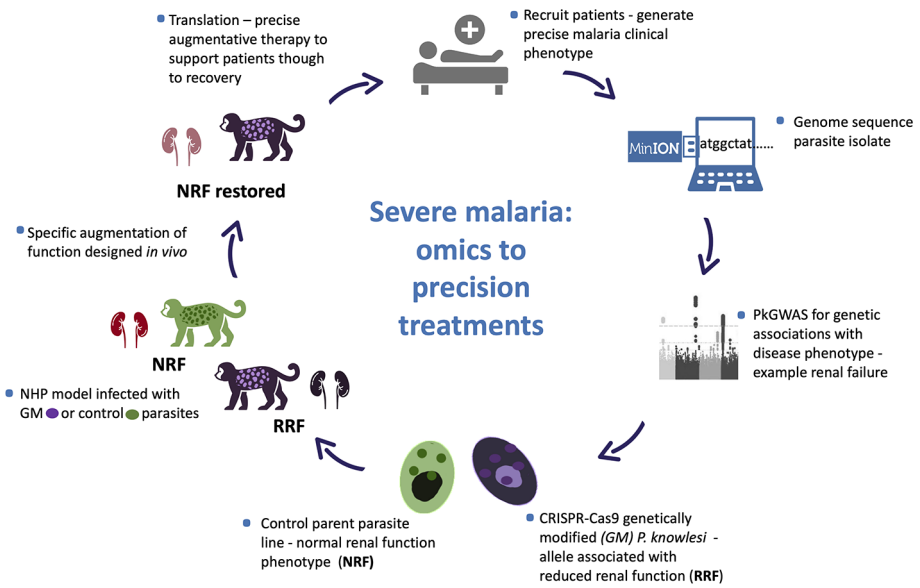

FIGURE 1 | *Plasmodium knowlesi* - proposed translational and dynamic model system for severe malaria. Precise clinical phenotyping malaria patients coupled with parasite genome sequencing "bed-side". Parasite genome wide association studies (pGWAS) with markers of disease – an example of renal impairment in severe *P. knowlesi* infection is used here. Associating alleles are superimposed onto an experimental parasite genetic background to produce genetically modified parasites (GM). GM parasites phenotyped *in vitro* and *in vivo* (non-human primate -NHP, model) for matched disease phenotype. NHP model used to develop strategies to specifically reduce the impact of the clinical phenotype for translation into therapies for patients with severe malaria.

progression (pGWAS) in malaria where disease phenotype precision is currently lacking. No matter how sophisticated the model system, mathematical, *in silico*, *in vitro*, or *in vivo*, the outputs can only be as precise as the input data.

Modelling malaria is especially difficult because malaria parasites have co-evolved with their vertebrate hosts each exerting selective forces on the other in a dynamic dance for survival (Loy et al., 2018). That dynamic is complicated further because malaria parasites are eucaryotic with a relatively large genome, 20–40 mega bases organised into 14 chromosomes (Gardner et al., 2002; Carlton et al., 2008; Pain et al., 2008; Ansari et al., 2016). Designing experiments to identify the drivers of pathogenesis, of parasite virulence and disease cause and effect are challenging.

The advent of "omics" may better inform models for malaria through multiple data generation platforms; genomics, transcriptomics and proteomics (Pinheiro et al., 2015; Campino et al., 2018; Benavente et al., 2019; Lindner et al., 2019). Even with these tools all too often, information is extrapolated. Rodent models and experimental lines that are unable to capture clinically relevant parasite diversity are much better characterised for markers of parasite virulence than diverse contemporary clinical isolates (Plewes et al., 2018). The value of supporting sophisticated forward genetic screens on laboratory isolates with clinical isolate genotyping was demonstrated in a recent study on *P. falciparum* gene clusters involved in erythrocyte invasion (Campino et al., 2018). Invasion phenotypes generated from crossing two experimental lines and phenotype-associated deletions were compared with long-read sequence data available from a small number of clinical isolates where indels in the same large locus were identified supporting invasion pathway variation in nature. Ignoring the impact of natural pathogen diversity on disease progression and virulence creates an inexcusable vacuum when analysing data for parasite association with disease severity.

P. knowlesi is an adaptable and naturally diverse parasite. A genetic study on clinical isolates of *P. knowlesi* identified an association between certain haplotypes of a short polymorphic fragment (~885bp) of the *Plasmodium knowlesi normocyte binding protein (Pknbp)xa* on chromosome 14 and continuous data on markers of disease severity (Ahmed et al., 2014). In addition to disease association, the fragment was dimorphic, clinical isolates clustered into one of two distinct genotypes at that locus, begging the question how far the dimorphism extended across the *Pknbpxa* 9578bp gene and chromosome 14.

Harnessing the power of next-generation sequencing seemed the obvious choice to take this work forward within the caveat that the clinical isolates of *P. knowlesi* available to study were small volume (<1mL) frozen whole blood. Undeterred and as proof of concept, we developed a method to deplete human DNA and concentrate parasite DNA in the samples. We produced *P. knowlesi* genome sequences from six clinical isolates using massively parallel Illumina short-read sequencing platforms (Pinheiro et al., 2015). The move from genetics to genomics for clinical isolate characterization unlocked a wealth of information. Subsequent analyses found that the *Pknbpxa* dimorphism extended along the gene and chromosome 14. Indeed, SNPs associated with the dimorphism were found on all chromosomes and involved more than half of all genes in *P. knowlesi* parasites isolated from patients. The work

demonstrated that *P. knowlesi* isolated from human infections in Sarawak, Malaysian Borneo are one of two distinct genotypes.

Both pieces of work unlocked hidden genome-wide characters in clinical isolates of *P. knowlesi*. The studies reinforced the idea that pathogen genome sequence data extracted from clinically well characterised infections provides a valuable resource for studies on the role of pathogen diversity in virulence and disease outcome.

P. knowlesi – A Model for Malaria

P. knowlesi was first described in a long tailed macaque in the 1930s (Knowles and Gupta, 1932). Early work demonstrated that *P. knowlesi* was an adaptable parasite and experimental lines were developed and maintained in rhesus macaques, *Macaca mulatta*, to model for malaria. The *P. knowlesi* – rhesus macaque malaria model was used extensively for studies on malaria antigenic variation, vaccine development, parasite invasion, and biology, recently reviewed (Butcher and Mitchell, 2018; Galinski et al., 2018; Pasini et al., 2018). Traditionally *P. knowlesi* was not favoured as a model for disease, pathophysiology, mostly because the *P. knowlesi* in *Macaca mulatta* was particularly aggressive and not representative of human malaria caused by *P. falciparum*. A view supported in more recent work on cytokine responses in *M. mulatta* experimentally infected with *P. knowlesi* where a dampened response, and if anything, an anti-inflammatory response was observed in this model, a response that is uncharacteristic of human-host *Plasmodium* infections (Praba-Egge et al., 2002). *P. falciparum* malaria and indeed *P. knowlesi* clinical infections, are characterised by vigorous pro- and anti-inflammatory responses depending on age and endemicity (Cox-Singh et al., 2011; Farrington et al., 2017). Taken together there was little support for the utility of *P. knowlesi* in *M. mulatta* as an *in vivo* model for severe malaria. *P. knowlesi* in other experimental non-human primates (NHP's) produces a disease more representative of human malaria and it is surprising that this opportunity to model severe malaria has not been taken forward (Langhorne and Cohen, 1979; Ozwara et al., 2003; Onditi et al., 2015). Unfortunately lack of support for using *P. knowlesi* to model for severe malaria is compounded by evolutionary distance. *P. knowlesi* and *P. falciparum* occupy distinct phylogenetic clades and phylogenetic distance is often used to argue against using *P. knowlesi* to model for *P. falciparum*. Evolutionary distance continues to be used to question the validity of comparing *P. knowlesi* with *P. falciparum* malaria, yet they are member-species of the same genus – by definition they are closely related. In practice, evolutionary distance often over-rides biological and comparable clinical characters and *P. knowlesi* is more often favourably viewed as a model for the phylogenetically closer yet phenotypically quite distinct *P. vivax* (Moon et al., 2013; Mohring et al., 2019; Verzier et al., 2019).

Neither *P. falciparum* nor *P. vivax* is permissive in intact experimental NHP hosts and to date, representative heterologous translational models for malaria are not available to interrogate pathways to pathology and to develop augmentative therapies. Consequently, the treatment and management of patients severely ill with malaria remain imprecise and generally supportive. We argue that clinical data collected from patients with naturally acquired severe *P. knowlesi* coupled with homologous laboratory adapted, well characterised and genetically adaptable experimental lines of *P. knowles*i can be exploited to discover the parasite drivers of severe malaria. Laboratory adapted lines of *P. knowlesi* are permissive in a range of NHP hosts, including olive baboons and common marmosets (Langhorne and Cohen, 1979; Ozwara et al., 2003; Onditi et al., 2015). Some of these *in vivo* models exhibit clinical characters representative of severe malaria caused by *P. falciparum* and, importantly, contemporary clinical descriptions of severe malaria caused by *P. knowlesi* (Cox-Singh et al., 2008; Daneshvar et al., 2009; Cox-Singh et al., 2010; Daneshvar et al., 2018). Notwithstanding NHP models are of ethical concern, expensive and valid only if the information obtained significantly advances knowledge, which often is not the case. Experimental lines of *P. knowlesi* even if modelled *in vivo* are effectively research silos lacking the power to inform clinical disease caused by genetically diverse contemporary wild-type zoonotic parasites (Ahmed et al., 2014; Assefa et al., 2015; Divis et al., 2015; Pinheiro et al., 2015).

Clinical descriptions of *P. knowlesi* malaria portray a spectrum of disease from uncomplicated – to severe and fatal infections and can be compared phenotypically with *P. falciparum* malaria (Cox-Singh et al., 2008; Daneshvar et al., 2009; Cox-Singh et al., 2010; Cox-Singh et al., 2011; Rajahram et al., 2012; Ahmed et al., 2014; Barber et al., 2018a; Barber et al., 2018b).

The duality of *P. knowlesi* as an adaptable experimental model and human pathogen offers a unique opportunity to develop a comprehensive representative translational model system for malaria informed by same-species clinical disease.

Two important advances enhance the utility of *P. knowlesi* as a model for disease. The first is the adaptation of an experimental line of *P. knowlesi* to *in vitro* growth in human erythrocytes (Moon et al., 2013). The second is transfection technology. *P. knowlesi* in macaque erythrocytes was already shown to be more amenable to transfection, meaning genetic modification, than experimental lines of *P. falciparum* (Kocken et al., 2002). The human erythrocyte adapted line is similarly receptive to transfection and indeed CRISPR-Cas9 targeted genetic modification technology, genome editing, has been developed for *P. knowlesi* (Moon et al., 2013; Mohring et al., 2019). These technologies together with genome sequence data, generated from clinical isolates, will facilitate the introduction of clinically relevant alleles of *P. knowlesi* into experimental lines for *in vitro* characterisation and the unique opportunity to take this work forward *in vivo* (Cox-Singh and Culleton, 2015).

A long journey to cause and effect harnessing omics, genetically modified parasites and comprehensive model systems to properly ascribe parasite virulence to malaria pathophysiology while possible is a long game, difficult, time-consuming and expensive. However, failure to make this effort is to perpetuate acceptance of clinical and

therapeutic blind-spots, imprecise and generally supportive treatment and management for severe malaria, that perhaps is only acceptable if there is no alternative.

In the first instance, the ability to genome sequence *Plasmodium* species isolated from clinically well-characterised malaria patients will facilitate *Plasmodium* Genome-Wide Associations Studies (*p*GWAS) and identify virulence gene candidates. We show how short and long-read *Plasmodium* genome sequence data can be generated from fresh or archived frozen samples held in the many malaria research centres worldwide. *Plasmodium* genome sequence outputs over time and space will facilitate the construction of a substantial genetic reference resource, based on diverse wild-type parasites isolated from patients, that will inform model systems (Milner et al., 2012; Ahmed et al., 2014; Pinheiro et al., 2015; Auburn et al., 2018; Campino et al., 2018; Divis et al., 2018; Otto et al., 2018; Su et al., 2019; Siao et al., 2020). Until now genome sequence data generated from clinical samples was more feasible using Illumina massively parallel short-read sequencing.

As highlighted in the *P. falciparum* invasion gene study described in an earlier section, prohibitively expensive and otherwise impractical long-read genome sequencing data from clinical isolates were required to validate study findings (Campino et al., 2018). We have already developed a method to extract *P. knowlesi* DNA from archived small volume clinical isolates suitable for Illumina short-read sequencing (Pinheiro et al., 2015). To overcome limitations of short-read genome sequencing that are problematic for multiple repeat regions and multiple gene families in *Plasmodium* spp., the method was further adapted for Oxford Nanopore MinION long-read sequencing, third-generation sequencing, that is accessible, affordable, mobile and suitable for low yield DNA samples (**Figure 2**). Briefly 200–400ul samples of archived whole blood from *P. knowlesi* patients was rapidly thawed and immediately diluted in 50mL cold PBS. The suspension was mixed gently before recovering parasites and any contaminating white blood cells (WBC's) by centrifugation: 2,000 x g; 20 minutes; 4°C (pellet 1). The supernatant was transferred to a fresh tube and centrifugation repeated to maximise parasite recovery (pellet 2). The pellets were combined and resuspended in 1.2mL of cold PBS. Surviving host WBCs, a source of human DNA (hDNA) contamination, were removed using magnetic beads coated with antibodies to the ubiquitous WBC surface marker CD45 (Dynabeads™ CD45, Invitrogen™). Dynabeads were prepared as per manufacturers' instruction and 100ul bead suspension added to the 1.2mL pellet suspension followed by incubation at 4°C with rotation for 30 minutes. WBC's bound to the beads were removed by placing in a magnetic field for two minutes.

The human WBC depleted eluate was carefully removed and transferred to a fresh Eppendorf tube and centrifuged at 2,000 x *g* for 20 min to recover the parasite enriched pellet (PEP). The PEP was suspended in 200ul PBS for DNA extraction (QIAamp DNA Blood Mini Kit, QIAGEN). Recovered DNA was eluted in 150ul of Buffer AE. Percent hDNA depletion and Plasmodium DNA recovery were determined using quantitative PCR (qPCR) (Klaassen et al., 2003; Divis et al., 2010). *P. knowlesi* qPCR *ct* values negatively correlated with genome coverage ($p = 0.0375$). *P. knowlesi* DNA enriched samples (post hDNA depletion) from isolates with a starting parasitaemia of <40,000 per ul had low parasite DNA yield and sequence coverage.

Twenty-one (21) samples from 15 different patients, median parasitaemia 193,600 parasites/ul (IQR 127,875 – 321,750; min 20,656; max 794,063) with >90% hDNA depletion were taken forward to PCR-free rapid barcoding library preparation (Oxford Nanopore, SQK-RBK004). SQK-RBK004 library preparation is suitable for small yield DNA samples in the region of 400ng and includes a tagmentation step that generates read lengths normally distributed around a mean length of 4,500 kb. Of 21 library preparations 13 (62%) had >10x genome sequence coverage and six of these >30x coverage. Coverage of 100x was achieved especially when >1 sequencing library was prepared per isolate.

For the first time it is possible to generate long-read *Plasmodium* genome sequence data from small clinical samples from malaria patients. Samples that are archived or collected prospectively can be sequenced in a cost-effective and time-efficient manner anywhere. The importance of this capability is the opportunity to move

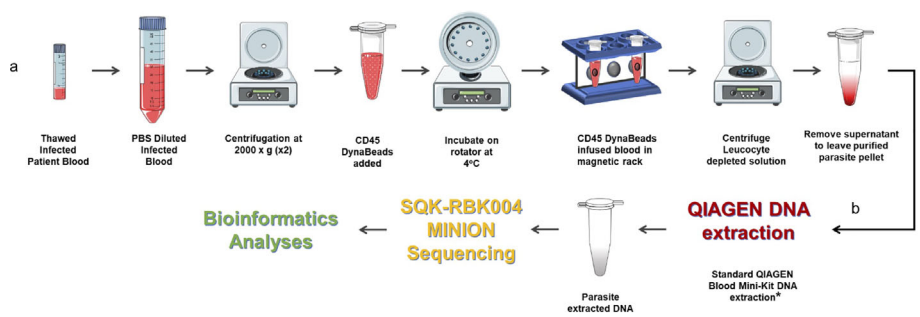

FIGURE 2 | Protocol for processing low volume frozen whole blood samples from patients with malaria in preparation for third generation genome sequencing. **(A)** Human leucocyte depletion and **(B)** sequencing pipeline. *Human DNA was quantified using qPCR (Klaassen et al., 2003) and a standard curve derived from Human Genomic Control DNA (Applied Biosystems®, TaqMan®). In the absence of pure control parasite DNA, cycle threshold (*ct*) values from *P. knowlesi* qPCR (Divis et al., 2010) were normalised by volume and used to estimate parasite DNA enrichment following human DNA depletion. *Parts of the figure are conceptualised and adapted using Servier Medical Art, Servier:* https://smart.servier.com.

forward from a necessary dependence on *Plasmodium* genome sequence generated from experimental lines to genome sequence generated from clinical samples with matched clinical data. The methodology we describe is particularly applicable to *P. knowlesi* infections that tend to be single genotype and reach relatively high parasitaemia. The methods can be applied to, albeit, relatively uncommon single genotype *P. falciparum* infections. Although multiple genotype infections present a limiting factor to the methods described here, the potential to generate valuable genome-wide information on even a small number of clinical isolates to inform studies on *P. falciparum* virulence should not be overlooked.

Subsequent *p*GWAS on long read sequence data from clinical isolates with matched high quality continuous clinical and laboratory data, relative to particular clinical manifestations of severe malaria, will help unravel the contribution of parasite diversity to virulence. In addition to accessibility and field application of low-cost real-time sequencing in-house, Nanopore MinION long-read sequencing can resolve important multiple gene family members, including the *P. knowlesi kirs* and *SICAvars* (Pain et al., 2008; Pinheiro et al., 2015; Lapp et al., 2018). These and other gene clusters encode surface antigens that are implicated in malaria parasite virulence and are difficult to sequence, formerly requiring expensive sequencing platforms equally prohibitive in cost and quantity of input DNA required (Campino et al., 2018).

Our particular interest is to use MinION sequence data from clinical isolates of *P. knowlesi* in *p*GWAS studies. We will analyse matched continuous clinical data predictive of precise characteristics of severe malaria to identify candidate alleles implicated in virulence to take forward in functional studies. CRISPR-Cas9 technology developed for *P. knowlesi* (Mohring et al., 2019) will facilitate locus-specific gene editing to superimpose clinically relevant alleles onto experimental lines and offer the opportunity for allele-specific phenotyping *in vitro*. Genetically modified lines with *in vitro* phenotypic characters that carry a high suspicion of involvement in parasite virulence and following exhaustive experimentation will be deemed suitable to take forward *in vivo* for clinical phenotyping and translational research (**Figure 1**).

Our immediate goal is to promote third-generation genome sequencing and capacity strengthening in bioinformatics for routine genetic studies on clinical malaria in endemic countries. The outputs will create a repository that captures diversity and information on multiple gene families hitherto outside the remit of all but large centres mostly working on model parasites. Our long-term vision is to develop a precise experimental model system for severe malaria pathophysiology informed by clinical infections and culminating in *in vivo* disease phenotyping and translational research. A model that, for the first time, will have the power to characterise parasite allele-specific cause and effect. A model system that exploits the utility of *P. knowlesi*, a laboratory model, and *P. knowlesi* that is responsible for naturally acquire human disease.

Not the end of the story or perfect by any standard but our sequencing capability represents a significant step forward towards creating the means to understand malaria pathophysiology and to inform the rational design and development of adjunctive therapies for patients with severe malaria.

DATA AVAILABILITY STATEMENT

The raw data supporting the conclusions of this article will be made available by the authors, without undue reservation.

ETHICS STATEMENT

The studies involving human participants were reviewed and approved by University of St. Andrews. The patients/participants provided their written informed consent to participate in this study.

AUTHOR CONTRIBUTIONS

JC-S and CD conceived the work and wrote the manuscript. DRO did sample processing, sequencing, and bioinformatics. All authors contributed to the article and approved the submitted version.

FUNDING

DRO is supported by the Wellcome Trust ISSF award 204821/Z/16/Z. Bioinformatics and computational biology analyses were supported by the University of St Andrews Bioinformatics Unit (AMD3BIOINF), funded by Wellcome Trust ISSF award 105621/Z/14/Z. The sample BioBank was compiled with informed consent (Medial Research Council, www.mrc.ac.uk, grant G0801971). Genome sequencing was supported by Tenovus Scotland (T16/03).

REFERENCES

Ahmed, A. M., Pinheiro, M. M., Divis, P. C., Siner, A., Zainudin, R., Wong, I. T., et al. (2014). Disease progression in Plasmodium knowlesi malaria is linked to variation in invasion gene family members. *PloS Negl. Trop. Dis.* 8 (8), e3086. doi: 10.1371/journal.pntd.0003086

Ansari, H. R., Templeton, T. J., Subudhi, A. K., Ramaprasad, A., Tang, J., Lu, F., et al. (2016). Genome-scale comparison of expanded gene families in Plasmodium ovale wallikeri and Plasmodium ovale curtisi with Plasmodium malariae and with other Plasmodium species. *Int. J. Parasitol.* 46 (11), 685–696. doi: 10.1016/j.ijpara.2016.05.009

Assefa, S., Lim, C., Preston, M. D., Duffy, C. W., Nair, M. B., Adroub, S. A., et al. (2015). Population genomic structure and adaptation in the zoonotic malaria parasite Plasmodium knowlesi. *Proc. Natl. Acad. Sci. U.S.A.* 112 (42), 13027–13032. doi: 10.1073/pnas.1509534112

Auburn, S., Benavente, E. D., Miotto, O., Pearson, R. D., Amato, R., Grigg, M. J., et al. (2018). Genomic analysis of a pre-elimination Malaysian Plasmodium vivax population reveals selective pressures and changing

transmission dynamics. *Nat. Commun.* 9 (1), 2585. doi: 10.1038/s41467-018-04965-4

Barber, B. E., William, T., Jikal, M., Jilip, J., Dhararaj, P., Menon, J., et al. (2011). Plasmodium knowlesi malaria in children. *Emerg. Infect. Dis.* 17 (5), 814–820. doi: 10.3201/eid1705.101489

Barber, B. E., Rajahram, G. S., Grigg, M. J., William, T., and Anstey, N. M. (2017). World Malaria Report: time to acknowledge Plasmodium knowlesi malaria. *Malar. J.* 16 (1), 135. doi: 10.1186/s12936-017-1787-y

Barber, B. E., Grigg, M. J., Piera, K. A., William, T., Cooper, D. J., Plewes, K., et al. (2018a). Intravascular haemolysis in severe Plasmodium knowlesi malaria: association with endothelial activation, microvascular dysfunction, and acute kidney injury. *Emerg. Microbes Infect.* 7 (1), 106. doi: 10.1038/s41426-018-0105-2

Barber, B. E., Russell, B., Grigg, M. J., Zhang, R., William, T., Amir, A., et al. (2018b). Reduced red blood cell deformability in Plasmodium knowlesi malaria. *Blood Adv.* 2 (4), 433–443. doi: 10.1182/bloodadvances.2017013730

Benavente, E. D., Gomes, A. R., De Silva, J. R., Grigg, M., Walker, H., Barber, B. E., et al. (2019). Whole genome sequencing of amplified Plasmodium knowlesi DNA from unprocessed blood reveals genetic exchange events between Malaysian Peninsular and Borneo subpopulations. *Sci. Rep.* 9 (1), 9873. doi: 10.1038/s41598-019-46398-z

Butcher, G. A., and Mitchell, G. H. (2018). The role of Plasmodium knowlesi in the history of malaria research. *Parasitology* 145 (1), 6–17. doi: 10.1017/S0031182016001888

Campino, S., Marin-Menendez, A., Kemp, A., Cross, N., Drought, L., Otto, T. D., et al. (2018). A forward genetic screen reveals a primary role for Plasmodium falciparum Reticulocyte Binding Protein Homologue 2a and 2b in determining alternative erythrocyte invasion pathways. *PloS Pathog.* 14 (11), e1007436. doi: 10.1371/journal.ppat.1007436

Carlton, J. M., Adams, J. H., Silva, J. C., Bidwell, S. L., Lorenzi, H., Caler, E., et al. (2008). Comparative genomics of the neglected human malaria parasite Plasmodium vivax. *Nature* 455 (7214), 757–763. doi: 10.1038/nature07327

Chin, A. Z., Maluda, M. C. M., Jelip, J., Jeffree, M. S. B., Culleton, R., and Ahmed, K. (2020). Malaria elimination in Malaysia and the rising threat of Plasmodium knowlesi. *J. Physiol. Anthropol.* 39 (1), 36. doi: 10.1186/s40101-020-00247-5

Cooper, D. J., Rajahram, G. S., William, T., Jelip, J., Mohammad, R., Benedict, J., et al. (2020). Plasmodium knowlesi Malaria in Sabah, Malaysi-2017: Ongoing Increase in Incidence Despite Near-elimination of the Human-only Plasmodium Species. *Clin. Infect. Dis.* 70 (3), 361–367. doi: 10.1093/cid/ciz237

Cox-Singh, J., and Culleton, R. (2015). Plasmodium knowlesi: from severe zoonosis to animal model. *Trends Parasitol.* 31 (6), 232–238. doi: 10.1016/j.pt.2015.03.003

Cox-Singh, J., Davis, T. M., Lee, K. S., Shamsul, S. S., Matusop, A., Ratnam, S., et al. (2008). Plasmodium knowlesi malaria in humans is widely distributed and potentially life threatening. *Clin. Infect. Dis.* 46 (2), 165–171. doi: 10.1086/524888

Cox-Singh, J., Hiu, J., Lucas, S. B., Divis, P. C., Zulkarnaen, M., Chandran, P., et al. (2010). Severe malaria - a case of fatal Plasmodium knowlesi infection with post-mortem findings: a case report. *Malar. J.* 9:10. doi: 10.1186/1475-2875-9-10

Cox-Singh, J., Singh, B., Daneshvar, C., Planche, T., Parker-Williams, J., and Krishna, S. (2011). Anti-inflammatory cytokines predominate in acute human Plasmodium knowlesi infections. *PloS One* 6 (6), e20541. doi: 10.1371/journal.pone.0020541

Daneshvar, C., Davis, T. M., Cox-Singh, J., Rafa'ee, M. Z., Zakaria, S. K., Divis, P. C., et al. (2009). Clinical and laboratory features of human Plasmodium knowlesi infection. *Clin. Infect. Dis.* 49 (6), 852–860. doi: 10.1086/605439

Daneshvar, C., William, T., and Davis, T. M. E. (2018). Clinical features and management of Plasmodium knowlesi infections in humans. *Parasitology* 145 (1), 18–31. doi: 10.1017/S0031182016002638

Divis, P. C., Shokoples, S. E., Singh, B., and Yanow, S. K. (2010). A TaqMan real-time PCR assay for the detection and quantitation of Plasmodium knowlesi. *Malar. J.* 9, 344. doi: 10.1186/1475-2875-9-344

Divis, P. C., Singh, B., Anderios, F., Hisam, S., Matusop, A., Kocken, C. H., et al. (2015). Admixture in Humans of Two Divergent Plasmodium knowlesi Populations Associated with Different Macaque Host Species. *PloS Pathog.* 11 (5), e1004888. doi: 10.1371/journal.ppat.1004888

Divis, P. C. S., Duffy, C. W., Kadir, K. A., Singh, B., and Conway, D. J. (2018). Genome-wide mosaicism in divergence between zoonotic malaria parasite subpopulations with separate sympatric transmission cycles. *Mol. Ecol.* 27 (4), 860–870. doi: 10.1111/mec.14477

Farrington, L., Vance, H., Rek, J., Prahl, M., Jagannathan, P., Katureebe, A., et al. (2017). Both inflammatory and regulatory cytokine responses to malaria are blunted with increasing age in highly exposed children. *Malar. J.* 16 (1), 499. doi: 10.1186/s12936-017-2148-6

Feachem, R. G. A., Chen, I., Akbari, O., Bertozzi-Villa, A., Bhatt, S., Binka, F., et al. (2019). Malaria eradication within a generation: ambitious, achievable, and necessary. *Lancet* 394 (10203), 1056–1112. doi: 10.1016/S0140-6736(19)31139-0

Galinski, M. R., Lapp, S. A., Peterson, M. S., Ay, F., Joyner, C. J., LE Roch, K. G., et al. (2018). Plasmodium knowlesi: a superb in vivo nonhuman primate model of antigenic variation in malaria. *Parasitology* 145 (1), 85–100. doi: 10.1017/S0031182017001135

Gardner, M. J., Hall, N., Fung, E., White, O., Berriman, M., Hyman, R. W., et al. (2002). Genome sequence of the human malaria parasite Plasmodium falciparum. *Nature* 419 (6906), 498–511. doi: 10.1038/nature01097

Grigg, M. J., William, T., Barber, B. E., Rajahram, G. S., Menon, J., Schimann, E., et al. (2018). Age-Related Clinical Spectrum of Plasmodium knowlesi Malaria and Predictors of Severity. *Clin. Infect. Dis.* 67 (3), 350–359. doi: 10.1093/cid/ciy065

Hussin, N., Lim, Y. A., Goh, P. P., William, T., Jelip, J., and Mudin, R. N. (2020). Updates on malaria incidence and profile in Malaysia from 2013 to 2017. *Malar. J.* 19 (1), 55. doi: 10.1186/s12936-020-3135-x

Jiram, A. I., Ooi, C. H., Rubio, J. M., Hisam, S., Karnan, G., Sukor, N. M., et al. (2019). Evidence of asymptomatic submicroscopic malaria in low transmission areas in Belaga district, Kapit division, Sarawak, Malaysia. *Malar. J.* 18 (1), 156. doi: 10.1186/s12936-019-2786-y

Klaassen, C. H., Jeunink, M. A., Prinsen, C. F., Ruers, T. J., Tan, A. C., Strobbe, L. J., et al. (2003). Quantification of human DNA in feces as a diagnostic test for the presence of colorectal cancer. *Clin. Chem.* 49 (7), 1185–1187. doi: 10.1373/49.7.1185

Knowles, R., and Gupta, B. M. D. (1932). A Study of Monkey-Malaria, and Its Experimental Transmission to Man. *Ind. Med. Gaz* 67 (6), 301–320.

Kocken, C. H., Ozwara, H., van der Wel, A., Beetsma, A. L., Mwenda, J. M., and Thomas, A. W. (2002). Plasmodium knowlesi provides a rapid in vitro and in vivo transfection system that enables double-crossover gene knockout studies. *Infect. Immun.* 70 (2), 655–660. doi: 10.1128/iai.70.2.655-660.2002

Langhorne, J., and Cohen, S. (1979). Plasmodium knowlesi in the marmoset (Callithrix jacchus). *Parasitology* 78 (1), 67–76. doi: 10.1017/s0031182000048599

Lapp, S. A., Geraldo, J. A., Chien, J. T., Ay, F., Pakala, S. B., Batugedara, G., et al. (2018). PacBio assembly of a Plasmodium knowlesi genome sequence with Hi-C correction and manual annotation of the SICAvar gene family. *Parasitology* 145 (1), 71–84. doi: 10.1017/S0031182017001329

Lee, K. S., Cox-Singh, J., Brooke, G., Matusop, A., and Singh, B. (2009a). Plasmodium knowlesi from archival blood films: further evidence that human infections are widely distributed and not newly emergent in Malaysian Borneo. *Int. J. Parasitol.* 39 (10), 1125–1128. doi: 10.1016/j.ijpara.2009.03.003

Lee, K. S., Cox-Singh, J., and Singh, B. (2009b). Morphological features and differential counts of Plasmodium knowlesi parasites in naturally acquired human infections. *Malar. J.* 8, 73. doi: 10.1186/1475-2875-8-73

Liew, J. W. K., Mahpot, R. B., Dzul, S., Abdul Razak, H. A. B., Ahmad Shah Azizi, N. A. B., Kamarudin, M. B., et al. (2018). Importance of Proactive Malaria Case Surveillance and Management in Malaysia. *Am. J. Trop. Med. Hyg.* 98 (6), 1709–1713. doi: 10.4269/ajtmh.17-1010

Lindner, S. E., Swearingen, K. E., Shears, M. J., Walker, M. P., Vrana, E. N., Hart, K. J., et al. (2019). Transcriptomics and proteomics reveal two waves of translational repression during the maturation of malaria parasite sporozoites. *Nat. Commun.* 10 (1), 4964. doi: 10.1038/s41467-019-12936-6

Loy, D. E., Liu, W., Li, Y., Learn, G. H., Plenderleith, L. J., Sundararaman, S. A., et al. (2017). Out of Africa: origins and evolution of the human malaria parasites Plasmodium falciparum and Plasmodium vivax. *Int. J. Parasitol.* 47 (2-3), 87–97. doi: 10.1016/j.ijpara.2016.05.008

Loy, D. E., Plenderleith, L. J., Sundararaman, S. A., Liu, W., Gruszczyk, J., Chen, Y. J., et al. (2018). Evolutionary history of human Plasmodium vivax revealed by genome-wide analyses of related ape parasites. *Proc. Natl. Acad. Sci. U.S.A.* 115 (36), E8450–E8459. doi: 10.1073/pnas.1810053115

MacRae, C. A. (2019). Closing the 'phenotype gap' in precision medicine: improving what we measure to understand complex disease mechanisms. *Mamm. Genome* 30 (7-8), 201–211. doi: 10.1007/s00335-019-09810-7

Mandl, J. N., Schneider, C., Schneider, D. S., and Baker, M. L. (2018). Going to Bat(s) for Studies of Disease Tolerance. *Front. Immunol.* 9, 2112. doi: 10.3389/fimmu.2018.02112

Mills, C. D., Ley, K., Buchmann, K., and Canton, J. (2015). Sequential Immune Responses: The Weapons of Immunity. *J. Innate Immun.* 7 (5), 443–449. doi: 10.1159/000380910

Milner, D.A. Jr., Vareta, J., Valim, C., Montgomery, J., Daniels, R. F., Volkman, S. K., et al. (2012). Human cerebral malaria and Plasmodium falciparum genotypes in Malawi. *Malar. J.* 11, 35. doi: 10.1186/1475-2875-11-35

Mohring, F., Hart, M. N., Rawlinson, T. A., Henrici, R., Charleston, J. A., Diez Benavente, E., et al. (2019). Rapid and iterative genome editing in the malaria parasite Plasmodium knowlesi provides new tools for P. vivax research. *Elife* 8, 1–29. doi: 10.7554/eLife.45829

Moon, R. W., Hall, J., Rangkuti, F., Ho, Y. S., Almond, N., Mitchell, G. H., et al. (2013). Adaptation of the genetically tractable malaria pathogen Plasmodium knowlesi to continuous culture in human erythrocytes. *Proc. Natl. Acad. Sci. U.S.A.* 110 (2), 531–536. doi: 10.1073/pnas.1216457110

Noordin, N. R., Lee, P. Y., Mohd Bukhari, F. D., Fong, M. Y., Abdul Hamid, M. H., Jelip, J., et al. (2020). Prevalence of Asymptomatic and/or Low-Density Malaria Infection among High-Risk Groups in Peninsular Malaysia. *Am. J. Trop. Med. Hyg.* 103 (3), 1107–1110. doi: 10.4269/ajtmh.20-0268

Numbers, M. B. (2011). Microbiology by numbers. *Nat. Rev. Microbiol.* 9 (9), 628–628. doi: 10.1038/nrmicro2644

Onditi, F. I., Nyamongo, O. W., Omwandho, C. O., Maina, N. W., Maloba, F., Farah, I. O., et al. (2015). Parasite accumulation in placenta of non-immune baboons during Plasmodium knowlesi infection. *Malar. J.* 14:118. doi: 10.1186/s12936-015-0631-5

Otto, T. D., Bohme, U., Sanders, M., Reid, A., Bruske, E. I., Duffy, C. W., et al. (2018). Long read assemblies of geographically dispersed Plasmodium falciparum isolates reveal highly structured subtelomeres. *Wellcome Open Res.* 3, 52. doi: 10.12688/wellcomeopenres.14571.1

Ozwara, H., Langermans, J. A., Maamun, J., Farah, I. O., Yole, D. S., Mwenda, J. M., et al. (2003). Experimental infection of the olive baboon (Paplio anubis) with Plasmodium knowlesi: severe disease accompanied by cerebral involvement. *Am. J. Trop. Med. Hyg.* 69 (2), 188–194. doi: 10.4269/ajtmh.2003.69.188

Pain, A., Bohme, U., Berry, A. E., Mungall, K., Finn, R. D., Jackson, A. P., et al. (2008). The genome of the simian and human malaria parasite Plasmodium knowlesi. *Nature* 455 (7214), 799–803. doi: 10.1038/nature07306

Pasini, E. M., Zeeman, A. M., Voorberg-VAN DER Wel, A., and Kocken, C. H. M. (2018). Plasmodium knowlesi: a relevant, versatile experimental malaria model. *Parasitology* 145 (1), 56–70. doi: 10.1017/S0031182016002286

Petersen, E., Koopmans, M., Go, U., Hamer, D. H., Petrosillo, N., Castelli, F., et al. (2020). Comparing SARS-CoV-2 with SARS-CoV and influenza pandemics. *Lancet Infect. Dis.* 20 (9), e238–e244. doi: 10.1016/S1473-3099(20)30484-9

Pinheiro, M. M., Ahmed, M. A., Millar, S. B., Sanderson, T., Otto, T. D., Lu, W. C., et al. (2015). Plasmodium knowlesi genome sequences from clinical isolates reveal extensive genomic dimorphism. *PloS One* 10 (4), e0121303. doi: 10.1371/journal.pone.0121303

Plewes, K., Turner, G. D. H., and Dondorp, A. M. (2018). Pathophysiology, clinical presentation, and treatment of coma and acute kidney injury complicating falciparum malaria. *Curr. Opin. Infect. Dis.* 31 (1), 69–77. doi: 10.1097/QCO.0000000000000419

Praba-Egge, A. D., Montenegro, S., Cogswell, F. B., Hopper, T., and James, M. A. (2002). Cytokine responses during acute simian Plasmodium cynomolgi and Plasmodium knowlesi infections. *Am. J. Trop. Med. Hyg.* 67 (6), 586–596. doi: 10.4269/ajtmh.2002.67.586

Raja, T. N., Hu, T. H., Kadir, K. A., Mohamad, D. S. A., Rosli, N., Wong, L. L., et al. (2020). Naturally Acquired Human Plasmodium cynomolgi and P. knowlesi Infections, Malaysian Borneo. *Emerg. Infect. Dis.* 26 (8), 1801–1809. doi: 10.3201/eid2608.200343

Rajahram, G. S., Barber, B. E., William, T., Menon, J., Anstey, N. M., and Yeo, T. W. (2012). Deaths due to Plasmodium knowlesi malaria in Sabah, Malaysia: association with reporting as Plasmodium malariae and delayed parenteral artesunate. *Malar. J.* 11, 284. doi: 10.1186/1475-2875-11-284

Shearer, F. M., Huang, Z., Weiss, D. J., Wiebe, A., Gibson, H. S., Battle, K. E., et al. (2016). Estimating Geographical Variation in the Risk of Zoonotic Plasmodium knowlesi Infection in Countries Eliminating Malaria. *PloS Negl. Trop. Dis.* 10 (8), e0004915. doi: 10.1371/journal.pntd.0004915

Siao, M. C., Borner, J., Perkins, S. L., Deitsch, K. W., and Kirkman, L. A. (2020). Evolution of Host Specificity by Malaria Parasites through Altered Mechanisms Controlling Genome Maintenance. *mBio* 11 (2), 1–6. doi: 10.1128/mBio.03272-19

Singh, B., and Daneshvar, C. (2013). Human infections and detection of Plasmodium knowlesi. *Clin. Microbiol. Rev.* 26 (2), 165–184. doi: 10.1128/CMR.00079-12

Singh, B., Kim Sung, L., Matusop, A., Radhakrishnan, A., Shamsul, S. S., Cox-Singh, J., et al. (2004). A large focus of naturally acquired Plasmodium knowlesi infections in human beings. *Lancet* 363 (9414), 1017–1024. doi: 10.1016/S0140-6736(04)15836-4

Su, X. Z., Lane, K. D., Xia, L., Sa, J. M., and Wellems, T. E. (2019). Plasmodium Genomics and Genetics: New Insights into Malaria Pathogenesis, Drug Resistance, Epidemiology, and Evolution. *Clin. Microbiol. Rev.* 32 (4), 1–29. doi: 10.1128/CMR.00019-19

Sutherland, C. J., Tanomsing, N., Nolder, D., Oguike, M., Jennison, C., Pukrittayakamee, S., et al. (2010). Two nonrecombining sympatric forms of the human malaria parasite Plasmodium ovale occur globally. *J. Infect. Dis.* 201 (10), 1544–1550. doi: 10.1086/652240

Verzier, L. H., Coyle, R., Singh, S., Sanderson, T., and Rayner, J. C. (2019). Plasmodium knowlesi as a model system for characterising Plasmodium vivax drug resistance candidate genes. *PloS Negl. Trop. Dis.* 13 (6), e0007470. doi: 10.1371/journal.pntd.0007470

White, N. J. (2018). Anaemia and malaria. *Malar. J.* 17 (1), 371. doi: 10.1186/s12936-018-2509-9

William, T., Menon, J., Rajahram, G., Chan, L., Ma, G., Donaldson, S., et al. (2011). Severe Plasmodium knowlesi malaria in a tertiary care hospital, Sabah, Malaysia. *Emerg. Infect. Dis.* 17 (7), 1248–1255. doi: 10.3201/eid1707.101017

Willmann, M., Ahmed, A., Siner, A., Wong, I. T., Woon, L. C., Singh, B., et al. (2012). Laboratory markers of disease severity in Plasmodium knowlesi infection: a case control study. *Malar. J.* 11, 363. doi: 10.1186/1475-2875-11-363

World-Health-Organization (2013). *Management of Severe Malaria - A Practical Handbook. 3rd ed* (Geneva: Worldhealth Organization).

World-Health-Organization (2019). *World Malaria Report 2019* (Geneva: Licence: CC BY-NC-SA 3.0 IGO.).

Conflict of Interest: The authors declare that the research was conducted in the absence of any commercial or financial relationships that could be construed as a potential conflict of interest.

frontiers in Cellular and Infection Microbiology

ORIGINAL RESEARCH
published: 24 March 2021
doi: 10.3389/fcimb.2021.637604

Sickle Cell Trait Modulates the Proteome and Phosphoproteome of *Plasmodium falciparum*-Infected Erythrocytes

Margaux Chauvet[1,2], *Cerina Chhuon*[3], *Joanna Lipecka*[3], *Sébastien Dechavanne*[2,4,5], *Célia Dechavanne*[1], *Murielle Lohezic*[1], *Margherita Ortalli*[1,2], *Damien Pineau*[1,2], *Jean-Antoine Ribeil*[6], *Sandra Manceau*[2,6], *Caroline Le Van Kim*[2,4,5], *Adrian J. F. Luty*[1], *Florence Migot-Nabias*[1], *Slim Azouzi*[2,4,5], *Ida Chiara Guerrera*[3] and *Anaïs Merckx*[1,2*]

[1] Université de Paris, MERIT, IRD, Paris, France, [2] Laboratoire d'Excellence GR-Ex, Paris, France, [3] Université de Paris, Proteomics Platform Necker, Structure Fédérative de Recherche Necker, Inserm US24/CNRS, UMS3633, Paris, France, [4] Université de Paris, Inserm, BIGR, Paris, France, [5] Institut National de la Transfusion Sanguine, Paris, France, [6] Biotherapy Department, Necker Children's Hospital, Assistance Publique-Hôpitaux de Paris, Paris, France

OPEN ACCESS

Edited by:
Deirdre A. Cunningham,
Francis Crick Institute,
United Kingdom

Reviewed by:
Hayley Bullen,
Burnet Institute, Australia
Jack Adderley,
RMIT University, Australia

***Correspondence:**
Anaïs Merckx
anais.merckx@parisdescartes.fr

Specialty section:
This article was submitted to Parasite and Host, a section of the journal Frontiers in Cellular and Infection Microbiology

Received: 03 December 2020
Accepted: 23 February 2021
Published: 24 March 2021

Citation:
Chauvet M, Chhuon C, Lipecka J, Dechavanne S, Dechavanne C, Lohezic M, Ortalli M, Pineau D, Ribeil JA, Manceau S, Le Van Kim C, Luty AJF, Migot-Nabias F, Azouzi S, Guerrera IC and Merckx A (2021) Sickle Cell Trait Modulates the Proteome and Phosphoproteome of Plasmodium falciparum-Infected Erythrocytes. Front. Cell. Infect. Microbiol. 11:637604. doi: 10.3389/fcimb.2021.637604

The high prevalence of sickle cell disease in some human populations likely results from the protection afforded against severe *Plasmodium falciparum* malaria and death by heterozygous carriage of HbS. *P. falciparum* remodels the erythrocyte membrane and skeleton, displaying parasite proteins at the erythrocyte surface that interact with key human proteins in the Ankyrin R and 4.1R complexes. Oxidative stress generated by HbS, as well as by parasite invasion, disrupts the kinase/phosphatase balance, potentially interfering with the molecular interactions between human and parasite proteins. HbS is known to be associated with abnormal membrane display of parasite antigens. Studying the proteome and the phosphoproteome of red cell membrane extracts from *P. falciparum* infected and non-infected erythrocytes, we show here that HbS heterozygous carriage, combined with infection, modulates the phosphorylation of erythrocyte membrane transporters and skeletal proteins as well as of parasite proteins. Our results highlight modifications of Ser-/Thr- and/or Tyr- phosphorylation in key human proteins, such as ankyrin, β-adducin, β-spectrin and Band 3, and key parasite proteins, such as RESA or MESA. Altered phosphorylation patterns could disturb the interactions within membrane protein complexes, affect nutrient uptake and the infected erythrocyte cytoadherence phenomenon, thus lessening the severity of malaria symptoms.

Keywords: ***Plasmodium falciparum*, hemoglobin S, erythrocyte, membrane phosphorylation, proteomics**

Abbreviations: BCA, Bi-cinchoninic acid; BSA, Bovine serum albumin; CPDA, Citrate-phosphate-dextrose with adenine; ECL, Electrochemiluminescence; FASP, Filter aided sample preparation; FDR, False discovery rate; G6PD, Glucose-6-phosphate dehydrogenase; Hb, Hemoglobin; HO, Hoechst; HPLC, High-performance liquid chromatography; iRBCs, infected RBCs; LFQ, Label-free quantification; MACS, Magnetic-activated cell sorting; MCs, Maurer's clefts; MESA, Mature parasite-infected erythrocyte surface antigen; MS, Mass spectrometry; PCR-RFLP, Polymerase chain reaction – restriction fragments length polymorphisms; *Pf*EMP1, *Plasmodium falciparum* erythrocyte membrane protein 1; RBCs, Red blood cells; RESA, Ring-infected erythrocyte surface antigen; ROM1, Rhomboid protease 1; Ser or S, Serine; TBS, Tris buffered saline; TFA, Trifluoroacetic acid; Thr or T, Threonine; Tyr or Y, Tyrosine.

INTRODUCTION

Hemoglobin (Hb) S erythrocyte abnormality is due to a genetic mutation resulting from the replacement of a glutamate at the sixth position within the β-globin chain by a valine in normal Hb (HbA) (Flint et al., 1998). The homozygous carriage of HbS (HbSS) results in sickle cell disease (SCD) which has serious pathological consequences such as anemia and vaso-occlusive crises and can be life-threatening. SCD is highly prevalent in human populations living in malaria endemic areas. The highest frequencies of HbS homozygous and heterozygous forms are indeed observed in sub-Saharan Africa, the Middle East, and India, reaching up to 25% (Migot-Nabias et al., 2000) and could result from the protection afforded by HbS heterozygous carriage (HbAS) against severe *Plasmodium falciparum* malaria-related symptoms and death without serious hematological disadvantage (Piel et al., 2010; Gonçalves et al., 2016). The HbAS genotype, commonly called sickle cell trait, is less clinically visible than the HbSS one.

P. falciparum asexual multiplication within human red blood cells (RBCs) leads to malaria symptoms. During this phase, *P. falciparum* exports proteins into the erythrocyte cytosol and membrane in order to remodel the host cell and allow it to prosper in this environment. Some of the most profound changes in infected erythrocytes comprise protrusions at the surface, termed « knobs », and vesicular cisternae in the RBC cytosol, called « maurer's clefts » (MCs). Export of proteins involves the remodeling of host actin by the parasite, to connect MCs and MCs-originated vesicles to the host cell cytoskeleton and membrane (Rug et al., 2014). Knobs display « *P. falciparum* erythrocyte membrane protein 1 » (*Pf*EMP1) that mediates the cytoadherence of infected RBCs (iRBCs) to microvascular blood vessel endothelium, thus preventing clearance of iRBCs by the spleen. The resulting obstruction of the microvasculature in the brain and other organs is considered to be one of the major contributors to the pathology associated with the most severe forms of malaria (Miller et al., 2002).

The molecular mechanisms of the protection conferred against severe malaria symptoms by abnormal HbS are still only partially understood and under active investigation. Previous studies showed that HbAS erythrocytes display impaired parasite-induced host actin reorganization and incompletely developed MCs, leading to reduced and impaired protein export (Cholera et al., 2008; Fairhurst et al., 2012). Furthermore, these RBCs display reduced amounts of adhesins which are aberrantly presented as they are anchored in enlarged and dispersed knobs, correlating with reduced cytoadherence capacity. Oxidative stress caused by HbS instability underlies the aberrant development of the parasite, insofar as an oxidative insult conferred to HbAA RBCs can promote the same phenotypic discrepancies (Cyrklaff et al., 2016).

The underlying erythrocyte membrane based-skeleton is known to play a major role in the function of the RBC membrane as well as in parasite knobs' organization. This cytoskeleton is physically linked to the membrane by vertical interactions at two key sites: the AnkyrinR and the 4.1R complexes (Mankelow et al., 2012). Abnormalities in erythrocyte membrane proteins have been observed in RBC disorders and are often associated with an increase of oxidative stress on proteins themselves or with perturbations in intracellular signaling pathways such as the balance between phosphatase/kinase functions (Pantaleo et al., 2010a). The phosphoproteome of the AnkyrinR complex and the erythrocyte membrane (George et al., 2010) is affected in HbSS RBCs. This altered phosphorylation of skeleton proteins may affect membrane deformability, increasing fragility and rigidity of the erythrocyte (George et al., 2010).

Both parasite infection and HbS promote oxidative stress in RBCs, which can subsequently modify the phosphorylative status of human and parasite proteins. Phosphorylation is indeed a key mechanism for parasite development and could be disturbed by HbS. Previous studies showed that the kinase/phosphatase equilibrium alteration could influence cytoadherence of iRBCs to endothelial receptors (Dorin-Semblat et al., 2019), erythrocyte membrane channel activities (Merckx et al., 2008) and membrane mechanical properties of iRBCs (Nunes et al., 2010). Therefore, we hypothesized that modulation of protein phosphorylation in iRBCs could be one mechanism underlying the relative protection conferred by HbS against malaria.

The present study has investigated the impact of heterozygous HbS carriage, as well as of *P. falciparum* infection, on the phosphorylative states of protein components of the erythrocyte cytoskeleton and membrane, and of parasite proteins. To this end, the phosphoproteome and the proteome of erythrocyte ghosts and parasite proteins from *P. falciparum* infected and non-infected homozygous HbAA and heterozygous HbAS RBCs were analyzed by mass spectrometry after TiO_2 enrichment, and by western blots.

The mass spectrometry analysis describes phosphorylation differences of both RBCs and parasite proteins. Those alterations concerned erythrocyte skeleton - interacting parasite proteins, erythrocyte transporters, membrane and skeletal proteins and could be involved in the regulation of molecular interactions within membrane protein complexes, such as the cytoadherence complex, and in the regulation of the functions of these proteins.

MATERIALS AND METHODS

Blood Samples

HbAA and HbAS erythrocytes were obtained from voluntary donors, after written informed consent obtained in accordance with the Declaration of Helsinki at Necker-Enfants-Malades hospital (Committee for the Protection of Persons n°DC 2014-2272). This study was approved and conducted according to institutional ethical guidelines of the National Institute for Blood Transfusion (INTS, Paris, France). Blood was collected in tubes containing citrate-phosphate-dextrose with adenine (CPDA). RBCs were then separated from plasma and leucocytes by three washings in RPMI 1640 medium (*Gibco-ThermoFisher Scientific*) and were stored maximum 24hrs at 4°C before use, or cryoconserved.

DNA Extraction

Genomic DNA was extracted from the donor's leucocytes with the DNeasy Blood and Tissue Kit (*Qiagen*). The concentration and

the quality of DNA were evaluated by measuring the absorbance at 260 nm and 280 nm with a Nanodrop spectrophotometer.

Hemoglobin Genotyping

Hemoglobin genotypes were determined by polymerase chain reaction – restriction fragments length polymorphisms (PCR-RFLP) adapted from Badaut et al. (2015), and according to the GoTaqFlexi DNA Polymerase (*Promega*) manufacturer requirements.

Plasmodium falciparum-Infected Erythrocyte Culture

P. falciparum strain 3D7 was grown *in vitro* in human HbAA and HbAS erythrocytes according to the procedures of "Methods in Malaria Research" (https://www.beiresources.org/portals/2/MR4/Methods_In_Malaria_Research-6th_edition.pdf) adapted from Trager and Jensen (1976). Briefly, infected erythrocytes were cultured in RPAS (RPMI-Albumax-Serum) medium (RPMI 1640 medium (*Gibco*) supplemented with 25 mM HEPES (*Gibco*), 2 mM L-glutamine (*Gibco*), 0.05 mg/ml gentamicin (*Gibco*), 2% human serum and 0.5% of Albumax). Cultures were maintained at 5% hematocrit in a gas mixture of 2% O_2, 5.5% CO_2 and 92.5% N_2 and incubated at 37°C. HbAA and HbAS RBCs from donors were infected with late trophozoite and schizont-infected HbAA erythrocytes obtained after magnetic-activated cell sorting (MACS) (*Miltenyi Biotec*), allowing the separation of erythrocytes infected with hemozoin expressing-parasites. Non-infected blood from the same donors was cultured in the same conditions and the media was changed every day. Infected RBCs were collected after 3 parasite life cycles. A MACS was performed when parasites were mainly late trophozoites and/or early schizonts. After MACS, parasitemia of infected RBCs was adjusted at 45% with non-infected RBCs providing from the same blood donor. Non-infected RBCs were also collected for ghost's production.

For proteome and phosphoproteome analysis, fresh blood from 3 HbAA and 3 HbAS donors was used. Ghosts and parasite proteins were prepared on three occasions, with one HbAA and one HbAS sample each time ($HbAA_1$ and $HbAS_1$ were used simultaneously, so as $HbAA_2$ with $HbAS_2$, and $HbAA_3$ with $HbAS_3$). As phosphorylation of proteins can change with time after blood collection (Azouzi et al., 2018), HbAA and HbAS blood were sampled the same day, washed, infected and collected at the same time. The same experimental procedure was performed for all coupled HbAA-HbAS samples.

Determination of *Plasmodium falciparum* Growth by Flow Cytometry

Growth assays were performed with cryoconserved erythrocytes (from $HbAA_1$, $HbAA_2$, $HbAS_1$ and $HbAS_2$ blood donors) that were thawed for this experiment. Parasitemia was determined by flow cytometry every 24hrs. For each condition, 100 µl of resuspended culture were sampled and fixed with phosphate-buffered saline (PBS)-1% paraformaldehyde for 30 minutes at room temperature. Then, 10^{11} cells (in PBS) per well were distributed in a 96-well plate. RBCs were labeled with PBS – Hoechst (BD Biosciences, Hoechst 34580) (HO) (1 µg/ml) and incubated 45 minutes at 37°C in the dark before acquisition and analysis by flow cytometry (FACS Canto II BD). Using FlowJo software, the geomean values of HO fluorescence were used to characterize the parasitemias.

For parasites growth in fresh blood for proteomics analysis, blood smears were also performed every 24hrs and observed by microscopy to follow *P. falciparum* growth and observe the parasite stages.

Preparation of Erythrocyte Ghosts

HbAA and HbAS erythrocyte ghosts (RBC membranes and cytoskeleton) were obtained by hypotonic lysis at 4°C of either infected or non-infected erythrocytes according to a protocol from Azouzi et al. (2015). The RBCs were first washed three times in PBS 1X and then incubated with 10 volumes of lysis buffer (5 mM Na_2HPO_4, 0.35 mM EDTA, pH 8.0 with proteases (*Roche Diagnostics*) and phosphatases inhibitors (*Sigma-Aldrich*)) for 5 minutes on ice. Solutions were afterwards centrifuged at 50,000 x g for 20 minutes at 4°C. For the infected samples, the ghost layer was collected in a new tube to separate ghosts from parasite pellet. The reddish supernatant (containing hemoglobin) was removed, and the ghosts and parasites were washed in lysis buffer until the pellets became colorless. Protein extraction from erythrocyte membranes and parasites was performed by adding one volume of extraction buffer 3X (3% NP40 (*Sigma-Aldrich*), 3% SDS (*Fluka*), 90 mM Tris pH 8, 3 mM EDTA, pH 8 with proteases (*Roche Diagnostics*) and phosphatases inhibitors (*Sigma-Aldrich*)) to two volumes of each pellet. For parasite extracts, a supplementary sonication step was realized to solubilize the proteins. The protein content was measured by BCA (bi-cinchoninic acid) assay (Micro BCA™ Protein Assay Kit, *ThermoFischer Scientific*). The preparations were finally stored at -80°C until analysis.

Sample Preparation and Mass Spectrometry

Proteins, from erythrocyte membrane or from parasite extracts, (100 µg) were first solubilized in 2% SDS pH 7.5 and heated at 95°C for 5 minutes. Samples were then reduced with 0.1 M dithiothreitol (*Sigma-Aldrich*) at 60°C for 1 hour. Mass spectrometry (MS) sample preparation was performed using a filter aided sample preparation (FASP) method according to Lipecka et al. (2016). We set aside 10% of the peptides for total ghost proteome analysis, while the remaining sample was used for phosphopeptide enrichment, according to the schematic workflow (**Figure 1**).

Phosphopeptide Enrichment by Titanium Dioxide (TiO_2)

Phosphopeptide enrichment was carried out using a Titansphere TiO_2 Spin tips (3 mg/200 µL, Titansphere PHOS-TiO (*GL Sciences Inc*) on the digested proteins for each biological replicate according to manufacturer's instructions. Samples were applied to the TiO_2 Spin tips three times in total in order to increase the adsorption of the phosphopeptides to the TiO_2. Phosphopeptides were eluted by the sequential

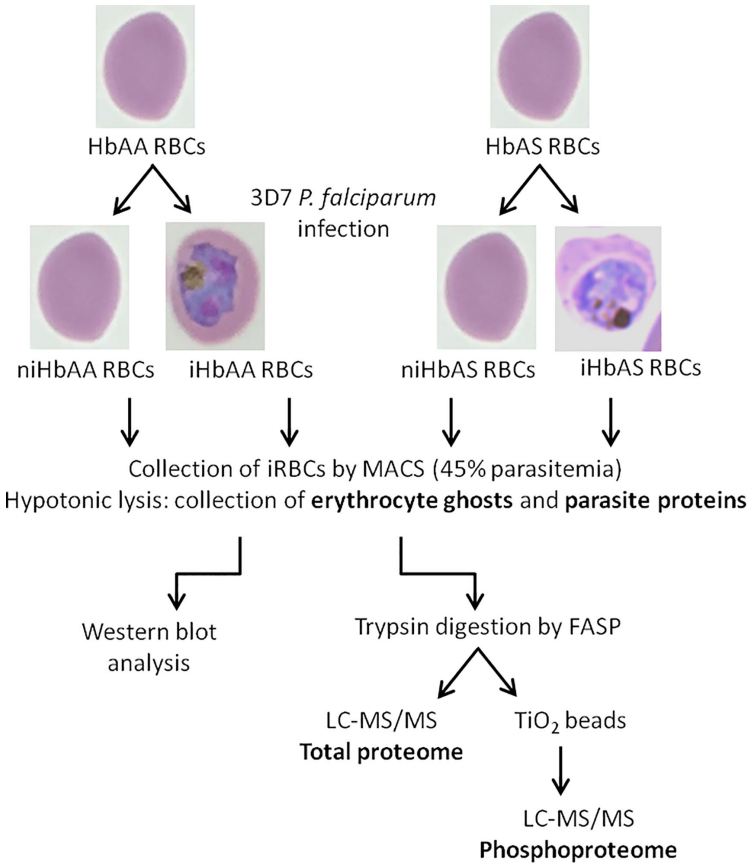

FIGURE 1 | Schematic workflow of infected and non-infected HbAA and HbAS erythrocytes proteome and phosphoproteome experimental procedures – HbAA and HbAS erythrocytes were collected and infected *in vitro* with the 3D7 *P. falciparum* strain. Mature trophozoite/schizont-infected RBCs were collected by MACS (45% parasitemia) and lysed to produce ghosts and collect parasites. Membrane erythrocyte lysates were analyzed by western blot. For mass spectrometry, after trypsin digestion of proteins, phosphopeptides were enriched on TiO_2 columns and analyzed by LC-MS/MS. Total proteomes of erythrocyte and parasite proteins were also generated. i, infected; ni, non-infected.

addition of 50 µL of 5% NH_4OH and 50 µL of 5% pyrrolidine. Phosphopeptides were washed and eluted with 70 µL of 0.1% trifluoroacetic acid (TFA), 80% acetonitrile high-performance liquid chromatography (HPLC)-grade (1,000 x g for 3 minutes) and vacuum dried.

NanoLC-MS/MS Protein Identification and Quantification

Samples were resuspended in 10 µL of 0.1% TFA in HPLC-grade water. For each run, 1 µL was injected in a nanoRSLC-Q Exactive PLUS (RSLC Ultimate 3000) (*Thermo Scientific*). Phosphopeptides were loaded onto a µ-precolumn (Acclaim PepMap 100 C18, cartridge, 300 µm i.d.×5 mm, 5 µm) (*Thermo Scientific*), and were separated on a 50 cm reversed-phase liquid chromatographic column (0.075 mm ID, Acclaim PepMap 100, C18, 2 µm) (*Thermo Scientific*). Phosphopeptides were analyzed using mass spectrometry parameters according to Meijer et al. (2017).

The MS files were processed with the MaxQuant software version 1.5.8.3 and searched with Andromeda search engine against a merged database of human from Swissprot 2011-10-19 and *P. falciparum* from Swissprot and PlasmoDB 8.1 (26047 entries in total). MS files from total ghosts (proteome) and from TiO_2 enriched peptides (phosphoproteome) were searched using two parameters groups. To search parent mass and fragment ions, we set a mass deviation of 4.5 ppm and 20 ppm respectively. Strict specificity for trypsin/P cleavage was required, allowing up to two missed cleavage sites. Carbamidomethylation (Cysteine) was set as fixed modification, whereas oxidation (Methionine) and N-term acetylation were set as variable modifications. For the analysis of MS files issued of TiO_2 enrichment, the variable modification of phosphorylation on S, T and Y was also added. The false discovery rates (FDRs) at the protein and peptide level were set to 1%. Scores were calculated in MaxQuant as described previously (Cox and Mann, 2008). Match between runs was allowed. The reverse hits were removed from MaxQuant output. Proteins were quantified according to the MaxQuant label-free algorithm using label-free quantification (LFQ) intensities (Cox and Mann, 2008; Cox et al., 2014) and phosphopeptides according to intensity; protein and peptide quantification were obtained using at least one peptide per protein.

Statistical and bioinformatic analysis, including heatmaps, profile plots and clustering, were performed with Perseus software (version 1.6.0.7) freely available at www.perseus-framework.org (Tyanova et al., 2016). For statistical comparison of the ghost proteome, we set four groups niHbAA, iHbAA, niHbAS, iHbAS. Each group contained three biological replicates (different donors). Each sample was also run in technical triplicates.

For total ghost proteome analysis, we analyzed the proteingroups.txt file. Protein LFQ intensities were transformed in log (2). Proteins were separated into *Plasmodium* and human to select the RBC derived proteins. We filtered the data to keep only proteins with at least three valid values in at least one group. Data were imputed to fill missing data points by creating a Gaussian distribution of random numbers with a standard deviation of 33% relative to the standard deviation of the measured values and 1.8 standard deviation downshift of the mean to simulate the distribution of low signal values. We performed an ANOVA test, p-value<0.01, S0 = 0.1.

For phosphopeptide analysis, we analyzed the Phospho (STY).txt file. Phosphopeptide intensities were transformed in log (2), site table was expanded to analyze all phosphosites separately. Phosphosites were separated into *Plasmodium* and human to select the RBC derived phosphoproteins. We filtered the data to keep only phosphosites with at least three valid values in at least one group. Only phosphosites with at least 0.75 of localization probability were retained. Phosphosite intensities were normalized by subtracting the median and adding a constant (25). Data were imputed to fill missing data as described above. We performed an ANOVA to compare the four groups, p-value<0.05, S0 = 0.1. To evaluate the influence of the genotype on the infection, and if it induces variations, we also performed a two-way ANOVA test, separating the infection and the genotype factors, interaction p-value<0.05. Data were imputed to fill missing values points by creating a Gaussian distribution of random numbers with a standard deviation of 33% relative to the standard deviation of the measured values and 3 standard deviation downshift of the mean to simulate the distribution of very low signal values. We performed a t-test to compare the parasite phosphoproteome after infection in HbAA vs HbAS, FDR<0.05, S0 = 0.5.

Hierarchical clustering of phosphosites/proteins that survived the tests was performed in Perseus on log-transformed LFQ intensities after z-score normalization of the data, using Euclidean distances.

The mass spectrometry proteomics data have been deposited to the ProteomeXchange Consortium *via* the PRIDE (Perez-Riverol et al., 2019) partner repository with the dataset identifier PXD023280.

SDS-PAGE and Western Blot

To complete our proteome and phosphoproteome analysis, all erythrocyte ghost samples were also analyzed by anti-Band 3 and anti-pY Band 3 western blots (**Figure 1**).

Ghost lysates (20 µg) were mixed with 5X loading buffer (1.25 mM sucrose, 20% SDS, 250 mM Tris-HCl, 25% β-mercaptoethanol, 1% bromophenol blue, pH 6.8) and heated at 70°C for 10 minutes. Proteins were separated by 4-12% gradient SDS-PAGE under reducing conditions and then transferred to nitrocellulose membrane (Trans-Blot® Turbo™ RTA Mini Nitrocellulose Transfer Kit) (*BioRad*). Blots were blocked with tris buffered saline (TBS) – 5% bovine serum albumin (BSA) (*Roche Diagnostics*), then probed with primary antibodies (mouse anti-Band 3 monoclonal IgG 1,20000 (*Sigma-Aldrich*), rabbit anti-pY^{359} Band 3 polyclonal IgG 1,10000 (*Abcam*), rabbit anti-pY^{21} Band 3 polyclonal IgG 1,10000 (*Abcam*) or rabbit anti-p55, 1,50000, used as a loading control, in TBS- 5% BSA) and finally with the appropriate peroxidase-conjugated secondary antibody (goat anti-rabbit polyclonal IgG 1,5000 (*Jackson ImmunoResearch (Interchim)*), or goat anti-mouse polyclonal IgG 1,5000 (*Jackson ImmunoResearch (Interchim))* applied in TBS - 5% BSA. Detection was performed using the electrochemiluminescence (ECL) Plus Western blotting detection system (*Amersham Biosciences*).

Anti-pY^{21} Band 3/- pY^{359} Band 3 and p55 western blots were performed on the same membrane. These membranes were then stripped and incubated with mouse anti-Band 3 antibody. After ensuring that the loading was similar for each condition with p55 western blots, Image Lab 6.0.1 software was used to measure the intensity of pY^{21} Band 3, pY^{359} Band 3 and Band 3 band signals. Subsequently, as inter-individual variations cannot be excluded, pY^{21} Band 3 or pY^{359} Band 3 intensities were normalized according to the corresponding Band 3 intensity for all donors.

RESULTS

Characterization of Hemoglobin Genotype of Blood Donors

For all the experiments, we obtained blood from three abnormal Hb carriers ($HbAS_1$, $HbAS_2$, and $HbAS_3$), and from three normal Hb carriers ($HbAA_1$, $HbAA_2$, $HbAA_3$). We verified their Hb genotype by PCR-RFLP and compared their profiles to control DNA. We confirmed that all the abnormal Hb carriers were HbAS and all the normal Hb ones were HbAA (**Supplementary Figure 1**). All information concerning the donors and their genotypes is summarized in **Supplementary Table 1**.

Parasite Growth Is Slower in HbS Heterozygous Carriage Than in HbAA Red Blood Cells

Before collecting infected erythrocytes in order to prepare ghosts and harvest parasites, we compared *P. falciparum* growth in HbAA versus HbAS RBCs. We assessed parasite replication rates by flow cytometry in RBCs provided from two HbAA and two HbAS donors. We observed a significant slower replication rate for *P. falciparum* grown in HbAS RBCs (**Figure 2**). Although parasite growth seems very low for parasites inside HbAS erythrocyte, parasites grew, and progressed from schizonts to ring and from ring to schizonts in HbAS erythrocytes. Microscopic observation revealed no difference in the proportions of different parasites developmental stages during the two first cycles of replication up to 96 h post-infection. From

the third cycle onwards, however, we observed a slight retardation of parasite growth in HbAS erythrocytes (**Figure 2B**).

Erythrocyte Membrane Proteome as a Function of *Plasmodium falciparum* Infection and/or Abnormal Hemoglobin S Carriage

Therefore, to investigate the proteome and phosphoproteome of *Plasmodium falciparum*-infected HbAA and HbAS erythrocytes, parasite development in the two types of RBCs was allowed to proceed for three cycles, and was assessed *via* sequential blood smears, to allow for adequate adaptation to the host cells. Infected RBCs were collected at the same parasite stage after 140 ± 2 h post-infection (**Figure 1**). We ensured that parasites were at the same stages (late trophozoites and early schizonts) in HbAA and HbAS RBCs, with blood smears made just prior to MACS (**Figure 2B**).

The total ghost proteome analyses led to identification of 1438 proteins across all samples, of which 910 were human (65%) (**Supplementary Table 2**) and 528 parasite proteins (35%). Most proteins identified were part of the erythrocyte cytoskeleton or transporters, confirming the enrichment in erythrocyte ghosts.

We observed significant differences in the quantity of 35 erythrocyte proteins according to infection and/or HbS carriage (**Supplementary Table 2**, in green) (p-value <0.05) after an ANOVA test. Performing hierarchical biclustering, we identified 4 main clusters of proteins according to their intensity variations (**Figure 3**). Some proteins were of particular interest because their quantity varied according to both *P. falciparum* infection and Hb genotype. Compared to infected RBC and heterozygous HbS carriage, i) the protein lin-7 homolog A/C (black arrow) was detected less frequently in

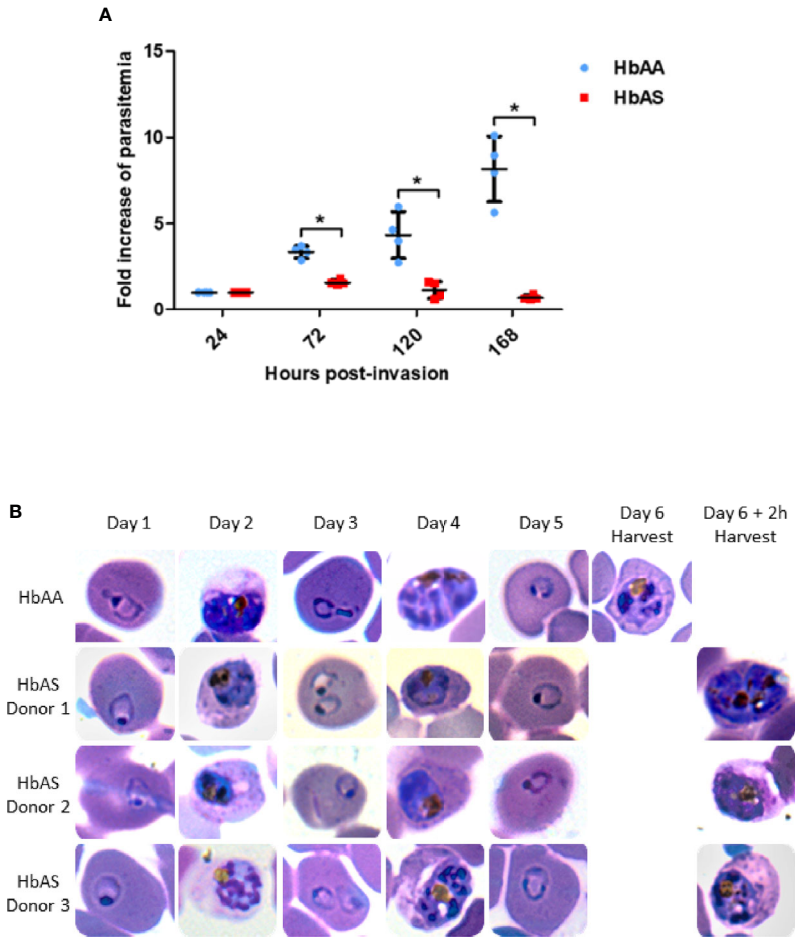

FIGURE 2 | Parasite replication in HbAA and HbAS RBCs assessed by flow cytometry **(A)** and by blood smears **(B)**. Invasion of 2 HbAA (HbAA1 and HbAA2) and 2 HbAS (HbAS1 and HbAS2) blood samples from the cryobank of the the French National Immunohematology Reference Laboratory (CNRGS), was realized at t = 0h. Parasitemia was assessed every 24h. To visualize the fold increase of parasitemia, all parasitemia values were divided by the initial parasitemia measured 24h post-infection. Technical duplicates were performed for each donor, and replicate values for each point were loaded on the graph. Unpaired Mann-Whitney t-test (p-value<0.05) was used to compare values from HbAA and HbAS groups at 24h, 72h, 120h and 168 h., asterisks (*) indicate significantly different values **(A)**. Parasite development in one HbAA (HbAA1 as a reference) and 3 HbAS (HbAS1, HbAS2 and HbAS3) blood donors erythrocytes. Invasion of fresh blood samples was realized at t = 0h. Blood smears were performed every 24h for six days. At day 6, blood smears were realized right before MACS collection **(B)**.

infected HbAA ghosts and ii) Heme-binding protein 1, and UPF0687 protein C20orf27 (Cluster 3), were detected more frequently in HbAA infected samples.

Erythrocyte Membrane Phosphoproteome as a Function of *Plasmodium falciparum* Infection and/or Abnormal Hemoglobin S Carriage

Phosphoproteomic analysis led to the quantification of 499 phosphosites from erythrocytic proteins, of which 413 serines (Ser or S), 81 threonines (Thr or T) and only 4 tyrosines (Tyr or Y). Performing an ANOVA test, we observed significant differences in the phosphorylation intensity of several erythrocyte proteins in association with *P. falciparum* infection and/or abnormal HbS carriage (p-value<0.05) (**Supplementary Table 3**). We identified 58 differentially phosphorylated sites corresponding to 33 distinct proteins (**Figure 4**). Most of the differential phosphosites were serine residues (44 serines, 13 threonines and 1 tyrosine). Among these phosphosites, 50 had already been described; the 8 remaining were identified in the present work for the first time, corresponding to 6 different new phosphoproteins. For each phosphosite, we ensured that its phosphorylation variation was not due to a different quantity of the corresponding protein, according to the global proteome analysis by LC-MS/MS of all samples (**Supplementary Table 2**).

Hierarchical clustering identified 5 residue phosphorylation modulation profiles (**Figure 4**). Cluster 1 is composed of 11 phosphosites over-phosphorylated in infected erythrocytes, including 5 sites that have already been described as "infection specific" in a meta-analysis of phosphoproteomic studies of *P. falciparum* iRBCs (Bouyer et al., 2016) (S^{726} and T^{724} of α-adducin, S^{1301} of β-spectrin, T^{238} of GLUT1 and S^{849} of protein 4.1), validating our analytical approach. Cluster 4 included sites presenting decreased phosphorylation intensities due to the infection of RBCs (Y^{359} of Band 3, S^{1381} of Tensin-1, S^{365} and S^{366} of Serine/threonine-protein kinase MARK2). First, these results confirmed previous data by detecting the same phosphorylation sites. Second, these results complete previous data by quantifying the phosphorylation intensities according to Hb genotypes and infection status. The decrease in phosphorylation intensities was not detected in previous studies that analyzed in some cases only infected RBCs. This analysis also identified two clusters containing phosphosites for which the phosphorylation state depended on Hb status, cluster 3 and cluster 5. Pattern 2 and two proteins (black arrows) were of particular interest because they were proteins for which the phosphorylation state was strongly modified depending on the combination of both infection and abnormal Hb carriage. The phosphorylation intensity of S^{31} of Serine/threonine protein kinase STK11 was stronger in non-infected HbAA RBCs. Cluster

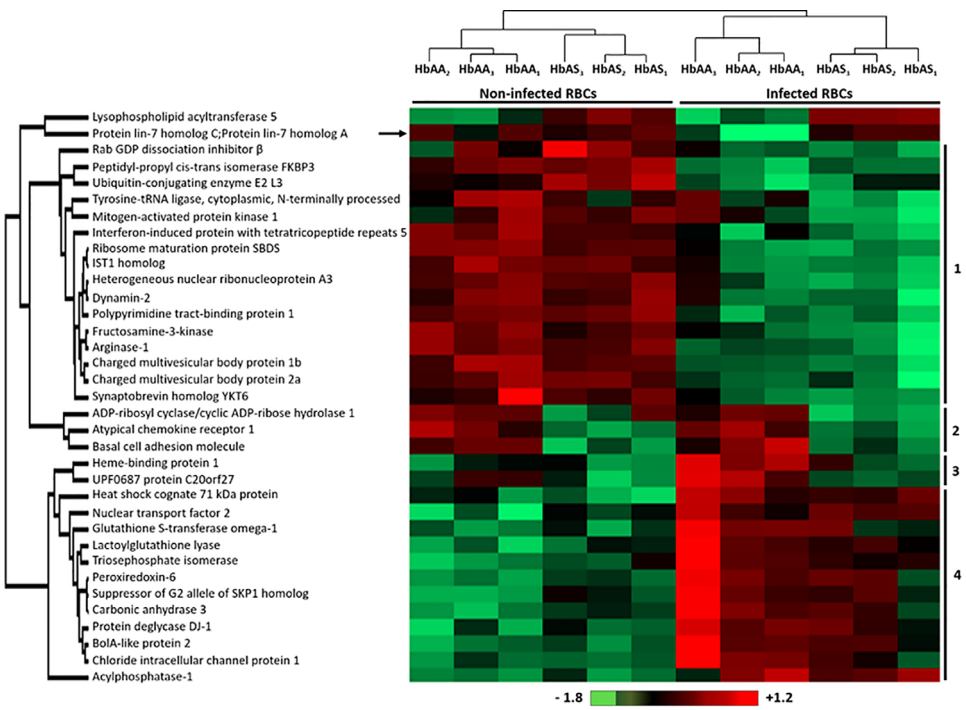

FIGURE 3 | Differentially detected human erythrocyte proteins as a function of *P. falciparum* infection and/or HbAS genotype. Six HbAA (non-infected and infected $HbAA_1$, $HbAA_2$, and $HbAA_3$) and six HbAS (non-infected and infected $HbAS_1$, $HbAS_2$, and $HbAS_3$) erythrocyte ghost samples were analyzed by hierarchical clustering based on the detected quantity of RBC proteins (ANOVA test, p-value < 0.05). Samples are displayed horizontally (columns) and proteins are shown vertically (rows). The more the protein is represented in light red, the more it is detected in the corresponding sample, and the more it is colored in light green, the less it is detected. The color bar represents $\log_2$ Z score fold-change. Proteins are clustered according to their quantity profile, represented by dendograms. Black arrow: protein profile that cannot be associated with a cluster.

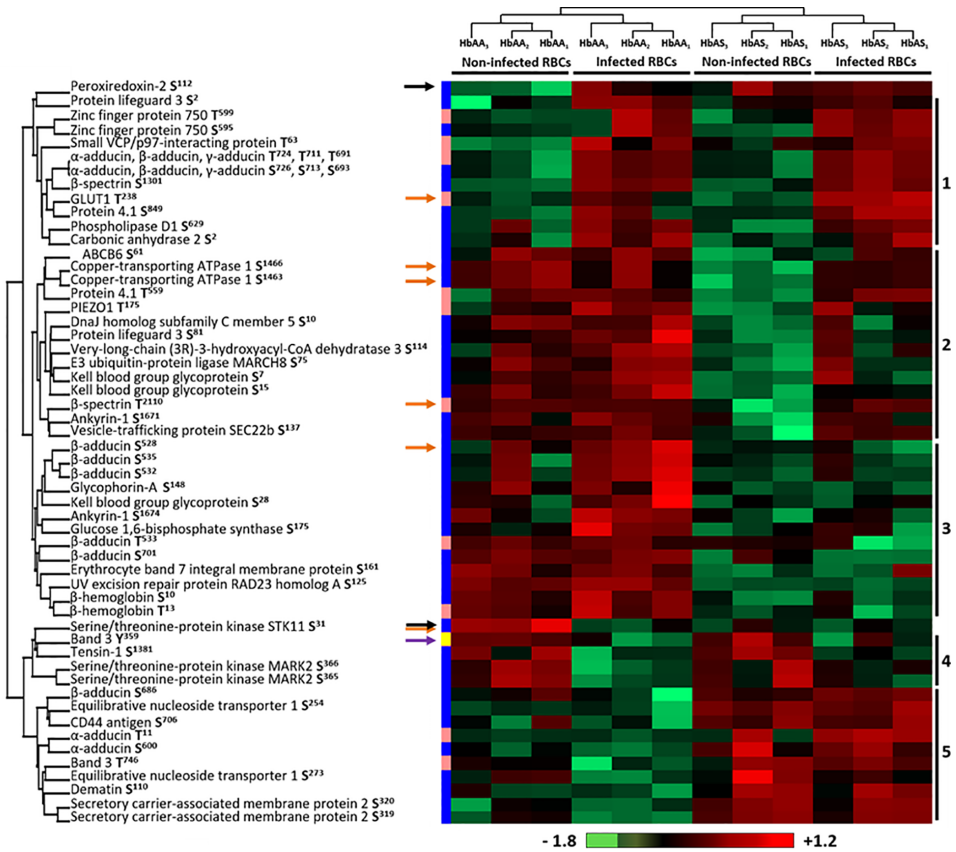

FIGURE 4 | Differentially phosphorylated sites of human erythrocyte proteins as a function of *P. falciparum* infection and/or HbAS genotype. Six HbAA (non-infected and infected $HbAA_1$, $HbAA_2$, and $HbAA_3$) and six HbAS (non-infected and infected $HbAS_1$, $HbAS_2$ and $HbAS_3$) were analyzed by hierarchical clustering based on the phosphorylation rate of a specific site of RBC proteins (ANOVA test, p-value < 0.05). Samples are displayed horizontally (columns) and proteins are shown vertically (rows). Sites are specified next to the protein name. The more the site is represented in light red, the more it is phosphorylated in the corresponding sample, and the more it is colored in light green, the less it is phosphorylated. The color bar represents $\log_2$ Z score fold-change. On the left, threonine (T) residues are in pink, serines (S) in blue and tyrosine (Y) in yellow. Proteins are clustered according to their phosphorylation profile, represented by dendograms. Black arrows: protein profiles that cannot be associated with a cluster, orange arrows: phosphosites differentially phosphorylated according to both *P. falciparum* infection and abnormal heterozygous HbS carriage.

2 was composed of S^{61} of ATP-binding cassette transporter subfamily B member 6, S^{1463} and S^{1466} of Copper-transporting ATPase 1, T^{559} of protein 4.1, T^{175} of PIEZO1, S^{10} of DnaJ homolog subfamily C member 5, S^{81} of Protein lifeguard 3, S^{114} of Very-long-chain (3R)-3-hydroxyacyl-CoA dehydratase 3, S^{75} of E3 ubiquitin-protein ligase MARCH8, S^{7} and S^{15} of Kell, T^{2110} of β-spectrin, S^{1671} of Ankyrin-1 and S^{137} of Vesicle-trafficking protein SEC22b. These sites displayed a lower intensity of phosphorylation specifically in non-infected HbAS RBCs. Finally, the phosphorylation intensity of S^{112} of Peroxiredoxin-2 increased in all HbAS samples and infected HbAA ghosts. This protein protects cells against oxidative stress and its function can be regulated by phosphorylation (Rhee and Kil, 2017). This result may be the consequence of the oxidative stress generated by both *P. falciparum* infection and HbS.

We then performed a two-ways ANOVA to visualize the phosphosites differentially phosphorylated according to both *P. falciparum* infection and abnormal heterozygous HbS carriage (**Supplementary Table 3**) (p-value<0.05). Six phosphosites were identified, corresponding to 5 different proteins (orange arrows).

Plasmodium falciparum Infection Modulates Band 3 Tyrosine-Phosphorylation

TiO_2-based enrichment has similar affinity for the serine, threonine and tyrosine, but the proportion of phosphosites is correlated with the frequency of these phosphosites in the cell. As tyrosine-phosphorylation is less represented, it would require additional steps to collect tyrosine-phosphopeptides or the use of alternative approaches.

For this reason, the erythrocyte ghosts were also investigated by anti-phospho-tyrosine western blot (**Figure 1**). Band 3 protein is the major known target of erythrocyte tyrosine kinases (Ferru et al., 2011), and the enhancement of its tyrosine-phosphorylation due to oxidative stress has been

described in previous reports (Pantaleo et al., 2010b; Ferru et al., 2011). Band 3 is known to be phosphorylated upon oxidative stress on several tyrosine residues including Y^{21} and Y^{359} by Syk and Lyn kinases, respectively. We confirmed the modulation of Band 3 Y^{359} phosphorylation in our mass spectrometry analysis (purple arrow in **Figure 4**). Thus, after ensuring that the same amount of protein was loaded for each sample using an anti-p55 western blot, we used specific anti-pY^{21} and anti-pY^{359} Band 3 antibodies (complete Western blots are provided in **Supplementary Figures 2** and **3**). Band 3 Y^{21} phosphorylation intensity increased with *P. falciparum* infection in both HbAA and HbAS erythrocytes (**Figures 5A, C**). We observed that Band 3 Y^{359} phosphorylation intensity decreased with infection in both HbAA and HbAS RBCs (**Figures 5B, D**). This result confirms the profile observed for the same phosphosite in mass spectrometry (**Figure 4**). Furthermore, the decreased phosphorylation intensity of Band 3 Y^{359} is significantly less marked in HbAS than in HbAA RBCs.

Parasite Phosphoproteome as a Function of Abnormal Hemoglobin S Carriage

Within the proteome and the phosphoproteome analysis, we also focused on the parasite proteins and we analyzed them according to Hb genotype of the erythrocyte in which *P. falciparum* grew (**Figure 1**). Proteome analysis revealed no significant difference in the protein amounts, with profiles showing individual variability. Phosphoproteome analysis identified 27 phosphosites that were differentially phosphorylated according to Hb genotype, corresponding to 14 different phosphoproteins (Student *t*-test, *p*-value<0.05) (**Supplementary Table 4**). Performing hierarchical clustering, we could identify two patterns of phosphorylation profiles (**Figure 6**). Cluster 1 included phosphorylation sites in 8 proteins such as ring-infected erythrocyte surface antigen (RESA), Antigen 332 – DBL like protein, mature parasite-infected erythrocyte surface antigen (MESA), and unknown proteins with the following PlasmoDB identifiers, MAL13P1.380 (PF3D7_1343800), PFI0345w (PF3D7_0907200), PFL0555c (PF3D7_1211200) for which phosphorylation intensities were greater when parasites were cultured in HbAS RBCs than in HbAA RBCs. Cluster 2 was composed of phosphosites from 8 proteins, including Rhomboid protease 1 (ROM1), PFE1485w (PF3D7_052980), PF07_0016 (PF3D7_0704300), PFL1930w (PF3D7_1239800), PF11_0233 (PF3D7_1122500), MAL8P1.29 (PF3D7_0825000), PF14_0343 (PF3D7_1436200) and PFF0535c (PF3D7_0610900). All the phosphosites of cluster 2 were serines and showed higher phosphorylation intensities in parasites grown in HbAA compare to HbAS erythrocytes.

DISCUSSION

This project aimed to measure the impact of HbS on proteomic and phosphoproteomic regulation of *P. falciparum*-infected

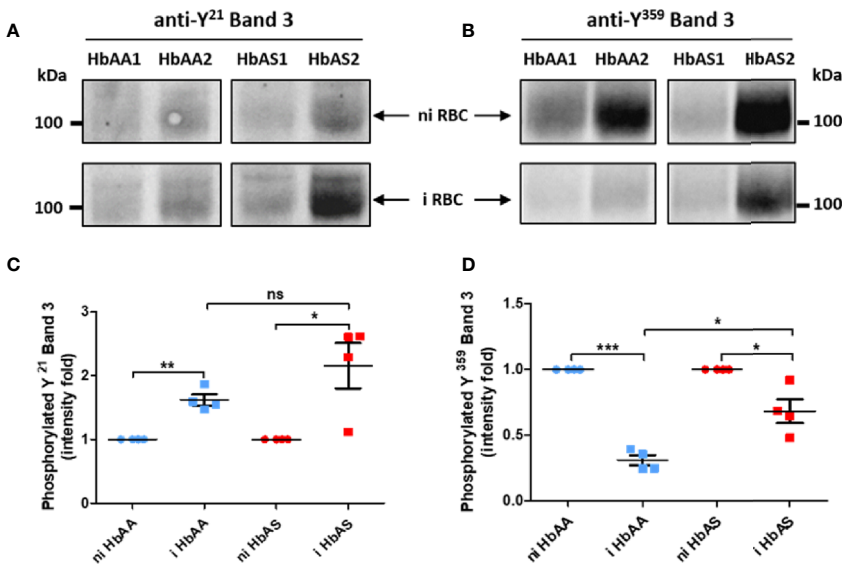

FIGURE 5 | Differences of Band 3 Y^{21} **(A, C)** and Y^{359} **(B, D)** phosphorylation according to P. falciparum infection and abnormal hemoglobin S carriage. 4-12% gradient gels were loaded with 20 µg/lane of ghost protein extracts from 2 HbAA (HbAA1 and HbAA2) and 2 HbAS (HbAS1 and HbAS2) donors. After separation of erythrocyte ghost lysate proteins by SDS-PAGE and transfer on nitrocellulose, tyrosine (Y)-phosphorylation was analyzed using anti-phosphoY21 **(A)** and anti-phosphoY359 **(B)** Band 3 antibodies. Tyrosine phosphorylation intensities were measured with Image Lab software, and these intensities were normalized to Band 3 quantity detected on the same membrane by western blot. For each sample, the phosphorylation intensity value of infected condition was reported to the non-infected condition intensity value **(C, D)**. Independent western blots were realized twice, and technical replicate values for each point were loaded on the graph. Phosphorylation fold intensities for HbAA and HbAS samples were represented in blue and red respectively, with non-infected (circles) and infected (square) ghosts. Paired t-test (*p-value < 0.05; **p-value < 0.01, and ***p-value < 0.001) were performed to compare intensities from the same genotype group (HbAA or HbAS) donors. Unpaired Mann-Whitney t-test (*p-value < 0.05; **p-value < 0.01, and ***p-value < 0.001) was used to compare intensities from infected HbAA and infected HbAS donors. i, infected; ni, non-infected; ns, not significant.

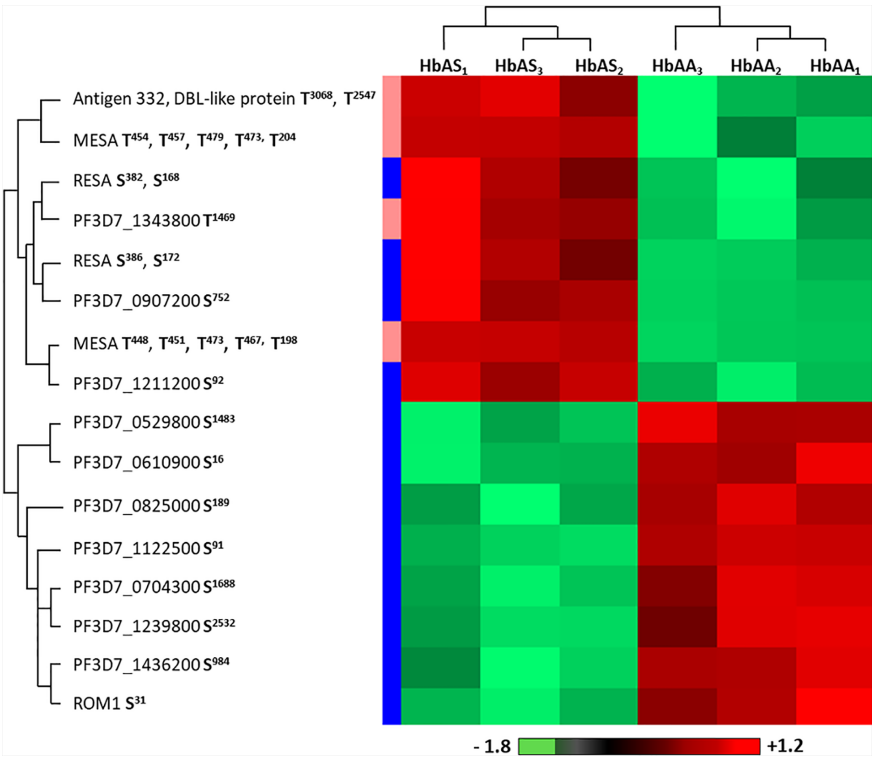

FIGURE 6 | Differentially phosphorylated sites of parasite proteins according to hemoglobin genotype. Parasites from three HbAA (infected $HbAA_1$, $HbAA_2$, and $HbAA_3$) and three HbAS (infected $HbAS_1$, $HbAS_2$, and $HbAS_3$) extracts were analyzed by hierarchical clustering based on the phosphorylation's rate of a specific site of RBC proteins (Student's *t*-test, *p*-value < 0.05). Samples are displayed horizontally (columns) and proteins are shown vertically (rows). Phosphosites are specified next to the protein name. The more the site is represented in dark red, the more it is phosphorylated in the corresponding sample, and the more it is colored in light green, the less it is phosphorylated. The color bar represents $\log_2$ Z score fold-change. On the left, threonine (T) residues are in pink and serines (S) in blue. Proteins are clustered according to their phosphorylation profile, represented by dendograms.

erythrocyte membrane proteins. We considered the impact of oxidative stress generated by both HbS heterozygous carriage and *P. falciparum* infection, because it could disturb the kinase/phosphatase equilibrium. Previous studies have investigated the phosphoproteome of HbSS and normal RBCs (George et al., 2010), or of HbAA erythrocytes after *P. falciparum* infection (Bouyer et al., 2016). To our knowledge, however, the phosphoproteome of HbAS RBCs has never been studied before. This study is also the first experimental, comparative and quantitative analysis of parasite and human protein phosphorylation of HbAA- and HbAS-infected erythrocyte membranes.

Other erythrocyte genetic abnormalities, such as α-thalassemia and glucose-6-phosphate dehydrogenase (G6PD) deficiency, can also confer protection against malaria (Taylor et al., 2013; Kakande et al., 2020) and coexist in populations affected by HbS in malaria endemic areas. Thus, the co-carriages of these other RBC disorders with HbS have been considered in this work (**Supplementary Figures S4–S6**). Investigation in the present study of cumulative erythrocyte disorders along with HbS led to the identification of G6PD deficiency carriages for the $HbAS_2$ and $HbAS_3$ donors. Also, $HbAS_2$ and $HbAS_3$ were heterozygous for α-thalassemia. We cannot exclude that these additional mutations may have an effect on *Plasmodium falciparum* infection. It is of note that the consequences of the interactions between sickle cell trait and G6PD deficiency with respect to malaria resistance conferred to carriers is still controversial. Further studies need to be performed to analyze and identify any epistasis between these two genetic disorders (Esoh and Wonkam, 2021). In our proteomics works, statistical analyses were performed in order to conserve only proteins that were differentially phosphorylated or abundant in all the HbAS samples compared to all HbAA samples. Moreover, our cohort, albeit small, reflects the reality, as the co-carriage of HbS with G6PD deficiency and alpha-thalassemia are frequently found in malaria endemic areas (Chauvet et al., 2019; Okafor et al., 2019). It is also important to note here that one of our donors, $HbAS_1$, only has sickle cell trait. However, to decipher accurately the impact of each mutation and of each combination of mutations on parasite development, further studies with large cohorts including individual carriage of these different genetic disorders, and all possible combinations of co-carriage of genetic disorders, should be conducted. Our own published work highlighted the importance of considering multiple RBC genotypes in studies of parasite antigen presentation at the erythrocyte surface.

P. falciparum growth was compared in HbAA and HbAS RBCs in our culture conditions. Indeed, parasite development in HbAS erythrocytes can be inhibited according to culture medium and atmospheric conditions, notably in hypoxia (Archer et al., 2018). We followed the course of parasite growth either by flow cytometry or blood smears over at least three cycles, in RBCs from HbAA and HbAS donors, and observed a lower replication rate for parasites grown in HbAS RBCs. These data could be seen as consistent with HbAS-conferred resistance against *P. falciparum* malaria. Although it is better to work with fresh blood, previous studies demonstrated similar results with cryoconserved erythrocytes (Egan et al., 2018; Kariuki et al., 2020), so for convenience, cryoconserved RBCs can be used.

Concerning erythrocyte proteins, modifications of both quantity and phosphorylation were identified, as summarized in **Figure 7**. Proteomic analysis revealed a group of proteins for which the quantity varied according to both infection and HbAS genotype. The current literature on Protein Lin-7 homolog A/C in red cells

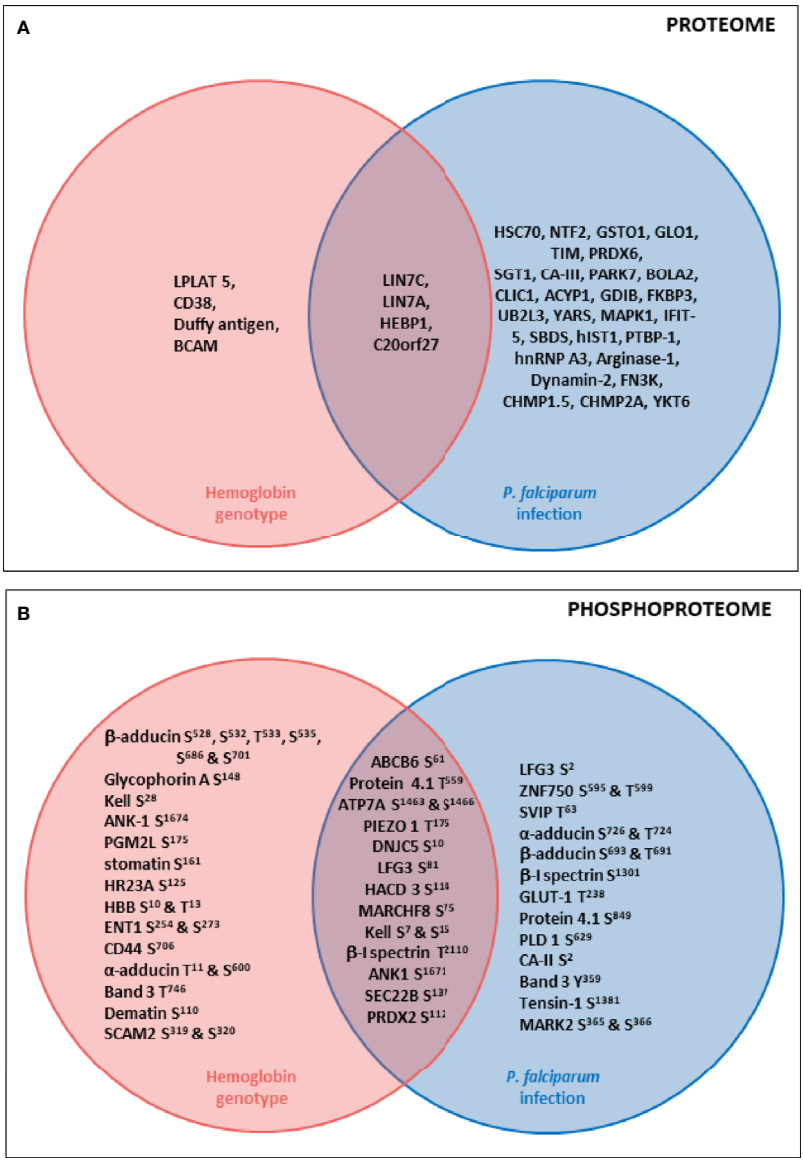

FIGURE 7 | Summary diagrams of proteome **(A)** and phosphoproteome **(B)** modulations of erythrocyte proteins according to *P. falciparum* infection and HbS carriage. Venn diagrams describing proteins whose quantity **(A)** or phosphorylation intensity **(B)** are varying according to hemoglobin genotype, *P. falciparum* infection or both parameters. Uniprot short names of proteins were represented, and phosphosites indicated. Erythrocyte proteins whose quantity **(A)** or phosphorylation intensity **(B)** was varying according to only hemoglobin genotype (ANOVA test) were presented in the pink circle. Erythrocyte proteins whose quantity **(A)** or phosphorylation intensity **(B)** was varying according to only *P. falciparum* infection (ANOVA test) were presented in the blue circle. Erythrocyte proteins whose quantity **(A)** or phosphorylation intensity **(B)** was varying according to both hemoglobin genotype and *P. falciparum* infection (ANOVA test) were presented in the junction between the pink and the blue circle.

does not allow us to explain the decrease in its quantity in iRBC HbAA. However, the HEBP1 protein was of particular interest. Indeed, this protein binds to free porphyrinogens and facilitates the elimination of elements potentially toxic for the cell (Jacob Blackmon et al., 2002). To our knowledge, no link between this protein and *P. falciparum* infection metabolism has ever been established. However, one can imagine that this protein could be necessary for the detoxification of the free heme generated during *P. falciparum* growth, because the quantity of this protein detected at the erythrocyte membrane increases with infection in HbAA RBCs. Heme detoxification is a key mechanism for parasite development, and is notably targeted in the development of drugs for malaria. However, the quantity of HEBP1 detected by mass spectrometry analysis does not increase in HbAS ghosts with *P. falciparum* infection. Therefore, it can be hypothesized that hemozoin formation and heme detoxification could be altered in HbAS RBCs.

Furthermore, the « Atypical chemokine receptor 1 » protein, also known as Duffy antigen, was detected at lower levels in the HbAS erythrocyte membrane. The Duffy antigen is known to be a receptor for the parasite *Plasmodium vivax*. Moreover, the Duffy null blood group confers protection against *P. vivax* malaria (Langhi and Bordin, 2006). To our knowledge, protection conferred by this blood group against *P. falciparum* malaria has never been described. A recent study reported a clinical case where a HbSS individual did not present any protection against *P. vivax* malaria (Moiz and Majeed, 2018). However, a more frequent association between HbS and Duffy null blood group has been observed, this combination being potentially selected in areas where *P. falciparum* and *P. vivax* malaria are both frequent (Gelpi and King, 1976), in particular in sub-Saharan Africa, a region from which the 3 HbAS blood donors originate. But for now, these observations don't allow us to suggest any mechanistic hypothesis regarding the potential role of a lower amount of Duffy antigen in conferring resistance to *P. falciparum* RBC invasion in HbAS carriers.

In our phosphoproteome analysis, proteins from 4 main groups were identified : (i) proteins from the Ankyrin-R complex (ankyrin, Band 3, β spectrin, stomatin, and glycophorin A); (ii) proteins from the junctional complex (protein 4.1, dematin, α, β and γ adducins, CD44, Duffy and Kell); (iii) carriers and channels (GLUT1, ENT1, PIEZO1, Secretory carrier-associated membrane protein 2, ABCB6 and Band 3); and (iv) kinases (Serine/threonine-protein kinase MARK2, Serine/threonine-protein kinase STK11). These phosphorylation changes could have an impact on the function of the different proteins, and thus on the structure and stability of the membrane of iRBCs. Indeed, phosphorylation of β spectrin by the casein kinase 1, associated with the membrane, leads to decreased mechanical stability of the membrane (Manno et al., 1995). Phosphorylation of dematin by the parasite kinase FIKK (Brandt and Bailey, 2013), or by a PKA, seems to disturb its function, interfering with its binding with actin and spectrin (Lalle et al., 2011). Finally, phosphorylation of protein 4.1 following infection (Chishti et al., 1994) inhibits its ability to promote the interaction between actin and spectrin, reducing membrane stability (Manno et al., 1995) and could participate in parasite-induced modifications of membrane properties.

These modifications could also modulate erythrocyte membrane permeability. During its intra-erythrocytic development, *P. falciparum* uses some of these transporters for its metabolism. In our work, we have shown that the protein ABCB6, a heme transporter, displayed lower phosphorylation intensity in non-infected HbAS RBCs, compared to infected HbAS, and infected or non-infected HbAA erythrocytes. However, a study recently observed that ABCB6-deficient RBCs were resistant to invasion by *P. falciparum* (Egan et al., 2018).

The two-way ANOVA test highlighted sites at which the phosphorylation intensity varied according to both infection and HbAS genotype. The lack of antibodies corresponding to those phosphosites did not allow us to validate the observed variations of phosphorylation intensities by western blot. All the identified modifications could thus be involved in regulation of *P. falciparum* development and in molecular interactions in the membrane protein complexes, such as the cytoadherence complex, which is associated with the cytoadherence of iRBCs and therefore with severe forms of malaria.

Concerning parasite proteins, although the proteome appeared unchanged according to our observations, the phosphorylation intensities of serines and threonines of some parasite proteins, such as RESA, MESA, *Pf*332 and ROM1, did vary according to the Hb genotype of the RBCs. RESA is a protein involved in parasite RBC invasion that is expressed from the ring stage, where it plays a major role in the reduction of membrane deformability. After invasion, RESA is phosphorylated and binds close to the site of auto-association of β spectrin dimers. This binding stabilizes the spectrin tetramer, by preventing the dimer dissociation that is necessary for invasion, strengthening the RBC membrane and preventing other invasion events (Pei et al., 2007). MESA is a phosphoprotein associated with the erythrocyte skeleton that interacts with 4.1 protein, at a position involved in the formation of the ternary complex (between p55, GPC and 4.1). MESA competes with p55 for the binding of 4.1 protein, and could thus impact iRBC membrane skeleton stability (Waller et al., 2003). Binding of MESA with 4.1 protein is crucial for parasite survival in the RBC, and also for correct localization of MESA in the erythrocyte skeleton (Black et al., 2008). MESA also binds to the cytoskeletal protein ankyrin (Kilili et al., 2019). Moreover, *Pf*332, a MCs resident peripheral protein, is associated with the erythrocyte cytoskeleton, at the schizont stage, where it binds to actin (Waller et al., 2010). *Pf*332 plays a role in membrane rigidity reduction, for *Pf*EMP1 trafficking and for iGRs adherence (Glenister et al., 2009). Indeed, RBCs infected by *Pf*332-deficient parasites are more rigid, express less *Pf*EMP1 and display lower adherence to CD36. Finally, ROM1 plays a role in the parasitophorous vacuole formation (Vera et al., 2011). It is also able to cleave AMA1, and adhesins during parasite invasion. There is no evidence in the literature of parasite-protein sites for which modifications of phosphorylation intensity have been described. However, the corresponding proteins play a role in iRBC membrane and cytoskeleton remodeling, in order to modify their rigidity and adherence properties. Thus, we can hypothesize that the altered cytoadherence and remodeling of HbAS iRBCs membranes could be linked to the alteration of the phosphorylation status of these proteins. Moreover, our results

suggest that HbS is also able to modulate parasite functions. One could also hypothesize that the parasite is able to adapt itself to the different environment of these abnormal RBCs by influencing the phosphorylation balance.

The parasite does not express any classical tyrosine kinase, but only tyrosine kinase-like (Abdi et al., 2013). Numerous studies have demonstrated the importance of the equilibrium in the tyrosine kinase and phosphatase activities during the intra-erythrocytic parasite life. Band 3 was chosen to study the potential Y phosphorylation differences due to HbAS genotype and infection. An increase of Band 3 Y^{21} phosphorylation intensity with infection was observed for HbAA and HbAS donors. However, a decrease of Band 3 Y^{359} phosphorylation intensity with infection was seen for these same donors. The number of donors is low, and we could not exclude individual variation. However, although not statistically detected in MS, the decreased Band 3 Y^{359} phosphorylation intensity appeared to be less important for HbAS donors than for HbAA donors in our western blot analysis. That the reduction of phosphorylation intensity in HbAS was less than that seen in HbAA iRBCs at the end of the parasite cycle could regulate Band 3 interactions with other erythrocyte membrane proteins and participate in the deregulation of erythrocyte membrane stability. Indeed, Y^{359} belongs to the Band 3 binding domain for 4.1 protein (Lux, 2016). Moreover, a recent study suggests that regulation of Band 3 phosphorylation is associated with the erythrocyte membrane destabilization needed for merozoite egress at the end of the intra-erythrocytic cycle (Pantaleo et al., 2017). Variations of Band 3 phosphorylation could be thus associated with altered parasite egress, and could explain the lower parasite replication rate observed in HbAS iRBCs.

Finally, this investigation of the proteome and the phosphoproteome of red cell membrane extracts from *P. falciparum* infected and non-infected erythrocytes, according to HbS heterozygous carriage, allowed us to point out a number of erythrocyte membrane transporters, skeletal proteins and parasite proteins for which phosphorylation was impacted by this genetic abnormality, combined with infection. This study, at the same time novel but also complicated by the use of freshly-collected RBCs, contributes to a better understanding of the biochemical mechanisms involved in conferring protection of HbAS carriers against disease caused by *P. falciparum*.

DATA AVAILABILITY STATEMENT

The datasets presented in this study can be found in online repositories. The name of the repository/repositories and accession number can be found below: ProteomeXchange *via* the PRIDE database, https://www.ebi.ac.uk/pride/, PXD023280.

ETHICS STATEMENT

The studies involving human participants were reviewed and approved by Necker-Enfants-Malades Hospital, Committee for the Protection of Persons n°DC 2014-2272. The patients/participants provided their written informed consent to participate in this study.

AUTHOR CONTRIBUTIONS

SA, IG, AL, AM, and FM-N conceived and designed the project. J-AR and SM collected the blood samples. MC, SD, CD, ML, AM, and MO performed the biochemical experiments. MC, AM, FM-N, and DP performed the genotyping. CC, IG, and JL performed the mass spectrometry experiments and analyses. SA, MC, IG, CLVK, AL, AM, and FM-N wrote the paper. All authors reviewed the manuscript before submission. All authors contributed to the article and approved the submitted version.

FUNDING

We thank the University of Paris for the doctoral scholarship awarded to MC. Funding came partly from the "Laboratoire d'Excellence GR-Ex," Paris, France, reference ANR-11-LABX-0051 that is funded by the program "Investissements d'avenir" of the French National Research Agency, reference ANR-11-IDEX-0005-02.

ACKNOWLEDGMENTS

We thank the voluntary blood donors for their participation in this project.

SUPPLEMENTARY MATERIAL

The Supplementary Material for this article can be found online at: https://www.frontiersin.org/articles/10.3389/fcimb.2021.637604/full#supplementary-material

REFERENCES

Abdi, A. I., Carvalho, T. G., Wilkes, J. M., and Doerig, C. (2013). A secreted Plasmodium falciparum kinase reveals a signature motif for classification of tyrosine kinase-like kinases. *Microbiol. Read. Engl.* 159, 2533–2547. doi: 10.1099/mic.0.070409-0

Archer, N. M., Petersen, N., Clark, M. A., Buckee, C. O., Childs, L. M., and Duraisingh, M. T. (2018). Resistance to Plasmodium falciparum in sickle cell trait erythrocytes is driven by oxygen-dependent growth inhibition. *Proc. Natl. Acad. Sci. U. S. A.* 115, 7350–7355. doi: 10.1073/pnas.1804388115

Azouzi, S., Collec, E., Mohandas, N., An, X., Colin, Y., and Le Van Kim, C. (2015). The human Kell blood group binds the erythroid 4.1R protein: new insights into the 4.1R-dependent red cell membrane complex. *Br. J. Haematol.* 171, 862–871. doi: 10.1111/bjh.13778

Azouzi, S., Romana, M., Arashiki, N., Takakuwa, Y., El Nemer, W., Peyrard, T., et al. (2018). Band 3 phosphorylation induces irreversible alterations of stored red blood cells. *Am. J. Hematol.* 93, E110–E112. doi: 10.1002/ajh.25044

Badaut, C., Guyonnet, L., Milet, J., Renard, E., Durand, R., Viwami, F., et al. (2015). Immunoglobulin response to Plasmodium falciparum RESA proteins in uncomplicated and severe malaria. *Malar. J.* 14, 278. doi: 10.1186/s12936-015-0799-8

Black, C. G., Proellocks, N. I., Kats, L. M., Cooke, B. M., Mohandas, N., and Coppel, R. L. (2008). In vivo studies support the role of trafficking and cytoskeletal-binding motifs in the interaction of MESA with the membrane skeleton of Plasmodium falciparum-infected red blood cells. *Mol. Biochem. Parasitol.* 160, 143–147. doi: 10.1016/j.molbiopara.2008.04.001

Bouyer, G., Reininger, L., Ramdani, G., D Phillips, L., Sharma, V., Egee, S., et al. (2016). Plasmodiumfalciparum infection induces dynamic changes in the erythrocyte phospho-proteome. *Blood Cells Mol. Dis.* 58, 35–44. doi: 10.1016/j.bcmd.2016.02.001

Brandt, G. S., and Bailey, S. (2013). Dematin, a human erythrocyte cytoskeletal protein, is a substrate for a recombinant FIKK kinase from Plasmodium falciparum. *Mol. Biochem. Parasitol.* 191, 20–23. doi: 10.1016/j.molbiopara.2013.08.003

Chauvet, M., Tétard, M., Cottrell, G., Aussenac, F., Brossier, E., Denoyel, L., et al. (2019). Impact of Hemoglobin S Trait on Cell Surface Antibody Recognition of Plasmodium falciparum-Infected Erythrocytes in Pregnancy-Associated Malaria. *Open Forum Infect. Dis.* 6, ofz156. doi: 10.1093/ofid/ofz156

Chishti, A. H., Maalouf, G. J., Marfatia, S., Palek, J., Wang, W., Fisher, D., et al. (1994). Phosphorylation of protein 4.1 in Plasmodium falciparum-infected human red blood cells. *Blood* 83, 3339–3345.

Cholera, R., Brittain, N. J., Gillrie, M. R., Lopera-Mesa, T. M., Diakité, S. A. S., Arie, T., et al. (2008). Impaired cytoadherence of Plasmodium falciparum-infected erythrocytes containing sickle hemoglobin. *Proc. Natl. Acad. Sci. U. S. A.* 105, 991–996. doi: 10.1073/pnas.0711401105

Cox, J., Hein, M. Y., Luber, C. A., Paron, I., Nagaraj, N., and Mann, M. (2014). Accurate proteome-wide label-free quantification by delayed normalization and maximal peptide ratio extraction, termed MaxLFQ. *Mol. Cell. Proteomics MCP* 13, 2513–2526. doi: 10.1074/mcp.M113.031591

Cox, J., and Mann, M. (2008). MaxQuant enables high peptide identification rates, individualized p.p.b.-range mass accuracies and proteome-wide protein quantification. *Nat. Biotechnol.* 26, 1367–1372. doi: 10.1038/nbt.1511

Cyrklaff, M., Srismith, S., Nyboer, B., Burda, K., Hoffmann, A., Lasitschka, F., et al. (2016). Oxidative insult can induce malaria-protective trait of sickle and fetal erythrocytes. *Nat. Commun.* 7, 13401. doi: 10.1038/ncomms13401

Dorin-Semblat, D., Tétard, M., Claës, A., Semblat, J.-P., Dechavanne, S., Fourati, Z., et al. (2019). Phosphorylation of the VAR2CSA extracellular region is associated with enhanced adhesive properties to the placental receptor CSA. *PloS Biol.* 17, e3000308. doi: 10.1371/journal.pbio.3000308

Egan, E. S., Weekes, M. P., Kanjee, U., Manzo, J., Srinivasan, A., Lomas-Francis, C., et al. (2018). Erythrocytes lacking the Langereis blood group protein ABCB6 are resistant to the malaria parasite Plasmodium falciparum. *Commun. Biol.* 1, 45. doi: 10.1038/s42003-018-0046-2

Esoh, K., and Wonkam, A. (2021). Evolutionary history of sickle cell mutation: implications for global genetic medicine. *Hum. Mol. Genet.* doi: 10.1093/hmg/ddab004

Fairhurst, R. M., Bess, C. D., and Krause, M. A. (2012). Abnormal PfEMP1/knob display on Plasmodium falciparum-infected erythrocytes containing hemoglobin variants: fresh insights into malaria pathogenesis and protection. *Microbes Infect. Inst. Pasteur* 14, 851–862. doi: 10.1016/j.micinf.2012.05.006

Ferru, E., Giger, K., Pantaleo, A., Campanella, E., Grey, J., Ritchie, K., et al. (2011). Regulation of membrane-cytoskeletal interactions by tyrosine phosphorylation of erythrocyte band 3. *Blood* 117, 5998–6006. doi: 10.1182/blood-2010-11-317024

Flint, J., Harding, R. M., Boyce, A. J., and Clegg, J. B. (1998). The population genetics of the haemoglobinopathies. *Baillieres Clin. Haematol.* 11, 1–51. doi: 10.1016/s0950-3536(98)80069-3

Gelpi, A. P., and King, M. C. (1976). Association of Duffy blood groups with the sickle cell trait. *Hum. Genet.* 32, 65–68. doi: 10.1007/BF00569977

George, A., Pushkaran, S., Li, L., An, X., Zheng, Y., Mohandas, N., et al. (2010). Altered phosphorylation of cytoskeleton proteins in sickle red blood cells: the role of protein kinase C, Rac GTPases, and reactive oxygen species. *Blood Cells Mol. Dis.* 45, 41–45. doi: 10.1016/j.bcmd.2010.02.006

Glenister, F. K., Fernandez, K. M., Kats, L. M., Hanssen, E., Mohandas, N., Coppel, R. L., et al. (2009). Functional alteration of red blood cells by a megadalton protein of Plasmodium falciparum. *Blood* 113, 919–928. doi: 10.1182/blood-2008-05-157735

Gonçalves, B. P., Gupta, S., and Penman, B. S. (2016). Sickle haemoglobin, haemoglobin C and malaria mortality feedbacks. *Malar. J.* 15, 26. doi: 10.1186/s12936-015-1077-5

Jacob Blackmon, B., Dailey, T. A., Lianchun, X., and Dailey, H. A. (2002). Characterization of a human and mouse tetrapyrrole-binding protein. *Arch. Biochem. Biophys.* 407, 196–201. doi: 10.1016/s0003-9861(02)00471-x

Kakande, E., Greenhouse, B., Bajunirwe, F., Drakeley, C., Nankabirwa, J. I., Walakira, A., et al. (2020). Associations between red blood cell variants and malaria among children and adults from three areas of Uganda: a prospective cohort study. *Malar. J.* 19, 21. doi: 10.1186/s12936-020-3105-3

Kariuki, S. N., Marin-Menendez, A., Introini, V., Ravenhill, B. J., Lin, Y.-C., Macharia, A., et al. (2020). Red blood cell tension protects against severe malaria in the Dantu blood group. *Nature* 585, 579–583. doi: 10.1038/s41586-020-2726-6

Kilili, G. K., Shakya, B., Dolan, P. T., Wang, L., Husby, M. L., Stahelin, R. V., et al. (2019). The Plasmodium falciparum MESA erythrocyte cytoskeleton-binding (MEC) motif binds to erythrocyte ankyrin. *Mol. Biochem. Parasitol.* 231, 111189. doi: 10.1016/j.molbiopara.2019.111189

Lalle, M., Currà, C., Ciccarone, F., Pace, T., Cecchetti, S., Fantozzi, L., et al. (2011). Dematin, a Component of the Erythrocyte Membrane Skeleton, Is Internalized by the Malaria Parasite and Associates with Plasmodium 14-3-3. *J. Biol. Chem.* 286, 1227–1236. doi: 10.1074/jbc.M110.194613

Langhi, D. M., and Bordin, J. O. (2006). Duffy blood group and malaria. *Hematol. Amst. Neth.* 11, 389–398. doi: 10.1080/10245330500469841

Lipecka, J., Chhuon, C., Bourderioux, M., Bessard, M.-A., van Endert, P., Edelman, A., et al. (2016). Sensitivity of mass spectrometry analysis depends on the shape of the filtration unit used for filter aided sample preparation (FASP). *Proteomics* 16, 1852–1857. doi: 10.1002/pmic.201600103

Lux, S. E. (2016). Anatomy of the red cell membrane skeleton: unanswered questions. *Blood* 127, 187–199. doi: 10.1182/blood-2014-12-512772

Mankelow, T. J., Satchwell, T. J., and Burton, N. M. (2012). Refined views of multi-protein complexes in the erythrocyte membrane. *Blood Cells Mol. Dis.* 49, 1–10. doi: 10.1016/j.bcmd.2012.03.001

Manno, S., Takakuwa, Y., Nagao, K., and Mohandas, N. (1995). Modulation of erythrocyte membrane mechanical function by beta-spectrin phosphorylation and dephosphorylation. *J. Biol. Chem.* 270, 5659–5665. doi: 10.1074/jbc.270.10.5659

Meijer, B. M., Jang, S. M., Guerrera, I. C., Chhuon, C., Lipecka, J., Reisacher, C., et al. (2017). Threonine eliminylation by bacterial phosphothreonine lyases rapidly causes cross-linking of mitogen-activated protein kinase (MAPK) in live cells. *J. Biol. Chem.* 292, 7784–7794. doi: 10.1074/jbc.M117.775940

Merckx, A., Nivez, M.-P., Bouyer, G., Alano, P., Langsley, G., Deitsch, K., et al. (2008). Plasmodium falciparum regulatory subunit of cAMP-dependent PKA and anion channel conductance. *PloS Pathog.* 4, e19. doi: 10.1371/journal.ppat.0040019

Migot-Nabias, F., Mombo, L. E., Luty, A. J., Dubois, B., Nabias, R., Bisseye, C., et al. (2000). Human genetic factors related to susceptibility to mild malaria in Gabon. *Genes Immun.* 1, 435–441. doi: 10.1038/sj.gene.6363703

Miller, L. H., Baruch, D. I., Marsh, K., and Doumbo, O. K. (2002). The pathogenic basis of malaria. *Nature* 415, 673–679. doi: 10.1038/415673a

Moiz, B., and Majeed, A. (2018). No risk reduction for Plasmodium vivax malaria in sickle cell disease. *Clin. Case Rep.* 6, 1187–1188. doi: 10.1002/ccr3.1507

Nunes, M. C., Okada, M., Scheidig-Benatar, C., Cooke, B. M., and Scherf, A. (2010). Plasmodium falciparum FIKK kinase members target distinct components of the erythrocyte membrane. *PloS One* 5, e11747. doi: 10.1371/journal.pone.0011747

Okafor, I. M., Okoroiwu, H. U., and Ekechi, C. A. (2019). Hemoglobin S and Glucose-6-Phosphate Dehydrogenase Deficiency Coinheritance in AS and SS Individuals in Malaria-Endemic Region: A Study in Calabar, Nigeria. *J. Glob. Infect. Dis.* 11, 118–122. doi: 10.4103/jgid.jgid_154_18

Pantaleo, A., De Franceschi, L., Ferru, E., Vono, R., and Turrini, F. (2010a). Current knowledge about the functional roles of phosphorylative changes of membrane proteins in normal and diseased red cells. *J. Proteomics* 73, 445–455. doi: 10.1016/j.jprot.2009.08.011

Pantaleo, A., Ferru, E., Carta, F., Mannu, F., Giribaldi, G., Vono, R., et al. (2010b). Analysis of changes in tyrosine and serine phosphorylation of red cell membrane proteins induced by P. falciparum growth. *Proteomics* 10, 3469–3479. doi: 10.1002/pmic.201000269

Pantaleo, A., Kesely, K. R., Pau, M. C., Tsamesidis, I., Schwarzer, E., Skorokhod, O. A., et al. (2017). Syk inhibitors interfere with erythrocyte membrane modification during P falciparum growth and suppress parasite egress. *Blood* 130, 1031–1040. doi: 10.1182/blood-2016-11-748053

Pei, X., Guo, X., Coppel, R., Bhattacharjee, S., Haldar, K., Gratzer, W., et al. (2007). The ring-infected erythrocyte surface antigen (RESA) of Plasmodium falciparum stabilizes spectrin tetramers and suppresses further invasion. *Blood* 110, 1036–1042. doi: 10.1182/blood-2007-02-076919

Perez-Riverol, Y., Csordas, A., Bai, J., Bernal-Llinares, M., Hewapathirana, S., Kundu, D. J., et al. (2019). The PRIDE database and related tools and resources in 2019: improving support for quantification data. *Nucleic Acids Res.* 47, D442–D450. doi: 10.1093/nar/gky1106

Piel, F. B., Patil, A. P., Howes, R. E., Nyangiri, O. A., Gething, P. W., Williams, T. N., et al. (2010). Global distribution of the sickle cell gene and geographical confirmation of the malaria hypothesis. *Nat. Commun.* 1, 104. doi: 10.1038/ncomms1104

Rhee, S. G., and Kil, I. S. (2017). Multiple Functions and Regulation of Mammalian Peroxiredoxins. *Annu. Rev. Biochem.* 86, 749–775. doi: 10.1146/annurev-biochem-060815-014431

Rug, M., Cyrklaff, M., Mikkonen, A., Lemgruber, L., Kuelzer, S., Sanchez, C. P., et al. (2014). Export of virulence proteins by malaria-infected erythrocytes involves remodeling of host actin cytoskeleton. *Blood* 124, 3459–3468. doi: 10.1182/blood-2014-06-583054

Taylor, S. M., Cerami, C., and Fairhurst, R. M. (2013). Hemoglobinopathies: slicing the Gordian knot of Plasmodium falciparum malaria pathogenesis. *PloS Pathog.* 9, e1003327. doi: 10.1371/journal.ppat.1003327

Trager, W., and Jensen, J. B. (1976). Human malaria parasites in continuous culture. *Science* 193, 673–675. doi: 10.1126/science.781840

Tyanova, S., Temu, T., Sinitcyn, P., Carlson, A., Hein, M. Y., Geiger, T., et al. (2016). The Perseus computational platform for comprehensive analysis of (prote)omics data. *Nat. Methods* 13, 731–740. doi: 10.1038/nmeth.3901

Vera, I. M., Beatty, W. L., Sinnis, P., and Kim, K. (2011). Plasmodium protease ROM1 is important for proper formation of the parasitophorous vacuole. *PloS Pathog.* 7, e1002197. doi: 10.1371/journal.ppat.1002197

Waller, K. L., Nunomura, W., An, X., Cooke, B. M., Mohandas, N., and Coppel, R. L. (2003). Mature parasite-infected erythrocyte surface antigen (MESA) of Plasmodium falciparum binds to the 30-kDa domain of protein 4.1 in malaria-infected red blood cells. *Blood* 102, 1911–1914. doi: 10.1182/blood-2002-11-3513

Waller, K. L., Stubberfield, L. M., Dubljevic, V., Buckingham, D. W., Mohandas, N., Coppel, R. L., et al. (2010). Interaction of the exported malaria protein Pf332 with the red blood cell membrane skeleton. *Biochim. Biophys. Acta* 1798, 861–871. doi: 10.1016/j.bbamem.2010.01.018

Conflict of Interest: The authors declare that the research was conducted in the absence of any commercial or financial relationships that could be construed as a potential conflict of interest.

frontiers in Cellular and Infection Microbiology

ORIGINAL RESEARCH
published: 16 June 2021
doi: 10.3389/fcimb.2021.672691

Isolation of Mutants With Reduced Susceptibility to Piperaquine From a Mutator of the Rodent Malaria Parasite *Plasmodium berghei*

Mie Ikeda[†], *Makoto Hirai*[*†], *Shin-Ichiro Tachibana*, *Toshiyuki Mori* and *Toshihiro Mita*[*]

Department of Tropical Medicine and Parasitology, Faculty of Medicine, Juntendo University, Tokyo, Japan

OPEN ACCESS

Edited by:
Takeshi Annoura, National Institute of Infectious Diseases (NIID), Japan

Reviewed by:
Johannes Theodorus Dessens, London School of Hygiene and Tropical Medicine, United Kingdom
Rapatbhorn Patrapuvich, Mahidol University, Thailand

***Correspondence:**
Makoto Hirai
m-hirai@juntendo.ac.jp
Toshihiro Mita
tmita@juntendo.ac.jp

[†]*These authors have contributed equally to this work and share first authorship*

Specialty section:
This article was submitted to Parasite and Host, a section of the journal Frontiers in Cellular and Infection Microbiology

Received: *01 March 2021*
Accepted: *19 April 2021*
Published: *16 June 2021*

Citation:
Ikeda M, Hirai M, Tachibana S-I, Mori T and Mita T (2021) Isolation of Mutants With Reduced Susceptibility to Piperaquine From a Mutator of the Rodent Malaria Parasite Plasmodium berghei. Front. Cell. Infect. Microbiol. 11:672691. doi: 10.3389/fcimb.2021.672691

Elucidation of the mechanisms of drug resistance in malaria parasites is crucial for combatting the emergence and spread of resistant parasites, which can be achieved by tracing resistance-associated mutations and providing useful information for drug development. Previously, we produced a novel genetic tool, a *Plasmodium berghei* mutator (PbMut), whose base substitution rate is 36.5 times higher than that of wild-type parasites. Here, we report the isolation of a mutant with reduced susceptibility to piperaquine (PPQ) from PbMut under PPQ pressure by sequential nine-cycle screening and named it PbMut-PPQ-R-P9. The ED_{50} of PbMut-PPQ-R-P9 was 1.79 times higher than that of wild-type parasites, suggesting that its PPQ resistance is weak. In the 1st screen, recrudescence occurred in the mice infected with PbMut but not in those infected with wild-type parasites, suggesting earlier emergence of PPQ-resistant parasites from PbMut. Whole-genome sequence analysis of PbMut-PPQ-R-P9 clones revealed that eight nonsynonymous mutations were conserved in all clones, including N331I in *PbCRT*, the gene encoding chloroquine resistance transporter (*CRT*). The PbCRT(N331I) mutation already existed in the parasite population after the 2nd screen and was predominant in the population after the 8th screen. An artificially inserted PbCRT(N331I) mutation gave rise to reduced PPQ susceptibility in genome-edited parasites (PbCRT-N331I). The PPQ susceptibility and growth rates of PbCRT-N331I parasites were significantly lower than those of PbMut-PPQ-R-P9, implying that additional mutations in the PbMut-PPQ-R9 parasites could compensate for the fitness cost of the PbCRT(N331I) mutation and contribute to reduced PPQ susceptibility. In summary, PbMut could serve as a novel genetic tool for predicting gene mutations responsible for drug resistance. Further study on PbMut-PPQ-R-P9 could identify genetic changes that compensate for fitness costs owing to drug resistance acquisition.

Keywords: piperaquine resistance, mutator, CRT, fitness, *Plasmodium berghei*, mutants with reduced PPQ susceptibility 2

INTRODUCTION

Malaria is one of the most life-threatening parasitic diseases worldwide. Its causative agents are *Plasmodium* spp., which are transmitted by anopheline mosquitoes. Among these, *P. falciparum* is the most malignant and threatens human life. It is responsible for 229 million clinical cases and 409,000 deaths, and its main victims are children under 5 years old living in sub-Saharan Africa (WHO and 2020, n.d). The obstacles for efficacious malaria control are the difficulty in development of effective vaccines and suppression of the emergence and spread of drug-resistant parasites. Regarding antimalarial drugs, the emergence of artemisinin-resistant malaria was confirmed in Cambodia in 2008 (Noedl et al., 2008), and the resistance has been spreading in the Greater Mekong subregion (Phyo et al., 2012; Kyaw et al., 2013). Since artemisinin is used in artemisinin-based combination therapy (ACT), treatment efficacy relies more heavily on the partner drug, which has induced the emergence of resistance to partner drugs, such as piperaquine (PPQ) (Amaratunga et al., 2016; Thanh et al., 2017). Moreover, the potential emergence of artemisinin-resistant *P. falciparum* parasites has been reported in Africa (Ikeda et al., 2018) and India (Das et al., 2018). The use of genetic markers is the most practical way to trace the emergence and spread of resistance. To identify genetic markers, a comparative genomics study between wild-type and drug-resistant parasites that emerged in the same area was performed. However, this approach is difficult and time-consuming because over 50,000 single-nucleotide polymorphisms (SNPs), corresponding to one SNP every 230 bp, are naturally detected in field isolates, e.g., from the border of China and Myanmar (Ye et al., 2019). In this context, isolation of drug-resistant parasites by *in vitro* evolution experiments could be simpler than the aforementioned approach. Moreover, isolation of drug-resistant parasites *in vitro* could predict mutations that will emerge in fields. For example, artemisinin-resistant parasites were isolated by *in vitro* under artemisinin pressure, and subsequent analysis identified a gene responsible for artemisinin resistance, *kelch13*. This attempt is still challenging because it took five years to isolate this mutant (Ariey et al., 2014). The reason for taking such a long time for the conventional *in vitro* evolution has been partly explained by the fact that the parasites amplify the genome surrounding the target genes through multiple steps, before the acquirement of mutations in the target genes (Guler et al., 2013). Therefore, it is anticipated that transgenic parasites producing spontaneous random nonsynonymous point mutations will produce drug-resistant parasites in a short time because several steps involved in genome amplification might be skipped. For this purpose, we previously generated a transgenic rodent malaria parasite, *P. berghei*, which possesses DNA polymerase δ with destructed proofreading activity (PbMut). The base substitution rate of PbMut is over 36.5-fold higher than that of wild-type parasites (Honma et al., 2014; Honma et al., 2016). Thus, PbMut could serve as a new tool for parasite drug resistance research (Hirai and Mita, 2015). In the present work, we attempted to isolate PPQ-resistant parasites from PbMut. As a result, we successfully isolated mutant clones exhibiting reduced susceptibility to PPQ and identified at least one SNP associated with this phenotype.

MATERIALS AND METHODS

Animals and Parasites

Two mouse strains, ddY and BALB/c mice (female, 5 weeks old), were purchased from a supplier (Sankyo Labo Service Corp., Japan). ddY and BALB/c mice were used for piperaquine (PPQ)-resistant mutant screening and other experiments, respectively. The rodent malaria parasite *Plasmodium berghei* ANKA (clone 2.34) was used for the generation of a *P. berghei* mutator (PbMut) in our previous study (Honma et al., 2014). In brief, PbMut possesses mutations in the *DNA polymerase δ* gene destructing the proofreading activity in the corresponding gene product. In wild-type *P. berghei* (PbWT), endogenous *DNA polymerase δ* was replaced by the wild-type gene. Both transgenic parasites possess a pyrimethamine resistance gene as a marker. The parasites were maintained by weekly passaging through mice. After 91 weeks of passaging, the parasite population (PbMut-P91) was composed of various mutants that were used in PPQ-resistant mutant screening. The protocols for animal and recombinant DNA experiments were approved by the Experimental Animal Ethics Committee and Recombinant DNA Committee of the School of Medicine, Juntendo University, and the assigned numbers were no. 290017 and no. 25-115, respectively.

Isolation of Piperaquine (PPQ)-Resistant Parasites From PbMut

The procedure for PPQ-resistant parasite screening is described in **Figure 1**. On the 1st screen, infected red blood cells (iRBCs, $1x10^6$) from the PbMut and PbWT populations were intravenously inoculated into two mice each. When parasitemia of the infected mice reached 1-2%, the mice infected with PbMut or PbWT were intraperitoneally administered PPQ tetraphosphate tetrahydrate (Sigma-Aldrich Co., USA) in Tween 80 (70%) and ethanol (30%) for four consecutive days. The drug administration start date was defined as day 0, and parasitemia was followed up until day 16. Parasitemia was quantified by counting over 2,000 erythrocytes on Giemsa-stained slides under a light microscope (1,000 x magnification). If infected erythrocytes were not detected by counting over 5,000 erythrocytes on day 16, we considered the mice to be cured. Recrudescence occurred in two mice carrying PbMut (PbMut-PPQ-R-P1a and b). These populations were passed to new mice, but the latter infection failed, and passaging was stopped thereafter. PbMut-PPQ-R-P1a was transferred to a mouse, which was treated with PPQ until passage 9 (P9), with PPQ doses of 15 and 30 mg/kg/day for P1 to P8 and P9, respectively. Four clones of PbMut-PPQ-R-P9 were isolated from the PbMut-PPQ-R-P9 population by limiting dilution.

To assess PPQ susceptibility, iRBCs ($1x10^3$) of PbMut-PPQ-R-P9 clones or PbWT were injected intravenously into each

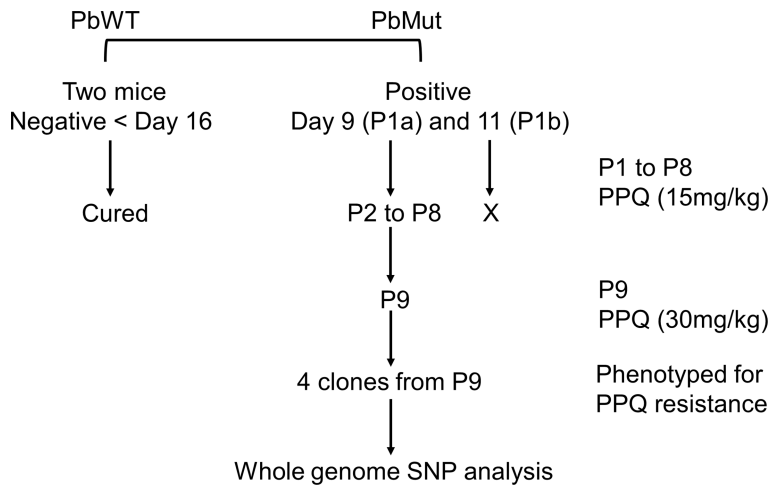

FIGURE 1 | Flow chart of nine-cycle screening for PPQ-resistant parasites. At passage 1 (P1), recrudescence was not confirmed in PbWT-infected mice until day 16, while it was detected in both mice infected with PbMut (P1a and b). P1b failed to be passaged to the next mouse (indicated by a cross). P1a proceeded to sequential passages until P9. The four clones from P9 and one clone from the original PbMut (PbMut-P91 clone) were subjected to SNP analysis.

mouse, which were administered PPQ (15 mg/kg/day) for 5 consecutive days. The parasitemia of PbMut-PPQ-R-P9 clones was monitored until day 11, while PbWT-infected mice were monitored until day 16.

Peters's four-day suppressive test (Peters, 1965) was performed to compare the efficacy of PPQ between PbMut-PPQ-R-P9 clones and PbWT. In brief, iRBCs ($1x10^6$) from three PbMut-PPQ-R-P9 clones or one PbWT clone were intravenously injected into five or fifteen BALB/c mice, respectively. Three mice infected with PbMut-PPQ-R-P9 or PbWT were then orally administered PPQ (2.5, 5, 7.5, or 10 mg/kg) at 4, 24, 48, and 72 hr post-infection. Three mice each were treated with 100 µl of Tween 80 (70%) and ethanol (30%) as a control. The parasitemia of all mice was quantified on day 4 post-infection. The 50% effective dose of PPQ (ED_{50}), which is defined as the dose that suppresses 50% of parasitemia, was calculated by ICEstimator ver.1.2 online (http://www.antimalarial-icestimator.net/).

Whole-Genome Sequencing and Single-Nucleotide Polymorphism (SNP) Analysis

In four PbMut-PPQ-R-P9 clones, and one PbMut-P91 clone which was obtained after 91 times serial passage through mice, genomic DNA was extracted from leukocyte-removed blood with a Plasmodipur filter (EuroProxima, The Netherlands) by using a QIAamp DNA Blood Mini Kit (QIAGEN, Germany) and sequenced with a HiSeq-2500 system (Illumina, USA). Analysis of genome-wide SNPs was conducted using CLC Genomics Workbench ver.11 (CLC-GW) (QIAGEN, Germany). Reads were mapped to the reference genome of *P. berghei* ANKA (PlasmoDB-49) with default parameters for detecting SNPs in samples. These steps for the selection of SNPs were performed using two variant detection tools (Basic Variant Detection and Fixed Ploidy Variant Detection) in CLC-GW. The PbMut-P91 SNPs were excluded from those of each PbMut-PPQ-R-P9 clone. The remaining nonsynonymous SNPs conserved in all clones were finally extracted as specific SNPs in PbMut-PPQ-R-P9 clones and were verified in all clones by Sanger sequencing. Multigene families were excluded from SNP analysis because of the high possibility of read mismapping.

Monitoring the PbCRT-N331I Mutant in PbMut-PPQ-R Populations

To investigate the association of the PbCRT(N331I) mutation with PPQ susceptibility, the presence of PbCRT(N331I) was monitored in nine parasite populations (PbMut-PPQ-R-P1 to 9) obtained from each screen. For this, genomic DNA was extracted from each population and used as a template for PCR. A fragment covering PbCRT(N331) was amplified using a pair of primers, PbCRT-checkF and PbCRT-checkR. The PCR product was Sanger sequenced by using the PbCRT-SeqF primer. The primer sequences are shown in **Figure S2**.

Generation of the PbCRT(N331I) Mutant by Genome Editing

The plasmid pYC for the CRISPR/Cas9 gene editing of *P. yoelii* was kindly gifted by Dr. Yuan (Zhang et al., 2014). To customize pYC for *P. berghei*, the U6 promoter of *P. yoelii* in pYC was excluded by inverse PCR using the primers A and B, which are designed in an outward direction from the *P. yoelii* U6 promoter region. The U6 promoter of *P. berghei* (PBANKA_1354380) was amplified with the primers C and D and ligated into the pYC PCR product by using an In-Fusion HD Cloning kit (TAKARA). The resultant plasmid, pBC, was used for *P. berghei* genome editing.

As donor DNA, a 1,343 bp fragment containing PbCRT (N331I) was synthesized (Genewiz, Japan) and ligated to the HindIII/AflII site in pBC by an In-Fusion HD Cloning kit. The candidate guide RNA (gRNA) was designed by the Eukaryotic Pathogen CRISPR Guide RNA Design Tool (http://grna.ctegd.

uga.edu/). A double-stranded DNA coding for the candidate gRNA was ligated into the BsmBI site of pBC; therefore, the gRNA was transcribed under the *P. berghei* U6 promoter. The resultant plasmid, pPbCRT(N331I), was electroporated into wild-type *P. berghei*. Transfection and subsequent parasite cloning followed a previously described protocol (Janse et al., 2006). The mutation in the resultant PbCRT-N331I parasite clone was verified by Sanger sequencing. The structure of PbCRT (N331) plasmid and the sequence of PbCRT(N331I) parasite clone, and the donor DNA sequence are shown in **Figures S1A, B**, respectively. The sequences of the gRNAs and primers are shown in **Figure S2**.

Comparison of PPQ Efficacy and Growth Rates Among PbMut-PPQ-R-P9, PbCRT-N331I, and PbWT Parasites

For the comparison of PPQ efficacy among PbMut-PPQ-R-P9, PbCRT-N331I, and PbWT, iRBCs ($1x10^6$) from three clones of PbMut-PPQ-R-P9 or PbCRT-N331I were intravenously inoculated into three mice each. For PbWT, iRBCs ($1x10^6$) were injected into nine mice. When the parasitemia reached 1-2%, PPQ (5, 15, and 30 mg/kg/day) was administered on day 0 for 5 consecutive days, and parasitemia was monitored until day 14. For PbWT-infected mice, parasitemia was followed up until day 16.

It is known that parasites acquire drug resistance at the expense of fitness (Rosenthal, 2013). Thus, the fitness of PbMut-PPQ-R-P9, PbCRT-N331I, and PbWT in each mouse was investigated. For this, iRBCs ($1x10^6$) infected with each of the three parasite clones were inoculated into one mouse each. For PbWT, iRBCs were inoculated into three mice. Parasitemia was monitored from days 3 to 6 under drug-free conditions.

Statistical Analysis

Comparisons between two or among three independent data groups were made by Student's t-test or analysis of variance test (ANOVA) followed by Tukey's multiple comparison test, respectively. Parasitemia is expressed as the mean ± standard deviation. $P<0.05$ was considered statistically significant.

RESULTS

Isolation of PPQ-Resistant Parasites From PbMut

To isolate PPQ-resistant parasites, two mice were infected with PbMut or PbWT parasites and were treated with PPQ (15 mg/kg/day, 4 days) on the 1st screen. For PbWT-infected mice, infected erythrocytes were undetectable from day 3 until day 16. In contrast, PbMut-infected mice showed recrudescence on days 9 and 11 (PbMut-PPQ-R-P1a and -P1b) (**Figure 2** and **Table S1**). PbMut-PPQ-R-P1a and -P1b were each passaged to another mouse, but the latter failed to cause infection. Thus, only PbMut-PPQ-R-P1a proceeded to serial passaging until P9. After nine cycles of serial passaging, PbMut-PPQ-R-P9 parasites survived under 30 mg/kg PPQ treatment for five consecutive days (**Table S1**). Four clones derived from the PbMut-PPQ-R-P9 population were assessed for susceptibility to PPQ. As shown in **Figure 3**, all the clones survived under PPQ pressure (15 mg/kg/day, 5 days), but PbWT did not, suggesting that all the clones were less susceptible than PbWT to PPQ. A four-day suppressive test was performed to quantitatively assess PPQ susceptibility. The ED_{50} of PbMut-PPQ-R-P9 was 2.06 mg/kg, which is 1.79 times higher than that of PbWT (1.15 mg/kg). Such a slight rise in the ED_{50} for PbMut-PPQ-R-P9 suggests that its PPQ resistance is weak.

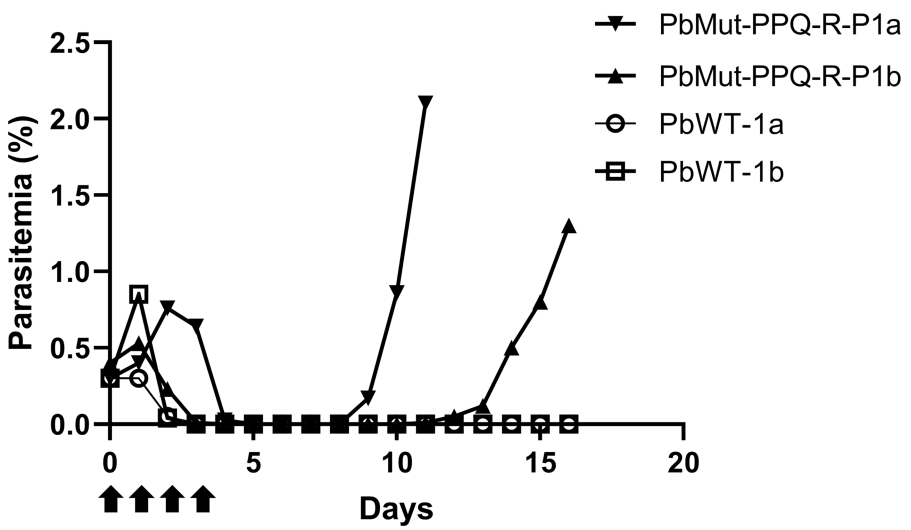

FIGURE 2 | Screening for PPQ-resistant parasites from PbMut. The first screen for PPQ-resistant parasites. Two mice each were infected with PbMut (PbMut-PPQ-R-P1a; closed inverted triangle, and PbMut-PPQ-R-P1b; closed triangle) or PbWT (PbWT-P1a; open circle, and PbWT-P1b; open square). The mice were administered PPQ (15 mg/kg/day) for 4 days (arrows), and parasitemia was monitored.

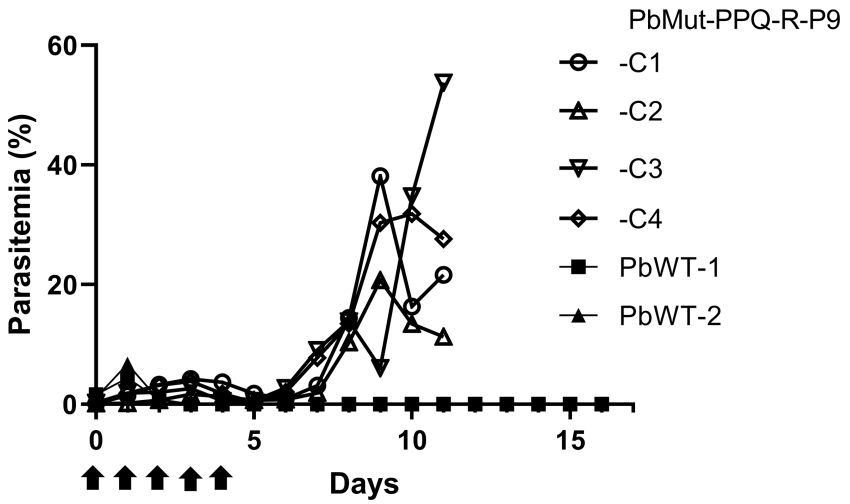

FIGURE 3 | Assessment of PPQ susceptibility in PbMut-PPQ-R-P9-derived clones. Erythrocytes ($1x10^3$) infected with two wild-type (PbWT-1 and PbWT-2, closed symbols) and four clones from PbMut-PPQ-R-P9 (open symbols) were transferred to each mouse. The mice were then treated with PPQ (15 mg/kg/day) for five consecutive days (arrows), and parasitemia was monitored.

Eight Nonsynonymous Mutations Shared Among the Four PbMut-PPQ-R-P9 Clones

To identify gene mutations responsible for the reduced PPQ susceptibility, we performed whole-genome SNP analysis in the four clones of PbMut-PPQ-R-P9 and one clone of PbMut-P91 as a control. Over three hundred redundant data points were obtained from each sample (**Table S2**). The numbers of nonsynonymous SNPs detected in PbMut-P91 and the four clones were 103, 113, 110, 123, and 117, respectively. SNPs of the four clones that were shared with PbMut-P91 were excluded, resulting in 20, 20, 31, and 25 SNPs for clones (**Table S3**). Of these, eight were conserved among all the clones (**Table 1**). Six of these eight nonsynonymous mutations were detected in the following genes*: exoribonuclease II* (SNP1), *tetratricopeptide repeat protein* (SNP3), *rhomboid protease ROM8* (SNP4) (Lin et al., 2013), *AP-2 complex subunit* α (SNP5), *chloroquine resistance transporter* (*CRT*) (SNP6) (Fidock et al., 2000; Martin et al., 2009; Juge et al., 2015) and *AAP4* (SNP8). Mutations in *CRT* of *P. falciparum* (*PfCRT*) have been suggested to be associated with resistance against several antimalarials, including PPQ (Agrawal, 2017; Ross et al., 2018). To investigate the association of PbCRT(N331I) with reduced PPQ susceptibility, the PbCRT(N331I) mutation in the nine parasite populations was monitored. This mutation was detected in the P2 population, and the wild-type allele was replaced by this mutation in the P8 and P9 populations (**Figure S3**), suggesting that this mutation might be selected by PPQ pressure.

Comparison of PPQ Susceptibility and Growth Rates Among PbMut-PPQ-R-P9, PbCRT-N331I, and PbWT Parasites

Transgenic PbCRT-N331I and PbMut-PPQ-R-P9, as well as PbWT parasites as controls, were inoculated into mice that were exposed to PPQ. Both PbMut-PPQ-R-P9 and PbCRT-N331I survived under PPQ pressure, but PbWT did not (**Figure 4**). Notably, the parasitemia of PbCRT-N331I was less than that of PbMut-PPQ-R-P9 (**Figure 4**). This result suggests that PbMut-PPQ-R-P9 could be less susceptible than PbCRT-N331I to PPQ. In addition, it is

TABLE 1 | Eight SNPs conserved in 4 clones of PbMut-PPQ-R-P9.

SNP site	Chr.	Position	Gene ID	Gene description	Amino acid change	Expression	KO
SNP1	4	552412	PBANKA_041530	exoribonuclease II, putative	K91N	A>S	×
SNP2	7	197615	PBANKA_070480	conserved Plasmodium protein	K349Q	A<S	?
SNP3	8	1048775	PBANKA_082730	tetratricopeptide repeat protein	K864N	A<S	?
SNP4	10	1225025	PBANKA_103130	rhomboid protease ROM8	P435S	A/S	×
SNP5	11	611718	PBANKA_111670	AP-2 complex subunit alpha, putative	L1128I	A/S	?
SNP6	12	722508	PBANKA_121950	chloroquine resistance transporter	N331I	A>S	×
SNP7	13	1765633	PBANKA_134480	conserved Plasmodium protein	R54K	A>S	?
SNP8	14	631065	PBANKA_141720	protein AAP4, putative	I773L	A<S	?

The SNPs are listed in order of chromosome number.

A, asexual; S, sexual stages; A>S, A<S and A/S represent the relative abundance of transcription between these two stages x and ○ represent failed and success for knockout.? is unknown. All data are referred from PlasmoDB.

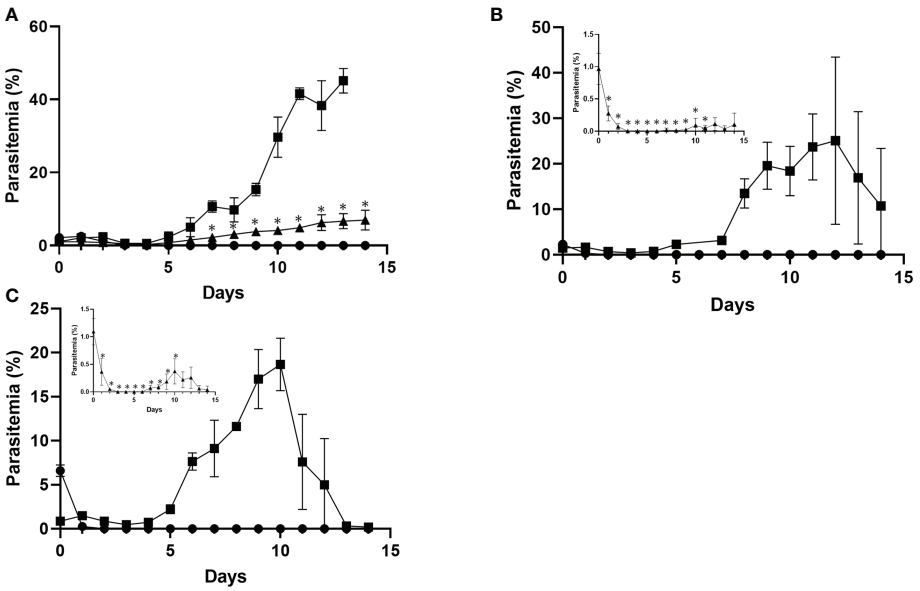

FIGURE 4 | Comparison of PPQ susceptibility among PbCRT-N331I, PbMut-PPQ-R-P9, and PbWT parasites. Three clones of PbMut-PPQ-R-P9 (closed square) or PbCRT-N331I (closed triangle) were intravenously inoculated into three BALB/c mice each. PbWT parasites (closed circle) were injected into nine mice. Three mice in each group were then treated with PPQ at doses of 5, 15, and 30 mg/kg/day **(A–C)** for five consecutive days starting on day 0. The parasitemia of PbCRT-N331I is shown in the insets of **(B, C)** because of low parasitemia. As shown in **(A)**, the parasitemia of PbMut-PPQ-R-P9 on day 14 was not determined because the mice died due to high parasitemia. The bar represents the standard deviation. The asterisks indicate that the parasitemia of PbCRT-N331I was significantly different from that of PbMut-PPQ-R-P9 ($p<0.05$).

interesting that no suppressive effect of a higher PPQ dose on parasitemia was detected for PbCRT-N331I (insets, **Figures 4B, C**). For PbMut-PPQ-R-P9, parasitemia continuously increased until mouse death on day 15 at a PPQ dose of 5 mg/kg/day (**Figure 4A**). At PPQ doses of 15 and 30 mg/kg/day, parasitemia peaked on day 12 (**Figure 4B**) and day 10 (**Figure 4C**) and then declined. The decrease in parasitemia might be due to host immunity and/or the accumulative effect of PPQ pressure, which could suppress parasite growth later in the follow-up period.

To investigate the possibility that the PbCRT(N331I) mutation imposes fitness costs on the parasite, the growth rates of PbMut-PPQ-R-P9 and PbCRT(N331I), as well as of PbWT, in mice were compared under drug-free conditions. The parasitemia of PbCRT-N331I and PbMut-PPQ-R-P9 was significantly less than that of PbWT on days 3 and 4 post-infection (* $p<0.05$, **Figure 5**). On days 5 and 6, the parasitemia of PbCRT-N331I was less than that of PbMut-PPQ-R-P9 (** $p<0.05$, **Figure 5**). This result demonstrates that the PbCRT(N331I) mutation partially impaired parasite growth in mice. This result also suggests that some genetic factors existing in PbMut-PPQ-R-P9 could compensate for the fitness cost imposed by the PbCRT(N331I) mutation.

DISCUSSION

In this study, we isolated PbMut-PPQ-R-P9 from PbMut after nine rounds of passaging with PPQ administration. The ED_{50} of PbMut-PPQ-R-P9 was 1.79 times higher than that of PbWT. Despite the weak PPQ resistance of PbMut-PPQ-R-P9, we successfully identified eight nonsynonymous SNPs that were conserved in all clones of PbMut-PPQ-R-P9 (**Table 1**). Four SNPs (SNP2, 3, 7, and 8) were detected in genes that are exclusively expressed at sexual stages and/or encode hypothetical proteins with no remarkable functional domain (PlasmoDB; https://plasmodb.org/plasmo/). SNP4 is in the rhomboid protein family gene (ROM8), which plays critical roles in host cell invasion in apicomplexan parasites (Lin et al., 2013) and is unlikely to be related to PPQ susceptibility. SNP1 is in the gene coding for PbRNase II. In *P. falciparum*, an ortholog of PbRNase II functions in posttranscriptional silencing of *upsA*, a *var* subgroup gene (Zhang et al., 2014) and has not been reported to have an association with PPQ resistance. Finally, either of the two remaining SNPs may be responsible for PPQ susceptibility, which is in *PbCRT* (SNP6) and *AP2-α* (SNP5).

We focused on PbCRT(N331I) because CRT is a well-known transporter on the food vacuole, a principal site of quinoline antimalarials, such as PPQ (Roepe, 2011; Ecker et al., 2012). To investigate the association of PbCRT(N331I) with PPQ susceptibility, we generated PbCRT-N331I parasites and confirmed that PbCRT-N331I exhibited reduced PPQ susceptibility (**Figure 4**). PbCRT (N331) corresponds to N330 in PfCRT (Kim et al., 2019). There is no evidence for the occurrence of PfCRT(N330I) in 3,488 *P. falciparum* genomes from 23 countries (Project, M. falciparum, 2016). Instead, a decrease in PPQ susceptibility or resistance has been significantly associated with particular mutations in *PfCRT*, including T93S, H97Y, F145I, I218F, M343L, and G353V in Southeast Asia and C350R in South America (Pelleau et al., 2015; Ross et al.,

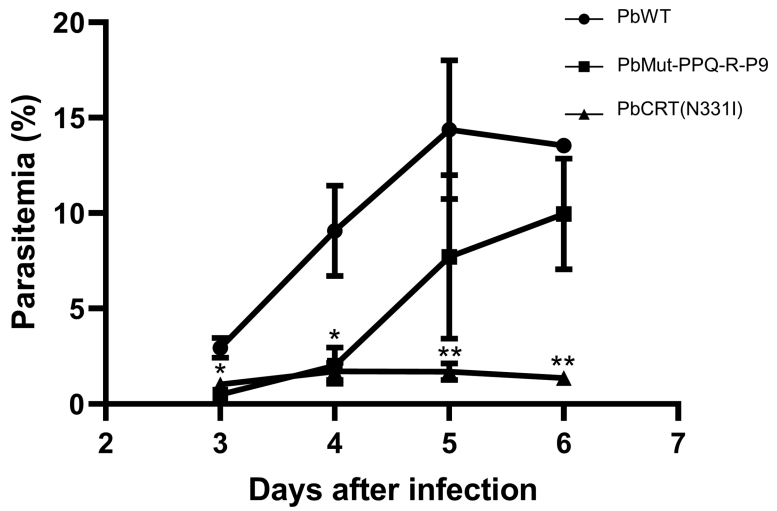

FIGURE 5 | Comparison of growth rates among PbCRT-N331I, PbMut-PPQ-R-P9 and PbWT parasites. Three clones of PbCRT-N331I (closed triangle) and PbMut-PPQ-R-P9 (closed square) were inoculated into one mouse each. PbWT (closed circle) was inoculated into three mice. Parasitemia was monitored from days 3 to 6 after infection. On days 3 and 4, the parasitemia of PbCRT-N331I and PbMut-PPQ-R-P9 was significantly lower than that of PbWT ($p < 0.05$, indicated by a single asterisk). On days 5 and 6, the parasitemia of the PbCRT-N331I parasite was significantly lower than that of PbMut-PPQ-R-P9 and PbWT ($p < 0.05$, indicated by double asterisks). The bar represents the standard deviation.

2018; Dhingra et al., 2019; Hamilton et al., 2019). Direct evidence of these associations from transfection studies using the Dd2 clone has been reported for all the above Southeast Asian mutations; T93S and I218F (Dhingra et al., 2019); H97Y, F145I, M343L, and G353V (Ross et al., 2018) and C350R using the 7G8 clone (Pelleau et al., 2015). Accumulating evidence has revealed that all these mutations reside within a negatively charged cavity in PfCRT where PPQ binds (Kim et al., 2019) and that these mutations change in the electrostatic potential to promote the escape of protonated PPQ from the food vacuole (Coppée et al., 2020), thereby contributing to PPQ resistance/susceptibility. According to the structural model of PfCRT (Kim et al., 2019), PfCRT(N330) appears to localize to the cavity (Protein Data Bank accession no. 6UKJ) (Kim et al., 2019). Thus, it is likely that PbCRT(N331) may also be located in the cavity and contribute to reduced PPQ susceptibility.

The growth of PbCRT-N331I parasites was much slower than that of wild-type parasites (**Figure 5**), suggesting that PbCRT (N331I) may impose a fitness cost. Relatedly, PfCRT(N330I) has not been detected in natural parasite populations (Project, M. falciparum, 2016). It is therefore likely that PfCRT-N330I parasites may not persist in natural populations because of the possible fitness cost of PfCRT(N330I). A supportive example was seen in the PPQ-resistant PfCRT-C101F mutant generated from *in vitro* culture (Eastman et al., 2011). PfCRT-C101F exhibited a much slower replication rate than wild-type parasites (Dhingra et al., 2017) and has not been detected in field samples (Project, M. falciparum, 2016). The absence of PfCRT-N330I in natural parasite populations does not mean that PbMut cannot reproduce PPQ-resistant mechanisms occurring in field parasites. Rather, PbMut could highlight the importance of CRT, especially mutations in the cavity of CRT, for PPQ resistance/susceptibility.

AP2-α (SNP5), a candidate SNP for reduced PPQ susceptibility, is a heterotetrameric complex that is involved in endocytosis (Mettlen et al., 2018). In *P. falciparum*, AP2 is composed of the α, β, μ, and σ subunits (Henrici et al., 2020), particular mutations in which were shown to be associated with drug resistance. The S160N mutation in *AP2-μ* enhanced parasite survival following ACT in Kenya (Henriques et al., 2014). A transfection study revealed that this mutation slightly decreased the *in vitro* sensitivity to quinine (Henriques et al., 2015). AP2-μ has been reported to interact with kelch13 and play roles in hemoglobin internalization and degradation, which regulates heme-dependent artemisinin activation (Yang et al., 2019; Birnbaum et al., 2020). Since the antimalarial action of PPQ is thought to inhibit the detoxification of toxic heme in food vacuoles (Blasco et al., 2017), we speculate that our identified AP2-α mutation might reduce PPQ potency *via* a decrease in hemoglobin uptake.

It has been proposed that copy number variation of *plasmepsin II/III* (*PfPmII/III*) is associated with PPQ susceptibility/resistance in *P. falciparum* (Amato et al., 2017; Witkowski et al., 2017; Bopp et al., 2018). In our study, however, *PbPmIV* (PBANKA_1034400), an ortholog of *PfPmII*, was encoded as a single copy in PbMut-PPQ-R-P9 (data not shown). In support of this finding, the introduction of several PfCRT mutations (H97Y, F145I, M343L, or G353V) into Dd2 gave rise to a PPQ-resistant phenotype without multicopying PfPmII/III (Ross et al., 2018). Overexpression of *PfPmII/III* in 3D7 did not confer PPQ resistance to the parasites (Loesbanluechai et al., 2018). These data suggest dispensable roles of multicopied *PfPmII/III* for PPQ resistance. Besides, PbMut-PPQ-R-P9 has weak PPQ resistance because its ED_{50} is low (2.06 mg/kg) and is much lower than that (168.08 mg/kg) of PPQ-resistant parasites previously

isolated by another group (Kiboi et al., 2009). Thus, PbMut is in the middle of an evolutionary process for acquiring potent PPQ resistance. Whether copy number elevation of *PbPmIV* occurs in PPQ-resistant PbMut parasites may answer the question of its association with PPQ resistance.

Overall, we provide evidence showing that PbMut could serve as a novel forward genetic tool. We previously showed that PbMut populations accumulated many mutations with an increase in the number of serial passages and that each clone had few overlapping mutations (Honma et al., 2016). Therefore, in this experiment, we used PbMut-P91, a high passage number PbMut library, to screen as many mutants as possible for quick isolation of mutants with reduced PPQ susceptibility. Indeed, recrudescence occurred in the mice infected with PbMut but not PbWT at the 1st screen (**Figure 2** and **Table S1**). PbCRT(N331I) already emerged in the parasite populations after the 2nd screen and then outcompeted wild-type parasites in the population after the 8th screen (**Figure S3**). Such rapid emergence of PbCRT(N331I) suggests that it may preexist in the PbMut-P91 population below the detectable limit. It is assumed that a drug-resistant phenotype imposes fitness costs that could be partially compensated by background gene mutations. Mutations such as those in ferredoxin, apicoplast ribosomal protein S10, multidrug resistance 2, and CRT are thought to create a genetic foundation suitable for kelch13 mutations in parasites from Southeast Asia (Miotto et al., 2015). In our study, the growth rate of PbMut-PPQ-R-P9 was higher than that of PbCRT-N331I (**Figure 5**), suggesting that background mutations might exist in PbMut-PPQ-R-P9 that compensate for fitness costs owing to PbCRT(N331I) acquisition. Currently, comparative SNP analysis among parasite populations obtained after each screen (PbMut-PPQ-R-P1 to P9) is ongoing. This study direction could provide clues for understanding genetic mechanisms in the fitness elevation of drug-resistant parasites, which is one of the critical factors for the spread and fixation of drug-resistant parasites in the field.

DATA AVAILABILITY STATEMENT

The datasets presented in this study can be found in online repositories. DDBJ repository (https://www.ddbj.nig.ac.jp/index-e.html), accession number: DRA010243.

ETHICS STATEMENT

The animal study was reviewed and approved by Experimental Animal Ethics Committee of the School of Medicine, Juntendo University, and the assigned numbers were no. 290017.

AUTHOR CONTRIBUTIONS

MI and MH performed the experiments. MH, SI-T, TMo and TMi analyzed the data. MH and TMi wrote the manuscript and supervised the work. All authors contributed to the article and approved the submitted version.

FUNDING

This work was supported by JSPS KAKENHI for Scientific Research (B) and (C) to TMi. (17H04074) and MH (18K07095), respectively. This work was also supported by the Research Program on Emerging and Re-emerging Infectious Diseases (21fk0108138s0402) from the Japan Agency for Medical Research and Development, AMED, to MH.

ACKNOWLEDGMENTS

We would like to thank Mrs. Kaisaki I. for helping with animal and molecular experiments. We also thank the Laboratory of Molecular and Biochemical Research, Research Support Centre, Juntendo University Graduate School of Medicine, for technical support with Sanger sequencing.

SUPPLEMENTARY MATERIAL

The Supplementary Material for this article can be found online at: https://www.frontiersin.org/articles/10.3389/fcimb.2021.672691/full#supplementary-material

REFERENCES

Agrawal, S. (2017). Association of a Novel Mutation in the Plasmodium Falciparum Chloroquine Resistance Transporter With Decreased Piperaquine Sensitivity. *J. Infect. Dis.* 216, 468–476. doi: 10.1093/infdis/jix334

Amaratunga, C., Lim, P., Suon, S., Sreng, S., Mao, S., Sopha, C., et al. (2016). Dihydroartemisinin–Piperaquine Resistance in Plasmodium Falciparum Malaria in Cambodia: A Multisite Prospective Cohort Study. *Lancet Infect. Dis.* 16, 357–365. doi: 10.1016/s1473-3099(15)00487-9

Amato, R., Lim, P., Miotto, O., Amaratunga, C., Dek, D., Pearson, R. D., et al. (2017). Genetic Markers Associated With Dihydroartemisinin–Piperaquine Failure in Plasmodium Falciparum Malaria in Cambodia: A Genotype–Phenotype Association Study. *Lancet Infect. Dis.* 17, 164–173. doi: 10.1016/s1473-3099(16)30409-1

Ariey, F., Witkowski, B., Amaratunga, C., Beghain, J., Langlois, A.-C., Khim, N., et al. (2014). A Molecular Marker of Artemisinin-Resistant Plasmodium Falciparum Malaria. *Nature* 505, 50–55. doi: 10.1038/nature12876

Birnbaum, J., Scharf, S., Schmidt, S., Jonscher, E., Hoeijmakers, W., Flemming, S., et al. (2020). A Kelch13-defined Endocytosis Pathway Mediates Artemisinin Resistance in Malaria Parasites. *Science* 367, 51–59. doi: 10.1126/science.aax4735

Blasco, B., Leroy, D., and Fidock, D. A. (2017). Antimalarial Drug Resistance: Linking Plasmodium Falciparum Parasite Biology to the Clinic. *Nat. Med.* 23, 917–928. doi: 10.1038/nm.4381

Bopp, S., Magistrado, P., Wong, W., Schaffner, S. F., Mukherjee, A., Lim, P., et al. (2018). Plasmepsin II–III Copy Number Accounts for Bimodal Piperaquine Resistance Among Cambodian Plasmodium Falciparum. *Nat. Commun.* 9, 1769. doi: 10.1038/s41467-018-04104-z

Coppée, R., Sabbagh, A., and Clain, J. (2020). Structural and Evolutionary Analyses of the Plasmodium Falciparum Chloroquine Resistance Transporter. *Sci. Rep-uk* 10, 4842. doi: 10.1038/s41598-020-61181-1

Das, S., Saha, B., Hati, A. K., and Roy, S. (2018). Evidence of Artemisinin-Resistant Plasmodium Falciparum Malaria in Eastern India. *N Engl. J. Med.* 379, 1962–1964. doi: 10.1056/nejmc1713777

Dhingra, S. K., Redhi, D., Combrinck, J. M., Yeo, T., Okombo, J., Henrich, P. P., et al. (2017). A Variant Pfcrt Isoform can Contribute to Plasmodium Falciparum Resistance to the First-Line Partner Drug Piperaquine. *Mbio* 8, e00303–e00317. doi: 10.1128/mbio.00303-17

Dhingra, S. K., Small-Saunders, J. L., Ménard, D., and Fidock, D. A. (2019). Plasmodium Falciparum Resistance to Piperaquine Driven by PfCRT. *Lancet Infect. Dis.* 19, 1168–1169. doi: 10.1016/s1473-3099(19)30543-2

Eastman, R. T., Dharia, N. V., Winzeler, E. A., and Fidock, D. A. (2011). Piperaquine Resistance Is Associated With a Copy Number Variation on Chromosome 5 in Drug-Pressured Plasmodium Falciparum Parasites †. *Antimicrob. Agents Chemother.* 55, 3908–3916. doi: 10.1128/aac.01793-10

Ecker, A., Lehane, A. M., Clain, J., and Fidock, D. A. (2012). PfCRT and its Role in Antimalarial Drug Resistance. *Trends Parasitol.* 28, 504–514. doi: 10.1016/j.pt.2012.08.002

Fidock, D. A., Nomura, T., Talley, A. K., Cooper, R. A., Dzekunov, S. M., Ferdig, M. T., et al. (2000). Mutations in the P. falciparum Digestive Vacuole Transmembrane Protein PfCRT and Evidence for Their Role in Chloroquine Resistance. *Mol. Cell.* 6, 861–871. doi: 10.1016/s1097-2765(05)00077-8

Guler, J. L., Freeman, D. L., Ahyong, V., Patrapuvich, R., White, J., Gujjar, R., et al. (2013). Asexual Populations of the Human Malaria Parasite, Plasmodium Falciparum, Use a Two-Step Genomic Strategy to Acquire Accurate, Beneficial DNA Amplifications. *PloS Pathog.* 9, e1003375. doi: 10.1371/journal.ppat.1003375

Hamilton, W. L., Amato, R., van der Pluijm, R. W., Jacob, C. G., Quang, H. H., Thuy-Nhien, N. T., et al. (2019). Evolution and Expansion of Multidrug Resistant Malaria in Southeast Asia: A Genomic Epidemiology Study. *Biorxiv* 19, 621763. doi: 10.1101/621763

Henrici, R. C., Edwards, R. L., Zoltner, M., van Schalkwyk, D. A., Hart, M. N., Mohring, F., et al. (2020). The Plasmodium Falciparum Artemisinin Susceptibility-Associated AP-2 Adaptin μ Subunit Is Clathrin Independent and Essential for Schizont Maturation. *Mbio* 11, e02918-19. doi: 10.1128/mbio.02918-19

Henriques, G., Hallett, R., and Beshir, K. (2014). Directional Selection at the pfmdr1, Pfcrt, pfubp1, and pfap2mu Loci of Plasmodium Falciparum in Kenyan Children Treated With ACT. *J. Infect. Dis.* 210, 2001–2008. doi: 10.1093/infdis/jiu358

Henriques, G., van Schalkwyk, D. A., Burrow, R., Warhurst, D. C., Thompson, E., Baker, D. A., et al. (2015). The Mu Subunit of Plasmodium Falciparum Clathrin-Associated Adaptor Protein 2 Modulates in Vitro Parasite Response to Artemisinin and Quinine. *Antimicrob. Agents Chemother.* 59, 2540–2547. doi: 10.1128/aac.04067-14

Hirai, M., and Mita, T. (2015). Challenging Malaria Control. *Juntendo Med. J.* 61, 370–377. doi: 10.14789/jmj.61.370

Honma, H., Hirai, M., Nakamura, S., Hakimi, H., Kawazu, S., Palacpac, N., et al. (2014). Generation of Rodent Malaria Parasites With a High Mutation Rate by Destructing Proofreading Activity of DNA Polymerase δ. *DNA Res.* 21, 439–446. doi: 10.1093/dnares/dsu009

Honma, H., Niikura, M., Kobayashi, F., Horii, T., Mita, T., Endo, H., et al. (2016). Mutation Tendency of Mutator Plasmodium Berghei With Proofreading-Deficient DNA Polymerase δ. *Sci. Rep-uk* 6, 36971. doi: 10.1038/srep36971

Ikeda, M., Kaneko, M., Tachibana, S.-I., Balikagala, B., Sakurai-Yatsushiro, M., Yatsushiro, S., et al. (2018). Artemisinin-Resistant Plasmodium Falciparum With High Survival Rates, Uganda 2014–2016. *Emerg. Infect. Dis.* 24, 718–726. doi: 10.3201/eid2404.170141

Janse, C. J., Ramesar, J., and Waters, A. P. (2006). High-Efficiency Transfection and Drug Selection of Genetically Transformed Blood Stages of the Rodent Malaria Parasite Plasmodium Berghei. *Nat. Protoc.* 1, 346–356. doi: 10.1038/nprot.2006.53

Juge, N., Moriyama, S., Miyaji, T., Kawakami, M., Iwai, H., Fukui, T., et al. (2015). Plasmodium falciparum Chloroquine Resistance Transporter Is a H+-coupled Polyspecific Nutrient and Drug Exporter. *Proc. Nat. Acad. Sci.* 112, 3356–3361. doi: 10.1073/pnas.1417102112

Kiboi, D. M., Irungu, B. N., Langat, B., Wittlin, S., Brun, R., Chollet, J., et al. (2009). Plasmodium Berghei ANKA: Selection of Resistance to Piperaquine and Lumefantrine in a Mouse Model. *Exp. Parasitol.* 122, 196–202. doi: 10.1016/j.exppara.2009.03.010

Kim, J., Tan, Y. Z., Wicht, K. J., Erramilli, S. K., Dhingra, S. K., Okombo, J., et al. (2019). Structure and Drug Resistance of the Plasmodium Falciparum Transporter PfCRT. *Nature* 576, 315–320. doi: 10.1038/s41586-019-1795-x

Kyaw, M. P., Nyunt, M. H., Chit, K., Aye, M. M., Aye, K. H., Aye, M. M., et al. (2013). Reduced Susceptibility of Plasmodium Falciparum to Artesunate in Southern Myanmar. *PloS One* 8, e57689. doi: 10.1371/journal.pone.0057689

Lin, J., Meireles, P., Prudêncio, M., Engelmann, S., Annoura, T., Sajid, M., et al. (2013). Loss-of-Function Analyses Defines Vital and Redundant Functions of the Plasmodium Rhomboid Protease Family. *Mol. Microbiol.* 88, 318–338. doi: 10.1111/mmi.12187

Loesbanluechai, D., Kotanan, N., de Cozar, C., Kochakarn, T., Ansbro, M. R., Chotivanich, K., et al. (2018). Overexpression of Plasmepsin II and Plasmepsin III Does Not Directly Cause Reduction in Plasmodium Falciparum Sensitivity to Artesunate, Chloroquine and Piperaquine. *Int. J. Parasitol. Drugs Drug Resist.* 9, 16–22. doi: 10.1016/j.ijpddr.2018.11.004

Martin, R. E., Marchetti, R. V., Cowan, A. I., Howitt, S. M., Bröer, S., and Kirk, K. (2009). Chloroquine Transport via the Malaria Parasite's Chloroquine Resistance Transporter. *Science* 325, 1680–1682. doi: 10.1126/science.1175667

Mettlen, M., Chen, P.-H., Srinivasan, S., Danuser, G., and Schmid, S. L. (2018). Regulation of Clathrin-Mediated Endocytosis. *Annu. Rev. Biochem.* 87, 871–896. doi: 10.1146/annurev-biochem-062917-012644

Miotto, O., Amato, R., Ashley, E. A., MacInnis, B., Almagro-Garcia, J., Amaratunga, C., et al. (2015). Genetic Architecture of Artemisinin-Resistant Plasmodium Falciparum. *Nat Genet.* 47, 226–234. doi: 10.1038/ng.3189

Noedl, H., Se, Y., Schaecher, K., Smith, B. L., Socheat, D., Fukuda, M. M., et al. (2008). Evidence of Artemisinin-Resistant Malaria in Western Cambodia. *N. Engl. J. Med.* 359, 2619–2620. doi: 10.1056/nejmc0805011

Pelleau, S., Moss, E. L., Dhingra, S. K., Volney, B., Casteras, J., Gabryszewski, S. J., et al. (2015). Adaptive Evolution of Malaria Parasites in French Guiana: Reversal of Chloroquine Resistance by Acquisition of a Mutation in Pfcrt. *Proc. Natl. Acad. Sci.* 112, 11672–11677. doi: 10.1073/pnas.1507142112

Peters, W. (1965). Drug Resistance in Plasmodium berghei Vincke and Lips 1948. I. Chloroquine Resistance. *Exp. Parasitol.* 17, 80–89. doi: 10.1016/0014-4894(65)90012-3

Phyo, A. P., Nkhoma, S., Stepniewska, K., Ashley, E. A., Nair, S., McGready, R., et al. (2012). Emergence of Artemisinin-Resistant Malaria on the Western Border of Thailand: A Longitudinal Study. *Lancet* 379, 1960–1966. doi: 10.1016/s0140-6736(12)60484-x

Project, M. falciparum (2016). Genomic Epidemiology of Artemisinin Resistant Malaria. *eLife* 5, e08714. doi: 10.7554/eLife.08714

Roepe, P. D. (2011). PfCRT-Mediated Drug Transport in Malarial Parasites. *Biochemistry-us* 50, 163–171. doi: 10.1021/bi101638n

Rosenthal, P. J. (2013). The Interplay Between Drug Resistance and Fitness in Malaria Parasites. *Mol. Microbiol.* 89, 1025–1038. doi: 10.1111/mmi.12349

Ross, L. S., Dhingra, S. K., Mok, S., Yeo, T., Wicht, K. J., Kümpornsin, K., et al. (2018). Emerging Southeast Asian PfCRT Mutations Confer Plasmodium Falciparum Resistance to the First-Line Antimalarial Piperaquine. *Nat. Commun.* 9, 3314. doi: 10.1038/s41467-018-05652-0

Thanh, N. V., Thuy-Nhien, N., Tuyen, N. T. K., Tong, N. T., Nha-Ca, N. T., Dong, L. T., et al. (2017). Rapid Decline in the Susceptibility of Plasmodium Falciparum to Dihydroartemisinin–Piperaquine in the South of Vietnam. *Malaria J.* 16, 27. doi: 10.1186/s12936-017-1680-8

WHO and 2020 (n.d.) *World Malaria Report 2020* (Geneva, Switzerland: WHO Press).

Witkowski, B., Duru, V., Khim, N., Ross, L. S., Saintpierre, B., Beghain, J., et al. (2017). A Surrogate Marker of Piperaquine-Resistant Plasmodium Falciparum Malaria: A Phenotype–Genotype Association Study. *Lancet Infect. Dis.* 17, 174–183. doi: 10.1016/s1473-3099(16)30415-7

Yang, T., Yeoh, L. M., Tutor, M. V., Dixon, M. W., McMillan, P. J., Xie, S. C., et al. (2019). Decreased K13 Abundance Reduces Hemoglobin Catabolism and Proteotoxic Stress, Underpinning Artemisinin Resistance. *Cell Rep.* 29, 2917–2928.e5. doi: 10.1016/j.celrep.2019.10.095

Ye, R., Tian, Y., Huang, Y., Zhang, Y., Wang, J., Sun, X., et al. (2019). Genome-Wide Analysis of Genetic Diversity in Plasmodium Falciparum Isolates From China–Myanmar Border. *Front. Genet.* 10:1065. doi: 10.3389/fgene.2019.01065

Zhang, Q., Siegel, N. T., Martins, R. M., Wang, F., Cao, J., Gao, Q., et al. (2014). Exonuclease-Mediated Degradation of Nascent RNA Silences Genes Linked to Severe Malaria. *Nature* 513, 431–435. doi: 10.1038/nature13468

Conflict of Interest: The authors declare that the research was conducted in the absence of any commercial or financial relationships that could be construed as a potential conflict of interest.

Advantages of publishing in Frontiers

OPEN ACCESS
Articles are free to read for greatest visibility and readership

FAST PUBLICATION
Around 90 days from submission to decision

HIGH QUALITY PEER-REVIEW
Rigorous, collaborative, and constructive peer-review

TRANSPARENT PEER-REVIEW
Editors and reviewers acknowledged by name on published articles

Frontiers
Avenue du Tribunal-Fédéral 34
1005 Lausanne | Switzerland

Visit us: www.frontiersin.org
Contact us: frontiersin.org/about/contact

REPRODUCIBILITY OF RESEARCH
Support open data and methods to enhance research reproducibility

DIGITAL PUBLISHING
Articles designed for optimal readership across devices

FOLLOW US
@frontiersin

IMPACT METRICS
Advanced article metrics track visibility across digital media

EXTENSIVE PROMOTION
Marketing and promotion of impactful research

LOOP RESEARCH NETWORK
Our network increases your article's readership